BNL 72009

National Synchrotron Light Source Activity Report 2003

National Synchrotron Light Source

Activity Report 2003

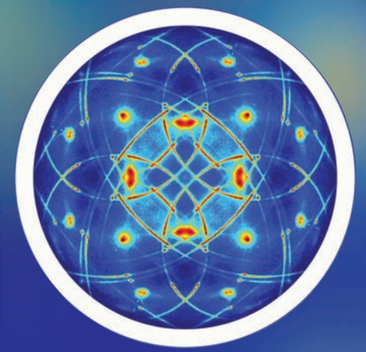

BNL-72009 - 2004
UC400
(General Energy Research)

Printed in the United States of America
Available from
National Technical Information Service
U.S. Department of Commerce
5285 Port Royal Road
Springfield, VA 22161

National Synchrotron Light Source
2003 Activity Report

Lisa M. Miller
managing editor

Laura Y. Mgrdichian
science editor

Nancye A. Wright, Stephen A. Giordano & Theresa A. Esposito
design & layout

The National Synchrotron Light Source is supported by the
Office of Basic Energy Sciences, United States Department of Energy, Washington, D.C.

Brookhaven National Laboratory, Brookhaven Science Associates, Inc., Upton, New York 11973
Under contract no. DE-AC02-98CH10886

BROOKHAVEN NATIONAL LABORATORY

nsls IR UV X

Office of Science U.S. DEPARTMENT OF ENERGY

Office of Basic Energy Sciences • Serving the Present, Shaping the Future •

Introduction

Science Highlights

Year in Review

NSLS Organization

Facility Report

Facts and Figures

Publications

Introduction

Chairman's Introduction

Steve Dierker
Chairman, National Synchrotron Light Source

The scientific productivity of the NSLS continues to be outstanding and the research conducted here has high impact. 2003 was no exception and some of the many highlights from this year's research activity are included in this Activity Report. We are especially pleased that one of our users, Professor Roderick MacKinnon (Rockefeller University), was the co-recipient of the 2003 Nobel Prize in Chemistry for work, much of which was done at the NSLS, explaining how proteins known as ion channels help to generate nerve impulses. It is also a particular pleasure to note that NSLS accelerator physicist Li Hua Yu was awarded the 2003 International Free Electron Laser Prize in recognition of his outstanding achievements, especially demonstrating High Gain Harmonic Generation (HGHG) at the DUV-FEL.

Our vision for the NSLS in the next five to 10 years is for it to continue to serve as a vital resource for the nation and especially for the strong Northeast research community. To accomplish this, we are working to preserve and enhance its outstanding scientific productivity by providing increased user support and upgrading beamline and endstation instrumentation. For example, this past year we collaborated with scientists from the Albert Einstein College of Medicine and the BNL Biology Department to develop a new undulator beamline, X29, to meet the needs of macromolecular crystallography for high brightness x-rays. A new endstation on the undulator beamline X13B is being equipped with optics and instrumentation for microdiffraction and microprobe experiments. The wiggler beamline, X21, is being upgraded to provide high intensity and increased capacity for small angle x-ray scattering experiments on nanotemplated soft matter, biomaterials, and other systems. We are collaborating with the BNL Center for Functional Nanomaterials to develop a beamline for LEEM/PEEM studies, which will add important new capabilities for nanoscience and catalysis research. A new high-speed, high-resolution curved position sensitive detector for powder diffraction was also developed and made available to users to enable time-resolved studies of reaction mechanisms, phase transformations, chemical kinetics, and material dynamics. At the DUV-FEL, this past year saw the achievement of HGHG light at 266 nm, with a substantial third harmonic at 89 nm. User science experiments were initiated and published in Physical Review Letters and a successful workshop was held to identify the new scientific opportunities in the chemical sciences enabled by this unique light source. These and many other important projects are described more fully in the Facility Report.

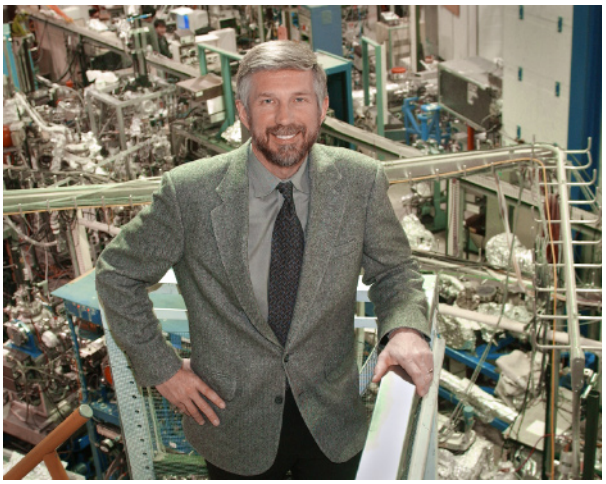

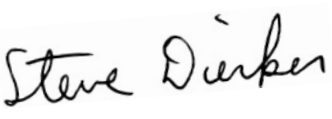

However, in spite of these efforts, the capabilities of the present NSLS are increasingly limiting the productivity of its user community. Continually updated over more than 20 years, with brightness several orders of magnitude higher than the initial design value, the performance of

the NSLS has reached its theoretical limit - its brightness cannot be increased significantly beyond its current value, and its eight-fold periodicity severely limits the number of insertion devices. Over the past two years we have engaged the user community in an extensive dialogue to answer the question, "What science will users do in 10+ years and what will they need to do it?" While predicting the future is always difficult, the user community responded enthusiastically, and in more than two dozen workshops (13 in 2003 alone) they identified the future 'grand challenge' problems in the fields of life science, nanoscience, materials and chemical sciences, geoscience, and environmental science. The clear result is that, in order for the legendary productivity of the NSLS to continue, and to tackle the 'grand challenge' problems of tomorrow, it is essential that the NSLS be upgraded to provide much higher average brightness and flux.

NSLS-II is a proposed new advanced third generation medium energy storage ring designed to deliver world leading brightness and flux with top-off operation for constant output. The facility will be able to produce x-rays up to 10,000 times brighter than those produced at the NSLS today.

To provide these capabilities, we submitted a proposal to the Department of Energy (DOE) for NSLS-II, a new National Synchrotron Light Source at BNL. Our initial proposal was reviewed in February 2003 by a DOE Basic Energy Sciences Subcommittee, convened as part of the process of formulating the 20-year facilities plan, and later released by the DOE. Recognizing the continued need for third generation x-ray sources, the subcommittee recommended that we work with DOE to formulate a plan for a new third generation ring to replace the current NSLS; now NSLS-II is one of the facilities listed on the 20-year DOE facilities plan. After collecting additional input from the user community and refining our concept, we will submit a full proposal describing the scientific opportunities enabled by NSLS-II, and its pre-conceptual design, in March 2004. NSLS-II will be a highly optimized, third generation medium energy storage ring with full energy injection for top-off mode operation. The x-ray brightness and flux of NSLS-II will be world leading and will be 10,000 times brighter and have 10 times more flux than the present NSLS across the energy spectrum from ~10 eV up to ~20 keV. The present VUV/IR ring will be relocated to the new facility to serve as a dedicated IR ring, which will provide world-leading brightness and flux in the important near- to far-IR spectral region.

Access to these new capabilities and the unique infrastructure envisioned for the new facility will have profound impact on a wide range of scientific disciplines and initiatives and lead to many exciting discoveries in the coming decades. NSLS-II will enable structural studies of the smallest crystals in structural biology and provide a wide range of nanometer resolution probes for nanoscience. It will make possible coherent beam scattering studies of the dynamics of condensed matter systems in an otherwise inaccessible regime of low frequencies and short length scales. It will introduce new methods for imaging the structure of biological systems and disordered materials, and greatly increase the applicability of inelastic x-ray scattering. The superlative character and combination of capabilities of NSLS-II will serve the cutting edge science of the nation, and will have a particularly dramatic impact as a vital resource for the strong academic and industrial research community of the Northeast United States.

Thus, our vision for NSLS in the next 10 to 30 years is to enable grand challenge science by providing world-leading capabilities. NSLS-II will accomplish this goal.

Users' Executive Committee Update

Anthony Lanzirotti
University of Chicago
NSLS Users' Executive Committee Chair

This has been a very exciting year at the NSLS and it has been an honor to serve as Chair of the Users' Executive Committee. As of May 18, 2004, I will pass on the mantle to Larry Shapiro. It has been a distinct pleasure to represent the NSLS user community in a very exciting time in our history, as we begin to take a hard look at our future.

And a very bright future it appears to be. This past year, we prepared for the submission of the NSLS-II proposal to DOE, a proposal highlighted by a large degree of user interaction. I believe it is clear to all of us that the likelihood of NSLS-II coming to fruition is very good indeed, and I feel confident that we will see a third generation light source here at BNL. But, perhaps, it is in these times of elevated expectations that it is most important for the user community to make its desires and concerns clear – not only to ensure that NSLS-II becomes a reality, but also to guarantee that the current NSLS continues to operate at its maximum potential in the interim period. It has been my experience while serving on the UEC that users can have a strong impact on how such projects are prioritized by participating in education and outreach efforts to our representatives and local community.

As we look to the future and NSLS-II, we also want to ensure that there are adequate funds and staff to upgrade and improve the current facility. For example, it has been a pleasure to see new beamlines come online over the past year, and others begin construction. These include the new X17B2 and B3 wiggler beamlines for high-pressure research, using large volume multi-anvil and diamond anvil cell presses. These were constructed as the result of NSLS collaborations with the NSF Consortium for Materials Properties Research in Earth Sciences (COMPRES). A new undulator-based protein crystallography beamline, X29, was constructed through a partnership between AECOM, BNL's Biology Department, and the NSLS. In 2003, construction also began on a new undulator-based x-ray micro-diffraction beamline, X13B, recently funded by DOE, and a new hard x-ray microprobe beamline operated at X27A, funded as a joint DOE/NSF collaboration with Stony Brook University's Center for Environmental Molecular Sciences, BNL's Environmental Sciences Department, and the NSLS.

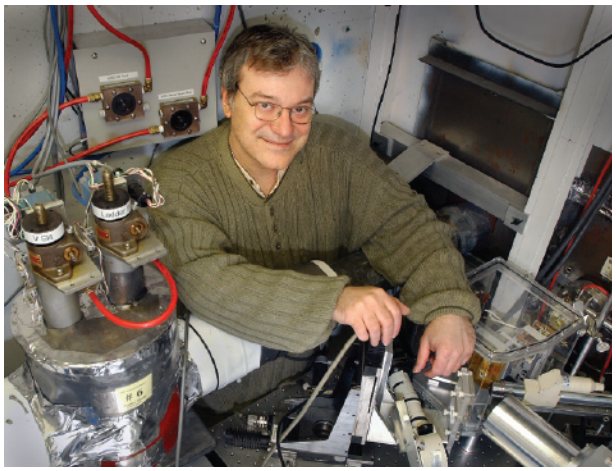

But many of the issues related to upgrading and maintaining the existing facility are not as obvious as the appearance of a new beamline. They include maintenance of an aging infrastructure, upgrades to beamline control and computing systems (particularly as older systems are no longer supported by manufacturers), detector upgrades, and adequate scientific and technical staffing at beamlines. I think these are areas where an increased level of dialog (and funding) is needed to keep the NSLS vibrant, and some hard questions must be asked about how DOE,

the NSLS, existing PRT's, and incoming Collaborative User groups will support these issues.

Over the past year, the UEC has also actively been involved in a number of administrative and policy changes that will directly affect how users obtain beamtime in the future. Arguably the most significant of these was the change in the User Access Policy, a re-definition of the modes of access to beamtime at the NSLS. The policy change saw the addition of Collaborative Users as groups that contribute to the beamline in terms of funding, instrumentation, or operations, but do not operate beamlines fully, like PRTs. We have also been involved in advising the NSLS on its development of an online Proposal, Allocation, Scheduling, and Safety (PASS) system that will dramatically change how requests for beamtime at the NSLS are submitted, reviewed, allocated, scheduled, and tabulated.

And of course the primary annual event organized by the UEC last year, with invaluable assistance from the Users' Office, was the 2003 NSLS Users' Meeting. Last year's meeting was held May 19-21. The UEC felt the meeting was a huge success with a record attendance of 396 registered participants. We all feel the attendance reflects our strong optimism about the future of the NSLS and synchrotron science at BNL. I assure you that this does not go unnoticed in Washington and I am confident that the 2004 attendance will far exceed what we achieved last year, thanks primarily to user and staff dedication and enthusiasm about the scientific accomplishments achieved at this facility. On behalf of the UEC, I wish to thanks everyone for a pivotal and successful year. Cheers!

Chairman's Introduction

Steve Dierker
Chairman, National Synchrotron Light Source

The scientific productivity of the NSLS continues to be outstanding and the research conducted here has high impact. 2003 was no exception and some of the many highlights from this year's research activity are included in this Activity Report. We are especially pleased that one of our users, Professor Roderick MacKinnon (Rockefeller University), was the co-recipient of the 2003 Nobel Prize in Chemistry for work, much of which was done at the NSLS, explaining how proteins known as ion channels help to generate nerve impulses. It is also a particular pleasure to note that NSLS accelerator physicist Li Hua Yu was awarded the 2003 International Free Electron Laser Prize in recognition of his outstanding achievements, especially demonstrating High Gain Harmonic Generation (HGHG) at the DUV-FEL.

Our vision for the NSLS in the next five to 10 years is for it to continue to serve as a vital resource for the nation and especially for the strong Northeast research community. To accomplish this, we are working to preserve and enhance its outstanding scientific productivity by providing increased user support and upgrading beamline and endstation instrumentation. For example, this past year we collaborated with scientists from the Albert Einstein College of Medicine and the BNL Biology Department to develop a new undulator beamline, X29, to meet the needs of macromolecular crystallography for high brightness x-rays. A new endstation on the undulator beamline X13B is being equipped with optics and instrumentation for microdiffraction and microprobe experiments. The wiggler beamline, X21, is being upgraded to provide high intensity and increased capacity for small angle x-ray scattering experiments on nanotemplated soft matter, biomaterials, and other systems. We are collaborating with the BNL Center for Functional Nanomaterials to develop a beamline for LEEM/PEEM studies, which will add important new capabilities for nanoscience and catalysis research. A new high-speed, high-resolution curved position sensitive detector for powder diffraction was also developed and made available to users to enable time-resolved studies of reaction mechanisms, phase transformations, chemical kinetics, and material dynamics. At the DUV-FEL, this past year saw the achievement of HGHG light at 266 nm, with a substantial third harmonic at 89 nm. User science experiments were initiated and published in Physical Review Letters and a successful workshop was held to identify the new scientific opportunities in the chemical sciences enabled by this unique light source. These and many other important projects are described more fully in the Facility Report.

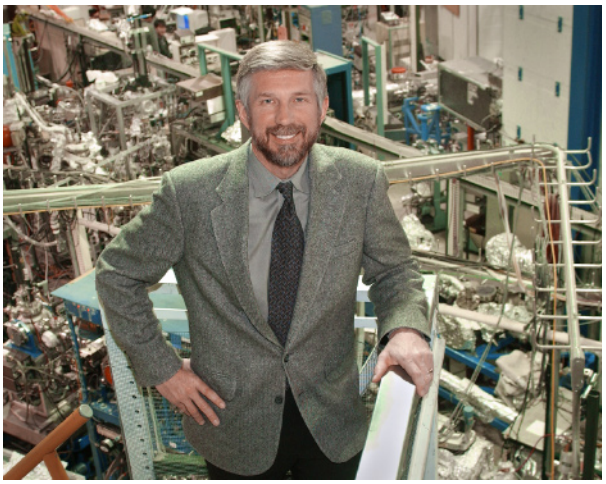

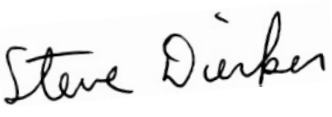

However, in spite of these efforts, the capabilities of the present NSLS are increasingly limiting the productivity of its user community. Continually updated over more than 20 years, with brightness several orders of magnitude higher than the initial design value, the performance of

the NSLS has reached its theoretical limit - its brightness cannot be increased significantly beyond its current value, and its eight-fold periodicity severely limits the number of insertion devices. Over the past two years we have engaged the user community in an extensive dialogue to answer the question, "What science will users do in 10+ years and what will they need to do it?" While predicting the future is always difficult, the user community responded enthusiastically, and in more than two dozen workshops (13 in 2003 alone) they identified the future 'grand challenge' problems in the fields of life science, nanoscience, materials and chemical sciences, geoscience, and environmental science. The clear result is that, in order for the legendary productivity of the NSLS to continue, and to tackle the 'grand challenge' problems of tomorrow, it is essential that the NSLS be upgraded to provide much higher average brightness and flux.

NSLS-II is a proposed new advanced third generation medium energy storage ring designed to deliver world leading brightness and flux with top-off operation for constant output. The facility will be able to produce x-rays up to 10,000 times brighter than those produced at the NSLS today.

To provide these capabilities, we submitted a proposal to the Department of Energy (DOE) for NSLS-II, a new National Synchrotron Light Source at BNL. Our initial proposal was reviewed in February 2003 by a DOE Basic Energy Sciences Subcommittee, convened as part of the process of formulating the 20-year facilities plan, and later released by the DOE. Recognizing the continued need for third generation x-ray sources, the subcommittee recommended that we work with DOE to formulate a plan for a new third generation ring to replace the current NSLS; now NSLS-II is one of the facilities listed on the 20-year DOE facilities plan. After collecting additional input from the user community and refining our concept, we will submit a full proposal describing the scientific opportunities enabled by NSLS-II, and its pre-conceptual design, in March 2004. NSLS-II will be a highly optimized, third generation medium energy storage ring with full energy injection for top-off mode operation. The x-ray brightness and flux of NSLS-II will be world leading and will be 10,000 times brighter and have 10 times more flux than the present NSLS across the energy spectrum from ~10 eV up to ~20 keV. The present VUV/IR ring will be relocated to the new facility to serve as a dedicated IR ring, which will provide world-leading brightness and flux in the important near- to far-IR spectral region.

Access to these new capabilities and the unique infrastructure envisioned for the new facility will have profound impact on a wide range of scientific disciplines and initiatives and lead to many exciting discoveries in the coming decades. NSLS-II will enable structural studies of the smallest crystals in structural biology and provide a wide range of nanometer resolution probes for nanoscience. It will make possible coherent beam scattering studies of the dynamics of condensed matter systems in an otherwise inaccessible regime of low frequencies and short length scales. It will introduce new methods for imaging the structure of biological systems and disordered materials, and greatly increase the applicability of inelastic x-ray scattering. The superlative character and combination of capabilities of NSLS-II will serve the cutting edge science of the nation, and will have a particularly dramatic impact as a vital resource for the strong academic and industrial research community of the Northeast United States.

Thus, our vision for NSLS in the next 10 to 30 years is to enable grand challenge science by providing world-leading capabilities. NSLS-II will accomplish this goal.

Users' Executive Committee Update

Anthony Lanzirotti
University of Chicago
NSLS Users' Executive Committee Chair

This has been a very exciting year at the NSLS and it has been an honor to serve as Chair of the Users' Executive Committee. As of May 18, 2004, I will pass on the mantle to Larry Shapiro. It has been a distinct pleasure to represent the NSLS user community in a very exciting time in our history, as we begin to take a hard look at our future.

And a very bright future it appears to be. This past year, we prepared for the submission of the NSLS-II proposal to DOE, a proposal highlighted by a large degree of user interaction. I believe it is clear to all of us that the likelihood of NSLS-II coming to fruition is very good indeed, and I feel confident that we will see a third generation light source here at BNL. But, perhaps, it is in these times of elevated expectations that it is most important for the user community to make its desires and concerns clear – not only to ensure that NSLS-II becomes a reality, but also to guarantee that the current NSLS continues to operate at its maximum potential in the interim period. It has been my experience while serving on the UEC that users can have a strong impact on how such projects are prioritized by participating in education and outreach efforts to our representatives and local community.

As we look to the future and NSLS-II, we also want to ensure that there are adequate funds and staff to upgrade and improve the current facility. For example, it has been a pleasure to see new beamlines come online over the past year, and others begin construction. These include the new X17B2 and B3 wiggler beamlines for high-pressure research, using large volume multi-anvil and diamond anvil cell presses. These were constructed as the result of NSLS collaborations with the NSF Consortium for Materials Properties Research in Earth Sciences (COMPRES). A new undulator-based protein crystallography beamline, X29, was constructed through a partnership between AECOM, BNL's Biology Department, and the NSLS. In 2003, construction also began on a new undulator-based x-ray micro-diffraction beamline, X13B, recently funded by DOE, and a new hard x-ray microprobe beamline operated at X27A, funded as a joint DOE/NSF collaboration with Stony Brook University's Center for Environmental Molecular Sciences, BNL's Environmental Sciences Department, and the NSLS.

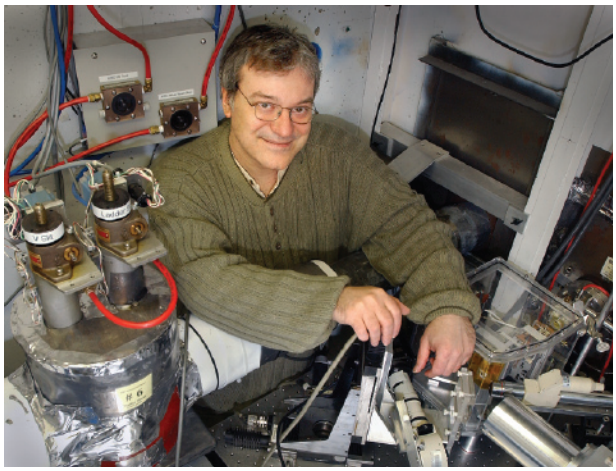

But many of the issues related to upgrading and maintaining the existing facility are not as obvious as the appearance of a new beamline. They include maintenance of an aging infrastructure, upgrades to beamline control and computing systems (particularly as older systems are no longer supported by manufacturers), detector upgrades, and adequate scientific and technical staffing at beamlines. I think these are areas where an increased level of dialog (and funding) is needed to keep the NSLS vibrant, and some hard questions must be asked about how DOE,

the NSLS, existing PRT's, and incoming Collaborative User groups will support these issues.

Over the past year, the UEC has also actively been involved in a number of administrative and policy changes that will directly affect how users obtain beamtime in the future. Arguably the most significant of these was the change in the User Access Policy, a re-definition of the modes of access to beamtime at the NSLS. The policy change saw the addition of Collaborative Users as groups that contribute to the beamline in terms of funding, instrumentation, or operations, but do not operate beamlines fully, like PRTs. We have also been involved in advising the NSLS on its development of an online Proposal, Allocation, Scheduling, and Safety (PASS) system that will dramatically change how requests for beamtime at the NSLS are submitted, reviewed, allocated, scheduled, and tabulated.

And of course the primary annual event organized by the UEC last year, with invaluable assistance from the Users' Office, was the 2003 NSLS Users' Meeting. Last year's meeting was held May 19-21. The UEC felt the meeting was a huge success with a record attendance of 396 registered participants. We all feel the attendance reflects our strong optimism about the future of the NSLS and synchrotron science at BNL. I assure you that this does not go unnoticed in Washington and I am confident that the 2004 attendance will far exceed what we achieved last year, thanks primarily to user and staff dedication and enthusiasm about the scientific accomplishments achieved at this facility. On behalf of the UEC, I wish to thanks everyone for a pivotal and successful year. Cheers!

Science Highlights

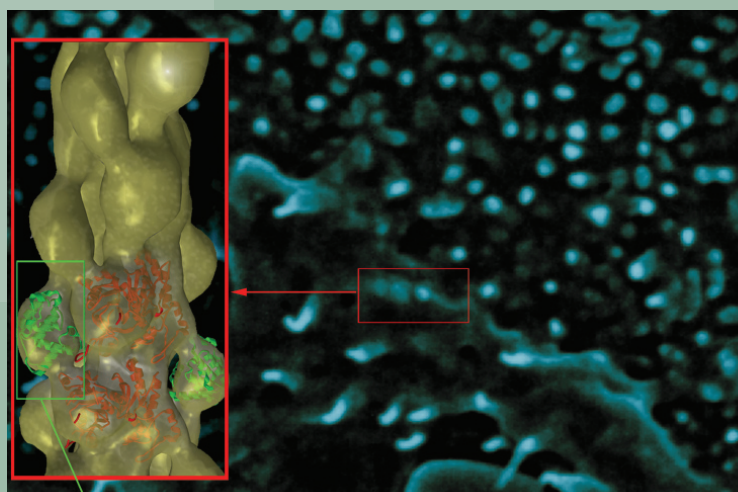

Science at the NSLS

Laura Mgrdichian
NSLS SCIENCE WRITER

As the new science writer at the NSLS, I am especially excited to introduce this year's Science Highlights and Feature Highlights sections. The articles presented in the following pages are just a sampling of the fantastic research performed at the NSLS in the chemical, material, environmental, physical, and life sciences.

Read on for summaries of highlighted work in these areas, such as research into a compound that could improve lithium ion batteries, the effect of nickel and uranium-contaminated soil on the growth of willow trees, the study of a material used in the microelectronics industry, and research that could lead to diabetes and obesity treatment drugs.

Of the hundreds of articles published by NSLS users each year in peer-reviewed journals, a few dozen are selected as potential Science Highlights. These Highlights, as we call them, are summarized versions of the published papers. They are written by the scientists themselves, and then sent to me to be edited and prepared for web posting. Highlights are intended for NSLS users and other readers with scientific background; Features are written by Brookhaven Lab science writers and are targeted at a general audience.

Because I joined the NSLS in October of 2003, I cannot take credit for all the editing and writing involved in creating these sections. To that end, I would like to acknowledge Lisa Miller, Mona S. Rowe, Karen McNulty Walsh, and Patrice Pages for their work.

Nonetheless, I am pleased to have contributed what I could, and I thank the scientists I've worked with and the NSLS staff for their cooperation and support. I think of myself as a valuable link between the NSLS and the outside community, and I look forward to championing the important research that is done here.

Science Highlights

■ Feature Highlights

■ Chemical Sciences

■ Condensed Matter Physics

■ GEOLOGICAL AND ENVIRONMENTAL SCIENCES

■ LIFE SCIENCES

■ Life Sciences (continued)

■ Soft Condensed Matter and Biophysics

■ SURFACES, INTERFACES, AND NANOMATERIALS

Feature Highlights

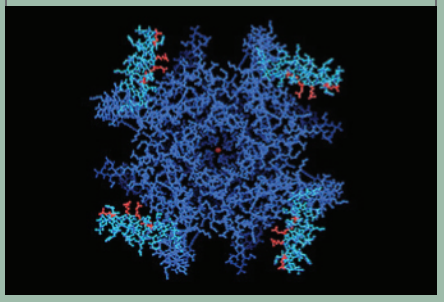

2003 Nobel Prize in Chemistry Awarded to NSLS User Roderick MacKinnon

Roderick MacKinnon, M.D., a professor at Rockefeller University, investigator at the Howard Hughes Medical Institute, and frequent NSLS user, shared this year's Nobel Prize in Chemistry for work explaining how a class of proteins helps to generate nerve impulses – the electrical activity that underlies all movement, sensation, and perhaps even thought. The work leading to the prize was done primarily at the Cornell High Energy Synchrotron Source (CHESS) and the NSLS.

"Without the synchrotrons, none of the work I do would be possible," MacKinnon told *Newsday.*

Rod MacKinnon

The proteins, called ion channels, are tiny pores that stud the surface of nearly all living cells. These channels allow the passage of potassium, calcium, sodium, and chloride molecules called ions. Rapid-fire opening and closing of these channels releases ions, moving electrical impulses from the brain in a wave to their destination in the body. The entire sequence of events takes only a few milliseconds, and occurs tens of thousands of times every day in human beings and organisms of all varieties.

Starting in 1998, after 10 years spent studying the biophysics of ion channels, MacKinnon and his research team surprised the entire research community when they published the very first potassium channel structure, which revealed the way that positively charged potassium ions flow easily through a pore formed by a protein that spans the cell membrane. Thanks to this contribution we can now "see" ions flowing through channels that open and close in response to different cellular signals.

In the five years following, the Rockefeller scientists have continued their research, revealing the inner workings of sodium and potassium channels, or the whys and hows of ion movement through a cell's membrane. This series of structural solutions, determined by x-ray crystallography, offers high resolution molecular-level "snapshots" of ion channels that literally showed the scientific community how electrical signaling occurs.

These structures not only portray an elusive ion channel structurally and mechanically, but also bring history full circle by showing, for the first time, the natural molecular mechanism that underlies the "action potential" theory. In 1952, the theory was demonstrated in a mathematical formulation by English physiologists Alan Hodgkin and Andrew Huxley, who identified a loop relationship between cell membrane permeability (the ability of a cell to open up via ion channels) and the voltage between the inside and outside of the cell.

In this theory, the "action potential" of nerve cells is generated when an ion channel on the surface of a nerve cell is opened by a chemical signal – a neurotransmitter called glutamate – which is sent from an adjacent nerve cell. As a result, positively charged sodium ions enter the cell's negatively charged interior. But this single event triggers an electrical pulse that propagates, like a chain reaction, along the surface of the nerve cell, causing sodium-conducting channels on the cell's surface to

open up. More sodium enters the cell, and the normal negative inside/positive outside voltage common to all living cells is upset. The whole process occurs in a matter of milliseconds.

The overall effect is an explosive, and then restorative, burst of energy to the otherwise placid cell membrane. As soon as the cascade of sodium channeling begins, hyper-sensitive voltage-dependent potassium channels along the same cell's surface sense the catastrophic switching of the charge value inside the cell. In their own domino effect, they open up to allow positively charged potassium ions to quickly flow out of the cell, restoring the negative inside/positive outside charge balance.

Until the research of MacKinnon and his group, however, no group of researchers had ever completed the loop by solving the riddle of how the membrane voltage determines the permeability. Their work widens a foot trail into an avenue for an entire new area of medical study on the hundreds of ion channel-related diseases and disorders, such as epilepsy, cystic fibrosis, and osteoporosis.

MacKinnon, a biophysicist and self-taught X-ray crystallographer, shares the 2003 Nobel Prize in Chemistry with Peter Agre, M.D., of Johns Hopkins University School of Medicine, who received his award for studies of another type of membrane channel protein.

—Karen McNulty Walsh, Laura Mgrdichian, and Lynn Love

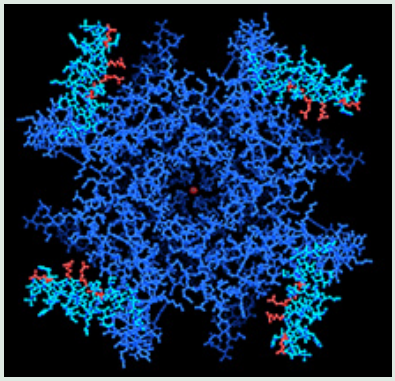

An overhead view of a voltage-dependent potassium ion channel shows four red-tipped "paddles" that open and close in response to positive and negative charges. This structure, discovered by Rockefeller scientists, shows for the first time the molecular mechanism by which potassium ions are allowed in and out of living cells during a nerve or muscle impulse.

NSLS Users Discover a New Material Texture Type

Researchers working at the National Synchrotron Light Source have identified a new way in which the orientation of the tiny grains that make up various materials can be classified. There were previously only three known types of grain orientation, and the discovery of a fourth type may have broad impact on technology research and the study of materials and crystals.

The results appeared in the December 11, 2003 issue of *Nature*.

At the microscopic level, most manufactured and naturally occurring materials, such as metals, are made of crystalline grains – tiny regions of ordered, symmetrical arrays of atoms or molecules. In the field of materials science, the way these grains fit together to form the overall material is referred to as the material's "texture."

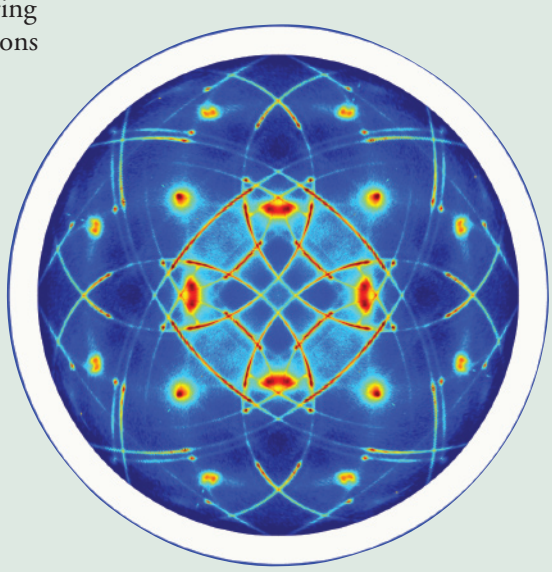

A pole figure of the NiSi thin film.

Until this discovery, there were three texture types, known as "random," "fiber," and "epitaxy" textures. To get a sense of these textures, picture a bucket of children's building blocks to represent the individual grains. If the blocks are dumped onto a table, the resulting jumbled pile, containing blocks in messy layers and many different positions, simulates a random texture. If the blocks are instead placed in layers such that the bottom face of each one is parallel to the table, but neighboring blocks are not parallel to each other, the configuration resembles a fiber texture. Finally, if the blocks are carefully placed in a series of neat, parallel stacks, like a three-dimensional checkerboard, an epitaxial texture is represented.

In materials science research, materials often take the form of "thin films" that are less than one-millionth of a meter thick. To be studied, these thin films must be produced on the surface of another material, called the "substrate." The region where the substrate meets the thin film is called the "interface." In our block example, the table acts like a substrate, and an interface exists between it and the blocks.

Keeping all this in mind, the new texture type, named "axiotaxy," is similar to fiber texture. However, instead of sitting flat on the table, each "block" is tilted upwards at the same angle, as if resting against an invisible sloped surface. This causes a special relationship to form between the orientation of the grains in the thin film and the substrate.

"The mechanism that causes the formation of this new type of texture is unique, and may help us to better understand the physics of thin film growth and phase transformations in thin films," said Christophe Detavernier, a materials scientist at the IBM T.J. Watson Research Center in Yorktown Heights, New York and the University of Ghent, Belgium. He is a member of the research group that discovered the new texture at the NSLS.

In the continuing development of portable electronics, such as cell phones, handheld computers, and digital music players, the study of thin films is crucial to creating the tiny electrical circuits that make these devices work. Therefore, gathering more knowledge of texture is just as important.

"The effect of texture on a material's physical properties is exploited in technology development in order to produce materials with specific characteristics," explained Detavernier.

"We focused on a class of materials called silicides that are used in integrated circuits. As the aggressive trend in miniaturization continues in silicon-based devices, controlling the properties of silicides becomes challenging. Therefore, understanding and controlling texture becomes critical in certain cases."

Authors Jean Jordan-Sweet and Ahmet Ozcan.

Details of the Discovery

The researchers discovered the new texture while studying a thin film of a nickel/silicon compound, called nickel silicide (NiSi). Starting with a substrate of pure silicon, they formed a NiSi thin film by depositing a small amount of pure nickel on the silicon substrate. During an annealing treatment, in which the sample was heated to 550 degrees Celsius in a furnace, a solid-state reaction occurred between the nickel and silicon. This caused all of the nickel to be consumed and a NiSi layer to form on the substrate.

Working at NSLS beamline X20A, the researchers shined x-rays at the film from several different angles and, using a computer, analyzed the pattern the rays created as they emerged from the material. The resulting image, known as a "pole figure," represents the distribution of the grain orientation in the film.

The researchers knew they had found a new texture when they noticed that their pole figures did not resemble those produced by materials with random, fiber, or epitaxy textures, or any combination of them (since many films contain elements of all three textures). They are now looking for axiotaxy in other thin films.

— Laura Mgrdichian

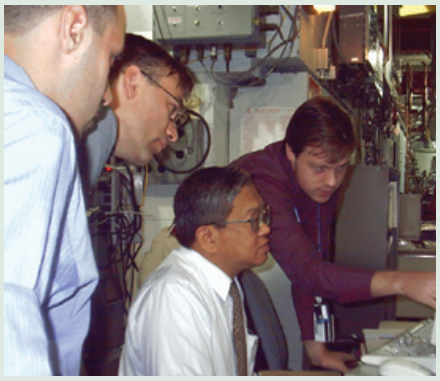

From left, IBM Researcher Cyril Cabral, Jr., Author Christian Lavoie, T.C. Chen (IBM Vice President, Silicon Technology), and Christophe Detavernier.

New Irreversible Expansion May Yield Better Pollution Trap

Scientists from Brookhaven National Laboratory and their collaborators have previously shown that certain zeolites — materials in which oxygen atoms are shared between tetrahedra-containing silicon and/or aluminium — can expand under pressure and take up more water to become superhydrated. These materials can exchange cations under pressure. Due to the pressure-induced expansion, larger molecules and cations — possibly pollutants — could be incorporated into the nano-sized pores of these "molecular sponges." When the pressure is released, the pollutants would become trapped.

However, in a reversible system, half of the water would be expelled again, making the sponges somewhat "leaky."

In a paper appearing in the December 5, 2002 issue of *Nature*, the scientists now describe a material that shows irreversible pressure-induced hydration. That is, when the pressure is released, the material stays superhydrated. This new finding opens up the possibility of using these "molecular sponges" to truly immobilize pollutants such as tritiated water.

"Our studies show that the irreversible pressure-induced hydration is associated with a rearrangement of the charge-balancing cations contained in the nanopores," says Brookhaven physicist Thomas Vogt, a co-author on the previous research and the Nature paper. "By understanding these cation migrations and rearrangments under pressure, we hope to be able to reduce the pressure at which the pressure-induced hydration occurs, and thereby open up new ways to use zeolites as "molecular sponges" for pollutants or as transport vessels for medical applications."

The collaborators on this research include Vogt and Yongjae Lee of the Physics Department and Jonathan Hanson of the Chemistry Department at Brookhaven Lab; Joe Hriljac of the University of Birmingham, U.K.; John B. Parise of Stony Brook University; and Sun Jin Kim of the Korean Institute of Science & Technology. The research was funded by the U.S. Department of Energy, which supports basic research in a variety of scientific fields.

—Mona Rowe

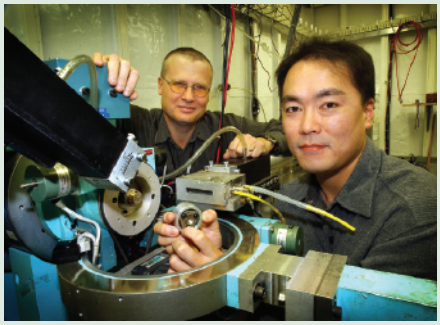

Physicist Tom Vogt (left) with postdoc Yongjae Lee at NSLS beamline X7A, where they determined the unusual structure of a new material that expands under pressure.

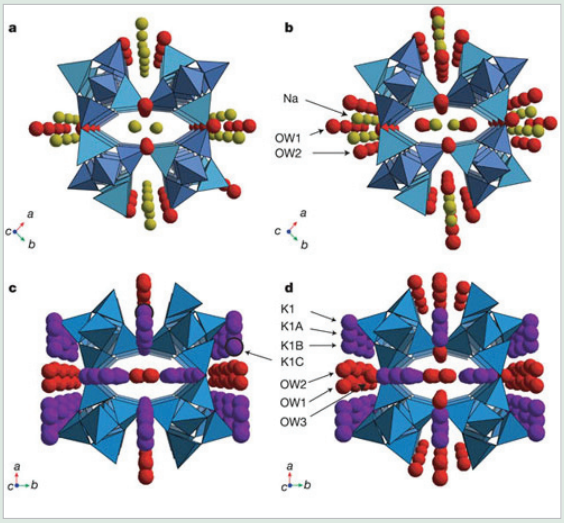

Polyhedral representations of two forms of natrolite: sodium aluminosilicate (Na-AlSi-NAT) and potassium gallosilicate (K-GaSi-NAT) before and after pressure-induced hydration, (a) Na-AlSi-NAT at 0.40 gigapascals; (b) Na-AlSi-NAT at 1.51 gigapascals; (c) K-GaSi-NAT as synthesized; (d) K-GaSi-NAT recovered from 1.9 gigapascals. Tetrahedra in Na-AlSi-NAT are shown in light and dark blue to illustrate the ordering aluminum and silicon ions over the framework tetrahedral sites, whereas the gallium and silicon ions in K-GaSi-NAT are disordered and shown in one color. OW1, OW2 and OW3 are water sites; K1A, K1B, and K1C are potassium ion sites.

Developing a Safer Way to Make One Class of Superconductors

A scientist at Brookhaven National Laboratory has developed a safer, more environmentally friendly way to create an experimental superconductor. This new process facilitates the study of superconductors, which are used in medical imaging machines and are expected to improve computer chips, electrical transmission lines, and many other devices. The findings appeared in the November 19, 2003, issue of *Physical Review B*.

Previously, creating the superconductor, called sodium cobalt oxyhydrate, required working with volatile and flammable liquids and created chemical waste. Now, BNL chemist Sangmoon Park has devised a cleaner synthesis method using plain water. Park works in the Physics Department's Materials Synthesis and Characterization group with his advisor, physicist Tom Vogt.

"We prepared the superconductor using an alternate route that does not require the special precautions necessary to handle hazardous substances," said Park. "Also, this method allows us to synthesize large amounts of the material, which will make it easier for us to further analyze its properties."

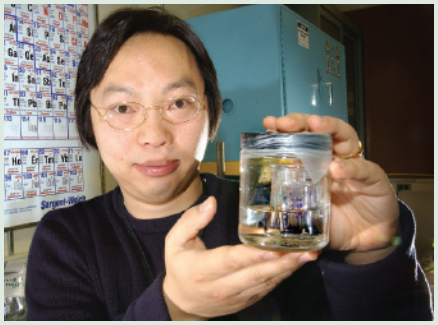

Sangmoon Park holds a sample of a superconducting compound.

Unlike metal-based superconductors, sodium cobalt oxyhydrate contains water. In 2003 researchers discovered that adding water to the initial cobalt-oxygen compound, called cobalt oxide, induced its superconductivity. This discovery, coupled with Park's method, may open a door to new superconductor research.

To synthesize the superconductor, Park dissolved a sodium/sulfur/oxygen compound into water, which caused sodium ions and sodium/oxygen (sulfate) ions to separate from it. This solution was mixed with a sodium/cobalt/oxygen compound. The resulting no-waste reaction created the superconductor. The material's structure and the amounts of its components, particularly the sodium and water, impart its superconducting properties. This was confirmed by measurements performed by chemist Arnold Moodenbaugh in the Materials Science Department.

The superconductor consists of hexagon-shaped layers: Cobalt oxide forms one layer and the sodium and water, together, form another – like a stack of pancakes and waffles, with each pair of thin cobalt oxide "pancakes" separated by a thick sodium/water "waffle." After surrounding it with an alcohol/water mixture, the material was subjected to pressure that distorted the layers by forcing alcohol or water molecules between them. This may further alter the material's behavior.

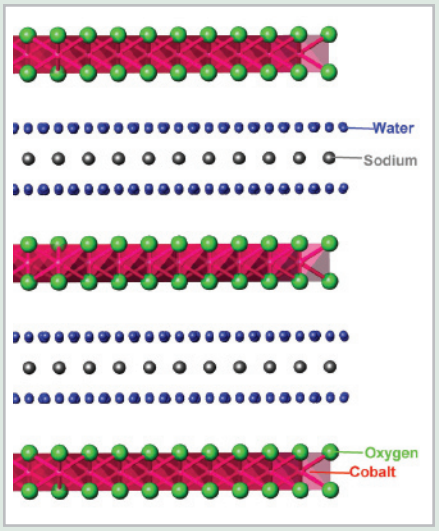

A cross-section representation of the superconductor's layer structure.

This distortion was studied using x-ray diffraction at NSLS beamline X7A by Yongjae Lee of the Materials Synthesis and Characterization Group. This revealed that, even at very low pressures, the superconductor's structure changed significantly. Park and his colleagues plan to investigate how these changes affect its superconductivity.

This research was funded by a BNL Laboratory Directed Research and Development (LDRD) grant.

—Laura Mgrdichian

Murder, Suicide, and a Trip to Princeton

Or how a virus can cause a cell to destroy itself, and how a meeting at Princeton University contributes to research at the NSLS

Viruses use actin, the most abundant protein in the cells that they are infecting, to break open the cells to allow new viruses to escape and infect others.

This discovery, described in the November 29, 2002, *Journal of Biological Chemistry*, was made by Walter Mangel, Biology Department, and his team, in collaboration with the laboratories of Nancy Reich, Stony Brook University, and Gerard Marriott, University of Wisconsin. The research is funded by the Office of Biological & Environmental Research in DOE's Office of Science and the National Institutes of Health (NIH).

The findings, which build upon Mangel's earlier research on how virus particles become infectious, may lead to better antiviral remedies.

Self-portrait by Wally Mangel, Biology Department, in graphite. The bar graph (upper left) shows the results of an experiment by Bill McGrath, Biology, in Mangel's lab, that was published in Nature. This was the first description of the two viral cofactors that stimulated the protease. Now, Mangel and his team have identified a third cofactor, the most abundant cellular protein, actin.

Murderous Intent

When a virus infects a cell, one of its objectives is to make new virus particles that can infect and reproduce in adjacent cells. One virus can produce thousands of virus particles within one cell.

The virus's next step is to cause the cell to lyse, or self-destruct, by breaking open and releasing newly synthesized virus particles that can infect adjacent cells. Different viruses employ different strategies in lysing cells late in infection. If cells with newly synthesized virus particles do not break open, then the virus infection is essentially aborted.

Hatchet-Job Enzymes

Mangel's group has been studying a protease made by human adenovirus, a virus that causes gastrointestinal and respiratory infections, and conjunctivitis. A protease is an enzyme that cleaves, or cuts, other proteins, making them shorter.

In human adenovirus infection, newly synthesized virus particles are not infectious. They contain precursor proteins, which are slightly larger than those that are seen in infectious virus. The precursor proteins act as "construction" parts, which are needed for virus particle assembly.

Mangel's group had shown that the adenovirus protease is synthesized in the cytoplasm of cells — the area between a cell's membrane and nucleus — in an inactive form. The protease migrates from the cytoplasm into the nucleus where it is incorporated into newly synthesized virus particles. Inside these particles, the protease activates by binding to the viral DNA and cleaving off a small fragment, pVIc, of a viral protein. The pVIc then binds to the protease and fully activates it.

Said Mangel, "Builders remove supportive scaffolding after completing a construction project. Similarly, the activated protease cleaves the viral precursor proteins, leaving infectious virus particles behind. Both the viral DNA and pVIc are cofactors for the adenovirus protease's becoming active in that their presence enhances its cleaving ability."

The Princeton Connection

A connection between cell lysis and the adenovirus protease was made serendipitously when Mangel gave a seminar on his protease research at Princeton University. He was invited by Clarence Schutt of the Chemistry Department, whom he had met while serving on a special study section at the NIH. During the talk, after Mangel showed the sequence, or formation, of pVIc, Schutt said that he had seen that sequence elsewhere.

"I found this hard to believe," Mangel admitted. "Ever since we'd discovered pVIc, our group had periodically searched the various databases to see if there were other proteins that contain the pVIc sequence — and we never found anything."

Later that day, Schutt showed Mangel the sequence of actin. Mangel saw that, of the last seven amino acids of actin, four are identical and three homologous to the sequence of pVIc.

At first, Mangel said, he was quite shocked by this revelation, but then he began to think of its implications.

"Wow! Can you spare some actin for me to take back to BNL tomorrow?" he asked. The next day, Mangel brought the actin to his lab, where Diana Toledo, formerly of Biology, was waiting. They tested to see if actin could be a cofactor.

"In the very first experiment, it was clear that actin can be a cofactor for the adenovirus protease," Mangel said. "Incubating actin and the adenovirus protease increases the cleaving activity of the adenovirus protease, just as pVIc can do."

Cell Suicide

Actin is the most abundant protein in a cell. Mangel explained that one of its functions is to form actin polymers that act as the steel girders in skyscrapers, giving rise to the structure of a cell. Conversely, if their actin is destroyed, cells lose their shape and eventually break open.

In the November 29 article, the authors show that the adenovirus protease binds to actin, and thus becomes activated. They also noted that the sequence of actin contains two sites that can be cleaved by the active adenovirus protease. Incubation of actin with the adenovirus protease not only activates the protease, but also allows it to cleave actin at those two sites.

"Thus, actin is a cofactor for its own destruction, a new and philosophically interesting way for a virus to lyse cells," Mangel commented.

Crystallizing the Future

Mangel's group has already set up crystallization trials of actin bound to the adenovirus protease. "If we can crystallize the complex, then we may be able to determine its atomic structure at the National Synchrotron Light Source," Mangel said. "That structure would then be used to find drugs to prevent the interaction between actin and the adenovirus protease. Such drugs could serve as a new type of antiviral agent."

—Karen McNulty Walsh

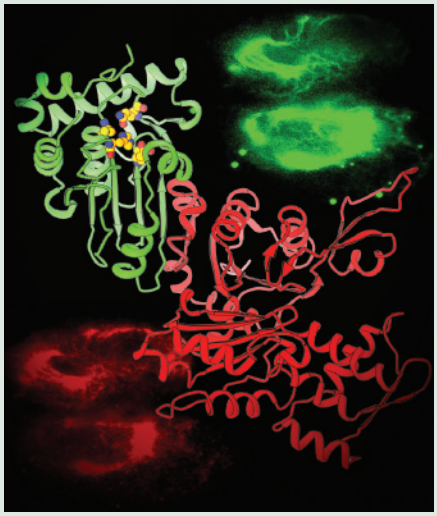

Predicted structure of the adenovirus proteinase (AVP)-actin complex and colocalization within cells of AVP and cytokeratin-18. The crystal structure of AVP (green) was docked onto a portion (blue) of the crystal structure of actin (red). The red green and yellow balls on AVP are the atoms involved in catalysis. In cells containing an AVP-green fluorescent protein complex, its fluorescence (green) colocalizes with the fluorescence (red) from an anti-cytokeratin-18 antibody, consistent with the cleavage of cytokeratin-18 by an AVP-actin complex.

Fabricating 2D Molecular Gradients with a Simple Mechanical Device

Scientists from North Carolina State University and the U.S. Department of Commerce's National Institute of Standards and Technology have used a silicon elastomer network in conjunction with a simple mechanical stretching device to produce two-dimensional molecular gradients for nanotechnology applications. The structure of these 2D molecular gradients was determined at the National Synchrotron Light Source. The research is described in the cover story of *Advanced Materials*, September 16, 2003.

Tuning the surface characteristics of materials has become of paramount interest in many fields of science and technology. While most applications involve surfaces that are chemically homogeneous, in other instances, surfaces are needed that comprise two or more chemically heterogeneous regions. Such heterogeneous structures can be applied as tools for chemical separations, substrates for selective adsorption, and specimens for lithography and other micro-fabrication technologies.

Authors (from left): Jan Genzer, Kirill Efimenko and Daniel Fischer

"We now see increased interest in generating and using 'gradient substrates,' in which the energy varies gradually across the sample surface," said Jan Genzer, a chemical engineer at North Carolina State and the lead author of the paper. "Numerous studies have shown that such structures offer a unique geometry for probing cell/substrate interactions, phase behavior in thin-liquid films, including those made of polymers, and directed motion of liquids. Recent reports also demonstrate that gradient substrates are useful in building molecular templates and exploring material characteristics using multi-variant approaches."

The scientists used a new synchrotron-based x-ray technique called combinatorial near edge x-ray absorption fine structure (NEXAFS) (cover story January 13, 2003, *Applied Physics Letters*) to map out the billionth-of-a-meter-thick molecular gradient with millimeter spatial resolution. According to Daniel Fischer, a physicist from the National Institute of Standards and Technology and co-author of the study, few techniques can be used to study the physical and chemical properties of chemically heterogeneous materials at the millimeter scale. In addition, most are limited in sensitivity, can damage the samples under study, or require special preparation protocols.

Said Fischer, "Combinatorial NEXAFS is non-invasive, does not require transparent samples, and provides simultaneous information about the chemical nature and orientation of the molecules on the surface. Also, we employed an in situ methodology, which is based on mechanical deformation of the substrate covered with a uniform array of grafted organosilane molecules."

Details of the Technique

A two-dimensional molecular gradient is produced by mechanically stretching a "dog bone"-shaped elastic poly(dimethylsiloxane) (PDMS) plastic sheet clamped in a simple screw-activated device (see figure).

As explained by Kirill Efimenko, a senior research associate at North Carolina State and a co-author of the study, turning the screw by hand stretches the PDMS sheet by 40 percent and produces a gradient of strains along the surface. The most strain occurs along the PDMS sheet that is continuous between the clamps. The asymmetrically stretched PDMS "dog bone" is then exposed to an ultraviolet ozone treatment, which sensitizes the PDMS, making it attractive to a gaseous organosilane monolayer deposited over the sheet's entire surface. After the monolayer deposition, the screw is turned backward, relieving the strain in the PDMS "dog bone." Doing so compacts the organosilane monolayer greatest at the position of highest original strain. The resulting 2D gradient in organosilane molecular density on the surface of the PDMS sheet was measured with combinatorial NEXAFS.

This research was funded by the Camille & Henry Dreyfus Foundation, 3M Company, the U.S. Department of Commerce, and the U.S. Department of Energy's Divisions of Materials Sciences and Chemical Sciences.

— Diane Greenberg

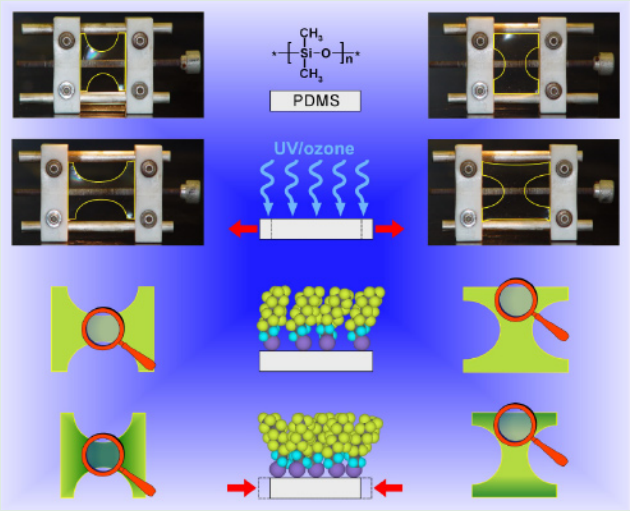

A two-dimensional molecular gradient is produced by mechanically stretching a "dog bone"-shaped elastic poly(dimethylsiloxane) (PDMS) plastic sheet clamped in a simple screw-activated device.

Scientists Image Soft Tissues With New X-Ray Technique

Provides more information than conventional x-rays or other scanning methods

Scientists at the NSLS, in collaboration with researchers at Rush Medical College, have demonstrated the effectiveness of a novel x-ray imaging technology to visualize soft tissues of the human foot that are not visible with conventional x-rays. The technique, called Diffraction Enhanced Imaging (DEI), provides all of the information imparted by conventional x-rays as well as detailed information on soft tissues previously accessible only with additional scanning methods such as ultrasound or magnetic resonance imaging (MRI). This study appeared in the May 2003 issue of the *Journal of Anatomy*.

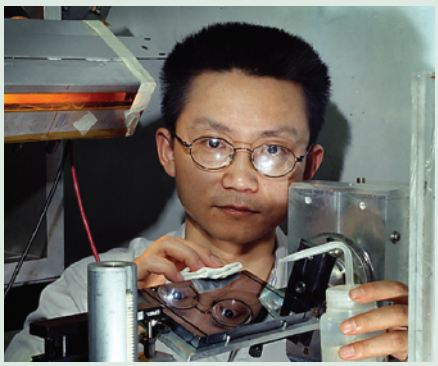

Zhong Zhong

"We've previously shown that this technique can visualize tumors in breast tissue and cartilage in human knee and ankle joints, but this is the first time we have shown it to be effective at visualizing a variety of soft tissues, such as skin, cartilage, ligaments, tendons, adipose pads, and even collagen and large blood vessels," said physicist Zhong Zhong, who works at the (NSLS). "The ability to visualize such a range of soft tissues as well as bone and other hard tissues with just one technique has many potential applications in diagnosis," Zhong said.

The technique makes use of the intense beams of x-rays available at synchrotron sources such as the NSLS. These beams are thousands of times brighter than those produced by conventional x-ray tubes, and provide enough monochromatic x-ray flux for imaging even after selection of a single wavelength.

In conventional x-ray images, the various shades of gray are produced because different tissues *absorb* different amounts of x-ray energy. "This works great in imaging bones and other calcified tissues," said Zhong, "but less satisfactorily in imaging soft-tissues that have similar and low x-ray absorption." In DEI, the scientists are more interested in the x-rays that *pass through* the tissue and how they bend and scatter as they do, because these properties vary more subtly between different types of tissue.

To analyze a specimen with DEI, the scientists place a perfect silicon crystal between the sample and the image detector. As x-rays from the synchrotron go through the sample, they bend, or refract, and scatter different amounts depending on the composition and microscopic structure of the tissue in the sample. Then, when the variously bent rays exit the sample and strike the silicon crystal, they are diffracted by different amounts according to their angular spread. So the silicon crystal helps convert the subtle differences in scattering angles produced by the different tissues into intensity differences, which can then be readily detected by a conventional x-ray detector. This results in extremely detailed images that are sensitive to soft tissue types.

For example, in the current study, a conventional radiograph of a human toe shows bones and a calcified blood vessel; except for the faint "shadow" of the surrounding soft tissues and calcification within a ten-

don, no other structures are visible. The DEI scan of the same specimen in the same position clearly shows skin, the fat pads beneath the bones, the blood vessel, the nail plate, and some tendons, which are clearly distinguishable from the surrounding connective tissue. Within one of the fat pads, even the organizational architecture of the collagen framework is visible. Moreover, the bones take on a three dimensional appearance because of the detail available in the scans.

In the current study, the DEI images were produced with a lower x-ray dose than that used for diagnostic x-rays and no contrast agent was needed, making the technique viable as a potential screening tool, said Zhong.

The scientists are still working on how to scale down the DEI design so that it can be used in a clinical setting. But they say this should be feasible and that the technique may eventually greatly enhance mammography and become increasingly important in the detection of other soft tissue pathologies such as osteoarthritis, breast cancer, and lung cancer.

Collaborators at Rush Medical College include Carol Muehleman, Jun Li, and Klaus Kuettner. This research was funded by the National Institutes of Health, GlaxoSmithKline, Inc., and the U.S. Department of Energy, which supports basic research in a variety of scientific fields.

— Karen McNulty Walsh

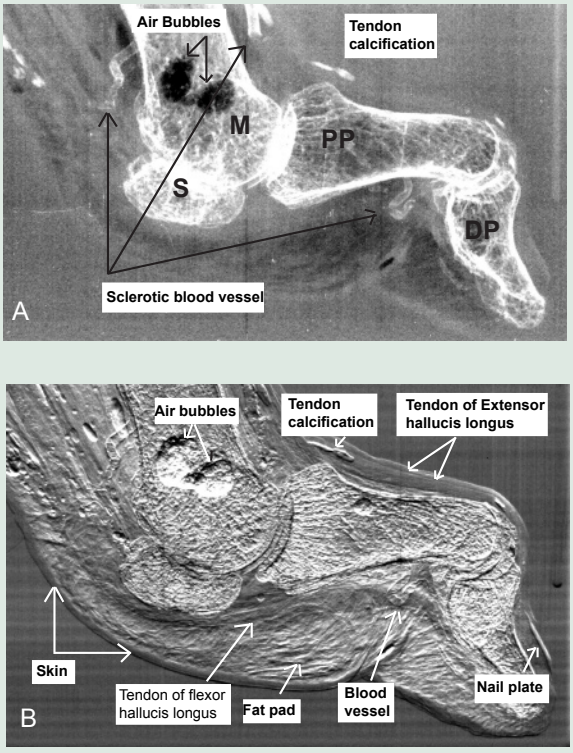

A conventional synchrotron radiography of a foot (A) and the same foot show with Diffraction Enhanced Imaging (B). Note the greater variety of soft tissues visible within the DEI frame.

Chemical Sciences

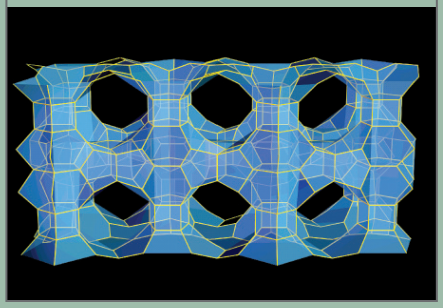

Photodegradation of a Ternary Iron(III)-Uranium(VI)-Citric Acid Complex

C.J. Dodge and A.J. Francis

Brookhaven National Laboratory

Scientists from Brookhaven National Laboratory have investigated how a mixture of compounds containing citric acid, iron, and uranium are degraded by light. Understanding the mechanisms involved in the photochemical degradation of metal-organic complexes should result in a process to treat uranium-containing waste streams while recovering the uranium.

Citric acid [$C_6H_8O_7$] is a naturally-occurring organic compound used to remove toxic metals and radionuclides from contaminated soils and sediments. It is easily dissolved in water and forms a variety of soluble complexes with metals. The nature of the metal-citrate complex formed depends upon the nature of the metal, the pH of the solution, and the stoichiometric ratio of metal to citric acid.

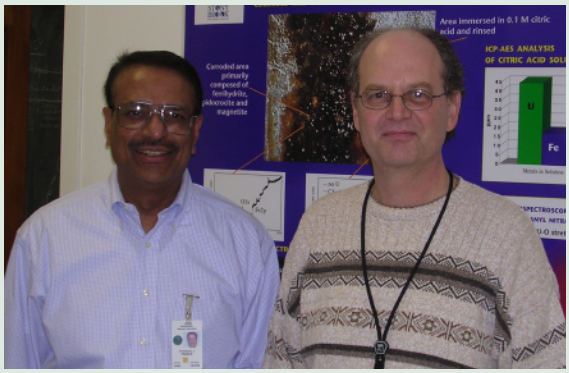

Authors (from left): Arokiasamy J. Francis and Cleveland J. Dodge

Biodegradation of the metal-citrate complexes by *Pseudomonas fluorescens* results in the production of carbon dioxide and water, and precipitation of the metal from the solution. In our laboratory, we have previously shown that the iron-citrate complex is readily biodegraded while the uranium-citrate complex is recalcitrant, but that, upon exposure to light, the uranium-citrate complex was photochemically degraded. When iron, uranium, and citric acid are present together, an iron-uranium-citrate complex is formed, which is also resistant to biodegradation.

To determine the mechanisms of light-induced degradation, or photodegradation, of iron-, uranium-, and iron-uranium-citrate complexes, we used extended x-ray absorption fine structure (EXAFS), with x-rays from beamline X11A at the NSLS. We established the molecular structure of each of the three complexes: iron-citrate, uranium-citrate and iron-uranium-citrate, and identified the nature of the metal precipitate formed following photodegradation.

The photodegradation mechanism for the complex depends upon its structure. The iron-citrate complex consists of a binuclear core containing two ferric [Fe^{3+}] ions bound together by a bridging group made of a terminal carboxylate group of citric acid [$C_5H_7O_5COO^-$] and an oxygen atom. Its photodegradation proceeds by a two-electron oxidation of citric acid to 3-oxoglutarate ($C_5H_4O_5$) with reduction of ferric ions to ferrous [Fe^{2+}] ions (**Figure 1A**). The ferrous ions are re-oxidized to ferric ions in the presence of photochemically generated hydrogen peroxide [H_2O_2] and the iron precipitates as ferrihydrite [$Fe(OH)_3$].

The uranium-citrate complex consists of a core of two uranium atoms bridged by hydroxyl groups (di-μ-OH bonding). In addition, attached to each uranium atom are three ligand groups from citric acid, which form a tridentate ring (chelate) to each uranyl ion [UO_2^{2+}]. Uranium-citrate photodegradation proceeds by a two-electron transfer mechanism with the oxidation of citric acid to acetoacetic acid [$C_4H_6O_3$] and the reduction of uranium to an insoluble tetravalent form (**Figure 1B**). The tetravalent uranium is subsequently re-oxidized to a hexavalent form by

BEAMLINE
X11A

Funding
U.S. Department of Energy, Office of Science, Office of Biological and Environmental Research; Environmental Management Science Program, Office of Science and Technology, Office of Environmental Management

Publication
C.J. Dodge and A.J. Francis, "Photodegradation of a Ternary Fe(III)-U(VI)-Citric Acid Complex," *Environ. Sci. Technol.*, 36, 2094 (2002).

Contact information
Cleveland Dodge, Associate Chemist, Environmental Research and Technology Division, Environmental Sciences Department, BNL

Email: dodge1@bnl.gov

reacting with a photochemically-generated hydroperoxy radical $\bullet O_2H$, and the uranium precipitates from solution as schoepite [$UO_3 \bullet 2H_2O$].

The ternary iron-uranium-citrate complex has a unique structure consisting of a citric acid molecule bound to a binuclear iron core similar to the iron-citrate complex, but the central carboxyl group [COOH] of each citric acid is bound to two uranyl ions. The remaining two citric acids form tridentate complexes with each uranyl ion. Photochemical degradation of the complex involves oxidation of citric acid and production of ferrous ions, similar to the iron-citrate complex (**Figure 1C**), but, in contrast to the uranium-citrate complex, no uranium reduction to the tetravalent form is observed. Iron and uranium precipitate as ferrihydrite and uranium hydroxide [$UO_2(OH)_2$], respectively.

These results show that the presence of iron affects not only the mechanism of photodegradation but also influences the nature, and thus the stability, of the precipitate formed.

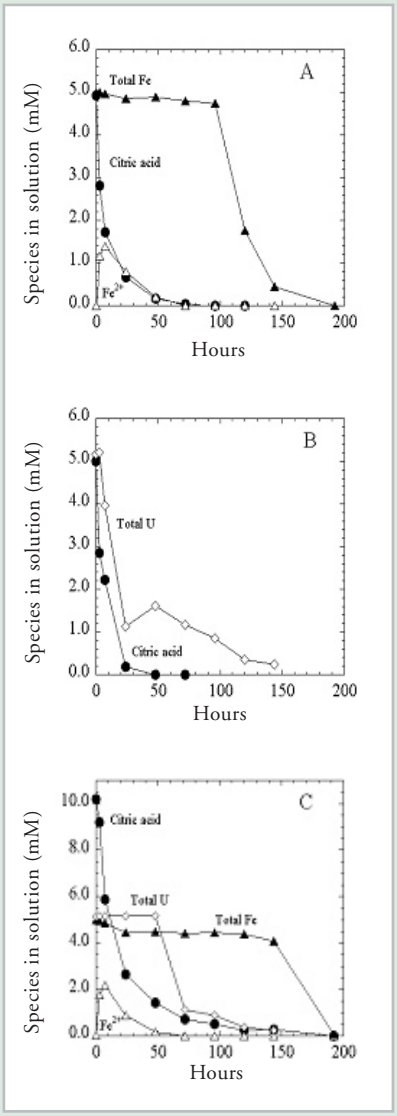

Figure 1. Organic metabolite production during photodegradation of: (A) 1:1 iron-citric acid, (B) 1:1 uranium-citric acid, and (C) 1:1:2 iron-uranium-citric acid complexes.

The Coordination Chemistry of Nickel Uptake Regulation in *Escherichia coli*

P.E. Carrington[1], P.T. Chivers[2,3], F. Al-Mjeni[1,4], R.T. Sauer[2], and M.J. Maroney[1]

[1]Department of Chemistry, University of Massachusetts; [2]Department of Biology, Massachusetts Institute of Technology; [3]Department of Biochemistry and Molecular Biophysics, Washington University School of Medicine; [4] Department of Chemistry, Sultan Qaboos University, Sultanate of Oman

Scientists from the University of Massachusetts in Amherst and the Massachusetts Institute of Technology in Cambridge have determined the structure of the high affinity nickel-binding site in NikR, a protein that regulates the uptake of nickel by the gut bacterium Escherichia coli. The scientists show that, in the NikR protein, nickel is bound in a novel four-coordinate planar site consisting of two histidines, one additional oxygen- or nitrogen-donor ligand, and one sulfur-donor (cysteine) ligand. The researchers also noticed that when NikR binds to DNA, the nickel-binding site becomes six-coordinate with ligands made of oxygen and nitrogen donors, but lacking cysteine.

Authors (from left): Sergio Chai, Faizah Al-Mjeni, Patrick DeCourcy, Paul Carrington, Michael Maroney, Peter Bryngelson, Jennifer Pinkham, and Arthur LaPlante

Microorganisms have developed high-affinity uptake systems to acquire metals, such as iron, copper, and zinc, from the environment. In the gut bacterium *Escherichia coli*, nickel plays a critical role in anaerobic metabolism, but it is usually present at low concentrations in the environment, so *E. coli* synthesizes a protein called NikABCDE, which acquires nickel from the environment and actively transports it into the cell. (The letters A to E label five proteins that assemble to form NikABCDE.)

This protein is produced via transcription of the *nik* operon (chromosomal functional unit acting like a gene) in response to a low oxygen level. When nickel concentration is high enough, the transcription process is repressed by NikR, a protein that appears to regulate nickel uptake in a number of bacteria and archaea.

NikR contains two distinct binding domains: an amino terminal, DNA-binding site and a carboxyl terminal high-affinity nickel-binding site. By using x-ray absorption spectroscopy (XAS) at beamline X9B at the NSLS, we have characterized the structure of the high-affinity nickel-binding site and have shown that the nickel-binding site is sensitive to the DNA-bound state of NikR.

Analysis of x-ray absorption near-edge structure (XANES) revealed that the nickel site is four-coordinate and planar, because it exhibits a 1s ➨ 3d electronic transition near 8332 electronvolts (eV) and a distinct maximum assigned to a 1s ➨ $4p_z$ transition near 8338 eV. This result was confirmed by the analysis of extended x-ray absorption fine structure (EXAFS), which revealed that the distances between nickel and other atoms are typical of planar four-coordinate nickel complexes, and also provided information about the ligands involved.

The nickel-binding domain of NikR contains a number of conserved amino acids that are potential nickel ligands. The structure that emerges from the combined XAS and mutagenesis of four of these amino acids is consistent with the planar four-coordinate N_2OS-donor site

BEAMLINE
X9B

Funding
U.S. Department of Energy; National Institutes of Health; American Chemical Society

Publication
P.E. Carrington, P.T. Chivers, F. Al-Mjeni, R.T. Sauer, and M.J. Maroney, "Nickel Coordination is Regulated by the DNA-Bound State of NikR," *Nat. Struct. Biol.*, 10, 126-130 (2003).

Contact information
Michael Maroney, Department of Chemistry, University of Massachusetts, Amherst, MA

Email: maroney@chem.umass.edu

shown in **Figure 2**. Since nickel is the only important biological metal ion that commonly adopts a square planar geometry, the results provide a structural basis for the specificity of NikR toward nickel ions.

Large structural changes were observed when NikR was bound to operator DNA (**Figure 1**). The XANES spectra of the NikR-DNA complexes (left) exhibit somewhat larger, but still small, peaks associated with 1s ➡ 3d electronic transitions near 8332 eV, while the peak assigned to the 1s ➡ $4p_z$ transition near 8338 eV is absent, indicating the presence of a six-coordinate nickel site. EXAFS analysis of the DNA complexes (right) shows that the best fits are obtained for six nitrogen and oxygen donors, including at least two histidine ligands, consistent with the XANES analysis.

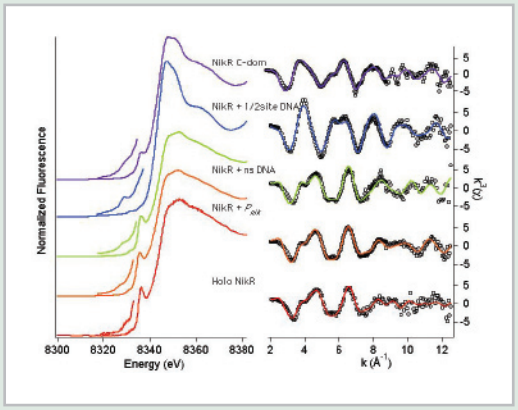

Figure 1. Nickel K-edge x-ray absorption near-edge spectroscopy (XANES) spectra (left) and unfiltered extended x-ray absorption fine structure (EXAFS) spectra (right). EXAFS data points are represented by open circles and the fit by a solid line.

NikR appears to be using the coordination chemistry characteristic of nickel not only to selectively bind nickel, but also to change the interaction between nickel and the protein. The change in nickel-coordination geometry has several potential consequences for NikR function, such as its role for NikR in buffering intracellular nickel at very low levels and controlling DNA transcription at higher concentrations of intracellular nickel.

Although the functional consequences of the change in nickel coordination remain to be elucidated, NikR provides a unique example of the role of metal ions in regulating DNA transcription.

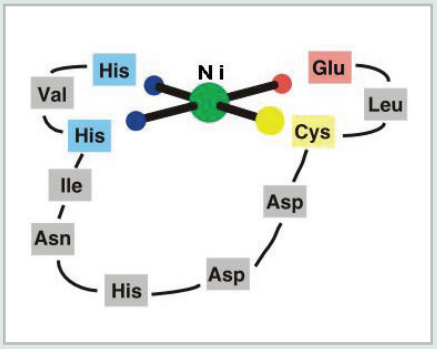

Figure 2. A model of the high-affinity nickel site in NikR based on x-ray absorption spectroscopy (XAS) and mutagenesis results. Residues are colored according to donor atom types (blue: nitrogen; red: oxygen; and orange: sulfur).

Electron Localization in a Mixed-Valent (+2/+3) Di-Iron Complex

F.B. Larsen[1], C.J. McKenzie[1], and R.C. Scarrow[2]

[1]University of Southern Denmark, Odense Campus; [2]Haverford College

Mixed-valence coordination complexes are molecules containing at least two of the same metal ions, where the formal oxidation state (charge) of the metal ions is different. Such complexes are of interest to inorganic chemists because of their unusual electronic and magnetic properties. An average (sometimes non-integral) charge may be the best assignment for the oxidation state due to the delocalization of electrons, such that the charge at each metal ion is effectively the same value. Accurate determination of bond lengths can be used to assess the extent of electronic delocalization. X-ray absorption spectroscopy (XAS) performed at the NSLS was used to determine that a mixed-valence complex with a $Fe_2(OH)_2$ core is best described as a complex with one Fe^{2+} and one Fe^{3+} ion. The XAS results were used along with X-ray diffraction to determine the crystal structure.

Authors (from left): Frank Larsen and Christine McKenzie

BEAMLINE
X18B

Funding
DANSYNC; Seimens Fund (CJM, FBL)

Publication
R.K. Egdal, A. Hazell, F.B. Larsen, C.J. McKenzie, and R.C. Scarrow, "A Dihydroxo-Bridged Fe(II)-Fe(III) Complex: A New Member of the Diiron Diamond Core Family," *J. Am. Chem. Soc.*, 125, 32-33 (2003).

Contact information
Christine McKenzie, University of Southern Denmark

Email: chk_chem@chem.sdu.dk

Dinuclear iron complexes containing a Fe_2O_2 rhombic core (top right) are of interest as models of the structure and function of the active site of the class of non-heme iron enzymes to which the hydroxylation protein of methane monooxygenase (MMOH) belongs. This enzyme is responsible for the bacterial conversion of methane to methanol. Recently, a mixed valence ($Fe^{II}Fe^{III}$) form of MMOH was structurally characterized as containing a triply-protonated rhombic core (i.e. one μ-OH and one μ-OH_2 bridging between the iron atoms).[Wittington, D. A. and Lippard, S. J., ````` *J. Am. Chem. Soc.,* 2001, *123*, 827-838.] While synthetic $Fe_2O_2(H)_{0-2}$ compounds with a rhombic core exist for the II-II, III-III, III-IV oxidation states, the II-III state was unknown.

Using the neutral capping ligand, *N,N'*-dimethyl-*N,N'*-bis(2-pyridylmethyl)ethane-1,2-diamine (L) (top right), to complete the coordination requirements of the iron atoms, and thus prevent an uncontrolled polymerization to form iron(III) hydroxides, we prepared and crystallized the first example of a synthetic diiron complex in the II-III iron oxidation state and containing a rhombic core. The compound, $[L_2Fe_2(OH)_2](ClO_4)_3 \bullet 3H_2O$, is unstable in solution. In the solid state, crystals decompose in weeks. The products of decomposition are iron (III) compounds. The initial structure of $[L_2Fe_2(OH)_2](ClO_4)_3 \bullet 3H_2O$, determined by single crystal X-ray diffraction, showed that the two iron atoms were related by symmetry, suggesting a delocalized mixed-valence complex ($Fe^{+2.5}Fe^{+2.5}$) with an average Fe-O distance of 1.98Å. All other things being equal, the metal-donor distances depend on metal oxidation state and are shorter for higher oxidation states. Given the chemical similarity of the local environment of each iron atom of the molecule, identical oxidation states (of +2.5) seemed plausible. The physical interpretation of such a non-integer oxidation state is that there is little barrier for electron transfer between the metal ions. However, an alternative explanation is that the compound can be regarded as a valence trapped Fe^{II}-Fe^{III} compound and the crystal structure is disordered.

In experiments performed at beamline X18B at the NSLS, we found that structural disorder in the crystal lattice is indeed the cause of the apparent equivalent oxidation states. The best fit of the X-ray absorp-

tion fine structure (XAFS) measurements was obtained by refining 2 Fe-O distances each to 1.90±0.03 and 2.12±0.08 Å rather than using the Fe-O distance found in the crystal structure (**Figure 1**). The refined Debye-Waller factor (σ^2) for these Fe-O shells was 0.004 Å^2, typical of what is found for compounds with only vibrational disorder in the bond lengths. The iron K-edge (XANES) spectrum could be well modeled as arising from 50% Fe^{2+} and 50% Fe^{3+} (**Figure 2**). The combined results from XANES and EXAFS analysis indicate that the iron atoms in $[L_2Fe_2(OH)_2](ClO_4)_3 \bullet 3H_2O$ are localized in their valence state on the X-ray time scale. Since the same time scale applies to X-ray diffraction, the apparent equivalence in Fe-O bond lengths in the crystal structure is ascribed to packing disorder.

Based on these results, the single crystal diffraction data of $[L_2Fe_2(OH)_2](ClO_4)_3 \bullet 3H_2O$ were re-fit using two half-occupancy isotropic oxygen atoms instead of the single anisotropic bridging oxygen atom (**Figure 3**). The two models fit the diffraction data equally well (R_w = 0.044) but the disordered model is obviously preferred because it explains the EXAFS and XANES results. In the disordered model, the averaged distances ascribed to Fe^{III}-O (1.89 Å) and to Fe^{II}-O (2.07 Å), as well as the Fe-Fe distance (2.95 Å), are within the uncertainty ranges for these parameters established by EXAFS analysis. These results show that, despite an ostensibly symmetrical chemical environment for both iron atoms of $[L_2Fe_2(OH)_2](ClO_4)_3 \bullet 3H_2O$, the electrons localize such that one Fe^{II} and one Fe^{III} are present in the complex.

A $Fe_2O_2(H)_{0-4}$ rhombic core.

Neutral capping ligand, N,N'-dimethyl-N,N'-bis (2-pyridylmethyl)ethane-1,2-diamine

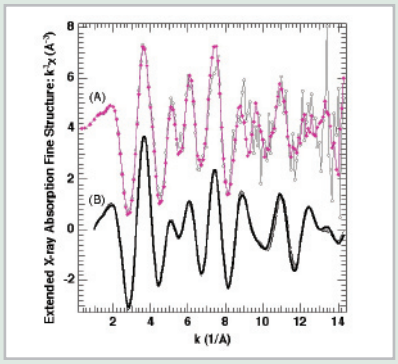

Figure 1. EXAFS analysis of $[L_2Fe_2(OH)_2](ClO_4)_3 \bullet 3H_2O$. (A) The fluorescence (circles) and transmission (diamond) detected EXAFS are compared (both are offset by +4 Å^{-3}; no systematic difference are evident). (B) Fourier filtered EXAFS (thick line) and simulation of the EXAFS to determine Fe-X distances discussed in this article.

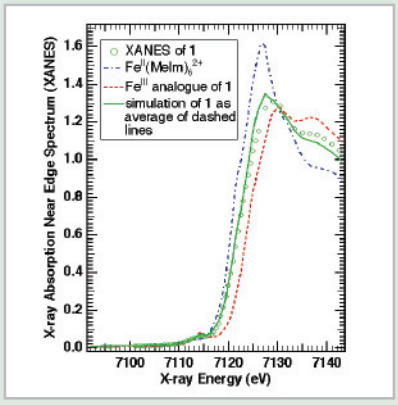

Figure 2. XANES of $[L_2Fe_2(OH)_2](ClO_4)_3 \bullet 3H_2O$ and its simulation representing contributions of 50% from Fe^{II} and 50% from Fe^{III} XANES shapes.

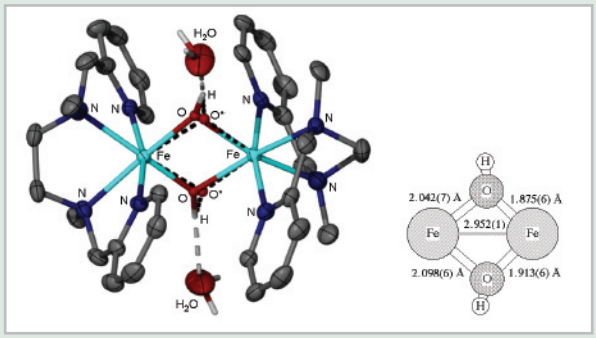

Figure 3. X-ray crystal structure of the cation of $[L_2Fe_2(OH)_2](ClO_4)_3 \bullet 3H_2O$, with enlarged geometry of the $Fe_2O_2H_2$ rhombic core inferred from a combination of XAS and X-ray diffraction experiments.

The Structure Solution of SSZ-58: A Novel Two-Dimensional 10-Member-Ring-Pore Zeolite with Previously Unseen Double Five-Member-Ring Subunits

A. Burton, S. Elomari, R.C. Medrud, I.Y. Chan, C.-Y. Chen, L.M. Bull, and E.S. Vittoratos

ChevronTexaco

Researchers at ChevronTexaco have recently prepared a novel zeolite (designated SSZ-58) with a ten-dimensional system of ten-membered ring pores. SSZ-58 is the first zeolite to possess a previously unobserved double five-membered ring unit. The structure of SSZ-58 was determined using the ab initio method FOCUS with powder diffraction data collected at beamline X7A. To date, SSZ-58 is the most complex zeolite (in terms of the number of atoms in the crystallographic asymmetric unit) to be solved from powder diffraction data.

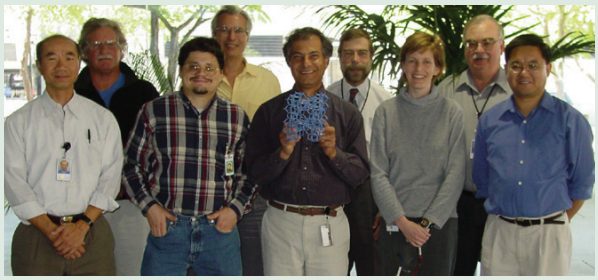

Authors (from left, front row): Ignatius Chan, Allen Burton, Saleh Elomari (holding a model of SSZ-58), Lucy Bull, and Cong-Yan Chen. (back row): Stacey Zones, Steven Vittoratos, Charles Wilson, and Charles Kibby

Zeolites are crystalline microporous aluminosilicates which find widespread use as catalysts, adsorbents, and ion-exchangers. New zeolites continue to emerge at an increasingly rapid pace. The syntheses of high-silica zeolites are usually performed hydrothermally in the presence of an organocationic structure directing agent (SDA). The size and shape of the SDA often correlate well with the dimensions of the zeolite micropores or cages. An understanding of molecular recognition effects in zeolite synthesis begins with identification of the structure or structures promoted by certain SDAs. A detailed knowledge of zeolite structure is also crucial for understanding catalytic and adsorptive properties. Once the structure of a zeolite is determined, applications based upon size or shape-selective processes may be targeted, or known properties of the material may be rationalized.

Although structure solutions of zeolites from single crystals have been reported, it is rare that zeolite crystals are large enough for single crystal structure analyses of novel zeolite phases. Investigators must therefore rely on powder diffraction data. *Ab initio* structure solution from powder data is difficult because of the high degree of peak overlap inherent to most powder patterns.

In the past, there was often a long time between the initial discovery of a zeolite and its structure elucidation. The investigators hoped to construct a model that was consistent with the unit cell parameters, the possible space group symmetries, and other physicochemical (*i.e.*, adsorption, catalytic, and density) data. These structure solutions often depended on simple modifications of previously known zeolite topologies. Model building continues to be an important tool to the zeolite crystallographer, particularly for the investigation of disordered materials. However, if an unsolved structure contains previously unobserved secondary building units, and especially if it possesses a large number of tetrahedral (T) atoms in its asymmetric unit, the success of model building is more dubious.

Recently, with the advent of the FOCUS· and ZEFSAII algorithms, there have been significant advances in *ab initio* structure solution of

BEAMLINE
X7A

Funding
Chevron Texaco Strategic Research

Publication
A. Burton, S. Elomari, R. Medrud, I. Chan, C. Chen, L. Bull, and E. Vittoratos, "The Synthesis of SSZ-58: A Novel Two-Dimensional 10-Ring Pore Zeolite with Previously Unseen Double 5-Ring Subunits," *J. Am. Chem. Soc.*, 125, 1633-1642 (2003).

Contact information
Allen Burton, Chevron Research & Technology Company

Email: buaw@chevrontexaco.com

zeolites from powder diffraction data. These methods incorporate the crystal chemical information inherent to most zeotype structures: *i.e.*, a fully connected, tetrahedral arrangement of the dominant x-ray scatterers. In this report we discuss the structure solution of the novel zeolite SSZ-58 by the FOCUS method.

SSZ-58 was synthesized using the 1-butyl-1-cyclooctylpyrrolidinium cation as a structure directing agent (SDA). Samples for detailed structural analysis were examined at beamline X7A. The synchrotron powder diffraction pattern (**Figure 1**) of SSZ-58 could be indexed in an orthorhombic unit cell in space group *Pmma*: a = 25.112 Å, b = 12.498 Å, c = 12.860 Å. **Figure 2** shows the topological structure of SSZ-58 (oxygen atoms have been omitted for clarity) determined from the FOCUS algorithm. This structure has 12 tetahedral (T) atoms and 26 oxygen atoms per asymmetric unit. In terms of the number of unique T atoms, SSZ-58 is the most complex zeolite or zeotype structure solved from powder diffraction data.

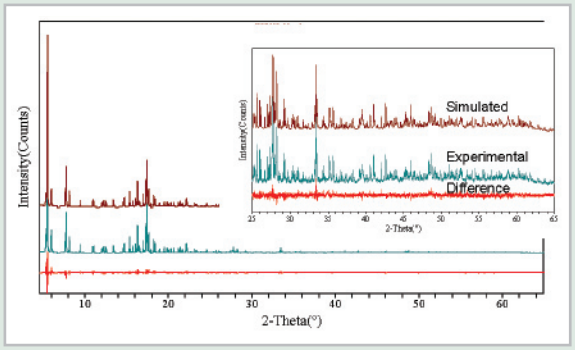

Figure 1. The simulated, experimental, and difference profiles of the synchrotron powder x-ray diffraction pattern (l = 1.1996 Angstrom) of SSZ-58.

SSZ-58 possesses a two-dimensional system of pores that intersect to form large cavities that are bound by two pairs of opposing 10-membered rings (10MRs). The pores along the *c*-direction are straight channels bound by 10-MRs with dimensions of 5.7 × 5.2 Å assuming an oxygen radius of 1.35 Å. The sinusoidal pores along the *a*-direction are bound by distorted elliptical 10MRs with dimensions of 4.8 × 5.7 Å. The structure of SSZ-58 is composed of columns that possess double five-member rings (D5MRs). Although the D5MR is a simple building unit, it surprisingly has not been observed in any other zeolite structures. The structure solution of SSZ-58 highlights the advances that have been made in structure elucidation of complex materials from powder data.

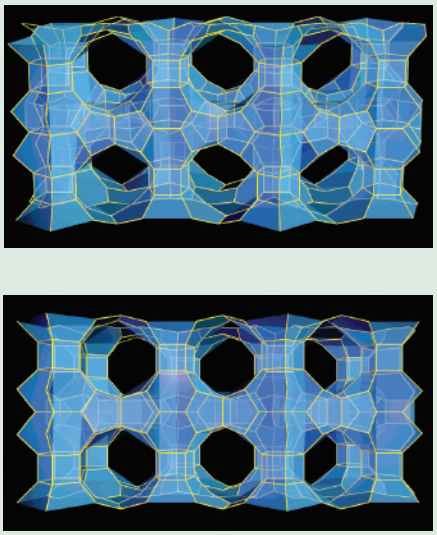

Figure 2. Models showing the two-dimensional pore system in SSZ-58 (top) along the c-axis and (bottom) along the a-axis. Tetrahedral atoms are represented by intersections of line segments. Oxygen atoms have been removed for visual clarity.

Experimental Electron Density Study of an Organozirconium Compound

S. Pillet[1], G. Wu[1], V. Kulsomphob[2], B.G. Harvey[2], R.D. Ernst[2], and P. Coppens[1]

[1]State University of New York, Buffalo; [2]University of Utah

Scientists at the State University of New York in Buffalo and at the University of Utah have synthesized a novel organozirconium complex and subjected it to a careful experimental electron density study at 16 K. The study demonstrates that it is now possible to achieve accurate results for such heavier atom-containing species when high intensity sources and small crystal sizes are employed. The analysis of the electron density distribution for the organozirconium complex has revealed unusual 4d orbital populations and provided insight both into the nature of the bonding of the zirconium center to its various ligands, and into a number of interatomic contacts between formally nonbonded atoms.

In electron deficient organometallic compounds, it is not uncommon for empty orbitals on a metal center to interact with electron pairs in nearby C-H bonds. That was certainly what was expected to be found in **Complex 1**, in which a very small Zr-N-C angle indicated there was some sort of interaction between Zr and the isopropyl group. However, spectroscopic data did not give any indication of such an interaction. This led the researchers to undertake an experimental electron density study of the compound, even though a truly accurate study of a compound with an atom as heavy as zirconium had never been achieved before. The high intensity X-rays provided by the NSLS and high-resolution single-crystal facilities at the SUNY X3 beamline were indispensable in this undertaking.

Despite the inherent obstacles to overcome in obtaining accurate data, the researchers were rewarded with a variety of interesting results, although ironically they ultimately did not find an unambiguous answer to the question that had prompted the study, which concerned the putative agostic interaction between the metal center and a proximal C,H region. To begin with, the d orbitals on zirconium were found to exhibit unusual populations based on ligand field considerations. Three orbitals (d_{z^2}, $d_{x^2-y^2}$, and d_{xz}) were found to be relatively highly populated, indicating σ donor interactions from the organic ligands, and both σ and π donor interactions from the nitrogen center, respectively.

The study also revealed significant details concerning the bonding electrons in the compound. A topological analysis of these electrons showed "bond paths" for all the expected bonds between the lighter atoms. However, bond paths were only found between the zirconium atom and three ligand atoms (N and two C). Many of the carbon atoms to which Zr is presumably bonded were not found to be connected to the Zr atom by bond paths. Thus, not only were there no bond paths connecting the Zr with the isopropyl group, but there were also no bond paths to four of the five dienyl carbon atoms (**Figure 1**), and three of the four diene carbon atoms. Nonetheless, the electron density distributions and ellipticities, together with the actual placement of the zirconium atom, provided clear evidence for the presence of interactions between these ligand atoms and the zirconium center. As topological analyses have

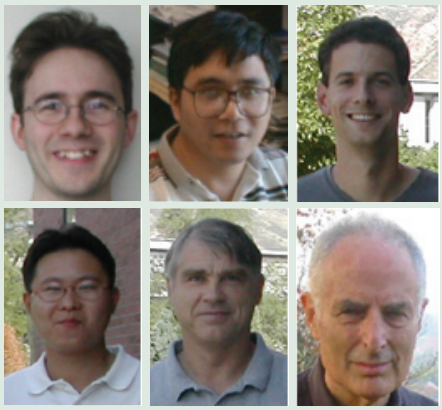

Authors (top row): S. Pillet, G. Wu, and B.G. Harvey, (bottom row): V. Kulsomphob, R.D. Ernst, and P. Coppens

BEAMLINE
X3A1

Funding
Department of Energy; National Science Foundation

Publication
S. Pillet, G. Wu, V. Kulsomphob, B.G. Harvey, R.D. Ernst, and P. Coppens, "Investigation of Zr-C, Zr-N and Potential Agostic Interactions in an Organozirconium Complex by Experimental Electron Density Analysis," *J. Am. Chem. Soc.*, 125, 1937-1949 (2003).

Contact information
Philip Coppens, Department of Chemistry, State University of New York, Buffalo

Email: coppens@acsu.buffalo.edu

only recently begun to be employed to characterize the bonding in types of organometallic compounds, this result provides guidance for further studies using this method.

An unexpected bonus was provided by the observation that the p-orbital electron densities of the diene and dienyl π systems were not oriented perpendicular to their atomic planes, but rather experienced "tilts" or rehybridizations in order to be directed more toward the zirconium center. Such tilts had previously been inferred from distortions exhibited by π ligand substituents, but this is the first direct experimental evidence for these reorientations. As noted above, the charge density analysis did not provide direct evidence for the existence of an agostic interaction (**Figure 2**).

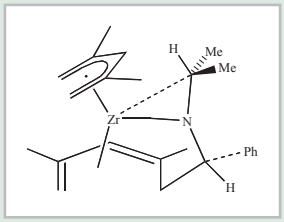

Complex 1

The topological analyses also revealed interesting interactions between some formally nonbonded atoms. Intermolecular CH/π and π/π interactions were observed between dienyl ligands in adjacent complexes, while a more unusual bond path was observed between opposing hydrogen atoms present on the dienyl ligand termini. This interaction may account for the observed tendency of pentadienyl ligands under some conditions to undergo loss of H_2, yielding the more common cyclopentadienyl ligand.

While this study has yielded substantial insight into the bonding of this compound, very few electron density studies have been carried out on organometallic compounds in general. One can therefore expect that a wealth of additional new information will be achieved through similar studies of a wide variety of organometallics.

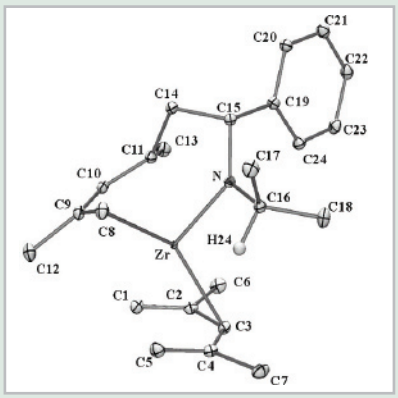

Figure 1. Illustration of the experimentally determined bond paths in the organozirconium complex.

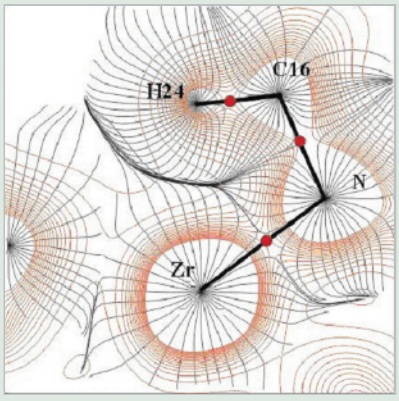

Figure 2. Electron density gradient trajectories (grey lines) and total electron density (red lines) for the Zr-N-C-H plane. Bond critical points are depicted as red circles. Contour levels of 0.1 eÅ^{-3} are used for the electron density.

In Situ X-ray Absorption Spectroscopic Study on the $LiNi_{0.5}Mn_{0.5}O_2$ Cathode Material During Electrochemical Cycling

W.-S. Yoon[1], C.P. Grey[2], M. Balasubramanian[1], X.-Q. Yang[1], and J. McBreen[1]

[1]Materials Science Department, Brookhaven National Laboratory; [2]Department of Chemistry, Stony Brook University

Lithium ion batteries consist of a layered-lithium first-row transition metal oxide cathode (positive) and a graphite anode (negative) that can intercalate lithium ions. In the intercalation process, Li^+ ions migrate into the empty space between the metal oxide or graphite layers. Oppositely, egress of the Li^+ ions is called deintercalation. During the repeated charging and discharging of the battery, called cycling, the lithium ions shuttle between the anode and cathode, electrons flow in the external circuit, and the metal in the cathode undergoes a redox process. In this process, the metal's oxidation state is changed. In situ x-ray absorption spectroscopy (XAS) was used to study the redox processes in $LiNi_{0.5}Mn_{0.5}O_2$. The results indicate that the redox process occurs on the nickel ions, with the conversion of Ni^{2+} to Ni^{3+} occurring first and the Ni^{3+} to Ni^{4+} conversion occurring second. The manganese remains Mn^{4+} during normal battery cycling.

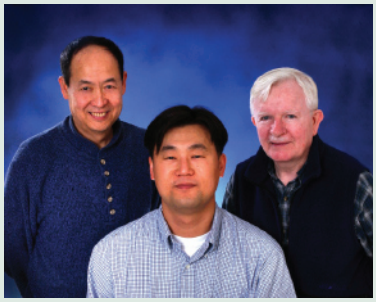

Authors (from left): Xiao-Qing Yang, Won-Sub Yoon, James McBreen, (top) Clare P. Grey, and (bottom) Mahalingam Balasubramanian

Rechargeable lithium ion batteries are a key component in portable electronic equipment, such as laptop computers and cellular phones. These batteries consist of a layered-lithium first-row transition metal oxide cathode (positive) and a graphite anode (negative) that can intercalate lithium ions. Commercial lithium ion batteries have $LiCoO_2$ cathodes. During cycling, the lithium ions shuttle between the anode and cathode through a non-aqueous electrolyte. During charging, Li^+ ions are removed from the cathode and inserted between the graphite layers in the anode. Concomitant with the removal of the Li^+, a Co^{4+}/Co^{3+} charge-compensation process converts Co^{3+} to Co^{4+}. This is called a redox process, and it causes electrons to flow in the external circuit from the cathode to the anode. Then, during discharging, all the processes are reversed. This type of reaction yields a long cycle life because no new phases crystallize on the electrodes and cause the battery to degrade and ultimately fail. For example, as a Pb-acid ($PbSO_4$) battery charges, lead metal with a textured consistency, called a lead sponge, forms on the anode and PbO_2 forms on the cathode. As the battery discharges, $PbSO_4$ forms on both electrodes. But in a lithium ion battery, the electrode materials do not undergo major structural changes. Instead, they merely act as intercalation hosts that accommodate the ingress and egress of Li^+ ions. This yields a long-life battery.

In practice, only 50 percent of the Li^+ ions are removed from the $LiCoO_2$ cathodes during the charging process. Removal of more than this severely limits the battery's cycle life. Fortunately, during charging, the cell voltage has a well-defined positive slope (**Figure 1**), making it possible to remove only 50 percent of the Li^+ ions by simply terminating the charge at 4.2 V. However, this results in the utilization of only half the theoretical charge capacity that could be obtained by completely removing the Li^+ ions. Because of the low cathode capacity and the cost of $LiCoO_2$, extensive research is underway to find alterna-

BEAMLINE
X18B

Funding
U.S. Department of Energy, Office of Energy Efficiency and Renewable Energy, Office of Freedom CAR and Vehicle Technologies

Publication
W.-S. Yoon, C.P. Grey, M. Balasubramanian, X.-Q. Yang, and J. McBreen, "*In Situ* X-ray Absorption Spectroscopic Study on the $LiNi_{0.5}Mn_{0.5}O_2$ Cathode Material During Electrochemical Cycling," *Chem. Mater.*, 15, 3161 (2003).

Contact information
Won-Sub Yoon, Materials Science Department, Brookhaven National Laboratory

Email: wonsuby@bnl.gov

tive cathode materials with larger operating capacities and lower costs. $LiNi_{0.5}Mn_{0.5}O_2$ is one of the more promising new materials. It has a lower cost, a higher capacity, and is more resistant to thermal abuse than $LiCoO_2$.

We reported an *in situ* XAS study of $LiNi_{0.5}Mn_{0.5}O_2$, at the Ni and Mn K-edges, as it was charged and discharged. The XAS study was done in the transmission mode in a two-electrode cell with thin mylar windows. The respective K-edges of Mn and Ni metal are at 6539 eV and 8333 eV. At these energies, the x-ray can eject *1s* core electrons and there is a large increase in the x-ray absorption. As the oxidation state of the metals increases, there are less electrons to screen the nucleus and the edge position shifts to higher energies because it becomes more difficult to eject the *1s* electrons. By monitoring the edge shifts, we can follow the redox processes on both Mn and Ni.

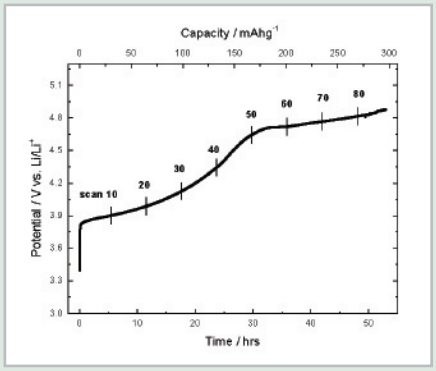

Figure 1. Voltage profile of cell on first charge. Representative XAS scans are indicated.

Figure 1 shows a voltage profile of the cell as it was charged over a 50-hour period to remove all the Li^+, while continuously recording XAS spectra. Representative XAS scans are indicated on the plot. **Figure 2a** shows the Mn K-edge x-ray absorption near-edge structure (XANES) and **Figure 2b** shows the Ni K-edge XANES. Even though there are changes in the Mn XANES during charging, there is no rigid shift of the Mn XANES to higher energies, indicating that the Mn remains Mn^{4+} throughout charging. However, the Ni XANES shows a rigid shift, indicating the conversion of the initial Ni^{2+} to Ni^{4+}. Analysis of the Mn extended x-ray absorption fine structure (EXAFS) shows very few changes in the Mn O first-shell interactions, which supports our conclusion from the XANES analysis that Mn remains Mn^{4+}. The Ni EXAFS shows major changes in the Ni O first-shell interactions, which is consistent with the XANES. All of this clearly indicates that charge compensation, during charging, occurs via the oxidation of Ni^{2+} to Ni^{4+}. Analysis of the EXAFS indicates that this occurs in two steps: first, from Ni^{2+} to Ni^{3+}, and then from Ni^{3+} to Ni^{4+}.

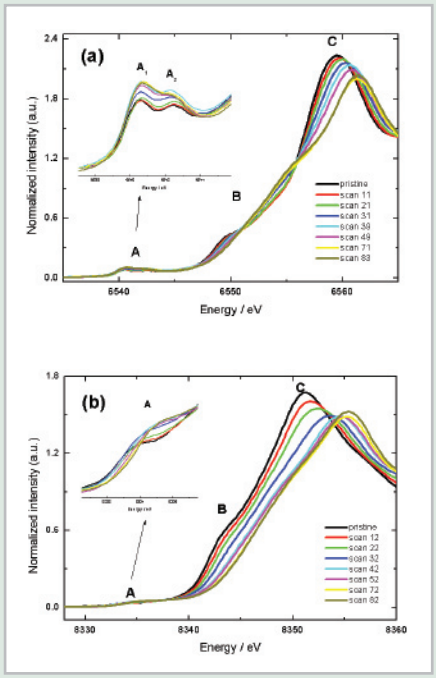

Figure 2. Normalized (a) Mn K-edge and (b) Ni K-edge XANES.

Condensed Matter Physics

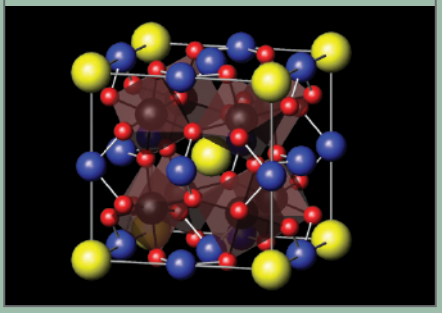

Palladium M_4-Valence-Valence and M_5-Valence-Valence Auger Spectra Determined by Auger-Photoelectron Coincidence Spectroscopy

M.T. Butterfield[1], R.A. Bartynski[1], and S.L. Hulbert[2]

[1]Department of Physics and Astronomy, Rutgers University; [2]National Synchrotron Light Source, Brookhaven National Laboratory

One of the best ways to probe electron correlations in the valence band of solids is to compare spectra of Auger decay processes with the predictions of various theories. But Auger spectra associated with different core levels are often closely spaced in energy and cannot be resolved by conventional means. Scientists from the NSLS and Rutgers University have recently succeeded in isolating the overlapping M_4-valence-valence and M_5-valence-valence Auger spectra of palladium metal by using vacuum ultraviolet synchrotron radiation from NSLS beamline U16B and a novel end station with two electron energy analyzers.

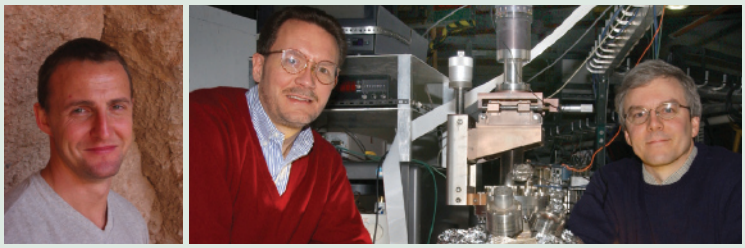

Authors (from left): Martin Butterfield, Robert Bartynski, and Steven Hulbert

One common way to probe the electronic structure of transition metals is through a mechanism called the Auger effect, which works as follows: An electron from a core electronic shell inside a metal atom is ejected by incoming radiation, leaving a vacant site, or hole, which is subsequently filled by another electron coming from a valence electronic shell (of higher energy than the core shell). By jumping into the hole, this second electron loses energy, which is then used to eject a third electron from another valence shell, called an Auger electron (**Figure 1**). Scientists can count the Auger electrons ejected as a function of their kinetic energy, called the Auger electron spectrum, which provides information on the correlations between the two holes left in the valence shell by the second and third electrons.

The kinetic energy distribution of Auger electrons, called the Auger line shape, is well understood when the electron-electron correlation energies in the valence band are either very large or very small. But palladium is an intermediate case that can test the ability to interpolate between these two extremes. Although an atom of palladium is an open-shell system (its outermost electronic shells are completely filled with electrons) in the solid form, it is missing only a fraction of an electron: It does not have a $4d^9$ but actually a $4d^{9+}$ configuration. So, palladium has what is called a marginally open shell. Thus, palladium should provide an interesting test of how theories formulated to explain the electronic properties of systems with totally filled, or closed, electronic shells can provide an accurate description of systems with marginally open shells.

Auger line shapes can be used to probe electron correlations in the valence band by comparing the measured Auger profiles against the prediction of various theories. But Auger spectra associated with different core levels are often closely spaced in energy and cannot be resolved by conventional means. With a technique called Auger-photoelectron coincidence spectroscopy, we have succeeded in distinguishing overlapping Auger spectra with different origins.

BEAMLINE
U16B

Funding
U.S. Department of Energy; National Science Foundation

Publication
M.T. Butterfield et al., "Pd M_{45} Auger Spectrum Determined by Auger-Photoelectron Coincidence Spectroscopy: Intrinsic Line Shape and Coster-Kroning Transitions," *Phys. Rev. B.*, 66, 115115 (2002).

Contact information
Steven Hulbert, NSLS, Brookhaven National Laboratory, Upton, NY

Email: hulbert1@bnl.gov

The importance of correlation effects in core-valence-valence Auger spectra can be quantified by the ratio of the Coulomb repulsion energy to the bandwidth, which, in transition metals, is usually the width of the *d* bands. If this quantity is small, the shape of the Auger spectrum will be band-like. In contrast, if this quantity is large, the lineshape will be atomic-like. Cini and Sawatzky independently developed a theoretical model of Auger transitions that describes the Auger line shape intermediate between these two extremes.

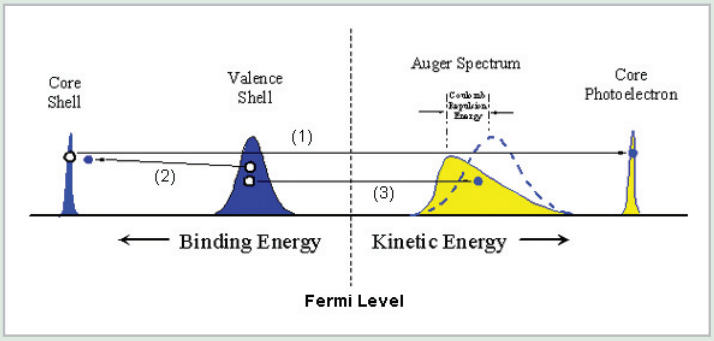

Figure 1. Energy level diagram for the Auger decay process. An electron in the core electronic shell is ejected (1) by a synchrotron soft x-ray and then an electron from the valence band fills (2) the hole previously occupied by the first electron. The energy released by this transition is transferred to the emission (3) of another valence electron, called an Auger electron. The Auger electron is produced by what is called core-valence-valence Auger decay. If the valence electrons are correlated via a Coulomb repulsion energy, the lineshape of the Auger spectrum can change shape as shown.

For palladium, the Cini-Sawatzky model cannot provide a complete description of our measured Auger spectra. We have succeeded in matching the entire Auger spectra by using an extension of the Cini-Sawatzky theory in which each electronic multiplet of the two-hole final state can be considered as having its own value of the Coulomb repulsion energy, so each will experience a different amount of distortion. The result of a fit using this approach is shown in **Figure 2**.

In the M_4-valence-valence Auger spectrum, we notice that excess emission above the theoretical curve accounts for a larger fraction of the spectrum than in the M_5-valence-valence line. This additional M_4 emission is attributed to a Coster-Kronig transition, whereby the palladium M_4 core hole is filled by an M_5 core electron, and then the remaining M_4 hole decays. We have recently found that the Coster-Kronig channel is dramatically enhanced in surface alloys of palladium and silver.

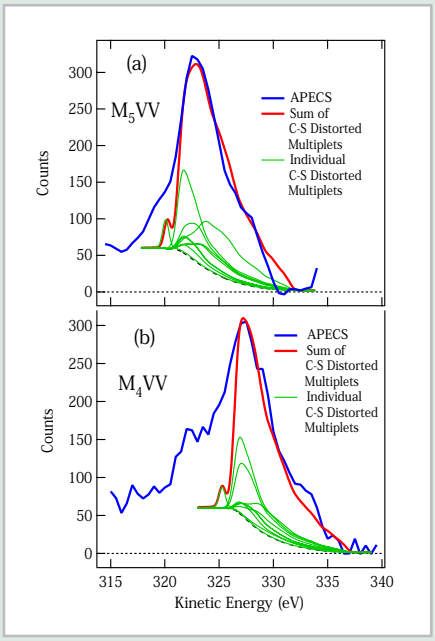

Figure 2. (a) Palladium M_4 valence-valence and (b) palladium M_5 valence-valence Auger spectra (blue curves) along with the individual (green curves) and the sum of the Cini-Sawatzky distorted final state multiplets (red curve) added to a simple inelastic background (black curve).

Superconductivity Induced Electronic Excitation and Phonon Anomalies in Trilayer $Bi_2Sr_2Ca_2Cu_3O_{10}$

A.V. Boris[1,2], D. Munzar[3], N.N. Kovaleva[1,2], B. Liang[1], C.T. Lin[1], A. Dubroka[3], A.V. Pimenov[1], T. Holden[1,4], B. Keimer[1], Y.-L. Mathis[5], and C. Bernhard[1]

[1]Max Planck Institute for Solid State Research, Stuttgart, Germany; [2]Institute of Solid State Physics, Chernogolovka, Russia; [3]Masaryk University, Brno, Czech Republic; [4]Brooklyn College; [5]ISS, Forschungszentrum Karlsruhe, Germany

Charge and lattice dynamics along the c axis perpendicular to the CuO_2 superconducting (SC) planes were studied in a Bi2223 crystal with infrared ellipsometry. The far-infrared (FIR) conductivity data reveal that a strong absorption band corresponding to a transverse Josephson plasmon develops as the crystal enters the SC state. The effect of the FIR spectral weight increase opposes the spectral weight decrease in conventional SC's. This unusual effect highlights that an anomalously large energy scale beyond the FIR range can be attributed to SC condensate formation in high-T_c superconductors. We also observe phonon anomalies, suggesting that the Josephson currents lead to a drastic variation of the local electric field within the closely spaced CuO_2 planes.

Alexander Boris

The transition from a normal metal to a superconductor (SC) below the critical temperature, T_c, is accompanied by a redistribution of spectral weight (*SW*) for the real part of the complex optical conductivity, $\sigma(\omega)$, from finite frequencies in the normal state (NS) into a δ-function at zero frequency in the SC state. For classical SC's, the energy gap determines the frequency range over which the *SW* of the δ-function is collected. That noticeable change occurs only for $\omega < 6\,\Delta$ (Ferrell-Glover-Tinkham (FGT) sum rule). Recently, it was found that the FGT sum rule is partially violated for the *c* axis response of some high-T_c cuprate compounds: The *SW* loss in the FIR below T_c is smaller than the *SW* of the δ-function at zero frequency. It implies that SC pairing involves a very large frequency scale and may rule out conventional mechanisms that rely on low-frequency bosons, such as phonons. Instead, it supports models where a decrease in the *c* axis kinetic energy below T_c provides a significant contribution to the SC condensation energy.

These far-reaching implications call for further experiments on a compound with a larger, more easily identified *SW* transfer. The best candidates are multilayer high-T_c compounds, which contain more than two CuO_2 planes per unit cell. Here we present ellipsometric data of the *c* axis dielectric response of the trilayer compound $Bi_2Sr_2Ca_2Cu_3O_{10}$ (Bi2223). The ellipsometric measurements have been performed at the infrared beamlines of the synchrotrons at ANKA in Karlsruhe, Germany and at NSLS. The brilliance of the synchrotrons enables us to obtain accurate data in the FIR spectral range, even on mm-sized samples.

Figure 1 shows the real part σ_1 of the *c* axis optical conductivity of Bi2223 at the three doping levels. The most prominent feature is the broad absorption band around 500 cm^{-1}, which appears below T_c and grows rapidly with decreasing temperature. The center of this band shifts towards higher frequencies with increasing doping. A similar band was previously identified in the bilayer compounds $YBa_2Cu_3O_{7-\delta}$ and $Bi_2Sr_2CaCu_2O_8$ where it has been attributed to a transverse Joseph-

BEAMLINE
U4IR

Funding
Max Planck Institute for Solid State Research; Alexander von Humboldt Foundation and Ministry of Education of Czech Republic

Publication
A.V. Boris et al., "Josephson Plasma Resonance and Phonon Anomalies in Trilayer $Bi_2Sr_2Ca_2Cu_3O_{10}$," *Phys. Rev. Letts.*, 89, 277001 (2002).

Contact information
Alexander Boris, Max Planck Institute for Solid State Research, Heisenberg-str. I, D-70569 Stuttgart, Germany

Email: A.Boris@fkf.mpg.de

son-plasma resonance (t-JPR). The *SW* of this feature in Bi2223 is very large and causes a considerable increase in the FIR-*SW* below T_c. This apparent increase in the *SW* is certainly not expected for any conventional SC where the FIR-*SW* should be removed and transferred to the δ-function at zero frequency (**Figure 2a**). **Figure 2b** shows the SC induced change of the FIR conductivity in Bi2223. The data represent a striking manifestation of the violation of the FGT sum rule. They highlight that a significant amount of *SW* is transferred from higher frequencies to the absorption band near 500 cm^{-1}. We emphasize that within the Josephson superlattice model (JSM) the *SW* of the t-JPR belongs to the SC condensate as much as the one of the δ-function at zero frequency.

Figure 1 shows that the t-JPR formation is also associated with an anomalous temperature dependence of the phonon modes. Particularly interesting are the contrasting *T* dependences of the modes at 360 and 400 cm^{-1}. As shown in **Figure 3a**, the mode at 360 cm^{-1} loses a significant amount of its SW below T_c, while the latter one gains in the *SW*. Both phonons are oxygen bond-bending modes with the eigenvector diagrams in **Figure 3b**. Their contrasting behavior is explained by the JSM. **Figure 3c** shows the charge dynamics corresponding to the t-JPR, where κ(ω) denotes the charge density that alternates from one outer plane to the other. The onset of the Josephson currents j_1 and j_2 between the CuO_2 layers below T_c can lead to a significant change of the dynamical local electric field inside the trilayer, E_1, inside the spacing layer that separates the trilayers, E_2, and at the outer CuO_2 layers, E_3. The strength of a given phonon mode is determined by the local field at the participating ions participating and by the mode polarizability. The main difference between the oxygen bond-bending modes is in the relative phase and amplitude of the inner and outer-plane oxygen vibrations: The mode at 360 cm^{-1} consists predominantly in the oxygens' vibration in the outer CuO_2 planes (O1), and the latter one involves vibrations in the middle CuO_2 (O4) plane. Following this model, we estimate that the average magnitude of E_3 at O1 ion sites is strongly suppressed below T_c, while the magnitude of E_1 inside the trilayer at O4 sites increases. The local field effect leads to the observed behavior of the oxygen bond-bending modes in the SC state. These phonon anomalies clearly reflect a transition from a confined state (incoherent intra-trilayer conductivity) to a state where the CuO_2 planes are Josephson-coupled. They demonstrate that, in the SC state, the local electric field can exhibit enormous unit cell variations.

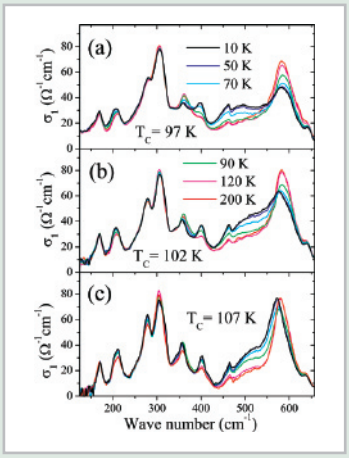

Figure 1. Real part, $\sigma_1(\omega)$, of the FIR c axis conductivity of Bi2223.

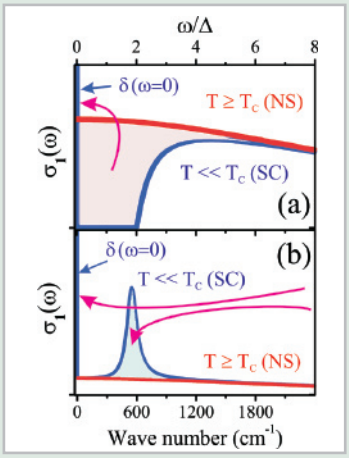

Figure 2. (a) Sketch of the SC induced change of the FIR conductivity (a) for classical materials with a s-wave SC order parameter. (b) as observed in Bi2223.

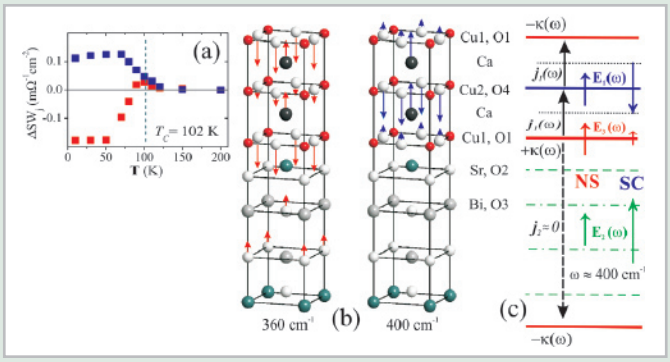

Figure 3. (a) Relative SW changes of the phonons at 360 cm^{-1} (red squares) and 400 cm^{-1} (blue squares) with decreasing temperature. (b) Calculated oxygen bond-bending A_{2u} eigenmodes of Bi2223. (c) Schematic representation of the charge density fluctuations associated with the IR active plasma mode and the related local electrical field in the normal and SC states in the frequency range of the bond-bending modes.

Polarized Light Drives Anisotropic Expansion in Chalcogenide Glasses

G. Chen[1], H. Jain[1], M. Vlcek[2], S. Khalid[3], D.A. Drabold[4], and S.R. Elliott[5]

[1]Department of Materials Science & Engineering, Lehigh University; [2]Department of General and Inorganic Chemistry, University of Pardubice, Pardubice, Czech Republic; [3]National Synchrotron Light Source, Brookhaven National Laboratory; [4]Department of Physics and Astronomy, Ohio University; [5]Department of Chemistry, University of Cambridge, United Kingdom

Common oxide glasses are transparent solids known for their inertness and stability. By contrast, their chalcogenide analogs (i.e. sulfides, selenides, and tellurides) exhibit unexpected sensitivity to bandgap light, leading to several novel photoinduced effects. Particularly fascinating are the anisotropic effects created in their random structure by the polarized light. The in situ EXAFS experiments at NSLS provide the first atomistic evidence of the origin of such structural changes where the local structure around Se in an arsenic selenide glass film expands anisotropically, depending on the polarization of the laser beam.

Authors (from left): H. Jain, G. Chen, and M. Vlcek

The exposure of solids to light leads to a number of important chemical reactions and physical phenomena in nature as well as in modern technology, e.g. photography, xerography, holography, photopolymerization, photosynthesis of plants, etc. In general, light interacts with a solid through its electronic states, which depend upon the constituent atoms and structure of the material. Light-induced change in the atomic structure involving displacement of atoms is unusual, except in special cases of *disordered* materials, including polymers and glasses. Such changes, when they occur, are expected to depend on the intensity and wavelength (λ) of light. However, recently light-induced mass transport, photocrystallization, and an opto-mechanical effect have been reported on glassy chalcogenide films, which imply a change in the atomic structure that depends also on the *polarization* of light. Atomistic, chemical specific experimental evidence about such changes has been missing. These so-called vector effects (because they depend on the direction of the electric field vector of light) are particularly intriguing because the starting structure of the unilluminated films is amorphous and isotropic.

To obtain atomistic insight into the light-induced structural changes that cause the newly discovered vector effects in chalcogenide glasses, it is necessary to have an experimental technique that is capable of probing the element-specific structure of amorphous materials in different directions as defined by the polarized laser beam. The extended x-ray absorption fine structure (EXAFS) analysis, which is conducted with a synchrotron light source, satisfies these requirements. Synchrotron light sources provide not only high-intensity but also *polarized* X-rays, which are essential for detecting anisotropic structures.

In the present work, the Lehigh University researchers, in collaboration with colleagues from Ohio, Pardubice (Czech Republic), and Cambridge (UK) universities and BNL, have used EXAFS analysis with polarized X-rays (in which the electrical field vector $\mathbf{E}_X$ // the ground plane) to probe the changes in the structure around Se and As atoms, and track the laser-polarization dependence of these changes in arsenic

BEAMLINE
X18B

Funding
National Science Foundation

Publication
G. Chen, H. Jain, M. Vlcek, S. Khalid, J. Li, D. Drabold, and S. Elliott, "Observation of Light Polarization-Dependent Structural Changes in Chalcogenide Glasses," *Appl. Phys. Lett.*, 82, 706 (2003).

Contact information
Professor Himanshu Jain,
Department of Materials Science & Engineering, Lehigh University,
Bethlehem, PA

Email: h.jain@lehigh.edu

selenide glasses. The experiments were performed at NSLS beamline X18B; the schematic for *in situ* observations is shown in **Figure 1**. A helium-neon laser beam (λ=633 nm) intercepts the X-ray beam on the sample. A half wave plate is used to change the polarization direction of the laser beam (identified by its electric field vector, $\mathbf{E}_L$) so that $\mathbf{E}_L$ // $\mathbf{E}_X$ or $\mathbf{E}_L \perp \mathbf{E}_X$. Two different spots of the same sample were separately illuminated by two orthogonal, linearly polarized laser beams, and the structural changes were probed *in situ* by the X-ray beam.

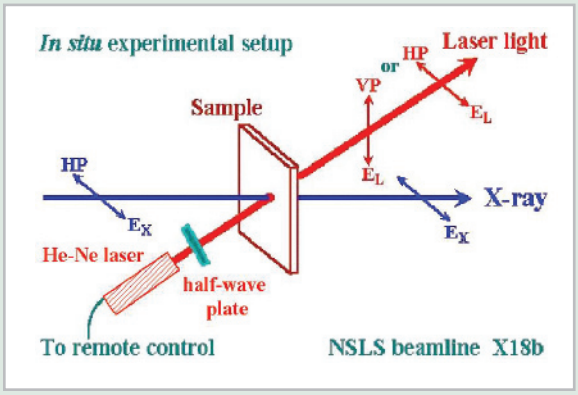

Figure 1. In situ EXAFS setup for studying laser-polarization-dependent photostructural changes. The amorphous As_2Se_3 film is irradiated with light of approximately the bandgap energy from a He-Ne laser (λ= 633 nm) and simultaneously observed by X-rays from the synchrotron. A half wave plate controls the polarization direction of the laser beam. HP: horizontal polarization. VP: vertical polarization.

Figure 2 shows an example of the light-induced structural changes for the two polarization directions of the laser beam. There is an expansion of the nearest-neighbor distance around the Se atoms - its magnitude depends on the direction of light polarization with larger expansion being observed when $\mathbf{E}_L$ // $\mathbf{E}_X$ than when $\mathbf{E}_L \perp \mathbf{E}_X$. Thus a vector structural change is observed *directly* for the first time for any amorphous material. The authors believe that the anisotropic local expansion around Se atoms occurs as the bandgap laser light excites and reorients the Se 4p lone pairs, and helps form anisotropic As-Se bonds. Their experiments provide an atomistic view of photo-induced vector phenomena in chalcogenide glasses, and guide the discovery of new materials with enhanced light-induced effects for photonic applications.

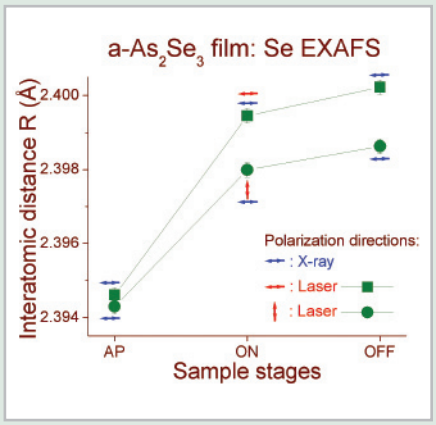

Figure 2: Effect of *in situ* laser irradiation on the interatomic distance from Se in amorphous As_2Se_3 film. Note a greater photoexpansion when $\mathbf{E}_L$ // $\mathbf{E}_X$ than when $\mathbf{E}_L \perp \mathbf{E}_X$. AP: as prepared; ON: laser beam is turned on; OFF: laser beam is switched off.

EXAFS, X-ray Diffraction and Neutron Diffraction Study of the Heusler Alloy Co_2MnSi

B. Ravel[1], M.P. Raphael[1], V.G. Harris[1], J.O. Cross[2], Q. Huang[3], R. Ramesh[4], and V.I. Saraf[4]

[1]Naval Research Laboratory; [2]Advanced Photon Source; [3]National Institute of Standards and Technology; [4]University of Maryland

Magnetoelectronics is an emerging field of electronics in which electron spin is used to control the properties of magnetic devices. More specifically, these devices exploit the imbalance of spin-up and spin-down conduction electrons in ferromagnetic materials. Band structure theory predicts that Heusler alloys, which are either Co_2MnSi or Co_2MnGe, have a complete spin imbalance in the conduction band. But the actual spin imbalance in bulk and thin film samples does not exceed 60, which might be explained by the swapping of lattice positions between cobalt and nickel atoms. We have used synchrotron and neutron techniques to confirm that extensive site-swapping occurs in Heusler alloys.

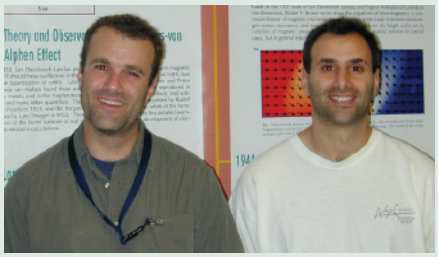

Authors (from left): Bruce Ravel and Marc Raphael

Magnetoelectronic devices have been proposed for a wide variety of applications, including magnetic recording, magnetic field sensors, and nonvolatile memory. The magnetoelectronic devices with the greatest economic impact have been hard disk read heads, which read signals encoded on a magnetic disk or tape. These read heads exploit the giant magnetoresistance (GMR) effect, which is the change in the electrical resistance of a material when it is subject to the application of a magnetic field.

A GMR device consists of ferromagnetic layers separated by a metallic layer, as shown in **Figure 1**. The resistance of the device varies according to how the two ferromagnetic layers are aligned with each other. In the low resistance state, the magnetic moments of the ferromagnetic layers are in the same direction and electron transport through the sample is enhanced because a spin-up transport electron in one ferromagnetic layer is more likely to find a same-spin state to scatter into in the other ferromagnetic layer. In the high resistance state, the two ferromagnetic layers are anti-aligned and electron transport is diminished.

A magnetic storage medium stores bits as magnetic grains whose spins point in opposite directions. So, as the read head passes over the medium, the spins of the bottom layer of the read head aligns to the spins of the magnetic grains, changing their resistance and thus reading the bits in the magnetic grains.

Currently, GMR read heads are made of ferromagnets composed of cobalt, nickel, iron, or an alloy. The read heads' efficiency is limited by the relatively small spin imbalance of 40 percent. With 100 percent spin imbalance – as predicted by band theory – Heusler alloys would be attractive candidates for future GMR devices that would be smaller and would feature an increased surface density. In practice, Heuslers have spin imbalances of around 55 percent.

Band theory predicts that this imbalance would be reduced if the manganese and cobalt atoms swapped their lattice positions (**Figure 2**), an effect also called anti-site disorder. Using neutron diffraction on bulk

BEAMLINE
X23B and X23A2

Funding
Office of Naval Research; U.S. Department of Energy, Office of Basic Energy Sciences

Publication
B. Ravel et al., "EXAFS and Neutron Diffraction Study of the Heusler Alloy Co_2MnSi," *Phys. Rev. B*, 65, 18, 184431 (2002).

Contact information
Bruce Ravel, Naval Research Laboratory, Washington, DC

Email: ravel@phys.washington.edu

Co_2MnSi, we found that about 15 percent of the manganese sites are occupied by cobalt. But neutron diffraction is impractical for the small sample volumes required for GMR devices. So we turned to synchrotron techniques to measure the anti-site disorder.

We used a technique called extended x-ray absorption fine structure spectroscopy (EXAFS) at NSLS beamlines X23B and X23A2 on powdered and thin film samples of Co_2MnSi. We found that about 15 percent of manganese sites are occupied by cobalt.

Because the photoelectron scattering amplitudes of cobalt and manganese are so similar, the anti-site disorder is measured with very poor precision by EXAFS. So we next turned to anomalous x-ray diffraction, and we were able to measure anti-site disorder in Heusler alloys in sample volumes comparable to those found in magnetoelectronic devices.

By using synchrotron measurement techniques, we sccessfully characterized a dominant form of disorder that limits the application of Heusler alloys to GMR devices.

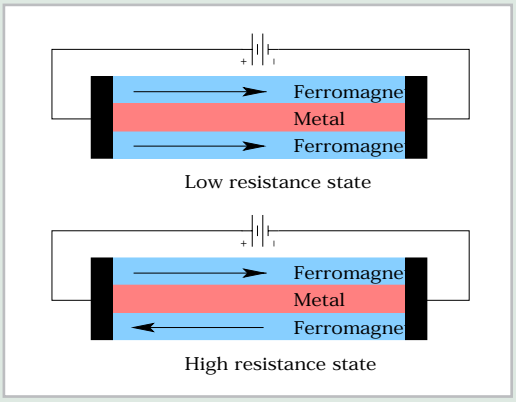

Figure 1. A giant resistive read head used in magnetic storage media consists of two ferromagnetic layers separated by a metallic layer. When the spins of the two ferromagnets are parallel (top), conduction electrons can easily scatter through the heterostructure, resulting in a low resistance. When the spins are anti-parallel, the resistance is high.

Additional Publication:

B. Ravel et al. "Atomic disorder in Heusler Co_2MnGe measured by anomalous x-ray diffraction," *Appl. Phys. Letts.,* **81**, 15, 2812 (2002).

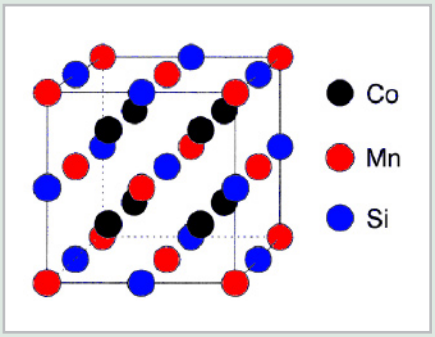

Figure 2. Crystal structure of the Heusler alloy Co_2MnSi.

Giant Dielectric Effect in $CaCu_3Ti_4O_{12}$ and Its Cd Analogue

C.C. Homes[1], T. Vogt[1], S.M. Shapiro[1], S. Wakimoto[1,2], M.A. Subramanian[3], and A.P. Ramirez[4]

[1]Department of Physics, Brookhaven National Laboratory; [2]Department of Physics, Massachusetts Institute of Technology; [3]DuPont Central Research & Development Experimental Station; [4]Materials Integration Science Laboratory, K764, Los Alamos National Laboratory

The perovskite-related material $CaCu_3Ti_4O_{12}$ has a very high static dielectric constant $\varepsilon_0 \sim 10^4$ at room temperature, which drops to about 100 at low temperature. Substituting Cd for Ca reduces the room temperature value by over an order of magnitude. The origin of the large ε_0 is not fully understood, but may be due to an internal barrier layer capacitance (IBLC) effect. Infrared measurements on the Ca and Cd compounds show dramatic changes in the nature of the normal modes at low temperature, suggesting that increasing electronic localization may lead to a breakdown of the IBLC effect.

Authors (from left): Tom Vogt, Christopher Homes, and Stephen Shapiro

Materials with large dielectric constants are highly sought after in the microelectronics industry for use in memory devices; the static dielectric constant ε_0 acts as a scaling factor and ultimately determines the level of miniaturization. One of the most commonly used dielectric materials is silicon nitride with $\varepsilon_0 \sim 7$; materials with $\varepsilon_0 > 7$ are generally referred to as high-dielectric constant materials. It was recently noted that the cubic perovskite-related material $CaCu_3Ti_4O_{12}$ shown in **Figure 1** had a tremendously high dielectric constant at room temperature, $\varepsilon_0 \sim 10^4$, which showed little temperature dependence until about 100 K, below which it decreased by nearly two orders of magnitude to $\varepsilon_0 \sim 100$, shown in **Figure 2a**. The substitution of Cd for Ca results in a large reduction of ε_0, shown in **Figure 2b**. It was initially suggested that this large value for ε_0 was a purely extrinsic effect due to Maxwell-Wagner-type depletion layers forming between the sample and the metal contacts used in the capacitive measurements of ε_0 in the kHz range. This effect has indeed been observed in a number of different materials. However, the addition of a thin a buffer layer of a dielectric with well-known electrical properties (aluminum oxide) has demonstrated that the large value for ε_0 persists in these materials, and is therefore a property of the bulk. The dramatic drop of ε_0 at low temperature is curious because it is not accompanied by any change in the long-range crystallographic structure when probed by high-resolution x-ray and neutron powder diffraction. In ferroelectric materials, large changes in ε_0 are usually accompanied by a structural distortion and soft-mode condensation.

Infrared (IR) spectroscopy is a powerful tool to study the lattice vibrations in insulators, in particular soft-mode condensation. The large change in ε_0 and the absence of any structural distortion suggested that the normal modes should be examined. The temperature dependence of the reflectance was determined over a wide frequency range using the spectrometer at NSLS beamline U10A and the complex optical properties determined from a Kramers-Kronig analysis. The real part of the dielectric function ε_1 is shown in **Figures 3a and 3b** for $CaCu_3Ti_4O_{12}$ and $CdCu_3Ti_4O_{12}$, respectively, at a variety of temperatures in the infrared region. The dielectric function is dominated by the infrared ac-

BEAMLINE
U10A

Funding
Department of Energy

Publication
C.C. Homes, et al., "Charge Transfer in the High Dielectric Constant Materials $CaCu_3Ti_4O_{12}$ and $CdCu_3Ti_4O_{12}$," *Phys. Rev. B*, 67, 092106 (2003).

Contact information
Christopher Homes, Department of Physics, Brookhaven National Laboratory, Upton, NY

Email: homes@bnl.gov

tive lattice modes. (The units of cm^{-1} are commonly used in IR spectroscopy, 1 THz = 30 cm^{-1}.) While these experiments are done in the THz range, the low-frequency value for ε_1 agrees with the values for ε_0 (kHz) at low temperature. It is clear from **Figure 3** that ε_1 at low frequency is also increasing at low temperature. Fits to simple Lorentzian oscillators describe these features quite well and indicate that many of the vibrational modes are gaining strength at low temperature, a violation of the partial ***f***-sum rule for oscillators. From this result, it may be inferred that the Born effective charge on the atoms is changing and that the material is becoming more ionic. We (along with others) have speculated that the large value of ε_0 is due to an internal barrier layer capacitance (IBLC) effect due to extensive twinning or grain boundaries. This view is consistent with impedance spectroscopy that indicates these materials may be described as semiconducting regions separated by insulating barriers. The increase in ionicity implies increasing charge localization at low temperatures. This localization may lead to an increase in the size of the insulating regions and a commensurate reduction of ε_0 within the IBLC picture, suggesting that the large value for ε_0 is, at least in part, due to "extrinsic" effects.

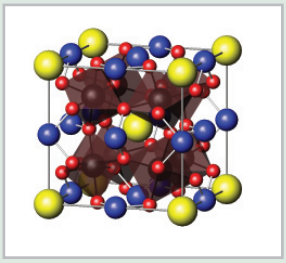

Figure 1. The unit cell of body-centered cubic $CaCu_3Ti_4O_{12}$, which consists of two formula units. The Ti atoms sit at the center of canted TiO_6 octahedra (the tilt angle is nominally 141°), with bridging Cu atoms and large Ca atoms sitting at the center and corners of the unit cell.

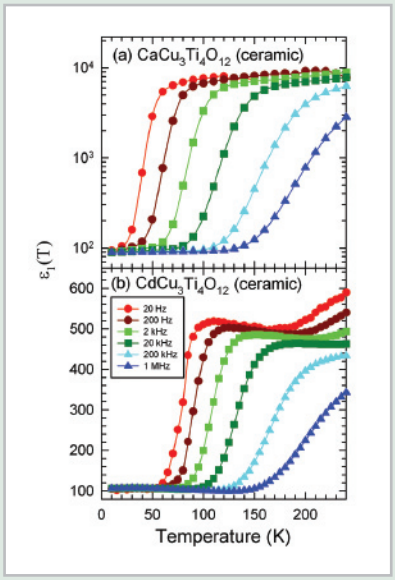

Figure 2. The temperature dependence of the real part of the dielectric constant of (a) $CaCu_3Ti_4O_{12}$ and (b) $CdCu_3Ti_4O_{12}$ ceramics for several fixed frequencies.

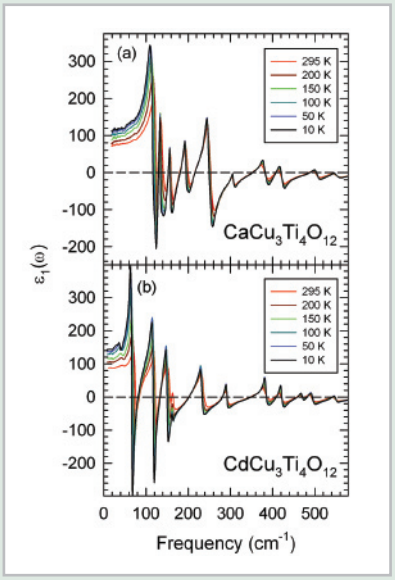

Figure 3. The temperature dependence of the real part of the dielectric function for (a) $CaCu_3Ti_4O_{12}$ and (b) $CdCu_3Ti_4O_{12}$ in the infrared region.

Electronic Structure of Thin Film Silicon Oxynitrides Measured Using Soft X-Ray Emission and Absorption Spectroscopies

C. McGuinness[1], D. Fu[1], J.E. Downes[1], K.E. Smith[1], G. Hughes[2], and J. Roche[2]

[1]Department of Physics, Boston University; [2]School of Physical Science, Dublin City University, Dublin, Ireland

The elementally-resolved valence band electronic structure of a thin film silicon oxynitride gate dielectric used in commercial device fabrication has been measured using soft x-ray emission and absorption spectroscopies. Specifically, the valence and conduction band partial density of states in the interfacial region of both the nitrogen and oxygen states was determined. The element-specific band gap for the O 2p states was measured to be 8.8 eV in the interfacial region, similar to that of pure SiO_2. However, the band gap for the N 2p states in the interfacial region was measured to be approximately 5 eV.

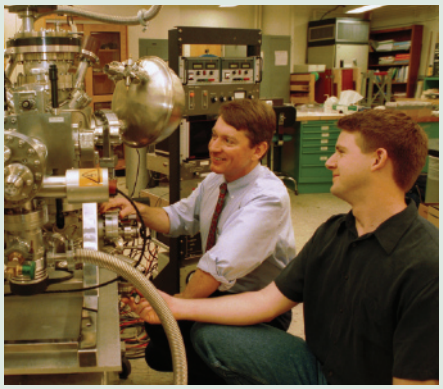

Authors (from left): Kevin Smith and James Downes

The material properties of SiO_2 gate dielectric are crucial to the behavior of metal-oxide-semiconductor field effect transistors. SiO_2 possesses a relatively low dielectric constant, which leads to increased leakage currents in submicron devices. One favored replacement dielectric material currently in use is SiO_xN_y (silicon oxynitride). While much progress has been made in understanding both the process of oxynitride film formation and the macroscopic dielectric and device properties of these films, the basic electronic structure of the nitrogen-rich interfacial layer remains poorly understood. We have made the first direct measurement of the element-specific O *2p* and N *2p* valence and conduction band partial densities of states for an ultrathin commercial SiO_xN_y layer. The measurements were made using synchrotron radiation-excited soft x-ray emission (SXE) spectroscopy and soft x-ray absorption (SXA) spectroscopy on beamline X1B at the NSLS. SXE is a unique probe of the bulk element-specific electronic structure of solids. SXE spectra reflect the occupied valence band partial density of states (PDOS — the valence band density of states resolved into its orbital angular momentum components). SXE measurements are also element-specific and are bulk-sensitive, with a sampling depth of well over 100 nm. Finally, as a "photon in - photon out" spectroscopy, SXE can be used to make electronic structure measurements on insulating samples, such as SiO_xN_y. Thus, SXE is in many ways a more useful probe of buried interfaces than photoemission spectroscopy, which, as a "photon in - electron out" spectroscopy, typically measures the electronic structure of solids within less than 1 nm of the vacuum-solid interface. Our SXE measurements were made with a Nordgren-type grating spectrometer, which is the only one of its kind at the NSLS.

The silicon oxynitride samples under investigation in this study were device-grade materials, where the nitration treatment consists of annealing the pre-grown SiO_2 in an NH_3 environment at elevated temperatures. This treatment results in a non-uniform distribution of nitrogen in the layer, with preferential build-up at both the Si-SiO_2 interface and the outer surface.

Figure 1 shows the N *2p* PDOS for SiO_xN_y as measured in this experi-

BEAMLINE
X1B

Funding
National Science Foundation; U.S. Army Research Office

Publication
C. McGuinness, D. Fu, J.E. Downes, K.E. Smith, G. Hughes, and J. Roche, "Electronic Structure of Thin Film Silicon Oxynitrides Measured Using Soft X-ray Emission and Absorption," *J. of Appl. Phys.*, 94, 3919 (2003).

Contact information
Kevin Smith, Department of Physics, Boston University

Email: ksmith@bu.edu

ment. Also shown are SXE spectra from bulk ∀ -Si_3N_4 and gas phase N_2. The ability of SXE and SXA to measure the elementally-resolved band gap in solids is immediately clear from **Figure 1**. The N *2p*-derived band gap for SiO_xN_y is approximately 5 eV, which is much less than the 8.8 eV for bulk SiO_2. Such elementally-resolved measurements are not possible using photoemission spectroscopy, which is the standard probe of solid-state electronic structure.

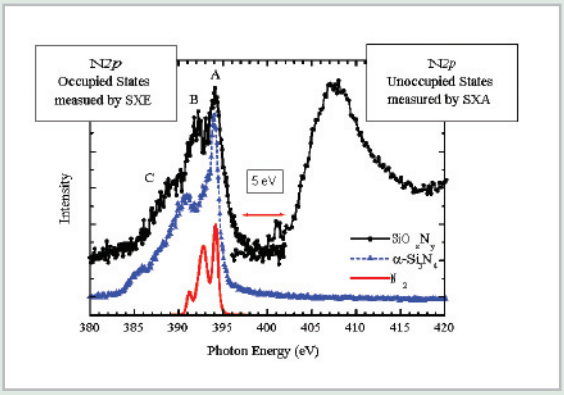

Figure 1. N K edge SXE and SXA spectra from the SiO_xN_y sample. The SXE spectrum reflects the occupied density of electronic states of N 2p character, while the SXA spectrum reflects the unoccupied density of electronic states of N 2p character. The SiO_xN_y SXE spectrum was obtained with an excitation energy of 435 eV. The N K edge SXE spectra obtained from ∀-Si_3N_4 (G. Wiech and A. Simunek, Phys. Rev. B 49, 5398 (1994)) and molecular N_2 (Glans et al, J. Elec. Spec. Related Phenom. 82, 193 (1996)) are also shown.

Geological and Environmental Sciences

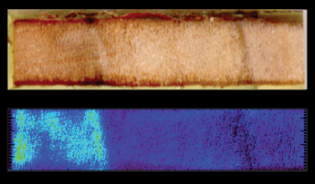

The Application of Synchrotron X-Ray Fluorescence Microanalysis to Dendroanalysis: Detecting a Contaminant Signature in Salix Nigra Annual Rings

T. Punshon[1], P.M. Bertsch[2], A. Lanzirotti[3], K.W. McLeod[2], and J. Burger[1]

[1]Consortium for Risk Evaluation with Stakeholder Participation, Environmental and Occupational Health Sciences Institute, Division of Life Sciences, Rutgers University; [2]Savannah River Ecology Laboratory, University of Georgia; [3]Consortium for Advanced Radiation Sources, The University of Chicago

Synchrotron X-Ray Fluorescence microanalysis (SXRF) was used to test the accuracy of dendroanalytical data using willows (Salix nigra L.) collected from an eroding U- and Ni-contaminated former settling pond and the impacted area downstream. Increases in background Ni concentration and enrichment in specific annual rings were in good agreement with contaminant history. High resolution spatial analysis showed that ring boundaries sharply separated differentially enriched annual rings, and revealed both a discrete and diffuse Ni distribution thought to be consistent with Ni transport within and binding to vessel elements in woody tissue, respectively.

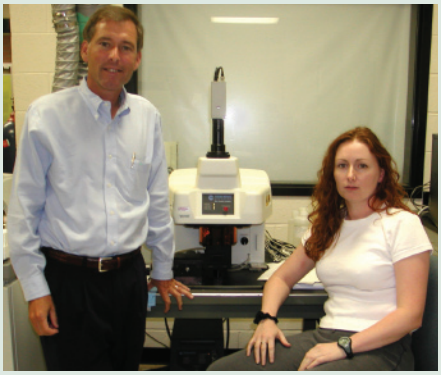

Authors (from left): Paul Bertsch and Tracy Punshon

Dendroanalysis, the measurement of the chemical composition of a tree's annual rings for retrospective biomonitoring, is a controversial area of study. For metals, the accuracy of the environmental record is based on the assumption that elemental distribution remains stable, however, reports of metal mobility have questioned this. Techniques capable of providing spatially-resolved elemental composition data, such as Synchrotron X-ray Fluorescence microanalysis (SXRF), can considerably enhance our understanding of metal transport and distribution within tree rings. In order to test the accuracy of dendroanalysis, annual rings from trees with a well-documented contaminant history, where metal concentrations have fluctuated in recent years, were investigated using SXRF at the dedicated microprobe beamline, X26A.

Steed Pond functioned as a de facto settling basin for uranium (U) and metal wastes discharged to a stream from a nuclear target and fuel fabrication facility on the Savannah River Site between 1954-1985, effectively retaining U (natural and depleted), Ni, Cu, Zn, and Al in its pond sediments. When the enclosing spillway breached in 1984, the water level fell and a pulse of contaminated sediments moved downstream, being redeposited in Lower Tims Branch; a process that continues during seasonal storms. We investigated whether willows collected from the contaminant source and sink areas, found to contain elevated metal concentrations in their leaves, contained the geochemical signature of contaminants in their annual rings.

Tree core samples were collected from Steed Pond and Lower Tims Branch, dated and analyzed using SXRF. One-dimensional line scans collected X-ray fluorescence data along the length of the core samples, from pith to cambium, to show changes in metal concentration throughout the lifetime of the trees. We found that samples from Steed Pond (source) contained higher concentrations of Ni than those collected from Lower Tims Branch (sink), indicating that SXRF can be used to provide quantitative data. Samples collected from Lower Tims Branch, pre-dating the spillway breach, clearly showed a large pulse in

BEAMLINE
X26A

Funding
Department of Energy Environmental Remediation Sciences Division, Office of Biological and Environmental Research

Publication
T. Punshon, P. M. Bertsch, A. Lanzirotti, K. W. McLeod, and J. Burger, "Geochemical Signature of Contaminated Sediment Remobilization Revealed by Spatially Resolved X-ray Microanalysis of Annual Rings of Salix nigra," Environ. Sci. Technol., 37 (9), 1766-1774 (2003).

Contact information
Tracy Punshon, Rutgers University

Email: punshon@srel.edu

Ni, Cu, and Zn in 1985, and again in 1991 (**Figure 1**), correlating with known contaminant pulses. In agreement with previous bioavailability studies, U was not detected in any of the samples.

Two-dimensional elemental maps of Ni closely resembled digital images of annual rings (**Figure 2**), and annual ring boundaries sharply separated differentially Ni-enriched zones. Elucidating this required a rigorous sample resolution and coverage, entailing a focused X-ray beam (10 × 15 µm) and small step size (30 µm); approximately 125,000 data points. Closer observation of the Ni-enriched ring revealed sporadically distributed, exclusively Ni-containing features, approximately 10-20 µm in diameter (**Figure 3**). Using the digital imaging capabilities at X26A, we could see this was a non-structural Ni-enriched substance within the lumen of vessel elements. Contrasting intense and diffuse Ni distributions may conceivably arise from Ni transport within and binding to annual rings, respectively, and are the subject of continued investigation using Size-Exclusion Chromatography and X-Ray Absorption Near Edge Spectroscopy (XANES).

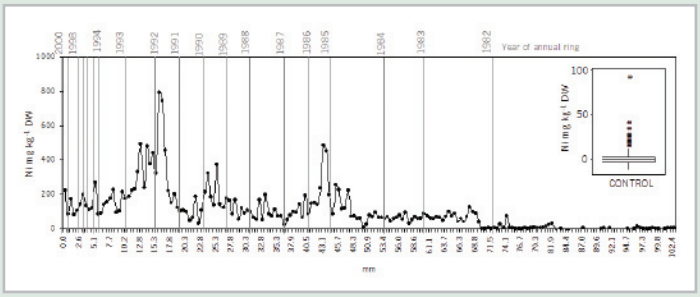

Figure 1. One-dimensional line scan of the Ni concentration (mg kg^{-1} d. wt) within annual rings of Salix nigra L. (black willow) collected from Lower Tims Branch referenced against the annual ring positions. Inset shows summarized control data.

This study demonstrates that micron-scale heterogeneity of metal distribution in the vascular system of woody plans can provide misleading data, but that the more rigorous two-dimensional elemental imaging obtainable with SXRF allows an accurate interpretation of dendroanalytical data with minimal sample preparation.

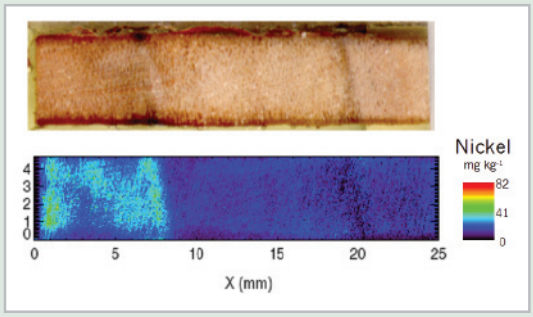

Figure 2. Digital photograph and compositional map of Ni fluorescence counts in the annual rings of Salix nigra L.

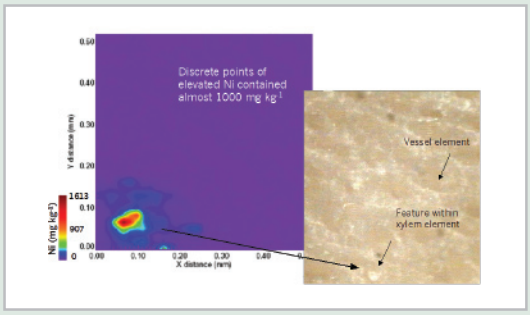

Figure 3. Discrete area of concentrated Ni distribution (shown as mg kg^{-1}), compared to digital photograph of the corresponding area, showing open ends of vessel elements and the location of the Ni feature.

Mechanisms of Selenate Adsorption on Iron Oxides and Hydroxides

D. Peak[1] and D.L. Sparks[2]

[1]University of Saskatchewan; [2]University of Delaware

Selenium is a naturally occurring element that occurs in rocks and soil and can also be released by manufacturing processes. In the environment, selenium combines with oxygen to form many different molecules, such as selenate (SeO_4^{2-}), which is known to bind to ferric oxides and hydroxides. Because of selenate's toxicity to animals and its mobility in the soil, the mechanism of selenate adsorption on iron oxides has been the subject of intense debate. Researchers from the University of Delaware have determined selenate bonding mechanisms on hematite (α-Fe_2O_3), goethite (α-FeOOH), and amorphous iron hydroxide ($Fe(OH)_3$).

Derek Peak

Selenate (SeO_4^{2-}) is the fully oxidized form of selenium, an essential micronutrient for plant growth. When soil selenate levels are high, it often accumulates in plants and can then prove toxic to animals that ingest this vegetation. Alternatively, deficiency symptoms are commonly seen in animals when selenium levels in plants are low. So, understanding the chemistry of selenate in soils is important for minimizing potentially hazardous environmental effects on animal populations.

In soils and sediments, selenate preferentially reacts with ferric [Fe(III)] oxides and hydroxides. However, the mechanism of selenate binding on iron oxides has been the subject of intense debate. Some researchers have proposed that the bonding is electrostatic and weak, while others have proposed that covalent chemical bonds form between selenate and iron oxides. The nature of bonding can have a large effect on the transport and availability of selenate in the environment, so we decided to investigate this adsorption mechanism when selenate binds to hematite (α-Fe_2O_3), goethite (α-FeOOH), and amorphous iron hydroxide ($Fe(OH)_3$).

The objectives of our work were to determine the effects of pH (the concentration of protons in solution), surface loading, and ionic strength (an average of the concentrations of the ions present) on selenate adsorption mechanisms. Hematite, goethite, and amorphous iron hydroxide were chosen due to their important differences in structure and their common occurance in soils.

Extended x-ray absorption fine structure (EXAFS) was the primary spectroscopic tool chosen due to its suitability to determine local bonding environments of selenate on all three sorbents. EXAFS spectra were collected at the selenium K-edge at beamline X11A. Additional information about selenate adsorption mechanisms on hematite was obtained using attenuated total reflectance-Fourier transform infrared (ATR-FTIR) spectroscopy.

Selenate forms different surface complexes on iron oxides, depending upon pH, ionic strength, and iron oxide structure. On hematite, we noticed that selenate ions directly interact with iron, with no intermediate water molecules present, a structure called an inner-sphere complex. Also, the adsorbed selenate ions form single covalent bonds (formed by sharing electrons) with the surface, a process known as monodentate.

BEAMLINE
X11A

Funding
National Science Foundation

Publication
J.D. Peak and D.L. Sparks, "Mechanisms of Selenate Adsorption on Iron Oxides and Hydroxides," *Environ. Sci. and Technol.*, 36, 1460-1466 (2002).

Contact information
Derek Peak, Assistant Professor, Department of Soil Science, University of Saskatchewan, Saskatoon, Canada

Email: derek.peak@usask.ca

These inner-sphere monodentate complexes were observed at all pH and ionic strength values considered in the study.

On goethite and amorphous iron hydroxide, we noticed that selenate forms outer-sphere complexes, in which a water molecule is positioned between each selenate and iron atom, at pH values of 6 (slightly acidic) and above (alkaline). For pH values between 3.5 and 6 (acidic), we noticed a mixture of outer- and inner-sphere monodentate complexes. ATR-FTIR spectroscopy also suggests that some hydrogen bonding is present in this inner-sphere complex.

The EXAFS spectra are shown for aqueous selenate (pH 4) and selenate adsorbed on goethite at pH values of 6 and 3.5 in **Figure 1**. A schematic representation of the outer- and inner-sphere monodentate complexes is provided in **Figure 2**.

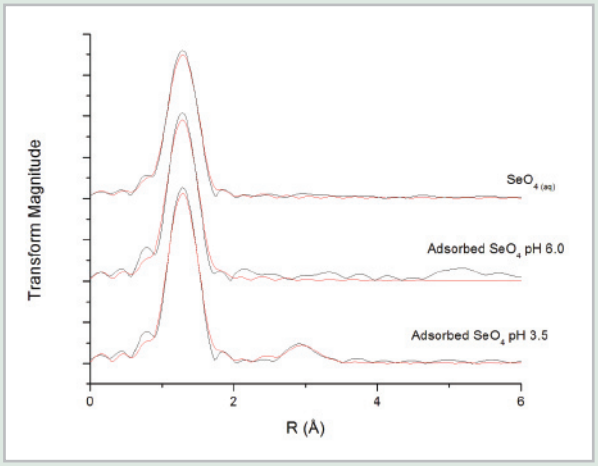

Figure 1. Selenium K-edge extended x-ray absorption fine structure (EXAFS) spectra of aqueous selenate, selenate adsorbed on goethite at pH = 6.0 (outer-sphere surface complex), and selenate adsorbed on goethite at pH = 3.5 (inner-sphere surface complex).

This study and others have shown that outer-sphere and inner-sphere complexation often occur simultaneously. We noticed that changes in the relative importance of different surface complexes depend on the pH and ionic strength of the solution containing the sorbent, as well as on the nature of the sorbent. So, to adequately characterize selenate reactivity at the molecular level, we consider it is necessary to conduct EXAFS studies over a wide range of reaction conditions and with a range of minerals. Such studies are expected to produce a far clearer picture of how selenate, and oxyanions in general, reacts under constantly changing conditions in the natural world.

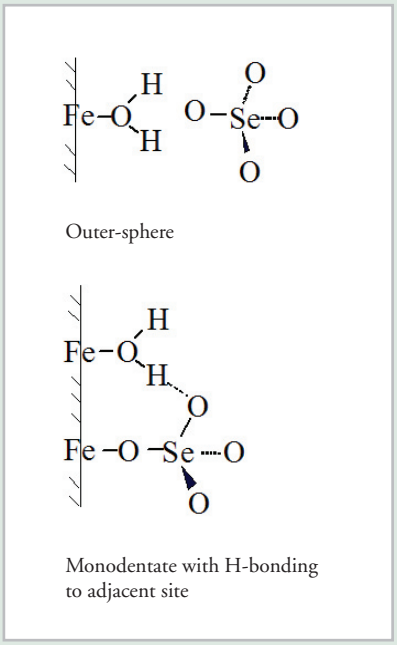

Figure 2. Bonding of selenate on goethite derived from EXAFS and attenuated total reflectance-Fourier transform infrared (ATR-FTIR) spectroscopy. (A) Outer-sphere complex (water molecule positioned between selenate and the iron atom); (B) Inner-sphere (no water molecule is positioned between selenate and the iron atom) and monodentate (shared electrons between selenate and the iron atom) complex.

Trapping Hydrogen in Ice

W.L. Mao[1,2], H.-k. Mao[2], A.F. Goncharov[2], V.V. Struzhkin[2], Q. Guo[2], J. Hu[2], J. Shu[2], R.J. Hemley[2], M. Somayazulu[3], and Y. Zhao[4]

[1]Department of the Geophysical Sciences, University of Chicago; [2]Geophysical Laboratory, Carnegie Institute of Washington; [3]HPCAT, Advanced Photon Source, Argonne National Laboratory; [4]LANSCE, Los Alamos National Laboratory

Until recently, scientists thought that molecular hydrogen was too small to be contained in clathrate hydrates — crystalline solids made of a crystalline lattice of water molecules enclosing molecules of another substance, usually a noble gas. Using x-rays produced at beamline X17B, scientists from the University of Chicago and the Carnegie Institution of Washington have reported the formation of a hydrogen clathrate hydrate – in which hydrogen molecules are completely enclosed in a lattice of water molecules – that is quenchable to ambient pressure at temperatures below 110 K. This material may have implications for research in hydrogen fuel storage, superfluidity, and astrophysics.

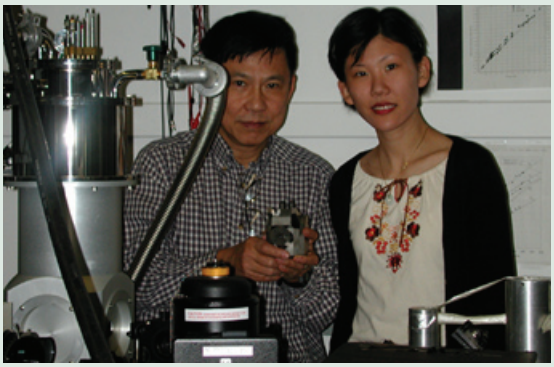

Authors (from left): Ho-kwang Mao and Wendy L. Mao

Hydrogen molecules are considered to be too small to be enclosed in one of four possible structures of clathrate hydrates, compounds in which molecules of a substance are completely enclosed within the crystal structure of water. The three clathrate structures that do not include hydrogen molecules are denoted sI, sII, and sH. Instead, hydrogen molecules have been found to fill small cavities in ice II and ice Ic at high pressures.

We have synthesized a hydrogen hydrate with the classical sII structure (HH-sII) and a high hydrogen:water ratio (= 0.45 ± 0.05). This high ratio shows that, unlike most clathrate hydrates, where only one molecule of a gas can be trapped inside the clathrate cage, many hydrogen molecules are entrapped in two types of cages (a small and a large one) within each clathrate compound. Two hydrogen molecules are enclosed in the small cages and four in the large cages (**Figure 1**).

HH-sII is stable or metastable – unstable in the absence of certain conditions that would induce stability – to ambient pressure and low temperature after initial synthesis at moderate pressure. We compressed a mixture of hydrogen and water to 180–220 megapascals (about 2,000 times the atmospheric pressure) at 300 K in a diamond anvil cell, which separated the samples into two regions: a hydrogen bubble and liquid water. We noticed that, upon cooling to 249 K, the two fluids reacted and formed a single, solid compound.

Using energy dispersive x-ray diffraction (EDXD) at beamline X17B, we observed 21 diffraction peaks at 220±30 megapascals and 234 K (**Figure 2**). The EDXD pattern reveals that the formed clathrate contains a face centered cubic (fcc) unit cell with a = 17.047 ± 0.010 angstrom, in excellent agreement with the sII clathrate. We attribute two hydrogen molecules to each pentagonal dodecahedron cage (structure with 12 pentagon faces) and four hydrogen molecules to each hexakaidodecahedron cage (structure with four hexagon faces and 12 pentagon faces).

Once HH-sII was synthesized at 200 megapascals, it showed remarkable stability or metastability and persisted to 280 K upon warming. The clathrate was also cooled to 78 K, and then pressure was released

BEAMLINE
X17B

Funding
National Science Foundation, Earth Science Division; National Aeronautics and Space Administration, Planetary Geology and Geophysics Division; U.S. Department of Energy, Office of Basic Energy Research; W.M. Keck Foundation

Publication
W.L. Mao, H.-k. Mao, A.F. Goncharov, V.V. Struzhkin, Q. Guo, J. Hu, J. Shu, R.J. Hemley, M. Somayazulu, and Y. Zhao, "Hydrogen Clusters in Clathrate Hydrate," Science, 297, 2247-2249 (2002).

Contact information
Wendy Mao, Department of Geophysical Sciences, University of Chicago, Chicago, IL

Email: wmao@uchicago.edu

completely. This sample was then exposed to vacuum in the cryostat, and the clathrate remained (did not decompose). The large hydrogen storage capacity and stability of HH-sII at ambient pressure make it a potential hydrogen fuel storage material.

Since HH-sII can be synthesized at a pressure of more than 180 megapascals, which is within the range of interior conditions of small, icy satellites, this clathrate could hold hydrogen to high temperatures in bodies which were previously thought to be incapable of retaining hydrogen.

The kinetics of possible *in-situ* formation of HH-sII at low-pressure interstellar conditions has not yet been explored. But this clathrate could be grown epitaxially (growth upon the surface of another crystal) on substrates of other sII clathrates or by annealing (heating to remove or prevent internal stress) hydrogen in amorphous ice. The intriguing physics and chemistry of filling large cages with clusters of small molecules also opens new directions in clathrate and ice research.

Confining hydrogen molecular clusters in cages also provides a new means for studying novel interactions and quantum effects, such as the proposed superfluidity and Bose-Einstein condensation of hydrogen molecular clusters.

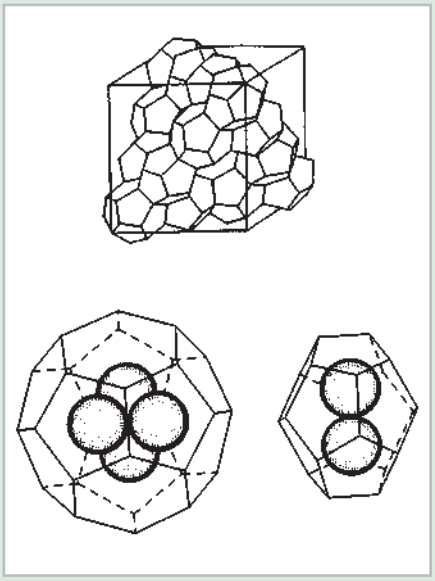

Figure 1. (Top) sII crystal structure consisting of large and small cages. (Bottom left) A tetrahedral cluster of four hydrogen molecules in a large cage. (Bottom right) A cluster of two hydrogen molecules in a small cage.

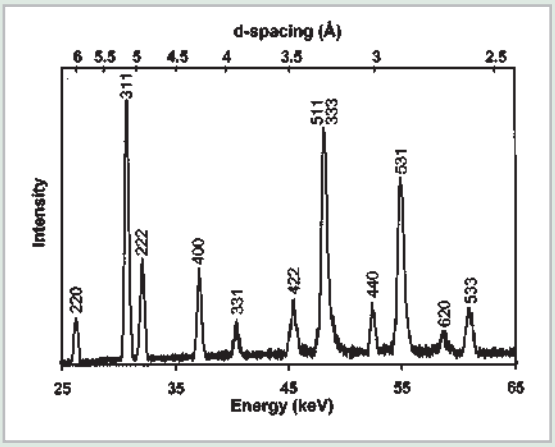

Figure 2. Energy dispersive x-ray diffraction pattern of HH-sII at 220 megapascals and 234 Kelvin (2q = 4.50 degrees). The Miller indices, *h*, *k*, and *l* are marked on each peak.

Zinc and Cadmium Associations with Reduced Forms of Sulfur in Organic Matter-Rich Aerobic Soils

C.E. Martínez[1], M.B. McBride[2], M.T. Kandianis[2], J.M. Duxbury[2], S. Yoon[3], and W.F. Bleam[3]

[1]The Pennsylvania State University; [2]Cornell University; [3]University of Wisconsin, Madison

Unusually high natural concentrations of zinc and cadmium have often been associated with soils high in organic matter and sulfur. For example, the soils from the Manning region of Western New York and from Guelph in Ontario concentrate zinc and cadmium by biogeochemical processes using sulfur. Scientists at The Pennsylvania State University in University Park, Cornell University in Ithaca, New York, and the University of Wisconsin in Madison have determined the oxidation states of sulfur in bulk soils, the distribution of these two metals in soil particles, and their solubility, toxicity, and bioavailability. The researchers used spectroscopic, chemical, and bioassay approaches and illustrated how the macroscopic behavior of metals in soils can be explained by knowledge of their forms at the microscopic scale.

Carmen Enid Martínez

Peat deposits, such as those overlying the dolomite bedrock that extends from eastern New York State into Ontario in Canada (**Figure 1**), contain unusually high concentrations of metals, such as zinc and cadmium, leading to potentially hazardous concentrations of cadmium in some crops. Scientists have determined that soluble zinc entered these wetlands by drainage and groundwater emanating from weathering dolomite [$CaMg(CO_3)_2$].

One possible concern with these metalliferous peats is the release of sulfur-bound cadmium and zinc during natural weathering conditions or when the bogs are drained for agricultural use. For example, in the Manning peatlands of western New York, this situation appears to have arisen as toxic metals were detected in vegetable crops in the early 1940s, not long after the bogs were drained for agriculture. Very high concentrations of zinc were measured in the plant shoots of some fields.

We recently collected peat soils from the Manning region and from Guelph in Ontario to investigate the processes controlling zinc and cadmium solubility, toxicity, and bioavailability in these soils.

Reduced forms of sulfur (compared to their oxidized forms) are potentially important to retain zinc and cadmium in organic soils. By using x-ray absorption near-edge spectroscopy (XANES) at NSLS beamline X19A, we have shown that 35 to 45 percent of sulfur in these soils exists in the most reduced electronic oxidation states 60 years after the soils were drained, while less than five percent of sulfur exist in the most oxidized forms (**Figure 2**). Although reduced forms of sulfur are not expected to prevail in aerobic soils for long periods of time, their presence may be the result of anaerobic microenvironments in otherwise apparent oxygen-rich soils, or of slow oxygen diffusion into soil aggregates.

Another technique called energy-dispersive x-ray absorption (EDX) also showed a close spatial distribution between zinc and sulfur in soil particles, thus suggesting their chemical association (**Figure 3**). But, despite this EDX evidence, conventional x-ray diffraction (XRD) analy-

BEAMLINE
X19A

Funding
U.S. Department of Agriculture, Agricultural Ecosystems Project

Publication
C.E. Martinez et al., "Zinc-Sulfur and Cadmium-Sulfur Association in Metalliferous Peats: Evidence from Spectroscopy, Distribution Coefficients and Phytoavailability," *Environ. Sci. Technol.*, 36, 3683 (2002).

Contact information
Carmen Enid Martinez, Asst. Professor of Environmental Soil Chemistry, Department of Crop and Soil Sciences, The Pennsylvania State University, University Park

Email: cem17@psu.edu

ses of the bulk soils did not detect a mineral phase of sphalerite (ZnS) in any of them.

Chemical data showed that cadmium binds relatively more strongly in these sulfur-rich organic soils than in most mineral soils, suggesting that reduced sulfur could be limiting cadmium solubility more than zinc. These data also showed that most of the high-zinc soils were very toxic to plants, and that such toxicity has persisted for decades since the soils were drained.

We have also demonstrated high zinc solubility and plant availability but relatively low cadmium solubility and plant uptake, despite very high soil cadmium concentrations, as well as both low mobility and bioavailability of cadmium relative to zinc in these soils.

We conclude that sulfur biogeochemical cycling may play an important role in zinc and cadmium retention in sulfur-rich organic soils.

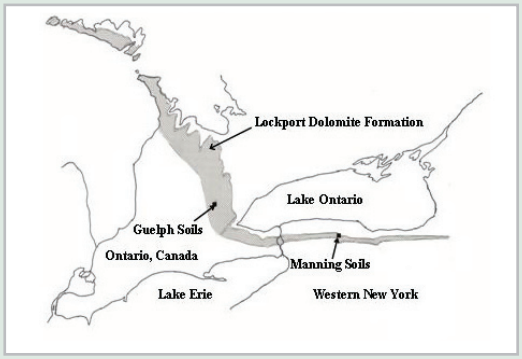

Figure 1. Lockport Dolomite formation: extension across New York and Ontario in Canada (gray area). The map shows the area where the Manning and Guelph peat soils were collected.

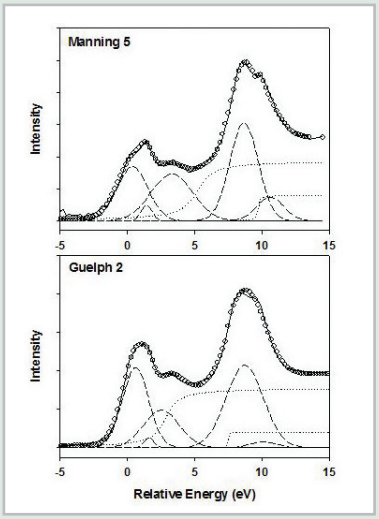

Figure 2. X-ray absorption near-edge spectroscopy (XANES) spectra for the Manning and Guelph soils used in this study. The solid line is the experimental spectrum, the circles represent the fit to the experimental spectrum, the broken lines are the Gaussian curves, and the dotted lines are the arctangents.

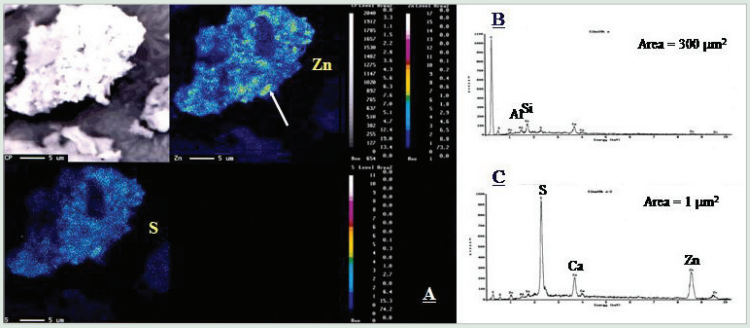

Figure 3. (A) X-ray maps obtained by energy-dispersive x-ray analysis (EDX), showing the backscattered image and the distribution of zinc and sulfur in a soil aggregate of the Manning soil containing 15800 milligrams of zinc per kilogram (top) and 7230 milligrams of sulfur per kilogram (bottom). (B) X-ray energy spectra showing the elemental composition of the whole aggregate (300-square-micrometer). (C) X-ray energy spectra showing the elemental composition of a one square-micrometer area (arrow in panel A) of the same soil particle.

Incorporation of Uranium with Iron Oxide Minerals

M.C. Duff, J. Urbanik Coughlin, and D.B. Hunter

Westinghouse Savannah River Company

The transport and biological availability of the toxic, radioactive element uranium (U) towards reduction to the less soluble U(IV) species may be limited by co-precipitation with Fe-oxide minerals. We examined the interaction dynamics between U(VI) and iron (Fe) oxides during crystallization by synthesizing Fe-oxide phases [0.5-5.4 mole %U/(U + Fe)] using U(VI) and Fe(III) solutions. Our studies show that U^{6+} is incorporated in Fe oxides as the uncommon uranate species (without axial O atoms) until saturation is reached, whereby U(VI) forms crystalline U(IV)O_2^{2+} phases.

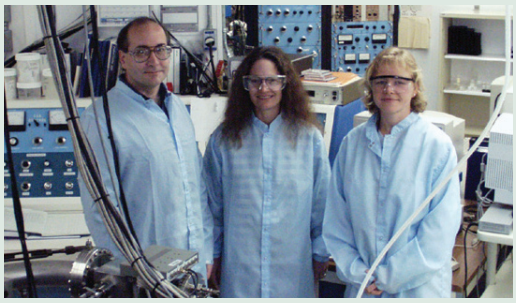

Authors (from left): Douglas B. Hunter, Martine C. Duff, and Jessica Coughlin

The geochemical speciation of uranium (U) influences its movement and biological availability in the environment. This information is often used to predict nuclear waste repository performance. In oxidized environments, U exists as the highly soluble uranyl [U(VI)O_2^{2+}] species with two axial U=O double bonds at ~1.8 Å. In contaminated materials, solid phase U(VI) typically exists as the uranyl mineral, schoepite [$UO_3 \cdot 2H_2O$]. Uranium(VI) can also exist as the less common uranate solid phase, which has at least three single U-O bonds and no axial double bonds. However, uranates have not been found in nature. The environmental mobility of U is influenced by many processes (**Figure 1**). Another process that may influence U mobility is co-precipitation with other host minerals (**Figure 1**). Uptake of U and other metals occurs during the formation of crystalline and amorphous Fe oxides but the local structure of U in these oxide materials has not been characterized.

Leaching of the synthetic U-Fe oxides typically removed most sorbed and solid phase U(VI) species, leaving on average ~0.6 mol % U. X-ray diffraction and infrared spectroscopic studies (**Figure 2A-B**) indicate that hematite (Fe_2O_3) formation is preferred over that of goethite (FeOOH) when the U level in the Fe-oxides exceeds 1 mol % U. Our studies with unleached U/Fe solids indicate a relationship between the mol % U in the Fe oxide, and the existence of the spectral features that can be assigned to uranyl species. These spectral features were undetectable in leached solids, suggesting solid phase and sorbed U(VI)O_2^{2+} species are extracted by leaching. Using uranium X-ray Absorption Fine Structure (XAFS) at NSLS beamlines X23A2 and X26A, analyses of unleached solids containing <1 mol % U revealed that U(VI) exists with four O atoms at radial distances of 2.21 and 2.36 Å and Fe atoms at 3.19 Å (**Figure 2C**). Due to the large size of UO_2^{2+} (~1.8 Å) relative to Fe^{3+} (0.65 Å), the UO_2^{2+} ion is unlikely to substitute for the Fe. Our results indicate that U^{6+} (~0.72-0.8 Å) is incorporated in the Fe oxides as uranate until a point of saturation is reached. Beyond this concentration, excess U precipitates as crystalline U(VI) phases resembling schoepite.

In summary, our findings indicate that the long-term association of U in the contaminated environment could result in the structural incorporation of U in Fe oxide host phases. In nature, precipitation of pure U phases should occur at a kinetically faster rate than the structural

BEAMLINE
X23A2, X26A

Funding
U.S. Department of Energy; University of Georgia Research Foundation

Publication
M.C. Duff, J.U. Coughlin, and D.B. Hunter, "Uranium Co-Precipitation with Fe Oxide Minerals," *Geochim. Cosmochim. Acta*, 66, 3533-3547 (2002).

Contact information
Martine C. Duff, Westinghouse Savannah River Company, Aiken, SC

Email: Martine.Duff@srs.gov

incorporation of U into Fe oxides. Precipitation of U as pure mineral phases should be favored at high dissolved U concentrations, whereas sorption and co-precipitation of U are most likely favored at lower U concentrations. In aged, U-contaminated Fe-rich soils, uptake of U by Fe oxides may be significant since ~1 mol % U can be incorporated. The importance of these mechanisms in U-contaminated materials has not been estimated.

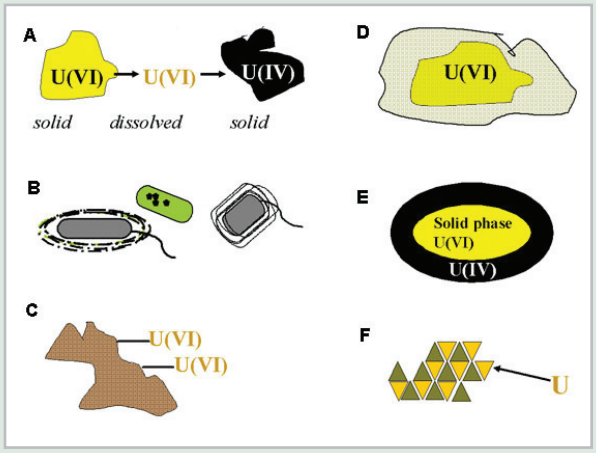

Figure 1. Mechanisms by which U mobility can be retarded in the surface and subsurface geologic environment. A) Precipitation of U(VI) and U(IV) phases. B) Microbial uptake (internal or external) of U. C) The sorption of U by organic or inorganic material such as humic acids and Fe oxides (respectively). D) Occlusion of U by clay and metal oxide coatings. E) Under reducing conditions, the formation of surface rinds of U(IV) on U(VI) minerals can also limit U mobility because U(IV) solids are less soluble. F) Co-precipitation of U with amorphous and crystalline host minerals may limit U mobility (adapted from Duff, Coughlin and Hunter, Uranium Co-precipitation with Fe Oxide Minerals. *Geochim. Cosmochim. Acta*, 66, 3533-3547 (2002.)

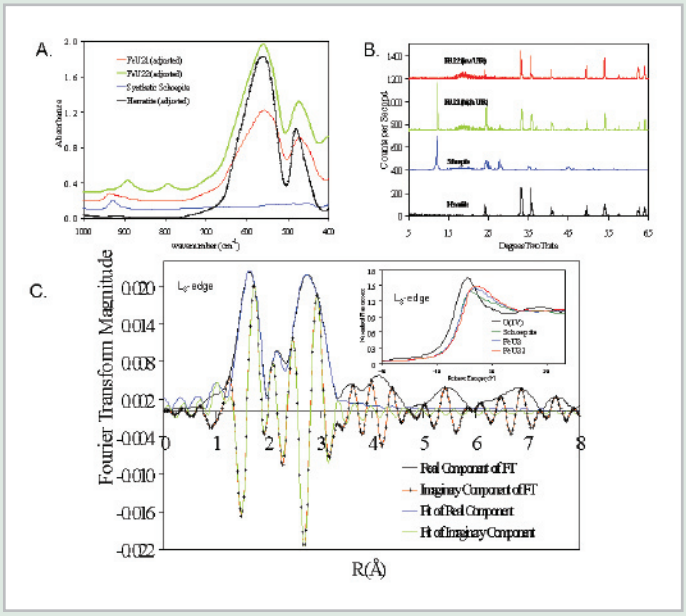

Figure 2. (A) Uranium XAFS spectra (L_3 edge) Fourier transform and fit data for the U-Fe oxide co-precipitate sample, FeU22. Inset: The U XANES spectra (L_3 edge) for $U(IV)O_2$, the U(VI) mineral meta-schoepite, the FeU2 and FeU22 U-Fe oxide co-precipitate samples. The XANES spectra for uranyl nitrate contained post-edge multiple scattering resonance (MSR) features typically observed for uranyl-containing solids (data not shown). (B) FTIR spectra for hematite, the synthetic U-Fe oxide co-precipitates (FeU21 and FeU22) and the synthetic mineral meta-schoepite. Three of the spectra for the samples are adjusted linearly so that their absorbance peaks are proportional to that of meta-schoepite and (C) Powder X-ray diffraction spectra for hematite, the synthetic U-Fe oxide co-precipitates and the synthetic (adapted from Duff, Coughlin and Hunter, 2002).

Coordination Chemistry of Methyl Mercury Bound in Natural Organic Matter Using Sulfur K-XANES and Mercury L_{III}-EXAFS

J. Qian[1,2], U. Skyllberg[1], W. Frech[2], W.F. Bleam[3], P.R. Bloom[4], and P-E. Petit[5]

[1]Swedish University of Agricultural Sciences; [2]Umeå University, Sweden; [3]University of Wisconsin; [4]University of Minnesota; [5]ESRF, France

Based on results from a combination of X-ray absorption near edge spectroscopy (XANES) and extended X-ray absorption fine structure (EXAFS) spectroscopy, we conclude that methyl mercury binds exclusively to high affinity reduced sulfur groups (RSH) in both stream and soil organic matter. Only when the RSH groups are saturated by methyl mercury, do oxygen (or nitrogen) groups take part in the bonding. Our results suggest that approximately 25-35% of reduced sulfur in natural organic matter, as determined by XANES, is represented by RSH groups with a high affinity for methyl mercury and likely other trace metals with soft Lewis acid properties.

Combustion of fossil fuels releases mercury into the atmosphere that may be long-range transported as Hg^0(g). After oxidation to Hg^{2+}, mercury is deposited and transformed to methyl mercury (CH_3Hg) in wetlands and soils. Subsequent accumulation of the highly bioavailable methyl mercury in organisms (e.g. fish) is a severe environmental problem at northern latitudes. In order to understand mechanisms behind the formation and decomposition of methyl mercury, as well as how it is transported and made available for organisms in soils and waters, detailed information about the coordination chemistry in natural organic matter (NOM) is crucial. We combined sulfur K-edge X-ray Absorption Near Edge Spectroscopy (K-XANES) and mercury L_{III}-edge Extended X-ray Absorption Fine Structure (L_{III}-EXAFS) spectroscopy in order to determine the coordination chemistry of methyl mercury in stream and soil NOM. Sulfur XANES was used to quantify the concentration of reduced sulfur groups (Org-S_{RED}). The same samples were added CH_3Hg to collect Hg EXAFS at varying Org-S_{RED} / CH_3Hg ratios.

Figure 1 shows the sulfur XANES spectrum for an organic soil. In the raw data spectrum, two large peaks appear: The left one is represented by reduced sulfur and the right peak represents oxidized sulfur. Raw data were fitted by a series of Gaussian peaks, using a least-square fitting procedure. The two peaks with highest oxidation states (electronic oxidation state 5.0 and 6.0) represent sulfonates and sulfate-esters, respectively. The red peak (Org-S_{RED}) represents sulfur functionalities of importance for trace metal binding, having an average electronic oxidation state of 0.2. This peak represents the sum of functional groups such as thiol (RSH), disulfane (RSSH), sulfide (RSR), and disulfide (RSSR).

Figure 2 shows Fourier-transformed Hg-EXAFS spectra for two NOM samples: a peat sample (FP) and dissolved organic substances gently extracted from an organic soil (PSOS). A comparison with the two peaks of the thiol resin model compound, showing a C–Hg bond (within the methyl mercury molecule) at 1.6 Å (corresponding to a bond length of 2.03 ± 0.02 Å) and a Hg–S bond at 2.0 Å (corresponding to a bond length of 2.34 ± 0.03 Å), suggests that CH_3Hg forms one covalent

Authors (from left, top): Jin Qian, Ulf Skyllberg, (bottom) Wolfgang Frech, and P. Bloom

BEAMLINE
X11A, X19A

Funding
Swedish Natural Science Research Council; Centre of Environmental Research, Umeå, Sweden; Europeon Synchrotron Radiation Facility and USDA-NIR Soils and Soil Biology Program

Publication
J. Qian et al., "Bonding of Methyl Mercury to Reduced Organic Sulfur Groups in Soil and Stream Organic Matter as Determined by X-ray Absorption Spectroscopy and Binding Affinity Studies," *Geochimica et Cosmochimica Acta*, 66, 3873-3885 (2002).

Contact information
Ulf Skyllberg, Swedish University of Agricultural Sciences, Umeå, Sweden

Email: Ulf.Skyllberg@sek.slu.se

bond with RSH groups in the peat and in the PSOS sample. Above a certain CH_3Hg / Org-S_{RED} ratio, oxygen (and possibly nitrogen, which cannot be separated from oxygen by EXAFS) functional groups also take part in the bonding, due to a saturation of RSH groups. This is illustrated by a decrease of the shoulder at 2.0 Å, while the peak at 1.6 Å is broadened and slightly shifted to 1.7Å for samples with CH_3Hg / Org-S_{RED} ratios of 0.47 and 0.95. The peak at 1.7 Å represents a mixture of C–Hg and Hg–O bonds, the latter having a bond length of 2.09 ± 0.01 Å. Exact coordination numbers and bond lengths were determined by the fitting of EXAFS data in *k*-space (not shown here).

In summary, our results show that methyl mercury binds to reduced sulfur groups in NOM of humic streams and organic soils. A consequence of the very strong CH_3Hg–S bond is that practically 100% of potentially mobile methyl mercury will be transported together with NOM in the aqueous phase and that concentrations of neutral methyl mercury forms that may pass biological membranes (e.g. CH_3HgCl, CH_3HgOH) are extremely low.

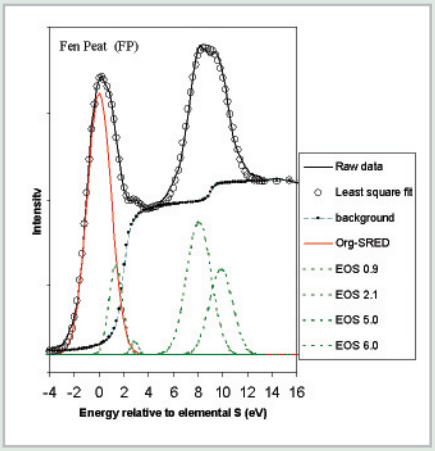

Figure 1. Sulfur K-edge XANES spectrum. The energy scale is relative to elemental sulfur (2472 eV). The raw spectrum was deconvoluted into five groups of sulfur functionalities with different electronic oxidation states (EOS).

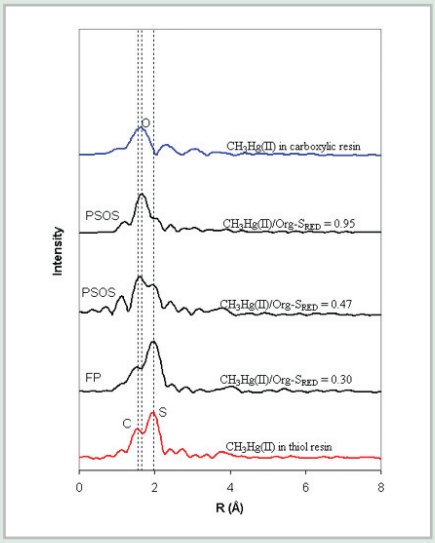

Figure 2. Fourier-transformed EXAFS spectra for two model compounds and two NOM samples. Spectra were not corrected for phase shift.

Chemical Forms of Zinc in a Smelter-Contaminated Soil

A.C. Scheinost[1], R. Kretzschmar[2], S. Pfister[2], D.R. Roberts[3], and D.L. Sparks[4]

[1]ROBL, European Synchrotron Radiation Facility, France; [2]Institute of Terrestrial Ecology, ETH Zurich, Switzerland; [3]Department of Physics, University of Ottawa, Canada; [4]Department of Plant and Soil Sciences, University of Delaware

Zinc is contained in many objects of our daily life, from baby care products to anti-corrosive coatings of cars. Concomitant of its frequent use, zinc is released into the environment and accumulates in soils. While zinc is benign to human health, it is phytotoxic at relatively modest concentrations, thereby reducing plant growth. In spite of its importance, relatively little is known on the chemistry of zinc in soils. We have used a combination of microscopic, spectroscopic, wet chemistry, and chemometric tools to investigate the chemical forms of zinc in a strongly acidic soil near the historic zinc smelter at Palmerton, Pennsylvania.

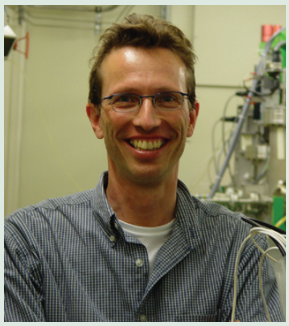

Andreas Scheinost

Due to the burning of coal and other fossil fuels, zinc ore smelting and processing, and the application of sewage sludge and agrochemicals, soils are increasingly contaminated with zinc. In Switzerland, and most likely also in other industrialized countries, zinc concentrations in soils may soon reach levels which could significantly reduce the production of food, fiber, and renewable energy sources. The problem of such predictions is, however, that the toxicity of plants for zinc, called phytotoxicity, in a given soil cannot be simply predicted from its concentration. For instance, aqueous zinc cations in soil solution are readily taken up by plant roots and are therefore very phytotoxic, while the incorporation of zinc into the crystal structure of recalcitrant (i.e. very insoluble) soil minerals may drastically reduce its solubility and hence phytotoxicity. Knowing the chemical forms of zinc is therefore a prerequisite for risk assessments and the development of effective remediation strategies.

Previous investigations have shown that Zn-bearing soil clay minerals, called phyllosilicates, may form after raising the soil pH to neutral values. Consequently, the bare soils in the vicinity of a zinc smelter in France could be re-vegetated by applications of lime and fly ash. On the other hand, a similar approach to remediate the Palmerton Superfund Site in Pennsylvania largely failed (**Figure 1**). The intention of our work was to determine the specific problems of this site by determining the chemical forms of zinc in a soil profile.

The zinc speciation was based on extended x-ray fine-structure absorption (EXAFS) spectroscopy performed at beamline X11A. While EXAFS is perhaps the only tool capable of identifying the various species possibly present in soils, it was complemented by additional methods to achieve unequivocal results. First, we made use of the non-homogeneous distribution of species at the micrometer scale, employing micro-focused x-rays for elemental mapping and microspectroscopy. Second, we made use of the different solubilities of species with respect to various solvents. We employed a sequence of six wet-chemical extraction procedures for a step-wise removal of increasingly recalcitrant species, while monitoring the remaining species with EXAFS spectroscopy. Third, we used statistical methods like principal component

BEAMLINE
X11B

Funding
Swiss Federal Institute of Technology; National Science Foundation

Publication
A.C. Scheinost et al, "Combining Selective Sequential Extractions, X-ray Absorption Spectroscopy and Principal Component Analysis for Quantitative Zinc Speciation in Soil," *Environ. Sci. Technol.*, 36, 5021 (2002).

Contact information
Andreas Scheinost, ROBL, European Synchrotron Radiation Facility, France

Email: scheinost@esrf.fr

analysis to extract the single components hidden in the experimental spectra of species mixtures.

Our results are summarized in **Figures 2** and **3**. In the topsoil with an extremely acidic pH of 3.1, most zinc atoms occur in franklinite, a zinc-iron oxide spinel-type mineral (**Figure 2**). Zinc sulfide (the mineral sphalerite) constitutes the second largest fraction. Divalent zinc cations dissolved in the soil water or exchangeably bound to clay minerals are the smallest fraction. The topsoil contains 6200 mg kg^{-1} zinc, however, this easily plant-available fraction still constitutes 620 mg kg^{-1}, a definitively phytotoxic concentration.

Both franklinite and sphalerite were part of the zinc ores smelted in the Palmerton furnaces. The deposition of these minerals by smelter-emitted dust initiated the geochemical cycle of zinc in the surrounding soils. While franklinite has a low solubility, sphalerite dissolves in the presence of oxygen releasing sulfuric acid. This ongoing release of protons explains the difficulty of raising the soil pH for longer than just a few years by applying lime and fly ash.

In the subsoil, the zinc concentration is lower (900 mg kg^{-1}). Due to the protective cover of the topsoil, no smelter-emitted minerals are present. Since the pH is still quite acidic (3.9), relatively stable inner-sphere sorption complexes and known zinc-bearing soil minerals cannot form. Therefore, we would have expected that all zinc is dissolved or easily exchangeable. Surprisingly, however, we found that 45% of zinc was bound by Al-hydroxide interlayers sandwiched between phyllosilicate layers (**Figure 3**). This clay mineral (HIM) is quite common in acidic soils, and may effectively scavenge a range of transition metals at low pH, thereby reducing their ecotoxicity.

Additional Publication:

D.R. Roberts et al., "Zn Speciation in a Smelter-Contaminated Soil Profile using Bulk and Micro-Spectroscopic Techniques," *Environ. Sci. Technol.*, 36, 1742 (2002).

Figure 1. Blue Ridge Mountains near Palmerton PA. What looks like a desert now was a lush green deciduous forest before the smelter operation began. Although the emissions were drastically reduced several decades ago, soil infertility still prevents re-vegetation.

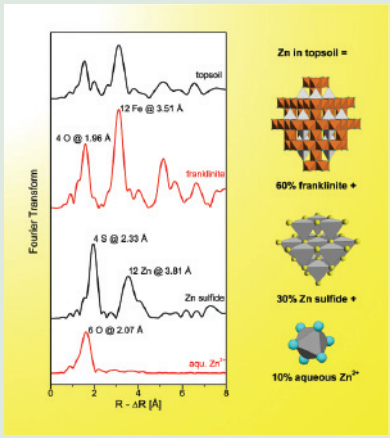

Figure 2. Zn speciation of topsoil sample. The graph on the left shows the Zn K-edge EXAFS spectra of the soil sample together with the spectra of the identified zinc species. The structure of the species and their quantity is given at the right.

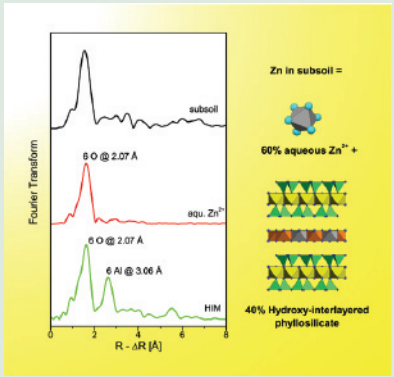

Figure 3. Zn speciation of subsoil sample (see Figure 2 for further explanations).

X-ray Absorption Study of the Uptake of Pb(II) at the Solid-Water Interface of Amorphous Silica

E.J. Elzinga[1,2] and D.L. Sparks[1]

[1]University of Delaware; [2]Stony Brook University

The bonding mechanism of Pb(II) at the amorphous silica surface was characterized with Extended X-Ray Absorption Fine Structure (EXAFS). The mode of Pb uptake was found to strongly depend on solution pH: At pH<4.4, monomeric complexes are formed by mostly electrostatic interactions with the silica surface, whereas dimeric covalent Pb surface complexes form at pH>6. These findings imply that the effectiveness of SiO_2 in retaining Pb^{2+} strongly depends on the conditions in the solution in contact with the SiO_2 surface.

Evert J. Elzinga

Characterizing the bonding mechanisms of trace metals on mineral surfaces is important in understanding and predicting their solubility and mobility in the environment. Dissolved metal concentrations in the pore water of soils and sediments are controlled by the extent of metal partitioning to the mineral matrix contacting the solution phase. Metal uptake at the mineral-water interface may occur via a number of different mechanisms. These include electrostatic interactions between oppositely charged metal ions and surface groups; direct chemical bonding of metal ions at the surface by the coordination to surface ligands; and the formation of metal precipitates at the surface. Distinguishing between these different modes of metal uptake is important, because they determine the stability of the partitioned metal ions. Electrostatically held complexes are weakly bound compared to chemically bonded complexes, and may therefore be more readily transferred back into solution, whereas precipitates are generally quite resistant to metal remobilization.

We investigated the interaction between Pb^{2+} and the surface of hydrous amorphous silica (SiO_2). Amorphous silica is abundant in marine environments, and serves as a high surface area analogue for quartz, a mineral found in essentially all soils and sediments. Experiments were run at low, intermediate, and high pH values, and at different concentration levels of co-adsorbing Na+ cations to simulate a range of environmentally relevant solution conditions.

Figure 1 shows the uptake of Pb^{2+} by silica as a function of pH and Na concentration. Both system parameters affect the amount of Pb held at the silica surface: Pb uptake increases with increasing pH, and decreasing Na+ concentration. The arrows in **Figure 1** indicate the samples for which we collected EXAFS data to characterize the bonding environment of Pb at the silica surface.

The EXAFS data shown in **Figure 2** indicate that the mechanism of Pb uptake by silica drastically changes as a function of pH. At low pH (<4.4), sorbed Pb has a first-shell O coordination similar to that of aqueous Pb^{2+} cations, which indicates that the interaction with the SiO_2 surface is mostly electrostatic. At high pH (>6.3), however, the surface-held Pb cations are in a covalent bonding state, as indicated by the similarity of their first-shell O coordination with that of aque-

BEAMLINE
X11A

Funding
DRP State, DuPont Company

Publication
E.J. Elzinga and D.L. Sparks, "X-ray Absorption Spectroscopy Study of the Effects of Ph and Ionic Strength on Pb(II) Sorption to Amorphous Silica," *Environ. Sci. & Technol.*, 36, 4352-4357 (2002).

Contact information
Evert J. Elzinga, Department of Geosciences, State University of New York, Stony Brook, NY

Email: eelzinga@notes.cc.sunysb.edu

ous $Pb_4(OH)_4^{4+}$ polymers; moreover, the presence of Pb atoms in the local coordination sphere of the sorbed Pb cations indicates that the Pb surface complexes formed at high pH are polymers, most likely dimers. The Pb surface complexes formed between pH 4.8 and 6.3 are intermediate between those observed at low and high pH, indicating that a mixed population of ionic (i.e. electrostatically held) and covalent Pb complexes is present at the silica surface in this pH range.

The presence of electrostatically held Pb surface complexes at low and intermediate pH implies that Pb may be effectively remobilized by competing with other cations for uptake at surface sites, as demonstrated by the decreased Pb uptake at high Na concentrations (**Figure 1**). With increasing pH, however, Pb becomes less susceptible to desorption due to the more covalent nature of the interaction with silica surface sites. The effectiveness of SiO_2 in retaining Pb^{2+} therefore strongly depends on the conditions in the solution in contact with the SiO_2 surface.

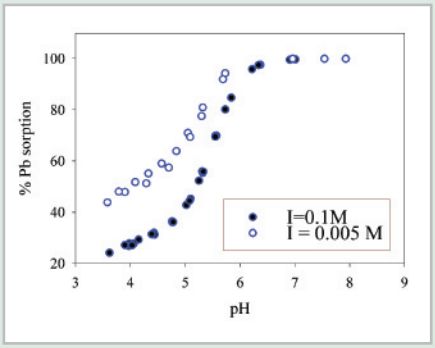

Figure 1. Comparison of the pH edges of Pb sorption at I = 0.1 and 0.005 M.

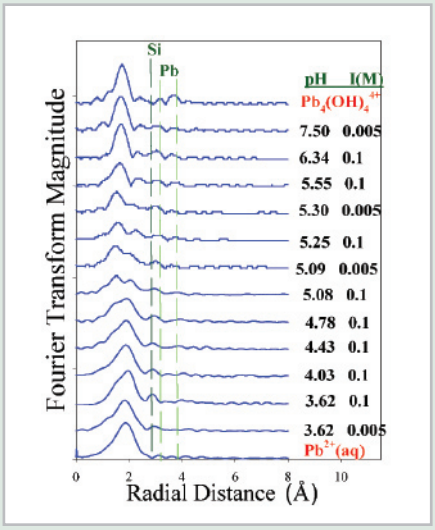

Figure 2. Radial structure functions (not corrected for phase shift) obtained by Fourier transforming the raw k^3-weighted spectra.

Superhard Materials Under Pressure: Strength and Elasticity of Stishovite

S.R. Shieh[1*], T.S. Duffy[1], and B. Li[2]

[1]Department of Geosciences, Princeton University; [2]Mineral Physics Institute, Stony Brook University

Stishovite, a six-coordinated form of SiO_2 and one of the hardest known oxides, was compressed in a diamond anvil cell to study its elastic and rheological behavior at extreme pressures. Our results show that the yield strength is surprising low at high pressures compared with other silicates. Furthermore, we provide experimental confirmation of the prediction that the transition from stishovite to the $CaCl_2$-type structure near 50 GPa is accompanied by an elastic instability. These results show that application of high pressures can greatly modify expectations of material behavior based on low-pressure considerations.

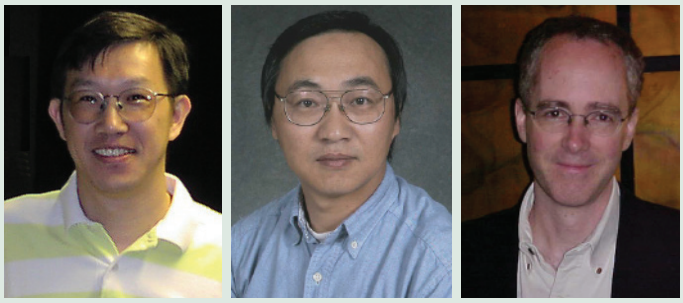

Authors (from left): Sean R. Shieh, Baosheng Li, and Thomas S. Duffy

Stishovite is likely to be an important constituent of the Earth's deep mantle. It is also a prototype for the six-coordinated silicates that are of fundamental importance in geophysics and materials science. The nature of the transformation of stishovite from the rutile structure to the $CaCl_2$-type structure near 50 GPa has been the focus of much recent interest. Stishovite is also among the strongest known oxides, and understanding its elastic and rheological properties is fundamental to the search for new superhard materials. In this study, we use new compression measurement techniques in a diamond anvil cell to examine the elasticity and yield strength of dense SiO_2 over a broad pressure range for the first time.

Stishovite was loaded into a diamond anvil cell and compressed non-hydrostatically. Energy dispersive x-ray diffraction experiments were conducted at beamline X17C (**Figure 1**). The sample was contained within an x-ray transparent (beryllium) gasket, which enabled us to measure the diffraction pattern at any angle with respect to the loading axis of the cell. The data were analyzed using lattice strain theory, which relates the anisotropy of the measured lattice strains to the yield strength and the elastic stiffness coefficients.

Figure 2 shows the yield strength of stishovite as a function of pressure from our x-ray diffraction data combined with theoretical predictions for the shear modulus. The yield strength was found to be nearly constant at pressures of 15-40 GPa and dropped sharply as the transition pressure was approached. The yield strength then increased rapidly in the $CaCl_2$-type phase. In contrast to its ambient-pressure behavior, our measurements indicate that the yield strength of stishovite is surprisingly low at high pressures especially when compared with other silicates (e.g. ringwoodite).

Our data also allow for inversion to recover a partial elastic stiffness tensor at high pressure. In general, our values of C_{11} and C_{12} (**Figure 3**) lie below theoretical values, but they are qualitatively consistent with theory in that C_{11}-C_{12} is markedly reduced near the transition pressure. This provides direct experimental support for the theoretical prediction

BEAMLINE
X17C

Funding
National Science Foundation; David and Lucille Packard Foundation

Publication
S. Shieh, T. Duffy, and B. Li, "Strength and Elasticity of SiO_2 Across the Stishovite-$CaCl_2$-type Structural Phase Boundary," *Phys. Rev. Lett.*, 89, 255507-1 (2002).

Contact information
Sean R. Shieh, Department of Geosciences, Princeton University

Email: shieh@princeton.edu

of an elastic instability involving C_{11}-C_{12} in stishovite near 50 GPa.

This study of stishovite provides an example of how recent developments in diamond anvil cell technology together with synchrotron x-ray diffraction techniques are yielding new advances in our understanding of fundamental quantities, such as elasticity and yield strength, of strong materials under extreme pressure conditions.

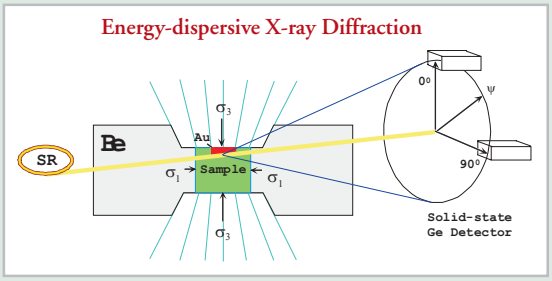

Figure 1. Sample configuration for radial x-ray diffraction experiments in a diamond anvil cell. The incident x-ray beam was directed through a beryllium gasket. Diffraction patterns are recorded by a solid-state Ge detector. The Au foil is used as a pressure marker, and σ_3 and σ_1 represent maximum and minimum stresses. Rotation of the sample allows lattice strains to be recorded at both the minimum and maximum stress directions.

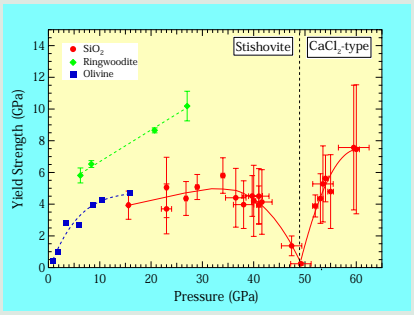

Figure 2. Yield strength of stishovite at high pressure. Red symbols and line are from this study; Squares and diamonds are olivine (α-Mg_2SiO_4) and ringwoodite (γ-Mg_2SiO_4) data, respectively. Dashed line shows the transition boundary of stishovite to the $CaCl_2$-type.

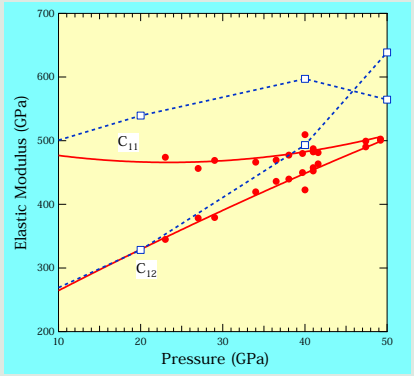

Figure 3. Selected elastic moduli of stishovite at high pressure. Red symbols and line are from this study; open symbols and dashed lines are from theoretical calculations.

The Effect of Phosphate on Lanthanide Sorption by an Oxide Mineral: X-ray Absorption and Magnetic Studies

S.-j. Yoon,[1] P.A. Helmke,[1] J.E. Amonette[2], and W.F. Bleam[1]

[1]Department of Soil Science, University of Wisconsin; [2]Environmental Molecular Sciences Laboratory, Pacific Northwest National Laboratory

The feasibility of using phosphate to enhance radionuclide immobilization on mineral surfaces was examined using trivalent lanthanide ions as chemical analogues of actinide radionuclides. Phosphate dramatically increased the amount of lanthanide sorbed on aluminum oxide surfaces at pH 5, the product apparently being ultra-fine particles of $LnPO_4$.

High-level radioactive wastes containing actinide elements have been introduced to the environment with the advent of nuclear weapons and nuclear energy. Sorption of the actinides by soil materials decreases their mobility and bioavailability. Understanding their sorption mechanism is important for forecasting their behavior in soils and designing environmental remediation procedures.

Authors (from left): Philip A. Helmke, James E. Amonette, Soh-joung Yoon, and William F. Bleam

Sorption studies involving radionuclides, such as ^{239}Pu, ^{240}Pu, and ^{241}Am, are relatively rare because the U.S. Nuclear Regulatory Commission grants few licenses for the possession and handling of these elements. Furthermore, it is difficult to control experimental conditions because their oxidation states are unstable. Other actinide ions ($^{232}Th^{4+}$, $^{237}Np^{5+}$, and $^{238}U^{6+}$) and non-radioactive lanthanide ions (Ln^{3+}) have served as chemical analogues for those unstable actinide ions in various environmental studies. The utility of these analogues, verified by numerous studies for solution chemistry, may also extend to mineral surface chemistry.

In this study, trivalent lanthanide ions (Eu^{3+}, Gd^{3+}, and Dy^{3+}) serve as chemical analogues of trivalent actinides to explore the sorption chemistry of actinide ions (Ac^{3+}) on mineral surfaces as affected by phosphate, a ubiquitous oxyanion found on all oxide mineral surfaces in nature. The *in situ* immobilization of actinides by phosphate may be feasible considering both actinide and lanthanide phosphates are highly insoluble and stable in geological formations.

Orthophosphate has proven effective for immobilizing lead (Pb^{2+}) as insoluble lead phosphate precipitates on phosphate minerals. Our study asked whether adsorbed phosphate anions at oxide mineral surfaces react with lanthanide ions, immobilizing lanthanide as phosphate surface precipitates analogous to the reaction observed with Pb^{2+}.

The amount of lanthanide ions sorbed on boehmite (γ-AlOOH) surfaces, estimated by neutron activation analysis, dramatically increased in the presence of phosphate at pH 5 (**Figure 1**). The structure of the sorbed lanthanide was determined by x-ray absorption spectroscopy (beamlines X23B and X10C), as well as by magnetic susceptibility measurements (Institute for Rock Magnetism at University of Minnesota and Kansas State University) and electron paramagnetic resonance (EPR) spectroscopy (EMSL, Pacific Northwest National Laboratory).

BEAMLINE
X10C, X23B

Funding
U.S. Department of Agriculture Hatch Program; U.S. Department of Energy through the William R. Wiley Environmental Molecular Sciences Laboratory

Publication
S. Yoon, P.A. Helmke, J.E. Amonette, and W.F. Bleam, "X-ray Absorption and Magnetic Studies of Trivalent Lanthanide Ions Sorbed on Pristine and Phosphate-Modified Boehmite Surfaces," *Langmuir*, 18, 10128-10136 (2002).

Contact information
Soh-joung Yoon, Environmental Sciences Department, Brookhaven National Laboratory, Upton, NY

Email: syoon@bnl.gov

The extended x-ray absorption fine structure (EXAFS) shows that the sorbed lanthanide ions react with phosphate to form lanthanide phosphate precipitates of indeterminate size on the oxide surface (**Figure 2**). The superparamagnetic behavior of dysprosium and gadolinium in the surface precipitates indicates the lanthanide phosphate precipitates are uniform, ultra-fine particles (radii less than 10 Å assuming spherical particles) distributed on the oxide surface. Even in the absence of phosphate, sorbed Gd^{3+} ions apparently form precipitates on boehmite surfaces rather than being adsorbed as isolated ions as evidenced in EPR spectra (not shown).

To the extent that Ln^{3+} ions serve as suitable chemical analogues for Ac^{3+} ions, the results of this study predict the ubiquitous phosphate, adsorbed to all mineral surfaces in the environment, would enhance the sorption of Ac^{3+} ions leading to the mineral-surface precipitation of ultra-fine $AcPO_4$ particles.

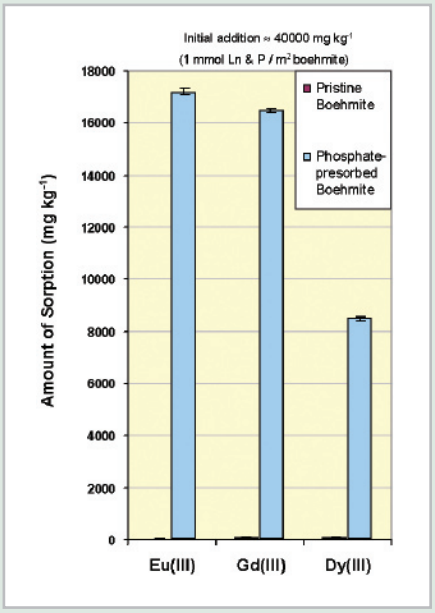

Figure 1. Amount of Ln^{3+} sorbed on boehmite (γ-AlOOH) in the absence and presence of phosphate at pH 5.

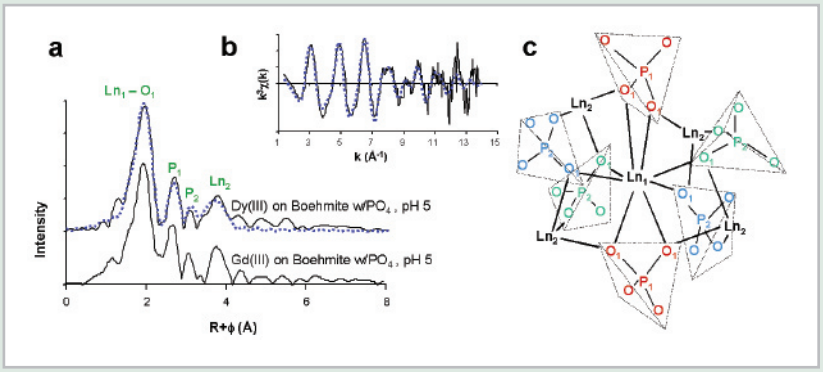

Figure 2. EXAFS data and proposed local chemical environment of Ln^{3+} ions sorbed on an aluminum oxide (boehmite) in the presence of phosphate: (a) experimental (solid lines) and simulated (dotted line) radial structure functions; (b) experimental (solid lines) and simulated (dotted line) scattering curve for Dy L_{III}-edge EXAFS; (c) local chemical environment showing proposed association of sorbed Ln^{3+} and phosphate.

Life Sciences

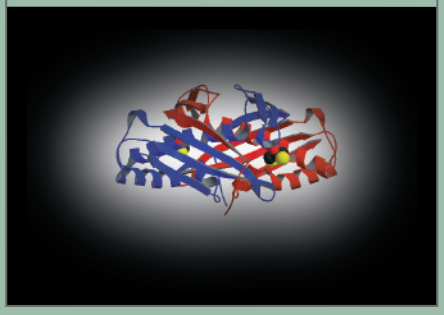

Structures of the Complexes of a Potent Anti-HIV Protein Cyanovirin-N and High-Mannose Oligosaccharides

I. Botos[1], A. Wlodawer[1], B.R. O'Keefe[2], S.R. Shenoy[2], L.K. Cartner[3], D.M. Ratner[4], P.H. Seeberger[4], and M.R. Boyd[5]

[1]Macromolecular Crystallography Laboratory, National Cancer Institute, National Institutes of Health; [2]Molecular Targets Drug Discovery Program, Center for Cancer Research, National Cancer Institute - Frederick; [3]Intramural Research Support Program, Science Applications International Corporation-Frederick; [4]Department of Chemistry, Massachusetts Institute of Technology; [5]USA Cancer Research Institute, College of Medicine, University of South Alabama

Using x-rays from beamline X9B, scientists have determined the structure of Cyanovirin-N (CV-N), a protein known for its ability to prevent viral infection. CV-N was complexed to high-mannose oligosaccharides, molecules located on the surface of the virus causing acquired immunodeficiency syndrome (AIDS). CV-N is a promising lead for the design of drugs against AIDS. The molecular structures generated in this study provide atomic details of how CV-N prevents infection by the human immunodeficiency virus (HIV), a virus causing AIDS.

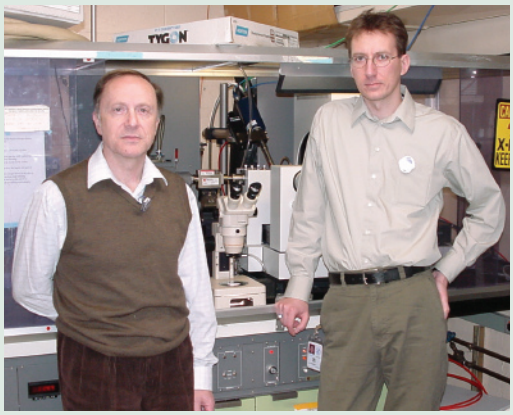

Authors (from left): Alexander Wlodawer and Istvan Botos

Of the more than 30 million people infected with human immunodeficiency virus (HIV) before 1997, 75 to 85 percent acquired the virus through heterosexual contact, making acquired immunodeficiency syndrome (AIDS) a continuing threat to the general population. Development of a vaccine active against HIV is complicated by the high mutation rate of the virus. So, another way of preventing HIV infection is the development of anti-HIV virucides, which are chemicals that prevent HIV infection. A unique natural product with anti-HIV properties was discovered while screening for new antiviral agents. This protein, originally isolated from cultures of the cyanobacterium (blue-green algae) *Nostoc ellipsosporum*, was named cyanovirin-N (CV-N).

CV-N potently inactivates the two most well known strains of HIV, HIV-1 and HIV-2, as well as their counterparts in monkeys, the simian immunodeficiency virus (SIV), and cats, the feline immunodeficiency virus (FIV). CV-N prevents HIV-1 from infecting host cells by interfering in key interactions between the glycoprotein gp120, which is present on the HIV-1 envelope, and receptors on cells that are about to be infected by HIV-1. Understanding the structural basis of such interactions is important for the potential development of CV-N as an anti-AIDS drug.

CV-N, a 101-amino acid protein, can exist in solution either as a monomer or a dimer. When in the form of a monomer, the protein consists of two similar domains with an overall ellipsoidal shape. Each domain contains mostly β-strands and loops (**Figure 1A**). A change of torsion angles in the central, or hinge, region between the two domains separates them into an extended form, in which they do not interact with each other (**Figure 1B**).

The CV-N dimer is formed by two extended monomers that swap their domains. By naming A and B the domains of the first monomer, and A' and B' those of the second monomer, the overall structure of CV-N is made of the combinations AB' and A'B, called pseudo-monomers,

BEAMLINE
X9B

Funding
National Cancer Institute, National Institutes of Health

Publication
I. Botos, B.R. O'Keefe, S.R. Shenoy, L.K. Cartner, D.M. Ratner, P.H. Seeberger, M.R. Boyd and A. Wlodawer, "Structures of the Complexes of a Potent Anti-HIV Protein Cyanovirin-N and High-Mannose Oligosaccharides," *J. Biol. Chem.*, 277, 34336-42 (2002).

Contact information
Istvan Botos, Macromolecular Crystallography Laboratory, National Cancer Institute, National Institutes of Health, Frederick, MD

Email: istvan@ncifcrf.gov
Web page: http://mc11.ncifcrf.gov/botos.html

which are linked to each other through a hinge region.

We investigated how the monomeric and dimeric forms of CV-N bind to two branched oligosaccharides (organic compounds that include sugars, starches, celluloses, and gums): oligomannose-9 (Man-9) and a synthetic hexamannoside, which have a high and low affinity to CV-N, respectively. Man-9 was derived from natural sources and its structure corresponds to that of glycoprotein gp120, the chemical present on the HIV-1 envelope. The synthetic hexamannoside has a similar core mannose structure to Man-9.

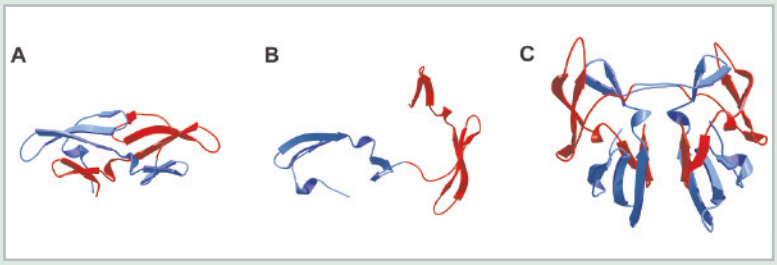

Figure 1. The monomeric form of cyanovirin-N (CV-N) (A) has two similar domains, A (red) and B (blue), linked by a hinge region. A change in torsion angles in the hinge region separates the domains into an extended form (B). A domain-swapped dimer (C) is formed by two such extended monomers. Each pseudo-monomer (AB' and A'B) is virtually identical to the compact monomer with the exception of the hinge residues.

A CV-N monomer can bind to oligosaccharides on two distinct sites: a high affinity, primary site, and a low affinity, secondary site (**Figure 2**). We have shown that the binding sites exhibit different affinities for the oligosaccharides. The CV-N domain-swapped dimer exhibits four sugar-binding sites: two primary sites near the hinge region, and two secondary sites on the opposite sides of the dimer (**Figure 3**).

In both monomeric and dimeric forms of CV-N, the primary sugar-binding site consists of a deep pocket in the close proximity of the hinge region. We have shown that the shape of this site is directly influenced by the hinge and relative orientation of the domains.

The secondary sugar-binding site, unaffected by the hinge region, has the same conformation in both the monomeric and dimeric CV-N. The molecular structures of CV-N bound to Man-9 and a synthetic hexamannoside show that the binding interface is formed by three mannose rings in the case of Man-9 and two in the case of the hexamannoside. So, the additional binding affinity of CV-N for Man-9, as compared to the hexamannoside, results from the additional binding energy of the third mannose ring's interaction with CV-N.

The ability of CV-N to target virus-associated oligosaccharides with high affinity, while binding mammalian oligosaccharides, such as Man-6, with comparably low affinity, is the basis for the potential use of CV-N to inhibit HIV infection.

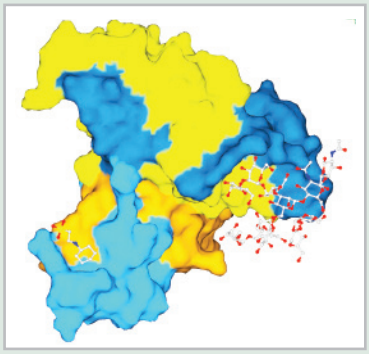

Figure 2. Crystal structure of the domain-swapped cyanovirin-N dimer. The molecular surface shows the primary and secondary oligosaccharide-binding sites, with a 2(Cyc lohexylamino)ethanesulfonic acid (CHES) molecule bound to primary site (left) and oligomannose-9 to the secondary site (right). Domains A and B of the first molecule are shown in dark and light blue, respectively, and domains A' and B' of the second molecule are shown in orange and yellow, respectively.

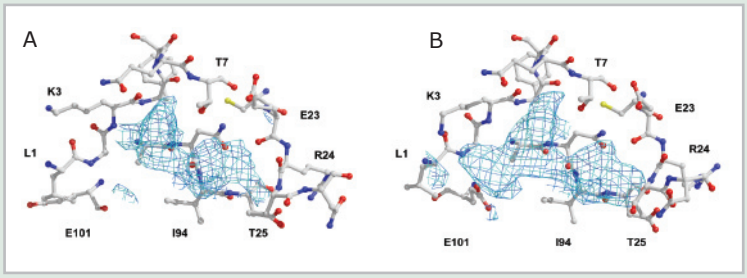

Figure 3. Sugar-binding areas on the surface of cyanovirin-N and the electron density maps of bound carbohydrate ligands: (A) cyanovirin-N and hexamannoside, and (B) cyanovirin-N and oligomannose-9. The binding interface is formed by three mannose rings in the case of oligomannose-9 and by two rings in the case of the hexamannoside, thus explaining the higher binding affinity of cyanovirin-N for oligomannose-9 than for the hexamannoside.

The Answer To a 100-Year Old Puzzle: The Structural Basis for Specificity in Human ABO(H) Blood Group Biosynthesis

S.I. Patenaude[1], N.O.L. Seto[1,2], S.N. Borisova[1], A. Szpacenko[3], S.L. Marcus[3], M.M. Palcic[3], and S.V. Evans[1]

[1]University of Ottawa; [2]National Research Council of Canada; [3]University of Alberta

Scientists working at beamlines X4A, X8C, and X12C have determined to a high resolution the structures of the enzymes that synthesize the human A and B blood group antigens. Although a mismatched blood transfusion could be fatal, the researchers found that the differences between the two enzymes are surprisingly small.

More than 100 years ago, Austrian pathologist Karl Landsteiner first investigated why some blood transfusions succeeded in reviving patients who had suffered severe blood loss while other transfusions killed. In 1901, he discovered the A, B, and O blood groups, for which he was rewarded with the Nobel Prize in physiology or medicine in 1930. Given the potentially fatal consequences of mismatched blood types, scientists presumed for more than half a century that the A and B blood groups must be significantly different from each other. But in 1956, the A, B, and O blood group antigens (antigens are molecules recognized by the immune system) were all found to be carbohydrate structures present on cell-surface glycoproteins (protein with attached sugars) and glycolipids (lipids with attached sugars).

Stephen V. Evans

The A and the B antigens were found to be modified from the carbohydrate corresponding to the O blood group by the addition of different monosaccharides (simple sugars). The A antigen was terminated by the sugar N-acetylgalactosmine (GalNAc) while the B antigen was terminated by galactose. In essence, these two blood groups, which were so immunologically distinct, differed only in the replacement of an acetamido group (-$NHCOCH_3$) by a hydroxyl group (-OH), as shown in **Figure 1**.

The inherited nature of the A, B, and O blood groups meant that the A and B antigens had to be produced by genetically encoded enzymes. In 1959, scientists postulated the existence of specific glycosyltransferases, enzymes that catalyze the transfer of sugar units between molecules. Their existence was later demonstrated in 1966, 1967, and 1968. In general, individuals with blood group A carried the gene for glycosyltransferase A (GTA), those with blood group B carried the gene for glycosyltransferase B (GTB), those with blood type AB carried both genes, and those with blood type O carried neither or an inactive gene.

In 1990, scientists cloned the genes corresponding to the glycosyltransferase enzymes that produce the A and B antigens and found that these enzymes are membrane-bound proteins of about 330 amino acids (elementary units of proteins) in length that differed from each other by only four amino acids. Both enzymes would recognize the disaccharide H antigen acceptor (corresponding to blood type O), so scientists thought that these four amino acid differences must serve to recognize the two different monosaccharide donors: uridine diphosphate-GalNAc for GTA, and uridine diphosphate-galactose for GTB.

BEAMLINE
X4A, X8C, X12C

Funding
Natural Sciences and Engineering Research Council of Canada, Canadian Institutes of Health Research

Publication
S. Patenaude, et al., "The Structural Basis for Specificity in Human ABO(H) Blood Group Biosynthesis," *Nat. Struct. Biol.*, 9, 685-690 (2002).

Contact information
Stephen V. Evans, Department of Biochemistry Microbiology & Immunology, University of Ottawa, Ontario, Canada

Email: evans@uottawa.ca

Later, kinetic characterization of GTA and GTB mutants revealed which of the four amino acid residues contributed most in distinguishing between the two donor molecules.

Using the very intense x-rays at beamlines X4A, X8C, and X12C, the structures of the GTA and GTB enzymes have been solved, in order to further characterize how they work.

Of the four amino acids that differ between GTA and GTB, only two (leucine/methionine 266 and glycine/alanine 268) are located in the active site pocket of both enzymes and well-positioned to contact the donor sugars, as shown in **Figure 2**. Remarkably, these small differences are enough to make the two enzymes use different mechanisms to recognize their respective donors.

The active site pocket of GTB contains the larger residues methionine 266 and alanine 268, used to exclude the GalNAc donor, and the active site in GTA contains the smaller residues leucine 266 and glycine 268, which can easily accommodate the galactose as well as GalNAc. GTA can easily recognize its donor because the smaller leucine 266 exposes the nearby residue histidine 233, which can form a strong hydrogen bond with the acetamido group of GalNAc, but cannot contact galactose. Thus, while GTB functions by excluding the incorrect donor, GTA functions by recognizing the correct donor.

Because such a small difference in enzyme and antigen structures has such large physiological consequences, GTA and GTB are paradigms for specificity in biosynthetic and immune recognition, paving the way for the design of enzymes with different specificities.

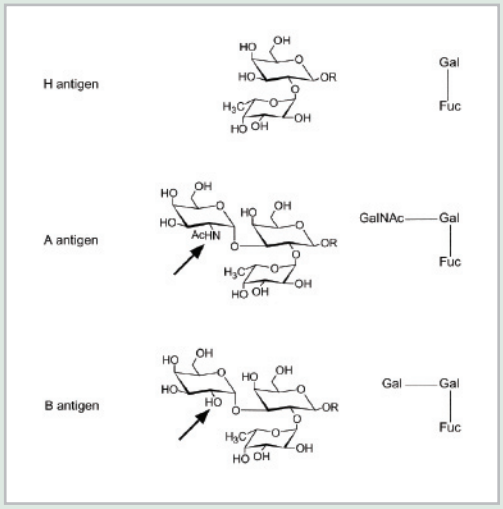

Figure 1. The antigens corresponding to the A, B, and O blood groups. The A and B antigens differ from the H antigen by the addition of different monosaccharides to the H antigen (corresponding to blood group O). Remarkably, the A and B antigens differ only by the replacement of an acetamido group (-NHCOCH$_3$) in A with a hydroxyl group (-OH) in B.

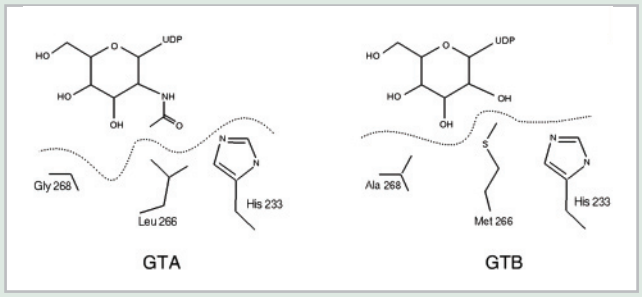

Figure 2. Leucine/methionine 266 and glycine/alanine 268 are the only amino acid residues that differ between the active sites of glycosyltransferase A (GTA) and glycosyltransferase B (GTB). While GTB excludes the A monosaccharide donor based on size, GTA selects the correct donor by forming a hydrogen bond with histidine 233.

Structural Basis of β-Lactam Resistance in Methicillin-Resistant Strains of "Superbug" Revealed

D. Lim and N.C.J. Strynadka

University of British Columbia

Some strains of the bacterium Staphylococcus aureus have developed resistance to multiple antibiotics and have emerged as major pathogens in hospitals worldwide. Resistance of these "superbugs" to the clinically important β-lactam class of antibiotics is mediated by a bacterial enzyme called penicillin-binding protein 2a (PBP2a). This enzyme catalyzes the formation of the bacterial cell wall, a process inhibited by β-lactam, thus weakening the bacterium, and ultimately killing it. The three-dimensional structure of PBP2a, determined by researchers at the University of British Columbia in Vancouver, Canada, reveals the structural basis of the resistance of S. aureus to β-lactam, and provides insights for the design of more effective inhibitors of the bacterium.

Authors (from left): Natalie C. J. Strynadka and Daniel Lim

The introduction of penicillin in the 1940s quickly selected for resistant strains of the bacterium *Staphylococcus aureus* that produced penicillinase, an enzyme that hydrolyzes β-lactam antibiotics, the most commonly used line of defense against bacterial infections. To counter these resistant bacterial strains, methicillin, a semisynthetic penicillinase-resistant penicillin derivative, was subsequently introduced.

Resistance to methicillin began to appear just one year after its introduction and has since spread to hospitals world-wide with alarmingly high prevalence of these strains, called methicillin-resistant strains of *Staphylococcus aureus* (MRSA), among clinical isolates in the United States and in a number of Asian and European countries. As MRSA strains are resistant to other classes of antibiotics, vancomycin has often been the treatment of choice against MRSA infections. But the appearance of vancomycin resistance in MRSA clinical isolates – first in Japan, and then in other countries, including the United States in recent months – underlines an urgent need for novel antibiotics.

β-lactams act as substrate analogs of bacterial enzymes called penicillin-binding proteins (PBPs) that catalyze the formation of peptide cross-links in the bacterial cell wall. By binding to PBPs, β-lactams irreversibly inhibit PBPs, resulting in a weakened cell wall and eventual cell death. Methicillin resistance in MRSA strains is due to the horizontal acquisition – from an unidentified species – of the *mecA* gene, which encodes PBP2a, a novel PBP distinct from the PBPs normally found in *S. aureus*. PBP2a is highly resistant to inhibition by all clinically used β-lactams and remains active to maintain cell wall synthesis at normally lethal β-lactam concentrations.

To identify the structural features of PBP2a that are responsible for *S. aureus* resistance, we determined the protein's crystal structure. To obtain crystals of PBP2a, a soluble derivative was constructed by removing the N-terminal transmembrane anchor – which does not affect its interaction with β-lactams. The excellent facilities at NSLS beamline X8C allowed us to collect data to 1.8 angstrom resolution for crystals of the

BEAMLINE
X8C

Funding
Canadian Institutes of Health Research; Howard Hughes Medical Institute; Burroughs Wellcome Fund; Canadian Bacterial Diseases Network

Publication
D. Lim and N.C.J. Strynadka, "Structural Basis for the β-Lactam Resistance of PBP2a from Methicillin-Resistant Staphylococcus aureus," *Nat. Struct. Bio.*, 9, 870 (2002).

Contact information
Natalie C.J. Strynadka, Department of Biochemistry and Molecular Biology, University of British Columbia, Vancouver, Canada

Email: natalie@byron.biochem.ubc.ca
Web page: http://byron.biochem.ubc.ca

apoenzyme (the enzyme with no inhibitor bound), and to 2.0 angstrom resolution for crystals of PBP2a bound to nitrocefin (a type of β-lactam). By comparing these structures, we noticed novel conformational changes at the active site that have not been observed in structures of β-lactam sensitive PBPs. Thus the active site of apoenzyme part of PBP2a is distorted relative to those of non-resistant PBPs.

Previous kinetic studies have shown that while the initial binding affinities of PBP2a for β-lactams are comparable to those of non-resistant PBPs, the subsequent acylation step, during which the PBP and β-lactam bind with an RCO- group (R being an organic group), is 1000 fold slower in PBP2a than in non-resistant PBPs. Acylation is key to the inhibition of PBPs by β-lactams, so the reduction of the acylation rate confers broad-spectrum resistance of *S. aureus* to antibiotics. But acylation is also key to the normal function of PBPs, so that the distorted active site of PBP2a provides a means of modulating the acylation rate to balance resistance while retaining activity.

Given that slow acylation is an intrinsic property of PBP2a, more effective inhibitors could be designed by improving their initial binding affinity to PBP2a. For example, novel forms of widely used antibiotics called cephalosporins provide a larger number of stabilizing interactions with and better shape complementarity to the narrow PBP2a active site groove, and thus show improved affinities for PBP2a. Optimization of cephalosporins and other inhibitors will be greatly facilitated by the structural information on the active site from our studies.

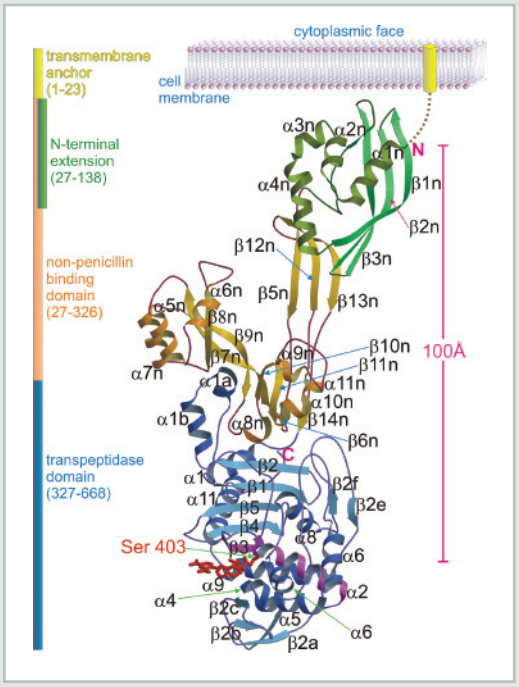

Figure 1. Structure of penicillin-binding protein of the bacterium *Staphylococcus aureus* (SauPBP2a*). The bilobed N-terminal (nPB) domain is colored orange with the N-terminal lobe (N-terminal extension) colored green. The transpeptidase domain is colored blue with the position of the active site indicated by the red nitrocefin adduct (shown in stick rendering). The secondary structure elements of the transpeptidase domain were labeled in accordance with the labeling scheme used for R6 PBP2x. The N- and C-termini are labeled N and C, respectively. Shown to the left of the ribbon representation is a linear representation of the domain structure of SauPBP2a* with residue numbers shown in parentheses.

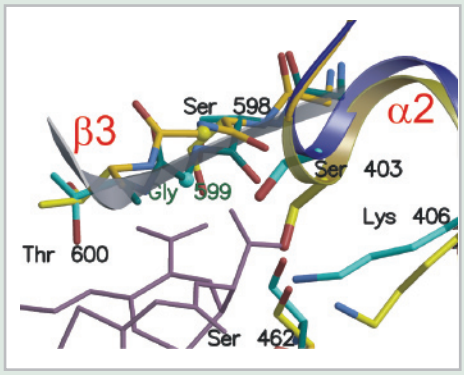

Figure 2. Superposition of the active site region from the native penicillin-binding protein of the bacterium *Staphylococcus aureus* (SauPBP2a*) and SauPBP2a* acylated with nitrocefin, shown in yellow and blue, respectively. Nitrocefin (purple) is shown in thin stick rendering. Covalent binding of nitrocefin to SauPBP2a* requires conformational changes at strand β3 and at the N-terminus of helix α2.

Structures of Two Kinetic Intermediates Reveal Species-Specificity of Penicillin-Binding Proteins

M.A. McDonough[1], J.W. Anderson[2], N.R. Silvaggi[1], R.F. Pratt[2], J.R. Knox[1], and J.A. Kelly[1]

[1]Department of Molecular and Cell Biology and Institute for Materials Science, University of Connecticut; [2] Department of Chemistry, Wesleyan University

β-lactam antibiotics are the most commonly used line of defense against bacterial infections, but the efficacy of antibiotics is threatened by the constant emergence of resistant bacteria. Scientists from the University of Connecticut in Storrs, and Wesleyan University in Middletown, Connecticut, have obtained the first crystallographic structures of complexes involving a peptide substrate and a penicillin-binding protein, which is the target of β-lactams. This research provides structural and mechanistic information to aid drug design efforts aimed at fighting β-lactam-resistant infections.

Authors (from left): Michael A. McDonough, Judith A. Kelly, and Nicholas R. Silvaggi

Most bacteria synthesize a rigid peptidoglycan cell wall that provides the characteristic cell shape and prevents destruction by osmotic lysis. Peptidoglycan is a polymer of carbohydrate units with branching peptide chains that usually terminate in D-alanyl-D-alanine. The final step in cell wall biosynthesis is a chemical reaction forming peptide bridges between neighboring peptidoglycan strands. The reaction is catalyzed by penicillin-binding proteins (PBPs), which also catalyze a carboxypeptidase reaction (**Figure 1**) that helps to maintain the proper degree of cell wall cross-linking.

β-lactam antibiotics are the most commonly used line of defense against bacterial infections. These antibiotics inhibit PBPs because they mimic the D-alanyl-D-alanine portion of peptidoglycan and form very long-lived covalent complexes, so that growing bacteria are unable to cross-link their cell walls and are vulnerable to cell lysis. Our research provides structural and mechanistic information to aid drug design efforts aimed at fighting β-lactam resistant infections.

By using x-rays at beamline X12C, we have obtained the first crystallographic structures of kinetic intermediates involving a peptide substrate and a PBP, the D-alanyl-D-alanine carboxypeptidase/transpeptidase from the bacterium Streptomyces R61. This enzyme is a model for membrane-bound PBPs that do the majority of cell wall synthesis.

Two members of our team, Rex F. Pratt and John W. Anderson, have recently identified a tetrapeptide substrate (**Figure 2**) that proved to be the most specific substrate yet for the R61 enzyme. This tetrapeptide corresponds exactly to a portion of Streptomyces peptidoglycan.

By soaking chemically cross-linked, inactive R61 crystals in a solution containing the tetrapeptide substrate, we were able to trap the noncovalent enzyme-substrate (ES) complex at 1.9 angstrom resolution. By performing the same experiment using active enzyme crystals, we determined the structure of the enzyme-products (EPs) complex with a 1.25 angstrom resolution.

With the ES structure (**Figure 3A**), we showed that the catalytic oxygen of the active serine, S62, is positioned 2.8 angstroms from the carbonyl carbon of the scissile peptide bond. Numerous noncovalent interactions

Beamline
X12C

Funding
State of Connecticut Critical Technologies Program in Drug Design; Connecticut Innovations, Inc.; National Institutes of Health; Pfizer

Publication
M.A. McDonough, J.W. Anderson, N.R. Silvaggi, R.F. Pratt, J.R. Knox, J.A. Kelly, "Structures of Two Kinetic Intermediates Reveal Species Specificity of Penicillin-Binding Proteins," *Journal of Molecular Biology,* 322, 111-122 (2002).

Contact information
Judith A. Kelly, Department of Molecular and Cell Biology, University of Connecticut, Storrs, CT

Email: Judith.Kelly@uconn.edu

between the enzyme and the tetrapeptide substrate explain the extraordinary specificity of this substrate. Indeed, the part of the substrate that changes from one species to another is bound tightly in a subsite of the active site. Presumably, PBPs of other species have analogous subsites complementary to their peptidoglycan. These species-specificity subsites could be exploited for species-specific antibiotics.

Figure 1. The carboxypeptidase reaction of the R61 DD-peptidase, where E is free enzyme, S is the substrate, ES is a non-covalent complex, ES* is a covalent complex, EP is a non-covalent complex between the enzyme and the hydrolyzed peptide, and P represents the free peptide product.

The EPs structure (**Figure 3B**) highlights conformational changes of both the tripeptide product and active site residues that ultimately lead to the ejection of products from the active site. The terminal D-alanine rotates 110 degrees about the nitrogen-alpha carbon bond, placing the carboxyl group (COOH) in a relatively hydrophobic environment, while the methyl (CH_3) side chain is moved into the plane of a hydrogen bond involving a conserved asparagine residue, weakening this interaction. Further, the main chain of threonine 301 is forced into a highly strained conformation. All these factors are likely to contribute to the destabilization of product binding.

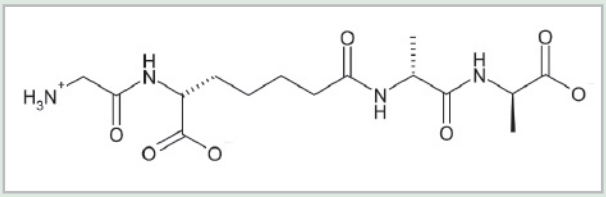

Figure 2. Tetrapeptide substrate that proved to be the most specific substrate yet for the R61 enzyme.

The two structures (ES and EPs) reveal detailed structural information about kinetic intermediates, providing insight into the catalytic mechanism of PBPs and critical information for future antibiotic design efforts.

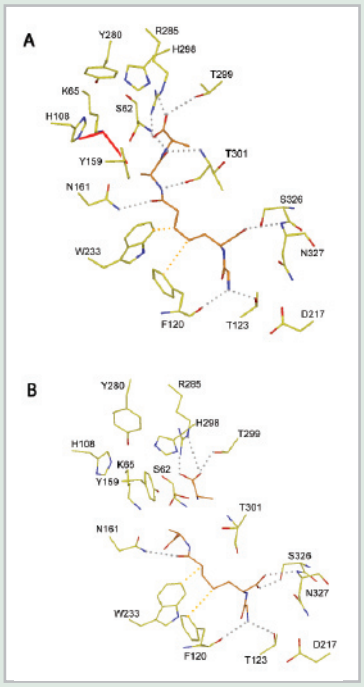

Figure 3. (A) The ES complex. Active site residues are yellow, the tetrapeptide substrate is orange. Hydrogen bonds are shown as gray dotted lines, hydrophobic interactions as yellow dotted lines, and the inactivating cross-links as solid red lines. (B) The EPs complex. Both the tripeptide product and free D-alanine are orange. The figure was produced by using XTALVIEW and Raster3D.

New Insights into Transcription Initiation in Bacteria

K.S. Murakami, E.A. Campbell, S. Masuda, O. Muzzin, M. Chlenov, J.L. Sun, C.A. Olson, O. Weinman, M.L. Trester-Zedlitz, and S.A. Darst

The Rockefeller University

Every cell of a living being contains an instruction manual, the genome, encoded in the form of messages called genes within a double helical molecule made of deoxyribonucleic acid (DNA). This information is read and interpreted in two steps, called transcription, in which the DNA is converted into ribonucleic acid (RNA), and translation, in which the RNA is converted into proteins, used by cells to function properly. Scientists from Rockefeller University have provided structural insights into the key machinery for controlling the initiation of transcription in bacteria.

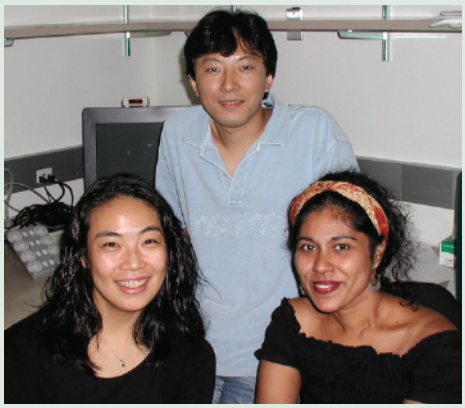

Authors (from left): Shoko Masuda, Katsuhiko S. Murakami, and Elizabeth A. Campbell

Beamline
X25, X9A

Funding
National Institutes of Health; Human Frontier Science Program; Norman and Rosita Winston Postdoctoral Fellowship; Burroughs Wellcome

Publication
E.A. Campbell, O. Muzzin, M. Chlenov, J.L. Sun, C.A. Olson, O. Weinman, M.L. Trester-Zedlitz, and S.A. Darst, "Structure of the Bacterial RNA Polymerase Promoter Specificity σ Subunit," *Mol. Cell,* 9, 527-539 (2002).

Contact information
Seth Darst, Lab. of Molecular Biophysics, The Rockefeller Univ., NY

Email: darst@mail.rockefeller.edu
Web page: http://www.rockefeller.edu/labheads/darst/darst.html

A genome is the complete "recipe" or set of instructions to make an organism. These instructions are stored in each cell of the organism in the form of a double helical molecule of deoxyribonucleic acid (DNA). The DNA information is read and decoded in two processes, called transcription, in which the DNA is converted into ribonucleic acid (RNA), and translation, in which the RNA is converted into proteins, necessary for the normal functioning of cells.

The conversion of DNA into RNA is performed by a protein called RNA polymerase, which slides along the DNA helix, unzipping the two strands as it goes, synthesizing complementary strands of RNA corresponding to packets of DNA information called genes.

In bacteria, the RNA polymerase has the shape of a 150-angstrom-long crab-claw, with a large cleft between the claws in which the RNA is produced. The RNA polymerase starts synthesizing RNA at defined DNA sequences called promoters, which are recognized by the combination of the RNA polymerase with a protein called the sigma factor. The RNA polymerase with sigma is called the holoenzyme. The sigma factor plays a central role in locating the promoter sequence and in separating the DNA strands, which is required for the RNA polymerase to decode the genetic messages.

Using data from the National Synchrotron Light Source, the Cornell High Energy Synchrotron Source, as well as the Advanced Photon Source, the Rockefeller researchers have provided high-resolution views of the sigma factor structure as well as of the entire holoenzyme bound to a promoter DNA fragment.

Three domains of sigma, labeled σ_2, σ_3, and σ_4, are connected by flexible linkers and are positioned across one face of the RNA polymerase, as shown in **Figure 1**.

One of the linkers connecting the σ_3 and σ_4 domains is particularly long, snaking into the cleft of the RNA polymerase active site and then out again through another channel, the RNA exit channel, that is occupied by the RNA during elongation (**Figure 1**). The linker suggests how sigma may assist in initiating transcription from nucleoside triphosphate (NTP) substrates – the basic units of RNA – by forming part of the initiating substrate-binding site.

The structures mentioned above also provide insights into the curious

phenomenon of abortive initiation, in which the initiating RNA polymerase generates large amounts of short RNA fragments while positioned at the promoter, but only rarely moves forward to elongate the entire RNA chain. During initiation, the elongating RNA must displace the sigma linker from the RNA exit channel. Only once in a while, when the RNA manages to push the linker completely out of the RNA exit channel, does abortive initiation cease and the transition into the elongation phase (which follows the initiation phase) occur.

The two structures above also provide a basis for modeling complexes with the entire promoter (**Figure 2**). Models of the initial 'closed' complex (where the DNA is not melted) and the final 'open' complex (where 14 base-pairs of DNA have been melted) provide a framework for designing further experiments to understand how the RNA polymerase operates.

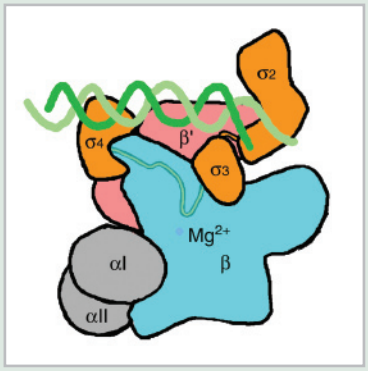

Figure 1. Cartoon model of a complex of the RNA polymerase holoenzyme and a fragment of the DNA promoter. The sigma subunit domains are labeled σ_2, σ_3, and σ_4, with the linker connecting σ_3 and σ_4 extending through the main RNA polymerase channel near the active site containing magnesium (purple sphere).

Additional Publications:

K.S. Murakami, S. Masuda, and S.A. Darst. "Structural Basis of Transcription Initiation: RNA Polymerase Holoenzyme at 4 Å Resolution," *Science,* 296, 1280-1284 (2002).

K.S. Murakami, S. Masuda, E.A. Campbell, O. Muzzin, and S.A. Darst. "Structural Basis of Transcription Initiation: An RNA Polymerase Holoenzyme/DNA Complex, *Science,* 296, 1285-1290 (2002).

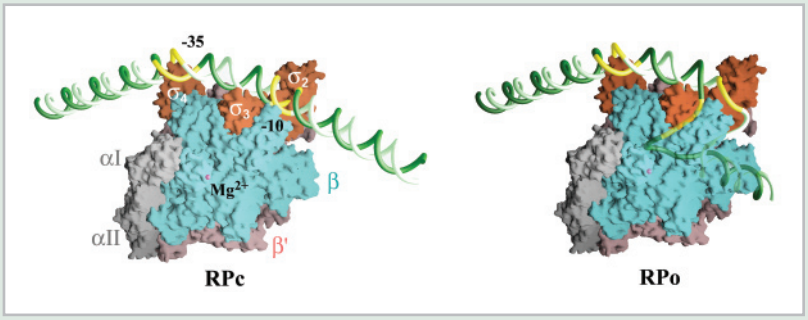

Figure 2. Models of RNA polymerase closed (RP_c) and open (RP_o) complexes with promoter DNA.

Novel Strategy for Stabilizing HIV Surface Proteins for AIDS Vaccine Development

J. Liu[1], S. Wang[1], M. Lu[1], C.C. LaBranche[2], and J.A. Hoxie[3]

[1]Weill Medical College of Cornell University; [2]Duke University; [3]University of Pennsylvania

Despite recent advances in retroviral drug therapy, the need for a vaccine that can slow or stop the spread of the human immunodeficiency virus (HIV), the causal agent of AIDS, remains urgent. The surface of the virus consists of three copies of glycoproteins (proteins and carbohydrate) in a trimeric configuration. This glycoprotein complex mediates entry of the virus into immune system cells. Vaccine candidates that mimic the HIV glycoproteins are expected to elicit antibodies able to block this viral-entry process and thus neutralize the virus. Scientists from the Weill Medical College of Cornell University in New York City, Duke University in Durham, North Carolina, and the University of Pennsylvania in Philadelphia have suggested a potential strategy for the production of HIV envelope proteins in a stably folded form that might serve as vaccine candidates.

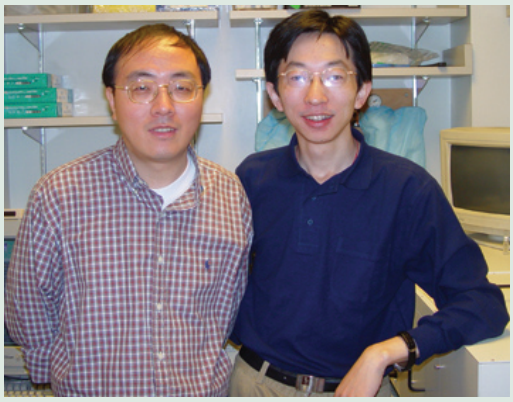

Authors (from left): Min Lu and Jie Liu

The current combination of drug therapies has not yet succeeded in eradicating the human immunodeficiency virus (HIV), the causal agent of AIDS. Even worse, new drug-resistant variants of HIV are emerging at an alarming rate. A vaccine that would block HIV's entry into host cells would thus most efficiently prevent the spread of HIV infection worldwide.

When either the human (HIV) or simian (SIV) immunodeficiency virus infect the human body, the viral membrane fuses with the membrane of a host cell, and then inserts the viral RNA (genetic information in the form of a single strand) inside the host cell. This RNA is used to create clones of the virus inside the host cell, and these new viruses then spread outside the host cell to invade other cells.

The virus harbors two types of glycoproteins (proteins and carbohydrate) on its membrane, called glycoprotein 120 (gp120) and gp41, that are assembled in the form of a trimer. When the virus attaches to a host cell, these glycoproteins bind by a lock-and-key mechanism to other proteins, called receptors, on the surface of the host cell.

When gp120 and gp41 bind to the host cell's surface receptors, the glycoproteins undergo a conformational change, creating a transient species called the pre-hairpin intermediate, in which gp41 is present simultaneously in both the viral and cellular membranes. The pre-hairpin intermediate ultimately transforms into a structure made of a trimer of hairpins (three hairpin-like structures assembled together) called the fusion-active state of gp41.

An anti-HIV vaccine would elicit antibodies from the host immune system that can neutralize HIV. Since gp120 is readily dissociated or shed from HIV because of its non-covalent association with the external portion, or ectodomain, of gp41, a major challenge in vaccine research has been to preserve completely the two types of glycoproteins together in vaccine preparations. To date, such efforts have relied on attempts to stabilize the glycoprotein complex by introducing disulfide bonds between the gp41 ectodomains or between the gp120 and gp41 subunits.

BEAMLINE
X25

Funding
National Institutes of Health; The Norman and Rosita Winston Foundation

Publication
J. Liu et al, "Mutations that Destabilize the gp41 Core are Determinants for Stabilizing the Simian Immunodeficiency Virus-CPmac Envelope Glycoprotein Complex," *J. Biol. Chem.*, 277, 12891 (2002).

Contact information
Min Lu, Weill Medical College of Cornell University, New York, NY

Email: mlu@med.cornell.edu

We have shown that a laboratory-created variant of SIVmac251, called CPmac, exhibits a remarkably stable association between the gp120 and gp41 subunits. In contrast to previously described HIV isolates, gp120 and gp41of this mutant remain associated during destruction of HIV by ionic detergents and can be isolated by monoclonal antibodies targeted to either gp120 or gp41. This unique property results from five amino acid substitutions in the gp41 ectodomain.

To understand why the gp120-gp41 structure was stable in CPmac, we sought to delineate the role of five CPmac mutations in the folding, thermodynamics, and conformation of the gp41 ectodomain. Crystallographic studies show that the CPmac mutant sequences fit to the trimer-of-hairpins structure of gp41. Thermal unfolding studies show that the gp41 trimer-of-hairpins structure is thermodynamically coupled to the stability of the gp120/gp41 complex.

Our results show that the gp120/gp41 complex could be stabilized by introducing mutations that destabilize the hairpin structure. If this idea proves correct, our results may lead to a novel strategy for stabilizing the HIV envelope glycoprotein complex and using it in structural and immunogenicity (induction of immune response) studies.

Crystal structure of the CPmac gp41 core. This structure is very similar to the trimer-of-hairpins structure present in the ectodomain of the glycoprotein 41 (gp41) of the parent simian immunodeficiency virus SIVmac251. (Left) Lateral view of superposition of the backbone traces for the wild-type (green) and CPmac (red) gp41 cores. The amino-terminal helices point toward the bottom of the page and carboxyl-terminal helices point toward the top. (Right) Axial view looking down the three-fold axis of the trimers.

Atomic Structures Reveal a Unique Molecular Mechanism for Initiating TRAF6 Signaling

H. Wu[1], H. Ye[1], M. Cirilli[1], D. Segal[1], O.K. Dzivenu[1], J.R. Arron[2], M. Vologodskaia[2], B. Lamothe[3], K. Du[3], B.G. Darney[3], T. Kobayashi[4], M. Yim[4], Y. Choi[4], N.K. Shevde[5], J.W. Pike[5], and S. Singh[6]

[1]Weill Medical College, Cornell University; [2]The Rockefeller University; [3]The University of Texas M.D. Anderson Cancer Center; [4]University of Pennsylvania School of Medicine; [5]University of Wisconsin, Madison; [6]Imgenex Corp

A family of proteins called TRAF is key to many cellular communication pathways. Although the six members of this family have certain structural and functional similarities, their differences are still being investigated. A team of scientists led by Hao Wu, an x-ray crystallographer at Cornell University's Weill Medical College in New York City, has now determined with high resolution the atomic structures of TRAF6 and its derivative structures. This finding is a continuation of four years of research into the elucidation of TRAF structures by Wu's team. Crucial structural and functional insights are presented via rigorous comparative analyses of these various TRAF structures.

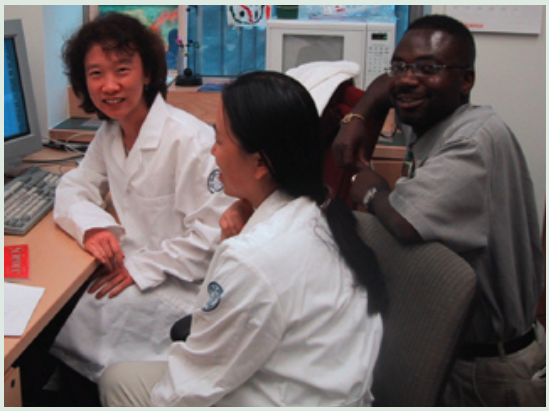

Authors (from left): Hao Wu, Hong Ye, and Oki Dzivenu

Cells talk to each other by exchanging molecules called messengers, such as growth factors (diffusible molecules affecting cellular growth), hormones (secreted in the blood by ductless glands), and neurotransmitters (molecules released between two neurons or a neuron and a muscle or a gland). On the cell surfaces, molecules called receptors bind to the exchanged molecules, activating proteins inside the cell. These proteins act together in an orderly fashion, defining what is called a signaling pathway.

One of the most potent cellular messengers, called tumor necrosis factor (TNF), binds to the TNF receptor (TNFR) located on the membrane surface of target cells and induces a wide range of cellular effects, such as cell survival, proliferation, differentiation, and death. A family of proteins that are major mediators of these effects is called TNF receptor associated factors (TRAFs).

To date, the TRAF family consists of six members that share certain common structural and functional domains. TRAFs can either directly interact with ligated TNFRs or indirectly form complexes with receptors binding to other signaling proteins. The binding of TRAFs to ligated TNFRs recruits more proteins, leading to multiprotein intracellular complexes that activate members of the families of proteins called necrosis-factor-kappa-B (NF-κ-B) and activator protein 1 (AP-1). NF-κ-B promotes the expression of genes involved in inflammatory and anti-apoptotic responses, while AP-1 can induce stress responses and cell death.

The signaling pathway of TRAF6 may be defined as follows: TRAF6 interacts with two members of the TNF receptor family, called clusters of differentiation 40 (CD40) and TNF-related activation-induced cytokine receptor (TRANCE-R). TRAF6 also participates in the interleukin-1 receptor (IL1-R)/Toll-like receptor (TLR) pathway by coupling to a protein called interleukin-1 receptor-associated kinase (IRAK).

We have recently revealed significant differences in the way receptors

BEAMLINE
X4A

Funding
National Institutes of Health; The Pew Charitable Trusts; Rita Allen Foundation; Medical Scientist Training Program Grant; Leukemia and Lymphoma Society; The Charles H. Revson Foundation

Publication
Ye et al., "Distinct Molecular Mechanism for Initiating TRAF6 Signalling," *Nature,* 418, 443-447 (2002).

Contact information
Hao Wu, Associate Professor of Biochemistry, Joan and Sanford I, Weill Medical College of Cornell University

Email: haowu@med.cornell.edu

bind to TRAF6 and TRAF2 (**Figure 1**). First, a receptor's peptide chain bound to TRAF6 deviates directionally from that bound to TRAF2 by about 40 degrees, so the reactive groups of the TRAF6-bound peptide latch onto pockets on TRAF6 that are very different than those on TRAF2. Second, the TRAF6-bound peptides assume extended β-conformations, unlike the poly-proline II (PPII) helix conformation adopted by the core region of TRAF2-binding peptides. Third, the TRAF6-bound peptides make more extensive main-chain hydrogen bonds with TRAF6.

Excessive activation of TRANCE-R can lead to significant resorption of bone, causing severe diseases such as osteoporosis and cancer-induced bone lesions. By using TRAF6-binding "decoy" peptides that we designed based on our structural studies and in collaboration with Bryant Darney at the MD Anderson Cancer Center in Houston, Texas, we have observed the inhibition of bond resorption in cells derived from mice (**Figure 2**).

We have identified a universal structural mechanism by which TRAF6 participates in adaptive immunity, innate immunity, and bone homeostasis. Our results may ultimately lead to drugs that modulate TRAF6-mediated signaling processes.

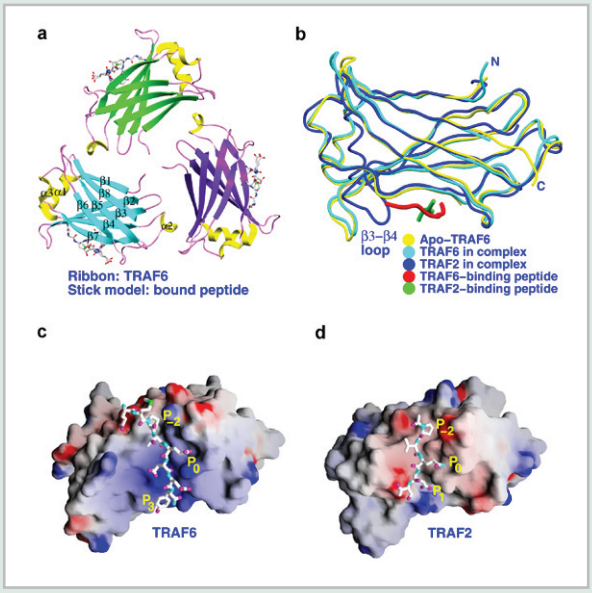

Figure 1. TRAF6 structures. (*a*) Ribbon diagram of the complex TRAF6 with TRANCE-R, shown as a trimeric model. (*b*) Worm representation of superimposed TRAF6 and TRAF2 structures. (*c*) Surface representation of TRAF6 and the bound TRANCE-R peptide. (*d*) Surface representation of TRAF2 and the bound core CD40 peptide.

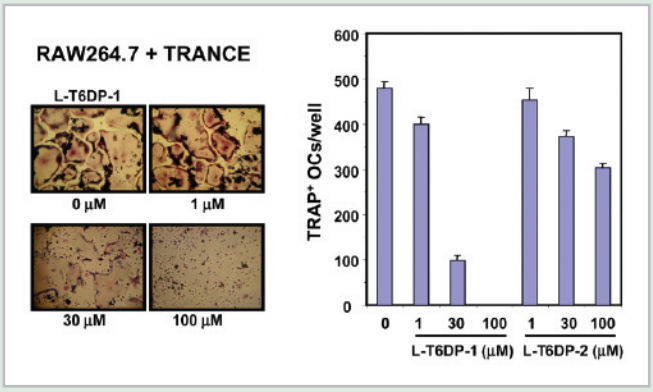

Figure 2. Co-treatment of RAW264.7 cells with TRAF6-binding "decoy" peptides, known here as L-T6DP-1 and L-T6DP-2, caused a dose-dependent decrease of osteoclasts – cells responsible for bone resorption – which are tartrate-resistant acid phosphatase-positive (TRAP⁺) and multinucleated.

The Last Piece of the Structural Puzzle in Bacterial Chemotaxis

R.B. Bourret[1], E.J. Collins[1], R.E. Silversmith[1], and R. Zhao[1,2]

[1]University of North Carolina at Chapel Hill; [2]University of Colorado Health Science Center in Denver

From the highest mammal to the simplest bacteria, cells respond to extracellular signals with appropriate responses. Signal transduction systems mediate this process and, in both prokaryotes and eukaryotes, phosphoryl groups reversibly attached to proteins provide a fundamental currency of information transfer. Chemotaxis, the signal transduction system that mediates the ability of Escherichia coli to swim towards nutrients and away from toxins, is arguably the best-studied signal transduction system in any organism. The detailed molecular picture of how chemotaxis works involves seven different proteins, six of which have solved atomic structures. The structure of the remaining protein, called CheZ, has long remained a mystery. Scientists at the University of North Carolina at Chapel Hill have determined the structure of CheZ.

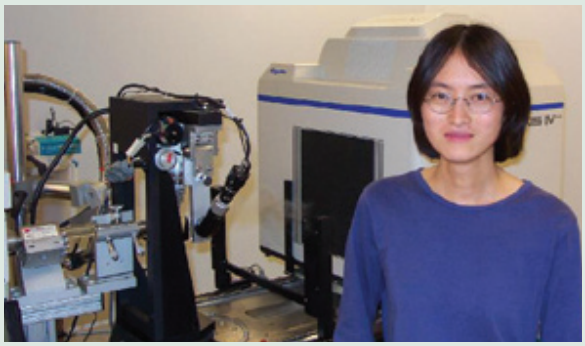

Rui Zhao

The gut bacterium *Escherichia coli* has the remarkable ability to rotate its flagella either counterclockwise, which results in forward swimming, or clockwise, which causes cell tumbling. The direction of flagellar rotation at any moment is determined by the degree of phosphorylation (addition of a phosphoryl group [$-PO_3^{2-}$]) to the chemotaxis signaling protein CheY, which binds to the base of the flagella. CheY is phosphorylated by the histidine kinase CheA and dephosphorylated by the CheZ phosphatase, the subject of our X-ray crystallographic studies.

Our initial efforts using crystals containing only CheZ were unsuccessful due to the poor diffraction of these crystals. We then shifted strategies and exploited a recent discovery that beryllium fluoride (BeF_3^-) binds to CheY to form a stable replica of phosphorylated CheY, the substrate of CheZ. We obtained crystals containing CheZ and CheY-BeF_3^--Mg^{2+}, and a cryoprotectant of 50% sucrose enabled us to improve the diffraction of these crystals from 8 angstrom (obtained with standard cryoprotectants) to 3.5 angstrom.

The CheZ dimer features an impressively long (105 angstrom) four-helix bundle composed of two helices from each chain, as shown in **Figure 1**. About 130 (of the 214) residues from each chain form an extended amphipathic (having both water-loving and water-repelling groups) alpha helix which folds on itself with a single hairpin turn. Two of these hairpins assemble to form the bundle. The amino-terminal of each chain forms an additional helix, as does the carboxyl-terminal, which interacts with a surface on CheY. The linker region between the carboxyl-terminal helix and the four-helix bundle was not visible in the electron density maps, implying that this region was disordered in the crystal.

For decades, scientists have debated whether CheZ acts as a positive allosteric effector of CheY's own autodephosphorylation activity by binding at a region of CheY away from the active site, or as a traditional phosphatase, which dephosphorylates CheY by binding to its active

BEAMLINE
X4A, X25

Funding
National Institutes of Health; Cancer Research Institute

Publication
R. Zhao, E.J. Collins, R.B. Bourret, and R.E. Silversmith, "Structure and Catalytic Mechanism of the *Escherichia coli* Chemotaxis Phosphatase CheZ," *Nat. Struct. Biol.*, 9, 570 (2002); P. Matsumura, "Last But Not Least," *Nat. Struct. Biol.*, 9, 563 (2002). (Commentary accompanying R. Zhao et al.'s article)

Contact information
Ruth Silversmith, Research Asst. Prof., Department of Microbiology and Immunology, University of North Carolina at Chapel Hill

Email: silversr@med.unc.edu

site. Our results showed two surfaces of interaction between CheY and CheZ. The carboxyl-terminal α-helix of CheZ binds to a surface on CheY that is distant from its active site, but a region of the four-helix bundle of CheZ interacts directly with the active site of CheY.

Strikingly, one residue from CheZ, called glutamine 147, inserts directly into the CheY active site. Mutagenesis studies showed that this residue was critical for catalytic activity. We now believe that glutamine 147 stimulates the CheY autodephosphorylation reaction by positioning a water molecule in an appropriate position to remove phosphoryl groups, as shown in **Figure 2**. So CheZ activity cannot be classified simply as an allosteric effector or true phosphatase, but instead contains features of both.

Our work provides structural information on the last of the seven proteins involved in *E. coli* chemotaxis. This new description of the CheZ structure and mechanism will enhance our understanding of bacterial chemotaxis.

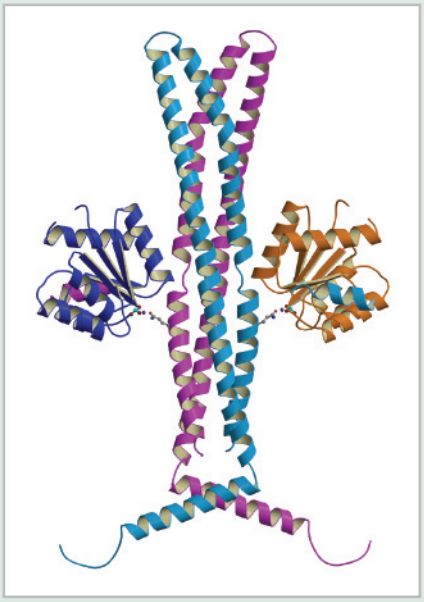

Figure 1. Ribbon representation of the structures of the chemotaxis protein CheZ and the complex between the chemotaxis protein CheY, beryllium fluoride (BeF_3^-) and magnesium (Mg^{2+}), showing the two chains of the CheZ dimer (light blue and magenta) and two symmetric CheY molecules (orange and dark blue). The active site of CheY is highlighted with ball and stick representations of BeF_3^- (green) and Mg^{2+} (purple). The essential catalytic residue from CheZ, glutamine 147 (gray ball and stick), inserts into the CheY active site.

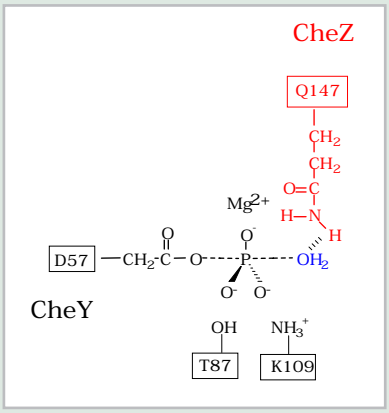

Figure 2. Model of the transition state in the dephosphorylation of CheY. In the absence of CheZ, CheY (black) catalyzes the reaction with active site residues threonine 87 (T87), lysine 109 (K109) and the bound magnesium ion (Mg^{2+}). In the presence of CheZ (red), the reaction is assisted by the glutamine 147 (Q147) side chain, which may help orient the "attacking" water molecule (purple) through a hydrogen-bonding interaction.

Structural and Functional Characterization of Ohr, an Organic Hydroperoxide Resistance Protein from *Pseudomonas aeruginosa*

J. Lesniak, W.A. Barton, and D.B. Nikolov

Memorial Sloan-Kettering Cancer Center

Pathogenic bacteria have developed complex strategies to detoxify and repair damage caused by reactive oxygen species. These compounds, produced during bacterial aerobic respiration, as well as by the host immune system cells as a defense mechanism against the infectious microorganisms, have the ability to damage nucleic acids, proteins, and phospholipid membranes. We have determined the crystal structure of Pseudomonas aeruginosa Ohr, a member of a recently discovered family of organic hydroperoxide resistance proteins. Using in vitro assays, we demonstrate that Ohr is a novel hydroperoxide reductase, converting both inorganic and organic hydroperoxides to less toxic metabolites. Structure-based mutagenesis reveal that the Ohr catalytic mechanism is similar to that of the structurally unrelated peroxiredoxins, directly utilizing highly reactive cysteine thiol groups to elicit hydroperoxide reduction.

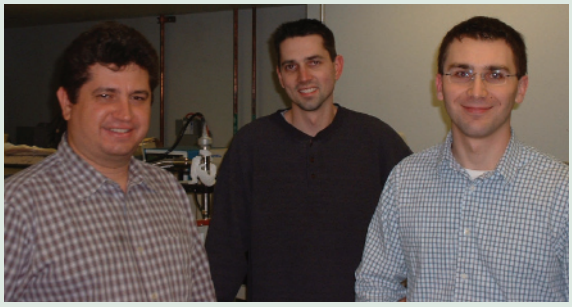

Authors (from left): Jacob Lesniak, William A. Barton, and Dimitar B. Nikolov

Pseudomonas aeruginosa, a versatile and ubiquitous Gram-negative bacterium, is one of the major causes of opportunistic human infections, such as bacteremia in burn victims, urinary tract infections in catheterized patients, pneumonia, and is a significant cause of morbidity and mortality in cystic fibrosis patients. During the course of host infection, *P. aeruginosa* is exposed to a variety of reactive oxygen species, including organic hydroperoxides. Their detoxification is essential for bacterial survival and proliferation, and genes involved in protection against organic peroxide toxicity play important roles in host-pathogen interactions.

A recently described family predicted to have such properties encompasses the organic hydroperoxide resistance (Ohr) and the osmotically inducible (OsmC) proteins. Prior to our experiments, the molecular mechanism that Ohr and OsmC utilize to protect bacteria from organic hydroperoxides had not been identified. We, therefore, determined the crystal structure of *P. aeruginosa* Ohr, revealing an oval-shaped molecule that lacks significant structural similarity to other proteins. Ohr is a tightly folded a/b homodimer with two putative active sites located at the monomer interface on opposite sides of the molecule. Each of the active sites contain two invariant cysteines, which are ideally located to form an intramolecular disulfide bond. The structural details of the Ohr active site suggest that the molecule functions as an organic hydroperoxide reductase, which was confirmed using *in vitro* enzyme assays.

Structure based mutagenesis was used to clarify the enzymatic mechanism and the role of the invariant cysteine residues, documenting that Cys-60 is indispensable for Ohr enzymatic activity, and that Cys-124, while not absolutely required for activity, is necessary for the maintenance of a high peroxidase reaction rate. We postulate that the interaction between Cys-60 and Arg-18 in Ohr has a major role in lowering the pK_a of the thiol side chain of Cys-60, polarizing and stabilizing it in the ionized state, which is more nucleophilic and therefore more reactive than the unionized form. The increased reactivity of the Cys-

BEAMLINE
X9A

Funding
The Bressler Foundation

Publication
J. Lesniak, W. Barton and D. Nikolov, "Structural and Functional Characterization of the Pseudomonas Hydroperoxide Resistance Protein Ohr," *EMBO J.*, 21, 6649-6659 (2002).

Contact information
Dimitar B. Nikolov, Memorial Sloan-Kettering Cancer Center, New York, NY

Email: dimitar@ximpact3.ski.mskcc.org

60 thiol group allows it to function as the initial attacking residue as follows: First, Cys-60 reacts with a peroxide molecule (ROOH), in the process becoming transiently oxidized to a cysteine sulfenic acid (Cys-60-SOH) intermediate. A molecule of peroxide is simultaneously reduced to its corresponding alcohol (ROH). Second, the Cys-60-SOH group quickly reacts with the reduced thiol group of Cys-124, forming an intramolecular disulfide bond and releasing a molecule of water: Cys-60-SOH + HS-Cys-124 → Cys-60-S-S-Cys-124 + H_2O. Finally, oxidized Ohr is regenerated back to its enzymatically active, reduced state using a yet unidentified endogenous protein or a small-molecule reductant.

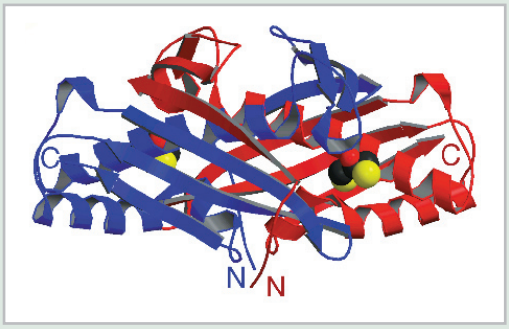

Figure 1. Structure of the Ohr dimer bound to dithiothreitol (DTT). One monomer is in red, the other in blue. DTT is shown in creatine phosphokinase (CPK) format, with oxygen atoms in red, carbon atoms in black, and sulfur atoms in yellow.

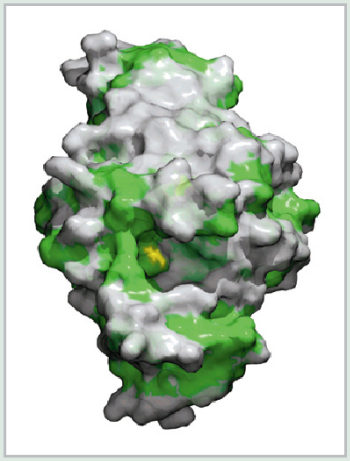

Figure 2. Molecular surface rendering of the Ohr dimer. The catalytically active Cys-60 (yellow) lies at the bottom of the active-site pocket, which is outlined with hydrophobic residues (green).

Insights into Antifolate Resistance from Malarial DHFR–TS Structures

J. Yuvaniyama[1], P. Chitnumsub[2], S. Kamchonwongpaisan[2], J. Vanichtanankul[2], W. Sirawaraporn[1], P. Taylor[3], M. Walkinshaw[3], and Y. Yuthavong[2]

[1]Department of Biochemistry, Faculty of Science, Mahidol University, Thailand; [2]BIOTEC, National Science and Technology Development Agency, Thailand Science Park, Thailand; [3]Institute of Cell and Molecular Biology, The University of Edinburgh, UK

Plasmodium falciparum dihydrofolate reductase-thymidylate synthase (PfDHFR–TS) is the main target of antimalarial antifolate drugs like pyrimethamine or cycloguanil, which inhibit the DHFR part of the bifunctional enzyme. Resistance to this class of drugs is now widespread due to mutations, which result in lower inhibitor binding affinities of DHFR. Scientists from the BIOTEC Center and Mahidol University in Thailand, and the University of Edinburgh, UK, have obtained the first crystallographic structures of wild-type and mutant PfDHFR-TS in complex with either pyrimethamine or WR99210, an inhibitor with high binding affinities with both wild-type and mutant enzymes. This research reveals the binding modes of the inhibitors with the target, and gives insights into the basis of antifolate resistance and possible approaches to the design of new drugs to overcome the resistance.

Authors (from left): Jarunee Vanichtanankul, Penchit Chitnumsub, Jirundon Yuvaniyama, Yongyuth Yuthavong, Worachart Sirawaraporn, and Sumalee Kamchonwongpaisan

Antifolate antimalarials, such as pyrimethamine and proguanil, a prodrug of cycloguanil, have long been used clinically in the treatment of malaria infection, especially that due to *Plasmodium falciparum*. The drugs act by inhibiting the dihydrofolate reductase activity of the *P. falciparum* enzyme dihydrofolate reductase–thymidylate synthase (PfDHFR–TS), and consequently preventing dTMP production and DNA synthesis. However, these drugs, as well as their combinations with sulfa drugs, have been compromised by parasite resistance. It is generally accepted that the resistance generally arises from mutations in PfDHFR–TS, first at residue 108 and subsequently at other residues, including 51, 59 and 164, resulting in increasingly poorer binding affinities of the enzyme with the inhibitors. However, WR99210, which differs from the compromised inhibitors in having a flexible side-chain, still binds tightly with the mutant enzymes and retains its antimalarial efficacy. Understanding the structural basis of interaction between drugs and the PfDHFR-TS, and the differences that determine drug efficacy, is important for the potential development of novel antimalarial drugs.

Structures of the wild-type, double mutant (C59R+S108N) and quadruple mutant (N51I+C59R+S108N+I164L) forms of PfDHFR–TS have been determined in complex with either pyrimethamine or WR99210 (**Figure 1**). The enzyme is a homodimer, with two TS domains (288 residues each) interacting extensively to form two active sites similar to TS from other species. The DHFR domain (231 residues) is attached to each TS directly and also through the interaction with the junction region (89 residues). While sharing overall features with DHFR from other species, PfDHFR has two extra inserts that interact with the TS domain and the junction region. The junction region moreover interacts extensively with both the TS and DHFR domains. These interdomain interactions help to pull the two DHFR domains closer to one another than those of *Leishmania major* DHFR–TS, the only other homologous, bifunctional enzyme with known structure,

BEAMLINE
X12C

Funding
Wellcome Trust; European Union Commission; Medicines for Malaria Ventrue; Special Programmed for Research and Training in Tropical Diseases; Thailand Tropical Diseases Research

Publication
J. Yavaniyama, P. Chitnumsub, S. Kamchonwongpaisan, J. Vanichtanankul, W. Sirawaraporn, P. Taylor, M.D. Walkinshaw, and Y. Yuthavong, "Insights into Antifolate Resistance from Malarial DHFR-TS Stuctures," *Nat. Struct. Biol.*, 10(5), 357-365 (2003).

Contact information
Yougyuth Yuthavong, BIOTEC

Email: yongyuth@nstda.or.th

and are probably responsible for the previously known fact that PfTS needs the presence of both DHFR and the junction region in order to express its activity. In addition, there are linings of positive electrostatic potentials on the molecular surface contributed by conserved basic amino acids that trace the paths between the DHFR and TS active sites. These may function as surface electrostatic channels that lead dihydrofolate from TS to DHFR active sites, similar to what was observed in the *L. major* DHFR–TS structure. Such substrate channeling may serve to promote effective dTMP production in the synthesis cycle.

The structure of the double-mutant enzyme with bound pyrimethamine shows that the S108N mutation causes steric conflict for binding of the rigid *p*-chlorophenyl side-chain of the inhibitor, especially around the Cl atom, in agreement with the previous prediction from modeling studies. In contrast, the structure of the quadruple-mutant enzyme with bound WR99210 shows that the flexible (2,4,5-trichlorophenoxy)propyloxy side-chain is oriented in such a way as to avoid this steric conflict (**Figure 2**). The flexible side-chain also interacts extensively with the enzyme, mainly through hydrophobic interactions. The quadruple mutant furthermore shows movement of residues 48–51 (0.5–2.2 Å) and residues 164–167 (0.3–0.5 Å), probably as the results of the N51I and I164L mutations, respectively, which widens the active-site gap between the C_α atoms of C50 and residue 164 from 16.0 Å to 17.3 Å. These changes likely contribute to the reduction in binding affinities of rigid inhibitors like pyrimethamine, but can be accommodated by flexible inhibitors like WR99210. The binding mode of WR99210 gives insight into the design of novel inhibitors that would be capable of averting the effects of mutations, which reduce the binding affinities of other, more rigid inhibitors.

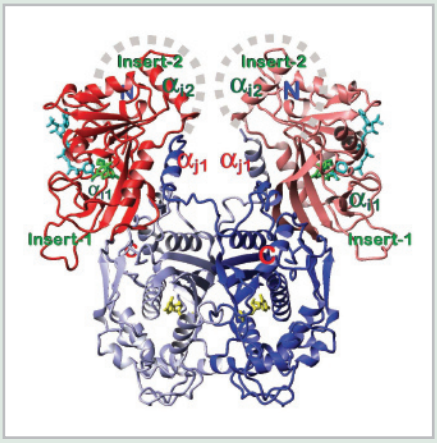

Figure 1. Ribbon diagram of the overall structure of the wild type PfDHFR-TS with bound WR99210, NADPH, and dUMP drawn in green, cyan, and yellow, respectively. N-terminal DHFR domains are in red, while C-terminal junction regions and TS domains are in blue. N and C termini and the inserts unique to plasmodial DHFR-TS are indicated. A short helix in Insert 1 and a long helix in Insert 2 are labeled as α_{i1} and α_{i2}, respectively. Termini and α_{i1} helix are on the back of the molecules in this orientation. The putative links between DHFR and TS domains shown as dashed gray curves are based on intermolecular spaces in crystal packing around the regions of unobserved residues. The helices α_{j1} in the junction region are involved in domain attachment, thus orienting the TS domains for dimerization into a functional unit.

Moreover, the structures provide clues to the design of novel types of inhibitors that act by interfering with interdomain interactions, which include interaction of TS with DHFR and Insert1, as well as the electrostatic attraction between the junction-region helix and the surface groove at the DHFR–TS domain interface. Since the activity of PfTS depends on these interactions, agents which interfere with them rather than the active sites per se may also cause the selective inhibition of malarial dTMP synthesis.

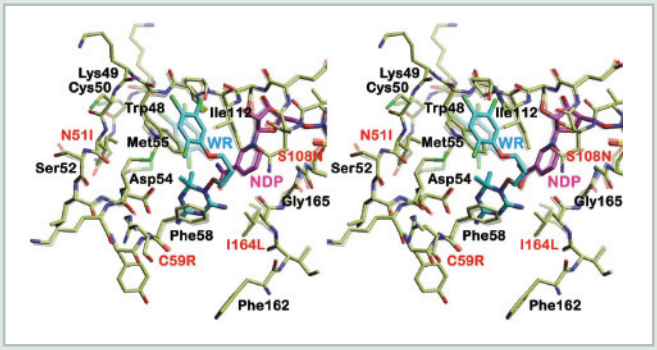

Figure 2. Comparison of enzyme-inhibitor interactions at the active sites of wild-type (lighter model) and V1/S quadruple mutant PfDHFR-TS in stereo view. Both enzymes are complexed with WR99210 (WR, in cyan) and NADPH (NDP, in magenta). The flexible tail of WR99210 allows it to bind in a conformation not affected by the pyrimethamine-resistant mutations (N51I+C59R+S108N+I164L), labeled in red.

Crystal Structure of the Carboxyltransferase Domain of Acetyl Coenzyme A Carboxylase

L. Tong, B. Tweel, Y. Shen, and H. Zhang

Department of Biological Sciences, Columbia University

Acetyl-CoA carboxylases are crucial for the biosynthesis and oxidation of long-chain fatty acids. They are targets for drug development against obesity and diabetes, and several herbicides function by inhibiting the carboxyltransferase (CT) domain of these enzymes in plants. We have determined the crystal structures of yeast CT free enzyme and the CoA complex at 2.7 Å resolution. The structure of CT comprises two domains, both belonging to the crotonase/ClpP superfamily. The active site is at the interface of a dimer. The herbicides target the active site of CT, providing a lead for inhibitor development against human ACCs.

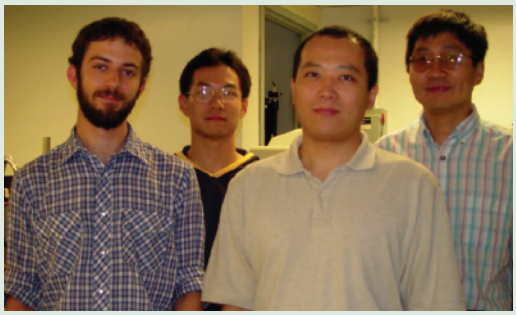

Authors (from left): Bengamin Tweel, Yang Shen, Hailong Zhang, and Liang Tong

Mammalian, yeast, and most other eukaryotic ACCs are large, multi-functional enzymes, containing the biotin carboxylase (BC) domain, the biotin carboxyl carrier protein (BCCP) domain, and the carboxyltransferase (CT) domain (**Figure 1a**). BC catalyzes the ATP-dependent carboxylation of a biotin group covalently linked to a lysine residue in BCCP, and then CT catalyzes the transfer of the carboxyl group from biotin to acetyl-CoA to produce malonyl-CoA (**Figure 1b**). In *E. coli* and other bacteria, ACCs are multi-subunit enzymes, with BC, BCCP, and two subunits for the CT (**Figure 1a**).

We have determined the crystal structures of the CT domain of yeast ACC, which constitutes the 90 kD fragment at the C-terminus of the protein (**Figure 1a**). Each CT domain molecule is made up of two sub-domains, N and C domains, that are intimately associated with each other (**Figure 1c**). The two domains share similar polypeptide backbone folds, with a central β-β-α super-helix. However, the amino acid sequence identity between the structurally equivalent residues of the two domains is only 12%, underscoring the lack of sequence conservation between them. The backbone fold is similar to that of the crotonase/ClpP superfamily, even though the amino acid sequence identity between CT domains and these other proteins is less than 14%.

A dimer of the CT domain is observed in the crystal as well as in solution. About 5300 $Å^2$ of the surface area of each monomer is buried in the dimer interface, involving mostly residues that are highly conserved among the ACCs. The dimer is formed by the side-to-side arrangement of the two monomers, such that the N domain of one molecule is placed next to the C domain of the other (**Figure 1c**).

The structure of the CoA complex shows that the active site of the enzyme is at the interface of the dimer (**Figures 1c, 2a**). Residues in this active site are well conserved among the various CT domains.

Herbicides that target the CT domain are powerful inhibitors of plastid ACC and can kill sensitive plants by shutting down fatty acid biosynthesis. Mutagenesis and biochemical studies showed that an Ile residue in the CT domain plays an important role in determining the sensitivity of the wheat enzyme to the commercial herbicides. An Ile→Leu mutation renders the wheat enzyme resistant to the herbicides,

BEAMLINE
X4A

Funding
Columbia University

Publication
Hailong Zhang, Zhiru Yang, Yang Shen, and Liang Tong, "Crystal Structure of the Carboxyltransferase Domain of Acetyl-Coenzyme A Carboxylase," Science, 299, 2064-2067 (2003).

Contact information
Prof. Liang Tong, Department of Biological Sciences, Columbia University

Email: tong@como.bio.columbia.edu

and plant ACCs that are insensitive to the herbicides have a Leu residue at this position. This residue is equivalent to Leu1705 in yeast ACC, which is located deep at the bottom of the active site cavity and also in the dimer interface. Thus, mutagenesis and structural information suggest that the herbicides target the active site of CT. Our kinetic experiments confirm that the herbicide haloxyfop is a competitive inhibitor of yeast CT with respect to the substrate malonyl-CoA (**Figure 2b**).

The successful development of inhibitors against the active site of the CT domain of plant ACCs holds promise for the development of inhibitors against other CT domains, especially those of human ACCs. Our structural information on the CT domain provides a starting point for understanding the catalysis by this enzyme as well as for designing and optimizing its inhibitors.

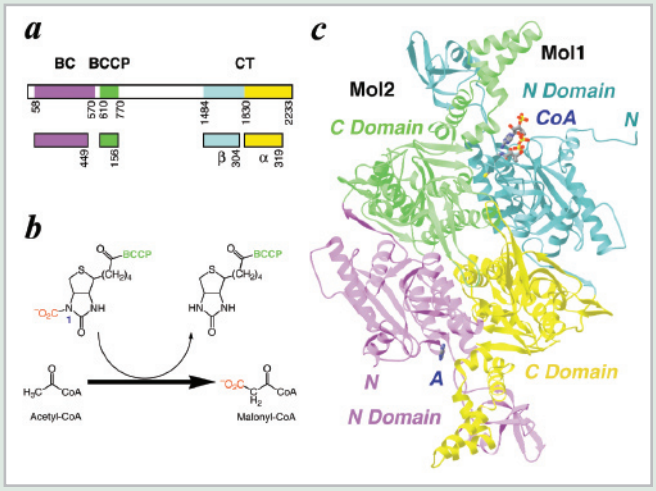

Figure 1. Structures of ACCs. (a) Schematic drawing of the primary structures of eukaryotic, multi-domain ACC and bacterial, multi-subunit ACC. (b) The chemical reaction catalyzed by CT. (c) Schematic drawing of the structure of the CT domain dimer of yeast ACC. The CoA molecule bound to one monomer is shown as a stick model.

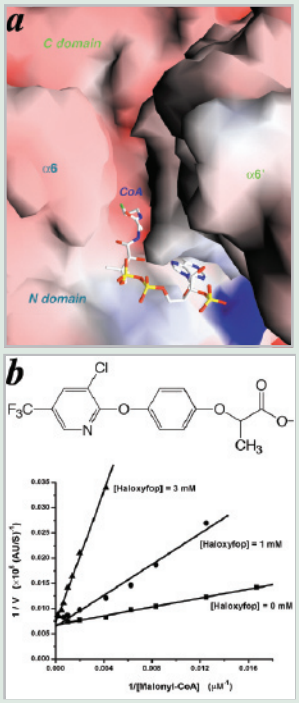

Figure 2. The active site of CT. (a) Molecular surface of the active site region of CT. (b) Double-reciprocal plot showing the competitive inhibition of the yeast CT domain by the herbicide haloxyfop.

A Salmonella Invasion Protein That Acts as a "Molecular Staple"

M. Lilic[2], V.E. Galkin[1], A. Orlova[1], M.S.VanLoock[1], E.H. Egelman[1], and C.E. Stebbins[2]

[1]University of Virginia; [2]The Rockefeller University

Salmonella invasion protein A (SipA) is an important virulence factor injected into host cells, where it modulates the cytoskeleton by polymerizing actin. By combining high resolution X-ray crystallography of SipA, reconstructions of electron micrographs of actin-SipA filaments, modeling, and structure-based mutagenesis, we demonstrate that SipA functions as a 'molecular staple,' in which a central globular domain and two non-globular 'arms' mechanically stabilize the filament by tethering actin subunits in opposing strands.

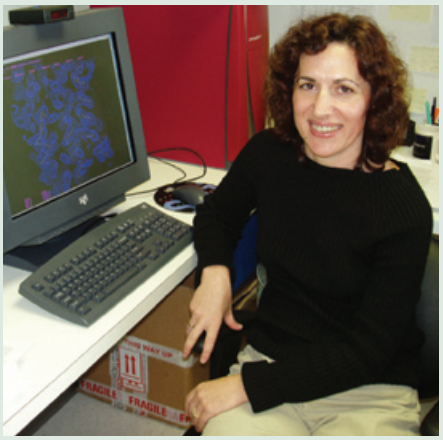

Mirjana Lilic

The etiological agents of plague, typhoid fever, certain food poisonings, and other medically relevant bacterial diseases utilize a type III protein-secretion system to translocate virulence factors, which modulate eukaryotic biochemical processes, into host cells. *Salmonella* species make use of a diverse repertoire of virulence factors, many that target and modulate the structure of the host actin cytoskeleton.

Mutants of *Salmonella typhimurium* with a disruption of the *sip*A gene show an attenuated virulence in bovine intestinal models, impaired ability to invade cells, and less robust and localized membrane ruffling as compared with the wild type strain. Biochemically, the SipA protein of *Salmonella* is able to bind to actin, reduce the critical concentration for the formation of F-actin, stabilize actin filaments, and potentiate the actin nucleating and bundling activity of other virulence factors.

The crystal structure of an active *S. typhimurium* C-terminal domain of SipA (residues 497-669, henceforth SipA$^{497\text{-}669}$) was solved using multiple anomalous dispersion (MAD) techniques on SeMet substituted protein and refined to 1.8Å resolution (**Figure 1**). SipA$^{497\text{-}669}$ possesses a novel three-dimensional structure that, in particular, has no relationship to any known actin binding proteins. This domain of SipA folds into a compact, heart-shaped molecule dominated by helical secondary structure with dimensions of roughly 30x40x40 Å. In the crystal, the protein is ordered only between residues 513 and 669 (leaving 15-20 amino acids disordered at the ends) and the N and C-termini are located at opposite ends of the molecule (the "bottom" and "top," respectively).

The compact nature of this domain of SipA was unexpected, as previous biophysical and electron microscopic (EM) reconstructions of the larger construct SipA$^{446\text{-}684}$ had indicated that the molecule was quite extended in conformation (~ 95Å). In order to reconcile these observations, EM studies of G and F-actin in the presence of SipA$^{497\text{-}669}$ were undertaken in collaboration with the group of Edward Egelman at the University of Virginia. These studies reveal that this smaller construct binds to actin as a globular structure with small non-globular extensions ("arms") that connect different actin monomers (**Figure 1**). Comparisons between EM densities from larger SipA constructs and SipA$^{497\text{-}669}$ reveal that they differ primarily in the length of the non-globular extensions, whereas the central globular density remains similar.

BEAMLINE
X9A

Funding
Rockefeller University; NIH; Burroughs-Welcome Foundation

Publication
Hailong Zhang, Zhiru Yang, Yang M. Lilic, V.E. Galkin, A. Orlova, M.S. VanLoock, E.H. Egelman, and C.E. Stebbins, "Salmonella SipA Polymerizes Actin by Stapling Filaments with Non-Globular Protein Arms," *Science*, 301, 1918-1921 (2003).

Contact information
Erec Stebbins, Assistant Professor and Head of Laboratory, The Rockefeller University

Email: Stebbins@rockefeller.edu

The fit of SipA$^{497\text{-}669}$ into the EM reconstructions places the SipA termini proximal to the linking arms, suggesting a model in which SipA would function as a kind of "molecular staple," centered upon the globular domain for binding actin and linking opposite strands using the non-globular extensions. This hypothesis was tested by a series of truncations designed to remove one or both of the "arms" of SipA. Deletion of the arms severely impaired the ability of SipA to polymerize actin, although not its ability to bind pre-formed F-actin, supporting our idea that the arms are key to the linking of actin protomers in the filament.

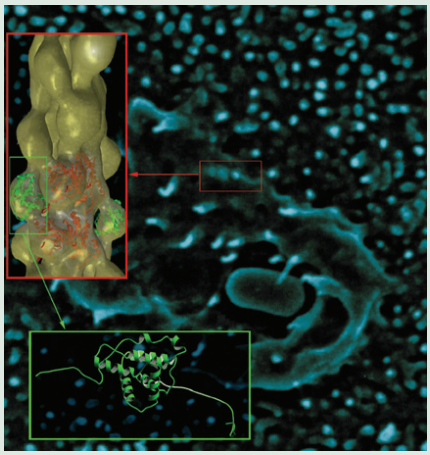

Figure 1. Superimposed on a background of Salmonella induced ruffling in intestinal cells is the EM density (red box) of SipA-actin with the actin (red) and SipA (green) crystal structures modeled. In the green box is a model of SipA showing hypothetical "arms" extending from the X-ray structure.

Soft Condensed Matter and Biophysics

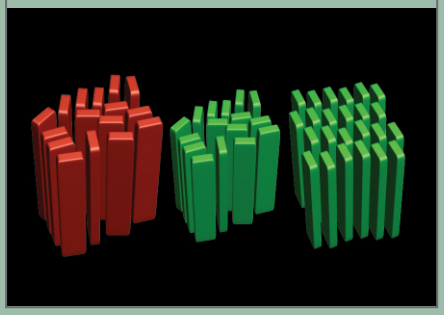

Polymers can Force Calcite to Form via Amorphous Mineral Precursors — and Synchrotron X-ray Studies can Reveal the Details

E. Dimasi[1], V.M. Patel[2], M. Sivakumar[2], M.J. Olszta[2], Y.P. Yang[2], and L.B. Gower[2]

[1]Brookhaven National Laboratory; [2]University of Florida

Scientists at Brookhaven National Laboratory and the University of Florida have used synchrotron x-ray scattering to monitor how mineral crystals and films form at an organic boundary surface, a process related to biological mineral formation. Beneath an organic monolayer, calcium carbonates crystallize rapidly from solution into calcite, but the addition of polymers produces an amorphous thin film and delays the conversion to crystalline calcite. The x-ray measurements reveal that the amorphous thin film forms through kinetic mechanisms rather than the previously assumed templating mechanism, where the atomic positions of organic functional groups match the lattice spacing of the mineral crystal.

Laurie Gower

In a process called biomineralization, some living organisms incorporate insoluble mineral compounds into their biological structures, creating biominerals that are usually hard but much less brittle than the inorganic (geological) minerals. Such biominerals are all the more fascinating because of the wealth of minerals having the same composition but different crystal structures used by animals. For example, calcium carbonates ($CaCO_3$) are abundant geologically but mainly as the stable minerals calcite and aragonite. But numerous marine invertebrates incorporate a broader range of calcium carbonates into their shells, such as the metastable vaterite and unstable amorphous hydrated calcium carbonates.

To study the biomineralization mechanisms, we have assembled organic molecules on a supersaturated $CaCO_3$ solution. The cations (Ca^{2+}) in solution are attracted to the negatively charged monolayer of organic molecules at the surface, creating an ion-rich region that eventually crystallizes into one or more crystal forms of $CaCO_3$ (**Figure 1**). Up to now, this process had never been monitored by a quantitative structural probe.

For the first time, we have determined the cation binding by analyzing the x-ray reflectivity from the initially assembled film. We found that, in the presence of polyacrylic acid – a soluble polymer which may mimic the action of biomolecules – the number of calcium cations bound to the surface layer was 80% less than in the case without polymer. Thus, the acidic macromolecules affect biomineralization primarily by reducing the concentration of cations at the monolayer. Instead, the charged polymer concentrates the ions to form a metastable amorphous layer, from which they can begin to crystallize against the overlying organic monolayer.

Without an appropriate organic template, this polymer-induced precursor initiates the formation of calcite homogeneously in solution, and, in some cases, we noticed that the amorphous precursor has a liquid-like consistency. This observation suggests that it may be possible for

BEAMLINE
X22B

Funding
National Science Foundation; National Institutes of Health; U.S. Department of Energy

Publication
E. DiMasi, M. Patel, M. Sivakumar, M.J. Olszta, Y.P. Yang, and L.B. Gower, "Polymer-Controlled Growth Rate of an Amorphous Mineral Precursor Film Nucleated at a Fatty Acid Monolayer," *Langmuir*, 18, 8902 (2002).

Contact information
Elaine DiMasi, BNL Physics Department, Upton, NY

Email: dimasi@bnl.gov

living organisms to "mold" biomineral crystals through a precursor mechanism. The organic substrate therefore controls the liquid-like or solid nature of the precursor material, a mechanism that may allow the fabrication of synthetic "biomimetic," or biomineral-inspired, materials.

At beamline X22B, we have measured both x-ray reflectivity – sensitive to the surface-normal density profile of the film – and grazing-incidence diffraction – probing in-plane structure – during the 20-hour biomineralization process. The time series of reflectivity curves (**Figure 2a**) displays interference patterns showing that a thick film grows beneath the organic monolayer. Fitting a structural model to this data indicates that the film has a density comparable to amorphous, hydrated $CaCO_3$ phases, half as dense as the anhydrous crystalline forms.

During the 20-hour biomineralization process, diffraction patterns within the layer plane (**Figure 2b**) show that the organic monolayer retains a tightly packed, two-dimensional structure, but no crystalline diffraction from the underlying mineral is observed.

These x-ray measurements provide important new information: Biomineralization can occur through an amorphous precursor, even when no structural alignment between the organic monolayer and the mineral is present. Also, simple variations in polymer concentration and supersaturation have pronounced effects on mineralization rate. These results are in contrast to suggestions in the literature, which have relied, up to now, upon assumptions regarding the alignment of crystals to organic monolayer templates. Our study shows that in-situ structural probes are increasingly important in illuminating the mechanisms of biomineralization.

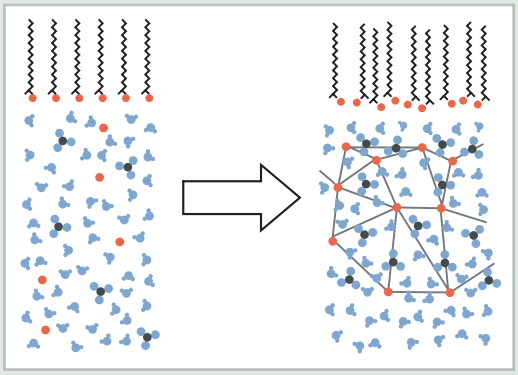

Figure 1. Scheme for biomineralization at an organic monolayer. A fatty acid, $CH_2(CH_3)_{18}COOH$, self-assembles at the surface of an aqueous layer supersaturated in calcium (Ca^{2+}) and carbonate (CO_3^{2-}) ions and containing dissolved poly(acrylic acid). At the negatively charged fatty acid headgroups, the ions that are sequestered by the polymer collect and heterogeneously form an amorphous hydrated mineral film, which reaches a thickness of more than 30 nanometers in 20 hours. The amorphous film subsequently crystallizes into calcite.

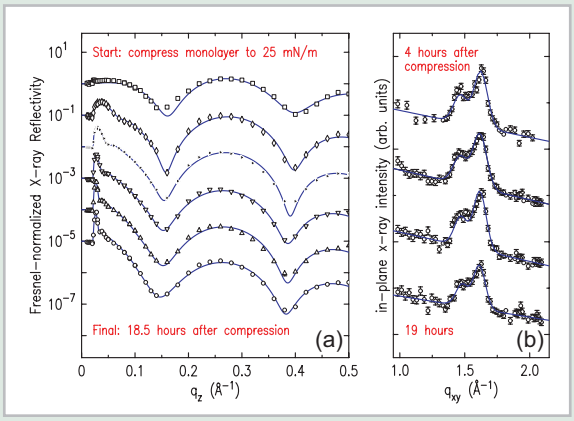

Figure 2. (a) Time series of normalized reflectivity curves from initial preparation of the sample through the growth of the mineral film. Oscillations in the data (symbols) are due to the reflection of x-rays from interfaces defined by the surface layers. Fit curves (lines) allow quantitative determination of the length scales and densities of both monolayer and mineral. The sharp peak near the origin is the main time-dependent feature, and provides a direct measure of the thickness of the mineral film. (b) Time series of in-plane scattering in a grazing incidence geometry, which is sensitive to the order of surface species within the layer plane. The observed peaks are consistent with tightly compressed fatty acid monolayers. Bragg diffraction peaks from crystalline calcium carbonate ($CaCO_3$) mineral species are not observed during this phase of mineral film growth, showing that the precursor film is amorphous.

Defects in Ethylene-Propylene Copolymer Crystals Drive Change in Lattice Geometry

W. Hu[1], S. Srinivas[1], and E.B. Sirota[2]

[1]ExxonMobil Chemical Company; [2]ExxonMobil Research and Engineering Company

By using x-ray light generated by the National Synchrotron Light Source, Exxon Mobil Corporation scientists have undertaken the challenging task of determining how defects affect the structure of crystals. Combining the power of wide-angle x-ray scattering and solid-state nuclear magnetic resonance, the scientists have shown how the incorporation of methyl branches in polyethylene crystals affect their transition from an orthorhombic to a hexagonal phase.

Authors (from left): Srivatsan Srinivas, Weiguo Hu, and Eric B. Sirota

Defects exist in all crystalline materials and exert a substantial effect on their physical and mechanical properties. The structure of defects in large-molecule crystals, such as polymers, is highly complex. So, many experimental and theoretical investigations have been and are still being very actively pursued.

In polymer crystals, scientists distinguish two types of defects, called dynamic and static. Dynamic defects are thermally-activated, large-amplitude chain motions that facilitate the deformation and mechanical damping of the crystals, whereas static defects are mostly due to the non-regularity of monomer units along polymer chains.

One example of static defect is that in ethylene (C_2H_4) copolymers, especially ethylene-propylene (EP) copolymers. By copolymerizing ethylene and propylene (C_3H_6), the polymer chain has mostly $(CH_2)_n$ units with randomly placed methyl (CH_3) side groups or branches. EP and other such "defected" polyethylenes, called linear low-density polyethylene (LLDPE), are of substantial commercial importance, with an annual U.S. production of more than 3.5 million tons.

With increasing defect concentration in the crystal, the crystalline lattice changes from an orthorhombic phase, with little or no methyl branches, to a hexagonal phase, with more methyl branches.

We studied the structure of static defects in EP copolymers at beamline X10A using wide-angle x-ray scattering (WAXS) and solid-state nuclear magnetic resonance (NMR), and found that chain motion in the crystal may serve as an important connection between the defect structure and change in the crystalline lattice.

WAXS data of a series of EP samples (**Figure 1**) show that the area per chain of the orthorhombic phase increases at increasing methyl branch content, and that the hexagonal phase emerges when the fraction of backbone carbons containing a methyl branch is larger than 0.095.

The hexagonal phase has an area per chain of 21Å^2, about 14 percent greater than that of the orthorhombic phase. The increased area in the hexagonal phase is probably due to a decrease in packing density caused by disorder and not merely due to lower density caused by packing of the branched chains. The abrupt change of area per chain upon the transition from an orthorhombic to a hexagonal phase indicates that the hexagonal phase is a distinct phase, rather than an inherently

BEAMLINE
X10A

Funding
Exxon Mobil Corporation

Publication
W. Hu, S. Srinivas, and E.B. Sirota, "Crystalline Structure and Properties of EP and EB Copolymers by WAXS, DSC, and Solid-State NMR," *Macromolecules*, 35, 5013-5024 (2002).

Contact information
Weiguo Hu, ExxonMobil Chemical Company, Baytown, TX

Email: weiguo.hu@exxonmobil.com

orthorhombic phase with a hexagonal geometry.

Solid-state nuclear magnetic resonance (NMR) spectra of several EP samples (**Figure 2**) show that the isotropic chemical shift (ICS), which is the slight difference between the intrinsic frequency at which each sample resonates and the frequency imposed by the NMR apparatus, changes from 32.8 parts per million (orthorhombic phase) to 33.4 parts per million (typical of rotator phase) at increasing propylene content. This can be interpreted as an increase in rotational freedom at higher defect levels, which occurs simultaneously with the expansion of the crystalline lattice seen in **Figure 1**. In the rotator phase, each chain has approximate rotational symmetry, and thus the packing of the chains is naturally hexagonal. So, the rotator phase observed by NMR should be the hexagonal phase detected by WAXS.

Combining the observations from the two techniques, we propose the following picture that seems to connect the observations for defect, molecular motion, and lattice geometry. In the polyethylene crystals that do not contain methyl branches, the motion of the chains is a 180-degree flip, followed by a slip by half the distance of a repeat unit. In crystals containing methyl branches, pure flip becomes less favorable because local segments containing methyl branches do not have the flip-and-slip symmetry as an ethylene chain without methyl branches. As a result, a certain amount of rotation is added to the motional mode. Since this component gives chains more cylindrical symmetry, it causes the lattice change from orthorhombic toward hexagonal. Eventually, the increase in rotation amplitude leads to the transition to the rotator/hexagonal phase.

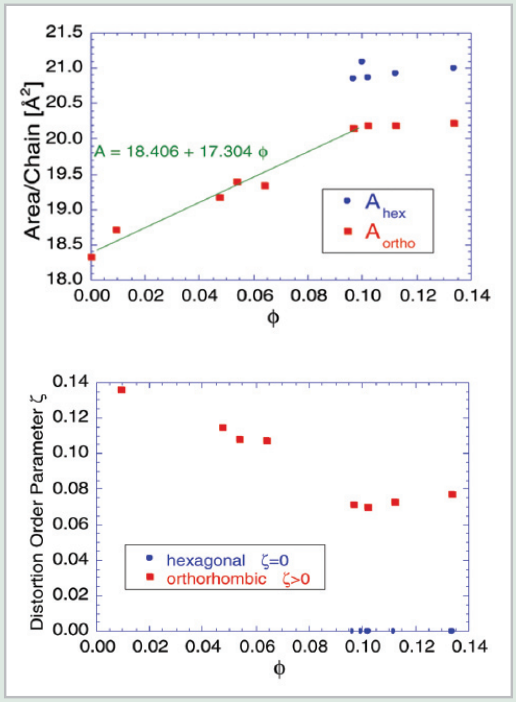

Figure 1. (Top) The computed area/chain, assuming the two peak orthorhombic structure (A_{ortho}) and single peak hexagonal phase (A_{hex}). (Bottom) The distortion order parameter, defined as a distortion away from hexagonal. ϕ is the fraction of backbone carbons containing a methyl (CH_3) branch.

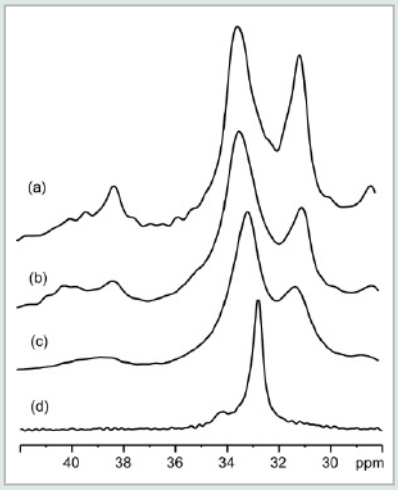

Figure 2. Cross polarization/magic angle spinning (CP/MAS) solid-state nuclear magnetic resonance spectra of ethylene-propylene copolymers for different values of ϕ, the fraction of backbone carbons containing a methyl (CH_3) branch: (a) 0.133, (b) 0.102, (c) 0.064, and (d) 0.

Structure of $V_2O_5 \cdot nH_2O$ Xerogel Solved by the Atomic Pair Distribution Function Technique

V. Petkov[1], P.N. Trikalitis[1], E.S. Bozin[1], S.J.L. Billinge[1], M.G. Kanatzidis[1], and T. Vogt[2]

[1]Michigan State University; [2]Brookhaven National Laboratory

The structure of most materials can be determined because they can be crystallized and thus studied by a technique called crystallography. But disordered materials lack the periodicity of crystals and show diffraction patterns that are much more diffuse. Scientists from BNL and Michigan State University have successfully applied a technique called atomic pair distribution function at NSLS beamline X7A to determine the structure of the $V_2O_5 \cdot nH_2O$ xerogel, a disordered material that could be used in chemical sensors, fast switching devices, and reversible lithium ion batteries.

Authors (from left): Valeri Petkov, Pantelis Trikalitis, and Mercouri Kanatzidis

The $V_2O_5 \cdot nH_2O$ xerogel, an organic polymer that can swell in suitable solvents to yield particles possessing a network of polymer chains, has fascinated researchers for many decades and inspired an intensive search for potential applications, such as chemical sensors, fast switching devices, and reversible lithium ion batteries. Despite decades of experimentation with this xerogel, its atomic structure has remained somewhat of a mystery because it does not form crystals but exists only as ribbon-like particles about 10 nanometers wide and one micrometer long, as shown in **Figure 1**.

The limited diffraction pattern of $V_2O_5 \cdot nH_2O$ makes it impossible to determine its three-dimensional structure using traditional crystallographic techniques. But the pattern contains a small number of features that indicate the presence of intermediate-range order and a pronounced diffused component. These are characteristics of "nanocrystalline" materials that have well-ordered local structures limited to the nanometer-length scale.

Scientists have put forward two competing structural models for $V_2O_5 \cdot nH_2O$. Jacques Livage of the University of Paris VI proposed that the xerogel, on the atomic scale, is a stack of corrugated single layers of VO_5 units, with the layers closely related to those occurring in crystalline V_2O_5. On the other hand, Y. Oka of Kyoto University proposed that the xerogel is made of V_2O_5 bilayers according to the crystalline structure of either $Na_xV_2O_5$ or $K_xV_2O_5$ (where x is an integer). But neither model can fully explain experimental observations made using the x-ray diffraction technique nor describe the atomic structure in terms of a unit cell and atomic coordinates.

We have determined the three-dimensional structure of $V_2O_5 \cdot nH_2O$ using the atomic pair distribution function (PDF) technique, which has emerged recently as a powerful and unique tool for the structural characterization of crystalline materials with significant disorder. The strength of the technique is that it takes into account all components of the diffraction pattern and thus reflects the longer-range structural order and the local deviations from it. The technique is gaining importance because of the availability of high energy, high flux synchrotron sources, such as the NSLS, that make accurate and fast data collection possible.

BEAMLINE
X7A

Funding
National Science Foundation; U.S. Department of Energy

Publication
V. Petkov, E.S. Bozin, S.J.L. Billinge, T. Vogt, P.N. Trikalitis, and .G. Kanatzidis, "Structure of V_2O_5 .OnH_2O Xerogel Solved by the Atomic Pair Distribution Function Technique," *J. Am. Chem. Soc.*, 124 (34), 10157-10162 (2002).

Contact information
Mercouri G. Kanatzidis, Department of Chemistry, Michigan State University, East Lansing, MI

Email: kanatzid@cem.msu.edu

We have shown that the structure of $V_2O_5 \cdot nH_2O$ can be well described as an assembly of almost perfect bilayers of single V_2O_5 layers made of square pyramidal VO_5 units with water molecules residing between them, as shown in **Figure 2**. The stacking sequence is imperfect because of the extensive turbostratic disorder in this material, meaning that the layers are stacked in one direction, but rotated every one way in the other two, similar to a deck of cards that has not been straightened after a game.

This structure explains almost all known spectroscopic, physical, and chemical properties of the material, and reveals the atomic ordering in the individual ribbon-like particles, as shown in **Figure 3**.

The most important outcome of the study is that it yields the three-dimensional structure of nanocrystalline $V_2O_5nH_2O$ in terms of a relatively simple model with only few meaningful parameters, such as its unit cell and symmetry. This work also shows that, even with a very low degree of structural coherence, at synchrotrons such as NSLS, using the right techniques, it is possible to determine nanoscale structures at the atomic level.

Although the PDF technique is not an *ab initio* structure determination technique, it can successfully distinguish between different structural possibilities, giving both local and long-range structural information.

Additional contact information:
Simon J. L. Billinge, Department of Physics and Astronomy, Michigan State University, East Lansing, MI
Email: billinge@pa.msu.edu

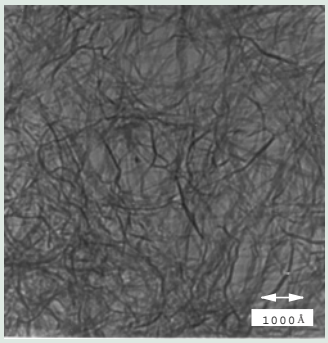

Figure 1. Transmission electron microscopy image of the $V_2O_5 \cdot nH_2O$ xerogel.

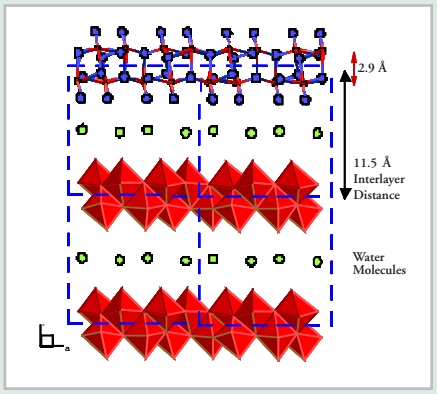

Figure 2. Structure of $V_2O_5 \cdot nH_2O$ xerogel (polyhedra and ball-stick model), as revealed by using the atomic pair distribution function technique. Characteristic distances are shown. Water molecules are shown in green.

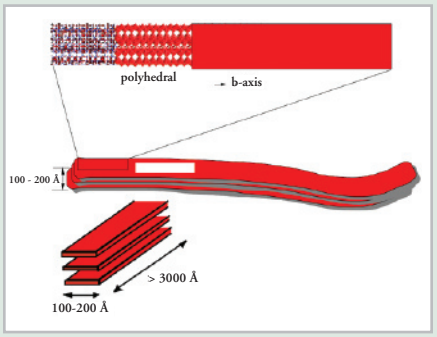

Figure 3. Ribbon-like representation of $V_2O_5 \cdot nH_2O$ xerogel showing intermediate structural makeup and overall V_2O_5 slab organization.

A Synchrotron WAXD Study on the Early Stages of Coagulation During PBO Fiber Spinning

S. Ran[1], C. Burger[1], D. Fang[1], X. Zong[1], B. Chu[1], B.S. Hsiao[1], Y. Ohta[2], K. Yabuki[2], and P.M. Cunniff[3]

[1]Department of Chemistry, State University of New York at Stony Brook; [2]Toyobo Research Center Co. Ltd., Katata, Ohtsu, Shiga, Japan; [3]Department of the U.S. Army, Soldier and Biological Chemical Command

The structural development at the very early stages of the coagulation process during PBO fiber spinning was investigated using synchrotron wide angle X-ray diffraction (WAXD). PBO was found to segregate into the PPA-free domains immediately upon the contact with water. Our results confirmed the hypothesis that the first step of the coagulation process during spinning was the formation of pure PBO stacks, with interstack order being formed later.

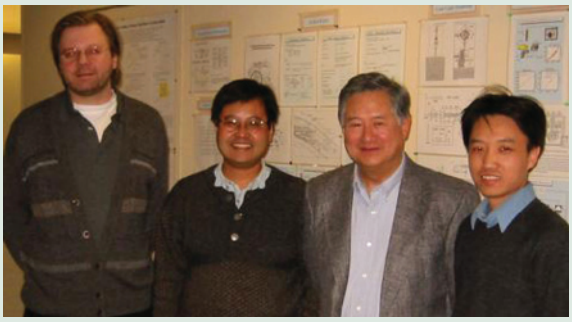

Authors (from left): Christian Burger, Benjamin S. Hsiao, Benjamin Chu, and Shaofeng Ran

Poly(*p*-phenylene benzobisoxazole) (PBO) fiber is known to be the strongest commercial synthetic polymer fiber. Its excellent mechanical properties and superb thermal stability make PBO the optimum material for high performance applications like lightweight bulletproof vests, helmets, and fire-resistant suits. The manufacturing process for PBO fibers involves dry-jet wet-spinning from a polymer solution in poly(phosphoric acid) (PPA). After spinning, the fiber is coagulated in water to remove the PPA component. Although the coagulation process was found to strongly affect the final PBO fiber properties, the structural evolution during the coagulation process had never been fully understood. In this work, a gel spinning apparatus was modified to study the fiber during coagulation with time resolution as short as 0.03 sec. The PBO/PPA dope was spun at 160 °C. Two-dimensional wide angle X-ray diffraction (WAXD) images were recorded using a CCD X-ray detector at beamline X27C.

Figure 1 shows the one-dimensional equatorial scattering profiles of the PBO filament before coagulation and at different coagulation times. Two scattering peaks were found on the equator before coagulation (**Figure 1A**), corresponding to *d*-spacings of 9.67 Å and 4.45 Å, respectively. These two equatorial peaks suggest that the molten dope structure is not simply nematic. The second peak was much stronger than the first one, excluding the possibility of a hexagonal-like disordered close packing. We attributed this structure to a "biaxial nematic" order, where the mesogenic unit was a well-defined complex between PBO and PPA molecules. After the fiber passed through the water bath, even if the coagulation time was as short as 0.03 sec (**Figure 1B**), an additional peak at d = 3.36 Å appeared, which corresponded to the eventual 010 reflection of the final PBO crystal structure, implying that PPA-free stacks of flat PBO molecules had been formed immediately at the very beginning (~0.03 sec) of the coagulation process. With increasing coagulation time, this peak became stronger, indicating that more PPA-free PBO regions had been formed.

We did not, however, observe the appearance of the 200 reflection of the final PBO crystal (d = 5.46 Å), even after the short coagulation time

Beamline
X27C

Funding
U.S. Army Research Office; National Science Foundation; U.S. Department of Energy; Toyobo, Inc. Japan

Publication
S. Ran, C. Burger, D. Fang, X. Zong, B. Chu, B.S. Hsiao, Y. Ohta, K. Yabuki, and P.M. Cunniff, "A Synchrotron WAXD Study on the Early Stages of Coagulation During PBO Fiber Spinning," *Macromolecules*, 35 (27), 9851-9853 (2002).

Contact information
Benjamin S. Hsiao, Professor, SUNY at Stony Brook, NY

Email: Benjamin.Hsiao@sunysb.edu

of 0.3 sec. This result confirms that the first step of coagulation is the formation of face-to-face stacks of PBO molecules on top of each other, separated by a 3.36 Å spacing. There is no significant lateral packing order between these stacks at this early stage of the coagulation, as shown schematically in **Figure 2A**. We assume that, after the PBO stacks accumulate to a certain critical fraction, the lateral packing ordering between the stacks would be formed, resulting in the appearance of the 200 reflection. When coagulation time is long enough, such that all of the PPA solvent is washed away, a (210) reflection will be observed, indicating that the order in the fiber cross section is no longer of short range nature only, but that a two-dimensional lattice with a certain degree of long-range order has been formed (**Figure 2B**).

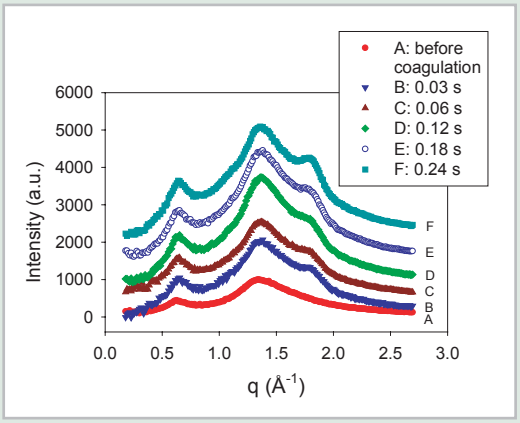

Figure 1. One-dimensional equatorial intensity profiles of PBO fiber at various coagulation times.

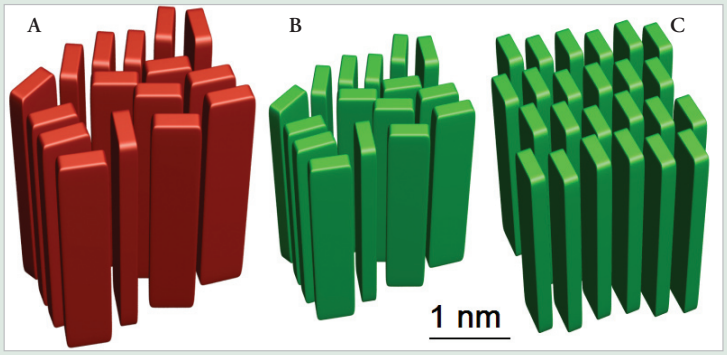

Figure 2. Schematic representation of sanidic or biaxial nematic packings: PBO-PPA solvate complexes (A) and pure PBO molecules (B), respectively, are represented by plank-shaped units with appropriately scaled cross-sections. The heights of these units are actually much larger than shown in the figure. The WAXD equator will show strong (0k0), weak (h00), and no mixed (hk0). (C) Two-dimensional long-range order in the cross-section (mixed (hk0) reflections) with translational disorder in the fiber direction (no mixed (hkl) reflections).

Visualizing the Ca^{2+} Dependent Activation of Gelsolin using Synchrotron Footprinting

J.G. Kiselar[1,3], P.A. Janmey[4], S.C. Almo[2,3], and M.R. Chance[1-3]

[1]Department of Physiology & Biophysics and [2]Biochemistry, and [3]Center for Synchrotron Biosciences, Albert Einstein College of Medicine; [4]Institute for Medicine and Engineering, University of Pennsylvania

Gelsolin is a Ca^{2+}-dependent protein composed of six homologous subdomains (denoted S1-S6) that severs actin filaments (F-actin) and caps the fast-growing barbed end with high affinity. The helical tail of S6, termed the "latch", interacts in a non-covalent manner with the F-actin binding helix of S2, making its actin-binding sites inaccessible in the absence of Ca^{2+}. Upon Ca^{2+} activation, the protein undergoes substantial changes in structure, involving a number of rearrangements that reveal actin filaments and actin monomer binding sites. Synchrotron protein footprinting was used to reveal detailed structural changes that occur in the Ca^{2+} dependent activation of gelsolin.

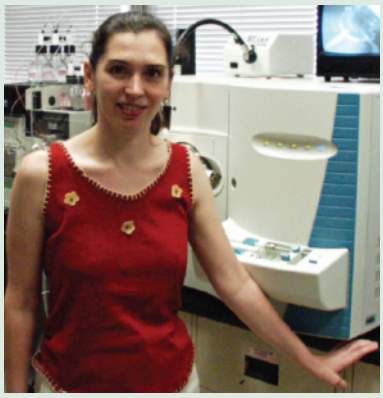

Janna G. Kiselar

Only modest structural information is available regarding the Ca^{2+}-induced reorganization accompanying gelsolin activation. Specifically, a structure of S4-S6 bound to Ca^{2+} and actin at 3.4 Å resolution shows details of specific rearrangements involving S4 and S6 (**Figure 1d**), which are thought to represent steps in the Ca^{2+} activation process. The most dramatic is the disruption of the extended β-sheet between S4 and S6 with S6 rotating away from S4 and moving adjacent to S5; however, it is unclear which of the above Ca^{2+}-binding processes induces this reorganization. There exists a need to develop experimental approaches that directly link Ca^{2+}-binding events with structural rearrangements at the atomic scale.

Synchrotron protein footprinting provides a quantitative approach to monitor changes in surface accessibility of specific amino acid side chains. Hydroxyl radicals generated from a millisecond exposure of aqueous solutions to unattenuated "white" synchrotron radiation result in the stable oxidative modification of solvent accessible amino acid side chains. The specific extents and sites of oxidative modification are quantified by proteolytic digestion and mass spectrometry. The most reactive residues, which represent the experimental probes for this method, include surface accessible cysteine, methionine, phenylalanine, tyrosine, tryptophan, histidine, proline, and leucine side chains.

More than 80 peptide segments within the structure, covering 95% of the sequence in the molecule, were examined using this approach for their solvent accessibility as a function of Ca^{2+} concentration in solution. Twenty-two of the peptides exhibited detectible oxidation; for seven, the oxidation extent was seen to be Ca^{2+} sensitive. Ca^{2+} titration isotherms (**Figure 2a-d**) monitoring the oxidation within residues 49-72 (within S1), 121-135 (S1), 162-166 (S2), and 722-748 (S6) indicate a three-state activation process with the intermediate that was populated at a Ca^{+2} concentration of 1-5 μM, which is competent for capping and severing activity. A second structural transition with a mid-point of ~60-100 μM (data shown in **Figure 2a-d**), where the accessibility of the above four peptides is further increased, is also observed.

Tandem mass spectrometry data showed that buried residues within the

BEAMLINE
X28C

Funding
National Institutes of Health

Publication
J.G. Kiselar, P.A. Janmey, S.C. Almo, and M.R. Chance, "Visualizing the Ca^{2+}-Dependent Activation of Gelsolin by Using Synchrotron Footprinting," *Proc. Natl. Acad. Sci. USA*, 100(7), 3942-3947 (2003).

Contact information
Prof. Mark R. Chance, Department of Physiology & Biophysics, Albert Einstein College of Medicine

Email: mrc@aecom.yu.edu

helical "latch" of S6 (including Pro745) that contact an F-actin binding site on S2 and buried F-actin binding residues within S2 (including Phe163) become exposed upon Ca^{2+} binding (**Figure 1b-c**), suggesting that the helical "latch" is released in the first transition coincident with the occupancy of a high-affinity Ca^{2+}-binding site in S6. However, residues within S4 that are part of an extended ß-sheet with S6 (including Tyr453 that is shown in **Figure 2c**) are revealed only in the subsequent transition at higher Ca^{2+} concentrations (**Figure 2e**); the disruption of this extended contact between S4 and S6 (and likely the analogous contact between S1 and S3) likely results in an extended structure permitting additional functions consistent with the fully activated gelsolin molecule. The location of eight amino acids that were oxidized in the presence of Ca^{2+} only are illustrated in **Figure 1a-c**.

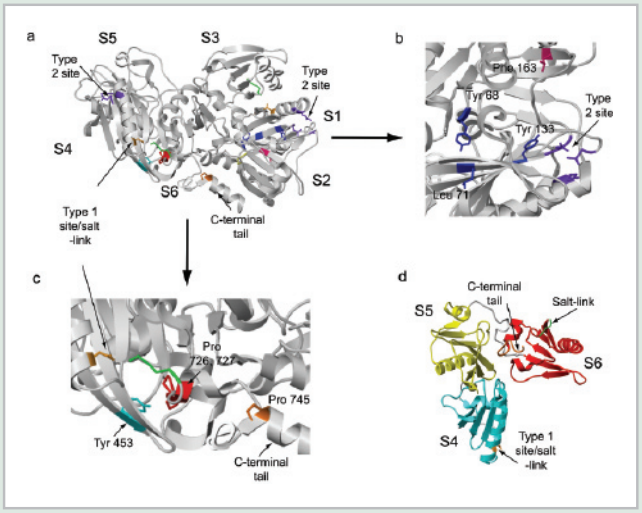

Figure 1. (a) The subunit structure of gelsolin. The buried residues that are revealed in the presence of Ca^{2+} are shown. The type 2 Ca^{2+} binding sites in S1 and S4 are colored in purple. The type 1 Ca^{2+} binding site in S4 and S6 are colored in gold and green, respectively. The residues from S4 and S6 form a salt-link between the sub-units. (b) A close-up of the S1 type 2 site with the adjacent reactive residues labeled. (c) A close-up of the S4 type 1 site with the reactive residues labeled. (d) The structure of the activated C-terminal half of gelsolin.

The results provide clear evidence for a three state, Ca^{2+}-induced activation process. State 1 corresponds to the "Ca^{2+}-free" form, state 2 is the intermediate observed in these studies that involves some unlatching of the structure, and state 3 is the Ca^{2+} saturated, fully activated form. The transition between states 1 and 2 occurs at sub-micromolar concentrations, which is in a good agreement with the previous biochemical studies and is accompanied by the binding of multiple Ca^{2+} ions. The transition between states 2 and 3 is mediated by occupancy of lower affinity binding sites and accompanied by the binding of 2-3 additional Ca^{2+} ions.

Additional Publications:
Kiselar, J.G., et al., *Int J Radiat Biol.*, 78, 101-14, (2002); Guan, J.Q., et al., *Biochemistry*, 41, 5765-75, (2002).

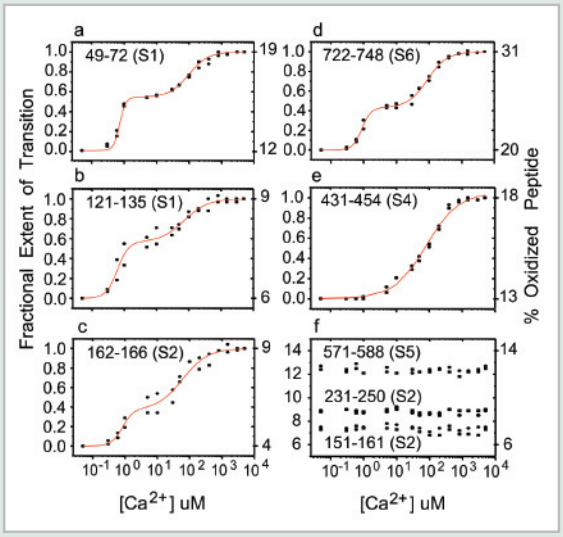

Figure 2. Ca^{2+} titration isotherms indicating changes in oxidation extent for specific peptides after exposure of gelsolin to the x-ray beam for 80 milliseconds. (a-e) The % oxidized peptide is shown on the right-hand side of the y-axis; on the left-hand side, the transition extent is indicated. The solid lines represent the fitting of the curves as described in the text. (f) oxidized peptides within gelsolin show no changes in oxidation upon titration by Ca^{2+}. The % oxidized peptide is shown on the right- and left-hand sides.

New Phases of Phospholipids and Implications to the Membrane Fusion Problem

L. Yang[1], L. Ding[2], and H.W. Huang[2]

[1]National Synchrotron Light Source, Brookhaven National Laboratory; [2]Department of Physics and Astronomy, Rice University

Membrane fusion is involved in many biological processes, such as cellular transportation, signal transduction, and viral infection. A key element of the study of membrane fusion is to understand the behavior of the primary structural component of the membrane, the lipid bilayer, in order to elucidate fusion proteins' regulatory role. In this study, we use x-ray diffraction at beamline X21 to study how the lipid composition affects bilayer fusion.

When two lipid bilayers fuse, they must undergo molecular rearrangements at the point of merging. The role of the fusion proteins that strictly control membrane fusion is therefore most likely to modify the relative free energy of different lipid configurations, and to exert mechanical work that shifts the system over the energy barriers along the fusion pathway. In order to understand the role of fusion proteins and how lipid structure transitions occur, researchers studied the phase transition of pure lipid membranes between the lamellar (L) phase (planar lipid layers) and the inverted hexagonal (H_{II}) phase (hexagonally stacked lipid tubes), based on the idea that lipid must undergo a similar rearrangement, as in fusion.

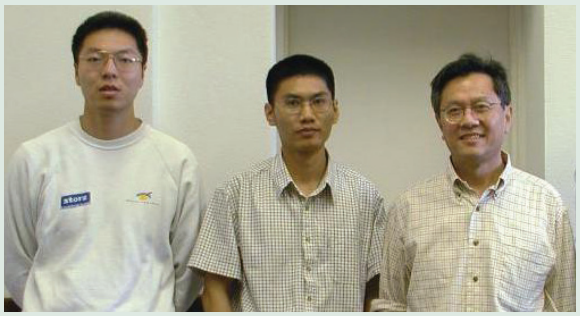

Authors (from left): Lai Ding, Lin Yang, and Huey Huang

However, previous investigations on the system of dioleoylphosphatidylcholine (DOPC) and dioleoylphosphatidylethanolamine (DOPE) did not reveal intermediate phases between the L and H_{II} phases. Recently, we found a rhombohedral phase (R) in diphytanoylphosphatidylcholine (DPhPC) between its L and H_{II} phases using substrate-supported samples. Here we report the observation of the rhombohedral phase, as well as a previously not observed distorted hexagonal phase in DOPC-DOPE mixtures.

The experiments were performed on model membranes that are made of hundreds of lipid bilayers prepared on silicon substrate. We observed the phase behavior of the lipid while varying the composition of the sample as well as its temperature and water content (**Figure 1**). The samples in general showed all three phases that were observed in DPhPC. However, depending on the sample composition, these three phases appeared at the different parts of the phase diagram.

It has been shown that the rhombohedral phase of DPhPC contains a lattice of stalk structure that was thought to be an intermediate structure during the fusion process. The existence of this phase in DOPC/DOPE mixtures once again confirms the stalk hypothesis for the L-H_{II} transition. Furthermore, the R phase exists only for a certain range of lipid composition (i.e. for a certain range of spontaneous curvature). This implies that the free energy barrier in the fusion pathway is directly determined by the spontaneous curvature of the lipid bilayer.

The samples with mixed DOPC and DOPE also showed (**Figure 2**) a distorted hexagonal phase (D). Though the detailed structure of this phase is yet to be determined, because of the symmetry of the structure and the fact that the D and H_{II} phases are neighbors in the phase

BEAMLINE
X21

Funding
National Institutes of Health; The Welch Foundation; LDRD, BNL

Publication
L. Yang, L. Ding, and H.W. Huang, "New Phases of Phospholipids and Implications to the Membrane Fusion Problem," *Biochemistry*, 42, 6631-6635 (2003).

Contact information
Lin Yang, NSLS, BNL, Upton, NY

Email: lyang@bnl.gov

diagram, the *D* phase very likely contains distorted lipid tubes. This implies that, under stress, lipids may partially demix to adjust its local spontaneous curvature in order to achieve energy minimum. Therefore demixing, or lipid sorting, may be a mechanism to promote membrane fusion.

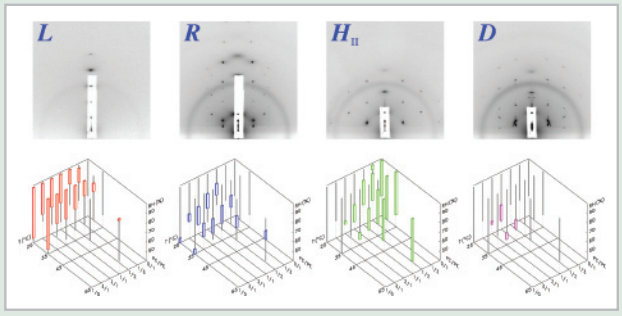

Figure 1. The phases diagrams of the structure of DOPC/DOPE multilayers as functions the composition, the temperature of the samples and the environmental relative humidity.

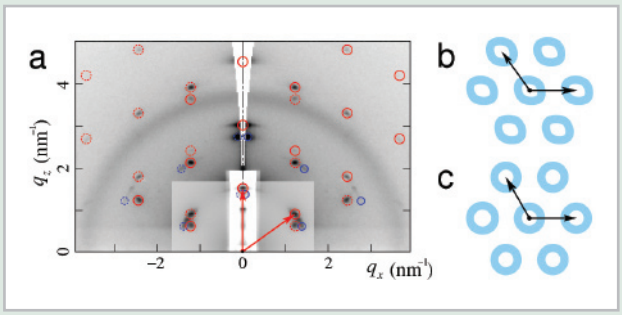

Figure 2. The diffraction pattern (a) from the distorted hexagonal phase of DOPC/DOPE suggests that the structure of this phase (model b) may contain distorted lipid tubes, much like those in the H_{II} phase (c).

A Monolayer of Ferritin Proteins at a Nanofilm Aqueous-Aqueous Interface

M. Li[1], D.J. Chaiko[2], and M.L. Schlossman[3]

[1]Department of Physics, University of Illinois; [2]Argonne National Laboratory; [3]Departments of Physics and Chemistry, University of Illinois

The formation of thin aqueous films on top of an aqueous subphase is demonstrated. The films form via a complex spreading process that results in the coexistence of macroscopic lenses and films that are several nanometers thick. Biomolecules, such as proteins, can be trapped at the aqueous-aqueous interface or in the thin film. This idea is demonstrated by an x-ray reflectivity study of ferritin proteins that form a two-dimensional assembly at the interface. It is shown that the electron density interfacial profile of the ferritin trapped in this thin film is consistent with the known crystal structure of ferritin.

Mark L. Schlossman

Although interfaces between bulk liquids are commonly formed between immiscible liquids, such as oil and water, it is also possible to form an interface between two aqueous solutions. For example, aqueous mixtures of polymers, salts, and water are known to separate into two or more equilibrium phases. Aqueous biphase systems (aqueous mixtures that form two phases) are used for the purification and separation of biological materials. This is possible because, although biological materials are soluble in both aqueous phases, they prefer to be in one or the other, and are therefore separated into one of the two. We have chosen to use mixtures of polyethylene glycol (PEG), potassium phosphates, and water to investigate the formation of protein assemblies in layers of aqueous solutions that are approximately four nanometers thick. Both the PEG and the potassium phosphates are compatible with many proteins, making the mixture an appropriate choice.

We have shown that thin layers of aqueous solutions supported on a bulk aqueous subphase can be formed from biphase mixtures by the following procedure: Upon mixing the PEG, salt, and water, the resulting bulk liquid separates into a lower salt-rich phase and an upper PEG-rich phase. After extracting the salt-rich phase into a separate container, a single drop of the PEG-rich phase is placed onto the surface of the salt-rich phase. The drop spreads across the entire surface, thins rapidly, and then breaks up into smaller drops that coarsen to form flat lenses with diameters on the order of one centimeter (**Figure 1**). Then, using a pipette, any lenses in the path of the x-ray beam are either aspirated off the surface or moved off to the side (at least one lens remains on the surface during the x-ray measurements). These macroscopic lenses function as reservoirs to supply the PEG-rich thin film.

We used x-ray reflectivity to demonstrate that a four nanometer-thick film exists in the region between the macroscopic lenses. This region is a thin layer of the bulk PEG-rich phase, rather than a monolayer of PEG. Since proteins retain their natural conformation in PEG solutions and protein dimensions are typically similar to the film thickness, it is natural to ask if this thin film can be used to collect proteins into two-dimensional assemblies.

In an experiment to test the proof of this principle, we demonstrated that ferritin proteins can be assembled into the PEG-rich thin film.

BEAMLINE
X19C

Funding
National Science Foundation Division of Materials Research; Petroleum Research Foundation administered by the American Chemical Society

Publication
Ming Li, David J. Chaiko, and Mark L. Schlossman, "An X-ray Reflectivity Study of a Monolayer of Ferritin Proteins at a Nano-Film Aqueous-Aqueous Interface," *J. of Phys. Chem. B*, 107, 9079-9085 (2003).

Contact information
Mark Schlossman, Department of Physics, University of Illinois at Chicago

Email: schloss@uic.edu

Ferritin is used for the storage of iron, and consists of a nearly spherical organic shell surrounding a nearly spherical core in which the iron is stored. The ferritin is prepared in a solution of water and PEG, whose composition mimics that of the PEG-rich solution in the biphase system. A few drops of the ferritin solution are added to the lower salt-rich bulk phase. Then, they rise to spread into the PEG-rich thin film. **Figure 2** illustrates the electron density profile of this film, as measured using x-ray reflectivity, and compares it to the predicted profile of a layer of ferritin calculated from the known molecular structure of the protein. The near-match of measured and calculated profiles indicates that the ferritin forms a two-dimensional film that is ordered normal to the interface.

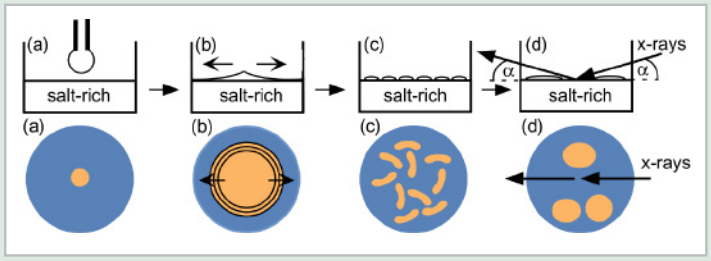

Figure 1. (a) Thin layer is formed by placing a drop of the PEG-rich phase on the surface of the salt-rich phase with a pipette (top illustrations are a side view, bottom are a top view). (b) Over a period of about one second the drop spreads and a ring of interference colors can be observed. (c) After about 10 seconds, small islands form a spinodal-like pattern (not as ordered as the illustration). (d) The pattern coarsens over a period of about one hour, leaving a few large (approximately one centimeter in diameter) lenses. The lenses are pushed aside with a pipette to allow access for the x-rays that probe the region between the lenses. This region consists of a four nanometer-thick film of a PEG-rich solution.

The overall method described here allows proteins or other biomolecules to be assembled two-dimensionally and studied with x-rays. This is significant because many proteins do not crystallize in three dimensions, or may be difficult to crystallize and, therefore, cannot be studied that way. Allowing proteins to assemble at an aqueous surface often results in protein denaturation, causing the loss of the protein's biological activity. Our method retains the natural shape of the protein at a liquid surface. Moreover, the formation of these two-dimensional arrays may be useful technologically because the arrays allow the biomolecules to interact with other molecules. This could be utilized in chemical sensing or catalytic applications.

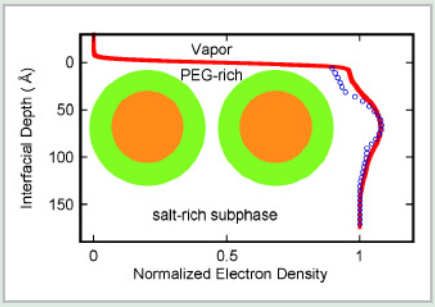

Figure 2. The electron density profile of ferritin adsorbed at the interface formed by the PEG-rich thin film and the salt-rich subphase. The solid curve is the profile determined by x-ray reflectivity, and the small circles are a calculation of the profile assuming a single layer of ferritin proteins. The illustration represents (nearly to scale) the position of the ferritin layer used for the calculation. The colored circular regions represent the core and shell of the ferritin.

Surfaces, Interfaces and Nanomaterials

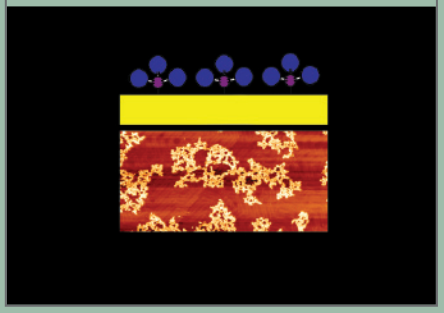

Direct Separation of Short Range Order in Intermixed Nanocrystalline and Amorphous Phases

A.I. Frenkel[1], A.V. Kolobov[2], I.K. Robinson[3], J.O. Cross[4], Y. Maeda[5], and C.E. Bouldin[6]

[1]Yeshiva University; [2]AIST, Tsukuba, Japan; [3]University of Illinois at Urbana-Champaign; [4]Argonne National Laboratory; [5]Osaka Prefecture University, Japan; [6]National Institute of Standards

Using intense x-rays from beamline X16C, scientists have developed a new method to determine the regularity in the arrangement of atoms, called short-range order, in heterogeneous mixtures of the same chemical element in amorphous and nanocrystalline states. The method combines two synchrotron techniques, X-ray Absorption Fine Structure (XAFS) and Diffraction Anomalous Fine Structure (DAFS). For a sample containing amorphous and nanocrystalline germanium supported by a silicon dioxide matrix, the XAFS-DAFS combination allowed the scientists to separately analyze the short-range order of the germanium atoms.

Anatoly Frenkel

Crystallization of amorphous materials and glasses is used to create commercial compact discs (CDs) and digital versatile disks (DVDs). The crystallization and amorphization rates can be increased, leading to faster and denser optical recording, by understanding how atoms interact within the material. Other possible applications resulting from this knowledge include studies of materials such as quantum dots, which are collections of between 100 and 1000 atoms, ion-damaged materials, and thin-film oxides.

We studied the local structure of a sample containing amorphous and crystalline germanium supported by a silicon dioxide matrix. The sample was annealed – heated and then slowly cooled down –, leading to the formation of tiny, roughly spherical crystals, or nanocrystals, about 15 to 20 nanometers in size (**Figure 1**).

In this sample, three phases: amorphous germanium, nanocrystalline germanium, as well as a fraction of germanium oxide, coexisted in small regions, each several tens of nanometers in size, within the silicon dioxide host matrix. The structural analysis of these regions was particularly challenging because of their small size, the heterogeneity of the mixture inside the region, and the interfacial disorder between the three phases.

Due to the absence of the long-range order – the existence of a pattern that is regularly repeated – in an amorphous phase, x-ray absorption fine structure (XAFS) is the technique usually used to solve the local structure in the amorphous germanium. In this technique, x-rays are projected onto the sample, and the ratio of absorbed photons versus total incident photons is measured at different x-ray energies to determine the nature and structure of the atoms in the sample. But because nanocrystalline germanium and germanium-oxide are also present in the sample, the XAFS signal is averaged over all germanium atoms.

Therefore, to disentangle the *local structures* of the amorphous and nanocrystalline germanium phases, as well as the germanium-oxide phase from the *average* structure around germanium atoms, it is essential to measure a partial XAFS signal from germanium atoms in the

BEAMLINE
X16C

Funding
Seitz Materials Research Laboratory; University of Illinois at Urbana-Champaign; Yeshiva University Research Foundation

Publication
A.I. Frenkel et al., "Direct Separation of Short Range Order in Intermixed Nanocrystalline and Amorphous Phases," *Physical Review Letters*, 89, 285503 (2002).

Contact information
Anatoly I. Frenkel, Physics Department, Yeshiva University, New York, NY

Email: frenkel@bnl.gov
Web page: http://www.yu.edu/faculty/afrenkel

nanocrystalline phase. Then, co-refinement of the two XAFS signals, the one pertaining to the average germanium and the one related to the nanocrystalline germanium phase, would provide information on the short range order – regularity in the arrangement of atoms relative to their close neighboring atoms – of germanium in all three phases.

A technique serving this purpose is called the Diffraction Anomalous Fine Structure (DAFS). It is a hybrid of x-ray diffraction (XRD), in which x-rays are scattered by the atoms of an *ordered* phase, and XAFS, where the x-rays probe the *local* structure around specific type of atoms only. Thus, by using DAFS, it is possible to *selectively* probe the structure of nanocrystals and completely ignore the other phases in the sample (**Figure 2**).

The XRD, XAFS, and DAFS measurements were performed using a custom-designed diffraction instrument, or diffractometer, at beamline X16C. From the co-refinement of nanocrystalline germanium XAFS and the average germanium XAFS data, the mixing fractions and the nearest neighbor bond distances in all three phases were obtained. Interestingly, we found that the germanium-germanium distance in the amorphous germanium phase is three percent longer than that in the nanocrystalline germanium phase. We believe that this difference is due to the large contribution of long germanium-germanium bonds located within the distorted amorphous-nanocrystalline interface layers.

This work illustrates that a combination of the DAFS and XAFS techniques can be used to determine the short-range order around a single atomic type in a sample of mixed ordered and disordered phases.

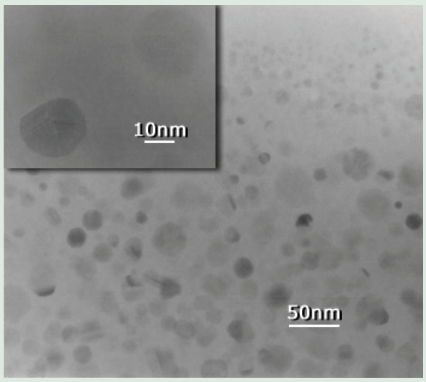

Figure 1. Image obtained by a transmission electron microscope of a sample of germanium nanocrystallites embedded in silicon dioxide.

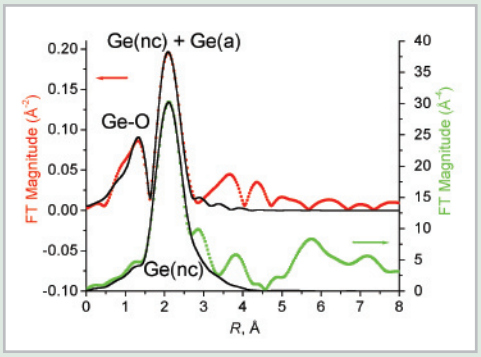

Figure 2. (Top curve): Experimental (red dots) and theoretical (solid, black) signals for germanium-oxide phase and the averaged nanocrystalline and amorphous germanium phase. (Bottom curve): Experimental (green dots) and theoretical (solid, black) signals by using the diffraction anomalous fine structure (DAFS) technique, showing that the contribution of the nanocrystalline phase is separated from the averaged nanocrystalline and amorphous phase.

Structure of Manganese Zinc Ferrite Nanomagnets

S. Calvin[1], S.A. Morrison[2], E.E. Carpenter[1], and V.G. Harris[1]

[1]Naval Research Laboratory; [2]George Washington University

Scientists at the Naval Research Laboratory have synthesized nanoscale manganese zinc ferrite (MZFO) particles using colloidal aggregates of amphiphilic molecules (having a water-soluble and a water-insoluble component). By using a technique called extended x-ray absorption fine structure (EXAFS) spectroscopy at beamline X11A, the scientists have determined the distribution of the manganese, zinc, and iron ions between the lattice sites of MZFO to a precision of eight percentage points.

Nanoscale magnets hold great promise for a wide range of future technologies: Aside from improving the performance of microwave filters and power supplies, they could be used in targeted delivery of pharmaceuticals and as biological sensors. Although scientists have been synthesizing nanoscale magnets for many years, the magnetic particles have generally been produced with a wide range of sizes, whereas most applications require particles with a narrow size distribution, called monodisperse particles.

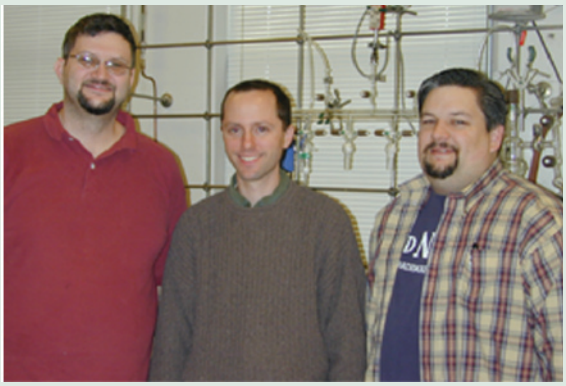

Authors (from left): Everett Carpenter, Scott Calvin, and Shannon Morrison

We created monodisperse nanoparticles made of manganese zinc ferrite (MZFO) by using micelles (**Figure 1**), which are colloidal aggregates of thousands of amphiphilic molecules (having a water-soluble and a water-insoluble component). The micelles were formed by adding a small amount of the surfactants nonylphenol poly(oxyethylene)$_5$ and nonylphenol poly(oxyethylene)$_9$ and water to cyclohexane. Micelle self-assembly sequesters the water into tiny droplets of a uniform size determined by the water-to-surfactant ratio, which limits the size of particles formed via aqueous reactions. In our case, the particles were approximately 11 nanometers in diameter.

In addition to the problem of monodispersion, the atomic-level structure of nanomagnets in their early development is not well known, so that the characteristics of devices made of nanomagnets are not well defined either. In the case of MZFOs, the manganese, zinc, and iron ions can each potentially reside in two different environments: tetrahedral sites surrounded by four oxygens, or octahedral sites surrounded by six oxygens. By knowing the distribution of the ions between these sites, scientists and engineers can better predict the performance of the materials made of MZFOs.

We studied the structure of MZFO by using extended x-ray absorption fine structure (EXAFS) spectroscopy at beamline X11A. In order to determine the distributions of the manganese, zinc, and iron ions, we first measured the ratio of absorbed photons versus the total incident photons. Then, we compared the experimental spectra to theoretical spectra, and developed a model of mixed ferrite materials for the purpose of extracting information from the absorption spectra.

Previous EXAFS studies of magnetic nanoparticles have looked at each metal absorption spectrum separately, allowing scientists to identify, for example, that the zinc ions were in a tetrahedral environment and that

BEAMLINE
X11A

Funding
DARPA Metamaterials Program

Publication
S. Calvin, et al., "Use of Multiple-Edge Refinement of Extended X-ray Absorption Fine Structure to Determine Site Occupancy in Mixed Ferrite Nanoparticles," *Appl. Phys. Letts.*, 81, 20, 3828-3830 (2003).

Contact information
Scott Calvin, Naval Research Laboratory, Code 6340, Washington, DC

Email: SCalvin100@aol.com

the iron and manganese were distributed between tetrahedral and octahedral environments. But, in these studies, scientists could not easily untangle the tetrahedral and octahedral contributions, and determine precise quantitative distributions.

In this study, we fit the models to all three metal edges simultaneously, so that the result was constrained to agree with the stoichiometry of the material and lead to a precision of about eight percentage points for the distribution of manganese, zinc, and iron ions. The technique outlined here promises to be an important tool in determining the structure of magnetic nanoparticle materials.

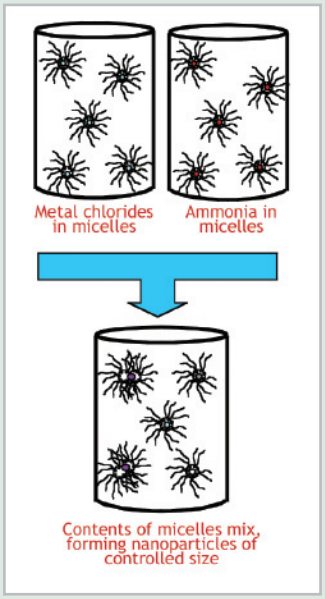

Figure 1. Schematic of reverse micellar method of nanoparticle synthesis.

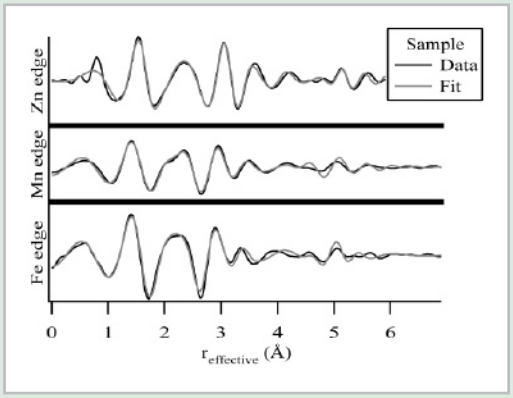

Figure 2. Real part of the Fourier transform of the EXAFS data for one sample, along with the fitted theoretical model. Above 1 Å the lower limit of validity for the fitting algorithm) the fitted models reproduce the data with high accuracy, confirming that the nanoparticles adopted the spinel ferrite structure.

Study of Amphiphilic Gold-Dendrimer Nanocomposite Monolayers

Y.-S. Seo[1], K.-S. Kim[1], K. Shin[1], H. White[1], M. Rafailovich[1], J. Sokolov[1], B. Lin[2], H.J. Kim[3], C. Zhang[4], and L. Balogh[4]

[1]SUNY at Stony Brook; [2]University of Chicago; [3]Argonne National Laboratory; [4]University of Michigan

Dendrimer-based nanocomposites are novel organic-inorganic hybrid molecular structures that are synthesized by dispersing very small inorganic molecules in nano-scaled branched polymeric networks and could be applied in catalysis and drug delivery. Since these nanocmomposites are often used both in aqueous media as well as coatings on solid substrates, we tried to determine how they respond to changes in their physical environment by using x-ray reflectivity. We find that the behavior of these structures significantly changes between aqueous and attractive solid substrates and that these structures are very sensitive to whether the solution is acidic or basic, so that they can be used either as sensors or drug delivery agents.

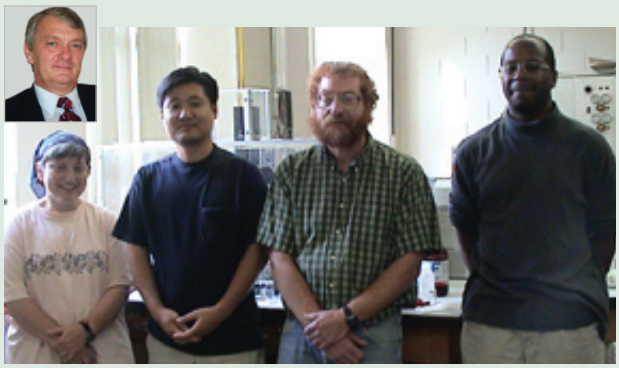

Authors (from left, top): Lajos Balogh, Miriam Rafailovich, Young-Soo Seo, Jonathan Sokolov, and Henry White

A dendrimer is a macromolecular structure containing connectors and branching units built around a small molecule or a linear polymer core, creating stepwise attachment of layers, called generations, that are nearly spherical. This highly symmetrical structure contains a large number of regularly spaced internal and external functional groups that interact with the molecular environment.

One well-studied dendrimer is poly(amidoamine) (PAMAM), which could be used as a building block for molecular-sized medical devices because it contains beta-alanine repeat units (which are amino acids, or basic units of proteins), and thus can be considered as spherical artificial proteins. The interaction of PAMAM with a biological object may be adjusted by modifying the dendrimer's surface properties. But it is extremely difficult to observe PAMAM dendrimers directly in cells or in tissue, because they do not easily give rise to color in organic substances.

Instead, another type of dendrimer, called dendrimer nanocomposite (DNC), can easily be observed by transmission electron microscopy and by other optical methods, so they are promising materials for biomedical nanotechnology.

We synthesized amphiphilic DNCs made of gold and PAMAM by dispersing gold atoms without covalent bonds inside dendrimer molecules (**Figure 1**). We investigated the properties of the DNC monolayer at the air/water interface at NSLS beamline X19C (**Figure 2a**) and on a solid substrate made of a Langmuir-Blodgett film (monomolecular layer containing molecules that are both water-loving and water-repelling) at NSLS beamline X10B (**Figure 2b**) using x-ray reflectivity.

Because of the small amount of gold present in the DNCs and the refractive index contrast between the gold domains and the water substrate, we successfully conducted *in situ* x-ray reflectivity measurements of the DNC. We found that the dendrimer layer is hydrated and the gold is uniformly distributed within the dendrimer body. The second-generation dendrimer was spherical on the water surface, while

BEAMLINE
X19C, X10B

Funding
Materials Research Science and Engineering Center, National Science Foundation; U.S. Department of Energy; Korea Science & Engineering Foundation (KOSEF)

Publication
Young-Soo Seo et al., "Morphology of Amphiphilic Gold-Dendrimer Nanocomposite Monolayers," *Langmuir*, 18, 5927-5932 (2002).

Contact information
Young-Soo Seo, Department of Materials Science, Stony Brook University, NY

Email: ysseo@nist.gov

the fourth-generation had a pancake-like, or oblate, structure at high pressures.

We also found that the shape of the DNCs was very sensitive to the acidity of the solution, indicating that these DNC could be used as detectors of biological activity or drug delivery systems.

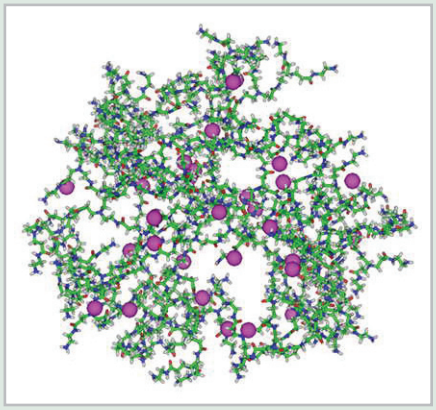

Figure 1. Computer simulation of the gold atom distribution in a dendrimer nanocomposite. (Courtesy of Inhan Lee, University of Michigan in Ann Arbor.)

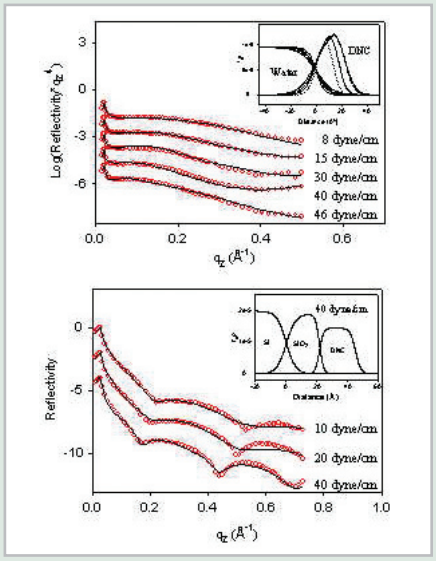

Figure 2. (a) X-reflectivity profiles of DNC monolayer at the air/water interface and (b) Langmuir-Blodgett films as a function of surface pressure and their corresponding scattering length density profiles in inset.

The Formation and the Spread of MoO_3 on Au(111): Study at a Molecular Level

Z. Song, T. Cai, Z. Chang, G. Liu, J.A. Rodriguez, and J. Hrbek

Chemistry Department, Brookhaven National Laboratory

The wetting and spreading of metal oxides on catalyst surfaces is one of the important processes for the preparation of highly dispersed monolayer catalytic particles. The formation and the spread of MoO_3 on Au(111) has been studied using photoemission and scanning transmission microscopy (STM). Molybdenum particles (~2 nm) on Au(111) were prepared by chemical vapor deposition (CVD) of $Mo(CO)_6$ and oxidized by NO_2 at elevated temperatures. The MoO_3 spread spontaneously over the surface to form two-dimensional fractal islands of amorphous MoO_3. A ramified-cluster-diffusion mechanism is proposed for the spreading of MoO_3.

Zhen Song

The spontaneous spread of many oxides and salts over catalytic supports has been used in the chemical industry to prepare highly dispersed monolayer catalysts, and to manufacture oxide films with specific electronic properties. Scientists have been discussing the spreading mechanism of oxides for two decades, trying to explain how the monolayer-thick film forms and spreads.

We prepared a model system for investigating the formation and the spread of MoO_3 on a Au(111) surface. We first deposited Mo on the Au surface and found by x-ray photoemission spectroscopy (XPS) that the Mo is metallic, and free of contaminants such as carbon or oxygen. The Mo growth on the Au surface is self-limited with narrow-sized metal particles about 1.8 nm in diameter. These Mo particles aggregate without coalescence, forming ramified islands with the arms extending preferentially along the fcc troughs or the domain boundaries of the Au(111) herringbone reconstruction (**Figure 1**).

O_2 is not efficient for the oxidation of the Mo on Au, especially for small Mo coverages. Thus, no oxidized Mo species is observed upon the reaction with O_2 at temperatures up to 850 K (**Figure 2**). Density function calculations suggest that the Mo particles may be capped by a layer of Au and therefore rendered inert. However, adsorption and dissociation of NO_2 on metal surfaces at elevated temperatures is known to generate a reactive form of chemisorbed atomic oxygen that can oxidize the Mo clusters to MoO_3 at 500 K readily, as we have shown in this work (**Figure 2**). The MoO_3 spreads over the Au surface along the troughs of the Au(111) surface at 500 K, and the spreading becomes random at 600 K. The important finding is that the MoO_3 spreads in a ramified way and forms *fractal* two-dimensional islands under ultra-high vacuum (UHV) conditions. Molecule-resolved scanning transmission microscopy (STM) images show the highly disordered arrangement of the MoO_3 molecules within the islands; the average distance between two adjacent molecules is ~0.38 nm. The island covered area increases by a factor of six compared with the original metallic Mo/Au sample (**Figure 1**).

Previous studies have suggested three mechanisms for the spontaneous spread of MoO_3 over surfaces, namely transportation via gas phase, unrolling-carpet, and free surface diffusion mechanisms. These mechanisms are mutually exclusive, and neither is capable of explaining all of

BEAMLINE
U7A

Funding
U.S. Department of Energy

Publication
Z. Song, T. Cai, Z. Chang, G. Liu, J.A. Rodriguez, and J. Hrbek, "Molecular Level Study of the Formation and the Spread of MoO_3 on Au (111) by Scanning Tunneling Microscopy and X-ray Photoelectron Spectroscopy," *J. Am. Chem. Soc.*, 125, 8059 (2003).

Contact information
Jan Hrbek, Chemistry Department, Brookhaven National Laboratory

Email: hrbek@bnl.gov

the experimental results alone. We suggest a ramified-cluster-diffusion mechanism for the spreading of MoO_3. The spread occurs via the diffusion of MoO_3 clusters detached from the bulk MoO_3 at temperatures above 500 K. This diffusion is a thermally activated process, and an anisotropic diffusion barrier at the edge of the island leads to the ramified spreading and the formation of the fractal islands. This mechanism explains the process of spreading on the nanoscale for all results in this and previous studies.

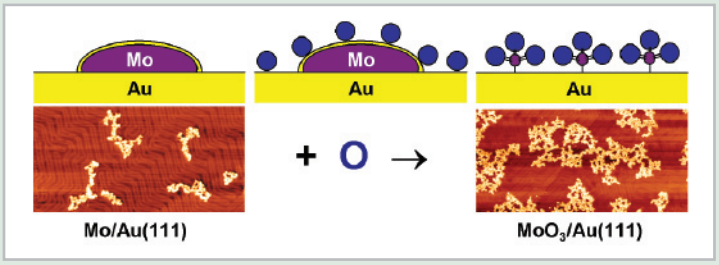

Figure 1. STM images of the Mo particles and MoO_3 submonolayer film on Au(111), and cartoons for the MoO_3 formation and spreading on the Au surface.

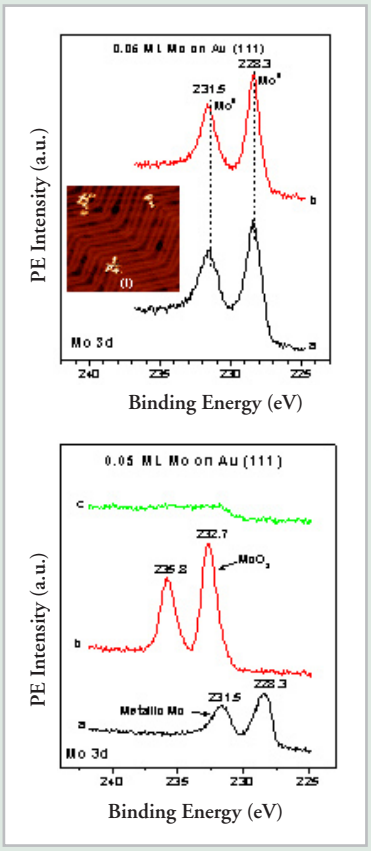

Figure 2. Mo nanoclusters after the interaction with O_2 (top panel) and NO_2 (bottom panel) at 500 K.

X-Ray Characterization of 3-Layer Assembly of 4 nm FePt Nanoparticles

S. Sun[1], S. Anders[2], T. Thomson[2], J.E.E. Baglin[2], M.F. Toney[2,3], H.F. Hamann[1], C.B. Murray[1], and B.D. Terris[2]

[1]IBM T.J. Watson Research Center; [2]IBM Almaden Research Center; [3]Stanford Synchrotron Radiation Laboratory, Stanford Linear Accelerator Center

Scientists from IBM's Thomas J. Watson Research Center in Yorktown Heights, New York and Almaden Research Center in San Jose, California have developed a chemical reduction process for making monodisperse 4 nm FePt nanoparticles. Further, they used polymer-mediated self-assembly approach to assemble the 4 nm FePt nanoparticles on various substrates. By using X-ray diffraction (XRD) in grazing incidence geometry at beamline X20C, the scientists have determined the structure of the assembly and the particles, and studied the aggregation behavior of the particles in an assembly of 3 nanoparticle layers under thermal annealing conditions.

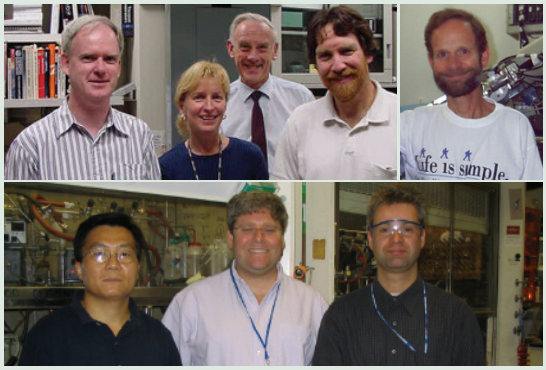

The authors (from left, top): Thomas Thomson, Simone Anders, John E.E. Baglin, Bruce D. Terris, and Mike F. Toney, (bottom) Shouheng Sun, C.B. Murray, and Hendrik F. Hamann

Hard magnetic FePt nanoparticles have attracted great interest because of their potential applications in ultrahigh density magnetic recording, highly sensitive magnetic sensors, and advanced nanocomposite permanent magnets. Recent advances in magnetic recording technology have indicated that if self-assembled in a tightly packed, exchange-decoupled array with controlled magnetic easy axis direction, these FePt nanoparticles would be a candidate for future ultrahigh density data storage media with potentially one bit per particle.

We report a simple chemical process for synthesizing FePt nanoparticles by the reduction of $FeCl_2$ and $Pt(acac)_2$. The particle growth is self-limited and 4 nm FePt nanoparticles are readily separated. The initial molar ratio of the metal precursors is carried over to the final product, and the FePt composition is easily tuned. We further demonstrated that alternate adsorption of polyethylenimine (PEI) and FePt nanoparticles on a hydroxyl (HO)-terminated surface via surface ligand exchange led to 4 nm FePt nanoparticle assemblies with controlled thickness. **Figure 1A** illustrates the general assembly approach.

We characterized the layered structure using X-ray reflectivity measurements using $CuK_{\alpha 1}$ radiation from an 18 kW X-ray generator. X-ray reflectivity measures the electron density of the nanoparticle assembly, which can be converted into mass density. The result of this analysis for a 3-layer assembly is shown in **Figure 1B**, which plots mass density as a function of position from the silicon substrate surface. The three layers are readily evident as regions of larger mass density than the PEI between the nanoparticle layers. The spacing between both the first-second and second-third layers is 6.5 nm.

We studied the structure of the FePt nanoparticles in a thin assembly using X-ray diffraction (XRD) measurements performed in grazing incidence geometry at beamline X20C. As shown in **Figure 2**, the XRD of the as-synthesized FePt particles reveals a typical chemically disordered fcc structure, in which Fe and Pt atoms randomly occupy the fcc lattice sites. Thermal annealing induces the Fe and Pt atoms to rearrange into the chemically ordered face-centered tetragonal structure,

BEAMLINE
X20C

Funding
U.S. Department of Energy

Publication
S. Sun, S. Anders, T. Thomson, J.E.E. Baglin, M.F. Toney, H.F. Hamann, C.B. Murray, and B.D. Terris, "Controlled Synthesis and Assembly of FePt Nanoparticles," *J. Phys. Chem. B*, 107, 5419 (2003).

Contact information
Shouheng Sun, IBM T.J. Watson Research Center, Yorktown Heights, NY

Email: ssun@us.ibm.com

which can be viewed as a natural superlattice of alternating Fe and Pt atomic planes along the (001) direction (**Figure 2**). From the line width of the (111) peak of the fct ordered FePt, we have also estimated the (111) coherence length that is related to the particle size. The average particle size increases with annealing temperature and duration. The particle size estimated from XRD line width for 3 layer assemblies (**Figure 2**) is 5 nm for the assemblies annealed at 580°C for 30 minutes, but rises to 17 nm for those annealed at 800°C for 5 minutes. The work demonstrates that synchrotron radiation is a powerful characterization tool for thin (~10 nm) FePt nanoparticle assemblies.

Additional Publication:

S. Anders, M.F. Toney, T. Thomson, R.F. Farrow, J.-U. Thiele, B.D. Terris, S. Sun, and C.B. Murray, "X-ray Absorption and Diffraction Studies of Thin Polymer/FePt Nanoparticle Assemblies," *J. Appl. Phys.*, 93, 6299 (2003).

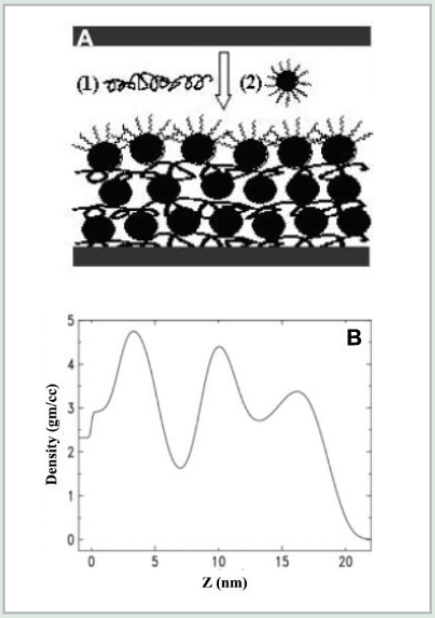

Figure 1. (A) Schematic illustration of polymer-mediated self-assembly of FePt nanoparticles by alternately adsorbing a layer of polymer (PEI) and a layer of nanoparticles on a solid surface; and (B) Mass density of a 3-layer FePt assembly, deduced from the X-ray reflectivity measurement, as a function of position from the silicon substrate (z). The silicon surface is arbitrarily defined as z = 0.

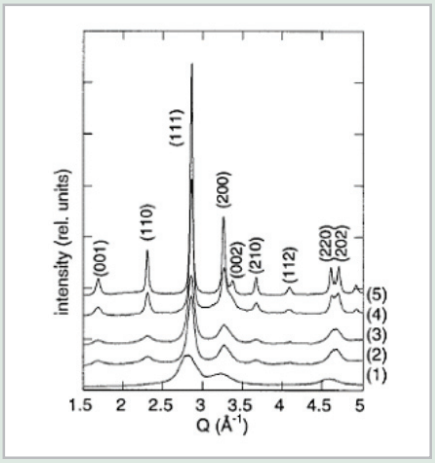

Figure 2. In-plane X-ray diffraction of 3-layer $Fe_{58}Pt_{42}$ assemblies as function of annealing: (a) as deposited, (b) 580°C for 30 min, (c) 650°C for 5 min, (d) 700°C for 5 min, (b) 800°C for 5 min. The ordinate is the scattering vector Q, which is the difference between incident and diffracted X-rays. It has magnitude Q= (4π/λ) sin θ, where λ is the X-ray wavelength (about 0.12 nm here) and θ is half the scattering angle. The index of diffraction peaks is marked.

Investigating a Surface Science Mystery: The Case of the Disappearing Monolayer

K.S. Schneider[1], T.M. Owens[1], D.R. Fosnacht[1], B.G. Orr[2,3], and M.M. Banaszak Holl[1,3]

[1]Chemistry Department, The University of Michigan; [2]Physics Department and the [3]Applied Physics Program, Harrison M. Randall Laboratory, The University of Michigan

A recent X-ray photoemission spectroscopy (XPS) and scanning tunneling microscopy (STM) investigation of an alkylsilane-based monolayer has yielded intriguing chemical and physical phenomena. In particular, oxidation of an octylsilane ($C_8H_{17}SiH_3$) monolayer chemisorbed to Au(111) via ambient atmosphere exposure yields two surprising results. First, the Au(111)-23×√3 surface reconstruction typical of a clean gold surface spontaneously regenerates underneath the oxidized (alkylsiloxane) monolayer. Furthermore, the physisorbed alkylsiloxane monolayer is completely transparent to STM imaging.

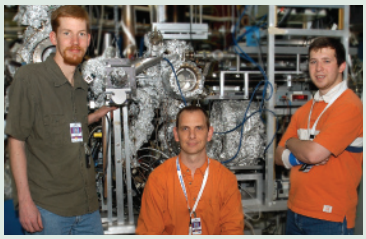

Authors (from left): Thomas M. Owens, Mark M. Banaszak Holl, Daniel R. Fosnacht, Kevin S. Schneider, and Bradford G. Orr

Frequently, the STM image contrast mechanism of organized organics—such as alkanethiols—on Au(111) is explained as a consequence of hydrocarbon chain crystallization and/or variations in chain angle or orientation. Similarly, subtle variations in alkyl chain angle or orientation may yield differing apparent heights of alkylsilane monolayer features as observed by STM. However, a recent XPS and STM investigation of an alkylsilane monolayer prior to and following oxidation suggests the alkyl chains are "transparent" to STM imaging and impart a negligible contrast contribution to the STM images.

A STM image of clean Au(111) displays the parallel striped features intrinsic to the 23×√3 surface reconstruction (**Figure 1a**). Monolayer formation via the exposure of Au(111)-23×√3 to a saturating gaseous pressure of octylsilane ($C_8H_{17}SiH_3$) in ultrahigh vacuum (UHV) yields a complex pattern of interwoven, sinuous ridge features containing numerous interstitial Au islands 20 – 40 Å in diameter (**Figure 1b**). The presence and quantity of the Au islands (~7% area coverage in **Figure 1b**) indicates the underlying 23×√3 surface reconstruction has fully relaxed to the unreconstructed Au(111)-1×1 phase.

Oxidation of the octylsilane monolayer via ambient atmosphere exposure results in the disappearance of monolayer features from the STM image (**Figure 1c**). The resulting substrate terraces are indistinguishable from clean Au(111)-23×√3 (having identical lateral and vertical dimensions) under the imaging conditions employed. STM image features of the exposed monolayer do not vary with changes in tunneling current (0.01 – 2 nA) or applied sample bias (± 2 V). However, exposure to additional octylsilane does not regenerate the image shown in **Figure 1b**. Instead, an image identical to clean Au(111)-23×√3 remains (**Figure 1d**). Therefore, the "clean gold" surface displayed in **Figure 1c** does not have identical chemical properties of the authentic clean gold surface illustrated in **Figure 1a**. On the basis of STM data alone, this set of results was mysterious!

Direct chemical analysis of oxidized sample surfaces has been performed using soft X-ray photoemission spectroscopy (SXPS) at beamline U8B.

BEAMLINE
U8B

Funding
Department of Energy; National Science Foundation; RHK Technology Inc.

Publication
K.S. Schneider, T.M. Owens, D.R. Fosnacht, B.G. Orr, and M.M. Banaszak Holl, "The Case of the Disappearing Monolayer: Alkylsilane Monolayer Formation, Oxidation, and Subsequent Transparency to Scanning Tunneling Microscopy," *ChemPhysChem.*, 4, 1111-1114, (2003).

Contact information
M.M. Banaszak Holl, Associate Professor, The University of Michigan

Email: mbanasza@umich.edu

Beamline U8B is perfectly suited to obtaining the high-resolution Si 2p core-level needed for this study, as well as the valence band region. Note that, due to the presence of an Au plasmon trailing the Au 4f core level, conventional XPS of the Si 2p core-level for these monolayers provides no information. Following exposure to ambient atmosphere, the Si 2p core level of the unoxidized octylsilane monolayer (**Figure 2a**) shifts by 2.3 eV to a higher binding energy and the peak full width at half-maximum (fwhm) increases (**Figure 2b**). The binding energy shift and peak broadening indicate the formation of a cross-linked $RSiO_3$ and/or $(ROSiO_{1.5})_n$ network. The C 2s features arising from the octyl chain are retained in the valence band data (-12 to -20 eV), indicating the presence of intact alkyl chains in the oxidized monolayer (**Figure 2d**). In summary, the XPS data indicate that exposure to ambient atmosphere effectively oxidizes the silicon head-groups; however, all of the silicon and alkyl chains are retained within the oxidized monolayer. Thus, the STM image displayed in **Figure 1c** does indeed have the monolayer present, albeit it in an oxidized form.

The combination of SXPS and STM data suggest the original octylsilane monolayer image in **Figure 1b** is the result of significant mixing of Au and Si states. Oxidation of the Si head-groups removes this interaction, causing the underlying substrate to regenerate the Au(111)-23×√3 surface reconstruction, and leaving only the Au states to image. In this case, the alkyl chains are "transparent" in both **Figures 1b** and **1c** and it is only the Au-Si interaction that changes upon oxidation. Since monolayer oxidation severs all Au-Si bonds, a completely "transparent" physisorbed alkylsiloxane layer remains on top of the reconstructed Au(111)-23×√3 surface.

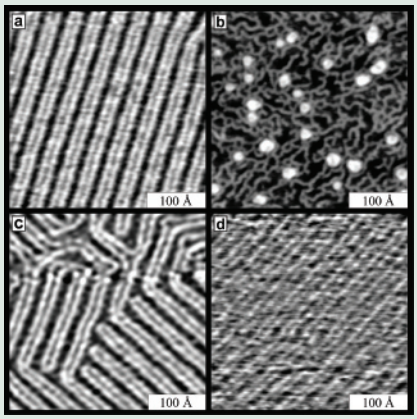

Figure 1. UHV-STM images of the same Au(111) sample (different sample areas), following successive experimental steps. All images are 35 nm × 35 nm. (a) Clean Au(111) 23×√3. (b) Chemisorbed octylsilane monolayer formed on (a) following exposure to 50 L (L = langmuir = 1 × 10^{-6} torr·s) gaseous octylsilane in UHV. (c) Oxidized physisorbed alkylsiloxane monolayer formed following exposure of (b) to ambient atmosphere for 15 minutes. (d) Oxidized physisorbed alkylsiloxane monolayer in (c) following exposure to 50 L gaseous octylsilane in UHV.

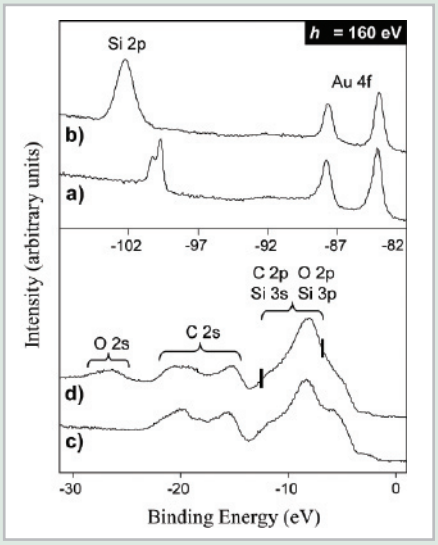

Figure 2. Soft X-ray photoemission spectra. (a) Si 2p and Au 4f core level spectrum of an octylsilane monolayer on Au(111). (b) Si 2p and Au 4f core level spectrum of the monolayer in (a), following exposure to ambient atmosphere for 15 minutes. (c) Valence band spectrum of an octlysilane monolayer on Au(111). (d) Valence band spectrum of the octylsilane monolayer in (c) following exposure to ambient atmosphere for 15 minutes.

Magnetic Switching in Multilayer 'Nanomagnets'

F.J. Castaño[1], Y. Hao[1], S. Haratani[1], C.A. Ross[1], B. Vögeli[2], H.I. Smith[2], C. Sánchez-Hanke[3], C-C. Kao[3], X. Zhu[4], and P. Grütter[4]

[1]Department of Materials Science and Engineering, MIT; [2]Department of Electrical Engineering and Computer Science, MIT; [3]NSLS, BNL; [4]Center for the Physics of Materials, Department of Physics, McGill University

This study investigated the magnetization reversal processes that take place in arrays of lithographically-patterned magnetic bars. Each bar is 70 nm x 550 nm in dimension, and is made from a NiFe 6 nm/ Cu 3 nm/ Co 4 nm multilayer stack. Arrays of these nanomagnets were characterized using a combination of magnetic force microscopy (MFM), alternating gradient magnetometry (AGM), and scattering experiments using synchrotron radiation. Both magnetic layers (i.e. the Co and the NiFe) form single-domain states at remanence and switch abruptly, but the collective magnetization reversal of the array shows a wide distribution of switching fields due to variability between the elements. Elementally-specific hysteresis loops obtained from synchrotron scattering experiments enable the separate reversal of the Ni, Fe, and Co to be followed.

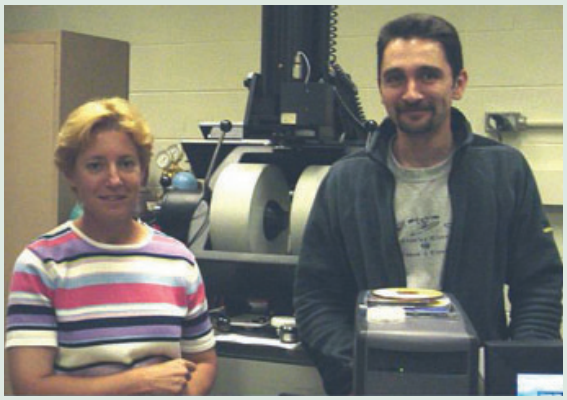

CA. Ross and F.J. Castaño

The magnetic properties of lithographically-defined multilayered magnetic solids are of considerable interest for the development of high-density magnetoresistive random access memory (MRAM) devices. The nanoscale bar-shaped magnets used as memory cells in MRAMs are composed of at least two magnetic layers sandwiching a non-magnetic insulating or metallic spacer. Future high-density MRAM devices will require layered magnetic structures with thicknesses below a few tens of nanometers and in-plane dimensions in the sub-100 nm regime. Within these structures, the individual magnetic layers are magnetized parallel to their length, and their switching field depends on their dimensions and compositions. Additionally, the magnetic layers interact by both exchange and magnetostatic coupling, which modifies the switching field and stabilizes specific remanent states.

In this work, we first used MFM to show that individual Co/Cu/NiFe sandwich nanomagnets could be magnetized into four distinct states, labelled A-D in **Figure 1**. For comparison, AGM measurements, measured on a piece of the array containing ~10^9 nanomagnets, show the structures switching from state A to B to D as the field is swept from +1000 Oe to –1000 Oe. As the field sweeps from –1000 Oe to +1000 Oe the structures switch from state D to C to A (**Figure 1**). Minor loops (shown as solid points) allow the switching field of the NiFe layers and the interaction field (i.e. the field that the Co exerts on the NiFe) to be measured. In this sample the Co hard layers reverse over a range of fields centered at 410 Oe. The interaction field was 60 Oe and the switching field of the NiFe layers was 125 Oe.

In addition, utilizing modulated circularly polarized soft x-rays from the X13A beamline, both reflectivity and magnetic circular dichroism (MCD) patterns were measured for these arrays. The magnetic parameters deduced from elementally-specific hysteresis loops, obtained from the difference signal close to the L_3 absorption edge of the Co and Ni present in the sample, agreed well with those measured by AGM. In the

BEAMLINE
X13A

Funding
MIT; TDK Corp., Japan; DARPA; McGill; NSERC and FCAR

Publication
F.J. Castano, Y. Hao, S. Haratani, C.A. Ross, B. Vogeli, H.I. Smith, C. Sanchez-Hanke, C.-C. Kao, X. Zhu, and P. Grutter, "Magnetic Force Microscopy and X-ray Scattering Study of 70 x 550 nm^2 Pseudo-spin-Valve Nanomagnets, *J. Appl. Phys.*, 93, 7927 (2003).

Contact information
Caroline Ross, Department of Materials Science and Engineering, Massachusetts Instititute of Technology

Email: caross@mit.edu

data of **Figure 2**, the reversal of the Ni and Fe occurs at identical fields, as expected, while the Co reverses at a higher field. The Ni and Fe loops are both offset from zero by 40 Oe, as a result of the interaction field. All three elements show a distribution of switching fields consistent with AGM data. The average coercive field for the Ni was 120 Oe and for the Co was 410 Oe, which is similar to the results obtained from AGM. These experiments show that synchrotron experiments provide a valuable measurement of magnetization reversal, even in buried layers, and can be used to track the behavior of complex multilayered magnetic structures.

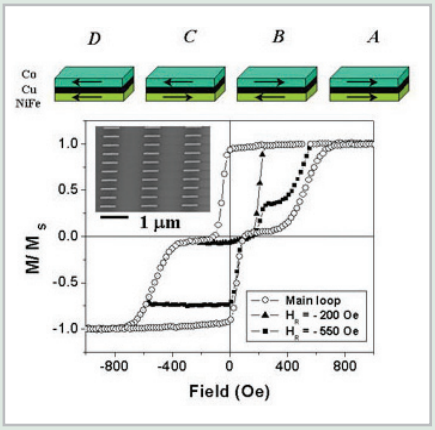

Figure 1. Room temperature hysteresis loops and minor loop measurements of a 70 x 550 nm² NiFe/Cu/Co PSV nanomagnet array. The reversing fields of the minor loops are -200 Oe (full triangles) and -550 Oe (full squares), respectively. The inset shows a scanning electron micrography of the sample. A schematic representation of the four possible orientations of the magnetization of both magnetic layers is also depicted.

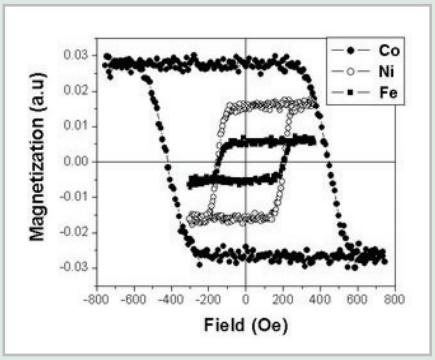

Figure 2. Elementally-specific hysteresis loops, deduced from magnetic circular dichroism-measurements, on an array of 70 x 180 nm² NiFe/Cu/Co PSV nanomagnets.

Year in Review

Workshop on Frontiers in Synchrotron X-Ray Microbeam Diffraction

January 10, 2003

The Workshop on Frontiers in Synchrotron X-Ray Microbeam Diffraction was held on January 10, 2003 in the Hamilton seminar room in the Chemistry Department at BNL, with a large gathering of over 40 people. The purpose of this workshop was to inform the scientific, university, and industrial community of the plans to design and install a state-of-the-art microdiffraction instrument at NSLS mini-gap undulator beamline X13B. This proposal was submitted to the DOE Office of Science towards the end of January and would be operated as a general user facility with an emphasis on nanoscale research. Opportunities in the cutting-edge science that could be accomplished with this instrument were explored, and user input was solicited.

The workshop was introduced and chaired by Dr. Elaine DiMasi (BNL Physics Dept.), who also outlined the motivation for the proposed instrument. The value of cutting-edge user facilities was described from the perspective of BNL management by Dr. Doon Gibbs, Associate Laboratory Director for Basics Energy Sciences (BES). He emphasized the importance to DOE and BNL of interacting with users at an early stage so that they can influence the evolutionary process by which new facilities are developed and built. He described the organizational structure of BNL BES as well as a number of exciting planned projects. Two such projects that will have a great impact on microbeam diffraction science at BNL are the proposed upgrade to the NSLS and the Center for Functional Nanomaterials (CFN). Dr. Gibbs concluded his presentation with a challenge to the audience to come up with ideas about scientific impacts that can be made by the future NSLS.

The CFN was further elaborated upon by NSLS scientist Dr. Ron Pindak. The CFN is one of five new DOE Nanoscale Science Research Centers (NSRCs). The user programs of the five centers were launched at a workshop in Washington DC on February 26-28, 2003. The CFN has six scientific themes that involve interdisciplinary research on diverse systems, which are listed and described on the CFN website, http://www.cfn.bnl.gov/. The instrumentation and capabilities of the CFN are organized into "lab clusters," such as materials synthesis, proximal probes, nanopatterning, etc. The CFN will be a user facility similar to the NSLS and both user programs will be coordinated through a common user office. Thus, one proposal can allow access to NSLS beamlines as well as CFN lab tools. Two of the NSLS beamlines, a SAXS beamline on X21 and the X13B microdiffraction beamline, will be optimized to service the needs of CFN General Users. The center, in addition to having the infrastructure to support state-of-the-art fabrication facilities, will provide offices and interaction areas for students and postdocs as well as regular staff.

Frontiers in Synchrotron X-Ray Microbeam Diffraction workshop attendees.

Dr. Patricia Mooney of IBM presented a talk on materials research for silicon CMOS technology using microbeam x-ray sources. Strain-relaxed SiGe "virtual substrates" for strained silicon CMOS transistors were described and results of studies characterizing the defect microstructure of these films were presented. Dr. Mooney remarked on how the divergent beam available at X20A of the NSLS limited the resolution at which "micrograins" could be observed, and that a sub-micron, more parallel beam would be of great advantage in her work.

A survey of synchrotron microdiffraction capabilities around the world was given by Prof. Cev Noyan of IBM. He pointed out that several synchrotrons, in particular the ESRF and ALS, have put great emphasis and resources into microbeam diffraction. The great vari-

ety in hard x-ray microfocusing optics and a number of designs for accessing reciprocal space (pink beam Laue, scanning monochromator Laue, small sphere-of-confusion six-circle, single-axis, etc.) were explained. The following two talks described in detail the microdiffraction capabilities currently available at the NSLS. Dr. Ken Evans-Lutterodt of Agere described the X16C microdiffraction beamline. He used the example of the selective growth of semiconductor materials on a patterned substrate to illustrate that microdiffraction combined with spectroscopy can be used to obtain strain and chemical composition information with micron-scale spatial resolution. Dr. Jean Jordan-Sweet of IBM next described the capabilities of beamline X20A. This capillary- and diffractometer-based instrument is primarily used to measure strain fields and mosaic structure by scanning diffraction topography. Results were presented on interfacial stress/strain in metal features on silicon and on electromigration-induced stress in narrow metal lines.

The proposed microdiffraction instrument to be built at X13B was described in the next two talks. Dr. James Ablett of the NSLS presented specifications and recently measured spectral plots of the new X13 Mini-Gap Undulator (MGU) source. He then described the plan to use a 4-bounce silicon monochromator and a variety of x-ray microfocusing optics for the proposed instrument. The monochromator can be removed for pink-beam studies, and the optics will be interchangeable between KB mirrors, capillary, pinholes, zone plates, and planar refractive lenses. The modular design will allow for great flexibility in beamsize and divergence selection. Dr. Ken Evans-Lutterodt further described the diffractometer and detector configurations. In order to minimize vibration and torque on the sample and optics, the detector arm will be a completely separate system. The entire microdiffraction instrument is being designed to be robust, easy to align and use, and modular, in order to serve a variety of users from students to busy experts.

After a break for lunch, the workshop resumed with presentations on scientific opportunities by researchers from a range of disciplines. Dr. Mehmet Sarikaya of the University of Washington began with an overview of the fascinating world of structural biomimetics. Biomaterials such as spiders' silk, mother-of-pearl, protein coats on certain bacteria, sea urchin spines, and sponge spicules exhibit nanoorganization. Understanding the structural, functional, and process design characteristics of these self-assembled structures will lead to the invention of engineered "bio-inspired" materials of the future. Next, Dr. DiMasi presented a talk prepared by Dr. Joanna Aizenberg of Lucent Technologies, which described how self-assembled nano structures of calcite crystals and other materials can be formed using organic alkane chain templates which have a variety of attached functional groups. These assemblies of crystals can be patterned and oriented in many ways by changing the functional group, chain tilt, and lithographic pattern. Following this talk, Prof. Valery Kiryukhin of Rutgers University described several correlated electronic systems that form functional materials, which exhibit large changes in electrical or magnetic properties (such as colossal magnetoresistance) under relatively weak external perturbations. He showed an example of strain mapping in the vicinity of a grain boundary taken at beamline 2ID-D at the APS. In order to study these systems, a microdiffraction instrument with temperature control, precise sample positioning, optical access, and tunable energy is needed. The scientific opportunity session was concluded with a talk by Dr. Jeffrey Kysar of Columbia University who discussed the difficulty in determining the relationship between stress and strain in materials. He has simplified the problem by reducing it from 3-D to 2-D by performing experiments using a line of applied force rather than the conventional point indenter on a metal

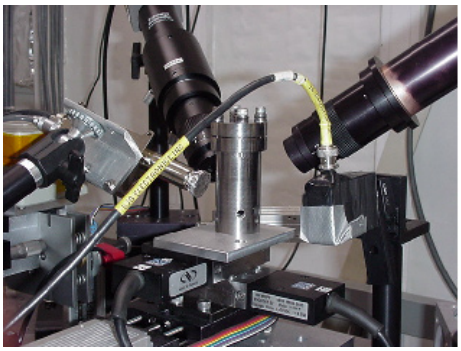

Microdiffraction setup at beamline X13B.

surface. A microbeam diffraction beamline would allow for the measurement of residual stresses and dislocation density on the surface of laser shock processed samples as a function of position from the "peened" line.

During the afternoon discussion session Dr. DiMasi read letters from members of the Clay Minerals Society email listserver. These researchers would like to see an instrument having high brilliance, a sensitive area detector, variable spot size, and control over temperature and humidity. Audience members also supported the desire for environmental control, citing the need to study self-assembly experiments in liquid solution rather than in just the dried post-assembly state. There is a need to get all information - tilt, chemical, lattice spacing, transformation temperature, etc., from single grains on the order of a micron in size. Many times the need for a parallel beam was mentioned. A discussion about the measurement of organic and bio-materials brought up legitimate concern over the possibility of beam damage. Another desired capability mentioned several times is computed tomography. Questions were asked about the time structure of the existing NSLS x-ray ring vs. the proposed upgrade. Pump-probe experiments are possible now with a ~0.5 nanosecond period, and in the future with ~20 femtosecond resolution. The APS currently has a 50 picosecond timing structure. It was pointed out that single-shot microdiffraction would not yield enough intensity, but a locked-in, repeated pump-probe setup would be able to accumulate enough signal.

The workshop concluded with committee members encouraging researchers to try microbeam experiments now on existing instruments, in order to see what is needed and what works. It is expected that the new microdiffraction beamline will constantly evolve over time, and experience now will lead to a better instrument in the future. Many components are available now or will be soon for experimental trials.

—Jean Jordan-Sweet

Two NSLS Scientists Win Engineering Awards

January 30, 2003

At the BNL Employee Recognition Award Ceremony on January 30, 17 Lab employees were rewarded with BNL's highest honors, including two NSLS scientists who won the $5,000 Engineering Awards, which are given to recognize distinguished contributions to engineering or computing over one or more years.

Donald Lynch, a project engineer who joined BNL in September 1991, and George Rakowsky, an electrical engineer who returned to BNL in July 1993, both at the NSLS, were recognized for their sustained contributions in the development of small-gap, in-vacuum undulators, a technology now adopted at most synchrotron radiation facilities in the world.

Pictured at right with Associate Laboratory Director for Facilities & Operations Mike Bebon (back, right) are the recipients of BNL's 2002 Engineering Award: (back, from left) Donald Lynch, NSLS Department; George Rakowsky, NSLS; Jack Fried, Instrumentation Division; (front, from left) George Ganetis, Magnet Division; Christopher Channing, Plant Engineering Division; and Joseph Levesque, Emergency Services Division.

The NSLS operates two electron storage rings: the 2.8-giga electron volt (GeV) x-ray ring and a 0.8-GeV vacuum ultraviolet ring, which contain periodic magnetic structures called wigglers and undulators, collectively known as insertion devices. Electrons are sent racing around the rings at nearly the speed of light. When they cross an insertion device, they emit a very intense, narrow beam of synchrotron radiation.

Earlier generations of undulators in medium-energy machines such as the NSLS x-ray ring are able to generate only "soft" x-rays, up to about 1 kilo electron volt (keV) of photon energy. The small-gap undulators generate tunable "hard" x-rays in the range of 3 to 20 keV, which are essential for decoding the structure of complex biological molecules in the rapidly expanding field of structural biology. Previously, tunable hard x-ray beams were available only at the very high-energy storage rings, such as the 7-GeV Advanced Photon Source at Argonne National Laboratory.

The idea of introducing a small-gap, short-period undulator in the NSLS

x-ray ring was originated in the late 1980s by Sam Krinsky, then NSLS Deputy Chair. Peter Stefan, then NSLS physicist, did the first proof-of-principle tests and developed the conceptual design of the small-gap undulator. Lynch worked with Stefan on the mechanical, structural, thermal, and vacuum design of the first two generations and on the latest version of the device.

Rakowsky proposed the magnetic design in 1991 and built a demonstration model, followed by the full-scale magnet arrays of the Prototype Small-Gap Undulator (PSGU) under contract for the NSLS, while he was employed at Rocketdyne, now part of Boeing, in California. After returning to BNL in 1993, Rakowsky worked with Lynch, Stefan and other collaborators at SPring8 in Japan, to develop the breakthrough In-Vacuum Undulator (IVUN).

Lynch and Rakowsky then developed the third-generation, higher-performance Mini-Gap Undulator (MGU), which has operated in the x-ray ring since January 2002. The MGU's compact size will allow the installation of two more MGUs, resulting in two new undulator beamlines. The next MGU was installed in May to serve a new beamline funded by the National Institutes of Health and dedicated to structural biology.

In developing these devices, still record-breakers as the smallest in their field, Rakowsky led the way in magnetic design and measurement, while Lynch provided the mechanical solutions to meet each challenge.

Their success has established the NSLS as the leader in small-gap undulator technology.

This innovation has dramatically changed light-source development world-wide to favor medium-energy machines of around 3-GeV over the more costly 6-to-8-GeV machines previously constructed as hard x-ray sources. The small-gap concept also serves as the basis for the NSLS 3-GeV upgrade proposal.

—Patrice Pages

BNL/Canadian Space Agency Experiment Lost in Tragic Columbia Accident

February 1, 2003

Among the 80 scientific experiments lost in the recent tragic accident involving the space shuttle Columbia, one was prepared by a team of scientists who would have studied the results at the NSLS. This experiment had been designed to provide insights into developing not only new drugs against cancer, but also drought-resistant plants.

The experiment is part of the Canadian Space Agency's Protein Crystal Growth (PCG) program, a project aimed at studying how proteins grow in space. A series of different protein crystal growth experiments were conducted in the recent Columbia mission, one of which is involved in a hallmark of cancer, called cachexia, which results in emaciation and muscle wasting. Another represented a protein used by plants to defend against environmental stress, such as drought and high salinity.

Protein crystal growth experiments were conducted on the Space Shuttle Columbia.

"Previous crystal growth experiments conducted in space have provided evidence that, when protein crystals grow in space, they are of higher quality, that is, they have fewer defects and may be of larger size than those grown on Earth," says Robert Sweet, BNL Biology Department and a PCG project collaborator. "But we know too little about the effectiveness of having crystals grow in space, where there is nearly no gravity. So we decided to compare crystals grown on Earth and in space."

Controlled Experiment

The PCG scientists, led by Jurgen Sygusch, a biochemist at the University of Montreal in Canada, designed a controlled experiment wherein duplicate samples of proteins in solution were taken to Kennedy Space Center (KSC), and one set of samples was taken into space on the space shuttle Columbia, one of five reusable spacecraft that had been employed by the National Aeronautics & Space Administration (NASA) since 1981.

While Columbia circled Earth from January 16 to 31, the protein samples on board were allowed to crystallize. At the same time, duplicate samples acting as controls were crystallized at KSC in the same type of crystallization hardware. If Columbia had returned to Earth, the two sets of samples were to have been compared with one another, using the intense light generated by the NSLS.

How Crystals Grow

"When crystals grow on Earth, gravity introduces disturbances that affect the way protein molecules assemble into a crystal lattice," Sygusch says. "But, in spacecraft such as Columbia, which orbit about 400 miles above Earth, crystal growth is subjected to only a millionth of Earth's gravity — called microgravity — so that the protein molecules during crystal growth are free of these disturbances, which is what we wanted to study."

In their experiment, the scientists planned to investigate two important disturbances, called convection and sedimentation, that occur during crystal growth.

"You can imagine a growing crystal being like layers of molecules that are piling up on each other," Sygusch says. "Non-crystalline aggregations of protein molecules that form naturally under crystal-growth conditions tend to disturb the deposition of these layers."

Sygusch explains that convection in the protein solution occurs because the protein is actually at a lower concentration, and therefore lower density, immediately adjacent to the growing crystal. This causes an upwelling of the solution that causes a surprisingly vigorous mixing of proteins and their aggregates.

As for sedimentation, once small crystallites have formed, they tend to sink to the bottom of the container, out of the zone of where they grew, and often cease growth.

Both convection and sedimentation affect crystal growth on Earth. In micro-gravity, the absence of convection eliminates solution mixing and reduces incorporation of protein aggregates into the crystal lattice, while no sedimentation allows crystallites to grow into larger crystals, leading to crystals of better quality. The higher crystallinity translates into a better definition of the atomic detail that can be obtained from synchrotron diffraction experiments.

"To get our results," Sweet says, "we had not only prepared two identical experiments, one on Earth and the other in space, but we had also decided that the data collected from both experiments would be analyzed in a double-blind fashion. After crystals had been recovered from Columbia, they would have been combined with the crystals grown on Earth in such a way that we could measure results without knowing until afterwards from which source the crystals came."

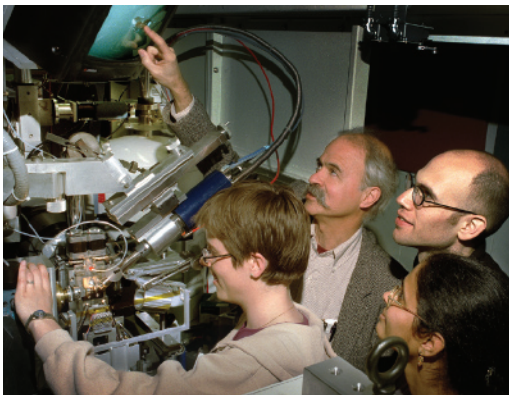

BNL scientist Bob Sweet demonstrates protein crystallography experiments underway at the NSLS.

Next Step

The PCG team is now waiting to know when they will be able to send new experiments in space, perhaps in an unmanned spacecraft. "Our experiment could easily be activated automatically," comments Sweet.

"Some perturbations, such as astronaut movements and orbit corrections, could be avoided if this experiment were performed in a free flyer or unmanned spacecraft," agrees Sygusch, who is confident that more chances to conduct experiments in space will arise in the near future.

"The latest Columbia mission was a tragic human disaster and a scientific catastrophe," Sygusch says. "But, once we understand what happened, we must continue. We will be able to investigate something never achieved before in the history of humankind: a glimpse of what life might look like in a world with a different level of gravity."

—Patrice Pages

U.S. Rep. John Sweeney Visits BNL and NSLS

February 24, 2003

U.S. Representative John Sweeney (R-20th District), visited BNL on February 24 with his aide Gaia Mishanta Ford. Sweeney serves on the House Appropriations Committee and on February 12 was named to the Select Committee on Homeland Security, which helps develop policy for the larger Homeland Security Committee.

Welcomed by BNL Interim Director Peter Paul, Sweeney met with Michael Holland, Manager of DOE's Brookhaven Area Office, and Marge Lynch, Assistant Laboratory Director for Community, Education, Government & Public Affairs. The Congressman then visited the NSLS, one of the world's most widely used scientific facilities. Researchers at the NSLS use sophisticated techniques to study the electronic and structural properties of materials and surfaces at the atomic level.

At the NSLS, Doon Gibbs, Interim Associate Laboratory Director for Basic Energy Sciences, and NSLS Chair Steven Dierker explained a proposed NSLS upgrade that will dramatically improve the capabilities available to the approximately 2,500 researchers from scientific institutions and industry who use the NSLS for their research each year. They also discussed plans for the new BNL Center for Functional Nanomaterials.

Later, on the NSLS experimental floor, Sweeney visited beamline U10B, where researchers use infrared light to study such diseases as Alzheimer's, osteoarthritis, and osteoporosis.

He next stopped at Berkner Hall, where Ralph James, Associate Laboratory Director for Energy, Environment & National Security, explained some of the Lab's work in the field of homeland security.

James focused on BNL capabilities in the areas of advanced sensor technology, particularly the Lab's research and development on nuclear, chemical, biological, and explosive detectors. Sweeney was also interested in seeing actual prototypes of BNL hardware that could detect more minute quantities of nuclear radiation from greater distances and without the false alarms attributed to many current approaches.

James described some of BNL's research suited to reducing the vulnerabilities of New York State, including better control of radioactive materials, advanced technologies to monitor cargo containers at national seaports, and sensor networks to help protect New York and its mass transportation systems.

BNL scientists' work to identify and prioritize risks, such as those connected with U.S. public water, bridges, banking and finance, electric power, gas, and oil and telecommunications infrastructures, was also presented.

On the experimental floor of the NSLS, U.S. Representative John Sweeney (center) and BNL Interim Director Peter Paul talk with NSLS scientist Lisa Miller about research on Alzheimer's disease being done at beamline U10B.

The Congressman conversed with Associate Director for Life Sciences Nora Volkow before concluding his visit. "The enthusiastic interest shown by Congressman Sweeney in the broad science of BNL, as well as his immediate understanding of the Lab's crucial role in the safety and securitiy of New York City, was impressive and refreshing," said BNL Interim Director Peter Paul.

— Liz Seubert

DOE Nanoscience Workshop Draws Crowd

February 27-28, 2003

More than 400 attendees of the first DOE Nanoscale Science Research Centers workshop, which was held February 27-28 in Washington D.C., were treated to a blue-ribbon lineup of political and scientific speakers. The message the participants heard was loud and clear: Nanotechnology research may involve the study of very small things, but it represents potentially very big things in terms of federal funding for the physical sciences.

"It's as if we all have the same speechwriter," observed former BNL Director John Marburger, who is now Director of the Office of Science & Technology Policy and President George W. Bush's science advisor, who delivered an address entitled "Nanoscience and the National Science Agenda."

In his speech, Marburger said that the governments of every major developed nation are now seeking to gain a competitive advantage by investing in nanotechnology research. "What gives our nation the edge are the five DOE nanoscale science research centers," he said.

Under the National Nanoscience Initiative which was launched in fiscal year 2001, DOE's Office of Science announced it would establish the five new centers to "support the synthesis, processing, fabrication, and analysis" of materials at the nanoscale. These centers are: Lawrence Berkeley National Laboratory's Molecular Foundry; the Center for Functional Nanomaterials at BNL; the Center for Integrated Nanotechnologies at Sandia National Laboratories and Los Alamos National Laboratory; the Center for Nanophase Materials Materials Sciences at Oak Ridge National Laboratory; and the Center for Nanoscale Materials at Argonne National Laboratory.

Marburger was introduced by Office of Science Director Raymond Orbach who, in his opening remarks, proclaimed that the five DOE nanoscience centers will be at the hub of national laboratory research efforts in nanorelated fields.

"All five centers are in the President's proposed FY2004 budget and all are well on their way to becoming a reality," Orbach said.

Before hearing from Orbach and Marburger, workshop attendees first heard from U.S. Representative Judy Biggert, a Republican who represents the 13th District of Illinois and who chairs the Energy Subcommittee of the House Science Committee.

Biggert recently introduced H.R. 34, the "Energy Science and Investment Act of 2003," which calls for the Office of Science to receive an overall increase in funding of nearly 62 percent by FY2007. This would mean a FY2007 authorization level of $5.31 billion, compared to the $3.3 billion funding for FY2003. According to the American Institute of Physics, her bill is one of the most important physics-related research bills that the new Congress will consider this year.

"Nanotechnology research is very important to our nation's future economic competitiveness," Biggert told workshop attendees. "The Office of Science is uniquely positioned to do nanotechnology research and I am convinced its nanoscience centers can only enhance our economic competitiveness."

The Congresswoman urged attendees to contact their Congressional representatives and get them to support H.R. 34, which now has 74 cosponsors. In addition to a substantial increase in funding for the Office of Science, her bill would also make some significant administrative changes in DOE. An Under Secretary of Energy & Research position would be created, with authority over all DOE funded civilian science at the non-weapons national laboratories and research universities. A new Assistant Secretary of Science would replace the current director position, and a Science Advisory Board would be established that would consist of the chairs of DOE's advisory panels.

Attendees at the DOE Nanoscale Science Research Centers workshop.

"I am a scientist wannabe who has always thought that scientists were very cool," Biggert said to enthusiastic applause.

The applause was also enthusiastic and vigorous for U.S. Representative Zach Wamp, a Republican who represents the 3rd District of Tennessee and serves on House Appropriations Committee

and the Energy and Water Subcommittees.

Speaking at a Thursday luncheon, Wamp told attendees, "If we want a balanced federal budget, we have to invest in technology. Investing in the physical sciences can give us another boom economy."

Wamp has won a "Champions of Science" award bestowed by the Science Coalition, an alliance of more than 400 organizations dedicated to sustaining the federal government's commitment to U.S. leadership in basic science. As a rousing speaker, Wamp energized the nanoscience audience.

Arguing that the national economic slump is a reason for more investment in the physical sciences rather than less, he cited the example of the Japanese government.

"The economy in Japan is bad, but that did not stop their government from investing in super-computing and taking the lead in that technology," he said. "New technologies are needed to solve problems not just today but for the long-term too. This takes leadership [in the physical sciences] and we're just not there now."

To get the resources needed to advance the development of nano and other technologies that can help solve persistent global problems, such as energy, Wamp said, "We need to do a much better job of marketing the physical sciences. We've got to brand the physical sciences in a different way. It is crucially important to the vitality of your science and this country's economy that we get people excited about and supportive of the physical sciences."

Attendees also heard from Senator Pete Domenici (R-New Mexico), another winner of the Champions of Science award. As chairman of the Senate Energy and Water Development Appropriations Subcommittee, Domenici has been a strong supporter of the physical sciences. He is especially keen on the promise of nanotechnology.

"Nanotechnology represents a new frontier, and it's harder to guess exactly where these new ultra-miniaturized technologies will make the greatest contribution," the Senator said. "Suggestions range from new generations of ultra-tough or ultra-light materials to new approaches to hydrogen storage for a future generation of hydrogen fueled vehicles. This is a truly exciting and revolutionary field."

Domenici also expressed confidence in DOE's ability to lead the development of nanotechnology. "The Department has led the nation in other major scientific initiatives in the past, from high performance computing to the human genome project," he said. "Nanoscience provides another golden opportunity for the Department to again lead the way into an important new area."

Scientific presentations were given by a number of the major names in nanotechnology research, and the directors of the five nanoscale science research centers each gave an overview of their centers, including BNL's Bob Hwang, who spoke about the Lab's Center for Functional Nanomaterials.

It was Patricia Dehmer, Director of DOE's Office of Basic Energy Sciences, who perhaps best summarized the anticipated role of the five new nanoscience centers with respect to the National Nanotechnology Initiative and the country's need to maintain economic competitiveness.

"The DOE centers are different from centers funded by the National Science Foundation and others, in that they are patterned after the same philosophy that guides our national user facilities: They are there to be used by everyone, including researchers from universities and private industry, as well as national laboratories," Dehmer said. "We will partner aggressively with NSF and others to get the job done. The importance of nanotechnology research and development cannot be overstated."

— Lynn Yarris, Lawrence Berkeley National Laboratory

John Marburger, Director of the Office of Science & Technology Policy, and Patricia Dehmer, Director of DOE's Office of Basic Energy Sciences.

SUNY Chancellor Robert King Visits Brookhaven

March 27, 2003

On Thursday, March 27, Robert King, Chancellor of the State University of New York (SUNY), visited BNL for an introduction to the Lab and its programs. As SUNY Chancellor, King oversees one of the nation's largest university systems, with about 500,000 students and an annual state budget of about $7 billion. After a welcome lunch with Interim BNL Director Peter Paul, BNL Director-designate Praveen Chaudhari, Manager of the DOE Brookhaven Area Office Michael Holland, and several Associate Lab Directors and Department Chairs, the Chancellor toured the Lab.

The first stop focused on atmospheric chemistry research in the Environmental Sciences (ES) Department chaired by Creighton Wirick. ES scientist Peter Daum of the Atmospheric Sciences Division talked about BNL's laboratory, field, and modeling program that has contributed to understanding the mechanism of photochemical smog formation. Judy Weinstein-Lloyd, a professor at SUNY Old Westbury who has a long-standing collaboration with BNL scientists, spoke of her program to develop new instrumentation for measuring atmospheric oxidants.

Ralph James, Associate Laboratory Director for Energy, Environment, & National Security, then described BNL homeland security initiatives, such as research and development on nuclear, chemical, biological, and explosive detectors. James showed King actual prototypes of BNL hardware that could detect small quantities of nuclear radiation from great distances.

King's second stop was at the Relativistic Heavy Ion Collider (RHIC), where Associate Laboratory Director Thomas Kirk, together with Collider-Accelerator (C-A) Department Chair Derek Lowenstein and Physics Department Chair Samuel Aronson described the program of RHIC and its four detectors. At one of these detectors, PHENIX, Ed O'Brien, PHENIX operations manager, and PHENIX analysis coordinator Thomas Hemmick, a physics professor at Stony Brook University outlined the scientific goals of the experiment and gave King a brief idea of how PHENIX collects RHIC data.

Next, King visited the NSLS, one of the Northeast's and New York State's most important scientific facilities. Interim Associate Laboratory Director for Basic Energy Science Doon Gibbs and NSLS Chair Steven Dierker explained a proposed upgrade that will dramatically improve the capabilities available to the NSLS's approximately 2,500 researchers from universities, scientific institutions, and industry.

Listening as Peter Daum (right) of the Environmental Sciences Department explains BNL research in atmospheric chemistry are: (from left) Ralph James, Associate Laboratory Director for Energy, Environment, & National Security; Creighton Wirick, Environmental Sciences Department Chair; Praveen Chaudhari, then designate BNL Director; Robert King, State University of New York (SUNY) Chancellor; Judy Weinstein-Lloyd, SUNY Professor at Old Westbury; Brian Giebel, SUNY Old Westbury; and Jun Zheng, Stony Brook University.

As King learned, researchers from SUNY at Albany, Buffalo, Plattsburgh, and Stony Brook used 20 NSLS beamlines during fiscal year 2002 for studies of, for example, materials characterization, materials in high magnetic fields and under extreme conditions, polymers, and biological and environmental systems. Plans for the new BNL Center for Functional Nanomaterials were also discussed.

The SUNY Chancellor moved on to BNL's NeuroImaging Center, where Linda Chang, Medical Department Chair, and Joanna Fowler, who heads the NeuroImaging Center, described some of the Lab's pioneering neuroimaging research on the brain chemistry of addiction; diseases such as Parkinson's and Alzheimer's; and aging. King also learned about the center's recent research on imaging awake animals, which has veterinary support from SUNY's Downstate Medical Center in Brooklyn.

King concluded his visit with discussions at the Director's Office, during which he stated how impressed he was with the programs of the Laboratory and its broad scope of research. He

pointed to a number of educational opportunities as good steps to increase the connections between the Lab and New York State. Interim Director Paul, who expressed his appreciation to the Chancellor for the visit to BNL, commented, "Chancellor King clearly recognized the importance of BNL for the economy of New York State and the education of the education of the State's students."

— Liz Seubert

RapiData Crystallography Course

April 6-11, 2003

Once again last spring, budding crystallographers from around the world gathered at BNL. They were attending RapiData 2003, a week-long course run by BNL's Biology and NSLS Departments. This course introduces students to the best people, newest equipment, and latest techniques in the field of macromolecular x-ray crystallography.

Emphasizing "Rapid Data Collection and Structure Solving at the NSLS," this "Practical Course in Macromolecular X-Ray Diffraction Measurement" ran from April 6 to 11. It consisted of two days of lectures and tutorials taught by scientists from BNL, industry, academia, and other national labs, followed by data collection and analysis at the NSLS. The same instructors and others act as hands-on advisors for a marathon sixty-hour data-collection session to close out the week. Half of this year's 48 students came as observers, while the other half arrived with specimens to analyze. Seven of the students left with solved structures, which will likely result in publications.

The course, which helps to train the next generation of NSLS users, is mostly organized by Bob Sweet and Denise Kranz of Biology, but they emphasize that its success absolutely depends on enthusiastic help from most of the twenty members of the PXRR (the Biology and NSLS Macromolecular Crystallography Research Resource), plus a dozen or so outside teachers.

Major funding for the course was from the National Institutes of Health through the National Center for Research Resources, and DOE's Office of Biological & Environmental Research, with support from the NSLS, and some interested equipment vendors and drug companies.

— Karen McNulty Walsh

Representatives of DOE Light Sources Meet with Elected Officials in Washington, D.C.

April 7-8, 2003

For the third consecutive year, a delegation of scientists representing the four U.S. Department of Energy (DOE) synchrotron light sources organized a successful lobbying trip to Washington, D.C. on April 7 and 8, 2003.

The visit was organized and coordinated by Leemor Joshua-Tor, the chair of the NSLS Users' Executive Committee (UEC). The delegation was comprised primarily of the chair and vice-chair of the UECs of the Advanced Light Source at Lawrence Berkeley National Laboratory (CA), the Advanced Photon Source at Argonne National Laboratory (IL), the NSLS, and the Stanford Synchrotron Radiation Laboratory at Stanford University (CA). Accompanying the delegation was Pat Fulton, Science Lobbyist for Stanford University. The NSLS scientists in the delegation were Tony Lanzirotti, UEC vice-chair, and Simon Bare, UEC lobbying coordinator.

A group of RapiData students seen with instructors Annie Héroux (standing, left), a BNL Biology Department structural biology scientist who works at NSLS beamline X26C, and Frank von Delft (foreground), Scripps Research Institute.

"The goal of these visits is to increase the visibility of the synchrotrons and the Department of Energy's Office of Science who funds them," Joshua-Tor says. "The Office of Science budget has remained essentially flat in recent years, forcing light source funding to remain flat as well, although the number of light source users nearly doubled."

"This office is by far the largest funding agency for the physical sciences in the U.S.," Bare says, " but its funding is buried within bills approved by the Senate Energy and Water Appropriations Subcommittee of the Senate Appropriations Committee and the House on Energy and Water Development Subcommittee of the House Appropriations Committee."

DOE's budget for fiscal year 2003 is $21.9 billion, of which only 15% ($3.3 billion) funds the Office of Science, and only one-third of this amount goes to Basic Energy Sciences, which is the primary funding agency for light source operations. "This amount does not reflect the real needs of the scientists working at the light sources," Bare says, "because the number of users keeps growing, but not the funding, so an infusion of operating funds is urgently required."

On the first day of the visit, the delegation met with Patricia Dehmer, Associate Director of Science for the Office of Basic Energy Sciences, which is one of six offices managed by the Office of Science; Joel Parriott, Budget Examiner from the Federal Office of Management and Budget; John Marburger, Director of the White House Office of Science and Technology Policy (OSTP) and science advisor to President George W. Bush; Kathie Olsen, Associate Director for Science at the OSTP; Michael Holland, Senior Policy Analyst at the OSTP; and Clay Sell and Drew Willison, both Staff members from the Senate Energy & Water Subcommittee of the Senate Appropriations Committee.

Marburger, who welcomed the delegation in his office in the morning of the first day, expressed his strong support for the four light sources, stating that he was holding them in high regard and considered them as the most productive user facilities by the scientific research community worldwide.

On the second day of the visit, the delegation met with senior staffers from the Senate Committee on Energy and Natural Resources, the Energy Subcommittee of House Science Committee, and the Energy and Water Development Subcommittee of the House Appropriations Committee.

The highlight of the visit was a meeting between NSLS user Martin Caffrey, professor of chemistry at Ohio State University in Columbus, and Representative David Hobson (R-OH), the new Chair of the House Energy and Water Development Subcommittee of the Appropriations Committee. Caffrey was accompanied by Simon Bare. The discussion focused on the wide variety of scientists working at the light sources, most of whom are not employees of the national laboratories housing the light sources, but come from universities, other federal agencies, and industry.

At the end of the second day, Bare and Lanzirotti visited with Sean Sweeney, a staffer in the office of Senator Hillary Rodham Clinton (D-NY) and expressed their interest in increasing funding for the DOE's Office of Science. The two scientists also reported to Sweeney that a proposal has been made to the Basic Energy Sciences Advisory Committee (BESAC) to build a new synchrotron at Brookhaven Lab, NSLS-II, which will provide a brighter beam for greatly improved scientific data and many new scientific discoveries.

The members of the delegation were generally satisfied with their visit. "We came away from our visit feeling positive and with many good suggestions on how to expand our efforts," Lanzirotti says. "We also noticed signs of support for increased funding for the Office of Science. For example, the bill introduced onto the floor of the House (H.R. 6) on April 10 provides for budget increases of approximately 15, 10, 15, and 15 percent over the next four years."

— Leemor Joshua-Tor and Simon Bare

NSLS's Youngest Scientists Learn from Light on "Take Our Daughters and Sons to Work" Day

April 24, 2003

On April 24, about 30 daughters and sons learned about some of the scientific programs at the NSLS, and even performed their own scientific experiments. The one-day visit was part of the national "Take our Daughters and Sons to Work Day."

At the NSLS, the children learned that the facility produces many types of light, from microwaves to x-rays, which have many applications in many fields, including electronics, catalysis, microscopes, and medicine. NSLS scientists Marc Allaire, Steve Hulbert, Lisa Miller, and Vivian Stojanoff offered a tour of the experimental floor to the boys and girls, who discovered how synchrotron light is used to design non-stick coatings for aluminum pans, study bone diseases like osteoporosis, and develop new drugs using protein crystallography.

After the tour, the daughters and sons had the chance to perform their own scientific experiments. Marc Allaire demonstrated simple reflection of light from a mirror and contrasted that with the process of diffraction, which was illustrated by reflecting red laser light from a CD-ROM -- the world's most popular diffraction grating. But perhaps the most exciting moment was when the boys and girls discovered that they could created their own rainbow patterns by diffracting visible white light from the CD-ROM.

The boys and girls then had the opportunity to learn from Lisa Miller about the wonders of liquid nitrogen. By immersing an inflated balloon in liquid nitrogen, they discovered that the air inside of the balloon contracts, and then re-expands when warmed up. Much to the amazement of the entire crowd, the balloon survived dozens of repeated freeze-thaw cycles without bursting. But perhaps one of the most memorable experiments involved freezing natural versus artificial daffodils in liquid nitrogen. Both the children and their parents learned that it is much more fun to freeze and crumble a living flower than to take it home as a souvenir.

— Lisa Miller

Simple reflection demonstrated with a flashlight, mirror, and a white board.

NSLS 2003 Annual Users' Meeting Highlights Scientific Successes, Exciting Future Plans

May 19-21, 2003

A spirit of optimism pervaded the 2003 annual meeting of National Synchrotron Light Source (NSLS) users, held at BNL May 19-21, 2003, with presentations on scientific successes and plans for new facilities.

About 30 sons and daughters visited the NSLS for "Take our sons & daughters to work" day.

"A lot of good things have happened at BNL in the last year," said Doon Gibbs, BNL's Interim Associate Laboratory Director for Basic Energy Sciences, as he welcomed NSLS users from around the country and the world to the Tuesday morning main meeting, chaired by Tony Lanzirotti of the University of Chicago, Chair-Elect of the Users' Executive Committee (UEC). Gibbs pointed out that BNL had made "great strides" toward establishing a new Center for Functional Nanomaterials (CFN) and toward significantly upgrading the NSLS. He also noted that several highly qualified people had been brought into BNL leadership positions, including Praveen Chaudhari, the new Laboratory Director.

Among speakers and attendees at the Annual National Synchrotron Light Source Users' Meeting are: (from left) Tony Lanzirotti, University of Chicago; Steven Dierker, BNL; Patricia Dehmer, DOE; Doon Gibbs, BNL; Pedro Montano, DOE; Peter Paul, BNL; Leemor Joshua-Tor, Cold Spring Harbor Laboratory; and Chi-Chang Kao, BNL.

In introducing Peter Paul, Deputy Director for Science & Technology, Gibbs also took the opportunity to thank Paul for his steadfast leadership as Interim Director during the past two years.

Paul, whose task was to give an overview

of BNL, echoed a statement made by Chaudhari at the previous week's RHIC & AGS Users' Meeting, that DOE program managers take a great risk when they build new facilities with the hope that users will come and do good science.

"Fortunately it has always seemed to work out, but we can't take it for granted," Paul said, emphasizing how important it is to have an active user community, such as that at the NSLS, to keep a facility strong. With such involved users and the new leadership at the Lab — including Chaudhari, Gibbs, James Misewich as Materials Science Department Chair, Robert Hwang as CFN Director, and Alex Harris as Chemistry Department Chair — "We are all set to move forward," Paul said.

After describing improvements in support services, housing, and other facilities for users, Paul spoke of the CFN, recent findings at the Relativistic Heavy Ion Collider, and the proposed NSLS-II, a third-generation light-source ring that would be the future center of synchrotron activity at BNL and in the Northeast. "The Laboratory will commit all the resources we can muster to make this a reality," he said.

Bob Hwang then presented details of the CFN, recognizing that "the current excitement in nanoscience is based on work that has been going on for decades at synchrotrons like the NSLS, and you, the users, are a big part of that." He asked NSLS users for help in shaping the new center, noting that the CFN, like DOE's four other nanoscience research centers, was co-located within an existing DOE research facility, in this case the NSLS, to build on existing strengths.

Like the NSLS, the CFN will be a user facility, with a similar process for reviewing proposals. With a range of complementary facilities focused on six scientific areas, the CFN will address the goal of tailoring materials' responses to achieve specific functionality based on an understanding of nanoscale phenomena.

Offering one example of what nanoscience might yield, Phaedon Avouris of IBM's T.J. Watson Research Center then gave the meeting's keynote address on "Carbon Nanotube Electronics."

With a break from science to focus on funding, UOP's Simon Bare, lobbying coordinator for the UEC, then urged all NSLS users to learn about the federal funding process and to get involved.

Users could help to "educate" their own legislators and the congressional committee members vital to science funding — via letters, phone calls, office visits, and even op-ed articles in newspapers — about the importance of research sponsored by DOE's Office of Science. Several bills that propose increased funding for the Office of Science are pending, he said, so to take action now is vital. For more information, see: http://www.nslsuec.org.

Robert Hwang (left), who is Director of the Lab's new Center for Functional Nanomaterials. Keynote speaker at the meeting was Phaedon Avouris (right) of IBM's T.J. Watson Research Center.

The meeting's next session was chaired by Ron Pindak, Head of Science Program Support for the NSLS. Patricia Dehmer, Associate Director of the Basic Energy Sciences (BES) within DOE's Office of Science, started the session. "After hearing this morning's talks," she said, "it strikes me that this is the beginning of a transition period for the Lab, and I'm very optimistic about the future of this institution."

Members of the 2003 planning committee for the NSLS Users' Meeting include: Ron Pindak, BNL; Annie Heroux, BNL; Dan Fischer, National Institute of Standards & Technology; Lisa Miller, BNL; Liz Flynn, BNL; Lydia Rogers, BNL; Mary Anne Corwin, BNL; Sue Wirick, Stony Brook University; and Tony Lanzirotti, University of Chicago.

Long-range planning within BES has resulted in a recommendation for a general upgrade to provide a full return on capital investments at existing light sources, Dehmer explained. Another recommendation was for the NSLS-II upgrade. "This rated very high," she said, encouraging the spontaneous applause that erupted, adding, "You can thank Steve [Dierker, NSLS Chair] for doing such a good job at the presentation."

Referring to the five DOE Nanoscale Science Research Centers, she said, "We are extremely happy that one of those is at Brookhaven. These [nanocenters] are

going to be a very, very important component of the BES family of facilities."

Dehmer then gave her "Totally Unsanctioned Safety Seminar," drawing partly from her own lab experience. The bottom line: "It is possible – and required – to run your laboratory safely, and Pat will become a pest [with investigations and possible cuts in funding] if you mess up."

Following Dehmer, Steve Dierker gave an overview of recent NSLS successes, including Roderick MacKinnon's "spectacular piece of work" on voltage-dependent potassium ion channels, featured on the cover of the May 1 issue of Nature; studies of materials that expand under pressure; and a paper on cell membrane fusion that explains "one of the most basis processes" of cell division. "This has been an action-packed year, with a lot of exciting developments," he said.

Dierker gave credit to the NSLS's support staff, saying, "None of these advances would have been possible if we could not deliver the photons to the end of the beamline. It takes a dedicated and talented staff and a determined effort to keep both rings running reliably."

Dierker then reviewed the many beamline and instrumentation improvements of the past year, and talked about the proposed NSLS-II.

This $400 million upgrade, featuring a new x-ray storage ring three times larger than the current NSLS, would be constructed on Brookhaven Avenue, across from the existing structure, featuring 21 superconducting undulator beamlines and providing the highest brightness of any existing light source, with much shorter pulses.

"Our goal is to build the ultimate medium-energy storage ring," Dierker said. "We would see a huge impact from these enhanced capabilities, especially in the areas of nanoscience and protein crystallography, as larger cells and smaller crystals could be analyzed."

The meeting continued with scientific talks on nanoscience, thin films, x-ray crystallography, and new x-ray sources. During the afternoon session chaired by Lisa Miller, Coordinator of the NSLS's Information & Outreach Office, the UEC Community Service Award was presented to Michael Sullivan, Chief Beamline Engineer for Albert Einstein College of Medicine, for service, innovation and dedication to NSLS users. The winners of the Student/Post Doc Poster Contest were also announced.

Poster prizewinners at the 2003 NSLS Users' Meeting are: (from left) Ally S.-Y. Chan, Rutgers University; David Linkous, George Mason University; Hidenori Tashiro, University of Florida; Henrik Loos, BNL; Daisuke Kawakami, Stony Brook University (SBU); and V.G. Alexandratos, SBU.

Users were then invited to hear more about the BNL nanocenter and encouraged to meet with CFN scientific and facility leaders before adjourning for the meeting's Western-theme banquet in Berkner Hall.

—Karen McNulty Walsh

Frontiers in Powder Diffraction Workshop

May 19, 2003

The theme of the workshop, "Frontiers in Powder Diffraction," held on May 19th at the 2003 NSLS Users' Meeting, was the growing practice and utility of powder diffraction and related techniques in a variety of contexts. Speakers covered work done with x-rays and neutrons, performed at the NSLS, Advanced Photon Source, European Synchrotron Radiation Facility, ISIS (spallation neutron source at Rutherford Appleton Lab, UK), the Intense Pulsed Neutron Source (Argonne National Lab), and the Institut Laue-Langevan, as well as laboratory x-ray instruments.

Enjoying the "Western" flavor banquet held at the 2003 NSLS Users' meeting are the NSLS User Office staff, past and present: (standing, from left) Gretchen Cisco, Eileen Pinkston, Susan Hatzel, Liz Flynn; (seated, from left) Lydia Rogers, Nancye Wright, Brian Bindert, Mary Anne Corwin, and Melissa Abramowitz.

The first speaker was Cam Hubbard of Oak Ridge National Lab, who spoke on *in situ* powder diffraction measurements at high temperatures. He discussed a variety of experimental systems, studied both in the High Temperature Materials Lab at ORNL and at the NSLS in

which the ability to follow phase transformations at high temperatures, under synthetic conditions, was key to solving practical problems in ceramics and other high performance materials. Richard Harlow (of Harlow, Inc.) followed with discussions of work performed at the APS on Fe metal catalysts that are used by DuPont in commercial scale manufacturing. These catalysts are activated at high temperature and pressure at the beginning of the process batch, and there was inadequate understanding of the chemical basis for the observed lot-to-lot variation of their performance. High energy x-rays were necessary to penetrate the stainless steel tube used to house the catalyst under process conditions, and high angular resolution was required to distinguish the processes of interest in the catalyst. Insights gained from the study of the state of the activated catalyst have given information useful to optimize the process in the chemical plant.

The next two talks addressed an extension of the domain of powder diffraction that is becoming increasingly important, pair distribution analysis. Briefly, this technique transforms the entire diffraction pattern into a radial distribution function. Instead of analyzing only the Bragg peaks to learn the periodically repeating component of the crystal structure, pair distribution analysis reveals the distribution of local environments throughout the sample. Accordingly, it is particularly valuable in materials that are only partially crystalline, such as nanoscale phases. Valeri Petkov of Central Michigan University provided an introduction to the technique, and discussed recent results from studies of nanophase $LiMoS_2$, $Ag_{0.4}MoS_2$, $(NH_4)_{0.5}V_2O_5$, magnetic $GdAl_2$, and Cs intercalated into zeolite. Jonathan Hanson (Brookhaven National Laboratory, Chemistry Department) continued with the theme of radial distribution structural refinements, combined with "conventional" Bragg peak analysis of diffraction patterns in studies of the reduction of (nominal) CuO and CeO_2, with measurements performed *in situ* at high temperature. This work shows the complementary information available from the two techniques, and the importance of both in unraveling complicated behavior in mixed phase materials with partial occupancy of several crystallographic sites.

After lunch, Bill David (Rutherford Appleton Laboratory, UK) woke the audience up with some startling new comments on a concept taken for granted by most practitioners: least squares analysis. While that would be the correct approach if the data errors obeyed a normal probability distribution governed by counting statistics and the hypothesized model was a correct description of the sample diffraction properties, these conditions are often not met. Starting with a formal description of least-squares analysis, David reviewed principles of experimental design to meet those criteria. He then presented some new results on techniques to deal with problems frequently observed: unknown impurities in a powder diffraction pattern handled with a new minimization criterion, and a maximum likelihood approach to analyze incomplete structures in which some atoms have not been located.

Frontiers in Powder Diffraction Workshop attendees.

The two following talks covered various perovskite-related materials in which the interplay of structural distortions, charge ordering, and magnetism require complementary application of neutron and x-ray powder diffraction. El'ad Caspi of Argonne National Laboratory discussed the phase diagram of the colossal magnetoresistance system $(Ca^{2+}_{1-x}Ce^{4+}_{x})MnO_3$. This is a two-electron doped system (in contrast to more familiar one-electron doped systems such as $(Ca^{2+},Bi^{3+})MnO_3$), and the faster change of electronic charge with ion substitution leads to a much more complicated interplay among charge ordering, orbital ordering, and spin ordering, which in turn causes phase separation over a much larger range than one-electron systems. Patrick

Woodward of Ohio State University opened his talk with several demonstrations that neutrons are often superior to x-rays in *ab initio* structure solutions of oxides and fluorides, even though the latter are much more widely used. He then discussed several neutron and x-ray experiments: Fe charge disproportionation in $CaFeO_3$, Mn orbital ordering in $NdSrMn_2O_6$, and the Verway transition on oxygen deficient double perovskites, $RBaFe_2O_{5+w}$ (R = Rb, Y, Ho, and Nd).

In the last session, Tom Vogt (BNL, Physics Department) discussed work on the high pressure chemistry of zeolites. The theme of his talk was the surprising discovery of materials that expand under pressure, due to increased incorporation of water into the zeolite cavities. Sodium aluminosilicate natrolite undergoes a reversibly pressure-induced lattice expansion, whereas a synthetic analog, potassium gallosilicate natrolite, expands irreversibly, retaining the expanded high pressure phase upon returning to ambient pressure. Vogt presented structure determinations showing the role of non-framework metal ions in distinguishing the two cases. Finally, Peter Stephens presented a talk largely prepared by Robert Von Dreele (Los Alamos and Argonne National Lab) on their work applying high resolution x-ray powder diffraction to proteins.

In all, the broad range of powder diffraction, pair distribution function, and single crystal analysis, and the large and growing user community at synchrotron and neutron facilities points towards increasing growth at the frontiers of powder diffraction. This in turn indicates continuing demand for improved instruments as well as improved access to the current generation of operating instruments.

—Peter Stephens

Workshop on Spectroscopy in High Magnetic Fields: ESR, Infrared, and Other Applications

May 19, 2003

The availability of high field magnets, combined with the development of high resolution/low energy spectroscopic techniques, provides new opportunities for probing materials with synchrotron light. In this workshop, a few selected applications of x-ray and infrared radiation for the study of superconductors, magnetic perovskites, semiconductor quantum wells and other systems were reviewed. x-ray scattering and spectroscopy, electron spin resonance, optically detected Hall effect, and far IR spectroscopy in high magnetic fields were also discussed. The speakers included current users as well as other leading experts from the U.S. and Europe.

Spectroscopy in High Magnetic Fields: ESR, Infrared and Other Applications Workshop attendees.

—Laszlo Mihaly

Processes in Environmental Sciences Workshop

May 19, 2003

Reliable long-term prediction of heavy element mobility in natural multi-component systems or construction of intelligent reactive barrier systems for waste confinement requires a fundamental process understanding. Application of a combination of macro- and microscopic techniques including EXAFS, XANES, FTIR, XRD, XRF and soft x-ray microscopy can provide atomic scale chemical information as well as information of nano- to microscopic spatial distribution in complex matrixes. New single crystal approaches on well defined crystallographic planes furthermore gives

Processes in Environmental Sciences Workshop attendees.

insight in redox-kinetics and sorption relevant mineral surfaces. The scope of this workshop will be to give a discussion platform as well as an overview of recent applications of synchrotron based techniques to elucidate important pathways in natural and anthropogenic influenced environmental systems.

—Thorsten Schaefer

Bio-Matters: from IR to X-rays Workshop

May 21, 2003

For the past two decades the NSLS has been increasingly contributing to structural biology. With the advent of a new facility the aim of this workshop was to discuss the contributions of different synchrotron radiation-based methods to the understanding of molecular structure and biomolecule function. The second goal was to focus on the complementary aspects between these techniques and different methods such as cryo-electron microscopy and neutron scattering methods. The workshop consisted of oral presentations, a poster session, and a panel discussion session on the future requirements and expectations of the NSLS user community. The talks presented are summarized below:

Wayne Hendrickson, Columbia University, *"Synchrotron Crystallography in Biological Discovery,"* introduced the subject of the workshop. In his talk he described the impact of synchrotron radiation on the field of biological crystallography, a number of technical advances, and the problems of radiation damage with the advent of more intense sources. Several examples were discussed in relation to the speed of solution provided by crystallography at synchrotron radiation sources, and the impact to biochemistry and molecular biology.

Chris Jacobsen, Stony Brook University, "*Soft X-ray Imaging and Spectromicroscopy,"* presented high resolution views of chemical contrast through the combination of soft x-ray microscopes and near-edge spectroscopy methods. This approach was illustrated with biomedical examples including microspectroscopy studies of human sperm, and imaging of several cell types.

Rob Scarrow, Haverford College, *"EXAFS Studies of Metalloproteins and the Usefulness of Model Coordination Complexes,"* discussed the application of EXAFS (Extended X-ray Absorption Fine Structure) analysis to a variety of metalloproteins. The determination of the nature of ligand atoms, the number and lengths of bonds, metal-metal distances, and how small molecule crystal structure databases are useful in the interpretation of the results was discussed using lipogenase and porphobilinogen synthase as examples.

Joannna Krueger, University of North Carolina at Charlotte, "*Small-Angle Scattering: Solutions in Protein Structural Analysis,"* discussed x-ray and neutron small angle scattering focusing on the complementary aspects of these techniques and other structural and biochemical approaches such as that obtained from selected-site mutagenesis, circular dichroism, NMR, and electron microscopy.

Bio-Matters from IR to x-rays Workshop attendees.

Udupi A. Ramagopal, Albert Einstein College of Medicine, and Zbigniew Dauter, NIH, "*SAD: Happy Phasing with Weak Anomalous Scatterers,"* described the single-wavelength anomalous diffraction (SAD) as an alternative to the multiple wavelength diffraction method (MAD) applied to sulfur-containing proteins and to radiation sensitive samples.

Uwe Bergmann, Stanford, "*Advances in High-Resolution Hard X-ray Spectroscopy: From Vibrational Studies to Identify ligands to the Local Structure of Water,*" explained that hard x-ray spectroscopy became possible in recent years due to intense sources and improvements in x-ray instrumentation. The application of x-ray fluorescence spectroscopy (XFS) of weak lines, resonant inelastic

x-ray scattering (RIXS), (non resonant) x-ray Raman scattering (XRS) and nuclear resonant vibrational spectroscopy (NRVS) to studies of the oxygen K-edge of water, metalloproteins and Fe containing systems was shown.

Mark Chance, Albert Einstein College of Medicine, "*Structure and Dynamics of Macromolecular Machines,"* described synchrotron footprinting to study the dynamics and interactions of proteins and nucleic acid structures with millisecond time resolution and high structural resolution using nanomoles to picomoles of material. He gave examples for the L-21 ribozyme from *Tetrahymena*, cofilin and time-resolved activation of the actin binding protein gelsolin.

Lisa Miller, NSLS, "*Chemical Imaging of Biological Tissues using a Combination of Infrared, UV-Visible Fluorescence, and X-ray Micro-Spectroscopy,"* discussed the application of synchrotron infrared (IR) micro-spectroscopy and fluorescence techniques for examining the inherent chemical makeup of biological cells and tissues at spatial resolutions not achieved by conventional IR microscopes. Comparisons with other techniques such as immunofluorescence and x-ray microspectroscopy were presented in light of Alzheimer's disease, scrapie, and bone disease.

Thomas C. Terwilliger, Los Alamos National Laboratory, "*Structural Genomics: Technology for Structural Biology,"* presented the future needs of structural genomics and the current status. He focused on the technological improvements needed from protein production to structure determination. Several of these developments are underway, one of the most important being the automation of data collection and analysis at x-ray beamlines worldwide. Other technologies such as the engineering of proteins for optimal solubility, automated structure solution, and phase improvement by x-ray crystallography were also discussed.

Several posters on different subjects ranging from imaging to scattering and from the NASA radiological program to Cryo Electron Microscopy were discussed over coffee and a lunch break.

Members of the panel (Wayne Hendrickson, Columbia; Thomas Terwilliger, Los Alamos; Joachim Frank, Wadsworth Center; and Naomi Chayen, Imperial College), and workshop participants addressed several technological problems such as instruments, detectors, methods, and software developments to subjects such as multiple assemblies and unstable systems. The main recommendations were related to the development of detectors, brighter sources, instrumentation to handle smaller crystals, software for automated structure determination, modeling, and docking.

Prior to the Bio-matters workshop, a workshop was held on the basic and advanced methods in protein crystallization. The aim of this one-day workshop was to allow participants to have a hands-on experience with the different crystal growth methods available to protein crystallographers. Naomi Chayen (Imperial College) explained the microbatch method and the oil method; Miroslawa Dauter (NIH) discussed the hanging drop method, co-crystallization of heavy atoms, and seeding; Zbigniew Dauter (NCI-NIH) presented strategies in choosing an optimal derivative and data collection; and Grahemen Williams (Brookhaven-Instruments) discussed the application of the light scattering technique to protein crystallization. Two parallel sessions were organized in the morning and in the afternoon where the 22 participants could experience the different crystallization methods. We thank our sponsors Nextal Biotechnologies, Brinkmann Instruments, Millipore, Fisher Scientific, Brookhaven Instruments Corporation, and New York New Jersey Scientific, Inc., for their kind support, without which the Crystallization Workshop, a satellite meeting to the NSLS Annual Users' Meeting, would not have been possible.

—Vivan Stojanoff

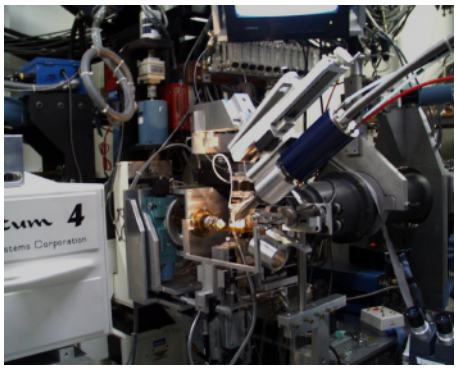

The majority of life science users at the NSLS perform protein crystallography experiments like the one shown here.

Workshop on High Pressure Mineral Physics Using Synchrotron Radiation

May 21, 2003

Most techniques for probing materials using synchrotron radiation can be applied to materials at high pressures and temperatures using either the Diamond Anvil Cell (DAC) or the Large Volume Press (LVP, also known as the Multianvil Press). These techniques include diffraction (both energy-dispersive using white radiation and angle-dispersive using white radiation); radiographic imaging; ultrasonic interferometry; stress and strain measurements; infrared spectroscopy; Raman spectroscopy; and inelastic scattering. Presentations will be made discussing most of these techniques and scientific applications of these technique.

—Michael Vaughan

Workshop on EXAFS Under Extreme Experimental Conditions: EXAFS in the Realms of Small Spot Size, Low Energy, Low Sample Concentration, or Fast Time Resolution

May 21, 2003

EXAFS is well established as a measurement technique used in a broad range of scientific disciplines. Within certain experimental constraints, high quality data is routinely obtained by users of synchrotrons around the world. In recent years, the scope of EXAFS has been expanded by advances in measurement techniques. At this year's NSLS Users' Meeting, these exciting developments were explored in a workshop titled, "EXAFS Under Extreme Experimental Conditions: EXAFS in the realms of small spot size, low energy, low sample concentration, and fast time resolution," organized by Bruce Ravel of the Naval Research Laboratory in Washington, DC. Just as EXAFS is commonly used by researchers from many different scientific disciplines, so too did our speakers present results from many different disciplines, including chemistry, environmental science, and materials physics.

Barukh Yaakobi of the University of Rochester began the workshop by discussing the use of laser-generated shocks with imploding targets as the radiation source for his EXAFS experiments. Dr. Yaakobi discussed measurements of an ultra-fast structural phase transition in titanium metal induced by the laser-generated shock and measured in dispersive mode. He was followed by Vadim Palshin from Louisiana State University and CAMD, who discussed the experimental challenges of low-energy EXAFS measurements. He presented detailed structural refinements on the silicon K-edge silicon-containing, thin, amorphous carbon films.

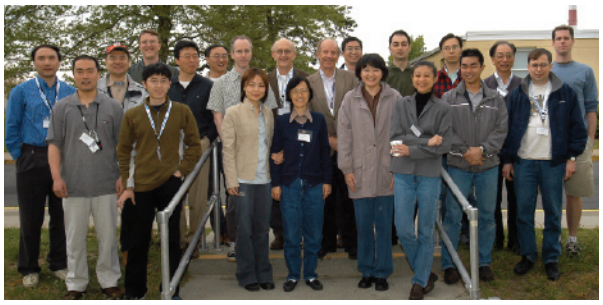

Attendees at the workshop on High Pressure Mineral Physics Using Synchrotron Radiation.

Lin Chen of Argonne National Laboratory spoke of using the time structure of a stored current to measure photo-excited molecular structures. In these experiments, very short-lived molecular states are measured in a pump-probe geometry wherein the molecular population is laser-excited and the excited state is measured by an x-ray pulse incident during its lifetime. Shelly Kelly also of Argonne National Laboratory spoke of uranium L_3-edge EXAFS at environmentally relevant concentrations. Environmentally relevant concentrations strain the limits of detectability even with third generation light sources and Dr. Kelly discussed the experimental concerns of low sample concentrations and addressed the limits of sample dilution

Attendees at the workshop on EXAFS Under Extreme Experimental Conditions: EXAFS in the Realms of Small Spot Size, Low Energy, Low Sample Concentration, or Fast Time Resolution.

for full analysis of the EXAFS signal. The final talk was by Ronald Cavell of the University of Alberta. He spoke on the use of microprobe EXAFS sources to map the composition of heterogeneous materials. He presented results of mapping and structural determination of the components of a meteor sample.

There is a rule of thumb that the measurements of elemental identification, XANES measurement, and EXAFS measurements require increasing orders of magnitude of photon flux or sample concentration. Consequently detailed EXAFS analysis in the limits of small spot size, low energy, low concentration, or fast time resolution requires special considerations for sample preparation and measurement. In many cases these experimental limitations have only been addressed since the advent of technical advances such as third generation sources. This workshop provided an excellent snapshot of the current state of the art technology for each of these extreme realms of EXAFS measurement and analysis.

—Bruce Ravel

UEC Community Service Award Presented to Michael Sullivan

May 20, 2003

Congratulations go out to Michael Sullivan, Chief Beamline Engineer for Albert Einstein College of Medicine. Mike is the second annual recipient of the NSLS Users' Executive Committee (UEC) Community Service Award. This award is given for service, innovation, and dedication to users of the NSLS.

Members of the NSLS user community nominated Mike for this award. Here are some of the comments that users sent about his wonderful contributions:

- "Mike is admired as a tireless, creative force dedicated to the principle of delivering user service."
- "In my opinion Mike is one of the most knowledgeable and extremely helpful engineers at NSLS floor, with very long experience [19 years] with dealing with all technical aspects of many different kinds of x-ray synchrotron research conducted at NSLS. He is a person who made it possible for very many staff and visitors to obtain top quality research results."
- "On several occasions, he has come in on weekends to help us salvage an experiment gone awry, or to bail us out of a technical problem. On one occasion, we reached him via his cell phone on his boat at sea, and he was able to come in and fix the problem to keep us running."
- "Mike is undoubtedly a gold standard of service, innovation, and dedication to users. Moreover, during this winter's biggest blizzard, I remember walking by the NSLS parking lot when Mike turned his car into a towing truck in order to help his users to pull out their car out of a huge pile of snow."

Leemor Joshua-Tor, the Chair of the NSLS UEC, presented the award to Mike at the NSLS Users' Meeting banquet on the evening of May 20th. Mike received a $250 gift certificate and his name was engraved on the plaque on display in the lobby of the NSLS.

—Leemor Joshua-Tor

Michael Sullivan, NSLS Users' Executive Committee (UEC) Community Service Award winner.

NSLS Scientist Ron Pindak Awarded Tenure

June 1, 2003

Brookhaven Science Associates (BSA) granted tenure on June 1 to nine Brookhaven scientists. They are: Mark Baker, Chemistry Department; Leslie Bland, Physics Department; Christopher Homes, Physics; Jean Logan, Chemistry; Ron Pindak, National Synchrotron Light Source Department; David Schlyer, Chemistry; Subramanyam Swaminathan, Biology Department; Dejan Trbojevic, Collider-Accelerator Department; and Gene-Jack Wang, Medical Department.

As described in the Scientific Staff Manual, "a tenure appointment constitutes recognition of independent accomplishment of a high order in the performance of original research or of other intellectually creative activity appropriate to Laboratory purposes."

Recognition may be earned through significant contributions to knowledge related to the purposes of the Laboratory and/or in furtherance of the Laboratory's aims, through continuing contributions of outstanding sig-

nificance to productive uses of the facilities, or outstanding and creative contributions to their design, development, and improvement.

For his outstanding contributions and sustained high-quality original research in the study of complex fluids, with particular emphasis on liquid crystals, Ron Pindak, NSLS Department, was awarded tenure.

"Ron consistently picks fundamentally important problems to work on and has an ability to design experiments to get at the heart of an issue," said Steven Dierker, NSLS Chair and Associate Laboratory Director for Light Sources. "He has amply demonstrated the versatility and expertise to practice whatever technique is necessary, sometimes by collaborating with others to learn the technique before applying it on his own, and in other cases by playing a lead role in developing a new technique."

Pindak's early work in forming free-standing liquid crystal films led to his experimental verification of the hexatic phase, a new state of matter with order intermediate between that of a liquid and of a solid. Later, he and collaborators discovered and characterized the "Twist Grain Boundary Phase," the liquid crystal analogue of the Abrikosov flux lattice in superconductors with screw dislocations playing the role of flux vortices.

Pindak joined BNL in 2001 as a physicist after a distinguished 24-year career at Bell Laboratories. During his career at Bell Labs, he had led a collaboration at the NSLS that pioneered the use of resonant x-ray scattering to elucidate molecular order in chiral ferri- and antiferro-electric liquid crystals. This required working in a low-energy x-ray region where air is very absorbing, so special instrumentation, a goniometer and x-ray polarization analyzer, which would operate in a helium atmosphere, had to be designed and constructed.

Said Dierker, "The unique insight provided by the measurements established by Ron's work has provided the motivation for developing this capability as a standard technique for the user program on one of the NSLS low-energy x-ray beamlines."

Most recently, Pindak has been a key contributor to the development of the Coherent Bragg Rod Analysis technique, which measures the phase of x-rays scattered by two-dimensional structures, such as epitaxial films or interfaces, to allow an absolute determination of the atomic positions. He is now exploring whether this technique can be extended to study two-dimensional protein crystals.

In addition, since joining the NSLS, Pindak has headed the Science Program Support Section of the User Science Division, and taken the lead in developing a soft condensed matter program. He also served as the Interim Associate Director for the BNL Nanocenter. Currently, together with Lin Yang, he is developing a small angle x-ray scattering beamline and starting soft matter and biophysics research relevant to understanding nanoscale device fabrication and operation.

Pindak received his Ph.D. in physics from the University of Pennsylvania in 1975.

— Liz Seubert

Ron Pindak

Dierker Named Associate Laboratory Director For BNL's New Light Sources Directorate

June 5, 2003

Steven Dierker, a forefront scientist and administrator in synchrotron light research, was named Associate Laboratory Director for the new Light Sources Directorate at BNL. Dierker, who is Chair of the NSLS, will also retain that position.

The NSLS at BNL is one of the world's most widely used scientific facilities. Each year, about 2,500 researchers from more than 400 universities, companies, and government labs use its bright beams of x-rays, ultraviolet light, and infrared light for research in such diverse fields as biology and physics,

Steven Dierker

chemistry and geophysics, medicine and materials science. For example, scientists have used the NSLS to produce imagesof the AIDS virus as it attacks a human cell, develop a method for breast cancer detection that is more accurate than mammography, and create a method to make faster, denser computer chips. The facility has 175 employees and a current annual budget of about $38 million.

"I am pleased about the continued growth of the NSLS Department," Dierker said. "Since its commissioning in 1982, the NSLS has continually updated and expanded its capabilities to remain at the forefront of science. Now we are proposing a major upgrade - essentially a new light source at Brookhaven."

BNL created the new Light Sources Directorate and promoted Dierker to his present position because of the importance of upgrading NSLS facilities within the next decade.

The project represents the next major step in the Lab's long history of building and operating world-class scientific facilities and is expected to have enormous impact in the life sciences, materials and chemical sciences, nanoscience, geoscience, environmental science, and other areas. Advanced light source capabilities would also complement the Center for Functional Nanomaterials at Brookhaven, which is due to be built starting in 2005 and to become fully operational by 2008.

After earning B.S. degrees in both physics and electrical engineering in 1977 from Washington University, Dierker earned both an M.S. and Ph.D. in physics from the University of Illinois, Urbana-Champaign, in 1978 and 1983, respectively. In 1983, he joined the Semiconductor and Chemical Physics Research Department at AT&T Bell Laboratories (now Lucent Technologies), and, in 1990, he joined the University of Michigan, where he was Professor of Physics and Applied Physics. He joined BNL in May 2001 to become Chair of the NSLS.

Since 1992, Dierker has been a member of the NSLS Users Group, and he performed initial experiments at the NSLS to develop a novel synchrotron technique called x-ray photon correlation spectroscopy, which uses coherent, or highly ordered, synchrotron beams to study colloidal systems, or particles dispersed in a solid, liquid, or gaseous medium, and polymers.

Since 1996, Dierker has been a member of the Advanced Photon Source (APS) Users Organization at Argonne National Laboratory, and he chaired that organization from 1998-2000. He also helped to plan the construction, design, and operation of beamlines at the APS, with funding from DOE and the National Science Foundation.

— Diane Greenberg

Yeshiva University Undergraduates Experience Hands-On Research at BNL

June 17, 2003

In June 2003, 12 students and 3 instructors from Yeshiva University (New York) spent a week at Brookhaven National Laboratory as part of an undergraduate course entitled "Experiments in Modern Physics". This course was developed by Yeshiva Physics Professor Anatoly Frenkel, in collaboration with his departmental colleagues Professors Gabriel Cwilich and Fredy Zypman. Professor Frenkel is also a long-time NSLS beamline scientist at X16C. The course was five weeks long, including four weeks on the Manhattan campus where students had lectures and labs introducing them to the foundations of modern physics, and one week of "mini-experiments" at BNL. Students participating in the course had widespread backgrounds, majoring in Physics, Political Science, English and Psychology.

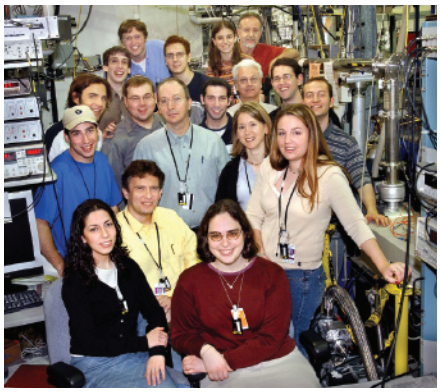

Yeshiva University undergraduates and faculty enjoy their summer mini-experiments at the NSLS.

The most attractive component of the new course was the Brookhaven visit. The purpose of this visit (and the entire course) was to help students under-

stand modern physics through a series of mini-experiments, while exposing them to the atmosphere of a National Lab where modern physics is practiced every day. The five BNL experiments were organized in collaboration with BNL scientists who helped to plan and run the experiments for several shifts of students. In this way teams of 3-4 students could rotate between all of the experiments during the week.

Three experiments, the "Photoelectric Effect," organized by Anatoly Frenkel, "Time-Resolved Chemistry," Jon Hanson (BNL-Chemistry), and "Fingerprinting of Fingerprints," organized by Lisa Miller (BNL-NSLS) were run at the NSLS beamlines X16C, X7B and U10B, respectively. The experiments were designed to show students both the laws of physics (photoelectric effect and x-ray absorption; x-ray diffraction and Bragg's law; absorption of infrared light by vibrating molecules) and elements of research. Two additional experiments, "Nuclear Decay" and "Electron-Positron Annihilation," were organized by Kathryn Kolsky and Leonard Mausner at BNL's Isotope Facility. There the students visited the Brookhaven LINAC Isotope Producer (BLIP) and spent two days studying properties of gamma radiation (absorption, element characterization, inverse square law and the law of radioactive decay) by operating the facility's germanium gamma ray detectors. They were particularly fascinated by utilizing the $E = mc^2$ law to obtain the electron mass from the characteristic "electron-position annihilation" peak at 511 MeV.

For most of the students it was the first experience of this kind. They endured working long shifts, participating in the ongoing laboratory research and enjoying the sense of "discovery" in learning. The entire group thanks the Brookhaven teams of scientists for their help and the NSLS for financial support. The course is now used as a prototype for a new course "Current Topics in Nanoscience" that is under development by the Yeshiva faculty.

— Anatoly Frenkel, Yeshiva University

'Mail-In' Crystallography at the NSLS Featured in *Nature*

June 19, 2003

BNL's Howard Robinson, Biology Department, who runs the "mail-in" crystallography program at the NSLS, got star billing (and photo prominence, right) in a news feature on the subject in the June 19, 2003, issue of *Nature*. Since 2000, Robinson and others at the NSLS have offered a mail-in data-collection service for scientists who want to solve protein structures without having to travel to a synchrotron themselves. According to the Nature article, such services are becoming increasingly popular for biologists without formal training in crystallography and for those who would rather not wait for time on a beamline. Robinson's team at the NSLS typically works on about 50 mail-in projects a year, free to academic scientists. Consistent with BNL's mission of making its highly specialized research facilities available to outside researchers, this mail-in program broadens BNL's service to science and is helping to speed up the process of biological research. The program is funded by the Office of Basic Energy Sciences and Office of Biological & Environmental Research within DOE's Office of Science and the National Institute of Health's National Center for Research Resources.

Howard Robinson

— Karen McNulty Walsh

NSLS EXAFS Data Collection and Analysis Short-Course Has Another Successful Year

July 14 - 17, 2003

A hands-on EXAFS Data Collection and Analysis Course was held July 14-17, 2003 at the NSLS. The course was co-organized by Bruce Ravel (Naval Research Laboratory) Simon Bare

(UOP LLC), with superb administrative support by Lisa Tranquada (SFA, Inc.). Twenty-eight eager participants (graduate students, postdocs, and institution and industrial scientists) representing universities, national laboratories, research institutes, and industry attended the course. Of these, there were ten new users to the NSLS. The participants had diverse research interests across a broad spectrum of scientific fields (materials science, geological and environmental sciences, catalysis, and biology) and attended to learn how XAFS may be applied to their research program.

The four-day course was divided into morning lectures, with two afternoons of hands-on data collection using seven different NSLS spectroscopy beamlines (X9B, X11A, X18B, X19A, X23A2, X23B, and X26A), and two afternoons of data analysis. The instructors on the beamlines were Faisal Alamgir, Wolfgang Caliebe, Scott Calvin, Syed Khalid, Tony Lanzirotti, Nebojsa Marinkovic, and Kaumudi Pandya.

The eight morning lectures were: "Introduction to XAFS," given by Matt Newville (University of Chicago), "Basics of sample preparation" by Scott Calvin, "XANES measurement and interpretation" by Simon Bare (UOP LLC), "Detectors and synchrotron radiation" by Peter Siddons (BNL), "Basics of data processing" by Shelly Kelly (Argonne National Laboratory), "Introduction to theory" by John Rehr (University of Washington), "Introduction to analysis" by Anatoly Frenkel (Yeshiva University), and "Applying XAFS into a research program" by Rich Reeder (Stony Brook University). The time allotted for the lectures allowed ample time for stimulating discussion, which often developed.

For the first two days of the course, after attending the morning lectures, the participants were divided into small groups by research discipline to conduct the experimental part of the course. Each student became familiar with beamline operation and collected real XAFS data on representative samples from their own individual research projects. On the last two days, following the morning lectures, the participants learned data analysis techniques using their own data they had just collected. The participants also enjoyed ample time for informal discussion over coffee and in the evenings over the excellent dinners that were included in the course fee.

There was a tremendous amount of information disseminated over the four days. All the participants left the course with new friends and armed with the basic tools to apply x-ray absorption spectroscopy to their own research programs.

Participants in the 2003 NSLS EXAFS course.

We plan to offer the course again in 2004 – check the NSLS website for updated information.

The course was sponsored by the NSLS, with support from the Center for Environmental Molecular Science at Stony Brook University.

— Simon Bare

NSLS Summer Sunday Draws a Record-Breaking Crowd

August 3, 2003

On Sunday August 3, 2003, over 750 visitors toured the NSLS as part of Brookhaven National Laboratory's Summer Sunday tour series. Thirty-five NSLS staff members, students, and users volunteered their time for the event, which was organized by NSLS scientist, Lisa Miller.

University of Chicago scientist Tony Lanzirotti animated scientific research at the NSLS to an overflowing NSLS seminar room crowd.

Each summer, BNL is open for tours on seven consecutive Sundays, feature exciting interactive exhibits and an inside look at a different Laboratory facility each week, including the NSLS.

Tours of the NSLS included presentations, demonstrations, and hands-on

exhibits. At Berkner Hall, visitors watched an introductory video about how a synchrotron works, narrated by NSLS Chairman Steve Dierker. After a short bus ride and tour of the Lab, visitors were dropped off at the NSLS. In the seminar room, NSLS scientists presented an introduction to "Science at the NSLS" by describing the many ways the NSLS is used to study scientific problems that affect everyday life. Improvements in biomedical imaging techniques, drug design, catalytic converters, environmental cleanup, and computer storage media were just a few of the topics discussed.

Visitors then toured the NSLS lobby, which was transformed into an exhibit area for numerous light- and synchrotron-related demonstrations. Visitors were able to experience "total internal reflection" as a laser beam was guided through a stream of falling water. A display on the principles of vacuum demonstrated its effect on a ringing bell, a balloon, a feather, and a marshmallow. The technique of diffraction was demonstrated using tiny metal grids and compact disks. Visitors had the opportunity to build their own "crystals" using gumdrops, and "see" the synchrotron light (at least the visible part of the spectrum) transported to the lobby through a fiber optic. But perhaps one of the all-time favorite features in the NSLS lobby was the view of the experimental floor from the display windows, which continues to amaze visitors year after year.

In addition to the many exhibits at the NSLS, BNL volunteers at Berkner Hall engaged visitors in a number of other activities. A hands-on exhibit called "Brain Matters," produced by the Oregon Museum of Science and Industry and funded by the National Institutes of Health, offered visitors the opportunity to explore the wonder of the brain and test their skills in solving challenging "brain twisters." Also, an exhibit about the 2002 Nobel Prize in Physics awarded to a Brookhaven Lab scientist was on display, and the Camp Upton Historical Collection featured memorabilia from World Wars I and II. The ever-popular "Whiz Bang Science Show" — popular with both adults and children — was also shown several times during the day. Both children and adults enjoyed lively interactive demonstrations of basic scientific principles. How does a "Bernoulli blower" float a beach ball in the air? What's a corrugaphone and how does sound travel through it? These were just a few of the intriguing items covered in the show.

—Lisa Miller

NSLS scientist Vivian Stojanoff, shows how much fun it can be to build crystal models out of gumdrops and toothpicks.

Fun with vacuum techniques was demonstrated by Alec Bernston (left), a Cornell University freshman that was a summer student at the NSLS.

In a series of articles published in the Bulletin, some research that was presented at the 226th meeting of the American Chemical Society (ACS), September 7-11, 2003, in New York City was featured.

Important Intermediate Isolated With Help From Reverse Reaction

September 7-11, 2003

BNL chemists have used a new way to isolate and study an important Intermediate in a chemical reaction: They run the reaction in reverse.

By starting with the final products — epoxides— and placing them on the surface of a model catalyst, the chemists are able to use surface chemistry techniques to "catch" the intermediate. Understanding this intermediate may ultimately help in developing improved or new catalysts for the forward reaction — a reaction that produces important "building blocks" in the manufacture of larger organic molecules.

In the forward direction, the interaction of the reactants with the surface is either too weak to allow direct study of the mechanism, or the intermediate — a ring structure on the surface of the silver catalyst — forms and transforms too quickly for scientists to study. But in reverse, the intermediate stays on the surface longer, so scientists

The NSLS lobby ws filled with visitors all day one on the NSLS Summer Sunday.

can apply various techniques to try to understand the reaction mechanism.

"If we find a general rule based on our studies with this model catalyst, then we can design a new catalyst, because we know how the reaction occurred on the surface," said the BNL Chemistry Department's Hong Piao, who is working on the project. The general goal is to improve the reactivity and selectivity of the catalyst for producing particular products.

Piao presented a talk on this work at the American Chemical Society's September meeting's Division of Colloid and Surface Chemistry poster session, "Fundamental Research in Colloid and Surface Chemistry." This work was funded by the Division of Chemical Sciences, Office of Basic Energy Sciences at DOE's Office of Science.

— Karen McNulty Walsh

Nanoscale Model Catalyst Paves Way Toward Atomic-Level Understanding

September 7-11, 2003

In an attempt to understand why ruthenium sulfide (RuS_2) is so good at removing sulfur impurities from fuels, BNL chemists have succeeded in making a model of this catalyst — nanoparticles supported on an inert surface — which can be studied under laboratory conditions.

"If we can understand why this catalyst is so active, we might be able to make it even better, or use what we learn to design other highly efficient catalysts," said Tanhong Cai of the BNL Chemistry Department, one of the scientists who made the model.

Removing sulfur from fossil fuels such as oil and coal is mandated because the resulting fuels burn more cleanly and efficiently. One common way of achieving this is to add hydrogen in the presence of a catalyst to release hydrogen sulfide (H_2S).

Recently, RuS_2 was found to be 100 times more active than the catalyst most commonly used for this "hydrodesulfurization" reaction. But studying the catalyst in action is nearly impossible because the reaction takes place at high temperatures and under extreme pressure.

The BNL team has therefore created a model of the catalyst via a chemical reaction that deposits nanosized particles of RuS_2 on a nonreactive gold surface. The small size of the particles maximizes the surface area available for the catalytic reaction to take place, and makes it ideal for analysis by classic surface chemistry techniques, such as scanning tunneling microscopy and x-ray photoemission spectroscopy. The entire model is being studied under well-defined ultrahigh vacuum conditions.

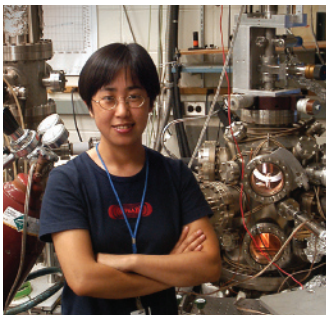

Hong Piao

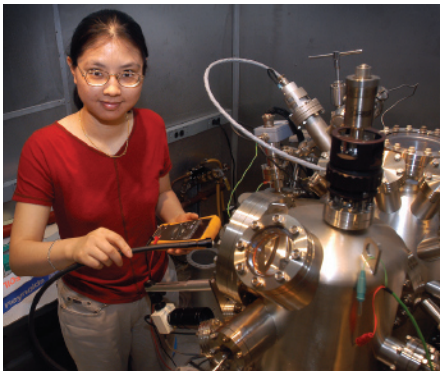

Tanhong Cai

Cai presented a talk on the preparation and characterization of this model catalyst at the American Chemical Society's September meeting during the "Size-Selected Clusters on Surfaces, Division of Physical Chemistry" session. The work was funded by the Division of Chemical Sciences, Office of Basic Energy Sciences at DOE's Office of Science.

— Karen McNulty Walsh

NYS Senators Balboni, Flanagan Visit BNL to Learn About Lab's Homeland Security Initiatives, More

September 12, 2003

On Friday, September 12, New York State Senator Michael Balboni, 7th District, who chairs the Senate Committee on Veterans, Homeland Security and Military Affairs, and New York State Senator John Flanagan, 2nd District, who, among other contributions, is a member of that same Committee, visited BNL with Jim Sherry, Counsel to Balboni.

After being welcomed by BNL Director Praveen Chaudhari, as well as DOE's Brookhaven Area Office Manager Michael Holland, Associate Laboratory Director for Energy, Environment & National Security Ralph James, and Assistant Laboratory Director for Community, Education, Government & Public Affairs Marge Lynch, the party was taken to the Lab's Radiation Detector Testing & Evaluation Facility (RADTEC).

There, Charles Finfrock of the Energy Sciences & Technology Department; Biays Bowerman of the Environmental Sciences Department; and Paul Moskowitz of the Nonproliferation & National Security (NNS) Department outlined the purpose of RADTEC, which is twofold — to assemble, operate, and test commercial and government off-the-shelf technologies targeted for various homeland security applications, and to provide baseline data for comparison purposes. At the facility, researchers collect baseline data on various types of detectors, and are available to provide assistance in training city, state, and federal officials to operate the detectors and interpret the results. RADTEC is open to all commercial and government technology vendors and is expected to become an important resource for local, county, state, and federal officials.

The visitors next stopped at the NSLS, to meet Associate Laboratory Director for Light Sources and NSLS Chair Steven Dierker and NSLS scientist Peter Siddons, who gave an overview of some of the research done in such diverse fields as biology and physics, chemistry and geophysics, materials science, and medicine. The group then saw beamline X12A, where detectors being developed by BNL and others in support of homeland security initiatives are inspected at a new testing station.

The tour continued at the Instrumentation Division, where, a collaboration including NNS is developing a detector that acts as a camera to make images of objects that emit low-energy neutrons. As Vanier explained, since there are very few natural background neutrons, and they are uniformly distributed, a concentrated source of neutrons is strong evidence of a manmade device, such as a plutonium weapon, or of spent nuclear fuel.

Graham Smith, Instrumentation, then showed the visitors a working prototype of a xenon-filled gamma ray spectrometer that BNL is developing to detect radioisotopes potentially in the terrorist arsenal, such as dirty bomb materials. Xenon detectors can be built in very large sizes, so as to pick up signals of radioisotopes more quickly and over a wider area than do instruments now available. Hence, these detectors will be suitable for homeland security applications.

At BNL's Radiation Detector Testing & Evaluation Facility are: (front, from left) NYS Senator John Flanagan, BNL's Ralph James and Paul Moskowitz, and NYS Senator Michael Balboni.

One of BNL's most enormous detectors, STAR, provided the next stop on the tour. The visitors learned from Tim Hallman, Collider Accelerator Department, that STAR tracks and analyzes thousands of particles, such as protons, neutrons, and pions, that may be produced in collisions of two beams of subatomic particles speeding around the tunnel at the Relativistic Heavy Ion Collider (RHIC). In the RHIC experiment, scientists expect to discover more about conditions that existed in the first few microseconds of the universe.

The visit concluded at the Positron Emission Tomography (PET) facility, where David Schlyer, Chemistry Department, described some of the Lab's pioneering neuroimaging research on the brain chemistry of addiction, aging, and diseases such as Parkinson's and Alzheimer's, and the recent PET research on imaging awake animals. Some of this work has veterinary support from the State University of New York's Downstate Medical Center in Brooklyn.

—Liz Seubert

2003 NSLS Annual Awards Ceremony and Picnic

September 17, 2003

On Wednesday, September 17, the NSLS had its annual Awards Ceremony and Picnic. Despite the impending arrival of Hurricane Isabel, the weather was spectacular and the pig roast was another big success. The picnic was coordinated by Laura Miller and executed by a number of NSLS staff members, including Charlie Nielson, Boyzie Singh, Bob Best, Joe Greco, Paul Humbert, Jim Lacy, Jim Newburgh, John Burke, Gerry Van Derlaske, and Bob Kiss, along with Ken Sutter "the pigman."

This year, Service Awards were given to 24 NSLS staff members: Al Almasy, Sam Krinsky, and Bob Casey (30 years); Roy D'Alsace, Walter De Boer, John Gallagher, Rick Greene, Chris Lanni, Payman Mortazavi, Jack Tallent, Frank Terrano, and Gerry VanDerlaske (25 years); Diane Hatton, Steve Hulbert, Jim Murphy, and Florin Staicu (20 years); Peter Gross, Alan Levine, Paul Montanez, Pauline Pearson, Eva Rothman, Brian Sheehy, Chris Stelmach, and Xijie Wang (10 years).

Spotlight Awards were presented to NSLS staff members for the completion of extraordinary accomplishments that were of significant benefit to the Department, Division, or Laboratory. This year's Spotlight Award winners were: (1) Brian Kushner for getting the x-ray ring's digital vertical feedback up and running, (2) Jim Newburgh for outstanding radio frequency cavity installation efforts during the winter 2002 shutdown, (3) Jack Tallent for designing a new beam profile monitor for the x-ray ring, (4) John Burke for completely rebuilding the fire-damaged Pulse Forming Network (PFN) section of the SDL modulator-A, and (5) Gary Nintzel for preparation, dismantling, and shipping of the U6 beamline.

—Lisa Miller

NSLS Physicist Wins 2003 Free Electron Laser Prize

October 10, 2003

Li Hua Yu, a physicist at the NSLS won the 2003 Free Electron Laser (FEL) Prize sponsored by the 25th International Free Electron Laser Conference. Yu received the award, which consists of $3,000, a certificate and a plaque, at the FEL conference held this year in Tsukuba, Japan.

NSLS Chairman Steve Dierker presented the Service and Spotlight Awards at the Annual Picnic.

Yu's award was given "in recognition of his outstanding contributions to FEL science and technology." Over the last 20 years, Yu and colleagues from Brookhaven contributed significantly in developing two types of lasers that are important for scientific investigations: the self-amplified spontaneous emission free electron laser (SASE FEL), and the high gain harmonic generation free electron laser (HGHG FEL).

NSLS Staff enjoying the barbeque.

In the SASE process, the light the laser emits for experiments starts from noise, or random signals. In contrast, in the HGHG process, the output light starts from fast-moving electrons interacting with a seeding laser that shifts the light to a higher frequency and makes it significantly more coherent, meaning electrons move in a coordinated way to emit light. The intense light of the HGHG FEL reveals the fine details of atomic interactions inside materials and the very fast motions of molecules in chemical reactions, all with an unsurpassed precision.

Yu explained, "The HGHG FEL combines the intensity and coherence of a laser with the broad spectrum of light available in a synchrotron, a type of accelerator. The invention of the laser provided a revolutionary source of coherent light that created many new fields of scientific research. The development of the HGHG FEL extends the reach of lasers to much shorter wavelengths, thus opening new research opportunities."

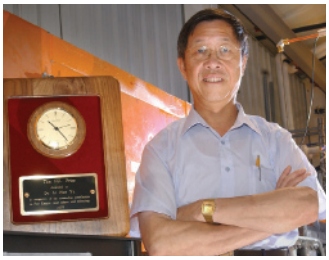

Li Hua Yu with FEL Prize

Yu continued, "I am very happy to

receive this award, and I am grateful for Brookhaven Lab's support and the excellent team who worked with me to make the HGHG FEL at Brookhaven the first and only one of its kind in the world."

At Brookhaven's Accelerator Test Facility in 1999, Brookhaven scientists, in collaboration with Argonne National Laboratory researchers, verified the theoretical foundation of the HGHG FEL operating in the infrared region of the light spectrum. In 2002, the technique was further developed to enable the HGHG FEL at Brookhaven to produce shorter wavelength light in the deep ultraviolet spectral region. This enabled researchers to perform new chemistry experiments.

The HGHG FEL may be a complementary research tool to synchrotrons around the world, including the Brookhaven's Laboratory Directed Research and Development Program, the U.S. Naval Research Laboratory, and the U.S. Air Force funded Yu's research on the DUV-FEL.

Li Hua Yu earned his undergraduate degree from Jilin University in China in 1970. He earned both an M.S. and Ph.D. in physics from Stony Brook University in 1980 and 1984, respectively. In 1984, he joined Brookhaven Lab as a research associate, and he rose through the ranks to become a senior physicist, in 2000. With a team of eight scientists and engineers from Brookhaven, Yu won an R&D 100 Award from R&D Magazine in 1989 for inventing the Real-Time Harmonic Closed-Orbit Feedback System, which stabilizes the orbit of electron beams in synchrotrons.

—Diane Greenberg

2003 Nobel Prize in Chemistry Awarded to NSLS User Roderick MacKinnon

October 8, 2003

Roderick MacKinnon, M.D., frequent NSLS user, won half of this year's Nobel Prize in Chemistry for work explaining how a class of proteins helps to generate nerve impulses -- the electrical activity that underlies all movement, sensation, and perhaps even thought. The work leading to the prize was done primarily at the Cornell High Energy Synchrotron Source and the National Synchrotron Light Source.

The proteins, called ion channels, are tiny pores that stud the surface of all of our cells. These channels allow the passage of potassium, calcium, sodium, and chloride molecules called ions. Rapid-fire opening and closing of these channels releases ions, moving electrical impulses from the brain in a wave to their destination in the body.

Starting in 1998, after 10 years studying the biophysics of ion channels, MacKinnon published a series of structural solutions — high-resolution molecular-level "snapshots" of ion channels, produced at Cornell and Brookhaven. These structures literally showed the scientific community how electrical signaling occurs.

MacKinnon, a biophysicist and self-taught x-ray crystallographer, is a professor at Rockefeller University and an investigator at the Howard Hughes Medical Institute. He shares this year's chemistry Nobel with Peter Agre, M.D., of Johns Hopkins University School of Medicine.

[Editor's note: For more information on MacKinnon's work, see the related Feature Highlight beginning on page 2-10]

—Karen McNulty Walsh

Rod MacKinnon. Photo courtesy of Chris Denney for the Howard Hughes Medical Institute, ©2003.

NSLS Shines Light on Disease

October 23, 2003

A group of four BNL scientists investigating the underpinnings of diseases from osteoporosis to botulism presented an overview of their work to a group of reporters in person and via live "webcast" on Thursday, October 23, at BNL. All the presenters use the extremely bright beams of energy (from infrared to x-rays) available at the NSLS.

NSLS Chair Steven Dierker gave an overview of the facility, which is used by more than 2,500 scientists from outside the Lab each year – including this year's chemistry Nobel Prize-winner, Rod MacKinnon of Rockefeller University, who used x-rays to determine the structure of proteins that help transmit nerve impulses throughout the body. Solving protein structures via the technique of x-ray crystallography can help scientists understand the proteins' functions and perhaps devise strategies to prevent them from causing disease.

That is the exact approach being pursued by the Biology Department's Walter Mangel and Subramanyam Swaminathan. Through x-ray crystallography and other techniques, Mangel has uncovered several parts of a viral enzyme that might be susceptible to antiviral drugs. "If you can block the activity of the enzyme," he says, "you can block the infection."

What is more, the sites Mangel has identified interact with one another. This led him to propose a new type of multi-drug therapy that viruses would not be able to "outsmart" via evolution of drug resistance. Using multiple drugs against several targets on the same enzyme might be effective against a range of viruses, including those that cause pink eye and AIDS, and against a range of bacteria, including those that cause Chlamydia, plague, and even malaria.

Swaminathan is using the NSLS x-rays to reveal components of botulinum toxin, the protein that causes botulism, that are central to its paralyzing effects. He is working to develop drugs that fit into the toxin's active sites to disrupt the potentially deadly process at three crucial steps. The result may be a vaccine and/or drugs that eliminate the toxin's potential as an agent of biowarfare or bioterrorism.

Shining the NSLS's beams on more traditional targets — bones and other body tissues — are the NSLS's biophysicist Lisa Miller and physicist Zhong Zhong. Miller is using the infrared beams to study bone composition, particularly that associated with areas of microscopic damage. She wants to know how bone composition changes in response to common osteoporosis treatments. Her work could lead to improvements in osteoporosis drugs.

Zhong uses the NSLS x-rays to look not just at bone, but at soft tissues like cartilage, blood vessels, skin, and fat deposits as well. His technique, called diffraction-enhanced imaging (DEI), uses higher energy x-rays that pass right through the sample without being absorbed, which results in a lower dose to the patient than traditional x-ray techniques. DEI makes soft tissues visible because each tissue type scatters the beam differently. A sensitive analyzer crystal can detect these subtle diffractions and translate them into different intensities, visible on x-ray film in magnificent detail. The technique could yield more accurate and earlier diagnosis of soft-tissue diseases such as breast cancer.

— Karen McNulty Walsh

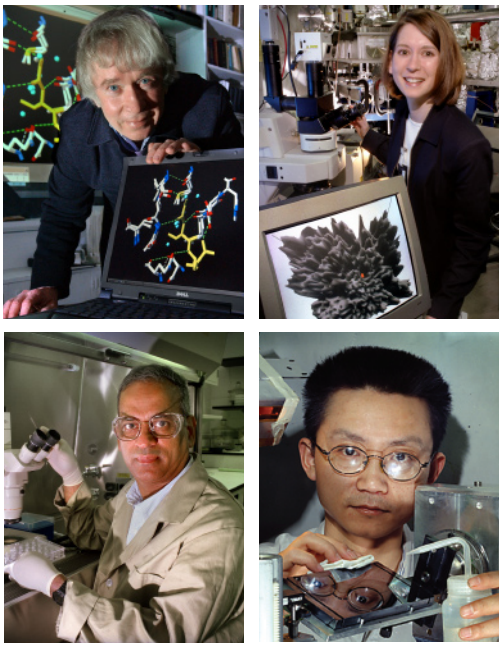

(Top, from left): Walter Mangel and Lisa Miller (bottom, left) Subramanyam Swaminathan and Zhong Zhong.

389th Brookhaven Lecture 'Nanoscale Twist in Liquid Crystal Miniature Video Displays'

December 17, 2003

Recently, commercial large-viewing angle flat panel displays, as well as miniature video displays for digital cameras, camcorders, head- and helmet-mounting, have been produced using ferroelectric liquid crystal (FLC) and antiferroelectric liquid crystal (AFLC) technology.

While developing materials for these devices, researchers noticed the thermal signature of a rich variety of new intermediate phases of the liquid crystals. The structures of these intermediate

Ron Pindak

phases look identical by conventional x-ray analysis and involves nanometer orientational properties that occur at smaller dimensions than can be observed using conventional optical microscopy.

To overcome this limitation of conventional investigative techniques, Ron Pindak, a physicist at the NSLS, and other researchers used a property of synchrotron x-ray sources — or more specifically, an intense beam of linearly polarized x-rays of a specific energy — to directly probe the nanometer-scale helical ordering of these new phases of liquid crystals.

Pindak gave a presentation on this research on Wednesday, December 17, at 4 p.m., the 389th Brookhaven Lecture, "Nanoscale Twist in Liquid Crystal Miniature Video Displays." Pindak was introduced by Steven Dierker, NSLS Chair and Associate Laboratory Director for Light Sources.

As Pindak explained in his talk, the x-ray scattering process is highly sensitive to the orientation of the chemical bonding of the atom, and therefore sensitive to the orientation of the molecule itself when using x-rays with an energy that excites electrons from the core of an atom within a molecule. He described how FLCs and AFLCs are used in devices and contrasted their behavior with more widely used liquid crystals.

Pindak joined BNL in 2001 as a physicist after 24 years at Bell Laboratories. Since then, he has headed the Science Program Support Section of the User Science Division, and taken the lead in developing a condensed matter program. He also served as the Interim Associate Director for the BNL Nanocenter.

Pindak received a B.S. in physics from Boston College in 1969 and a Ph.D. in physics from the University of Pennsylvania in 1975.

— Ron Pindak and John Galvin

Workshop on Frontiers in Synchrotron X-Ray Microbeam Diffraction

January 10, 2003

The Workshop on Frontiers in Synchrotron X-Ray Microbeam Diffraction was held on January 10, 2003 in the Hamilton seminar room in the Chemistry Department at BNL, with a large gathering of over 40 people. The purpose of this workshop was to inform the scientific, university, and industrial community of the plans to design and install a state-of-the-art microdiffraction instrument at NSLS mini-gap undulator beamline X13B. This proposal was submitted to the DOE Office of Science towards the end of January and would be operated as a general user facility with an emphasis on nanoscale research. Opportunities in the cutting-edge science that could be accomplished with this instrument were explored, and user input was solicited.

The workshop was introduced and chaired by Dr. Elaine DiMasi (BNL Physics Dept.), who also outlined the motivation for the proposed instrument. The value of cutting-edge user facilities was described from the perspective of BNL management by Dr. Doon Gibbs, Associate Laboratory Director for Basics Energy Sciences (BES). He emphasized the importance to DOE and BNL of interacting with users at an early stage so that they can influence the evolutionary process by which new facilities are developed and built. He described the organizational structure of BNL BES as well as a number of exciting planned projects. Two such projects that will have a great impact on microbeam diffraction science at BNL are the proposed upgrade to the NSLS and the Center for Functional Nanomaterials (CFN). Dr. Gibbs concluded his presentation with a challenge to the audience to come up with ideas about scientific impacts that can be made by the future NSLS.

The CFN was further elaborated upon by NSLS scientist Dr. Ron Pindak. The CFN is one of five new DOE Nanoscale Science Research Centers (NSRCs). The user programs of the five centers were launched at a workshop in Washington DC on February 26-28, 2003. The CFN has six scientific themes that involve interdisciplinary research on diverse systems, which are listed and described on the CFN website, http://www.cfn.bnl.gov/. The instrumentation and capabilities of the CFN are organized into "lab clusters," such as materials synthesis, proximal probes, nanopatterning, etc. The CFN will be a user facility similar to the NSLS and both user programs will be coordinated through a common user office. Thus, one proposal can allow access to NSLS beamlines as well as CFN lab tools. Two of the NSLS beamlines, a SAXS beamline on X21 and the X13B microdiffraction beamline, will be optimized to service the needs of CFN General Users. The center, in addition to having the infrastructure to support state-of-the-art fabrication facilities, will provide offices and interaction areas for students and postdocs as well as regular staff.

Frontiers in Synchrotron X-Ray Microbeam Diffraction workshop attendees.

Dr. Patricia Mooney of IBM presented a talk on materials research for silicon CMOS technology using microbeam x-ray sources. Strain-relaxed SiGe "virtual substrates" for strained silicon CMOS transistors were described and results of studies characterizing the defect microstructure of these films were presented. Dr. Mooney remarked on how the divergent beam available at X20A of the NSLS limited the resolution at which "micrograins" could be observed, and that a sub-micron, more parallel beam would be of great advantage in her work.

A survey of synchrotron microdiffraction capabilities around the world was given by Prof. Cev Noyan of IBM. He pointed out that several synchrotrons, in particular the ESRF and ALS, have put great emphasis and resources into microbeam diffraction. The great vari-

ety in hard x-ray microfocusing optics and a number of designs for accessing reciprocal space (pink beam Laue, scanning monochromator Laue, small sphere-of-confusion six-circle, single-axis, etc.) were explained. The following two talks described in detail the microdiffraction capabilities currently available at the NSLS. Dr. Ken Evans-Lutterodt of Agere described the X16C microdiffraction beamline. He used the example of the selective growth of semiconductor materials on a patterned substrate to illustrate that microdiffraction combined with spectroscopy can be used to obtain strain and chemical composition information with micron-scale spatial resolution. Dr. Jean Jordan-Sweet of IBM next described the capabilities of beamline X20A. This capillary- and diffractometer-based instrument is primarily used to measure strain fields and mosaic structure by scanning diffraction topography. Results were presented on interfacial stress/strain in metal features on silicon and on electromigration-induced stress in narrow metal lines.

The proposed microdiffraction instrument to be built at X13B was described in the next two talks. Dr. James Ablett of the NSLS presented specifications and recently measured spectral plots of the new X13 Mini-Gap Undulator (MGU) source. He then described the plan to use a 4-bounce silicon monochromator and a variety of x-ray microfocusing optics for the proposed instrument. The monochromator can be removed for pink-beam studies, and the optics will be interchangeable between KB mirrors, capillary, pinholes, zone plates, and planar refractive lenses. The modular design will allow for great flexibility in beamsize and divergence selection. Dr. Ken Evans-Lutterodt further described the diffractometer and detector configurations. In order to minimize vibration and torque on the sample and optics, the detector arm will be a completely separate system. The entire microdiffraction instrument is being designed to be robust, easy to align and use, and modular, in order to serve a variety of users from students to busy experts.

After a break for lunch, the workshop resumed with presentations on scientific opportunities by researchers from a range of disciplines. Dr. Mehmet Sarikaya of the University of Washington began with an overview of the fascinating world of structural biomimetics. Biomaterials such as spiders' silk, mother-of-pearl, protein coats on certain bacteria, sea urchin spines, and sponge spicules exhibit nanoorganization. Understanding the structural, functional, and process design characteristics of these self-assembled structures will lead to the invention of engineered "bio-inspired" materials of the future. Next, Dr. DiMasi presented a talk prepared by Dr. Joanna Aizenberg of Lucent Technologies, which described how self-assembled nano structures of calcite crystals and other materials can be formed using organic alkane chain templates which have a variety of attached functional groups. These assemblies of crystals can be patterned and oriented in many ways by changing the functional group, chain tilt, and lithographic pattern. Following this talk, Prof. Valery Kiryukhin of Rutgers University described several correlated electronic systems that form functional materials, which exhibit large changes in electrical or magnetic properties (such as colossal magnetoresistance) under relatively weak external perturbations. He showed an example of strain mapping in the vicinity of a grain boundary taken at beamline 2ID-D at the APS. In order to study these systems, a microdiffraction instrument with temperature control, precise sample positioning, optical access, and tunable energy is needed. The scientific opportunity session was concluded with a talk by Dr. Jeffrey Kysar of Columbia University who discussed the difficulty in determining the relationship between stress and strain in materials. He has simplified the problem by reducing it from 3-D to 2-D by performing experiments using a line of applied force rather than the conventional point indenter on a metal

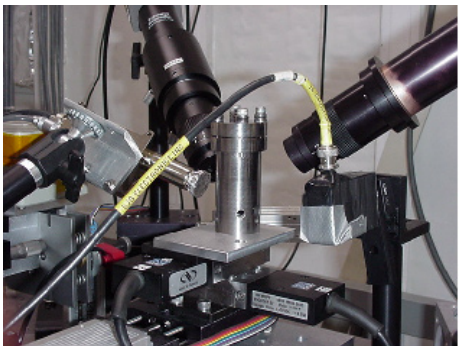

Microdiffraction setup at beamline X13B.

surface. A microbeam diffraction beamline would allow for the measurement of residual stresses and dislocation density on the surface of laser shock processed samples as a function of position from the "peened" line.

During the afternoon discussion session Dr. DiMasi read letters from members of the Clay Minerals Society email listserver. These researchers would like to see an instrument having high brilliance, a sensitive area detector, variable spot size, and control over temperature and humidity. Audience members also supported the desire for environmental control, citing the need to study self-assembly experiments in liquid solution rather than in just the dried post-assembly state. There is a need to get all information - tilt, chemical, lattice spacing, transformation temperature, etc., from single grains on the order of a micron in size. Many times the need for a parallel beam was mentioned. A discussion about the measurement of organic and bio-materials brought up legitimate concern over the possibility of beam damage. Another desired capability mentioned several times is computed tomography. Questions were asked about the time structure of the existing NSLS x-ray ring vs. the proposed upgrade. Pump-probe experiments are possible now with a ~0.5 nanosecond period, and in the future with ~20 femtosecond resolution. The APS currently has a 50 picosecond timing structure. It was pointed out that single-shot microdiffraction would not yield enough intensity, but a locked-in, repeated pump-probe setup would be able to accumulate enough signal.

The workshop concluded with committee members encouraging researchers to try microbeam experiments now on existing instruments, in order to see what is needed and what works. It is expected that the new microdiffraction beamline will constantly evolve over time, and experience now will lead to a better instrument in the future. Many components are available now or will be soon for experimental trials.

—Jean Jordan-Sweet

Two NSLS Scientists Win Engineering Awards

January 30, 2003

At the BNL Employee Recognition Award Ceremony on January 30, 17 Lab employees were rewarded with BNL's highest honors, including two NSLS scientists who won the $5,000 Engineering Awards, which are given to recognize distinguished contributions to engineering or computing over one or more years.

Donald Lynch, a project engineer who joined BNL in September 1991, and George Rakowsky, an electrical engineer who returned to BNL in July 1993, both at the NSLS, were recognized for their sustained contributions in the development of small-gap, in-vacuum undulators, a technology now adopted at most synchrotron radiation facilities in the world.

Pictured at right with Associate Laboratory Director for Facilities & Operations Mike Bebon (back, right) are the recipients of BNL's 2002 Engineering Award: (back, from left) Donald Lynch, NSLS Department; George Rakowsky, NSLS; Jack Fried, Instrumentation Division; (front, from left) George Ganetis, Magnet Division; Christopher Channing, Plant Engineering Division; and Joseph Levesque, Emergency Services Division.

The NSLS operates two electron storage rings: the 2.8-giga electron volt (GeV) x-ray ring and a 0.8-GeV vacuum ultraviolet ring, which contain periodic magnetic structures called wigglers and undulators, collectively known as insertion devices. Electrons are sent racing around the rings at nearly the speed of light. When they cross an insertion device, they emit a very intense, narrow beam of synchrotron radiation.

Earlier generations of undulators in medium-energy machines such as the NSLS x-ray ring are able to generate only "soft" x-rays, up to about 1 kilo electron volt (keV) of photon energy. The small-gap undulators generate tunable "hard" x-rays in the range of 3 to 20 keV, which are essential for decoding the structure of complex biological molecules in the rapidly expanding field of structural biology. Previously, tunable hard x-ray beams were available only at the very high-energy storage rings, such as the 7-GeV Advanced Photon Source at Argonne National Laboratory.

The idea of introducing a small-gap, short-period undulator in the NSLS

x-ray ring was originated in the late 1980s by Sam Krinsky, then NSLS Deputy Chair. Peter Stefan, then NSLS physicist, did the first proof-of-principle tests and developed the conceptual design of the small-gap undulator. Lynch worked with Stefan on the mechanical, structural, thermal, and vacuum design of the first two generations and on the latest version of the device.

Rakowsky proposed the magnetic design in 1991 and built a demonstration model, followed by the full-scale magnet arrays of the Prototype Small-Gap Undulator (PSGU) under contract for the NSLS, while he was employed at Rocketdyne, now part of Boeing, in California. After returning to BNL in 1993, Rakowsky worked with Lynch, Stefan and other collaborators at SPring8 in Japan, to develop the breakthrough In-Vacuum Undulator (IVUN).

Lynch and Rakowsky then developed the third-generation, higher-performance Mini-Gap Undulator (MGU), which has operated in the x-ray ring since January 2002. The MGU's compact size will allow the installation of two more MGUs, resulting in two new undulator beamlines. The next MGU was installed in May to serve a new beamline funded by the National Institutes of Health and dedicated to structural biology.

In developing these devices, still record-breakers as the smallest in their field, Rakowsky led the way in magnetic design and measurement, while Lynch provided the mechanical solutions to meet each challenge.

Their success has established the NSLS as the leader in small-gap undulator technology.

This innovation has dramatically changed light-source development world-wide to favor medium-energy machines of around 3-GeV over the more costly 6-to-8-GeV machines previously constructed as hard x-ray sources. The small-gap concept also serves as the basis for the NSLS 3-GeV upgrade proposal.

—Patrice Pages

BNL/Canadian Space Agency Experiment Lost in Tragic Columbia Accident

February 1, 2003

Among the 80 scientific experiments lost in the recent tragic accident involving the space shuttle Columbia, one was prepared by a team of scientists who would have studied the results at the NSLS. This experiment had been designed to provide insights into developing not only new drugs against cancer, but also drought-resistant plants.

The experiment is part of the Canadian Space Agency's Protein Crystal Growth (PCG) program, a project aimed at studying how proteins grow in space. A series of different protein crystal growth experiments were conducted in the recent Columbia mission, one of which is involved in a hallmark of cancer, called cachexia, which results in emaciation and muscle wasting. Another represented a protein used by plants to defend against environmental stress, such as drought and high salinity.

Protein crystal growth experiments were conducted on the Space Shuttle Columbia.

"Previous crystal growth experiments conducted in space have provided evidence that, when protein crystals grow in space, they are of higher quality, that is, they have fewer defects and may be of larger size than those grown on Earth," says Robert Sweet, BNL Biology Department and a PCG project collaborator. "But we know too little about the effectiveness of having crystals grow in space, where there is nearly no gravity. So we decided to compare crystals grown on Earth and in space."

Controlled Experiment

The PCG scientists, led by Jurgen Sygusch, a biochemist at the University of Montreal in Canada, designed a controlled experiment wherein duplicate samples of proteins in solution were taken to Kennedy Space Center (KSC), and one set of samples was taken into space on the space shuttle Columbia, one of five reusable spacecraft that had been employed by the National Aeronautics & Space Administration (NASA) since 1981.

While Columbia circled Earth from January 16 to 31, the protein samples on board were allowed to crystallize. At the same time, duplicate samples acting as controls were crystallized at KSC in the same type of crystallization hardware. If Columbia had returned to Earth, the two sets of samples were to have been compared with one another, using the intense light generated by the NSLS.

How Crystals Grow

"When crystals grow on Earth, gravity introduces disturbances that affect the way protein molecules assemble into a crystal lattice," Sygusch says. "But, in spacecraft such as Columbia, which orbit about 400 miles above Earth, crystal growth is subjected to only a millionth of Earth's gravity — called microgravity — so that the protein molecules during crystal growth are free of these disturbances, which is what we wanted to study."

In their experiment, the scientists planned to investigate two important disturbances, called convection and sedimentation, that occur during crystal growth.

"You can imagine a growing crystal being like layers of molecules that are piling up on each other," Sygusch says. "Non-crystalline aggregations of protein molecules that form naturally under crystal-growth conditions tend to disturb the deposition of these layers."

Sygusch explains that convection in the protein solution occurs because the protein is actually at a lower concentration, and therefore lower density, immediately adjacent to the growing crystal. This causes an upwelling of the solution that causes a surprisingly vigorous mixing of proteins and their aggregates.

As for sedimentation, once small crystallites have formed, they tend to sink to the bottom of the container, out of the zone of where they grew, and often cease growth.

Both convection and sedimentation affect crystal growth on Earth. In micro-gravity, the absence of convection eliminates solution mixing and reduces incorporation of protein aggregates into the crystal lattice, while no sedimentation allows crystallites to grow into larger crystals, leading to crystals of better quality. The higher crystallinity translates into a better definition of the atomic detail that can be obtained from synchrotron diffraction experiments.

"To get our results," Sweet says, "we had not only prepared two identical experiments, one on Earth and the other in space, but we had also decided that the data collected from both experiments would be analyzed in a double-blind fashion. After crystals had been recovered from Columbia, they would have been combined with the crystals grown on Earth in such a way that we could measure results without knowing until afterwards from which source the crystals came."

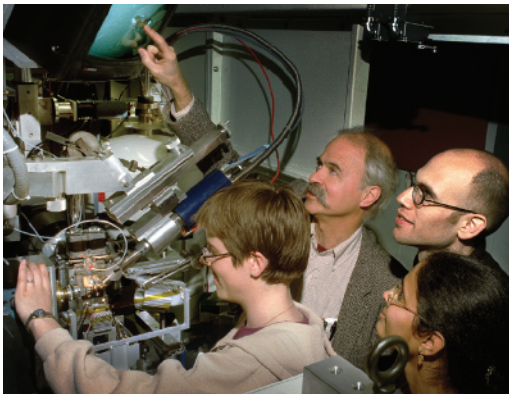

BNL scientist Bob Sweet demonstrates protein crystallography experiments underway at the NSLS.

Next Step

The PCG team is now waiting to know when they will be able to send new experiments in space, perhaps in an unmanned spacecraft. "Our experiment could easily be activated automatically," comments Sweet.

"Some perturbations, such as astronaut movements and orbit corrections, could be avoided if this experiment were performed in a free flyer or unmanned spacecraft," agrees Sygusch, who is confident that more chances to conduct experiments in space will arise in the near future.

"The latest Columbia mission was a tragic human disaster and a scientific catastrophe," Sygusch says. "But, once we understand what happened, we must continue. We will be able to investigate something never achieved before in the history of humankind: a glimpse of what life might look like in a world with a different level of gravity."

—Patrice Pages

U.S. Rep. John Sweeney Visits BNL and NSLS

February 24, 2003

U.S. Representative John Sweeney (R-20th District), visited BNL on February 24 with his aide Gaia Mishanta Ford. Sweeney serves on the House Appropriations Committee and on February 12 was named to the Select Committee on Homeland Security, which helps develop policy for the larger Homeland Security Committee.

Welcomed by BNL Interim Director Peter Paul, Sweeney met with Michael Holland, Manager of DOE's Brookhaven Area Office, and Marge Lynch, Assistant Laboratory Director for Community, Education, Government & Public Affairs. The Congressman then visited the NSLS, one of the world's most widely used scientific facilities. Researchers at the NSLS use sophisticated techniques to study the electronic and structural properties of materials and surfaces at the atomic level.

At the NSLS, Doon Gibbs, Interim Associate Laboratory Director for Basic Energy Sciences, and NSLS Chair Steven Dierker explained a proposed NSLS upgrade that will dramatically improve the capabilities available to the approximately 2,500 researchers from scientific institutions and industry who use the NSLS for their research each year. They also discussed plans for the new BNL Center for Functional Nanomaterials.

Later, on the NSLS experimental floor, Sweeney visited beamline U10B, where researchers use infrared light to study such diseases as Alzheimer's, osteoarthritis, and osteoporosis.

He next stopped at Berkner Hall, where Ralph James, Associate Laboratory Director for Energy, Environment & National Security, explained some of the Lab's work in the field of homeland security.

James focused on BNL capabilities in the areas of advanced sensor technology, particularly the Lab's research and development on nuclear, chemical, biological, and explosive detectors.

Sweeney was also interested in seeing actual prototypes of BNL hardware that could detect more minute quantities of nuclear radiation from greater distances and without the false alarms attributed to many current approaches.

James described some of BNL's research suited to reducing the vulnerabilities of New York State, including better control of radioactive materials, advanced technologies to monitor cargo containers at national seaports, and sensor networks to help protect New York and its mass transportation systems.

BNL scientists' work to identify and prioritize risks, such as those connected with U.S. public water, bridges, banking and finance, electric power, gas, and oil and telecommunications infrastructures, was also presented.

On the experimental floor of the NSLS, U.S. Representative John Sweeney (center) and BNL Interim Director Peter Paul talk with NSLS scientist Lisa Miller about research on Alzheimer's disease being done at beamline U10B.

The Congressman conversed with Associate Director for Life Sciences Nora Volkow before concluding his visit. "The enthusiastic interest shown by Congressman Sweeney in the broad science of BNL, as well as his immediate understanding of the Lab's crucial role in the safety and securitiy of New York City, was impressive and refreshing," said BNL Interim Director Peter Paul.

— Liz Seubert

DOE Nanoscience Workshop Draws Crowd

February 27-28, 2003

More than 400 attendees of the first DOE Nanoscale Science Research Centers workshop, which was held February 27-28 in Washington D.C., were treated to a blue-ribbon lineup of political and scientific speakers. The message the participants heard was loud and clear: Nanotechnology research may involve the study of very small things, but it represents potentially very big things in terms of federal funding for the physical sciences.

"It's as if we all have the same speechwriter," observed former BNL Director John Marburger, who is now Director of the Office of Science & Technology Policy and President George W. Bush's science advisor, who delivered an address entitled "Nanoscience and the National Science Agenda."

In his speech, Marburger said that the governments of every major developed nation are now seeking to gain a competitive advantage by investing in nanotechnology research. "What gives our nation the edge are the five DOE nanoscale science research centers," he said.

Under the National Nanoscience Initiative which was launched in fiscal year 2001, DOE's Office of Science announced it would establish the five new centers to "support the synthesis, processing, fabrication, and analysis" of materials at the nanoscale. These centers are: Lawrence Berkeley National Laboratory's Molecular Foundry; the Center for Functional Nanomaterials at BNL; the Center for Integrated Nanotechnologies at Sandia National Laboratories and Los Alamos National Laboratory; the Center for Nanophase Materials Materials Sciences at Oak Ridge National Laboratory; and the Center for Nanoscale Materials at Argonne National Laboratory.

Marburger was introduced by Office of Science Director Raymond Orbach who, in his opening remarks, proclaimed that the five DOE nanoscience centers will be at the hub of national laboratory research efforts in nanorelated fields.

"All five centers are in the President's proposed FY2004 budget and all are well on their way to becoming a reality," Orbach said.

Before hearing from Orbach and Marburger, workshop attendees first heard from U.S. Representative Judy Biggert, a Republican who represents the 13th District of Illinois and who chairs the Energy Subcommittee of the House Science Committee.

Biggert recently introduced H.R. 34, the "Energy Science and Investment Act of 2003," which calls for the Office of Science to receive an overall increase in funding of nearly 62 percent by FY2007. This would mean a FY2007 authorization level of $5.31 billion, compared to the $3.3 billion funding for FY2003. According to the American Institute of Physics, her bill is one of the most important physics-related research bills that the new Congress will consider this year.

"Nanotechnology research is very important to our nation's future economic competitiveness," Biggert told workshop attendees. "The Office of Science is uniquely positioned to do nanotechnology research and I am convinced its nanoscience centers can only enhance our economic competitiveness."

The Congresswoman urged attendees to contact their Congressional representatives and get them to support H.R. 34, which now has 74 cosponsors. In addition to a substantial increase in funding for the Office of Science, her bill would also make some significant administrative changes in DOE. An Under Secretary of Energy & Research position would be created, with authority over all DOE funded civilian science at the non-weapons national laboratories and research universities. A new Assistant Secretary of Science would replace the current director position, and a Science Advisory Board would be established that would consist of the chairs of DOE's advisory panels.

Attendees at the DOE Nanoscale Science Research Centers workshop.

"I am a scientist wannabe who has always thought that scientists were very cool," Biggert said to enthusiastic applause.

The applause was also enthusiastic and vigorous for U.S. Representative Zach Wamp, a Republican who represents the 3rd District of Tennessee and serves on House Appropriations Committee

and the Energy and Water Subcommittees.

Speaking at a Thursday luncheon, Wamp told attendees, "If we want a balanced federal budget, we have to invest in technology. Investing in the physical sciences can give us another boom economy."

Wamp has won a "Champions of Science" award bestowed by the Science Coalition, an alliance of more than 400 organizations dedicated to sustaining the federal government's commitment to U.S. leadership in basic science. As a rousing speaker, Wamp energized the nanoscience audience.

Arguing that the national economic slump is a reason for more investment in the physical sciences rather than less, he cited the example of the Japanese government.

"The economy in Japan is bad, but that did not stop their government from investing in super-computing and taking the lead in that technology," he said. "New technologies are needed to solve problems not just today but for the long-term too. This takes leadership [in the physical sciences] and we're just not there now."

To get the resources needed to advance the development of nano and other technologies that can help solve persistent global problems, such as energy, Wamp said, "We need to do a much better job of marketing the physical sciences. We've got to brand the physical sciences in a different way. It is crucially important to the vitality of your science and this country's economy that we get people excited about and supportive of the physical sciences."

Attendees also heard from Senator Pete Domenici (R-New Mexico), another winner of the Champions of Science award. As chairman of the Senate Energy and Water Development Appropriations Subcommittee, Domenici has been a strong supporter of the physical sciences. He is especially keen on the promise of nanotechnology.

"Nanotechnology represents a new frontier, and it's harder to guess exactly where these new ultra-miniaturized technologies will make the greatest contribution," the Senator said. "Suggestions range from new generations of ultra-tough or ultra-light materials to new approaches to hydrogen storage for a future generation of hydrogen fueled vehicles. This is a truly exciting and revolutionary field."

Domenici also expressed confidence in DOE's ability to lead the development of nanotechnology. "The Department has led the nation in other major scientific initiatives in the past, from high performance computing to the human genome project," he said. "Nanoscience provides another golden opportunity for the Department to again lead the way into an important new area."

Scientific presentations were given by a number of the major names in nanotechnology research, and the directors of the five nanoscale science research centers each gave an overview of their centers, including BNL's Bob Hwang, who spoke about the Lab's Center for Functional Nanomaterials.

It was Patricia Dehmer, Director of DOE's Office of Basic Energy Sciences, who perhaps best summarized the anticipated role of the five new nanoscience centers with respect to the National Nanotechnology Initiative and the country's need to maintain economic competitiveness.

"The DOE centers are different from centers funded by the National Science Foundation and others, in that they are patterned after the same philosophy that guides our national user facilities: They are there to be used by everyone, including researchers from universities and private industry, as well as national laboratories," Dehmer said. "We will partner aggressively with NSF and others to get the job done. The importance of nanotechnology research and development cannot be overstated."

— Lynn Yarris, Lawrence Berkeley National Laboratory

John Marburger, Director of the Office of Science & Technology Policy, and Patricia Dehmer, Director of DOE's Office of Basic Energy Sciences.

SUNY Chancellor Robert King Visits Brookhaven

March 27, 2003

On Thursday, March 27, Robert King, Chancellor of the State University of New York (SUNY), visited BNL for an introduction to the Lab and its programs. As SUNY Chancellor, King oversees one of the nation's largest university systems, with about 500,000 students and an annual state budget of about $7 billion. After a welcome lunch with Interim BNL Director Peter Paul, BNL Director-designate Praveen Chaudhari, Manager of the DOE Brookhaven Area Office Michael Holland, and several Associate Lab Directors and Department Chairs, the Chancellor toured the Lab.

The first stop focused on atmospheric chemistry research in the Environmental Sciences (ES) Department chaired by Creighton Wirick. ES scientist Peter Daum of the Atmospheric Sciences Division talked about BNL's laboratory, field, and modeling program that has contributed to understanding the mechanism of photochemical smog formation. Judy Weinstein-Lloyd, a professor at SUNY Old Westbury who has a long-standing collaboration with BNL scientists, spoke of her program to develop new instrumentation for measuring atmospheric oxidants.

Ralph James, Associate Laboratory Director for Energy, Environment, & National Security, then described BNL homeland security initiatives, such as research and development on nuclear, chemical, biological, and explosive detectors. James showed King actual prototypes of BNL hardware that could detect small quantities of nuclear radiation from great distances.

King's second stop was at the Relativistic Heavy Ion Collider (RHIC), where Associate Laboratory Director Thomas Kirk, together with Collider-Accelerator (C-A) Department Chair Derek Lowenstein and Physics Department Chair Samuel Aronson described the program of RHIC and its four detectors. At one of these detectors, PHENIX, Ed O'Brien, PHENIX operations manager, and PHENIX analysis coordinator Thomas Hemmick, a physics professor at Stony Brook University outlined the scientific goals of the experiment and gave King a brief idea of how PHENIX collects RHIC data.

Next, King visited the NSLS, one of the Northeast's and New York State's most important scientific facilities. Interim Associate Laboratory Director for Basic Energy Science Doon Gibbs and NSLS Chair Steven Dierker explained a proposed upgrade that will dramatically improve the capabilities available to the NSLS's approximately 2,500 researchers from universities, scientific institutions, and industry.

Listening as Peter Daum (right) of the Environmental Sciences Department explains BNL research in atmospheric chemistry are: (from left) Ralph James, Associate Laboratory Director for Energy, Environment, & National Security; Creighton Wirick, Environmental Sciences Department Chair; Praveen Chaudhari, then designate BNL Director; Robert King, State University of New York (SUNY) Chancellor; Judy Weinstein-Lloyd, SUNY Professor at Old Westbury; Brian Giebel, SUNY Old Westbury; and Jun Zheng, Stony Brook University.

As King learned, researchers from SUNY at Albany, Buffalo, Plattsburgh, and Stony Brook used 20 NSLS beamlines during fiscal year 2002 for studies of, for example, materials characterization, materials in high magnetic fields and under extreme conditions, polymers, and biological and environmental systems. Plans for the new BNL Center for Functional Nanomaterials were also discussed.

The SUNY Chancellor moved on to BNL's NeuroImaging Center, where Linda Chang, Medical Department Chair, and Joanna Fowler, who heads the NeuroImaging Center, described some of the Lab's pioneering neuroimaging research on the brain chemistry of addiction; diseases such as Parkinson's and Alzheimer's; and aging. King also learned about the center's recent research on imaging awake animals, which has veterinary support from SUNY's Downstate Medical Center in Brooklyn.

King concluded his visit with discussions at the Director's Office, during which he stated how impressed he was with the programs of the Laboratory and its broad scope of research. He

pointed to a number of educational opportunities as good steps to increase the connections between the Lab and New York State. Interim Director Paul, who expressed his appreciation to the Chancellor for the visit to BNL, commented, "Chancellor King clearly recognized the importance of BNL for the economy of New York State and the education of the education of the State's students."

— Liz Seubert

RapiData Crystallography Course

April 6-11, 2003

Once again last spring, budding crystallographers from around the world gathered at BNL. They were attending RapiData 2003, a week-long course run by BNL's Biology and NSLS Departments. This course introduces students to the best people, newest equipment, and latest techniques in the field of macromolecular x-ray crystallography.

Emphasizing "Rapid Data Collection and Structure Solving at the NSLS," this "Practical Course in Macromolecular X-Ray Diffraction Measurement" ran from April 6 to 11. It consisted of two days of lectures and tutorials taught by scientists from BNL, industry, academia, and other national labs, followed by data collection and analysis at the NSLS. The same instructors and others act as hands-on advisors for a marathon sixty-hour data-collection session to close out the week. Half of this year's 48 students came as observers, while the other half arrived with specimens to analyze. Seven of the students left with solved structures, which will likely result in publications.

The course, which helps to train the next generation of NSLS users, is mostly organized by Bob Sweet and Denise Kranz of Biology, but they emphasize that its success absolutely depends on enthusiastic help from most of the twenty members of the PXRR (the Biology and NSLS Macromolecular Crystallography Research Resource), plus a dozen or so outside teachers.

Major funding for the course was from the National Institutes of Health through the National Center for Research Resources, and DOE's Office of Biological & Environmental Research, with support from the NSLS, and some interested equipment vendors and drug companies.

— Karen McNulty Walsh

Representatives of DOE Light Sources Meet with Elected Officials in Washington, D.C.

April 7-8, 2003

For the third consecutive year, a delegation of scientists representing the four U.S. Department of Energy (DOE) synchrotron light sources organized a successful lobbying trip to Washington, D.C. on April 7 and 8, 2003.

The visit was organized and coordinated by Leemor Joshua-Tor, the chair of the NSLS Users' Executive Committee (UEC). The delegation was comprised primarily of the chair and vice-chair of the UECs of the Advanced Light Source at Lawrence Berkeley National Laboratory (CA), the Advanced Photon Source at Argonne National Laboratory (IL), the NSLS, and the Stanford Synchrotron Radiation Laboratory at Stanford University (CA). Accompanying the delegation was Pat Fulton, Science Lobbyist for Stanford University. The NSLS scientists in the delegation were Tony Lanzirotti, UEC vice-chair, and Simon Bare, UEC lobbying coordinator.

A group of RapiData students seen with instructors Annie Héroux (standing, left), a BNL Biology Department structural biology scientist who works at NSLS beamline X26C, and Frank von Delft (foreground), Scripps Research Institute.

"The goal of these visits is to increase the visibility of the synchrotrons and the Department of Energy's Office of Science who funds them," Joshua-Tor says. "The Office of Science budget has remained essentially flat in recent years, forcing light source funding to remain flat as well, although the number of light source users nearly doubled."

"This office is by far the largest funding agency for the physical sciences in the U.S.," Bare says, " but its funding is buried within bills approved by the Senate Energy and Water Appropriations Subcommittee of the Senate Appropriations Committee and the House on Energy and Water Development Subcommittee of the House Appropriations Committee."

DOE's budget for fiscal year 2003 is $21.9 billion, of which only 15% ($3.3 billion) funds the Office of Science, and only one-third of this amount goes to Basic Energy Sciences, which is the primary funding agency for light source operations. "This amount does not reflect the real needs of the scientists working at the light sources," Bare says, "because the number of users keeps growing, but not the funding, so an infusion of operating funds is urgently required."

On the first day of the visit, the delegation met with Patricia Dehmer, Associate Director of Science for the Office of Basic Energy Sciences, which is one of six offices managed by the Office of Science; Joel Parriott, Budget Examiner from the Federal Office of Management and Budget; John Marburger, Director of the White House Office of Science and Technology Policy (OSTP) and science advisor to President George W. Bush; Kathie Olsen, Associate Director for Science at the OSTP; Michael Holland, Senior Policy Analyst at the OSTP; and Clay Sell and Drew Willison, both Staff members from the Senate Energy & Water Subcommittee of the Senate Appropriations Committee.

Marburger, who welcomed the delegation in his office in the morning of the first day, expressed his strong support for the four light sources, stating that he was holding them in high regard and considered them as the most productive user facilities by the scientific research community worldwide.

On the second day of the visit, the delegation met with senior staffers from the Senate Committee on Energy and Natural Resources, the Energy Subcommittee of House Science Committee, and the Energy and Water Development Subcommittee of the House Appropriations Committee.

The highlight of the visit was a meeting between NSLS user Martin Caffrey, professor of chemistry at Ohio State University in Columbus, and Representative David Hobson (R-OH), the new Chair of the House Energy and Water Development Subcommittee of the Appropriations Committee. Caffrey was accompanied by Simon Bare. The discussion focused on the wide variety of scientists working at the light sources, most of whom are not employees of the national laboratories housing the light sources, but come from universities, other federal agencies, and industry.

At the end of the second day, Bare and Lanzirotti visited with Sean Sweeney, a staffer in the office of Senator Hillary Rodham Clinton (D-NY) and expressed their interest in increasing funding for the DOE's Office of Science. The two scientists also reported to Sweeney that a proposal has been made to the Basic Energy Sciences Advisory Committee (BESAC) to build a new synchrotron at Brookhaven Lab, NSLS-II, which will provide a brighter beam for greatly improved scientific data and many new scientific discoveries.

The members of the delegation were generally satisfied with their visit. "We came away from our visit feeling positive and with many good suggestions on how to expand our efforts," Lanzirotti says. "We also noticed signs of support for increased funding for the Office of Science. For example, the bill introduced onto the floor of the House (H.R. 6) on April 10 provides for budget increases of approximately 15, 10, 15, and 15 percent over the next four years."

— Leemor Joshua-Tor and Simon Bare

NSLS's Youngest Scientists Learn from Light on "Take Our Daughters and Sons to Work" Day

April 24, 2003

On April 24, about 30 daughters and sons learned about some of the scientific programs at the NSLS, and even performed their own scientific experiments. The one-day visit was part of the national "Take our Daughters and Sons to Work Day."

At the NSLS, the children learned that the facility produces many types of light, from microwaves to x-rays, which have many applications in many fields, including electronics, catalysis, microscopes, and medicine. NSLS scientists Marc Allaire, Steve Hulbert, Lisa Miller, and Vivian Stojanoff offered a tour of the experimental floor to the boys and girls, who discovered how synchrotron light is used to design non-stick coatings for aluminum pans, study bone diseases like osteoporosis, and develop new drugs using protein crystallography.

After the tour, the daughters and sons had the chance to perform their own scientific experiments. Marc Allaire demonstrated simple reflection of light from a mirror and contrasted that with the process of diffraction, which was illustrated by reflecting red laser light from a CD-ROM -- the world's most popular diffraction grating. But perhaps the most exciting moment was when the boys and girls discovered that they could created their own rainbow patterns by diffracting visible white light from the CD-ROM.

The boys and girls then had the opportunity to learn from Lisa Miller about the wonders of liquid nitrogen. By immersing an inflated balloon in liquid nitrogen, they discovered that the air inside of the balloon contracts, and then re-expands when warmed up. Much to the amazement of the entire crowd, the balloon survived dozens of repeated freeze-thaw cycles without bursting. But perhaps one of the most memorable experiments involved freezing natural versus artificial daffodils in liquid nitrogen. Both the children and their parents learned that it is much more fun to freeze and crumble a living flower than to take it home as a souvenir.

— Lisa Miller

Simple reflection demonstrated with a flashlight, mirror, and a white board.

NSLS 2003 Annual Users' Meeting Highlights Scientific Successes, Exciting Future Plans

May 19-21, 2003

A spirit of optimism pervaded the 2003 annual meeting of National Synchrotron Light Source (NSLS) users, held at BNL May 19-21, 2003, with presentations on scientific successes and plans for new facilities.

About 30 sons and daughters visited the NSLS for "Take our sons & daughters to work" day.

"A lot of good things have happened at BNL in the last year," said Doon Gibbs, BNL's Interim Associate Laboratory Director for Basic Energy Sciences, as he welcomed NSLS users from around the country and the world to the Tuesday morning main meeting, chaired by Tony Lanzirotti of the University of Chicago, Chair-Elect of the Users' Executive Committee (UEC). Gibbs pointed out that BNL had made "great strides" toward establishing a new Center for Functional Nanomaterials (CFN) and toward significantly upgrading the NSLS. He also noted that several highly qualified people had been brought into BNL leadership positions, including Praveen Chaudhari, the new Laboratory Director.

Among speakers and attendees at the Annual National Synchrotron Light Source Users' Meeting are: (from left) Tony Lanzirotti, University of Chicago; Steven Dierker, BNL; Patricia Dehmer, DOE; Doon Gibbs, BNL; Pedro Montano, DOE; Peter Paul, BNL; Leemor Joshua-Tor, Cold Spring Harbor Laboratory; and Chi-Chang Kao, BNL.

In introducing Peter Paul, Deputy Director for Science & Technology, Gibbs also took the opportunity to thank Paul for his steadfast leadership as Interim Director during the past two years.

Paul, whose task was to give an overview

of BNL, echoed a statement made by Chaudhari at the previous week's RHIC & AGS Users' Meeting, that DOE program managers take a great risk when they build new facilities with the hope that users will come and do good science.

"Fortunately it has always seemed to work out, but we can't take it for granted," Paul said, emphasizing how important it is to have an active user community, such as that at the NSLS, to keep a facility strong. With such involved users and the new leadership at the Lab — including Chaudhari, Gibbs, James Misewich as Materials Science Department Chair, Robert Hwang as CFN Director, and Alex Harris as Chemistry Department Chair — "We are all set to move forward," Paul said.

After describing improvements in support services, housing, and other facilities for users, Paul spoke of the CFN, recent findings at the Relativistic Heavy Ion Collider, and the proposed NSLS-II, a third-generation light-source ring that would be the future center of synchrotron activity at BNL and in the Northeast. "The Laboratory will commit all the resources we can muster to make this a reality," he said.

Bob Hwang then presented details of the CFN, recognizing that "the current excitement in nanoscience is based on work that has been going on for decades at synchrotrons like the NSLS, and you, the users, are a big part of that." He asked NSLS users for help in shaping the new center, noting that the CFN, like DOE's four other nanoscience research centers, was co-located within an existing DOE research facility, in this case the NSLS, to build on existing strengths.

Like the NSLS, the CFN will be a user facility, with a similar process for reviewing proposals. With a range of complementary facilities focused on six scientific areas, the CFN will address the goal of tailoring materials' responses to achieve specific functionality based on an understanding of nanoscale phenomena.

Offering one example of what nanoscience might yield, Phaedon Avouris of IBM's T.J. Watson Research Center then gave the meeting's keynote address on "Carbon Nanotube Electronics."

With a break from science to focus on funding, UOP's Simon Bare, lobbying coordinator for the UEC, then urged all NSLS users to learn about the federal funding process and to get involved.

Users could help to "educate" their own legislators and the congressional committee members vital to science funding — via letters, phone calls, office visits, and even op-ed articles in newspapers — about the importance of research sponsored by DOE's Office of Science. Several bills that propose increased funding for the Office of Science are pending, he said, so to take action now is vital. For more information, see: http://www.nslsuec.org.

Robert Hwang (left), who is Director of the Lab's new Center for Functional Nanomaterials. Keynote speaker at the meeting was Phaedon Avouris (right) of IBM's T.J. Watson Research Center.

The meeting's next session was chaired by Ron Pindak, Head of Science Program Support for the NSLS. Patricia Dehmer, Associate Director of the Basic Energy Sciences (BES) within DOE's Office of Science, started the session. "After hearing this morning's talks," she said, "it strikes me that this is the beginning of a transition period for the Lab, and I'm very optimistic about the future of this institution."

Members of the 2003 planning committee for the NSLS Users' Meeting include: Ron Pindak, BNL; Annie Heroux, BNL; Dan Fischer, National Institute of Standards & Technology; Lisa Miller, BNL; Liz Flynn, BNL; Lydia Rogers, BNL; Mary Anne Corwin, BNL; Sue Wirick, Stony Brook University; and Tony Lanzirotti, University of Chicago.

Long-range planning within BES has resulted in a recommendation for a general upgrade to provide a full return on capital investments at existing light sources, Dehmer explained. Another recommendation was for the NSLS-II upgrade. "This rated very high," she said, encouraging the spontaneous applause that erupted, adding, "You can thank Steve [Dierker, NSLS Chair] for doing such a good job at the presentation."

Referring to the five DOE Nanoscale Science Research Centers, she said, "We are extremely happy that one of those is at Brookhaven. These [nanocenters] are

going to be a very, very important component of the BES family of facilities."

Dehmer then gave her "Totally Unsanctioned Safety Seminar," drawing partly from her own lab experience. The bottom line: "It is possible – and required – to run your laboratory safely, and Pat will become a pest [with investigations and possible cuts in funding] if you mess up."

Following Dehmer, Steve Dierker gave an overview of recent NSLS successes, including Roderick MacKinnon's "spectacular piece of work" on voltage-dependent potassium ion channels, featured on the cover of the May 1 issue of Nature; studies of materials that expand under pressure; and a paper on cell membrane fusion that explains "one of the most basis processes" of cell division. "This has been an action-packed year, with a lot of exciting developments," he said.

Dierker gave credit to the NSLS's support staff, saying, "None of these advances would have been possible if we could not deliver the photons to the end of the beamline. It takes a dedicated and talented staff and a determined effort to keep both rings running reliably."

Dierker then reviewed the many beamline and instrumentation improvements of the past year, and talked about the proposed NSLS-II.

This $400 million upgrade, featuring a new x-ray storage ring three times larger than the current NSLS, would be constructed on Brookhaven Avenue, across from the existing structure, featuring 21 superconducting undulator beamlines and providing the highest brightness of any existing light source, with much shorter pulses.

"Our goal is to build the ultimate medium-energy storage ring," Dierker said. "We would see a huge impact from these enhanced capabilities, especially in the areas of nanoscience and protein crystallography, as larger cells and smaller crystals could be analyzed."

The meeting continued with scientific talks on nanoscience, thin films, x-ray crystallography, and new x-ray sources. During the afternoon session chaired by Lisa Miller, Coordinator of the NSLS's Information & Outreach Office, the UEC Community Service Award was presented to Michael Sullivan, Chief Beamline Engineer for Albert Einstein College of Medicine, for service, innovation and dedication to NSLS users. The winners of the Student/Post Doc Poster Contest were also announced.

Poster prizewinners at the 2003 NSLS Users' Meeting are: (from left) Ally S.-Y. Chan, Rutgers University; David Linkous, George Mason University; Hidenori Tashiro, University of Florida; Henrik Loos, BNL; Daisuke Kawakami, Stony Brook University (SBU); and V.G. Alexandratos, SBU.

Users were then invited to hear more about the BNL nanocenter and encouraged to meet with CFN scientific and facility leaders before adjourning for the meeting's Western-theme banquet in Berkner Hall.

—Karen McNulty Walsh

Frontiers in Powder Diffraction Workshop

May 19, 2003

The theme of the workshop, "Frontiers in Powder Diffraction," held on May 19th at the 2003 NSLS Users' Meeting, was the growing practice and utility of powder diffraction and related techniques in a variety of contexts. Speakers covered work done with x-rays and neutrons, performed at the NSLS, Advanced Photon Source, European Synchrotron Radiation Facility, ISIS (spallation neutron source at Rutherford Appleton Lab, UK), the Intense Pulsed Neutron Source (Argonne National Lab), and the Institut Laue-Langevan, as well as laboratory x-ray instruments.

Enjoying the "Western" flavor banquet held at the 2003 NSLS Users' meeting are the NSLS User Office staff, past and present: (standing, from left) Gretchen Cisco, Eileen Pinkston, Susan Hatzel, Liz Flynn; (seated, from left) Lydia Rogers, Nancye Wright, Brian Bindert, Mary Anne Corwin, and Melissa Abramowitz.

The first speaker was Cam Hubbard of Oak Ridge National Lab, who spoke on *in situ* powder diffraction measurements at high temperatures. He discussed a variety of experimental systems, studied both in the High Temperature Materials Lab at ORNL and at the NSLS in

which the ability to follow phase transformations at high temperatures, under synthetic conditions, was key to solving practical problems in ceramics and other high performance materials. Richard Harlow (of Harlow, Inc.) followed with discussions of work performed at the APS on Fe metal catalysts that are used by DuPont in commercial scale manufacturing. These catalysts are activated at high temperature and pressure at the beginning of the process batch, and there was inadequate understanding of the chemical basis for the observed lot-to-lot variation of their performance. High energy x-rays were necessary to penetrate the stainless steel tube used to house the catalyst under process conditions, and high angular resolution was required to distinguish the processes of interest in the catalyst. Insights gained from the study of the state of the activated catalyst have given information useful to optimize the process in the chemical plant.

The next two talks addressed an extension of the domain of powder diffraction that is becoming increasingly important, pair distribution analysis. Briefly, this technique transforms the entire diffraction pattern into a radial distribution function. Instead of analyzing only the Bragg peaks to learn the periodically repeating component of the crystal structure, pair distribution analysis reveals the distribution of local environments throughout the sample. Accordingly, it is particularly valuable in materials that are only partially crystalline, such as nanoscale phases. Valeri Petkov of Central Michigan University provided an introduction to the technique, and discussed recent results from studies of nanophase $LiMoS_2$, $Ag_{0.4}MoS_2$, $(NH_4)_{0.5}V_2O_5$, magnetic $GdAl_2$, and Cs intercalated into zeolite. Jonathan Hanson (Brookhaven National Laboratory, Chemistry Department) continued with the theme of radial distribution structural refinements, combined with "conventional" Bragg peak analysis of diffraction patterns in studies of the reduction of (nominal) CuO and CeO_2, with measurements performed *in situ* at high temperature. This work shows the complementary information available from the two techniques, and the importance of both in unraveling complicated behavior in mixed phase materials with partial occupancy of several crystallographic sites.

After lunch, Bill David (Rutherford Appleton Laboratory, UK) woke the audience up with some startling new comments on a concept taken for granted by most practitioners: least squares analysis. While that would be the correct approach if the data errors obeyed a normal probability distribution governed by counting statistics and the hypothesized model was a correct description of the sample diffraction properties, these conditions are often not met. Starting with a formal description of least-squares analysis, David reviewed principles of experimental design to meet those criteria. He then presented some new results on techniques to deal with problems frequently observed: unknown impurities in a powder diffraction pattern handled with a new minimization criterion, and a maximum likelihood approach to analyze incomplete structures in which some atoms have not been located.

Frontiers in Powder Diffraction Workshop attendees.

The two following talks covered various perovskite-related materials in which the interplay of structural distortions, charge ordering, and magnetism require complementary application of neutron and x-ray powder diffraction. El'ad Caspi of Argonne National Laboratory discussed the phase diagram of the colossal magnetoresistance system $(Ca^{2+}_{1-x}Ce^{4+}_{x})MnO_3$. This is a two-electron doped system (in contrast to more familiar one-electron doped systems such as $(Ca^{2+},Bi^{3+})MnO_3$), and the faster change of electronic charge with ion substitution leads to a much more complicated interplay among charge ordering, orbital ordering, and spin ordering, which in turn causes phase separation over a much larger range than one-electron systems. Patrick

Woodward of Ohio State University opened his talk with several demonstrations that neutrons are often superior to x-rays in *ab initio* structure solutions of oxides and fluorides, even though the latter are much more widely used. He then discussed several neutron and x-ray experiments: Fe charge disproportionation in $CaFeO_3$, Mn orbital ordering in $NdSrMn_2O_6$, and the Verway transition on oxygen deficient double perovskites, $RBaFe_2O_{5+w}$ (R = Rb, Y, Ho, and Nd).

In the last session, Tom Vogt (BNL, Physics Department) discussed work on the high pressure chemistry of zeolites. The theme of his talk was the surprising discovery of materials that expand under pressure, due to increased incorporation of water into the zeolite cavities. Sodium aluminosilicate natrolite undergoes a reversibly pressure-induced lattice expansion, whereas a synthetic analog, potassium gallosilicate natrolite, expands irreversibly, retaining the expanded high pressure phase upon returning to ambient pressure. Vogt presented structure determinations showing the role of non-framework metal ions in distinguishing the two cases. Finally, Peter Stephens presented a talk largely prepared by Robert Von Dreele (Los Alamos and Argonne National Lab) on their work applying high resolution x-ray powder diffraction to proteins.

In all, the broad range of powder diffraction, pair distribution function, and single crystal analysis, and the large and growing user community at synchrotron and neutron facilities points towards increasing growth at the frontiers of powder diffraction. This in turn indicates continuing demand for improved instruments as well as improved access to the current generation of operating instruments.

—Peter Stephens

Workshop on Spectroscopy in High Magnetic Fields: ESR, Infrared, and Other Applications

May 19, 2003

The availability of high field magnets, combined with the development of high resolution/low energy spectroscopic techniques, provides new opportunities for probing materials with synchrotron light. In this workshop, a few selected applications of x-ray and infrared radiation for the study of superconductors, magnetic perovskites, semiconductor quantum wells and other systems were reviewed. x-ray scattering and spectroscopy, electron spin resonance, optically detected Hall effect, and far IR spectroscopy in high magnetic fields were also discussed. The speakers included current users as well as other leading experts from the U.S. and Europe.

Spectroscopy in High Magnetic Fields: ESR, Infrared and Other Applications Workshop attendees.

—Laszlo Mihaly

Processes in Environmental Sciences Workshop

May 19, 2003

Reliable long-term prediction of heavy element mobility in natural multi-component systems or construction of intelligent reactive barrier systems for waste confinement requires a fundamental process understanding. Application of a combination of macro- and microscopic techniques including EXAFS, XANES, FTIR, XRD, XRF and soft x-ray microscopy can provide atomic scale chemical information as well as information of nano- to microscopic spatial distribution in complex matrixes. New single crystal approaches on well defined crystallographic planes furthermore gives

Processes in Environmental Sciences Workshop attendees.

insight in redox-kinetics and sorption relevant mineral surfaces. The scope of this workshop will be to give a discussion platform as well as an overview of recent applications of synchrotron based techniques to elucidate important pathways in natural and anthropogenic influenced environmental systems.

—Thorsten Schaefer

Bio-Matters: from IR to X-rays Workshop

May 21, 2003

For the past two decades the NSLS has been increasingly contributing to structural biology. With the advent of a new facility the aim of this workshop was to discuss the contributions of different synchrotron radiation-based methods to the understanding of molecular structure and biomolecule function. The second goal was to focus on the complementary aspects between these techniques and different methods such as cryo-electron microscopy and neutron scattering methods. The workshop consisted of oral presentations, a poster session, and a panel discussion session on the future requirements and expectations of the NSLS user community. The talks presented are summarized below:

Wayne Hendrickson, Columbia University, *"Synchrotron Crystallography in Biological Discovery,"* introduced the subject of the workshop. In his talk he described the impact of synchrotron radiation on the field of biological crystallography, a number of technical advances, and the problems of radiation damage with the advent of more intense sources. Several examples were discussed in relation to the speed of solution provided by crystallography at synchrotron radiation sources, and the impact to biochemistry and molecular biology.

Chris Jacobsen, Stony Brook University, "*Soft X-ray Imaging and Spectromicroscopy,"* presented high resolution views of chemical contrast through the combination of soft x-ray microscopes and near-edge spectroscopy methods. This approach was illustrated with biomedical examples including microspectroscopy studies of human sperm, and imaging of several cell types.

Rob Scarrow, Haverford College, *"EXAFS Studies of Metalloproteins and the Usefulness of Model Coordination Complexes,"* discussed the application of EXAFS (Extended X-ray Absorption Fine Structure) analysis to a variety of metalloproteins. The determination of the nature of ligand atoms, the number and lengths of bonds, metal-metal distances, and how small molecule crystal structure databases are useful in the interpretation of the results was discussed using lipogenase and porphobilinogen synthase as examples.

Joannna Krueger, University of North Carolina at Charlotte, "*Small-Angle Scattering: Solutions in Protein Structural Analysis,"* discussed x-ray and neutron small angle scattering focusing on the complementary aspects of these techniques and other structural and biochemical approaches such as that obtained from selected-site mutagenesis, circular dichroism, NMR, and electron microscopy.

Bio-Matters from IR to x-rays Workshop attendees.

Udupi A. Ramagopal, Albert Einstein College of Medicine, and Zbigniew Dauter, NIH, "*SAD: Happy Phasing with Weak Anomalous Scatterers,"* described the single-wavelength anomalous diffraction (SAD) as an alternative to the multiple wavelength diffraction method (MAD) applied to sulfur-containing proteins and to radiation sensitive samples.

Uwe Bergmann, Stanford, "*Advances in High-Resolution Hard X-ray Spectroscopy: From Vibrational Studies to Identify ligands to the Local Structure of Water,*" explained that hard x-ray spectroscopy became possible in recent years due to intense sources and improvements in x-ray instrumentation. The application of x-ray fluorescence spectroscopy (XFS) of weak lines, resonant inelastic

x-ray scattering (RIXS), (non resonant) x-ray Raman scattering (XRS) and nuclear resonant vibrational spectroscopy (NRVS) to studies of the oxygen K-edge of water, metalloproteins and Fe containing systems was shown.

Mark Chance, Albert Einstein College of Medicine, "*Structure and Dynamics of Macromolecular Machines,"* described synchrotron footprinting to study the dynamics and interactions of proteins and nucleic acid structures with millisecond time resolution and high structural resolution using nanomoles to picomoles of material. He gave examples for the L-21 ribozyme from *Tetrahymena*, cofilin and time-resolved activation of the actin binding protein gelsolin.

Lisa Miller, NSLS, "*Chemical Imaging of Biological Tissues using a Combination of Infrared, UV-Visible Fluorescence, and X-ray Micro-Spectroscopy,"* discussed the application of synchrotron infrared (IR) micro-spectroscopy and fluorescence techniques for examining the inherent chemical makeup of biological cells and tissues at spatial resolutions not achieved by conventional IR microscopes. Comparisons with other techniques such as immunofluorescence and x-ray microspectroscopy were presented in light of Alzheimer's disease, scrapie, and bone disease.

Thomas C. Terwilliger, Los Alamos National Laboratory, "*Structural Genomics: Technology for Structural Biology,"* presented the future needs of structural genomics and the current status. He focused on the technological improvements needed from protein production to structure determination. Several of these developments are underway, one of the most important being the automation of data collection and analysis at x-ray beamlines worldwide. Other technologies such as the engineering of proteins for optimal solubility, automated structure solution, and phase improvement by x-ray crystallography were also discussed.

Several posters on different subjects ranging from imaging to scattering and from the NASA radiological program to Cryo Electron Microscopy were discussed over coffee and a lunch break.

Members of the panel (Wayne Hendrickson, Columbia; Thomas Terwilliger, Los Alamos; Joachim Frank, Wadsworth Center; and Naomi Chayen, Imperial College), and workshop participants addressed several technological problems such as instruments, detectors, methods, and software developments to subjects such as multiple assemblies and unstable systems. The main recommendations were related to the development of detectors, brighter sources, instrumentation to handle smaller crystals, software for automated structure determination, modeling, and docking.

Prior to the Bio-matters workshop, a workshop was held on the basic and advanced methods in protein crystallization. The aim of this one-day workshop was to allow participants to have a hands-on experience with the different crystal growth methods available to protein crystallographers. Naomi Chayen (Imperial College) explained the microbatch method and the oil method; Miroslawa Dauter (NIH) discussed the hanging drop method, co-crystallization of heavy atoms, and seeding; Zbigniew Dauter (NCI-NIH) presented strategies in choosing an optimal derivative and data collection; and Grahemen Williams (Brookhaven-Instruments) discussed the application of the light scattering technique to protein crystallization. Two parallel sessions were organized in the morning and in the afternoon where the 22 participants could experience the different crystallization methods. We thank our sponsors Nextal Biotechnologies, Brinkmann Instruments, Millipore, Fisher Scientific, Brookhaven Instruments Corporation, and New York New Jersey Scientific, Inc., for their kind support, without which the Crystallization Workshop, a satellite meeting to the NSLS Annual Users' Meeting, would not have been possible.

—Vivan Stojanoff

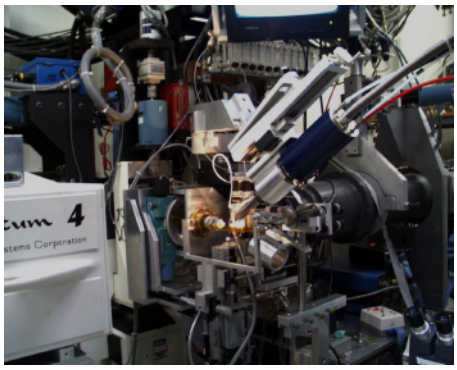

The majority of life science users at the NSLS perform protein crystallography experiments like the one shown here.

Workshop on High Pressure Mineral Physics Using Synchrotron Radiation

May 21, 2003

Most techniques for probing materials using synchrotron radiation can be applied to materials at high pressures and temperatures using either the Diamond Anvil Cell (DAC) or the Large Volume Press (LVP, also known as the Multianvil Press). These techniques include diffraction (both energy-dispersive using white radiation and angle-dispersive using white radiation); radiographic imaging; ultrasonic interferometry; stress and strain measurements; infrared spectroscopy; Raman spectroscopy; and inelastic scattering. Presentations will be made discussing most of these techniques and scientific applications of these technique.

—Michael Vaughan

Workshop on EXAFS Under Extreme Experimental Conditions: EXAFS in the Realms of Small Spot Size, Low Energy, Low Sample Concentration, or Fast Time Resolution

May 21, 2003

EXAFS is well established as a measurement technique used in a broad range of scientific disciplines. Within certain experimental constraints, high quality data is routinely obtained by users of synchrotrons around the world. In recent years, the scope of EXAFS has been expanded by advances in measurement techniques. At this year's NSLS Users' Meeting, these exciting developments were explored in a workshop titled, "EXAFS Under Extreme Experimental Conditions: EXAFS in the realms of small spot size, low energy, low sample concentration, and fast time resolution," organized by Bruce Ravel of the Naval Research Laboratory in Washington, DC. Just as EXAFS is commonly used by researchers from many different scientific disciplines, so too did our speakers present results from many different disciplines, including chemistry, environmental science, and materials physics.

Barukh Yaakobi of the University of Rochester began the workshop by discussing the use of laser-generated shocks with imploding targets as the radiation source for his EXAFS experiments. Dr. Yaakobi discussed measurements of an ultra-fast structural phase transition in titanium metal induced by the laser-generated shock and measured in dispersive mode. He was followed by Vadim Palshin from Louisiana State University and CAMD, who discussed the experimental challenges of low-energy EXAFS measurements. He presented detailed structural refinements on the silicon K-edge silicon-containing, thin, amorphous carbon films.

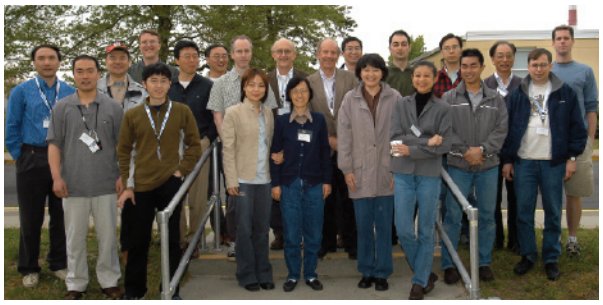

Attendees at the workshop on High Pressure Mineral Physics Using Synchrotron Radiation.

Lin Chen of Argonne National Laboratory spoke of using the time structure of a stored current to measure photo-excited molecular structures. In these experiments, very short-lived molecular states are measured in a pump-probe geometry wherein the molecular population is laser-excited and the excited state is measured by an x-ray pulse incident during its lifetime. Shelly Kelly also of Argonne National Laboratory spoke of uranium L_3-edge EXAFS at environmentally relevant concentrations. Environmentally relevant concentrations strain the limits of detectability even with third generation light sources and Dr. Kelly discussed the experimental concerns of low sample concentrations and addressed the limits of sample dilution

Attendees at the workshop on EXAFS Under Extreme Experimental Conditions: EXAFS in the Realms of Small Spot Size, Low Energy, Low Sample Concentration, or Fast Time Resolution.

for full analysis of the EXAFS signal. The final talk was by Ronald Cavell of the University of Alberta. He spoke on the use of microprobe EXAFS sources to map the composition of heterogeneous materials. He presented results of mapping and structural determination of the components of a meteor sample.

There is a rule of thumb that the measurements of elemental identification, XANES measurement, and EXAFS measurements require increasing orders of magnitude of photon flux or sample concentration. Consequently detailed EXAFS analysis in the limits of small spot size, low energy, low concentration, or fast time resolution requires special considerations for sample preparation and measurement. In many cases these experimental limitations have only been addressed since the advent of technical advances such as third generation sources. This workshop provided an excellent snapshot of the current state of the art technology for each of these extreme realms of EXAFS measurement and analysis.

—Bruce Ravel

UEC Community Service Award Presented to Michael Sullivan

May 20, 2003

Congratulations go out to Michael Sullivan, Chief Beamline Engineer for Albert Einstein College of Medicine. Mike is the second annual recipient of the NSLS Users' Executive Committee (UEC) Community Service Award. This award is given for service, innovation, and dedication to users of the NSLS.

Members of the NSLS user community nominated Mike for this award. Here are some of the comments that users sent about his wonderful contributions:

- "Mike is admired as a tireless, creative force dedicated to the principle of delivering user service."
- "In my opinion Mike is one of the most knowledgeable and extremely helpful engineers at NSLS floor, with very long experience [19 years] with dealing with all technical aspects of many different kinds of x-ray synchrotron research conducted at NSLS. He is a person who made it possible for very many staff and visitors to obtain top quality research results."
- "On several occasions, he has come in on weekends to help us salvage an experiment gone awry, or to bail us out of a technical problem. On one occasion, we reached him via his cell phone on his boat at sea, and he was able to come in and fix the problem to keep us running."
- "Mike is undoubtedly a gold standard of service, innovation, and dedication to users. Moreover, during this winter's biggest blizzard, I remember walking by the NSLS parking lot when Mike turned his car into a towing truck in order to help his users to pull out their car out of a huge pile of snow."

Leemor Joshua-Tor, the Chair of the NSLS UEC, presented the award to Mike at the NSLS Users' Meeting banquet on the evening of May 20th. Mike received a $250 gift certificate and his name was engraved on the plaque on display in the lobby of the NSLS.

—Leemor Joshua-Tor

Michael Sullivan, NSLS Users' Executive Committee (UEC) Community Service Award winner.

NSLS Scientist Ron Pindak Awarded Tenure

June 1, 2003

Brookhaven Science Associates (BSA) granted tenure on June 1 to nine Brookhaven scientists. They are: Mark Baker, Chemistry Department; Leslie Bland, Physics Department; Christopher Homes, Physics; Jean Logan, Chemistry; Ron Pindak, National Synchrotron Light Source Department; David Schlyer, Chemistry; Subramanyam Swaminathan, Biology Department; Dejan Trbojevic, Collider-Accelerator Department; and Gene-Jack Wang, Medical Department.

As described in the Scientific Staff Manual, "a tenure appointment constitutes recognition of independent accomplishment of a high order in the performance of original research or of other intellectually creative activity appropriate to Laboratory purposes."

Recognition may be earned through significant contributions to knowledge related to the purposes of the Laboratory and/or in furtherance of the Laboratory's aims, through continuing contributions of outstanding sig-

nificance to productive uses of the facilities, or outstanding and creative contributions to their design, development, and improvement.

For his outstanding contributions and sustained high-quality original research in the study of complex fluids, with particular emphasis on liquid crystals, Ron Pindak, NSLS Department, was awarded tenure.

"Ron consistently picks fundamentally important problems to work on and has an ability to design experiments to get at the heart of an issue," said Steven Dierker, NSLS Chair and Associate Laboratory Director for Light Sources. "He has amply demonstrated the versatility and expertise to practice whatever technique is necessary, sometimes by collaborating with others to learn the technique before applying it on his own, and in other cases by playing a lead role in developing a new technique."

Pindak's early work in forming free-standing liquid crystal films led to his experimental verification of the hexatic phase, a new state of matter with order intermediate between that of a liquid and of a solid. Later, he and collaborators discovered and characterized the "Twist Grain Boundary Phase," the liquid crystal analogue of the Abrikosov flux lattice in superconductors with screw dislocations playing the role of flux vortices.

Pindak joined BNL in 2001 as a physicist after a distinguished 24-year career at Bell Laboratories. During his career at Bell Labs, he had led a collaboration at the NSLS that pioneered the use of resonant x-ray scattering to elucidate molecular order in chiral ferri- and antiferro-electric liquid crystals. This required working in a low-energy x-ray region where air is very absorbing, so special instrumentation, a goniometer and x-ray polarization analyzer, which would operate in a helium atmosphere, had to be designed and constructed.

Said Dierker, "The unique insight provided by the measurements established by Ron's work has provided the motivation for developing this capability as a standard technique for the user program on one of the NSLS low-energy x-ray beamlines."

Most recently, Pindak has been a key contributor to the development of the Coherent Bragg Rod Analysis technique, which measures the phase of x-rays scattered by two-dimensional structures, such as epitaxial films or interfaces, to allow an absolute determination of the atomic positions. He is now exploring whether this technique can be extended to study two-dimensional protein crystals.

In addition, since joining the NSLS, Pindak has headed the Science Program Support Section of the User Science Division, and taken the lead in developing a soft condensed matter program. He also served as the Interim Associate Director for the BNL Nanocenter. Currently, together with Lin Yang, he is developing a small angle x-ray scattering beamline and starting soft matter and biophysics research relevant to understanding nanoscale device fabrication and operation.

Pindak received his Ph.D. in physics from the University of Pennsylvania in 1975.

— Liz Seubert

Ron Pindak

Dierker Named Associate Laboratory Director For BNL's New Light Sources Directorate

June 5, 2003

Steven Dierker, a forefront scientist and administrator in synchrotron light research, was named Associate Laboratory Director for the new Light Sources Directorate at BNL. Dierker, who is Chair of the NSLS, will also retain that position.

The NSLS at BNL is one of the world's most widely used scientific facilities. Each year, about 2,500 researchers from more than 400 universities, companies, and government labs use its bright beams of x-rays, ultraviolet light, and infrared light for research in such diverse fields as biology and physics,

Steven Dierker

chemistry and geophysics, medicine and materials science. For example, scientists have used the NSLS to produce imagesof the AIDS virus as it attacks a human cell, develop a method for breast cancer detection that is more accurate than mammography, and create a method to make faster, denser computer chips. The facility has 175 employees and a current annual budget of about $38 million.

"I am pleased about the continued growth of the NSLS Department," Dierker said. "Since its commissioning in 1982, the NSLS has continually updated and expanded its capabilities to remain at the forefront of science. Now we are proposing a major upgrade - essentially a new light source at Brookhaven."

BNL created the new Light Sources Directorate and promoted Dierker to his present position because of the importance of upgrading NSLS facilities within the next decade.

The project represents the next major step in the Lab's long history of building and operating world-class scientific facilities and is expected to have enormous impact in the life sciences, materials and chemical sciences, nanoscience, geoscience, environmental science, and other areas. Advanced light source capabilities would also complement the Center for Functional Nanomaterials at Brookhaven, which is due to be built starting in 2005 and to become fully operational by 2008.

After earning B.S. degrees in both physics and electrical engineering in 1977 from Washington University, Dierker earned both an M.S. and Ph.D. in physics from the University of Illinois, Urbana-Champaign, in 1978 and 1983, respectively. In 1983, he joined the Semiconductor and Chemical Physics Research Department at AT&T Bell Laboratories (now Lucent Technologies), and, in 1990, he joined the University of Michigan, where he was Professor of Physics and Applied Physics. He joined BNL in May 2001 to become Chair of the NSLS.

Since 1992, Dierker has been a member of the NSLS Users Group, and he performed initial experiments at the NSLS to develop a novel synchrotron technique called x-ray photon correlation spectroscopy, which uses coherent, or highly ordered, synchrotron beams to study colloidal systems, or particles dispersed in a solid, liquid, or gaseous medium, and polymers.

Since 1996, Dierker has been a member of the Advanced Photon Source (APS) Users Organization at Argonne National Laboratory, and he chaired that organization from 1998-2000. He also helped to plan the construction, design, and operation of beamlines at the APS, with funding from DOE and the National Science Foundation.

— Diane Greenberg

Yeshiva University Undergraduates Experience Hands-On Research at BNL

June 17, 2003

In June 2003, 12 students and 3 instructors from Yeshiva University (New York) spent a week at Brookhaven National Laboratory as part of an undergraduate course entitled "Experiments in Modern Physics". This course was developed by Yeshiva Physics Professor Anatoly Frenkel, in collaboration with his departmental colleagues Professors Gabriel Cwilich and Fredy Zypman. Professor Frenkel is also a long-time NSLS beamline scientist at X16C. The course was five weeks long, including four weeks on the Manhattan campus where students had lectures and labs introducing them to the foundations of modern physics, and one week of "mini-experiments" at BNL. Students participating in the course had widespread backgrounds, majoring in Physics, Political Science, English and Psychology.

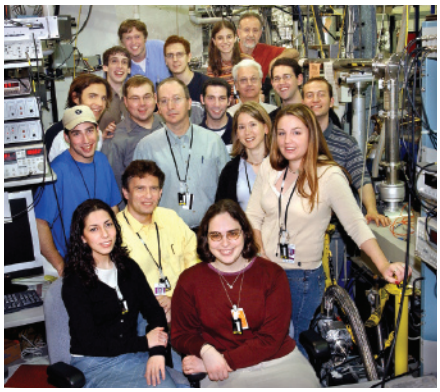

Yeshiva University undergraduates and faculty enjoy their summer mini-experiments at the NSLS.

The most attractive component of the new course was the Brookhaven visit. The purpose of this visit (and the entire course) was to help students under-

stand modern physics through a series of mini-experiments, while exposing them to the atmosphere of a National Lab where modern physics is practiced every day. The five BNL experiments were organized in collaboration with BNL scientists who helped to plan and run the experiments for several shifts of students. In this way teams of 3-4 students could rotate between all of the experiments during the week.

Three experiments, the "Photoelectric Effect," organized by Anatoly Frenkel, "Time-Resolved Chemistry," Jon Hanson (BNL-Chemistry), and "Fingerprinting of Fingerprints," organized by Lisa Miller (BNL-NSLS) were run at the NSLS beamlines X16C, X7B and U10B, respectively. The experiments were designed to show students both the laws of physics (photoelectric effect and x-ray absorption; x-ray diffraction and Bragg's law; absorption of infrared light by vibrating molecules) and elements of research. Two additional experiments, "Nuclear Decay" and "Electron-Positron Annihilation," were organized by Kathryn Kolsky and Leonard Mausner at BNL's Isotope Facility. There the students visited the Brookhaven LINAC Isotope Producer (BLIP) and spent two days studying properties of gamma radiation (absorption, element characterization, inverse square law and the law of radioactive decay) by operating the facility's germanium gamma ray detectors. They were particularly fascinated by utilizing the $E = mc^2$ law to obtain the electron mass from the characteristic "electron-position annihilation" peak at 511 MeV.

For most of the students it was the first experience of this kind. They endured working long shifts, participating in the ongoing laboratory research and enjoying the sense of "discovery" in learning. The entire group thanks the Brookhaven teams of scientists for their help and the NSLS for financial support. The course is now used as a prototype for a new course "Current Topics in Nanoscience" that is under development by the Yeshiva faculty.

— Anatoly Frenkel, Yeshiva University

'Mail-In' Crystallography at the NSLS Featured in *Nature*

June 19, 2003

BNL's Howard Robinson, Biology Department, who runs the "mail-in" crystallography program at the NSLS, got star billing (and photo prominence, right) in a news feature on the subject in the June 19, 2003, issue of *Nature*. Since 2000, Robinson and others at the NSLS have offered a mail-in data-collection service for scientists who want to solve protein structures without having to travel to a synchrotron themselves. According to the Nature article, such services are becoming increasingly popular for biologists without formal training in crystallography and for those who would rather not wait for time on a beamline. Robinson's team at the NSLS typically works on about 50 mail-in projects a year, free to academic scientists. Consistent with BNL's mission of making its highly specialized research facilities available to outside researchers, this mail-in program broadens BNL's service to science and is helping to speed up the process of biological research. The program is funded by the Office of Basic Energy Sciences and Office of Biological & Environmental Research within DOE's Office of Science and the National Institute of Health's National Center for Research Resources.

Howard Robinson

— Karen McNulty Walsh

NSLS EXAFS Data Collection and Analysis Short-Course Has Another Successful Year

July 14 - 17, 2003

A hands-on EXAFS Data Collection and Analysis Course was held July 14-17, 2003 at the NSLS. The course was co-organized by Bruce Ravel (Naval Research Laboratory) Simon Bare

(UOP LLC), with superb administrative support by Lisa Tranquada (SFA, Inc.). Twenty-eight eager participants (graduate students, postdocs, and institution and industrial scientists) representing universities, national laboratories, research institutes, and industry attended the course. Of these, there were ten new users to the NSLS. The participants had diverse research interests across a broad spectrum of scientific fields (materials science, geological and environmental sciences, catalysis, and biology) and attended to learn how XAFS may be applied to their research program.

The four-day course was divided into morning lectures, with two afternoons of hands-on data collection using seven different NSLS spectroscopy beamlines (X9B, X11A, X18B, X19A, X23A2, X23B, and X26A), and two afternoons of data analysis. The instructors on the beamlines were Faisal Alamgir, Wolfgang Caliebe, Scott Calvin, Syed Khalid, Tony Lanzirotti, Nebojsa Marinkovic, and Kaumudi Pandya.

The eight morning lectures were: "Introduction to XAFS," given by Matt Newville (University of Chicago), "Basics of sample preparation" by Scott Calvin, "XANES measurement and interpretation" by Simon Bare (UOP LLC), "Detectors and synchrotron radiation" by Peter Siddons (BNL), "Basics of data processing" by Shelly Kelly (Argonne National Laboratory), "Introduction to theory" by John Rehr (University of Washington), "Introduction to analysis" by Anatoly Frenkel (Yeshiva University), and "Applying XAFS into a research program" by Rich Reeder (Stony Brook University). The time allotted for the lectures allowed ample time for stimulating discussion, which often developed.

For the first two days of the course, after attending the morning lectures, the participants were divided into small groups by research discipline to conduct the experimental part of the course. Each student became familiar with beamline operation and collected real XAFS data on representative samples from their own individual research projects. On the last two days, following the morning lectures, the participants learned data analysis techniques using their own data they had just collected. The participants also enjoyed ample time for informal discussion over coffee and in the evenings over the excellent dinners that were included in the course fee.

There was a tremendous amount of information disseminated over the four days. All the participants left the course with new friends and armed with the basic tools to apply x-ray absorption spectroscopy to their own research programs.

Participants in the 2003 NSLS EXAFS course.

We plan to offer the course again in 2004 – check the NSLS website for updated information.

The course was sponsored by the NSLS, with support from the Center for Environmental Molecular Science at Stony Brook University.

— Simon Bare

NSLS Summer Sunday Draws a Record-Breaking Crowd

August 3, 2003

On Sunday August 3, 2003, over 750 visitors toured the NSLS as part of Brookhaven National Laboratory's Summer Sunday tour series. Thirty-five NSLS staff members, students, and users volunteered their time for the event, which was organized by NSLS scientist, Lisa Miller.

University of Chicago scientist Tony Lanzirotti animated scientific research at the NSLS to an overflowing NSLS seminar room crowd.

Each summer, BNL is open for tours on seven consecutive Sundays, feature exciting interactive exhibits and an inside look at a different Laboratory facility each week, including the NSLS.

Tours of the NSLS included presentations, demonstrations, and hands-on

exhibits. At Berkner Hall, visitors watched an introductory video about how a synchrotron works, narrated by NSLS Chairman Steve Dierker. After a short bus ride and tour of the Lab, visitors were dropped off at the NSLS. In the seminar room, NSLS scientists presented an introduction to "Science at the NSLS" by describing the many ways the NSLS is used to study scientific problems that affect everyday life. Improvements in biomedical imaging techniques, drug design, catalytic converters, environmental cleanup, and computer storage media were just a few of the topics discussed.

Visitors then toured the NSLS lobby, which was transformed into an exhibit area for numerous light- and synchrotron-related demonstrations. Visitors were able to experience "total internal reflection" as a laser beam was guided through a stream of falling water. A display on the principles of vacuum demonstrated its effect on a ringing bell, a balloon, a feather, and a marshmallow. The technique of diffraction was demonstrated using tiny metal grids and compact disks. Visitors had the opportunity to build their own "crystals" using gumdrops, and "see" the synchrotron light (at least the visible part of the spectrum) transported to the lobby through a fiber optic. But perhaps one of the all-time favorite features in the NSLS lobby was the view of the experimental floor from the display windows, which continues to amaze visitors year after year.

In addition to the many exhibits at the NSLS, BNL volunteers at Berkner Hall engaged visitors in a number of other activities. A hands-on exhibit called "Brain Matters," produced by the Oregon Museum of Science and Industry and funded by the National Institutes of Health, offered visitors the opportunity to explore the wonder of the brain and test their skills in solving challenging "brain twisters." Also, an exhibit about the 2002 Nobel Prize in Physics awarded to a Brookhaven Lab scientist was on display, and the Camp Upton Historical Collection featured memorabilia from World Wars I and II. The ever-popular "Whiz Bang Science Show" — popular with both adults and children — was also shown several times during the day. Both children and adults enjoyed lively interactive demonstrations of basic scientific principles. How does a "Bernoulli blower" float a beach ball in the air? What's a corrugaphone and how does sound travel through it? These were just a few of the intriguing items covered in the show.

—Lisa Miller

NSLS scientist Vivian Stojanoff, shows how much fun it can be to build crystal models out of gumdrops and toothpicks.

Fun with vacuum techniques was demonstrated by Alec Bernston (left), a Cornell University freshman that was a summer student at the NSLS.

In a series of articles published in the Bulletin, some research that was presented at the 226th meeting of the American Chemical Society (ACS), September 7-11, 2003, in New York City was featured.

Important Intermediate Isolated With Help From Reverse Reaction

September 7-11, 2003

BNL chemists have used a new way to isolate and study an important Intermediate in a chemical reaction: They run the reaction in reverse.

By starting with the final products — epoxides— and placing them on the surface of a model catalyst, the chemists are able to use surface chemistry techniques to "catch" the intermediate. Understanding this intermediate may ultimately help in developing improved or new catalysts for the forward reaction — a reaction that produces important "building blocks" in the manufacture of larger organic molecules.

In the forward direction, the interaction of the reactants with the surface is either too weak to allow direct study of the mechanism, or the intermediate — a ring structure on the surface of the silver catalyst — forms and transforms too quickly for scientists to study. But in reverse, the intermediate stays on the surface longer, so scientists

The NSLS lobby ws filled with visitors all day one on the NSLS Summer Sunday.

can apply various techniques to try to understand the reaction mechanism.

"If we find a general rule based on our studies with this model catalyst, then we can design a new catalyst, because we know how the reaction occurred on the surface," said the BNL Chemistry Department's Hong Piao, who is working on the project. The general goal is to improve the reactivity and selectivity of the catalyst for producing particular products.

Piao presented a talk on this work at the American Chemical Society's September meeting's Division of Colloid and Surface Chemistry poster session, "Fundamental Research in Colloid and Surface Chemistry." This work was funded by the Division of Chemical Sciences, Office of Basic Energy Sciences at DOE's Office of Science.

— Karen McNulty Walsh

Nanoscale Model Catalyst Paves Way Toward Atomic-Level Understanding

September 7-11, 2003

In an attempt to understand why ruthenium sulfide (RuS_2) is so good at removing sulfur impurities from fuels, BNL chemists have succeeded in making a model of this catalyst — nanoparticles supported on an inert surface — which can be studied under laboratory conditions.

"If we can understand why this catalyst is so active, we might be able to make it even better, or use what we learn to design other highly efficient catalysts," said Tanhong Cai of the BNL Chemistry Department, one of the scientists who made the model.

Removing sulfur from fossil fuels such as oil and coal is mandated because the resulting fuels burn more cleanly and efficiently. One common way of achieving this is to add hydrogen in the presence of a catalyst to release hydrogen sulfide (H_2S).

Recently, RuS_2 was found to be 100 times more active than the catalyst most commonly used for this "hydrodesulfurization" reaction. But studying the catalyst in action is nearly impossible because the reaction takes place at high temperatures and under extreme pressure.

The BNL team has therefore created a model of the catalyst via a chemical reaction that deposits nanosized particles of RuS_2 on a nonreactive gold surface. The small size of the particles maximizes the surface area available for the catalytic reaction to take place, and makes it ideal for analysis by classic surface chemistry techniques, such as scanning tunneling microscopy and x-ray photoemission spectroscopy. The entire model is being studied under well-defined ultrahigh vacuum conditions.

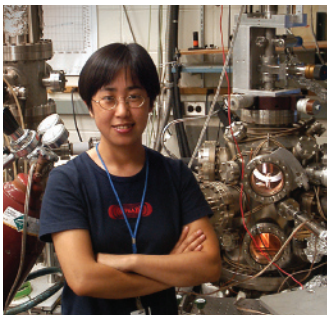

Hong Piao

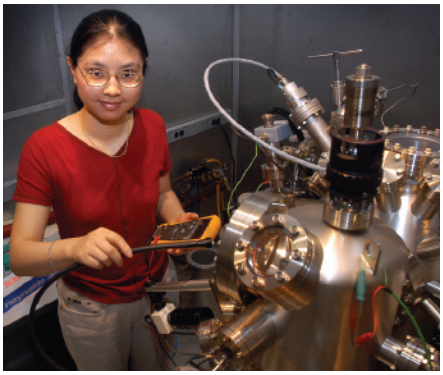

Tanhong Cai

Cai presented a talk on the preparation and characterization of this model catalyst at the American Chemical Society's September meeting during the "Size-Selected Clusters on Surfaces, Division of Physical Chemistry" session. The work was funded by the Division of Chemical Sciences, Office of Basic Energy Sciences at DOE's Office of Science.

— Karen McNulty Walsh

NYS Senators Balboni, Flanagan Visit BNL to Learn About Lab's Homeland Security Initiatives, More

September 12, 2003

On Friday, September 12, New York State Senator Michael Balboni, 7th District, who chairs the Senate Committee on Veterans, Homeland Security and Military Affairs, and New York State Senator John Flanagan, 2nd District, who, among other contributions, is a member of that same Committee, visited BNL with Jim Sherry, Counsel to Balboni.

After being welcomed by BNL Director Praveen Chaudhari, as well as DOE's Brookhaven Area Office Manager Michael Holland, Associate Laboratory Director for Energy, Environment & National Security Ralph James, and Assistant Laboratory Director for Community, Education, Government & Public Affairs Marge Lynch, the party was taken to the Lab's Radiation Detector Testing & Evaluation Facility (RADTEC).

There, Charles Finfrock of the Energy Sciences & Technology Department; Biays Bowerman of the Environmental Sciences Department; and Paul Moskowitz of the Nonproliferation & National Security (NNS) Department outlined the purpose of RADTEC, which is twofold — to assemble, operate, and test commercial and government off-the-shelf technologies targeted for various homeland security applications, and to provide baseline data for comparison purposes. At the facility, researchers collect baseline data on various types of detectors, and are available to provide assistance in training city, state, and federal officials to operate the detectors and interpret the results. RADTEC is open to all commercial and government technology vendors and is expected to become an important resource for local, county, state, and federal officials.

The visitors next stopped at the NSLS, to meet Associate Laboratory Director for Light Sources and NSLS Chair Steven Dierker and NSLS scientist Peter Siddons, who gave an overview of some of the research done in such diverse fields as biology and physics, chemistry and geophysics, materials science, and medicine. The group then saw beamline X12A, where detectors being developed by BNL and others in support of homeland security initiatives are inspected at a new testing station.

The tour continued at the Instrumentation Division, where, a collaboration including NNS is developing a detector that acts as a camera to make images of objects that emit low-energy neutrons. As Vanier explained, since there are very few natural background neutrons, and they are uniformly distributed, a concentrated source of neutrons is strong evidence of a manmade device, such as a plutonium weapon, or of spent nuclear fuel.

Graham Smith, Instrumentation, then showed the visitors a working prototype of a xenon-filled gamma ray spectrometer that BNL is developing to detect radioisotopes potentially in the terrorist arsenal, such as dirty bomb materials. Xenon detectors can be built in very large sizes, so as to pick up signals of radioisotopes more quickly and over a wider area than do instruments now available. Hence, these detectors will be suitable for homeland security applications.

At BNL's Radiation Detector Testing & Evaluation Facility are: (front, from left) NYS Senator John Flanagan, BNL's Ralph James and Paul Moskowitz, and NYS Senator Michael Balboni.

One of BNL's most enormous detectors, STAR, provided the next stop on the tour. The visitors learned from Tim Hallman, Collider Accelerator Department, that STAR tracks and analyzes thousands of particles, such as protons, neutrons, and pions, that may be produced in collisions of two beams of subatomic particles speeding around the tunnel at the Relativistic Heavy Ion Collider (RHIC). In the RHIC experiment, scientists expect to discover more about conditions that existed in the first few microseconds of the universe.

The visit concluded at the Positron Emission Tomography (PET) facility, where David Schlyer, Chemistry Department, described some of the Lab's pioneering neuroimaging research on the brain chemistry of addiction, aging, and diseases such as Parkinson's and Alzheimer's, and the recent PET research on imaging awake animals. Some of this work has veterinary support from the State University of New York's Downstate Medical Center in Brooklyn.

—Liz Seubert

2003 NSLS Annual Awards Ceremony and Picnic

September 17, 2003

On Wednesday, September 17, the NSLS had its annual Awards Ceremony and Picnic. Despite the impending arrival of Hurricane Isabel, the weather was spectacular and the pig roast was another big success. The picnic was coordinated by Laura Miller and executed by a number of NSLS staff members, including Charlie Nielson, Boyzie Singh, Bob Best, Joe Greco, Paul Humbert, Jim Lacy, Jim Newburgh, John Burke, Gerry Van Derlaske, and Bob Kiss, along with Ken Sutter "the pigman."

This year, Service Awards were given to 24 NSLS staff members: Al Almasy, Sam Krinsky, and Bob Casey (30 years); Roy D'Alsace, Walter De Boer, John Gallagher, Rick Greene, Chris Lanni, Payman Mortazavi, Jack Tallent, Frank Terrano, and Gerry VanDerlaske (25 years); Diane Hatton, Steve Hulbert, Jim Murphy, and Florin Staicu (20 years); Peter Gross, Alan Levine, Paul Montanez, Pauline Pearson, Eva Rothman, Brian Sheehy, Chris Stelmach, and Xijie Wang (10 years).

Spotlight Awards were presented to NSLS staff members for the completion of extraordinary accomplishments that were of significant benefit to the Department, Division, or Laboratory. This year's Spotlight Award winners were: (1) Brian Kushner for getting the x-ray ring's digital vertical feedback up and running, (2) Jim Newburgh for outstanding radio frequency cavity installation efforts during the winter 2002 shutdown, (3) Jack Tallent for designing a new beam profile monitor for the x-ray ring, (4) John Burke for completely rebuilding the fire-damaged Pulse Forming Network (PFN) section of the SDL modulator-A, and (5) Gary Nintzel for preparation, dismantling, and shipping of the U6 beamline.

—Lisa Miller

NSLS Physicist Wins 2003 Free Electron Laser Prize

October 10, 2003

Li Hua Yu, a physicist at the NSLS won the 2003 Free Electron Laser (FEL) Prize sponsored by the 25th International Free Electron Laser Conference. Yu received the award, which consists of $3,000, a certificate and a plaque, at the FEL conference held this year in Tsukuba, Japan.

NSLS Chairman Steve Dierker presented the Service and Spotlight Awards at the Annual Picnic.

Yu's award was given "in recognition of his outstanding contributions to FEL science and technology." Over the last 20 years, Yu and colleagues from Brookhaven contributed significantly in developing two types of lasers that are important for scientific investigations: the self-amplified spontaneous emission free electron laser (SASE FEL), and the high gain harmonic generation free electron laser (HGHG FEL).

NSLS Staff enjoying the barbeque.

In the SASE process, the light the laser emits for experiments starts from noise, or random signals. In contrast, in the HGHG process, the output light starts from fast-moving electrons interacting with a seeding laser that shifts the light to a higher frequency and makes it significantly more coherent, meaning electrons move in a coordinated way to emit light. The intense light of the HGHG FEL reveals the fine details of atomic interactions inside materials and the very fast motions of molecules in chemical reactions, all with an unsurpassed precision.

Yu explained, "The HGHG FEL combines the intensity and coherence of a laser with the broad spectrum of light available in a synchrotron, a type of accelerator. The invention of the laser provided a revolutionary source of coherent light that created many new fields of scientific research. The development of the HGHG FEL extends the reach of lasers to much shorter wavelengths, thus opening new research opportunities."

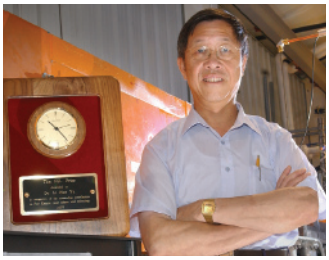

Li Hua Yu with FEL Prize

Yu continued, "I am very happy to

receive this award, and I am grateful for Brookhaven Lab's support and the excellent team who worked with me to make the HGHG FEL at Brookhaven the first and only one of its kind in the world."

At Brookhaven's Accelerator Test Facility in 1999, Brookhaven scientists, in collaboration with Argonne National Laboratory researchers, verified the theoretical foundation of the HGHG FEL operating in the infrared region of the light spectrum. In 2002, the technique was further developed to enable the HGHG FEL at Brookhaven to produce shorter wavelength light in the deep ultraviolet spectral region. This enabled researchers to perform new chemistry experiments.

The HGHG FEL may be a complementary research tool to synchrotrons around the world, including the Brookhaven's Laboratory Directed Research and Development Program, the U.S. Naval Research Laboratory, and the U.S. Air Force funded Yu's research on the DUV-FEL.

Li Hua Yu earned his undergraduate degree from Jilin University in China in 1970. He earned both an M.S. and Ph.D. in physics from Stony Brook University in 1980 and 1984, respectively. In 1984, he joined Brookhaven Lab as a research associate, and he rose through the ranks to become a senior physicist, in 2000. With a team of eight scientists and engineers from Brookhaven, Yu won an R&D 100 Award from R&D Magazine in 1989 for inventing the Real-Time Harmonic Closed-Orbit Feedback System, which stabilizes the orbit of electron beams in synchrotrons.

—Diane Greenberg

2003 Nobel Prize in Chemistry Awarded to NSLS User Roderick MacKinnon

October 8, 2003

Roderick MacKinnon, M.D., frequent NSLS user, won half of this year's Nobel Prize in Chemistry for work explaining how a class of proteins helps to generate nerve impulses -- the electrical activity that underlies all movement, sensation, and perhaps even thought. The work leading to the prize was done primarily at the Cornell High Energy Synchrotron Source and the National Synchrotron Light Source.

The proteins, called ion channels, are tiny pores that stud the surface of all of our cells. These channels allow the passage of potassium, calcium, sodium, and chloride molecules called ions. Rapid-fire opening and closing of these channels releases ions, moving electrical impulses from the brain in a wave to their destination in the body.

Starting in 1998, after 10 years studying the biophysics of ion channels, MacKinnon published a series of structural solutions — high-resolution molecular-level "snapshots" of ion channels, produced at Cornell and Brookhaven. These structures literally showed the scientific community how electrical signaling occurs.

MacKinnon, a biophysicist and self-taught x-ray crystallographer, is a professor at Rockefeller University and an investigator at the Howard Hughes Medical Institute. He shares this year's chemistry Nobel with Peter Agre, M.D., of Johns Hopkins University School of Medicine.

[Editor's note: For more information on MacKinnon's work, see the related Feature Highlight beginning on page 2-10]

—Karen McNulty Walsh

Rod MacKinnon. Photo courtesy of Chris Denney for the Howard Hughes Medical Institute, ©2003.

NSLS Shines Light on Disease

October 23, 2003

A group of four BNL scientists investigating the underpinnings of diseases from osteoporosis to botulism presented an overview of their work to a group of reporters in person and via live "webcast" on Thursday, October 23, at BNL. All the presenters use the extremely bright beams of energy (from infrared to x-rays) available at the NSLS.

NSLS Chair Steven Dierker gave an overview of the facility, which is used by more than 2,500 scientists from outside the Lab each year – including this year's chemistry Nobel Prize-winner, Rod MacKinnon of Rockefeller University, who used x-rays to determine the structure of proteins that help transmit nerve impulses throughout the body. Solving protein structures via the technique of x-ray crystallography can help scientists understand the proteins' functions and perhaps devise strategies to prevent them from causing disease.

That is the exact approach being pursued by the Biology Department's Walter Mangel and Subramanyam Swaminathan. Through x-ray crystallography and other techniques, Mangel has uncovered several parts of a viral enzyme that might be susceptible to antiviral drugs. "If you can block the activity of the enzyme," he says, "you can block the infection."

What is more, the sites Mangel has identified interact with one another. This led him to propose a new type of multi-drug therapy that viruses would not be able to "outsmart" via evolution of drug resistance. Using multiple drugs against several targets on the same enzyme might be effective against a range of viruses, including those that cause pink eye and AIDS, and against a range of bacteria, including those that cause Chlamydia, plague, and even malaria.

Swaminathan is using the NSLS x-rays to reveal components of botulinum toxin, the protein that causes botulism, that are central to its paralyzing effects. He is working to develop drugs that fit into the toxin's active sites to disrupt the potentially deadly process at three crucial steps. The result may be a vaccine and/or drugs that eliminate the toxin's potential as an agent of biowarfare or bioterrorism.

Shining the NSLS's beams on more traditional targets — bones and other body tissues — are the NSLS's biophysicist Lisa Miller and physicist Zhong Zhong. Miller is using the infrared beams to study bone composition, particularly that associated with areas of microscopic damage. She wants to know how bone composition changes in response to common osteoporosis treatments. Her work could lead to improvements in osteoporosis drugs.

Zhong uses the NSLS x-rays to look not just at bone, but at soft tissues like cartilage, blood vessels, skin, and fat deposits as well. His technique, called diffraction-enhanced imaging (DEI), uses higher energy x-rays that pass right through the sample without being absorbed, which results in a lower dose to the patient than traditional x-ray techniques. DEI makes soft tissues visible because each tissue type scatters the beam differently. A sensitive analyzer crystal can detect these subtle diffractions and translate them into different intensities, visible on x-ray film in magnificent detail. The technique could yield more accurate and earlier diagnosis of soft-tissue diseases such as breast cancer.

— Karen McNulty Walsh

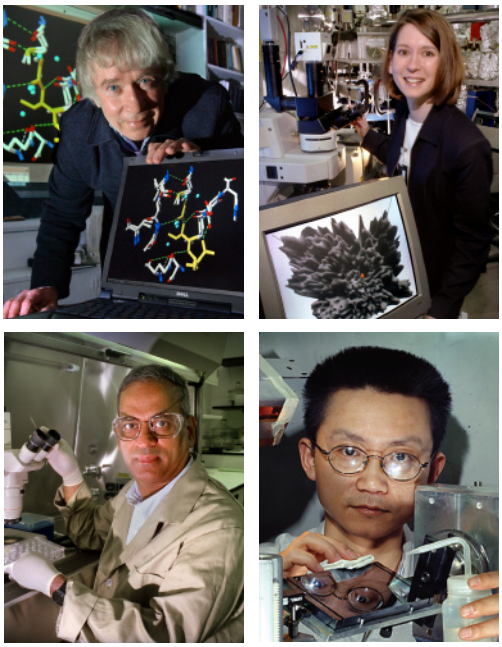

(Top, from left): Walter Mangel and Lisa Miller (bottom, left) Subramanyam Swaminathan and Zhong Zhong.

389th Brookhaven Lecture 'Nanoscale Twist in Liquid Crystal Miniature Video Displays'

December 17, 2003

Recently, commercial large-viewing angle flat panel displays, as well as miniature video displays for digital cameras, camcorders, head- and helmet-mounting, have been produced using ferroelectric liquid crystal (FLC) and antiferroelectric liquid crystal (AFLC) technology.

While developing materials for these devices, researchers noticed the thermal signature of a rich variety of new intermediate phases of the liquid crystals. The structures of these intermediate

Ron Pindak

phases look identical by conventional x-ray analysis and involves nanometer orientational properties that occur at smaller dimensions than can be observed using conventional optical microscopy.

To overcome this limitation of conventional investigative techniques, Ron Pindak, a physicist at the NSLS, and other researchers used a property of synchrotron x-ray sources — or more specifically, an intense beam of linearly polarized x-rays of a specific energy — to directly probe the nanometer-scale helical ordering of these new phases of liquid crystals.

Pindak gave a presentation on this research on Wednesday, December 17, at 4 p.m., the 389th Brookhaven Lecture, "Nanoscale Twist in Liquid Crystal Miniature Video Displays." Pindak was introduced by Steven Dierker, NSLS Chair and Associate Laboratory Director for Light Sources.

As Pindak explained in his talk, the x-ray scattering process is highly sensitive to the orientation of the chemical bonding of the atom, and therefore sensitive to the orientation of the molecule itself when using x-rays with an energy that excites electrons from the core of an atom within a molecule. He described how FLCs and AFLCs are used in devices and contrasted their behavior with more widely used liquid crystals.

Pindak joined BNL in 2001 as a physicist after 24 years at Bell Laboratories. Since then, he has headed the Science Program Support Section of the User Science Division, and taken the lead in developing a condensed matter program. He also served as the Interim Associate Director for the BNL Nanocenter.

Pindak received a B.S. in physics from Boston College in 1969 and a Ph.D. in physics from the University of Pennsylvania in 1975.

— Ron Pindak and John Galvin

Organization

NATIONAL SYNCHROTRON LIGHT SOURCE ORGANIZATION

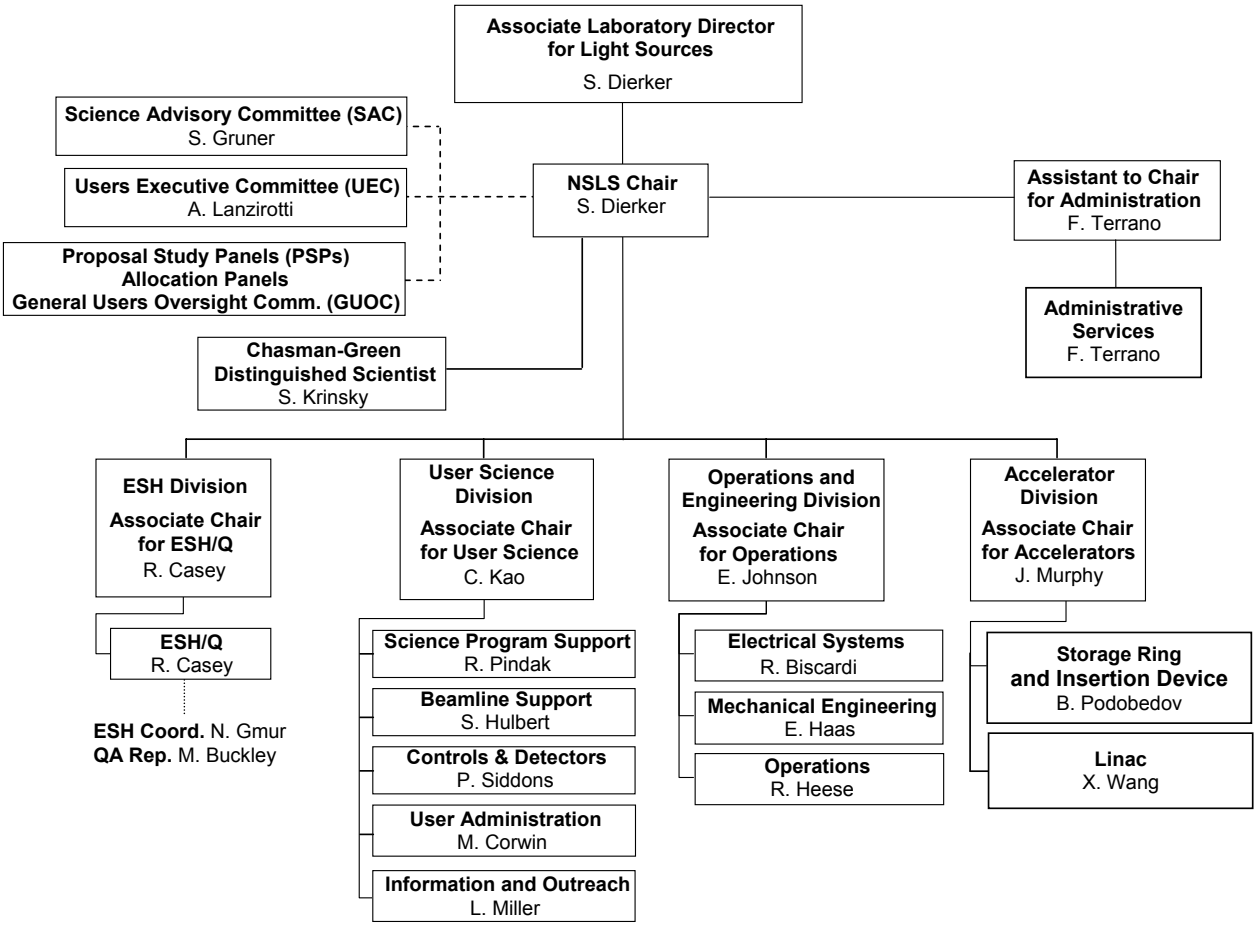

NSLS Advisory Committees

Users' Executive Committee

The Users Executive Committee (UEC) provides for organized discussions among the user community, NSLS administration and laboratory directorate. It aims to communicate current and future needs, concerns, trends within the user community to NSLS staff and management, and to disseminate to the users information about the NSLS and BNL plans.

Chair
Antonio Lanzirotti
University of Chicago

Past Chair
Leemor Joshua-Tor
Cold Spring Harbor Laboratory

Member
Fred Dyda
National Institute of Health

Member
Daniel Fischer
NIST

Member
Anatoly Frenkel
Yeshiva University

Member
Dean Hesterberg
North Carolina State University

Member
Richard Reeder
Stony Brook University

Vice Chair
Larry Shapiro
Columbia University

Secretary
Peter Stephens
Stony Brook University

Ex-Officio
Chi-Chang Kao
NSLS User Science Division

Ex-Officio
Mary Anne Corwin
NSLS User Administration Office

Ex-Officio
Lisa Miller
NSLS Information & Outreach

Special Interest Group Representatives

Special Interest Groups in areas of common concern communicate with NSLS management through the UEC.

Biological Scattering & Diffraction
Vivian Stojanoff, BNL-NSLS

Industrial Users
Simon Bare, UOP LLC

Imaging
Jerry Delaney, Rutgers University

Infrared Users
Larry Carr, BNL-NSLS

Nuclear Physics
Mahbub Khandaker, Thomas Jefferson Nat. Lab.

Students and Post Docs
Aaron Celestian, Stony Brook University

XAFS

Kumi Pandya, North Carolina State University

X-ray Scattering & Crystallography
Peter Stephens, Stony Brook University

Time Resolved Spectroscopy
John Sutherland, BNL-Biology

Topography
Michael Dudley, Stony Brook University

UV Photoemission & Surface Science

Peter Johnson, BNL-Physics

Science Advisory Committee

The Science Advisory Committee (SAC) evaluates science programs at the NSLS and makes recommendations to the Chairman.

M. Blume, BNL

S. Burley, Structural GenomiX

S. Gruner Chess, Cornell University

F. Himpsel, University of Wisconsin, Madison

K. Hodgson, SLAC

J. Schneider, HASYLAB, DESY Germany

A. Sievers, Cornell University

S. Sinha, University of California, San Diego

A. Lanzirotti, University of Chicago (UEC Chair, Ex-Officio)

NSLS Advisory Committees

General User Proposal Study Panel

The Proposal Study Panel (PSP) reviews and rates General User Proposals. Members are drawn from the scientific community and generally serve a two-year term.

X-ray Scattering

Ben Hsiao, Stony Brook University

Rainer Kolb, ExxonMobil

Karl Ludwig, Boston University

X-ray Spectroscopy

Anatoly Frenkel, Yeshiva University

Douglas Hunter, University of Georgia

Trevor Tyson, New Jersey Institute of Technology

X-ray Biology

Rui-Ming Xu, Cold Spring Harbor Laboratory

DaXiong Fu, BNL-Biology

Da-Neng Wang, New York University

Daniel Leahy, John Hopkins University

Imaging/Other

Richard Reeder, Stony Brook University

George Flynn, SUNY @ Platts-burgh

VUV Science

Daniel Fischer, NIST

Friedrich Hoffmann, Sci.-Med.

Jan Hrbek, BNL-Chemistry

Allocation Panel

The Allocation Panel allocates General User beam time to both new proposals and Beam Time Requests based on ratings provided by the Proposal Study Panels. Members are drawn from the scientific community and generally serve a two-year term.

VUV

Laszlo Mihaly
Stony Brook University

Elio Vescovo
BNL-NSLS

X-ray

Marc Allaire
BNL-NSLS

Annie Heroux
BNL-Biology

Jean Jordan-Sweet
IBM

Elaine DiMasi
BNL-Physics

Syed Khalid
BNL-NSLS

Wolfgang Caliebe
BNL-NSLS

General User Oversight Committee

The General User Oversight Committee resolves disputes between General Users, PRTs, and NSLS staff.

Simon Bare
UOP

Mark Chance
AECOM

Barbara Illman
University of Wisconsin

Dale Sayers
North Carolina State University

NATIONAL SYNCHROTRON LIGHT SOURCE ORGANIZATION

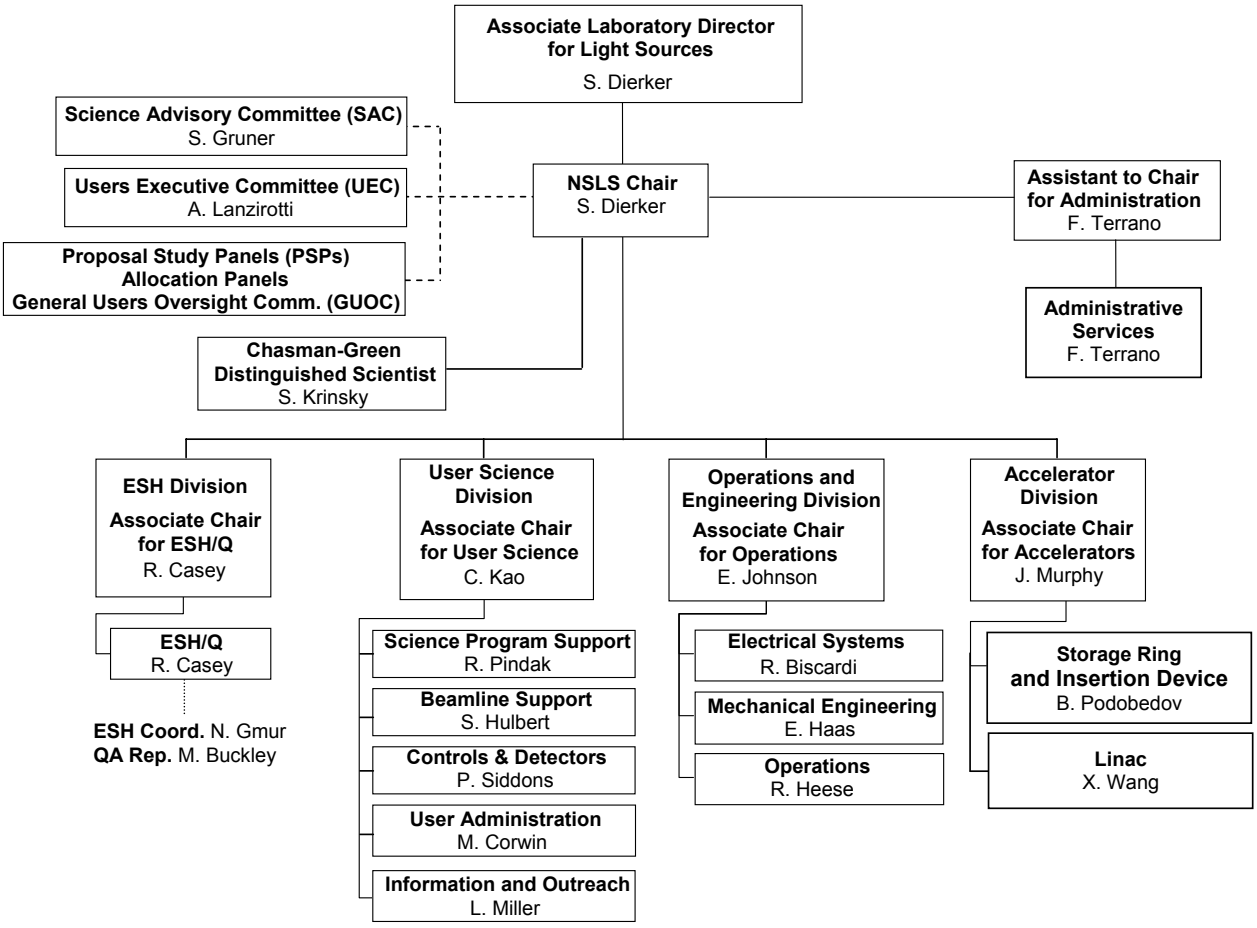

NSLS Advisory Committees

Users' Executive Committee

The Users Executive Committee (UEC) provides for organized discussions among the user community, NSLS administration and laboratory directorate. It aims to communicate current and future needs, concerns, trends within the user community to NSLS staff and management, and to disseminate to the users information about the NSLS and BNL plans.

Chair
Antonio Lanzirotti
University of Chicago

Past Chair
Leemor Joshua-Tor
Cold Spring Harbor Laboratory

Member
Fred Dyda
National Institute of Health

Member
Daniel Fischer
NIST

Member
Anatoly Frenkel
Yeshiva University

Member
Dean Hesterberg
North Carolina State University

Member
Richard Reeder
Stony Brook University

Vice Chair
Larry Shapiro
Columbia University

Secretary
Peter Stephens
Stony Brook University

Ex-Officio
Chi-Chang Kao
NSLS User Science Division

Ex-Officio
Mary Anne Corwin
NSLS User Administration Office

Ex-Officio
Lisa Miller
NSLS Information & Outreach

Special Interest Group Representatives

Special Interest Groups in areas of common concern communicate with NSLS management through the UEC.

Biological Scattering & Diffraction
Vivian Stojanoff, BNL-NSLS

Industrial Users
Simon Bare, UOP LLC

Imaging
Jerry Delaney, Rutgers University

Infrared Users
Larry Carr, BNL-NSLS

Nuclear Physics
Mahbub Khandaker, Thomas Jefferson Nat. Lab.

Students and Post Docs
Aaron Celestian, Stony Brook University

XAFS

Kumi Pandya, North Carolina State University

X-ray Scattering & Crystallography
Peter Stephens, Stony Brook University

Time Resolved Spectroscopy
John Sutherland, BNL-Biology

Topography
Michael Dudley, Stony Brook University

UV Photoemission & Surface Science

Peter Johnson, BNL-Physics

Science Advisory Committee

The Science Advisory Committee (SAC) evaluates science programs at the NSLS and makes recommendations to the Chairman.

M. Blume, BNL

S. Burley, Structural GenomiX

S. Gruner Chess, Cornell University

F. Himpsel, University of Wisconsin, Madison

K. Hodgson, SLAC

J. Schneider, HASYLAB, DESY Germany

A. Sievers, Cornell University

S. Sinha, University of California, San Diego

A. Lanzirotti, University of Chicago (UEC Chair, Ex-Officio)

NSLS Advisory Committees

General User Proposal Study Panel

The Proposal Study Panel (PSP) reviews and rates General User Proposals. Members are drawn from the scientific community and generally serve a two-year term.

X-ray Scattering

Ben Hsiao, Stony Brook University

Rainer Kolb, ExxonMobil

Karl Ludwig, Boston University

X-ray Spectroscopy

Anatoly Frenkel, Yeshiva University

Douglas Hunter, University of Georgia

Trevor Tyson, New Jersey Institute of Technology

X-ray Biology

Rui-Ming Xu, Cold Spring Harbor Laboratory

DaXiong Fu, BNL-Biology

Da-Neng Wang, New York University

Daniel Leahy, John Hopkins University

Imaging/Other

Richard Reeder, Stony Brook University

George Flynn, SUNY @ Platts-burgh

VUV Science

Daniel Fischer, NIST

Friedrich Hoffmann, Sci.-Med.

Jan Hrbek, BNL-Chemistry

Allocation Panel

The Allocation Panel allocates General User beam time to both new proposals and Beam Time Requests based on ratings provided by the Proposal Study Panels. Members are drawn from the scientific community and generally serve a two-year term.

VUV

Laszlo Mihaly
Stony Brook University

Elio Vescovo
BNL-NSLS

X-ray

Marc Allaire
BNL-NSLS

Annie Heroux
BNL-Biology

Jean Jordan-Sweet
IBM

Elaine DiMasi
BNL-Physics

Syed Khalid
BNL-NSLS

Wolfgang Caliebe
BNL-NSLS

General User Oversight Committee

The General User Oversight Committee resolves disputes between General Users, PRTs, and NSLS staff.

Simon Bare
UOP

Mark Chance
AECOM

Barbara Illman
University of Wisconsin

Dale Sayers
North Carolina State University

Facility Report

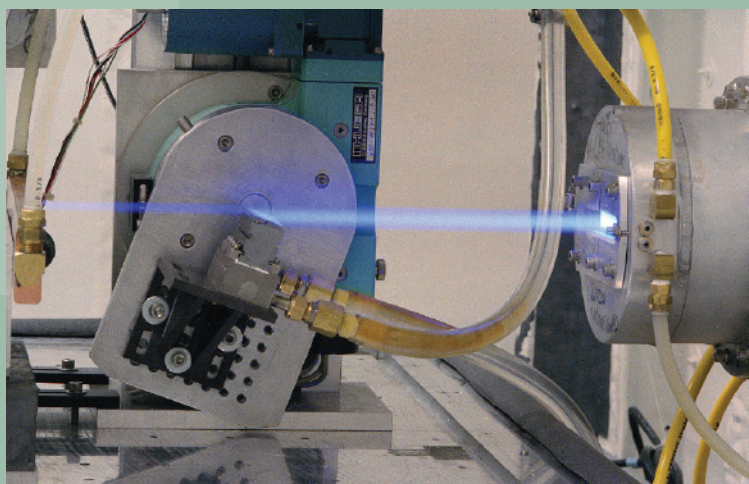

Operations and Engineering Division Report

Erik D. Johnson
ASSOCIATE CHAIR FOR OPERATIONS AND ENGINEERING

Organization and Mission

The largest of the NSLS Divisions, Operations and Engineering consists of three sections: Operations, which is led by Richard Heese, Electrical Systems, led by Richard Biscardi, and Mechanical Engineering, led by Ed Haas. The mission of our division falls into three main areas:

- Operation of the NSLS 24 hours a day, 7 days a week, an average of 44 weeks a year.
- Design, fabrication, and maintenance of the NSLS accelerators and utilities, including upgrades and modifications to meet changing needs.
- Engineering and technical support for the other NSLS divisions and the NSLS user community.

As the department continues to emphasize beamline operations, we are increasingly relying upon a department-wide matrixed management approach: The Operations and Engineering Division (OED) draws resources from other divisions to support operations, and we provide special expertise to support development for other divisions.

2003 Activities This report provides a transition to reporting activities by the calendar year. Hence, three major shutdowns are included as well as operations throughout the year. Operational performance statistics will continue to be reported on a fiscal year basis. An overview of machine performance for Fiscal Year 2003 is provided in section 6, 'Facility Facts and Figures.'

X29: A series of major installation tasks spanning several shutdowns revolved around the development of an insertion device based program at beamline X29. A new ring vacuum chamber for an insertion device beamline had previously been installed in the x-ray ring. During December 2002, our third new RF cavity was installed in the X29 straight section. With this installation, two new cavities reside in the straight, providing space for the installation of a Mini Gap Undulator (MGU), identical to that already in service at X13. Shield wall modifications were also made during the December 2002 shutdown that allowed construction of the beamline on the floor to commence.

During the May 2003 shutdown, the MGU itself was moved into place between the RF cavities. The installation of the MGU controls, active interlock electronics, and beamline front-end was completed in the December 2003 shutdown, with commissioning starting in January of 2004. The X29 MGU project exercised the 'matrix organization' concept to the fullest, as its success depended upon significant contributions from every NSLS division and the collaboration building the beamline. While X29 was a major activity for the OED, it is an achievement for the entire NSLS.

NSLS-II: A major initiative for the NSLS community, NSLS-II has been a high priority for the department throughout the year. The OED has contributed primarily through the development of engineering

conceptual designs, project schedules, and cost estimates to meet the requirements established by the User Science and Accelerator Divisions.

Surprises and Triage: Nearly every parameter of the NSLS has been expanded beyond its original design goals. Careful evaluation of changes as well as diligent maintenance of the machines has allowed our user community to enjoy a very high degree of reliability. However, as the machine ages, problems do crop up, and 2003 seemed to be a bumper year for surprises.

On the X-ray ring, the increase in operating energy to 2.8 GeV and the implementation of the high brightness optical configuration required the current of the defocusing string of sextupole magnets to be raised from 500 amperes to over 800 amps. This almost tripled the power dissipated in the magnet string. The change was carefully evaluated before it was instituted several years ago, but it was known that the magnets would become more sensitive to flow disruptions. Coming out of the December 2003 shutdown, we experienced a failure of a coil in one of the magnets in the string. This particular magnet is buried within the LEGS area of the machine, making it both a 'one of a kind' and very difficult to access. Removing and repairing the magnet took nearly two weeks, cutting significantly into January 2003 operations. Later in the year, another magnet in the same string started overheating, although it did not fail. In the December 2003 shutdown, during preparations to replace the magnet, a blockage was discovered (and removed) from the magnet buss work, alleviating the overheating.

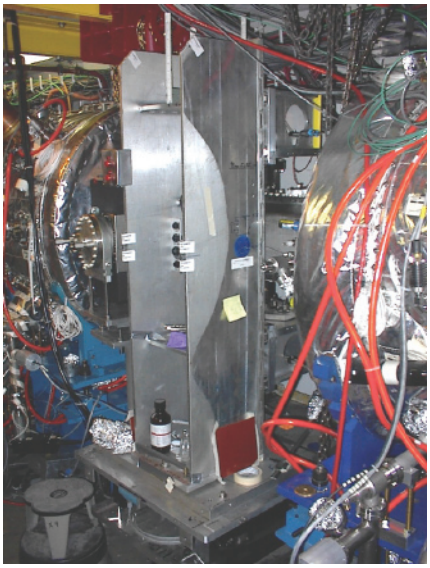

The new MGU between the RF cavities in the X29 straight section.

Various vacuum problems also contributed to operational headaches in 2003. In the month running up to the May 2003 shutdown, a small leak developed in a stripline monitor in the X-ray ring, causing a reduced beam lifetime, which led us to start the shutdown two days early. The leak was successfully repaired during the shutdown. During the summer, we also had a user vacuum venting accident and a leak in an ion pump feedthrough. It failed when it was sprayed by a fine mist of water from a pinhole leak in the body of a brass fitting four feet away that had been in place for over 15 years!

This also happened to be the year of the Northeast black out in August, causing nearly three days of X-ray operations downtime. This year the 'unusual' problems on the X-ray ring accounted for more than 12 days of down time, with just over six days due to the more typical operations problems. Overall, for fiscal year 2003, machine reliability was 89% for X-ray, although UV reliability remained high at 98%.

These very visible events tend to overshadow the failures that didn't happen because of the vigilance of the staff that maintains and repairs the machines out of the sight of the user community. Examples include the repair of the U14 water cooled mask during the May 2003 shutdown, the U4IR mirror rebuild during the December 2003 shutdown, and the upgrade of the X17 wiggler controls in December 2003. Magnet power systems, injection control, and diagnostic systems were also upgraded without fanfare; these are all systems that are essential to maintaining the performance and reliability of the NSLS. As we look forward to NSLS-II, the staff of the OED is prepared to meet the challenge of keeping the current NSLS performing at its best for another decade.

Accelerators Report

James Murphy
ASSOCIATE CHAIR FOR ACCELERATORS

Organization and Mission

The NSLS Accelerator Division (AD) was established in late 2001 through the reorganization of the NSLS and is headed by James B. Murphy. The division is organized into two sections: the Linear Accelerator (Linac) Section, headed by Xijie Wang, and the Storage Ring & Insertion Device Section, headed by Boris Podobedov. The staff consists of eight accelerator physicists, two engineers, three technicians, and two postdocs.

The NSLS Accelerator Division (AD) has a four-part mission:

- To ensure the quality of the electron beam in the existing NSLS booster, linear accelerator, and x-ray and vacuum ultraviolet (VUV) storage rings
- To operate the deep ultraviolet free electron laser (DUV-FEL) and Magnet Measurement facilities
- To participate in the NSLS-II project
- To perform fundamental research and development in accelerator and free electron laser physics

2003 Activities

NSLS-II: A major activity of the AD staff was the initial design of the new storage ring source for the NSLS-II project. The AD staff worked in conjunction with the other divisions of the NSLS to develop the machine concept for an ultra-high brightness (~10^{21}) 3 GeV electron storage ring design. The preliminary design is based on a 24-cell triple bend achromat lattice with a horizontal emittance in the range of 1.5 nm (**Figure 1**). Such a ring would more than triple the number of insertion devices available to the user community and provide 10,000 times higher brightness. A machine advisory committee was established to provide feedback on the machine design.

Storage Rings: Significant effort by the AD staff went into studying how the installation of more Mini Gap Undulators (MGU) in the x-ray ring would affect accelerator performance. In particular, MGUs may limit the beam current due to various collective effects induced by the strong impedance of the mini-gap chamber and transitions. The recent installation of the X29 MGU chamber gave us an opportunity to measure and compare some of these effects before and after the installation. While we did observe increased betatron tuneshifts with current at low energy, fortunately the increase turned out to be quite small and should not hinder operations. Single bunch currents of up to 125 mA are still possible, with the (administrative) limit set due to heat in vacuum chamber components unrelated to MGUs. We are also numerically calculating the impedance of the MGU chamber with electromagnetic field simulators. These studies should also provide valuable insights into the possible effect of MGUs on the future performance of the NSLS-II storage ring.

Another area of activity emphasized improvements to the storage ring lattices of the X-ray and VUV rings. The LOCO code, originally developed at the NSLS by James Safranek, allows calibrating and correcting the ring lattice from the measured beam response matrix. With James' help, a new, more powerful MATLAB-based version of this code was extensively debugged at the NSLS last year and is now used for both rings. This work has also shown some limitations of our existing diagnostics and resulted in the installation of new Hall probes into some of the X-ray ring magnets.

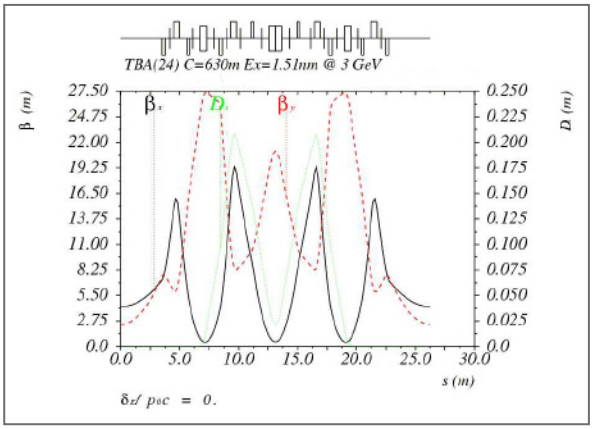

Figure 1. Storage ring lattice functions for the preliminary design of the NSLS-II ring (β_x in black, β_y in red and D_x in green).

Other work on the VUV ring included setting up shorter electron bunch configurations for time-resolved experiments as requested by the IR users. The challenge is to get a stable configuration of the ring lattice and RF system (with the harmonic cavity set for compression) that produces short bunches at substantial beam currents. Bunch lengths on the order of 400 ps FWHM with ~100 mA/bunch have been achieved. Work is continuing on yet another challenging configuration that produces mm-scale periodic ~10 Hz orbit motion at beamline U4IR while keeping stable orbit throughout the rest of the ring. This motion fills the very-far IR spectral gaps that are produced by the interference between the direct synchrotron radiation and (orbit-dependent) reflections off the walls of the vacuum chamber. To provide for the very localized orbit distortion, we are reconfiguring the VUV ring digital orbit feedback system.

Magnetic Measurement Lab: Early in FY 2003, a second in-vacuum, mini-gap undulator (designated MGU-29) was assembled, measured, and magnetically shimmed to minimize magnetic field errors and to optimize its spectral performance. The Mechanical Group installed it in the X-ray ring in the space between a pair of accelerating cavities in the X29 straight section. The magnet gap was left open to temporarily reduce the x-ray output to a negligible amount pending installation of front-end and optical components of the new NIH-funded protein crystallography beamline. These components were installed in the winter 2003-04 shutdown.

An FY 2002 design study to replace the aging X1 soft x-ray undulator identified several options that were presented to the X1 users and User Science Division staff. The preferred option was a pair of 1.4 m long undulators in tandem, canted to produce two photon beams, separated by about 1 milliradian, serving beamlines X1A and X1B independently, with independent control of each device by the respective users. One device would be a variable-polarization undulator, the other a planar one. However, this solution was predicated on a significant reduction of the height of the vacuum chamber in these devices. To verify the impact of a reduced chamber height on machine operations, particularly during injection, and to determine the minimum allowed vertical aperture in the new undulators, we decided to experimentally simulate the reduced aperture. A motorized beam scraper assembly was refurbished and installed in a chamber to be shared with an existing photon absorber, just upstream of the MGU-13 in-vacuum undulator. The combination of the variable-gap MGU-13 in the center of the straight and the scraper, approximately one meter upstream, will allow the characterization of

the vertical beam profile in a typical straight section under all operating conditions. This scraper assembly was installed during the December 2003 shutdown.

As an important part of our efforts to develop a superconducting undulator (SCU), a state-of-the-art SCU measurement apparatus was designed by the Magnetic Measurement and Mechanical Engineering staff, and is now under construction (**Figure 2**). It is designed to perform both magnetic and calorimetric measurements on SCU models up to about 0.4 m in length, cooled either by immersion in liquid helium (LHe) or by conduction. Three independently instrumented helium channels will allow detailed calorimetric measurement of both the SCU magnet windings and the beampipe under various thermal conditions, including simulated beam heating. A motorized, multi-element Hall sensor assembly for detailed magnetic field mapping has been constructed and bench-tested. The Hall sensors will be calibrated off-line against an NMR standard in a laboratory magnet, both at room temperature and at 77K in a liquid nitrogen bath. A small superconducting magnet within the cryostat will also permit in-situ calibration checks of the sensors at 4K. The Hall probe mapper will be interchangeable with a stretched wire sensor, instrumented to operate in either the pulsed-wire or vibrating-wire mode, and will provide complementary measurements of field errors, trajectory errors, and integrated field errors.

Figure 2. Vertical Test Facility for magnetic measurements of future superconducting undulators.

Together with the BNL Magnet Division, we plan to develop a SCU design using advanced "APC-type" NbTi superconductors, which can operate at higher currents and fields than conventional NbTi. We also plan to investigate a means of correcting phase errors in SCU's, critical for achieving high brightness at high harmonics for full coverage of the 2-20 keV photon range.

An improved magnetic design was developed for a new in-vacuum undulator to replace the aging X25 wiggler. The new device, designated "MGU-25," will be one meter long with an 18 mm period and a minimum gap of 5.6 mm, and will cover 1.9 – 20 keV, using the fundamental, 2^{nd} (present due to the rather high emittance), 3^{rd}, 5^{th}, and 7^{th} harmonics. The latest NdFeB materials with higher remanent field and very high intrinsic coercivity will be used to maximize the tuning range. The Mechanical Engineering group designed a longer vacuum chamber and a "twin-tower" support structure derived from the successful "single-tower" and chamber designs used in MGU-13 and MGU-29. A make-or-buy decision, development of detailed specifications, and procurement of just the magnets or the complete undulator are expected in FY 2004.

We continued our collaboration with A. Temnykh of Cornell in developmenting a vibrating-wire magnetic probe for use in small-gap undulators. This technique will be adapted for insertion into the SCU test apparatus described above. Magnetic Measurement staff also supported the Cascaded High-Gain Harmonic Generation X-ray FEL proposal by modeling and developing wiggler designs for the five modulator and amplifier stages. Magnetic Measurement staff contributed to the development of the NSLS-II lattice design via 3D magnetic modeling of candidate magnet designs, such as combined-function gradient dipole electromagnets and permanent magnet-driven gradient dipoles.

DUV-FEL: The Deep Ultra Violet Free Electron Laser (DUV-FEL) provides unique capabilities to the NSLS user community. The accelerator system of the DUV-FEL consists of a 1.6-cell BNL photo injector driven by a Ti:Sapphire laser system, and a four section 2856 MHz SLAC-type traveling wave linac capable of producing a 200 MeV electron beam. The magnetic chicane bunch compressor at the DUV-FEL produces sub picosecond (ps) long electron bunches with a peak current of a few hundred amperes. The high brightness electron beam transits the 10 meter long NISUS undulator to generate UV light with a fundamental wavelength of 266 nanometers (nm).

In FY03, the DUV-FEL achieved a unique mode of operation known as High Gain Harmonic Generation (HGHG), whereby the electron beam is energy modulated with the Ti:Sapphire laser at 800 nm, the energy modulation is converting into spatial bunching in a dispersive magnet, and then the bunched electron beam radiates coherently at 266 nm in the NISUS undulator.

After successfully lasing at 266 nm with the 800 nm laser seeding, experiments were carried out at the DUV-FEL to further characterize the properties of the HGHG FEL, and to demonstrate its stability and controllability. The narrower spectrum and better stability of HGHG compared to a SASE FEL were observed (**Figure 3**). Both the second and the third harmonic of the HGHG FEL radiation were experimentally characterized using a vacuum monochromator. The pulse energy for both harmonics (133 and 89 nm) was measured to be about 1 μJ, which is about 1% of the fundamental at 266 nm. A two-photon absorption auto-correlator with 100 fs resolution was developed to characterize the HGHG output pulse length. It was experimentally demonstrated that the HGHG output pulse length can be controlled using the seed laser from a picosecond down to 250 fs (FWHM). Experiments to investigate a chirped HGHG FEL were also initialized in 2003. Preliminary results are very promising, and the chirped FEL could lead to even shorter pulses of HGHG output.

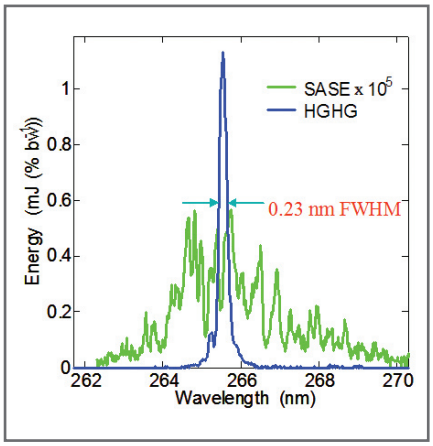

Figure 3. Experimental comparison between unsaturated Self Amplified Spontaneous Emission (SASE) and High Gain Harmonic Generation (HGHG) spectra.

One of the most important milestones in the last year at the DUV-FEL is the initialization and completion of the first DUV-FEL user experiment by Arthur Suits and his collaborators from the BNL Chemistry Department. The first chemical science experiment – ion pair imaging – used the third harmonic (89 nm) of the HGHG output to study the super excited states of methyl fluoride. Velocity mapped ion images of the fluoride ion, obtained with excitation via intense, coherent, sub-picosecond pulses of 86-89 nm radiation, reveal low translational energy, implying very high internal excitation in the methyl cation cofragment (**Figure 4**). The report on this experiment has been published in Physical Review Letters. To advance the user science program at the DUV-FEL, the NSLS hosted a very productive chemical science user workshop in July 2003.

There is increasing interest in high intensity THz radiation because of its potential applications in homeland security and material characterization. Two experiments were performed at the DUV-FEL to explore the possibility of using the bright electron beam to generate coherent THz radiation. In the first experiment, the electron beam with a sub-mm modulation was produced via temporal modulation of the photoinjec-

tor drive laser. The spatially modulated electron beam then is used to generate coherent THz radiation. Pulses in excess of 80 μJ of coherent THz radiation, using a transition radiation mechanism, were measured in the second experiment using sub-picosecond electron bunches containing about 0.7 nano-coulombs of charge. This intensity is about two orders of magnitude higher than the laser-based THz sources, and field strengths on the order 500 kV/cm are expected from such an intense THz source.

High-brightness electron beam generation and preservation is the key to the success of all future linac-based light sources. Investigations performed at the DUV-FEL revealed the possibility of strong longitudinal spatial modulation driven by a space-charge oscillation during the electron beam bunch compression. Comparison between experiments and simulation confirmed the amplification of an existing modulation during bunch compression. A femtosecond electron bunch monitor based on the electron-optical effect was successfully commissioned at the DUV-FEL to study the electron beam longitudinal distribution and the timing jitter between the electron beam and the HGHG seed laser. Using this technique, the timing jitter between the electron beam and the HGHG seed laser was measured to be 150 fs.

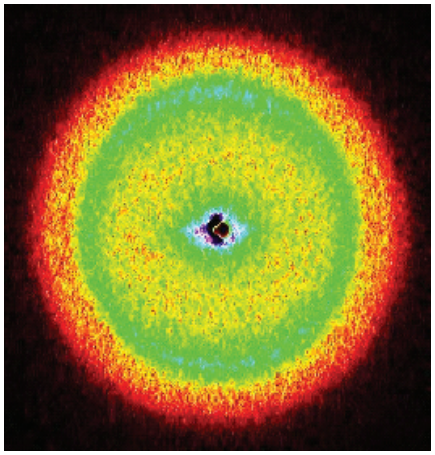

Figure 4. Ion pair image from the first DUV-FEL user experiment.

Beam Line Operations and Safety Awareness (BLOSA) training and many other procedures were developed at the DUV-FEL to improve acceleration operation and laser safety.

In September 2003, Dr. L.H. Yu of the NSLS Accelerator Division was awarded the 2003 International FEL Prize for his outstanding contributions to “High Gain Free Electron Lasers and High Gain Harmonic Generation.”

User Science Report

Chi-Chang Kao
Associate Chair for User Science Division

Organization and Mission

The User Science Division coordinates major facility activities related to users so that we can be more effective in communicating with the user community, strengthen existing scientific programs, foster the growth of new scientific programs, and raise the visibility of the exciting science produced by our users. The division consists of five sections: User Administration (Mary Anne Corwin), Information and Outreach (Lisa Miller), Beamline Development and Support (Steve Hulbert), Scientific Program Support (Ron Pindak), and Detectors and Controls (Peter Siddons). The major initiatives and accomplishments of the User Science Division and the NSLS user community for 2003 are summarized briefly below.

2003 Activities

This year has been eventful for the User Science Division. The year began with coordinating the user community in response to a Department of Energy /Basic Energy Sciences (DOE/BES) call for proposals to "Enhanced Research Capabilities at DOE X-ray and Neutron Facilities." Thanks to the effort of a large number of users and NSLS staff members, several major instrumentation proposals were submitted, including a new micro-beam x-ray diffraction instrument, an undulator-based small angle x-ray scattering beamline, and instrumentation upgrades for a number of powder/single crystal diffraction beamlines. Among them, the micro-diffraction instrument was funded in 2003, and the small angle scattering beamline will be funded in 2004. Both projects will take full advantage of the high brightness provided by the in-vacuum small gap undulator developed at the NSLS, and will provide two new world-class capabilities at the NSLS that are particularly important for nanoscience research. In addition, the input from the user community during the preparation of these proposals has been extremely valuable and will help us serve them better.

We soon turned our attention to working on the NSLS response to the DOE/BES "twenty-year facilities roadmap" review, and subsequently the science case for the NSLS-II proposal, an ultra-high brightness, medium energy storage ring. With the help of a large number of users, we organized more than a dozen scientific workshops, ranging from life sciences, materials/chemical sciences, and nanoscience to earth and environmental sciences. These focused workshops were very successful in identifying the grand challenges in the individual fields of research, and the impact of NSLS-II on them, as well as the technical challenges in the accelerator, insertion devices, optics and detectors. More importantly, these workshops have clearly demonstrated a great deal of excitement and support in the user community about the NSLS-II project.

The year continued with the exciting news that NSLS user Roderick MacKinnon from Rockefeller University shared the 2003 Nobel Prize in chemistry for his work on ion channel proteins. A very important part of

his work, the determination of numerous protein crysal structures, was done primarily at the Cornell High Energy Synchrotron Source and the NSLS. More good news this year for the NSLS macromolecular crystallography user community came when the BNL Biomedical Technology Research Resource for Macromolecular Crystallography, a center sponsored by the National Center for Research Resources (NCRR) of the National Institutes of Health (NIH), received its renewal funding for another five-year period. This supplements another grant sponsored by the Department of Energy (DOE) Office of Biological and Environmental Research (BER) for the same period. These two grants will fund a number of activities, including the support of full-time operation of the X25 wiggler beamline, the completion of construction and the ensuing commissioning and operation of a new undulator beamline for macromolecular crystallography at X29, and a major upgrade of beamline X25, which involves the replacement of its wiggler source by a novel small-gap undulator source and appropriate beamline optics upgrades to take advantage of the properties of the new source.

In between these exciting events, we have also completed a number of major beamline construction and upgrade projects:

- X6A beamline construction: A new bending magnet beamline, X6A, has been completed and started user operation. The beamline was funded by the National Institutes of General Medical Sciences of the National Institutes of Health (NIH-NIGMS) to meet the increasing demand in protein crystallography.

- X6B beamline construction: X6B is a new powder/single crystal diffraction beamline, designed to perform (1) time-resolved powder diffraction experiments, (2) combined x-ray spectroscopy and x-ray diffraction experiments, (3) single crystal diffraction experiments, and (4) electron density of excited states.

- X17 superconducting wiggler beamline upgrade: The upgrade involved the construction of two new experimental hutches to allow a dedicated hutch for a materials science instrument, a large volume press instrument, and a diamond anvil cell instrument. This upgrade will significantly increase the amount of beam time available to these user communities.

- X19A beamline upgrade: X19A is the premier low-energy x-ray beamline at the NSLS and has very high user demand. In 2003, a new monochromator was designed and installed to improve the cooling of the monochromator crystals. The new design has led to better energy and intensity stability of the beamline and ease of beamline operation.

- U5UA beamline upgrade: A refocusing mirror was added to provide the possibility of providing radiation to a second endstation. The focused beam size is on the order of 10 microns, making it ideally suited for the planned combined low-energy electron and photoemission microscopy endstation.

In addition, we have initiated several new beamline upgrade projects this year, including the X1A undulator beamline, the X13A elliptical polarizing wiggler beamline, the X21 wiggler beamline, and the X27 microprobe beamline. The completion of these projects will be very

Figure 1. Beamline X6A, a new macromolecular crystallography beamline funded by the National Institutes of General Medical Sciences of the National Institutes of Health.

important for the development of new scientific programs in nanoscience, soft and biomaterials, magnetism, advanced materials growth, and environmental science. We are also very fortunate to have seven very talented scientific and technical staff joining us this year to take on these projects and lead the development of new scientific programs.

There has also been steady progress in the detector development area this year. After successful a demonstration last year, several copies of the fast avalanche photodiode (APD) detector-electronics units have been installed at x-ray scattering beamlines. The large-angle curved gas proportional counter detector for time-resolved x-ray powder diffraction has been installed on two beamlines, one for testing purposes and the second for a user run. New software enabling time-slicing down to the microsecond time scale has also been implemented. Finally, several 96-element prototype silicon detectors with custom-designed integrated circuits, which each parallel-process input from 32 detector elements, are being assembled and will be deployed soon.

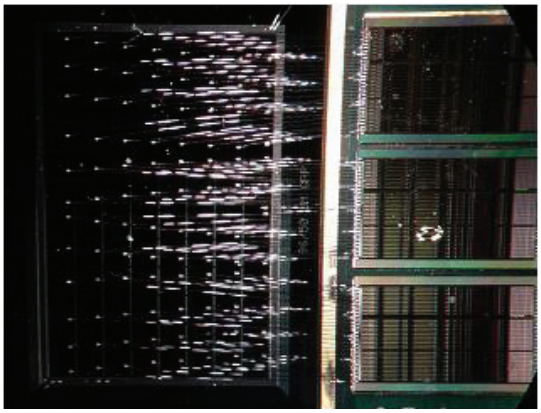

Figure 2. Three of the new 32-channel custom integrated circuits bonded to 96 silicon diode detectors. This configuration provides <250 eV resolution at 4 microseconds shaping time, or a count rate of >100 kHz per element at 0.5 microseconds shaping time.

With the addition of a full-time programmer this year, the User Administration office has made significant progress in the development of a new online proposal system to integrate proposal submission, safety approval, proposal review, beamtime allocation, and beamtime scheduling. We appreciate greatly the effort by a large number of participating research teams (PRTs), users, and NSLS staff, who provided valuable input and recommendations throughout the process. Testing of the system will begin in 2004.

Finally, we continue to take more immediate steps to enhance user science at NSLS. First, a short course on EXAFS data collection and analysis was held again this past summer with the help of many experienced users. This hands-on workshop provided both new and experienced users with exposure to EXAFS theory, data collection, and analysis. Feedback on the EXAFS short course has been so extremely positive that it has become an annual event. Second, a regular series of science highlight articles is now published on the NSLS website to facilitate the dissemination of exciting scientific results obtained at NSLS beamlines to the NSLS user community, as well as the wider scientific community. Third, a new symposium series has been established at the NSLS to give staff and users an opportunity to hear about cutting-edge synchrotron research that is performed worldwide. Upcoming seminars are now listed on the NSLS homepage for easy access to the schedule. In addition to these activities, the NSLS staff has been helping the BNL Center for Functional Nanomaterials (CFN) establish and launch a CFN user program, exploring ways to coordinate the NSLS and CFN user programs.

User Administration Report

Mary Anne Corwin
USER ADMINISTRATION HEAD

User Statistics

During the past year, 2206 badged users performed experiments at the NSLS, almost a third of them (681 users) for the first time.

For users who conducted experiments at the NSLS facility during the year, 31% indicated their primary field of research as materials sciences, 37% as life sciences, 8% chemical sciences, 9% geosciences and ecology, 10% applied science and engineering, and 5% optical/nuclear/general physics.

While the number of users in particular fields of science is indicative of *who* is using the facility, it does not show *how* the facility is used. Since 1999, the NSLS has reported statistical data based on actual usage of the facility. This information is extracted from beam time used by each of the 1145 experiments performed in FY03. This year, nearly 42% of the beam time used was utilized by experiments conducted in the field of materials sciences. The remaining beam time was utilized by biological and life sciences (18%), physics, except condensed matter (4%), chemistry excluding materials chemistry (5%), polymers (3%), medical applications (2%), earth sciences (6%), environmental sciences (4%), optics (3%), engineering (3%), instrumentation (5%), particle accelerator R&D (1%), radiation source R&D (2%), and other (1%). The primary difference in the number of users versus the amount of beam time utilized for a given field of research is explained by the fact that materials sciences experiments utilize considerably more beam time than other experiments. This is particularly true for experiments in the biological/life sciences. In addition, there are generally a lower number of experimenters utilizing the facility for materials experiments than there are for biological/life sciences experiments.

The primary source of user funding can also be determined based on beam time usage at the facility. During FY03, experiments funded by the Department of Energy's Office of Basic Energy Sciences (DOE/BES) within the Office of Science utilized 33% of the facility's beam time. Other programs in the DOE complex utilized an additional 7% of the beam time. Facility usage by other *primary sources* of user support included NSF (16%), NIH (11%), and Industry (10%).

More than 67% of our users are affiliated with U.S. and foreign academic institutions. Other affiliations include BNL employees who are facility users (11%), other DOE contractor employees (2%), other federal agencies (5%), industry (7%), and other (8%).

The 2206 users who visited our facility in FY03 are affiliated with 376 unique U.S. and foreign institutions, including 233 academic institutions, 65 industrial institutions, 24 federal government agencies, 25 non-governmental laboratories, and 29 other institutions.

Faculty members at universities or colleges, professional staff and scientists at private, and national or industrial laboratories account for

the greatest population of users (38%), followed by graduate students (33%), postdoctoral research associates (19%), undergraduate students (5%), and retired, self-employed, or other (4%).

Users come to the NSLS from around the globe. Though half are citizens of other countries, only 13% of all our users physically arrive from outside the U.S. to perform research here at the NSLS. All others are affiliated with a U.S. institution. About 36% arrive from New York institutions and another 27% are affiliated with institutions in the northeast. Our remaining users come from U.S. institutions outside of the northeast.

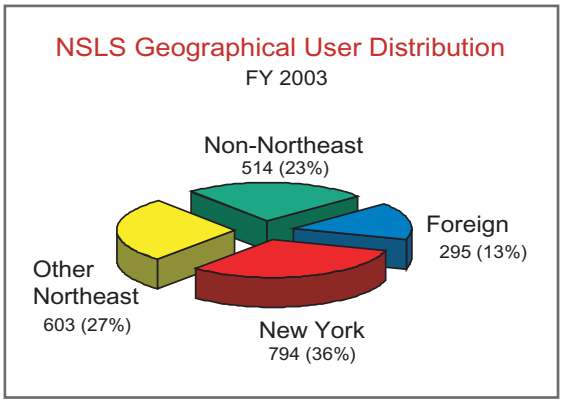

Security Compliance

A laboratory directive was issued in FY03 requiring strict adherence to DOE Notice 142.1 pertaining to requirements for unclassified visits, assignments, and activities by foreign nationals to DOE facilities. Our users were subsequently notified of new site access policies and requirements. Though the NSLS had hoped to see little disruption in our programs and use of the facility, we found that many users encountered problems accessing the site and others were required to leave BNL until appropriate documentation and/or approvals were secured. The most common problems experienced by our users are detailed below. The number of occurrences has decreased quite a bit over the last year, but there are still two or three users each month experiencing considerable delays.

Visa Problems: Upon entering the U.S., a user possessed appropriate paperwork for a work visa, but Immigration incorrectly issued documentation pertaining to a tourist visa. The user arrived at User Administration the same day but could not finalize the appointment. The process required that the user return to the airport within 24 hours of entry to correct the documentation. Unfortunately, if the documents are not corrected within 24 hours, the user is unable to work at BNL.

Approval Lead Time: A scientist from a northeastern university arrived at BNL after submitting the online registration form less than one week earlier. The form indicated an arrival date five days later. More than eight reviews are required before approval is granted and, at times, the process can take up to 45 days. User Administration immediately notified the scientist that he could not access the site until approval was granted. Disregarding the information, the scientist arrived the following weekend expecting to begin his experiment. After learning that access to the facility could not be granted, he returned to the university.

Appointment Renewals: A Ph.D. from a local institution arrived at BNL with an expired BNL identification badge without having submitted the registration form requesting an extension to his appointment. The user was required to leave the BNL site until his extension was requested and approval had been granted. A review of his file indicated he was previously notified that his appointment was terminated and was provided instructions on how to extend his appointment.

Visa Status: Although users receive two-year appointments, their termination date may extend beyond their visa expiration date. When that date arrives, the next time the user enters the main gate at BNL, the

badge scanning system will display a "yellow" light indicating that the user's passport and/or visa are out of status. One of our guest scientists arrived at BNL with a valid appointment and valid BNL identification badge. The badge scanned "yellow" and the guard advised the user to check in at User Administration to update his visa information. Once entered, the scanning system will display a "green" light. However, the user's documentation was at home, more than 200 miles away, and he was required to leave BNL until the documentation could be presented.

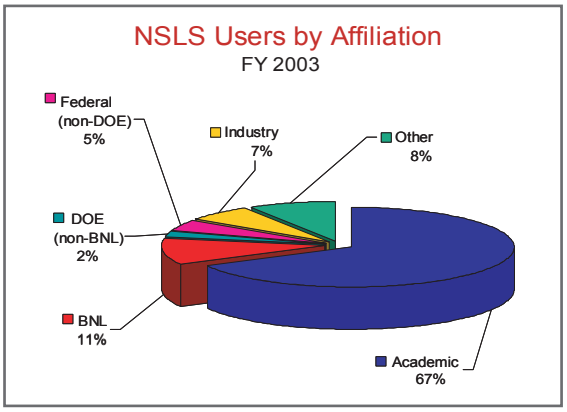

Escorting at the NSLS and Open to the Public Events: Historically, the NSLS has permitted non-users to be escorted onto the experimental floor provided certain safety requirements have been met. With the lab's new directive to come into compliance with DOE Order 142.1, changes took place in laboratory accessibility and escorting procedures, and with regard to "open to the public" events, especially for our foreign national users and visitors.

BNL management has indicated that foreign nationals attending "open to the public" events may tour other facilities while on site provided the tour is part of the event (not a separate event). There is no provision to permit a foreign national to be escorted onto the NSLS experimental floor unless the visitor (1) has a valid BNL ID badge, (2) is attending an "open to the public" event that specifically includes a tour of the experimental floor, or (3) has registered in the BNL's Guest Information System and their appointment and record have been activated. Additionally, foreign nationals performing any type of work or observing experiments at the NSLS must register and receive approval prior to arrival.

I would like to thank our users for their cooperation in helping the NSLS to maintain compliance with DOE requirements. Please contact our office at (631) 344-8737 with any questions.

Safety Report

Bob Casey
Associate Chair for ESH

Organization and Mission

Environmental, Safety, and Health (ESH) performance within the NSLS and at BNL in general remains an important issue for all NSLS staff, PRT members, and general users. The Annual Report provides an excellent opportunity to comment on past ESH performance and important changes in program requirements, and to identify issues that will be of importance in the year ahead.

2003 Activities

Calendar year 2003 was particularly dynamic for ESH in a number of important areas:

ESH Responsibilities of PRT Members and Beamline Staff: The ESH responsibilities of PRT members, beamline staff members, and investigators/users were better defined in 2003 to ensure that roles were clearly understood by all. A summary of the roles and responsibilities can be found at: *http://www.nsls.bnl.gov/organization/ESH/safety/r2a2.htm*.

Training: There has been a major emphasis at BNL on training for all staff members and guests. This year we increased the previous training requirements for resident beamline staff and users routinely present at the NSLS to provide a more detailed understanding of ESH requirements that are applicable to common situations in our work place. These training requirements can be found at: *http://www.nsls.bnl.gov/training/Requirements/Resident-User-Training.htm*. Training for our short-term users can be found at: *http://www.nsls.bnl.gov/training/Requirements/User-Training.htm* and is unchanged from previous years.

Work Planning: Work planning is the process for evaluating work to ensure identification of hazards and the establishment of appropriate controls. The work planning process for experimental research at the NSLS has worked well for many years and is implemented through the Safety Approval Form (*http://130.199.76.84/safety/default.asp*) process. Work at the beamlines, however, can involve beamline staff in routine activities that are not reviewed as a part of the SAF process (e.g. day-to-day work in maintaining a beamline, and modifications or additions to beamline components). Work planning requirements were revised this year to capture these type of activities and are identified at *http://www.nsls.bnl.gov/newsroom/publications/manuals/eshguide/D*. The requirements are graded based on the level of training of beamline staff. More detailed NSLS guidance may be obtained at: *http://www.nsls.bnl.gov/newsroom/publications/manuals/prm/LS-ESH-PRM-1.3.5a.html* and *http://www.nsls.bnl.gov/newsroom/publications/manuals/prm/LS-ESH-PRM-1.3.6.html*.

TLD Requirements for Access to the Experimental Floor: The requirements for wearing a TLD while working on the experimental floor were relaxed this year for many of our short-term users. Only users routinely working at the NSLS throughout the year, or those who fall into special

categories (e.g. working with radioactive materials, women with declared pregnancies, minors, or those working in the Bldg. 729 Controlled Area) are required to wear a TLD. Details of the new requirements can be found at: *http://www.nsls.bnl.gov/organization/ESH/temp/tldchange.htm*. It is very important to note that training requirements for access to the floor remain the same as previous years.

Laser Use: A serious eye injury occurred to a graduate student working in a different department at BNL when he inadvertently exposed himself to a high power laser. All laser use at BNL was suspended by the Laboratory Deputy Director pending a review to confirm that practices with each laser complied with the requirements of the BNL Standard for Lasers (*https://sbms.bnl.gov/standard/2g/2g00t011.htm*). All lasers at the NSLS were eventually restarted, but extensive stoppages were experienced. All users who plan to bring or use existing lasers should anticipate detailed reviews and contact the NSLS Safety Officer well in advance of arrival. Users of Class 3b/4 lasers must prepare written procedures, receive additional training, and complete a medical eye examination prior to use of the laser. These requirements are time consuming. Whenever possible, use of lower power lasers (i.e. Class 2 or 3a) will greatly simplify review requirements. Use of any laser in an experiment must be described in the Safety Approval Form (*http://130.199.76.84/safety/default.asp*). Additional NSLS guidance may be obtained at: *http://www.nsls.bnl.gov/newsroom/publications/manuals/prm/LS-ESH-PRM-2.3.1.html* (Laser Safety Program Requirements).

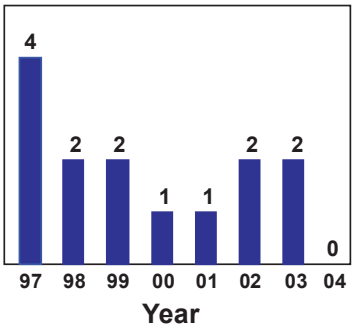

Lost time injuries per year since 1997. In 2004, we are striving for zero injuries.

Conclusion: The user community has responded well to the high level of expectations for safety performance at the NSLS. Prominent and high level presentations were made at the Annual Users' Meeting, and safety is a topic at every Town Meeting. On the other hand, we have had our share of problems, and the BNL Director and the head of the DOE Office of Science have stated on several occasions that science carried out in an unsafe environment will not be supported. It is important for everyone to understand that a safe environment is much more than just an injury-or incident-free environment - positive attitudes and compliance with requirements are equally important.

I think our ESH program continues to be strong, and the improvements of the past year will serve us well. We need a successful safety program, and that requires ongoing awareness, involvement, and commitment from everyone. One incident or injury can quickly over-ride and outshine many successes. Whether at your home institution or at the NSLS, keep an eye on the workplace and your co-workers. Make sure that all requirements are respected and that work is conducted safely. We all have a stake in safety performance.

Please let me know if you have any comments or suggestions.

Building Administration Report

Gerry Van Derlaske
NSLS Building Manager

The new mini-gap undulator, sextupole repair, the installation of the x-ray radio-frequency circulator, the continuing construction of cutting-edge beamlines, and the announcement that one of our users received the Nobel Prize in Chemistry for his NSLS research – It has been more than twenty years since the first operational beamlines were commissioned here, and, due to the efforts of many individuals and multiple service and support groups, the future of the NSLS is as bright as ever.

Safety and security issues remain at the forefront of daily operations, and facility improvements range from the physical plant infrastructure to a new user network outside of the current BNL firewall. Various beamline and ring upgrades have been fully commissioned and additions to the NSLS scientific staff have made for a very productive and interesting year.

Safety:

NSLS staff and users are reminded that working safely is a top priority at BNL. In accordance with this basic principal, the past year saw the introduction of new work planning elements for scientists and technicians. Work planning and control procedures require that work being performed at the NSLS above the "skill of the craft" level be reviewed by the appropriate subject matter experts and scheduled accordingly through available resources. Meetings are held weekly, or as needed in emergency cases, to review, approve, and authorize work that does not fall within this "skill of the craft" category. Using a graduated approach for hazard determinations, formal work permits will be issued for work deemed hazardous. Users and staff should contact the building manager with any questions pertaining to whether a formal work permit is required.

In October, the entire laboratory underwent a full OSHA walk-through inspection. Teams of OSHA personnel, from all areas of expertise and backgrounds in industrial safety, toured virtually every building at BNL. The NSLS fared reasonably well, receiving 61 citations, compared with some several thousand lab-wide. Many of the NSLS citations were corrected prior to this article, and we are tracking the few remaining open items. Our target goal remains set at zero citations in the future. The NSLS safety teams, paired with Tier 1 inspections, experimental reviews, and the work planning and control process, manage one of the busiest user facilities in the world and have the resources to achieve this objective. Accordingly, everyone must continue to intervene and act appropriately if observing any unsafe conditions.

Security:

This year, America has cycled between the Code Yellow (elevated) and Code Orange (high) terrorism awareness levels. We therefore ask everyone to be constantly vigilant when performing common, everyday tasks

at the NSLS. For example, lock your parked vehicle and do not leave it in the parking lot for long periods of time when you are absent from the NSLS. Do not leave your packages unattended, even for a few moments. There have been several instances of items found unattended and unidentified in the following areas: the main lobby, the entrance vestibule, and the drop-off zone inside the circular driveway of building 725. We urge all personnel to follow security measures when entering both BNL and the NSLS. Vehicle inspections at all gates leading off-site have increased, and the Department of Energy requires that all non-expendable property at BNL have bar codes or property tags affixed to indicate ownership. These tags are available free of charge from the NSLS stockroom.

While transparent to the casual observer, behind-the-scene work by many employees continues to provide our staff and users with a very safe and secure workplace. Again, we extend our gratitude to everyone for their patience and cooperation in conforming to the newly-implemented rules and regulations.

Some of the many talented members of the NSLS Plant Engineering Support Staff, Work Control Coordinators, and Facility Support/ Work Planning Team, who work together to keep the facility safe and sound.

Facility Upgrades:

New furniture, complimented by matching NSLS logo rugs, has been installed in the main lobby. Additionally, a satellite dish network was installed to feed the LCD projection monitor video wall and second floor conference rooms with a commercial signal that can provide live feeds to the NSLS community. The NSLS building manager will be the point of contact for submitting requests to activate the signal for viewing during evening and weekend hours. For special occasions or events, requests for viewing sporting events and educational, cultural, and informative programming can be sent to the chairman through the building manager for review and approval.

The RF penthouse air conditioning upgrade increased output cooling, reducing the heat load onto working power supplies and virtually eliminating power supply trips on hot summer days. All experimental floor steam re-heat coils located within the AC duct works were cleaned and serviced, providing better flow through ventilation. Due to the cleaning process, heat and air conditioning delivery is expected to become more stable.

Special maintenance funding from Plant Engineering provided the necessary resources to install replacement wall-to-wall carpeting in the seminar room, directorate wing hallway, and conference room A. Maintenance crews refurbished the restroom in building 726 and applied fresh coats of paint to many areas of building 725. The roof over MER 2, as well as the pitch pockets and galvanized trays surrounding the power feeders near the RF penthouse, were sealed and subjected to various proof tests during the summer downpours. The remaining areas of suspected roof leaks are now marked for repair once the winter freeze/ thaw cycles have ended.

As requested by users utilizing very sensitive detector equipment, the two-ton stock room overhead crane was modified with an infinitely-

variable speed controller. This allows for extremely smooth vertical lifts, making the positioning of delicate equipment more precise and operator-friendly.

The nslsusers.org network is up and fully operational. This network provides users with an option to route connections to the World Wide Web without passing through the BNL firewall. Wireless access points (WAP's) are activated in conference and seminar rooms located on the second floor of 725.

Office Space/Storage:

Available NSLS user office space in building 535 has been completely allocated. Occupants previously located in buildings 510E, 129, 728, and the NSLS trailer park are now settled into nicely-appointed areas of the instrumentation facility. A notable occurrence is the relocation of the NSLS Controls and Detector Group, headed by Peter Siddons. The close proximity of this group to the specialists located within the Instrumentation Division makes for excellent idea-sharing while developing prototype devices and designing layouts for PC boards.

An all-inclusive undertaking to visually account for items being stored by both staff and users took place during the first quarter of the new fiscal year. A very good response ratio from the user community was compiled, along with a 100% physical inventory account rate from targeted NSLS sections.

Conclusion:

The NSLS continues to thrive in today's environment by relying on talented and dedicated individuals from within the department and across the laboratory, providing our Users with high quality, reliable beam time. The NSLS remains a world-class research center, often referred to as a jewel amongst DOE facilities. In closing, I wish to extend my thanks to everyone who assists in the daily operations and maintenance of all the facilities within the NSLS complex.

Stockroom Upgrade

Donna Buckley
Budget/Administration

The NSLS Stockroom database has recently been upgraded from a dated "Rbase" system into one using a Visual Basic and Oracle database. New barcode scanners have also been incorporated, allowing customers to easily scan their BNL ID badge for their life/guest number and their default project/activity number. The new system is user friendly and makes withdrawals faster and easier.

The number of NSLS stock items has increased over the past few years and continues to do so, due to changes in the BNL main stockroom and the reduction in the number of credit cards issued at BNL. Please remember to fill out the "Request For Additional NSLS Stockroom Inventory" forms located in the stockroom, with any suggestions for items to be stocked. All suggestions are presented to and considered by the NSLS Stockroom Committee.

Operations and Engineering Division Report

Erik D. Johnson
ASSOCIATE CHAIR FOR OPERATIONS AND ENGINEERING

Organization and Mission

The largest of the NSLS Divisions, Operations and Engineering consists of three sections: Operations, which is led by Richard Heese, Electrical Systems, led by Richard Biscardi, and Mechanical Engineering, led by Ed Haas. The mission of our division falls into three main areas:

- Operation of the NSLS 24 hours a day, 7 days a week, an average of 44 weeks a year.
- Design, fabrication, and maintenance of the NSLS accelerators and utilities, including upgrades and modifications to meet changing needs.
- Engineering and technical support for the other NSLS divisions and the NSLS user community.

As the department continues to emphasize beamline operations, we are increasingly relying upon a department-wide matrixed management approach: The Operations and Engineering Division (OED) draws resources from other divisions to support operations, and we provide special expertise to support development for other divisions.

2003 Activities This report provides a transition to reporting activities by the calendar year. Hence, three major shutdowns are included as well as operations throughout the year. Operational performance statistics will continue to be reported on a fiscal year basis. An overview of machine performance for Fiscal Year 2003 is provided in section 6, 'Facility Facts and Figures.'

X29: A series of major installation tasks spanning several shutdowns revolved around the development of an insertion device based program at beamline X29. A new ring vacuum chamber for an insertion device beamline had previously been installed in the x-ray ring. During December 2002, our third new RF cavity was installed in the X29 straight section. With this installation, two new cavities reside in the straight, providing space for the installation of a Mini Gap Undulator (MGU), identical to that already in service at X13. Shield wall modifications were also made during the December 2002 shutdown that allowed construction of the beamline on the floor to commence.

During the May 2003 shutdown, the MGU itself was moved into place between the RF cavities. The installation of the MGU controls, active interlock electronics, and beamline front-end was completed in the December 2003 shutdown, with commissioning starting in January of 2004. The X29 MGU project exercised the 'matrix organization' concept to the fullest, as its success depended upon significant contributions from every NSLS division and the collaboration building the beamline. While X29 was a major activity for the OED, it is an achievement for the entire NSLS.

NSLS-II: A major initiative for the NSLS community, NSLS-II has been a high priority for the department throughout the year. The OED has contributed primarily through the development of engineering

conceptual designs, project schedules, and cost estimates to meet the requirements established by the User Science and Accelerator Divisions.

Surprises and Triage: Nearly every parameter of the NSLS has been expanded beyond its original design goals. Careful evaluation of changes as well as diligent maintenance of the machines has allowed our user community to enjoy a very high degree of reliability. However, as the machine ages, problems do crop up, and 2003 seemed to be a bumper year for surprises.

On the X-ray ring, the increase in operating energy to 2.8 GeV and the implementation of the high brightness optical configuration required the current of the defocusing string of sextupole magnets to be raised from 500 amperes to over 800 amps. This almost tripled the power dissipated in the magnet string. The change was carefully evaluated before it was instituted several years ago, but it was known that the magnets would become more sensitive to flow disruptions. Coming out of the December 2003 shutdown, we experienced a failure of a coil in one of the magnets in the string. This particular magnet is buried within the LEGS area of the machine, making it both a 'one of a kind' and very difficult to access. Removing and repairing the magnet took nearly two weeks, cutting significantly into January 2003 operations. Later in the year, another magnet in the same string started overheating, although it did not fail. In the December 2003 shutdown, during preparations to replace the magnet, a blockage was discovered (and removed) from the magnet buss work, alleviating the overheating.

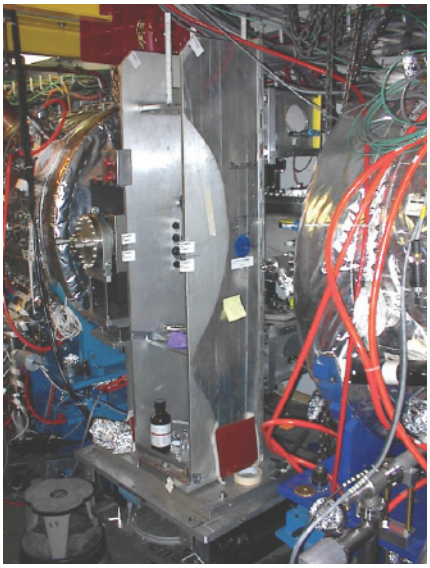

The new MGU between the RF cavities in the X29 straight section.

Various vacuum problems also contributed to operational headaches in 2003. In the month running up to the May 2003 shutdown, a small leak developed in a stripline monitor in the X-ray ring, causing a reduced beam lifetime, which led us to start the shutdown two days early. The leak was successfully repaired during the shutdown. During the summer, we also had a user vacuum venting accident and a leak in an ion pump feedthrough. It failed when it was sprayed by a fine mist of water from a pinhole leak in the body of a brass fitting four feet away that had been in place for over 15 years!

This also happened to be the year of the Northeast black out in August, causing nearly three days of X-ray operations downtime. This year the 'unusual' problems on the X-ray ring accounted for more than 12 days of down time, with just over six days due to the more typical operations problems. Overall, for fiscal year 2003, machine reliability was 89% for X-ray, although UV reliability remained high at 98%.

These very visible events tend to overshadow the failures that didn't happen because of the vigilance of the staff that maintains and repairs the machines out of the sight of the user community. Examples include the repair of the U14 water cooled mask during the May 2003 shutdown, the U4IR mirror rebuild during the December 2003 shutdown, and the upgrade of the X17 wiggler controls in December 2003. Magnet power systems, injection control, and diagnostic systems were also upgraded without fanfare; these are all systems that are essential to maintaining the performance and reliability of the NSLS. As we look forward to NSLS-II, the staff of the OED is prepared to meet the challenge of keeping the current NSLS performing at its best for another decade.

Accelerators Report

James Murphy
ASSOCIATE CHAIR FOR ACCELERATORS

Organization and Mission

The NSLS Accelerator Division (AD) was established in late 2001 through the reorganization of the NSLS and is headed by James B. Murphy. The division is organized into two sections: the Linear Accelerator (Linac) Section, headed by Xijie Wang, and the Storage Ring & Insertion Device Section, headed by Boris Podobedov. The staff consists of eight accelerator physicists, two engineers, three technicians, and two postdocs.

The NSLS Accelerator Division (AD) has a four-part mission:

- To ensure the quality of the electron beam in the existing NSLS booster, linear accelerator, and x-ray and vacuum ultraviolet (VUV) storage rings
- To operate the deep ultraviolet free electron laser (DUV-FEL) and Magnet Measurement facilities
- To participate in the NSLS-II project
- To perform fundamental research and development in accelerator and free electron laser physics

2003 Activities

NSLS-II: A major activity of the AD staff was the initial design of the new storage ring source for the NSLS-II project. The AD staff worked in conjunction with the other divisions of the NSLS to develop the machine concept for an ultra-high brightness (~10^{21}) 3 GeV electron storage ring design. The preliminary design is based on a 24-cell triple bend achromat lattice with a horizontal emittance in the range of 1.5 nm (**Figure 1**). Such a ring would more than triple the number of insertion devices available to the user community and provide 10,000 times higher brightness. A machine advisory committee was established to provide feedback on the machine design.

Storage Rings: Significant effort by the AD staff went into studying how the installation of more Mini Gap Undulators (MGU) in the x-ray ring would affect accelerator performance. In particular, MGUs may limit the beam current due to various collective effects induced by the strong impedance of the mini-gap chamber and transitions. The recent installation of the X29 MGU chamber gave us an opportunity to measure and compare some of these effects before and after the installation. While we did observe increased betatron tuneshifts with current at low energy, fortunately the increase turned out to be quite small and should not hinder operations. Single bunch currents of up to 125 mA are still possible, with the (administrative) limit set due to heat in vacuum chamber components unrelated to MGUs. We are also numerically calculating the impedance of the MGU chamber with electromagnetic field simulators. These studies should also provide valuable insights into the possible effect of MGUs on the future performance of the NSLS-II storage ring.

Another area of activity emphasized improvements to the storage ring lattices of the X-ray and VUV rings. The LOCO code, originally developed at the NSLS by James Safranek, allows calibrating and correcting the ring lattice from the measured beam response matrix. With James' help, a new, more powerful MATLAB-based version of this code was extensively debugged at the NSLS last year and is now used for both rings. This work has also shown some limitations of our existing diagnostics and resulted in the installation of new Hall probes into some of the X-ray ring magnets.

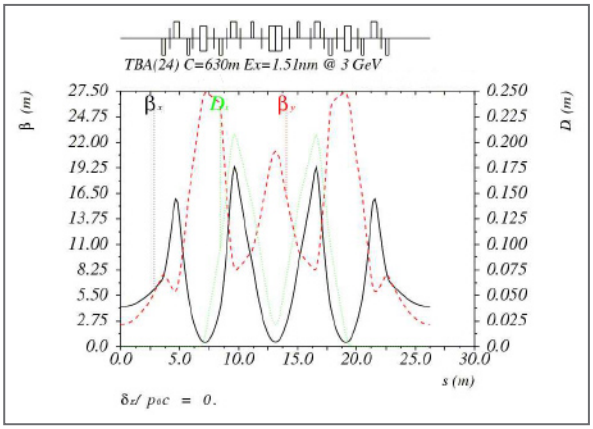

Figure 1. Storage ring lattice functions for the preliminary design of the NSLS-II ring (β_x in black, β_y in red and D_x in green).

Other work on the VUV ring included setting up shorter electron bunch configurations for time-resolved experiments as requested by the IR users. The challenge is to get a stable configuration of the ring lattice and RF system (with the harmonic cavity set for compression) that produces short bunches at substantial beam currents. Bunch lengths on the order of 400 ps FWHM with ~100 mA/bunch have been achieved. Work is continuing on yet another challenging configuration that produces mm-scale periodic ~10 Hz orbit motion at beamline U4IR while keeping stable orbit throughout the rest of the ring. This motion fills the very-far IR spectral gaps that are produced by the interference between the direct synchrotron radiation and (orbit-dependent) reflections off the walls of the vacuum chamber. To provide for the very localized orbit distortion, we are reconfiguring the VUV ring digital orbit feedback system.

Magnetic Measurement Lab: Early in FY 2003, a second in-vacuum, mini-gap undulator (designated MGU-29) was assembled, measured, and magnetically shimmed to minimize magnetic field errors and to optimize its spectral performance. The Mechanical Group installed it in the X-ray ring in the space between a pair of accelerating cavities in the X29 straight section. The magnet gap was left open to temporarily reduce the x-ray output to a negligible amount pending installation of front-end and optical components of the new NIH-funded protein crystallography beamline. These components were installed in the winter 2003-04 shutdown.

An FY 2002 design study to replace the aging X1 soft x-ray undulator identified several options that were presented to the X1 users and User Science Division staff. The preferred option was a pair of 1.4 m long undulators in tandem, canted to produce two photon beams, separated by about 1 milliradian, serving beamlines X1A and X1B independently, with independent control of each device by the respective users. One device would be a variable-polarization undulator, the other a planar one. However, this solution was predicated on a significant reduction of the height of the vacuum chamber in these devices. To verify the impact of a reduced chamber height on machine operations, particularly during injection, and to determine the minimum allowed vertical aperture in the new undulators, we decided to experimentally simulate the reduced aperture. A motorized beam scraper assembly was refurbished and installed in a chamber to be shared with an existing photon absorber, just upstream of the MGU-13 in-vacuum undulator. The combination of the variable-gap MGU-13 in the center of the straight and the scraper, approximately one meter upstream, will allow the characterization of

the vertical beam profile in a typical straight section under all operating conditions. This scraper assembly was installed during the December 2003 shutdown.

As an important part of our efforts to develop a superconducting undulator (SCU), a state-of-the-art SCU measurement apparatus was designed by the Magnetic Measurement and Mechanical Engineering staff, and is now under construction (**Figure 2**). It is designed to perform both magnetic and calorimetric measurements on SCU models up to about 0.4 m in length, cooled either by immersion in liquid helium (LHe) or by conduction. Three independently instrumented helium channels will allow detailed calorimetric measurement of both the SCU magnet windings and the beampipe under various thermal conditions, including simulated beam heating. A motorized, multi-element Hall sensor assembly for detailed magnetic field mapping has been constructed and bench-tested. The Hall sensors will be calibrated off-line against an NMR standard in a laboratory magnet, both at room temperature and at 77K in a liquid nitrogen bath. A small superconducting magnet within the cryostat will also permit in-situ calibration checks of the sensors at 4K. The Hall probe mapper will be interchangeable with a stretched wire sensor, instrumented to operate in either the pulsed-wire or vibrating-wire mode, and will provide complementary measurements of field errors, trajectory errors, and integrated field errors.

Figure 2. Vertical Test Facility for magnetic measurements of future superconducting undulators.

Together with the BNL Magnet Division, we plan to develop a SCU design using advanced "APC-type" NbTi superconductors, which can operate at higher currents and fields than conventional NbTi. We also plan to investigate a means of correcting phase errors in SCU's, critical for achieving high brightness at high harmonics for full coverage of the 2-20 keV photon range.

An improved magnetic design was developed for a new in-vacuum undulator to replace the aging X25 wiggler. The new device, designated "MGU-25," will be one meter long with an 18 mm period and a minimum gap of 5.6 mm, and will cover 1.9 – 20 keV, using the fundamental, 2^{nd} (present due to the rather high emittance), 3^{rd}, 5^{th}, and 7^{th} harmonics. The latest NdFeB materials with higher remanent field and very high intrinsic coercivity will be used to maximize the tuning range. The Mechanical Engineering group designed a longer vacuum chamber and a "twin-tower" support structure derived from the successful "single-tower" and chamber designs used in MGU-13 and MGU-29. A make-or-buy decision, development of detailed specifications, and procurement of just the magnets or the complete undulator are expected in FY 2004.

We continued our collaboration with A. Temnykh of Cornell in developmenting a vibrating-wire magnetic probe for use in small-gap undulators. This technique will be adapted for insertion into the SCU test apparatus described above. Magnetic Measurement staff also supported the Cascaded High-Gain Harmonic Generation X-ray FEL proposal by modeling and developing wiggler designs for the five modulator and amplifier stages. Magnetic Measurement staff contributed to the development of the NSLS-II lattice design via 3D magnetic modeling of candidate magnet designs, such as combined-function gradient dipole electromagnets and permanent magnet-driven gradient dipoles.

DUV-FEL: The Deep Ultra Violet Free Electron Laser (DUV-FEL) provides unique capabilities to the NSLS user community. The accelerator system of the DUV-FEL consists of a 1.6-cell BNL photo injector driven by a Ti:Sapphire laser system, and a four section 2856 MHz SLAC-type traveling wave linac capable of producing a 200 MeV electron beam. The magnetic chicane bunch compressor at the DUV-FEL produces sub picosecond (ps) long electron bunches with a peak current of a few hundred amperes. The high brightness electron beam transits the 10 meter long NISUS undulator to generate UV light with a fundamental wavelength of 266 nanometers (nm).

In FY03, the DUV-FEL achieved a unique mode of operation known as High Gain Harmonic Generation (HGHG), whereby the electron beam is energy modulated with the Ti:Sapphire laser at 800 nm, the energy modulation is converting into spatial bunching in a dispersive magnet, and then the bunched electron beam radiates coherently at 266 nm in the NISUS undulator.

After successfully lasing at 266 nm with the 800 nm laser seeding, experiments were carried out at the DUV-FEL to further characterize the properties of the HGHG FEL, and to demonstrate its stability and controllability. The narrower spectrum and better stability of HGHG compared to a SASE FEL were observed (**Figure 3**). Both the second and the third harmonic of the HGHG FEL radiation were experimentally characterized using a vacuum monochromator. The pulse energy for both harmonics (133 and 89 nm) was measured to be about 1 μJ, which is about 1% of the fundamental at 266 nm. A two-photon absorption auto-correlator with 100 fs resolution was developed to characterize the HGHG output pulse length. It was experimentally demonstrated that the HGHG output pulse length can be controlled using the seed laser from a picosecond down to 250 fs (FWHM). Experiments to investigate a chirped HGHG FEL were also initialized in 2003. Preliminary results are very promising, and the chirped FEL could lead to even shorter pulses of HGHG output.

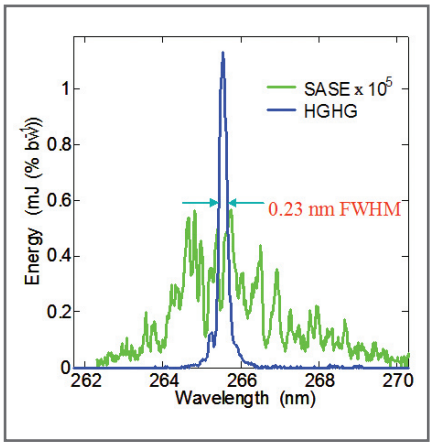

Figure 3. Experimental comparison between unsaturated Self Amplified Spontaneous Emission (SASE) and High Gain Harmonic Generation (HGHG) spectra.

One of the most important milestones in the last year at the DUV-FEL is the initialization and completion of the first DUV-FEL user experiment by Arthur Suits and his collaborators from the BNL Chemistry Department. The first chemical science experiment – ion pair imaging – used the third harmonic (89 nm) of the HGHG output to study the super excited states of methyl fluoride. Velocity mapped ion images of the fluoride ion, obtained with excitation via intense, coherent, sub-picosecond pulses of 86-89 nm radiation, reveal low translational energy, implying very high internal excitation in the methyl cation cofragment (**Figure 4**). The report on this experiment has been published in Physical Review Letters. To advance the user science program at the DUV-FEL, the NSLS hosted a very productive chemical science user workshop in July 2003.

There is increasing interest in high intensity THz radiation because of its potential applications in homeland security and material characterization. Two experiments were performed at the DUV-FEL to explore the possibility of using the bright electron beam to generate coherent THz radiation. In the first experiment, the electron beam with a sub-mm modulation was produced via temporal modulation of the photoinjec-

tor drive laser. The spatially modulated electron beam then is used to generate coherent THz radiation. Pulses in excess of 80 μJ of coherent THz radiation, using a transition radiation mechanism, were measured in the second experiment using sub-picosecond electron bunches containing about 0.7 nano-coulombs of charge. This intensity is about two orders of magnitude higher than the laser-based THz sources, and field strengths on the order 500 kV/cm are expected from such an intense THz source.

High-brightness electron beam generation and preservation is the key to the success of all future linac-based light sources. Investigations performed at the DUV-FEL revealed the possibility of strong longitudinal spatial modulation driven by a space-charge oscillation during the electron beam bunch compression. Comparison between experiments and simulation confirmed the amplification of an existing modulation during bunch compression. A femtosecond electron bunch monitor based on the electron-optical effect was successfully commissioned at the DUV-FEL to study the electron beam longitudinal distribution and the timing jitter between the electron beam and the HGHG seed laser. Using this technique, the timing jitter between the electron beam and the HGHG seed laser was measured to be 150 fs.

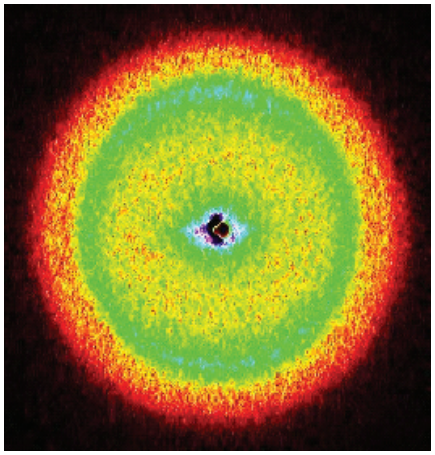

Figure 4. Ion pair image from the first DUV-FEL user experiment.

Beam Line Operations and Safety Awareness (BLOSA) training and many other procedures were developed at the DUV-FEL to improve acceleration operation and laser safety.

In September 2003, Dr. L.H. Yu of the NSLS Accelerator Division was awarded the 2003 International FEL Prize for his outstanding contributions to “High Gain Free Electron Lasers and High Gain Harmonic Generation.”

User Science Report

Chi-Chang Kao
Associate Chair for User Science Division

Organization and Mission

The User Science Division coordinates major facility activities related to users so that we can be more effective in communicating with the user community, strengthen existing scientific programs, foster the growth of new scientific programs, and raise the visibility of the exciting science produced by our users. The division consists of five sections: User Administration (Mary Anne Corwin), Information and Outreach (Lisa Miller), Beamline Development and Support (Steve Hulbert), Scientific Program Support (Ron Pindak), and Detectors and Controls (Peter Siddons). The major initiatives and accomplishments of the User Science Division and the NSLS user community for 2003 are summarized briefly below.

2003 Activities

This year has been eventful for the User Science Division. The year began with coordinating the user community in response to a Department of Energy /Basic Energy Sciences (DOE/BES) call for proposals to "Enhanced Research Capabilities at DOE X-ray and Neutron Facilities." Thanks to the effort of a large number of users and NSLS staff members, several major instrumentation proposals were submitted, including a new micro-beam x-ray diffraction instrument, an undulator-based small angle x-ray scattering beamline, and instrumentation upgrades for a number of powder/single crystal diffraction beamlines. Among them, the micro-diffraction instrument was funded in 2003, and the small angle scattering beamline will be funded in 2004. Both projects will take full advantage of the high brightness provided by the in-vacuum small gap undulator developed at the NSLS, and will provide two new world-class capabilities at the NSLS that are particularly important for nanoscience research. In addition, the input from the user community during the preparation of these proposals has been extremely valuable and will help us serve them better.

We soon turned our attention to working on the NSLS response to the DOE/BES "twenty-year facilities roadmap" review, and subsequently the science case for the NSLS-II proposal, an ultra-high brightness, medium energy storage ring. With the help of a large number of users, we organized more than a dozen scientific workshops, ranging from life sciences, materials/chemical sciences, and nanoscience to earth and environmental sciences. These focused workshops were very successful in identifying the grand challenges in the individual fields of research, and the impact of NSLS-II on them, as well as the technical challenges in the accelerator, insertion devices, optics and detectors. More importantly, these workshops have clearly demonstrated a great deal of excitement and support in the user community about the NSLS-II project.

The year continued with the exciting news that NSLS user Roderick MacKinnon from Rockefeller University shared the 2003 Nobel Prize in chemistry for his work on ion channel proteins. A very important part of

his work, the determination of numerous protein crysal structures, was done primarily at the Cornell High Energy Synchrotron Source and the NSLS. More good news this year for the NSLS macromolecular crystallography user community came when the BNL Biomedical Technology Research Resource for Macromolecular Crystallography, a center sponsored by the National Center for Research Resources (NCRR) of the National Institutes of Health (NIH), received its renewal funding for another five-year period. This supplements another grant sponsored by the Department of Energy (DOE) Office of Biological and Environmental Research (BER) for the same period. These two grants will fund a number of activities, including the support of full-time operation of the X25 wiggler beamline, the completion of construction and the ensuing commissioning and operation of a new undulator beamline for macromolecular crystallography at X29, and a major upgrade of beamline X25, which involves the replacement of its wiggler source by a novel small-gap undulator source and appropriate beamline optics upgrades to take advantage of the properties of the new source.

In between these exciting events, we have also completed a number of major beamline construction and upgrade projects:

- X6A beamline construction: A new bending magnet beamline, X6A, has been completed and started user operation. The beamline was funded by the National Institutes of General Medical Sciences of the National Institutes of Health (NIH-NIGMS) to meet the increasing demand in protein crystallography.

- X6B beamline construction: X6B is a new powder/single crystal diffraction beamline, designed to perform (1) time-resolved powder diffraction experiments, (2) combined x-ray spectroscopy and x-ray diffraction experiments, (3) single crystal diffraction experiments, and (4) electron density of excited states.

- X17 superconducting wiggler beamline upgrade: The upgrade involved the construction of two new experimental hutches to allow a dedicated hutch for a materials science instrument, a large volume press instrument, and a diamond anvil cell instrument. This upgrade will significantly increase the amount of beam time available to these user communities.

- X19A beamline upgrade: X19A is the premier low-energy x-ray beamline at the NSLS and has very high user demand. In 2003, a new monochromator was designed and installed to improve the cooling of the monochromator crystals. The new design has led to better energy and intensity stability of the beamline and ease of beamline operation.

- U5UA beamline upgrade: A refocusing mirror was added to provide the possibility of providing radiation to a second endstation. The focused beam size is on the order of 10 microns, making it ideally suited for the planned combined low-energy electron and photoemission microscopy endstation.

In addition, we have initiated several new beamline upgrade projects this year, including the X1A undulator beamline, the X13A elliptical polarizing wiggler beamline, the X21 wiggler beamline, and the X27 microprobe beamline. The completion of these projects will be very

Figure 1. Beamline X6A, a new macromolecular crystallography beamline funded by the National Institutes of General Medical Sciences of the National Institutes of Health.

important for the development of new scientific programs in nanoscience, soft and biomaterials, magnetism, advanced materials growth, and environmental science. We are also very fortunate to have seven very talented scientific and technical staff joining us this year to take on these projects and lead the development of new scientific programs.

There has also been steady progress in the detector development area this year. After successful a demonstration last year, several copies of the fast avalanche photodiode (APD) detector-electronics units have been installed at x-ray scattering beamlines. The large-angle curved gas proportional counter detector for time-resolved x-ray powder diffraction has been installed on two beamlines, one for testing purposes and the second for a user run. New software enabling time-slicing down to the microsecond time scale has also been implemented. Finally, several 96-element prototype silicon detectors with custom-designed integrated circuits, which each parallel-process input from 32 detector elements, are being assembled and will be deployed soon.

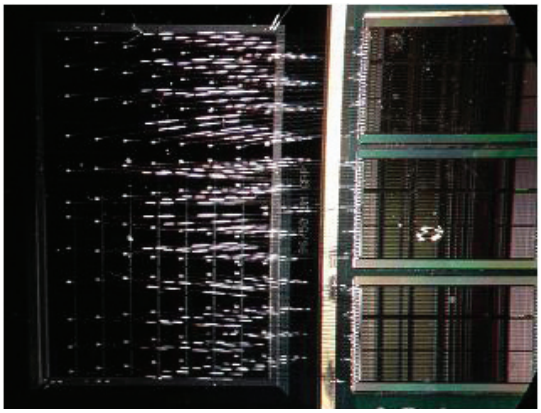

Figure 2. Three of the new 32-channel custom integrated circuits bonded to 96 silicon diode detectors. This configuration provides <250 eV resolution at 4 microseconds shaping time, or a count rate of >100 kHz per element at 0.5 microseconds shaping time.

With the addition of a full-time programmer this year, the User Administration office has made significant progress in the development of a new online proposal system to integrate proposal submission, safety approval, proposal review, beamtime allocation, and beamtime scheduling. We appreciate greatly the effort by a large number of participating research teams (PRTs), users, and NSLS staff, who provided valuable input and recommendations throughout the process. Testing of the system will begin in 2004.

Finally, we continue to take more immediate steps to enhance user science at NSLS. First, a short course on EXAFS data collection and analysis was held again this past summer with the help of many experienced users. This hands-on workshop provided both new and experienced users with exposure to EXAFS theory, data collection, and analysis. Feedback on the EXAFS short course has been so extremely positive that it has become an annual event. Second, a regular series of science highlight articles is now published on the NSLS website to facilitate the dissemination of exciting scientific results obtained at NSLS beamlines to the NSLS user community, as well as the wider scientific community. Third, a new symposium series has been established at the NSLS to give staff and users an opportunity to hear about cutting-edge synchrotron research that is performed worldwide. Upcoming seminars are now listed on the NSLS homepage for easy access to the schedule. In addition to these activities, the NSLS staff has been helping the BNL Center for Functional Nanomaterials (CFN) establish and launch a CFN user program, exploring ways to coordinate the NSLS and CFN user programs.

User Administration Report

Mary Anne Corwin
USER ADMINISTRATION HEAD

User Statistics

During the past year, 2206 badged users performed experiments at the NSLS, almost a third of them (681 users) for the first time.

For users who conducted experiments at the NSLS facility during the year, 31% indicated their primary field of research as materials sciences, 37% as life sciences, 8% chemical sciences, 9% geosciences and ecology, 10% applied science and engineering, and 5% optical/nuclear/general physics.

While the number of users in particular fields of science is indicative of *who* is using the facility, it does not show *how* the facility is used. Since 1999, the NSLS has reported statistical data based on actual usage of the facility. This information is extracted from beam time used by each of the 1145 experiments performed in FY03. This year, nearly 42% of the beam time used was utilized by experiments conducted in the field of materials sciences. The remaining beam time was utilized by biological and life sciences (18%), physics, except condensed matter (4%), chemistry excluding materials chemistry (5%), polymers (3%), medical applications (2%), earth sciences (6%), environmental sciences (4%), optics (3%), engineering (3%), instrumentation (5%), particle accelerator R&D (1%), radiation source R&D (2%), and other (1%). The primary difference in the number of users versus the amount of beam time utilized for a given field of research is explained by the fact that materials sciences experiments utilize considerably more beam time than other experiments. This is particularly true for experiments in the biological/life sciences. In addition, there are generally a lower number of experimenters utilizing the facility for materials experiments than there are for biological/life sciences experiments.

The primary source of user funding can also be determined based on beam time usage at the facility. During FY03, experiments funded by the Department of Energy's Office of Basic Energy Sciences (DOE/BES) within the Office of Science utilized 33% of the facility's beam time. Other programs in the DOE complex utilized an additional 7% of the beam time. Facility usage by other *primary sources* of user support included NSF (16%), NIH (11%), and Industry (10%).

More than 67% of our users are affiliated with U.S. and foreign academic institutions. Other affiliations include BNL employees who are facility users (11%), other DOE contractor employees (2%), other federal agencies (5%), industry (7%), and other (8%).

The 2206 users who visited our facility in FY03 are affiliated with 376 unique U.S. and foreign institutions, including 233 academic institutions, 65 industrial institutions, 24 federal government agencies, 25 non-governmental laboratories, and 29 other institutions.

Faculty members at universities or colleges, professional staff and scientists at private, and national or industrial laboratories account for

the greatest population of users (38%), followed by graduate students (33%), postdoctoral research associates (19%), undergraduate students (5%), and retired, self-employed, or other (4%).

Users come to the NSLS from around the globe. Though half are citizens of other countries, only 13% of all our users physically arrive from outside the U.S. to perform research here at the NSLS. All others are affiliated with a U.S. institution. About 36% arrive from New York institutions and another 27% are affiliated with institutions in the northeast. Our remaining users come from U.S. institutions outside of the northeast.

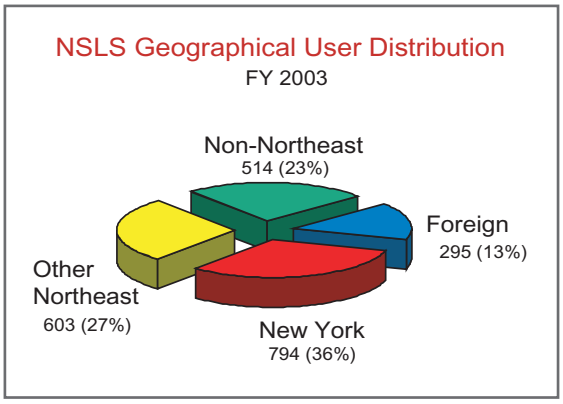

Security Compliance

A laboratory directive was issued in FY03 requiring strict adherence to DOE Notice 142.1 pertaining to requirements for unclassified visits, assignments, and activities by foreign nationals to DOE facilities. Our users were subsequently notified of new site access policies and requirements. Though the NSLS had hoped to see little disruption in our programs and use of the facility, we found that many users encountered problems accessing the site and others were required to leave BNL until appropriate documentation and/or approvals were secured. The most common problems experienced by our users are detailed below. The number of occurrences has decreased quite a bit over the last year, but there are still two or three users each month experiencing considerable delays.

Visa Problems: Upon entering the U.S., a user possessed appropriate paperwork for a work visa, but Immigration incorrectly issued documentation pertaining to a tourist visa. The user arrived at User Administration the same day but could not finalize the appointment. The process required that the user return to the airport within 24 hours of entry to correct the documentation. Unfortunately, if the documents are not corrected within 24 hours, the user is unable to work at BNL.

Approval Lead Time: A scientist from a northeastern university arrived at BNL after submitting the online registration form less than one week earlier. The form indicated an arrival date five days later. More than eight reviews are required before approval is granted and, at times, the process can take up to 45 days. User Administration immediately notified the scientist that he could not access the site until approval was granted. Disregarding the information, the scientist arrived the following weekend expecting to begin his experiment. After learning that access to the facility could not be granted, he returned to the university.

Appointment Renewals: A Ph.D. from a local institution arrived at BNL with an expired BNL identification badge without having submitted the registration form requesting an extension to his appointment. The user was required to leave the BNL site until his extension was requested and approval had been granted. A review of his file indicated he was previously notified that his appointment was terminated and was provided instructions on how to extend his appointment.

Visa Status: Although users receive two-year appointments, their termination date may extend beyond their visa expiration date. When that date arrives, the next time the user enters the main gate at BNL, the

badge scanning system will display a "yellow" light indicating that the user's passport and/or visa are out of status. One of our guest scientists arrived at BNL with a valid appointment and valid BNL identification badge. The badge scanned "yellow" and the guard advised the user to check in at User Administration to update his visa information. Once entered, the scanning system will display a "green" light. However, the user's documentation was at home, more than 200 miles away, and he was required to leave BNL until the documentation could be presented.

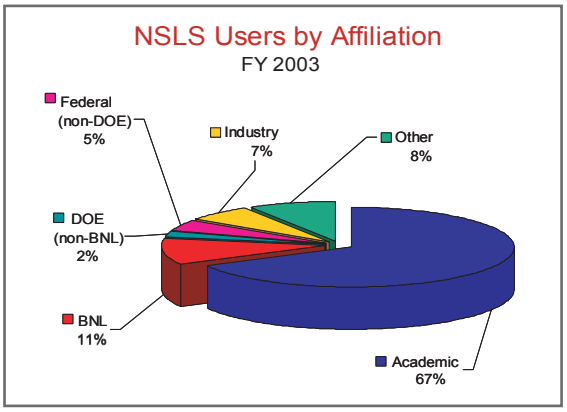

Escorting at the NSLS and Open to the Public Events: Historically, the NSLS has permitted non-users to be escorted onto the experimental floor provided certain safety requirements have been met. With the lab's new directive to come into compliance with DOE Order 142.1, changes took place in laboratory accessibility and escorting procedures, and with regard to "open to the public" events, especially for our foreign national users and visitors.

BNL management has indicated that foreign nationals attending "open to the public" events may tour other facilities while on site provided the tour is part of the event (not a separate event). There is no provision to permit a foreign national to be escorted onto the NSLS experimental floor unless the visitor (1) has a valid BNL ID badge, (2) is attending an "open to the public" event that specifically includes a tour of the experimental floor, or (3) has registered in the BNL's Guest Information System and their appointment and record have been activated. Additionally, foreign nationals performing any type of work or observing experiments at the NSLS must register and receive approval prior to arrival.

I would like to thank our users for their cooperation in helping the NSLS to maintain compliance with DOE requirements. Please contact our office at (631) 344-8737 with any questions.

Safety Report

Bob Casey
Associate Chair for ESH

Organization and Mission

Environmental, Safety, and Health (ESH) performance within the NSLS and at BNL in general remains an important issue for all NSLS staff, PRT members, and general users. The Annual Report provides an excellent opportunity to comment on past ESH performance and important changes in program requirements, and to identify issues that will be of importance in the year ahead.

2003 Activities

Calendar year 2003 was particularly dynamic for ESH in a number of important areas:

ESH Responsibilities of PRT Members and Beamline Staff: The ESH responsibilities of PRT members, beamline staff members, and investigators/users were better defined in 2003 to ensure that roles were clearly understood by all. A summary of the roles and responsibilities can be found at: *http://www.nsls.bnl.gov/organization/ESH/safety/r2a2.htm*.

Training: There has been a major emphasis at BNL on training for all staff members and guests. This year we increased the previous training requirements for resident beamline staff and users routinely present at the NSLS to provide a more detailed understanding of ESH requirements that are applicable to common situations in our work place. These training requirements can be found at: *http://www.nsls.bnl.gov/training/Requirements/Resident-User-Training.htm*. Training for our short-term users can be found at: *http://www.nsls.bnl.gov/training/Requirements/User-Training.htm* and is unchanged from previous years.

Work Planning: Work planning is the process for evaluating work to ensure identification of hazards and the establishment of appropriate controls. The work planning process for experimental research at the NSLS has worked well for many years and is implemented through the Safety Approval Form (*http://130.199.76.84/safety/default.asp*) process. Work at the beamlines, however, can involve beamline staff in routine activities that are not reviewed as a part of the SAF process (e.g. day-to-day work in maintaining a beamline, and modifications or additions to beamline components). Work planning requirements were revised this year to capture these type of activities and are identified at *http://www.nsls.bnl.gov/newsroom/publications/manuals/eshguide/D*. The requirements are graded based on the level of training of beamline staff. More detailed NSLS guidance may be obtained at: *http://www.nsls.bnl.gov/newsroom/publications/manuals/prm/LS-ESH-PRM-1.3.5a.html* and *http://www.nsls.bnl.gov/newsroom/publications/manuals/prm/LS-ESH-PRM-1.3.6.html*.

TLD Requirements for Access to the Experimental Floor: The requirements for wearing a TLD while working on the experimental floor were relaxed this year for many of our short-term users. Only users routinely working at the NSLS throughout the year, or those who fall into special

categories (e.g. working with radioactive materials, women with declared pregnancies, minors, or those working in the Bldg. 729 Controlled Area) are required to wear a TLD. Details of the new requirements can be found at: *http://www.nsls.bnl.gov/organization/ESH/temp/tldchange.htm*. It is very important to note that training requirements for access to the floor remain the same as previous years.

Laser Use: A serious eye injury occurred to a graduate student working in a different department at BNL when he inadvertently exposed himself to a high power laser. All laser use at BNL was suspended by the Laboratory Deputy Director pending a review to confirm that practices with each laser complied with the requirements of the BNL Standard for Lasers (*https://sbms.bnl.gov/standard/2g/2g00t011.htm*). All lasers at the NSLS were eventually restarted, but extensive stoppages were experienced. All users who plan to bring or use existing lasers should anticipate detailed reviews and contact the NSLS Safety Officer well in advance of arrival. Users of Class 3b/4 lasers must prepare written procedures, receive additional training, and complete a medical eye examination prior to use of the laser. These requirements are time consuming. Whenever possible, use of lower power lasers (i.e. Class 2 or 3a) will greatly simplify review requirements. Use of any laser in an experiment must be described in the Safety Approval Form (*http://130.199.76.84/safety/default.asp*). Additional NSLS guidance may be obtained at: *http://www.nsls.bnl.gov/newsroom/publications/manuals/prm/LS-ESH-PRM-2.3.1.html* (Laser Safety Program Requirements).

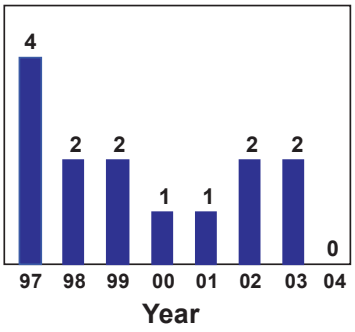

Lost time injuries per year since 1997. In 2004, we are striving for zero injuries.

Conclusion: The user community has responded well to the high level of expectations for safety performance at the NSLS. Prominent and high level presentations were made at the Annual Users' Meeting, and safety is a topic at every Town Meeting. On the other hand, we have had our share of problems, and the BNL Director and the head of the DOE Office of Science have stated on several occasions that science carried out in an unsafe environment will not be supported. It is important for everyone to understand that a safe environment is much more than just an injury-or incident-free environment - positive attitudes and compliance with requirements are equally important.

I think our ESH program continues to be strong, and the improvements of the past year will serve us well. We need a successful safety program, and that requires ongoing awareness, involvement, and commitment from everyone. One incident or injury can quickly over-ride and outshine many successes. Whether at your home institution or at the NSLS, keep an eye on the workplace and your co-workers. Make sure that all requirements are respected and that work is conducted safely. We all have a stake in safety performance.

Please let me know if you have any comments or suggestions.

Building Administration Report

Gerry Van Derlaske
NSLS Building Manager

The new mini-gap undulator, sextupole repair, the installation of the x-ray radio-frequency circulator, the continuing construction of cutting-edge beamlines, and the announcement that one of our users received the Nobel Prize in Chemistry for his NSLS research – It has been more than twenty years since the first operational beamlines were commissioned here, and, due to the efforts of many individuals and multiple service and support groups, the future of the NSLS is as bright as ever.

Safety and security issues remain at the forefront of daily operations, and facility improvements range from the physical plant infrastructure to a new user network outside of the current BNL firewall. Various beamline and ring upgrades have been fully commissioned and additions to the NSLS scientific staff have made for a very productive and interesting year.

Safety:

NSLS staff and users are reminded that working safely is a top priority at BNL. In accordance with this basic principal, the past year saw the introduction of new work planning elements for scientists and technicians. Work planning and control procedures require that work being performed at the NSLS above the "skill of the craft" level be reviewed by the appropriate subject matter experts and scheduled accordingly through available resources. Meetings are held weekly, or as needed in emergency cases, to review, approve, and authorize work that does not fall within this "skill of the craft" category. Using a graduated approach for hazard determinations, formal work permits will be issued for work deemed hazardous. Users and staff should contact the building manager with any questions pertaining to whether a formal work permit is required.

In October, the entire laboratory underwent a full OSHA walk-through inspection. Teams of OSHA personnel, from all areas of expertise and backgrounds in industrial safety, toured virtually every building at BNL. The NSLS fared reasonably well, receiving 61 citations, compared with some several thousand lab-wide. Many of the NSLS citations were corrected prior to this article, and we are tracking the few remaining open items. Our target goal remains set at zero citations in the future. The NSLS safety teams, paired with Tier 1 inspections, experimental reviews, and the work planning and control process, manage one of the busiest user facilities in the world and have the resources to achieve this objective. Accordingly, everyone must continue to intervene and act appropriately if observing any unsafe conditions.

Security:

This year, America has cycled between the Code Yellow (elevated) and Code Orange (high) terrorism awareness levels. We therefore ask everyone to be constantly vigilant when performing common, everyday tasks

at the NSLS. For example, lock your parked vehicle and do not leave it in the parking lot for long periods of time when you are absent from the NSLS. Do not leave your packages unattended, even for a few moments. There have been several instances of items found unattended and unidentified in the following areas: the main lobby, the entrance vestibule, and the drop-off zone inside the circular driveway of building 725. We urge all personnel to follow security measures when entering both BNL and the NSLS. Vehicle inspections at all gates leading off-site have increased, and the Department of Energy requires that all non-expendable property at BNL have bar codes or property tags affixed to indicate ownership. These tags are available free of charge from the NSLS stockroom.

While transparent to the casual observer, behind-the-scene work by many employees continues to provide our staff and users with a very safe and secure workplace. Again, we extend our gratitude to everyone for their patience and cooperation in conforming to the newly-implemented rules and regulations.

Some of the many talented members of the NSLS Plant Engineering Support Staff, Work Control Coordinators, and Facility Support/ Work Planning Team, who work together to keep the facility safe and sound.

Facility Upgrades:

New furniture, complimented by matching NSLS logo rugs, has been installed in the main lobby. Additionally, a satellite dish network was installed to feed the LCD projection monitor video wall and second floor conference rooms with a commercial signal that can provide live feeds to the NSLS community. The NSLS building manager will be the point of contact for submitting requests to activate the signal for viewing during evening and weekend hours. For special occasions or events, requests for viewing sporting events and educational, cultural, and informative programming can be sent to the chairman through the building manager for review and approval.

The RF penthouse air conditioning upgrade increased output cooling, reducing the heat load onto working power supplies and virtually eliminating power supply trips on hot summer days. All experimental floor steam re-heat coils located within the AC duct works were cleaned and serviced, providing better flow through ventilation. Due to the cleaning process, heat and air conditioning delivery is expected to become more stable.

Special maintenance funding from Plant Engineering provided the necessary resources to install replacement wall-to-wall carpeting in the seminar room, directorate wing hallway, and conference room A. Maintenance crews refurbished the restroom in building 726 and applied fresh coats of paint to many areas of building 725. The roof over MER 2, as well as the pitch pockets and galvanized trays surrounding the power feeders near the RF penthouse, were sealed and subjected to various proof tests during the summer downpours. The remaining areas of suspected roof leaks are now marked for repair once the winter freeze/ thaw cycles have ended.

As requested by users utilizing very sensitive detector equipment, the two-ton stock room overhead crane was modified with an infinitely-

variable speed controller. This allows for extremely smooth vertical lifts, making the positioning of delicate equipment more precise and operator-friendly.

The nslsusers.org network is up and fully operational. This network provides users with an option to route connections to the World Wide Web without passing through the BNL firewall. Wireless access points (WAP's) are activated in conference and seminar rooms located on the second floor of 725.

Office Space/Storage:

Available NSLS user office space in building 535 has been completely allocated. Occupants previously located in buildings 510E, 129, 728, and the NSLS trailer park are now settled into nicely-appointed areas of the instrumentation facility. A notable occurrence is the relocation of the NSLS Controls and Detector Group, headed by Peter Siddons. The close proximity of this group to the specialists located within the Instrumentation Division makes for excellent idea-sharing while developing prototype devices and designing layouts for PC boards.

An all-inclusive undertaking to visually account for items being stored by both staff and users took place during the first quarter of the new fiscal year. A very good response ratio from the user community was compiled, along with a 100% physical inventory account rate from targeted NSLS sections.

Conclusion:

The NSLS continues to thrive in today's environment by relying on talented and dedicated individuals from within the department and across the laboratory, providing our Users with high quality, reliable beam time. The NSLS remains a world-class research center, often referred to as a jewel amongst DOE facilities. In closing, I wish to extend my thanks to everyone who assists in the daily operations and maintenance of all the facilities within the NSLS complex.

Stockroom Upgrade

Donna Buckley
Budget/Administration

The NSLS Stockroom database has recently been upgraded from a dated "Rbase" system into one using a Visual Basic and Oracle database. New barcode scanners have also been incorporated, allowing customers to easily scan their BNL ID badge for their life/guest number and their default project/activity number. The new system is user friendly and makes withdrawals faster and easier.

The number of NSLS stock items has increased over the past few years and continues to do so, due to changes in the BNL main stockroom and the reduction in the number of credit cards issued at BNL. Please remember to fill out the "Request For Additional NSLS Stockroom Inventory" forms located in the stockroom, with any suggestions for items to be stocked. All suggestions are presented to and considered by the NSLS Stockroom Committee.

Facts and Figures

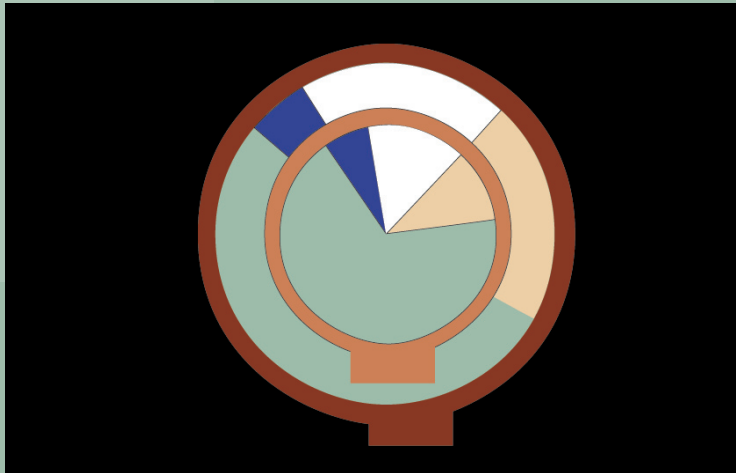

Facility Facts & Figures

The National Synchrotron Light Source (NSLS) is a national user research facility funded by the U.S. Department of Energy's Office of Basic Energy Science. The NSLS operates two electron storage rings: an X-ray ring (2.8 GeV, 280 mA) and a Vacuum Ultraviolet (VUV) ring (800 meV, 1.0 A) which provide intense light spanning the electromagnet spectrum from the infrared through x-rays. The properties of this light, and the specially designed experimental stations, called beamlines, allow scientists in many fields of research to perform experiments not otherwise possible at their own laboratories.

Over 2200 scientists representing almost 400 institutions, 65 of them corporations, come to Brookhaven National Laboratory annually to conduct research at the NSLS. The facility operates 7 days a week, 24 hours a day, throughout the year, except during periods of maintenance and studies.

As a national user facility, the NSLS does not charge for its beamtime, providing that the research results are published in the open literature. Proprietary research is conducted on a full cost recovery basis.

There are two ways to obtain beamtime at the NSLS: either as a General User or as a member of a Participating Research Team (PRT). General Users are independent investigators interested in using the NSLS for their research. Access is gained through a peer-reviewed proposal system. All operational beamlines at the NSLS reserve at least 25% of their available beamtime for General Users. PRTs are groups of researchers with related interests from one or more institutions. Membership in a PRT is open to all members of the scientific community who can contribute significantly to the program of the PRT, (i.e., funding, contribution of equipment, scientific program, design and engineering, operations manpower, etc).

The NSLS currently has 58 X-Ray and 22 VUV operational beamlines for performing a wide range of experiments. The following pages list the operational beamlines at the NSLS and their unique characteristics.

BEAMLINE GUIDE

TECHNIQUE	DESCRIPTION
ARPES	UV PHOTOELECTRON SPECTROSCOPY, ANGLE-RESOLVED
DAFS	X-RAY DIFFRACTION ANOMALOUS FINE STRUCTURE
DEI	DIFFRACTION-ENHANCED IMAGING
EXAFS	X-RAY ABSORPTION SPECTROSCOPY, EXTENDED FINE STRUCTURE
HARMST	HIGH ASPECT RATIO MICROSYSTEMS TECHNOLOGY
IRMS	INFRARED MICROSPECTROSCOPY
MAD	MULTI-WAVELENGTH ANOMOLOUS DISPERSION
NEXAFS	NEAR EDGE X-RAY ABSORPTION SPECTROSCOPY
SAXS	SMALL ANGLE X-RAY SCATTERING
SPARPES	UV PHOTOELECTRON SPECTROSCOPY, SPIN- AND ANGLE-RESOLVED
STXM	SCANNING TRANSMISSION X-RAY MICROSCOPY
UPS	UV PHOTOELECTRON SPECTROSCOPY
UV-CD	ULTRAVIOLET CIRCULAR DICHROISM
WAXD	WIDE-ANGLE X-RAY DIFFRACTION
WAXS	WIDE-ANGLE X-RAY SCATTERING
XAS	X-RAY ABSORPTION SPECTROSCOPY
XMCD	X-RAY MAGNETIC CIRCULAR DICHROISM
XPS	X-RAY PHOTOELECTRON SPECTROSCOPY
XRD	X-RAY DIFFRACTION
XSW	X-RAY STANDING WAVES

BEAMLINE	SOURCE	TYPE OF RESEARCH	ENERGY RANGE	ORGANIZATION
U1A	Bend	NEXAFS XAS	20-900 eV	ExxonMobil Research and Engineering Co.
U2A	Bend	High Pressure Research IRMS IR spectroscopy	30-8000 cm-1	Carnegie Institute of Washington
U2B	Bend	IRMS IR spectroscopy	50-4000 cm-1	Albert Einstein College of Medicine
U3C	Bend	XPS	50-1000 eV	Bechtel Nevada Lawrence Livermore National Laboratory Los Alamos National Laboratory Sandia National Laboratory
U4A	Bend	UPS	10-300 eV	Army Research Laboratory BNL-NSLS Boston University North Carolina State University Rutgers University University of North Carolina
U4B	Bend	XMCD X-ray scattering, resonant X-ray scattering, magnetic X-ray florescence XPS UPS	20-1200 eV	BNL-NSLS Montana State University
U4IR	Bend	IR spectroscopy IRMS	20-3000 cm-1	BNL-Chemistry BNL-NSLS
U5UA	Insertion Device	UPS ARPES SPARPES Magnetospectroscopy	15-150 eV	BNL-NSLS
U7A	Bend	NEXAFS XPS	180-1200 eV	BNL-Chemistry BNL-Physcis Dow Chemical Company National Institute of Standards & Technology Rutgers University Texas A&M University University of Michigan
U7B	Bend	XPS UPS NEXAFS	15-300 eV	BNL-NSLS
U8B	Bend	NEXAFS X-ray photoemission ARPES	100-1000 eV	IBM Research Division University of California @ Riverside University of Michigan
U9A	Bend	Photon-stim. Desorption	White Beam	BNL-NSLS
U9B	Bend	UV florescence UV-CD	0.8 - 8.0 eV	BNL-Biology BNL-NSLS
U10A	Bend	IR spectroscopy	30-20000 cm-1	BNL-NSLS BNL-Physics
U10B	Bend	IRMS	50-4000 cm-1	BNL-NSLS University of Saskatchewan
U11	Bend	UPS UV photoabsorption UV photoionization	3-30 eV	BNL-Biology BNL-NSLS

BEAMLINE	SOURCE	TYPE OF RESEARCH	ENERGY RANGE	ORGANIZATION
U12A	Bend	XAS	100-800 eV	BNL-NSLS Oak Ridge National Laboratory
U12IR	Bend	IR spectroscopy Time-resolved spectroscopy	2-400 cm-1	BNL-NSLS SUNY @ Stony Brook University of Florida
U13UA	Insertion Device	Focused white beam	3-1000 eV White Beam	BNL-NSLS
U13UB	Insertion Device	UPS ARPES	3-30 eV	BNL-NSLS BNL-Physics Boston University
U14A	Bend	XPS UPS	15-300 eV	BNL-NSLS
U16B	Bend	XPS	50-1000 eV	BNL-NSLS Rutgers University University of Texas Arlington
X1A1	Insertion Device	STXM	.25-.50 keV	BNL-Environmental Science BNL-NSLS ExxonMobil Research and Engineering Co. SUNY @ Plattsburgh SUNY @ Stony Brook University of Texas
X1A2	Insertion Device	STXM	.25-1 keV	SUNY @ Stony Brook
X1B	Insertion Device	X-ray scattering, resonant X-ray scattering, coherent ARPES UV fluorescence XAS	.2-1.6 keV	Boston University BNL-NSLS University of Groningen
X2B	Bend	X-ray microtomography	8-35 keV	ExxonMobil Research and Engineering Co.
X3A2	Bend	XAS SAXS XRD, single-crystal MAD	3-31 keV	SUNY @ Stony Brook
X3B1	Bend	XAS XRD, powder EXAFS	6-30 keV	SUNY @ Buffalo SUNY @ Stony Brook
X4A	Bend	MAD	3.5-20 keV	Albert Einstein College of Medicine City University of New York Columbia University Memorial Sloan-Kettering Cancer Center Mount Sinai School of Medicine New York Structural Biology Center New York University SUNY @ Buffalo The Wadsworth Center of the NYS Dept of Health Weill Medical College of Cornell University

BEAMLINE	SOURCE	TYPE OF RESEARCH	ENERGY RANGE	ORGANIZATION
X4C	Bend	MAD	7-20 keV	Albert Einstein College of Medicine City University of New York Columbia University Memorial Sloan-Kettering Cancer Center Mount Sinai School of Medicine New York Structural Biology Center New York University Rockefeller University SUNY @ Buffalo The Wadsworth Center of the NYS Dept of Health Weill Medical College of Cornell University
X5A	Bend	Laser backscattering	150-470 MeV	BNL-Physics Forschungszentrum Juelich (KFA) Norfolk State University Ohio University Syracuse University University of Paris University of Rome II University of South Carolina University of Virginia Virginia Polytechnic Inst. & State University
X6A	Bend	MAD	7-20 keV	BNL-NSLS
X6B	Bend	XRD, powder XRD, single-crystal	7-20 keV	BNL-NSLS
X7A	Bend	XRD, powder	5-45 keV	BNL-Physics Chevron Research & Technology Company Ohio State University SUNY @ Stony Brook University of Birmingham University of California @ Santa Barbara University of Pennsylvania
X7B	Bend	XRD, single-crystal XRD, time-resolved WAXS or WAXD	5-21 keV	BNL-Chemistry
X8A	Bend	Metrology	.26-5.9 keV	Bechtel Nevada Lawrence Livermore National Laboratory Los Alamos National Laboratory Sandia National Laboratory
X8C	Bend	MAD	5-19 keV	Biogen Incorporated BNL-Biology Hoffmann-La Roche National Research Council of Canada
X9A	Bend	MAD	5-15 keV	Albert Einstein College of Medicine Rockefeller University Sloan-Kettering Institute for Cancer Research
X9B	Bend	EXAFS XAS MAD NEXAFS	5-15 keV	Albert Einstein College of Medicine National Institutes of Health
X10A	Bend	XRD, time-resolved WAXS or WAXD XRD, powder X-ray reflectivity SAXS	6-15.2 keV	ExxonMobil Research and Engineering Co.
X10B	Bend	XRD, surface WAXS or WAXD XRD, powder X-ray reflectivity	14 keV	ExxonMobil Research and Engineering Co.

BEAMLINE	SOURCE	TYPE OF RESEARCH	ENERGY RANGE	ORGANIZATION
X10C	Bend	XAS NEXAFS EXAFS	4-24 keV	ExxonMobil Research and Engineering Co.
X11A	Bend	EXAFS NEXAFS XAS	4.5-35 keV	BNL-Environmental Science Canadian Light Source Hunter College Naval Research Laboratory Naval Surface Warfare Center New Jersey Institute of Technology North Carolina State University Northeastern University Paul Scherrer Institute U.S. Enivronmental Protection Agency Virginia Union University
X11B	Bend	EXAFS NEXAFS XAS	5.0-30 keV	BNL-Environmental Science Canadian Light Source Hunter College Naval Research Laboratory Naval Surface Warfare Center New Jersey Institute of Technology North Carolina State University Northeastern University Paul Scherrer Institute U.S. Enivronmental Protection Agency University of Connecticut Virginia Union University
X12A	Bend	Optics R&D	5-50 keV	BNL-NSLS
X12B	Bend	MAD	5-20 keV	BNL-Biology
X12C	Bend	MAD	5.5-20.0 keV	BNL-Biology
X13A	Insertion Device	Magnetospectroscopy XMCD X-ray scattering, resonant	.2-1.8 keV	BNL-NSLS
X13B	Insertion Device	Microdiffraction imaging X-ray microprobe	4-16 KeV	BNL-NSLS
X14A	Bend	XRD, single-crystal	5-26 keV	Oak Ridge National Laboratory University of Tennessee
X15A	Bend	XSW DEI	3-25 keV 10-60 keV	Argonne National Laboratory BNL-NSLS Canadian Light Source Illinois Institute of Technology North Carolina State University Northwestern University University of North Carolina University of Saskatchewan
X15B	Bend	NEXAFS XAS EXAFS	1.5-15 keV	SUNY @ Stony Brook
X16A	Bend	XRD, surface	4-12 keV	University of Illinois @ Chicago
X16B	Bend	XRD, powder XRD, surface	7.85 keV	
X16C	Bend	XAS	4.5-25 keV	University of Illinois @ Chicago
X17B1	Insertion Device	XRD, powder	67 keV 20-100 keV	BNL-Medical BNL-NSLS

BEAMLINE	SOURCE	TYPE OF RESEARCH	ENERGY RANGE	ORGANIZATION
X17B2	Insertion Device	XRD, powder High Pressure Research	20-100 keV	SUNY @ Stony Brook
X17B3	Insertion Device	High Pressure Research	20-100 keV	Brookhaven National Laboratory Carnegie Institute of Washington
X17C	Insertion Device	High Pressure Research XRD, powder XRD, single-crystal	5-80 keV	Carnegie Institute of Washington Lawrence Livermore National Laboratory Naval Research Laboratory University of Chicago
X18A	Bend	XRD, surface XRD, powder X-ray reflectivity XRD, single-crystal WAXS or WAXD	4-19 keV	BNL-Environmental Science Pennsylvania State University Purdue University University of Maryland University of Missouri
X18B	Bend	NEXAFS XAS EXAFS	5.7-40 keV	BNL-Chemistry BNL-NSLS Chevron Research & Technology Company General Electric North Carolina State University Rutgers University University of Kentucky UOP
X19A	Bend	EXAFS XAS NEXAFS	2-8 keV	BNL-Chemistry BNL-NSLS Chevron Research & Technology Company General Electric North Carolina State University Rutgers University University of Kentucky UOP
X19C	Bend	X-ray topography X-ray scattering, liquid X-ray reflectivity XRD, surface	6-17 keV	Army Research Laboratory Carnegie Mellon University Dartmouth College Johns Hopkins University National Aeronautical and Space Agency SUNY @ Stony Brook University of Chicago University of Illinois @ Chicago University of Wisconsin
X20A	Bend	Microdiffraction imaging XRD, surface	4.5-13 keV	IBM Research Division
X20B	Bend	XRD, surface	17.4 keV	IBM Research Division
X20C	Bend	XRD, surface XRD, time-resolved	5-11 keV	IBM Research Division
X21	Insertion Device	SAXS X-ray florescence X-ray inelastic scattering	5-10 keV	BNL-NSLS
X22A	Bend	XRD, surface XRD, time-resolved WAXS or WAXD X-ray reflectivity XRD, single-crystal	10 keV 32 keV	BNL-Environmental Science BNL-Physics Rutgers University University of Maryland
X22B	Bend	X-ray scattering, liquid XRD, surface	6.5-10 keV	BNL-Physics Harvard University Rutgers University

BEAMLINE	SOURCE	TYPE OF RESEARCH	ENERGY RANGE	ORGANIZATION
X22C	Bend	X-ray scattering, magnetic X-ray reflectivity XRD, surface XRD, single-crystal	3-12 keV	BNL-Physics Rutgers University University of Maryland
X23A2	Bend	DAFS XAS XRD, powder NEXAFS EXAFS	4.7-30 keV	BNL-NSLS
X23B	Bend	XAS XRD, powder EXAFS NEXAFS	3-10.5 keV	BNL-Environmental Science Canadian Light Source Hunter College Naval Research Laboratory Naval Surface Warfare Center New Jersey Institute of Technology North Carolina State University Northeastern University Paul Scherrer Institute U.S. Enivronmental Protection Agency Virginia Union University
X24A	Bend	XPS Auger spectroscopy XSW EXAFS X-ray fluorescence	1.8-5 keV	BNL-NSLS National Institute of Standards & Technology
X24C	Bend	XPS	.006-1.8 keV	Naval Research Laboratory
X25	Insertion Device	MAD	3-28 keV	BNL-Biology BNL-NSLS
X26A	Bend	X-ray microprobe Microdiffraction imaging	3-30 keV	BNL-Environmental Science University of Chicago University of Georgia
X26C	Bend	MAD	5-20 keV	BNL-Biology Cold Spring Harbor Laboratory SUNY @ Stony Brook
X27A	Bend	X-ray microtomography	8-40 keV	BNL-NSLS
X27B	Bend	HARMST	White Beam	BNL-NSLS
X27C	Bend	SAXS WAXS or WAXD XRD, time-resolved	9 KeV	Basell USA, Inc. (formerly Montell) Honeywell International National Institute of Standards & Technology National Institutes of Health Naval Surface Warfare Center New Jersey Institute of Technology SUNY @ Stony Brook U.S. Air Force
X28C	Bend	X-ray footprinting	White Beam	Albert Einstein College of Medicine

NSLS Linac Parameters as of December 2003

Injection Energy	100 keV
Final Energy	120 MeV
Number of Sections	3
Number of Klystrons	3
Frequency	2856 MHz

NSLS Booster Parameters

Injection Energy	120 MeV
Extraction Energy	750 MeV
Circumference	28.35 m
Number of Superperiods	4
Dipole Bending Radius	1.91 m
Nominal Horizontal Tune	2.42
Nominal Vertical Tune	1.37
Maximum Horizontal Beta	8.63 m
Minimum Horizontal Beta	1.01 m
Maximum Vertical Beta	5.26 m
Minimum Vertical Beta	1.73 m
Maximum Dispersion	1.21 m
Minimum Dispersion	0.41 m
Momentum Compaction	0.106
Peak RF Voltage	25 kV
RF Frequency	52.88 MHz
Horizontal Acceptance	1.66E-04 m-rad
Vertical Acceptance	6.11E-05 m-rad
Momentum Acceptance	±0.0025

Booster Magnetic Elements (Fields at 750 MeV)

Name	Type	Quantity	B (kG)	B’ (kG/m)	B” (kG/m)	Effective Length (m)
BB	Dipole	8	13.099	-7.97	-125	1.5
Q1	Quadrupole	4		68.82		0.3
Q2	Quadrupole	4		93.60		0.3
SF	Sextupole	4			1223.7	0.2

VUV STORAGE RING PARAMETERS AS OF DECEMBER 2003

Normal Operating Energy	0.808 GeV
Peak Operating Current (multibunch ops.)	1.0 amp
Circumference	51.0 meters
Number of Beam Ports on Dipoles	18
Number of Insertion Devices	2
Maximum Length of Insertion Devices	~ 2.25 meters
$\lambda_c(E_c)$	19.9 Å (622 eV)
$B(\rho)$	1.41 Tesla (1.91 meters)
Electron Orbital Period	170.2 nanoseconds
Damping Times	$\tau_x=\tau_y$= 13 msec; τ_ε = 7 msec
Lifetime @ 200 mA with 52 MHz	360 min
(with 211 MHz Bunch Lengthening)	(590 min)
Lattice Structure (Chasman-Green)	Separated Function, Quad, Doublets
Number of Superperiods	4
Magnet Complement	8 Bending (1.5 meters each) 24 Quadrupole (0.3 meters each) 12 Sextupole (0.2 meters each)
Nominal Tunes (ν_x,ν_y)	3.14, 1.26
Momentum Compaction	0.0235
RF Frequency	52.887 MHz
Radiated Power	20.4 kW/amp of Beam
RF Peak Voltage with 52 MHz (with 211 MHz)	80 kV (20kV)
Design RF Power with 52 MHz (with 211 MHz)	50 kW (10 kW)
Synchrotron Tune (ν_s)	0.0018
Natural Energy Spread (σ_e/E)	5.0×10^{-4} , I_b< 20 mA
Bunch Length (2σ)	9.7 cm (I_b < 20 mA)
($2L_{rms}$ with 211 MHz Bunch Lengthening)	(36 cm)
Number of RF Buckets	9
Typical Bunch Mode	7
Horizontal Damped Emittance (ε_x)	160 nm-rad
Vertical Damped Emittance (ε_y)	≥ 0.35 nm-rad (4nm-rad in normal ops.)*
Power per Horizontal Milliradian (@ 1A)	3.2 Watts

ARC SOURCE PARAMETERS

Betatron Function (β_x,β_y)	1.18 to 2.25 m, 10.26 to 14.21 m
Dispersion Function (η_x,η'_x)	0.500 to 0.062 m, 0.743 to 0.093 m
$\alpha_{x,y} = -\beta'_{x\,y}/2$	-0.046 to 1.087, 3.18 to -0.96
$\gamma_{x,y} = (1+\alpha^2_{x,y})/\beta_{x,y}$	0.738 to 0.970 m^{-1}, 1.083 to 0.135 m^{-1}
Source Size (σ_x,σ_y)	536 to 568 μm, >60 to >70 μm (170-200 μm in normal ops.)*
Source Divergence (σ'_x,σ'_y)	686 to 373 μrad, 19.5 to 6.9 μrad (55-20 μrad in normal ops.)*

INSERTION DEVICE PARAMETERS

Betatron Function (β_x,β_y)	11.1 m, 5.84 m
Source Size (σ_x,σ_y)	1240 μm, >45 μm (220 μm in normal ops.)*
Source Divergence (σ'_x, σ'_y)	112 μrad, >7.7 μrad (22 μrad in normal ops.)*

* ε_y is adjustable

X-Ray Storage Ring Parameters as of December 2003

Normal Operating Energies	2.800 GeV
Maximum Operating Current	280 mA
Lifetime	~20 hours
Circumference	170.1 meters
Number of Beam Ports on Dipoles	30
Number of Insertion Devices	6
Maximum Length of Insertion Devices	< 4.50 meters
$\lambda_c(E_c)$ at 1.36 T	1.75 Å (7.1 keV)
$\lambda_c(E_c)$ at 5.0 T (W)	0.48 Å (26.1 keV)
$B(\rho)$	1.36 Tesla (6.875 meters)
Electron Orbital Period	567.2 nanoseconds
Damping Times	$\tau_x = \tau_y$ =4 msec; τ_ε =2 msec
Lattice Structure (Chasman-Green)	Separated Function, Quad Triplets
Number of Superperiods	8
Magnet Complement	16 Bending (2.7 meters each) 40 Quadrupole (0.45 meters each) 16 Quadrupole (0.80 meters each) 32 Sextupole (0.20 meters each)
Nominal Tunes (ν_x,ν_y)	9.8, 5.7
Momentum Compaction	4.10^{-3}
RF Frequency	52.88 MHz
Radiated Power for Bending Magnets	198 kW (0.25A)
RF Peak Voltage	1120 kV
Design RF Power	450 kW
Synchrotron Tune (ν_s)	0.0023
Natural Energy Spread (σ_e/E)	9.2×10^{-4}
Natural Bunch Length (2σ)	8.7 cm
Number of RF Buckets	30
Typical Bunch Mode	25
Horizontal Damped Emittance (ε_x)	7.5×10^{-8} meter-rad
Vertical Damped Emittance (ε_y)	1.5×10^{-10} meter-rad
Power per Horizontal Milliradian (0.25A)	32W

Arc Source Parameters

Betatron Function (β_x,β_y)	1.0 to 3.8 m, 7.9 to 26.5 m
Dispersion Function (η_x,η'_x)	0.47 to -0.11, -0.39 to 0.22
$\alpha_{x,y} = -\beta'_{x,y}/2$	-0.49 to 1.62, -3.4 to 4.5
$\gamma_{x,y} = (1+\alpha^2_{x,y})/\beta_{x,y}$	0.952 to 0.962 m^{-1}, 0.81 to 0.52 m^{-1}
Source Size (σ_x,σ_y)	371 to 612 μm, 27 to 53 μm
Source Divergence (σ_x',σ_y')	476 to 324 μrad, 9 to 7 μrad

Insertion Device Parameters

Betatron Function (β_x, β_y)	1.60 m, 0.35 m
Source Size (σ_x,σ_y)	300 μm, 6 μm
Source Divergence (σ_x', σ_y')	260 μrad, 35 μrad

FY 2003 NSLS Machine Activities

Activity	UV/IR	X-ray
Operations	67.0%	52.2%
Unscheduled Operations	7.2%	6.1%
Maintenance	14.6%	20.4%
Other	11.2%	21.2%

Full Year 8760 hours 100 hours=1.1%

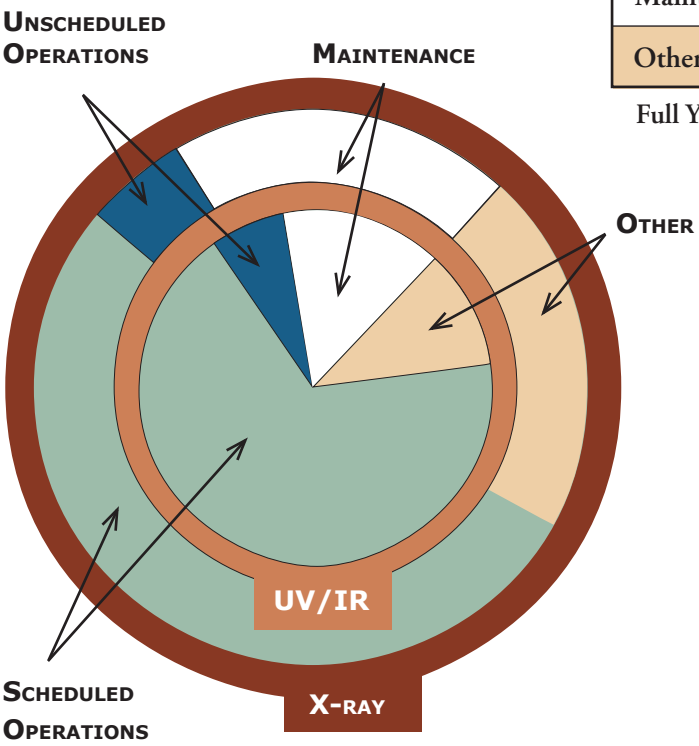

"Other" FY 2003 Activities

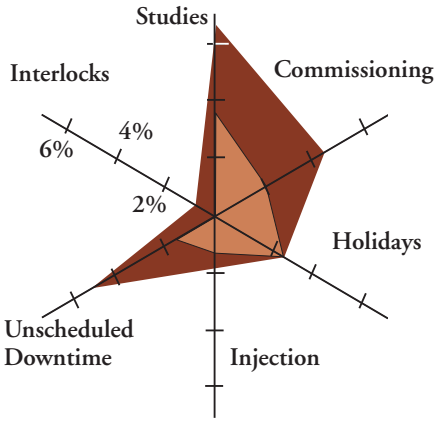

Fiscal Year 2003

Month	VUV Actual FY 03			X-Ray Actual FY 03		
	Planned Hours	Reliability[1]	Availability[2]	Planned Hours	Reliability[1]	Availability[2]
October	617	99.8%	104.7%	532	96.2%	114.9%
November	521	98.2%	101.3%	457	96.0%	101.7%
December	0	-	-	0	-	-
January	440	99.3%	122.6%	214	16.0%	24.4%
February	546	99.6%	106.6%	492	96.5%	108.3%
March	617	99.4%	107.9%	556	99.0%	107.2%
April	595	97.3%	106.2%	552	83.3%	94.6%
May	338	95.1%	112.3%	256	65.4%	65.4%
June	597	98.6%	106.2%	535	95.6%	101.8%
July	515	99.4%	111.4%	510	99.9%	105.3%
August	615	90.5%	103.5%	547	82.1%	96.3%
September	592	99.9%	115.0%	495	94.6%	112.0%
	5993			**5146**		
Fiscal 2003 Delivered	5871	98.0%	108.4%	4575	88.9%	99.3%

Note: Delivered hours are only those accumulated during scheduled operations. Unscheduled operations do not contribute to this total.

[1] Operations during scheduled time
[2] Operations compared to total scheduled time

Facility Facts & Figures

The National Synchrotron Light Source (NSLS) is a national user research facility funded by the U.S. Department of Energy's Office of Basic Energy Science. The NSLS operates two electron storage rings: an X-ray ring (2.8 GeV, 280 mA) and a Vacuum Ultraviolet (VUV) ring (800 meV, 1.0 A) which provide intense light spanning the electromagnet spectrum from the infrared through x-rays. The properties of this light, and the specially designed experimental stations, called beamlines, allow scientists in many fields of research to perform experiments not otherwise possible at their own laboratories.

Over 2200 scientists representing almost 400 institutions, 65 of them corporations, come to Brookhaven National Laboratory annually to conduct research at the NSLS. The facility operates 7 days a week, 24 hours a day, throughout the year, except during periods of maintenance and studies.

As a national user facility, the NSLS does not charge for its beamtime, providing that the research results are published in the open literature. Proprietary research is conducted on a full cost recovery basis.

There are two ways to obtain beamtime at the NSLS: either as a General User or as a member of a Participating Research Team (PRT). General Users are independent investigators interested in using the NSLS for their research. Access is gained through a peer-reviewed proposal system. All operational beamlines at the NSLS reserve at least 25% of their available beamtime for General Users. PRTs are groups of researchers with related interests from one or more institutions. Membership in a PRT is open to all members of the scientific community who can contribute significantly to the program of the PRT, (i.e., funding, contribution of equipment, scientific program, design and engineering, operations manpower, etc).

The NSLS currently has 58 X-Ray and 22 VUV operational beamlines for performing a wide range of experiments. The following pages list the operational beamlines at the NSLS and their unique characteristics.

Beamline Guide

Technique	Description
ARPES	UV photoelectron spectroscopy, angle-resolved
DAFS	X-ray diffraction anomalous fine structure
DEI	Diffraction-enhanced imaging
EXAFS	X-ray absorption spectroscopy, extended fine structure
HARMST	High aspect ratio microsystems technology
IRMS	Infrared Microspectroscopy
MAD	Multi-Wavelength anomolous dispersion
NEXAFS	Near edge x-ray absorption spectroscopy
SAXS	Small angle x-ray scattering
SPARPES	UV photoelectron spectroscopy, spin- and angle-resolved
STXM	Scanning transmission x-ray microscopy
UPS	UV photoelectron spectroscopy
UV-CD	Ultraviolet circular dichroism
WAXD	Wide-angle x-ray diffraction
WAXS	Wide-angle x-ray scattering
XAS	X-ray absorption spectroscopy
XMCD	X-ray magnetic circular dichroism
XPS	X-ray photoelectron spectroscopy
XRD	X-ray diffraction
XSW	X-ray standing waves

BEAMLINE	SOURCE	TYPE OF RESEARCH	ENERGY RANGE	ORGANIZATION
U1A	Bend	NEXAFS XAS	20-900 eV	ExxonMobil Research and Engineering Co.
U2A	Bend	High Pressure Research IRMS IR spectroscopy	30-8000 cm-1	Carnegie Institute of Washington
U2B	Bend	IRMS IR spectroscopy	50-4000 cm-1	Albert Einstein College of Medicine
U3C	Bend	XPS	50-1000 eV	Bechtel Nevada Lawrence Livermore National Laboratory Los Alamos National Laboratory Sandia National Laboratory
U4A	Bend	UPS	10-300 eV	Army Research Laboratory BNL-NSLS Boston University North Carolina State University Rutgers University University of North Carolina
U4B	Bend	XMCD X-ray scattering, resonant X-ray scattering, magnetic X-ray florescence XPS UPS	20-1200 eV	BNL-NSLS Montana State University
U4IR	Bend	IR spectroscopy IRMS	20-3000 cm-1	BNL-Chemistry BNL-NSLS
U5UA	Insertion Device	UPS ARPES SPARPES Magnetospectroscopy	15-150 eV	BNL-NSLS
U7A	Bend	NEXAFS XPS	180-1200 eV	BNL-Chemistry BNL-Physcis Dow Chemical Company National Institute of Standards & Technology Rutgers University Texas A&M University University of Michigan
U7B	Bend	XPS UPS NEXAFS	15-300 eV	BNL-NSLS
U8B	Bend	NEXAFS X-ray photoemission ARPES	100-1000 eV	IBM Research Division University of California @ Riverside University of Michigan
U9A	Bend	Photon-stim. Desorption	White Beam	BNL-NSLS
U9B	Bend	UV florescence UV-CD	0.8 - 8.0 eV	BNL-Biology BNL-NSLS
U10A	Bend	IR spectroscopy	30-20000 cm-1	BNL-NSLS BNL-Physics
U10B	Bend	IRMS	50-4000 cm-1	BNL-NSLS University of Saskatchewan
U11	Bend	UPS UV photoabsorption UV photoionization	3-30 eV	BNL-Biology BNL-NSLS

BEAMLINE	SOURCE	TYPE OF RESEARCH	ENERGY RANGE	ORGANIZATION
U12A	Bend	XAS	100-800 eV	BNL-NSLS Oak Ridge National Laboratory
U12IR	Bend	IR spectroscopy Time-resolved spectroscopy	2-400 cm-1	BNL-NSLS SUNY @ Stony Brook University of Florida
U13UA	Insertion Device	Focused white beam	3-1000 eV White Beam	BNL-NSLS
U13UB	Insertion Device	UPS ARPES	3-30 eV	BNL-NSLS BNL-Physics Boston University
U14A	Bend	XPS UPS	15-300 eV	BNL-NSLS
U16B	Bend	XPS	50-1000 eV	BNL-NSLS Rutgers University University of Texas Arlington
X1A1	Insertion Device	STXM	.25-.50 keV	BNL-Environmental Science BNL-NSLS ExxonMobil Research and Engineering Co. SUNY @ Plattsburgh SUNY @ Stony Brook University of Texas
X1A2	Insertion Device	STXM	.25-1 keV	SUNY @ Stony Brook
X1B	Insertion Device	X-ray scattering, resonant X-ray scattering, coherent ARPES UV fluorescence XAS	.2-1.6 keV	Boston University BNL-NSLS University of Groningen
X2B	Bend	X-ray microtomography	8-35 keV	ExxonMobil Research and Engineering Co.
X3A2	Bend	XAS SAXS XRD, single-crystal MAD	3-31 keV	SUNY @ Stony Brook
X3B1	Bend	XAS XRD, powder EXAFS	6-30 keV	SUNY @ Buffalo SUNY @ Stony Brook
X4A	Bend	MAD	3.5-20 keV	Albert Einstein College of Medicine City University of New York Columbia University Memorial Sloan-Kettering Cancer Center Mount Sinai School of Medicine New York Structural Biology Center New York University SUNY @ Buffalo The Wadsworth Center of the NYS Dept of Health Weill Medical College of Cornell University

BEAMLINE	SOURCE	TYPE OF RESEARCH	ENERGY RANGE	ORGANIZATION
X4C	Bend	MAD	7-20 keV	Albert Einstein College of Medicine City University of New York Columbia University Memorial Sloan-Kettering Cancer Center Mount Sinai School of Medicine New York Structural Biology Center New York University Rockefeller University SUNY @ Buffalo The Wadsworth Center of the NYS Dept of Health Weill Medical College of Cornell University
X5A	Bend	Laser backscattering	150-470 MeV	BNL-Physics Forschungszentrum Juelich (KFA) Norfolk State University Ohio University Syracuse University University of Paris University of Rome II University of South Carolina University of Virginia Virginia Polytechnic Inst. & State University
X6A	Bend	MAD	7-20 keV	BNL-NSLS
X6B	Bend	XRD, powder XRD, single-crystal	7-20 keV	BNL-NSLS
X7A	Bend	XRD, powder	5-45 keV	BNL-Physics Chevron Research & Technology Company Ohio State University SUNY @ Stony Brook University of Birmingham University of California @ Santa Barbara University of Pennsylvania
X7B	Bend	XRD, single-crystal XRD, time-resolved WAXS or WAXD	5-21 keV	BNL-Chemistry
X8A	Bend	Metrology	.26-5.9 keV	Bechtel Nevada Lawrence Livermore National Laboratory Los Alamos National Laboratory Sandia National Laboratory
X8C	Bend	MAD	5-19 keV	Biogen Incorporated BNL-Biology Hoffmann-La Roche National Research Council of Canada
X9A	Bend	MAD	5-15 keV	Albert Einstein College of Medicine Rockefeller University Sloan-Kettering Institute for Cancer Research
X9B	Bend	EXAFS XAS MAD NEXAFS	5-15 keV	Albert Einstein College of Medicine National Institutes of Health
X10A	Bend	XRD, time-resolved WAXS or WAXD XRD, powder X-ray reflectivity SAXS	6-15.2 keV	ExxonMobil Research and Engineering Co.
X10B	Bend	XRD, surface WAXS or WAXD XRD, powder X-ray reflectivity	14 keV	ExxonMobil Research and Engineering Co.

BEAMLINE	SOURCE	TYPE OF RESEARCH	ENERGY RANGE	ORGANIZATION
X10C	Bend	XAS NEXAFS EXAFS	4-24 keV	ExxonMobil Research and Engineering Co.
X11A	Bend	EXAFS NEXAFS XAS	4.5-35 keV	BNL-Environmental Science Canadian Light Source Hunter College Naval Research Laboratory Naval Surface Warfare Center New Jersey Institute of Technology North Carolina State University Northeastern University Paul Scherrer Institute U.S. Enivronmental Protection Agency Virginia Union University
X11B	Bend	EXAFS NEXAFS XAS	5.0-30 keV	BNL-Environmental Science Canadian Light Source Hunter College Naval Research Laboratory Naval Surface Warfare Center New Jersey Institute of Technology North Carolina State University Northeastern University Paul Scherrer Institute U.S. Enivronmental Protection Agency University of Connecticut Virginia Union University
X12A	Bend	Optics R&D	5-50 keV	BNL-NSLS
X12B	Bend	MAD	5-20 keV	BNL-Biology
X12C	Bend	MAD	5.5-20.0 keV	BNL-Biology
X13A	Insertion Device	Magnetospectroscopy XMCD X-ray scattering, resonant	.2-1.8 keV	BNL-NSLS
X13B	Insertion Device	Microdiffraction imaging X-ray microprobe	4-16 KeV	BNL-NSLS
X14A	Bend	XRD, single-crystal	5-26 keV	Oak Ridge National Laboratory University of Tennessee
X15A	Bend	XSW DEI	3-25 keV 10-60 keV	Argonne National Laboratory BNL-NSLS Canadian Light Source Illinois Institute of Technology North Carolina State University Northwestern University University of North Carolina University of Saskatchewan
X15B	Bend	NEXAFS XAS EXAFS	1.5-15 keV	SUNY @ Stony Brook
X16A	Bend	XRD, surface	4-12 keV	University of Illinois @ Chicago
X16B	Bend	XRD, powder XRD, surface	7.85 keV	
X16C	Bend	XAS	4.5-25 keV	University of Illinois @ Chicago
X17B1	Insertion Device	XRD, powder	67 keV 20-100 keV	BNL-Medical BNL-NSLS

BEAMLINE	SOURCE	TYPE OF RESEARCH	ENERGY RANGE	ORGANIZATION
X17B2	Insertion Device	XRD, powder High Pressure Research	20-100 keV	SUNY @ Stony Brook
X17B3	Insertion Device	High Pressure Research	20-100 keV	Brookhaven National Laboratory Carnegie Institute of Washington
X17C	Insertion Device	High Pressure Research XRD, powder XRD, single-crystal	5-80 keV	Carnegie Institute of Washington Lawrence Livermore National Laboratory Naval Research Laboratory University of Chicago
X18A	Bend	XRD, surface XRD, powder X-ray reflectivity XRD, single-crystal WAXS or WAXD	4-19 keV	BNL-Environmental Science Pennsylvania State University Purdue University University of Maryland University of Missouri
X18B	Bend	NEXAFS XAS EXAFS	5.7-40 keV	BNL-Chemistry BNL-NSLS Chevron Research & Technology Company General Electric North Carolina State University Rutgers University University of Kentucky UOP
X19A	Bend	EXAFS XAS NEXAFS	2-8 keV	BNL-Chemistry BNL-NSLS Chevron Research & Technology Company General Electric North Carolina State University Rutgers University University of Kentucky UOP
X19C	Bend	X-ray topography X-ray scattering, liquid X-ray reflectivity XRD, surface	6-17 keV	Army Research Laboratory Carnegie Mellon University Dartmouth College Johns Hopkins University National Aeronautical and Space Agency SUNY @ Stony Brook University of Chicago University of Illinois @ Chicago University of Wisconsin
X20A	Bend	Microdiffraction imaging XRD, surface	4.5-13 keV	IBM Research Division
X20B	Bend	XRD, surface	17.4 keV	IBM Research Division
X20C	Bend	XRD, surface XRD, time-resolved	5-11 keV	IBM Research Division
X21	Insertion Device	SAXS X-ray florescence X-ray inelastic scattering	5-10 keV	BNL-NSLS
X22A	Bend	XRD, surface XRD, time-resolved WAXS or WAXD X-ray reflectivity XRD, single-crystal	10 keV 32 keV	BNL-Environmental Science BNL-Physics Rutgers University University of Maryland
X22B	Bend	X-ray scattering, liquid XRD, surface	6.5-10 keV	BNL-Physics Harvard University Rutgers University

BEAMLINE	SOURCE	TYPE OF RESEARCH	ENERGY RANGE	ORGANIZATION
X22C	Bend	X-ray scattering, magnetic X-ray reflectivity XRD, surface XRD, single-crystal	3-12 keV	BNL-Physics Rutgers University University of Maryland
X23A2	Bend	DAFS XAS XRD, powder NEXAFS EXAFS	4.7-30 keV	BNL-NSLS
X23B	Bend	XAS XRD, powder EXAFS NEXAFS	3-10.5 keV	BNL-Environmental Science Canadian Light Source Hunter College Naval Research Laboratory Naval Surface Warfare Center New Jersey Institute of Technology North Carolina State University Northeastern University Paul Scherrer Institute U.S. Enivronmental Protection Agency Virginia Union University
X24A	Bend	XPS Auger spectroscopy XSW EXAFS X-ray fluorescence	1.8-5 keV	BNL-NSLS National Institute of Standards & Technology
X24C	Bend	XPS	.006-1.8 keV	Naval Research Laboratory
X25	Insertion Device	MAD	3-28 keV	BNL-Biology BNL-NSLS
X26A	Bend	X-ray microprobe Microdiffraction imaging	3-30 keV	BNL-Environmental Science University of Chicago University of Georgia
X26C	Bend	MAD	5-20 keV	BNL-Biology Cold Spring Harbor Laboratory SUNY @ Stony Brook
X27A	Bend	X-ray microtomography	8-40 keV	BNL-NSLS
X27B	Bend	HARMST	White Beam	BNL-NSLS
X27C	Bend	SAXS WAXS or WAXD XRD, time-resolved	9 KeV	Basell USA, Inc. (formerly Montell) Honeywell International National Institute of Standards & Technology National Institutes of Health Naval Surface Warfare Center New Jersey Institute of Technology SUNY @ Stony Brook U.S. Air Force
X28C	Bend	X-ray footprinting	White Beam	Albert Einstein College of Medicine

NSLS Linac Parameters as of December 2003

Injection Energy	100 keV
Final Energy	120 MeV
Number of Sections	3
Number of Klystrons	3
Frequency	2856 MHz

NSLS Booster Parameters

Injection Energy	120 MeV
Extraction Energy	750 MeV
Circumference	28.35 m
Number of Superperiods	4
Dipole Bending Radius	1.91 m
Nominal Horizontal Tune	2.42
Nominal Vertical Tune	1.37
Maximum Horizontal Beta	8.63 m
Minimum Horizontal Beta	1.01 m
Maximum Vertical Beta	5.26 m
Minimum Vertical Beta	1.73 m
Maximum Dispersion	1.21 m
Minimum Dispersion	0.41 m
Momentum Compaction	0.106
Peak RF Voltage	25 kV
RF Frequency	52.88 MHz
Horizontal Acceptance	1.66E-04 m-rad
Vertical Acceptance	6.11E-05 m-rad
Momentum Acceptance	±0.0025

Booster Magnetic Elements (Fields at 750 MeV)

Name	Type	Quantity	B (kG)	B’ (kG/m)	B” (kG/m)	Effective Length (m)
BB	Dipole	8	13.099	-7.97	-125	1.5
Q1	Quadrupole	4		68.82		0.3
Q2	Quadrupole	4		93.60		0.3
SF	Sextupole	4			1223.7	0.2

VUV STORAGE RING PARAMETERS AS OF DECEMBER 2003

Normal Operating Energy	0.808 GeV
Peak Operating Current (multibunch ops.)	1.0 amp
Circumference	51.0 meters
Number of Beam Ports on Dipoles	18
Number of Insertion Devices	2
Maximum Length of Insertion Devices	~ 2.25 meters
$\lambda_c(E_c)$	19.9 Å (622 eV)
$B(\rho)$	1.41 Tesla (1.91 meters)
Electron Orbital Period	170.2 nanoseconds
Damping Times	$\tau_x=\tau_y$= 13 msec; τ_ε = 7 msec
Lifetime @ 200 mA with 52 MHz	360 min
(with 211 MHz Bunch Lengthening)	(590 min)
Lattice Structure (Chasman-Green)	Separated Function, Quad, Doublets
Number of Superperiods	4
Magnet Complement	8 Bending (1.5 meters each) 24 Quadrupole (0.3 meters each) 12 Sextupole (0.2 meters each)
Nominal Tunes (ν_x,ν_y)	3.14, 1.26
Momentum Compaction	0.0235
RF Frequency	52.887 MHz
Radiated Power	20.4 kW/amp of Beam
RF Peak Voltage with 52 MHz (with 211 MHz)	80 kV (20kV)
Design RF Power with 52 MHz (with 211 MHz)	50 kW (10 kW)
Synchrotron Tune (ν_s)	0.0018
Natural Energy Spread (σ_e/E)	5.0×10^{-4} , I_b< 20 mA
Bunch Length (2σ)	9.7 cm (I_b < 20 mA)
($2L_{rms}$ with 211 MHz Bunch Lengthening)	(36 cm)
Number of RF Buckets	9
Typical Bunch Mode	7
Horizontal Damped Emittance (ε_x)	160 nm-rad
Vertical Damped Emittance (ε_y)	≥ 0.35 nm-rad (4nm-rad in normal ops.)*
Power per Horizontal Milliradian (@ 1A)	3.2 Watts

ARC SOURCE PARAMETERS

Betatron Function (β_x,β_y)	1.18 to 2.25 m, 10.26 to 14.21 m
Dispersion Function (η_x,η'_x)	0.500 to 0.062 m, 0.743 to 0.093 m
$\alpha_{x,y} = -\beta'_{x\,y}/2$	-0.046 to 1.087, 3.18 to -0.96
$\gamma_{x,y} = (1+\alpha^2_{x,y})/\beta_{x,y}$	0.738 to 0.970 m^{-1}, 1.083 to 0.135 m^{-1}
Source Size (σ_x,σ_y)	536 to 568 μm, >60 to >70 μm (170-200 μm in normal ops.)*
Source Divergence (σ'_x,σ'_y)	686 to 373 μrad, 19.5 to 6.9 μrad (55-20 μrad in normal ops.)*

INSERTION DEVICE PARAMETERS

Betatron Function (β_x,β_y)	11.1 m, 5.84 m
Source Size (σ_x,σ_y)	1240 μm, >45 μm (220 μm in normal ops.)*
Source Divergence (σ'_x, σ'_y)	112 μrad, >7.7 μrad (22 μrad in normal ops.)*

* ε_y is adjustable

X-Ray Storage Ring Parameters as of December 2003

Normal Operating Energies	2.800 GeV
Maximum Operating Current	280 mA
Lifetime	~20 hours
Circumference	170.1 meters
Number of Beam Ports on Dipoles	30
Number of Insertion Devices	6
Maximum Length of Insertion Devices	< 4.50 meters
$\lambda_c(E_c)$ at 1.36 T	1.75 Å (7.1 keV)
$\lambda_c(E_c)$ at 5.0 T (W)	0.48 Å (26.1 keV)
$B(\rho)$	1.36 Tesla (6.875 meters)
Electron Orbital Period	567.2 nanoseconds
Damping Times	$\tau_x = \tau_y$ =4 msec; τ_ε =2 msec
Lattice Structure (Chasman-Green)	Separated Function, Quad Triplets
Number of Superperiods	8
Magnet Complement	16 Bending (2.7 meters each) 40 Quadrupole (0.45 meters each) 16 Quadrupole (0.80 meters each) 32 Sextupole (0.20 meters each)
Nominal Tunes (ν_x,ν_y)	9.8, 5.7
Momentum Compaction	4.10^{-3}
RF Frequency	52.88 MHz
Radiated Power for Bending Magnets	198 kW (0.25A)
RF Peak Voltage	1120 kV
Design RF Power	450 kW
Synchrotron Tune (ν_s)	0.0023
Natural Energy Spread (σ_e/E)	9.2×10^{-4}
Natural Bunch Length (2σ)	8.7 cm
Number of RF Buckets	30
Typical Bunch Mode	25
Horizontal Damped Emittance (ε_x)	7.5×10^{-8} meter-rad
Vertical Damped Emittance (ε_y)	1.5×10^{-10} meter-rad
Power per Horizontal Milliradian (0.25A)	32W

Arc Source Parameters

Betatron Function (β_x,β_y)	1.0 to 3.8 m, 7.9 to 26.5 m
Dispersion Function (η_x,η'_x)	0.47 to -0.11, -0.39 to 0.22
$\alpha_{x,y} = -\beta'_{x,y}/2$	-0.49 to 1.62, -3.4 to 4.5
$\gamma_{x,y} = (1+\alpha^2_{x,y})/\beta_{x,y}$	0.952 to 0.962 m^{-1}, 0.81 to 0.52 m^{-1}
Source Size (σ_x,σ_y)	371 to 612 μm, 27 to 53 μm
Source Divergence (σ_x',σ_y')	476 to 324 μrad, 9 to 7 μrad

Insertion Device Parameters

Betatron Function (β_x, β_y)	1.60 m, 0.35 m
Source Size (σ_x,σ_y)	300 μm, 6 μm
Source Divergence (σ_x', σ_y')	260 μrad, 35 μrad

FY 2003 NSLS Machine Activities

Activity	UV/IR	X-ray
Operations	67.0%	52.2%
Unscheduled Operations	7.2%	6.1%
Maintenance	14.6%	20.4%
Other	11.2%	21.2%

Full Year 8760 hours 100 hours=1.1%

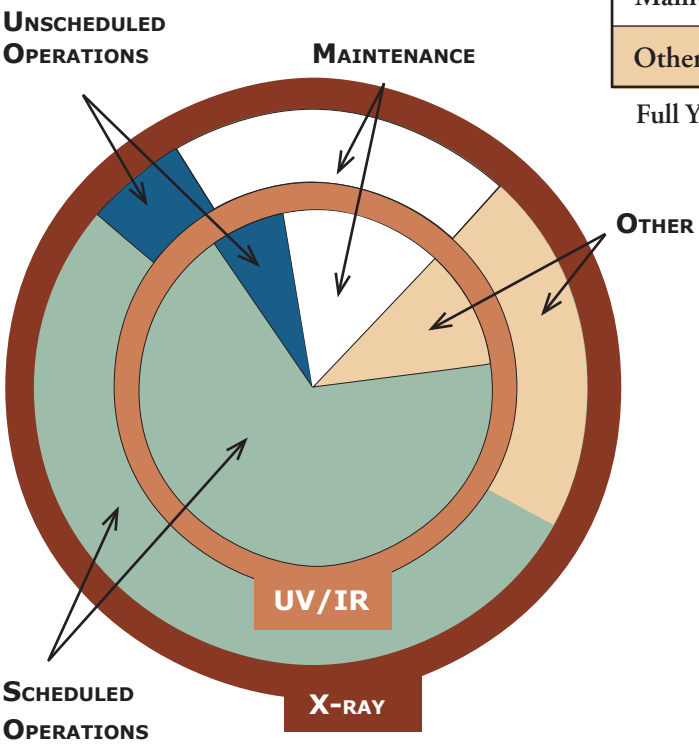

"Other" FY 2003 Activities

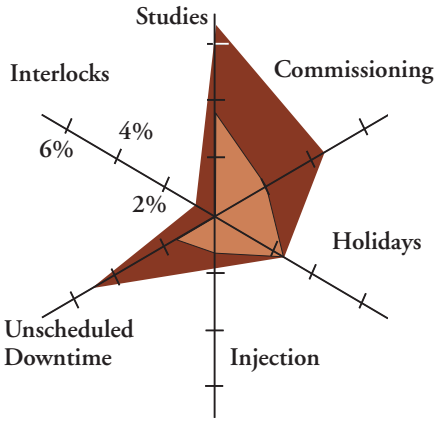

Fiscal Year 2003

Month	VUV Actual FY 03			X-Ray Actual FY 03		
	Planned Hours	Reliability[1]	Availability[2]	Planned Hours	Reliability[1]	Availability[2]
October	617	99.8%	104.7%	532	96.2%	114.9%
November	521	98.2%	101.3%	457	96.0%	101.7%
December	0	-	-	0	-	-
January	440	99.3%	122.6%	214	16.0%	24.4%
February	546	99.6%	106.6%	492	96.5%	108.3%
March	617	99.4%	107.9%	556	99.0%	107.2%
April	595	97.3%	106.2%	552	83.3%	94.6%
May	338	95.1%	112.3%	256	65.4%	65.4%
June	597	98.6%	106.2%	535	95.6%	101.8%
July	515	99.4%	111.4%	510	99.9%	105.3%
August	615	90.5%	103.5%	547	82.1%	96.3%
September	592	99.9%	115.0%	495	94.6%	112.0%
	5993			**5146**		
Fiscal 2003 Delivered	5871	98.0%	108.4%	4575	88.9%	99.3%

Note: Delivered hours are only those accumulated during scheduled operations. Unscheduled operations do not contribute to this total.

[1] Operations during scheduled time
[2] Operations compared to total scheduled time

Publications

The following pages list all publication citations reported to the NSLS in FY 2003 (October 1, 2002 through September 30, 2003). Citations are listed in order of beamline number and then alphabetically by the last name of the first author. This list contains unique citations for journal, published conference proceedings, books, chapters in books, formal reports, informal reports, technical reports, theses, dissertations, and patents when reported. For citation submissions where research was performed on more than one beamline, the citation is listed under each beamline. However, each citation was only counted once. Citations bearing publication dates prior to the Year 2003 are listed only if they had not been previously reported to the NSLS and did not appear in a prior fiscal year's activity report. Diligent effort has been made to ensure that each reference is unique and complete. For journal articles, online searches were performed to locate missing reference information (e.g., year of publication, volume, issue or page numbers). With regard to conference papers, considerable effort was put into ensuring that the citations appeared in published proceedings. Many citations for conferences papers have been omitted from this list if verification could not be made. We apologize to our users and authors for any citations incorrectly omitted.

Several types of journal articles are reported in this list, including premiere journals, peer-reviewed journals and a few that are not peer-reviewed. Premiere journals include: Physical Review Letters, Science, Nature, Cell, EMBO Journal, Nature Structural Biology, Proceedings of the National Academy of Sciences of the United States of America, Structure, and Applied Physics Letters.

In FY 2003, the following types and numbers of publication citations were reported to the NSLS where research was performed in part or in whole at the NSLS.

Journals, peer-reviewed, premiere	113
Journals, other peer-reviewed	440
Journals, non peer-reviewed	22
Total Journals and Magazines	575
Books/Chapters in Books	17
Published Conference Proceedings	59
Reports: Technical, Formal, Informal	1
Theses/Dissertations	9
Patents	1
Total Misc. Publications	87
Total Citations Listed	**662**

NSLS VUV User Publications	76
NSLS X-Ray User Publications	489
NSLS Staff Publications	97
	662

NSLS Users

Beamline U1A

M Zwahlen, D Brovelli, W Caseri, G Haehner. Orientation and Electronic Structure of Ion-Exchanged Pyridinium Compounds on Mica. *J. Colloid Interface Sci.*. **256**, 262 (2002).

Beamline U2A

B Chen, D Muthu, Z Liu, A Sleight, M Kruger. High-pressure Optical Study of HfW2O8. *J. Phys.: Condens. Matter*. **14**, 13911-13916 (2002).

E Gregoryanz, A Goncharov, R Hemley, H Mao, M Somayazulu, G Shen. Raman. Infrared, and x-ray evidence for new phases of. *Phys. Rev. B: Condens. Matter*. **66**, 224108 (2002).

R Hemley, Z Liu, E Gregoryanz, H Mao. Infrared and Raman Microspectroscopy of Materials Under Pressure. *Microscopy and Microanalysis*, Vol 9, p. 1098, (2003).

R Hemley, H Mao. Overview of static high pressure science, in High-Pressure Phenomena. *Proceedings of the International School of Physics, "Enrico Fermi" Course CXLVII*, p. 3-40, IOS Press, Amsterdam. (2002).

R Hemley, H Mao. New window on earth and planetary interiors. *Miner. Mag.*. **66**, 791-811 (2002).

Z Liu, J Hu, H Yang, H Mao, R Hemley. High-pressure Synchrotron X-ray Diffraction and Infrared Microspectroscopy: Application to Dense Hydrous Phases. *J. Phys.: Condens. Matter*. **14**, 10641-10646 (2002).

Z Liu, G Lager, R Hemley, N Ross. Synchrotron Infrared Spectroscopic Study of OH-chondrodite and OH-clinohumite at High Pressure. *Am. Mineral.*. **88**, 1412 (2003).

Y Song, R Hemley, Z Liu, M Mosayazulu, H Mao, D Herschbach. High-pressure stability, transformations, and vibrational dynamics of nitrosonium nitrate from synchrotron infrared and Raman spectroscopy. *J. Chem. Phys.*. **119** (4), 2232 (2002).

H Yang, C Prewitt, Z Liu. Crystal structures and infrared spectra of two Fe-bearing hydrous magnesium silicates synthesized at high temperature and pressure. *J. Miner. Petrological Sci.*. **97**, 137-143 (2002).

Beamline U2B

L Cho, J Reffner, B Gatewood, D Wetzel. Single Fiber Analysis by Internal Reflection Infrared Microspectroscopy. *J. of Forsensic Sci.*. **46** (6), 1309-1314 (2001).

A Eilert, J Sweat, D Wetzel. Parabolic Concentration of Diffusely Transmitted Near-IR Radiation in an Acousto-Optic Tunable Filter Spectrometer. *J. Near Infrared Spectrosc.*. **8**, 239-250 (2000).

A Eilert, D Wetzel. Optics and Sample Handling for Near-Infrared Diffuse Reflection. *Handbook of Vibrational Spectroscopy*, p. 436-452, Wiley, Chichester. (2002).

R Huang, L Miller, C Carlson, M Chance. FTIR Analysis of Tibia Bone from Ovariectomized Cynomolgus Monkeys (Macaca fascialaris) and the Effect of Nandrolone Deconoate Treatment. *Bone*. **30** (2), 492-497 (2002).

S Judex, S Boyd, Y Qin, L Miller, R Muller, C Rubin. Combining High-Resolution MicroCT with Material Composition to Define the Quality of Bone Tissue. *Curr. Osteoporosis Reports*. **1**, 11-19 (2003).

J Radel, J Homan, D Wallace, D Wetzel, S LeVine. FT-IR Microspectroscopic Chemical Analysis of Photoreceptor Outer Segment Changes Resulting from Oxidative Stress. *Invest. Opht. Vis. Sci.*. **41** (4), S23 (2000).

J Sweat, D Wetzel. Near Infrared Acousto-Optic Tunable Filter Based Instrumentation for the Measurement of Dynamic Spectra of Polymers. *Rev. Sci. Instrum.*. **72** (4), 2153-2158 (2001).

D Wetzel, A Eilert, J Sweat. Tunable Filter and Discrete Filter Near-IR Spectrometers. *Handbook of Vibrational Spectroscopy*, p. 436-452, Wiley, Chichester. (2002).

D Wetzel, S LeVine. Biological Applications of Infrared Microspectroscopy. *Infrared and Raman Spectroscopy of Biological Materials*, p. 101-142, Marcel Dekkar, New York. (2000).

D Wetzel, J Reffner. Infrared Spectroscopy goes Microscopic. *Chem. Ind.*. **9** (8), 308-313 (2000).

D Wetzel, P Srivarin, J Finney. Revealing Protein Infrared Spectral Detail in a Heterogenous Matrix Dominated by Starch. *Vib. Spectrosc.*. **31**, 109-114 (2003).

D Wetzel, S LeVine. Spatially Resolved Improved FT-IR Microspectroscopy of Deuterated Species in Tissue. *Microscopy and Microanalysis*, Vol 8, p. 1502, (2002).

D Wetzel, G Williams. Synchrotron Infrared Microspectroscopy of Retinal Layers. *Vib. Spectrosc.*. **30**, 101-109 (2002).

D Wetzel. A New Approach to the Problem of Dispersive Windows in Infrared Microspectroscopy. *Vib. Spectrosc.*. **29**, 291-297 (2002).

D Wetzel. Sensitive Infrared Narrow Band Optimized Microspectrometer. *Vib. Spectrosc.*. **29**, 291-297 (2002).

D Wetzel. Contemporary Near-Infrared Instrumentation. *Near Infrared Technology in the Agricultural and Food Industries*, p. 129-144, Am. Assoc. Cereal Chem., St. Paul. (2001).

Beamline U4B

M Harris, G Appel, H Ade. Surface Morphology of Annealed Polystyrene and Poly(methyl methacrylate) Thin Film Blends and Bilayers. *Macromolecules*. **36**, 3307-3314 (2003).

A Lussier, Y Idzerda, S Stadler, S Ogale, S Shinde, V Venkatesan. Characterization for Strontium Titanate/Fe3O4 and TiN/Fe3O4 Interfaces. *J. Vac. Sci. Technol., B*. **20** (4), 1609-1613 (2002).

Beamline U4IR

A Boris, D Munzar, N Kovaleva, B Liang, C Lin, A Dubroka, T Holden, B Keimer, C Bernhard, et al.. Josephson Plasma Resonanse and Phonon Anomalies in Trilayer Bi2Sr2Ca2Cu3O10. *Phys. Rev. Lett.*. **89** (27), 277001 (2002).

G Carr. Dynamics of GaAs photocarriers probed with pulsed infrared synchrotron radiation. *Nucl. Instrum. Meth. B*. **199**, 323 (2003).

G Flynn, L Keller. Synchrotron FTIR Examination of Interplanetary Dust Particles: An Effort to Determine the Compounds and Minerals in Interstellar and Circumstellar Dust. *Laboratory Astrophysics Workshop*, Vol NASA CP-2002-211863, p. 201-203, sponsored by NASA. (2002).

L Miller, G Smith, G Carr. Synchrotron-based Biological Microspectroscopy: From the Mid- to the Far-Infrared Regimes. *J. Biol. Phys.*. **29** (1), 219-230 (2003).

Beamline U5UA

I Baek, H Lee, H Kim, E Vescovo. Spin Reorientation Transition in Fe(110) Thin Films: The Role of Surface Anisotropy. *Phys. Lett. B*. **67**, 075401 (2003).

Beamline U7A

D Abraham, R Twesten, M Balasubramanian, J Kropf, D Fischer, J McBreen, I Petrov, K Amine. The Electrochemistry of Germanium Nitride with Lithium. *J. Electrochem. Soc.*. **150** (11), A1450-A1456 (2003).

L Andruzzi, W Senaratne, A Hexemer, C Ober, E Kramer. PEG-Based Biostable Surfaces by Controlled Radical Polymerization. *Polymeric Materials: Science & Engineering*, Vol 88, p. 604-605, sponsored by ACS. (2003).

R Bhat, J Genzer, B Chaney, H Sugg, A Liebmann-Vinson. Controlling the Assemblies of Nanoparticles using Molecular and Macromolecular Gradients. *Nanotech.*. **14**, 1145-1152 (2003).

R Bubeck, L Thomas, W Burghardt, S Rendon, A Hexemer, B Hart. Mechanical and Morphological Anisotropy in a Thermotropic Liquid Crystalline Polymer. *12th International Conference on Deformation, Yield, and Fracture of Polymers*, Vol 12, p. 155 - 158, sponsored by The Plastics and Rubber Division of the Institute of Materials, Minerals, and Mining. (2003).

J Genzer, D Fischer, K Efimenko. Combinatorial near-edge x-ray absorption fine structure: Simultaneous determination of molecular orientation and bond concentration on chemically heterogeneous surfaces. *Appl. Phys. Lett.*. **82**, 266 (2003).

J Genzer, K Efimenko, D Fischer. Molecular Orientation and Grafting Density in Semifluorinated Self-Assembled Monolayers of Mono-, Di-, and Trichloro Silanes on Silica Substrates. *Langmuir*. **18**, 9307-9311 (2002).

J Genzer, D Fischer, K Efimenko. Fabricating Two-Dimensional Molecular Gradients via Asymmetric Deformation of Uniformly-Coated Elastomer Sheets. *Advanced Materials*. **15** (18), 1545-1547 (2003).

J Genzer, E Kramer, D Fischer. Application of near-edge absorption fine structure (NEXAFS) to studies of surface molecular orientation of model organic molecules. *J. Appl. Phys.*. **92**, 7070 (2002).

S Kang, M Liang, X Li, F Chiellini, C Ober, E Kramer. Surface Active Block Copolymers (SABC): Biofouling Resistant Coatings from Chemically Modified Polymers. *Polymeric Materials: Science & Engineering*, Vol 84, p. 14-15, sponsored by ACS. (2001).

J Lenhart, R Jones, E Lin, C Soles, W Wu, S Sambasivan, D Goldfarb, M Angelopoulos. Probing Surface and Bulk Chemistry in Resist Films using near-edge x-ray absorption fine structure. *J. Vac. Sci. Technol., B*. **20** (6), 2920-2926 (2002).

Q Li, L Wu, Y Zhu, A Moodenbaugh, G Gu, M Suenaga, Z Ye, D Fischer. Comparitive studies fo MgB2/Mg Nano-composites and press-sintered MgB2 pellets. *IEEE Trans. Appl. Superconductivity*. **13**, 3051-3055 (2003).

X Li. Studies of Block Copolymers in Surface Engineering and Nanotechnology. Ph.D. Thesis. Cornell University, Ithaca. (2003).

G Liu, J Rodriguez, J Hrbek, B Long, D Chen. Interaction of Thiophene with Titania Surfaces. *J. Mol. Catal. A: Chem.*. **202**, 215-227 (2003).

P Liu, J Rodriguez, J Muckerman, J Hrbek. Interaction of CO, O, and S with metal nanoparticles on Au(111): A theoretical study. *Phys. Rev. B*. **67**, 155416-1-155416-10 (2003).

G Long, A Allen, D Black, H Burdette, D Fischer, R Spal, J Woicik. National Institute of Standards and Technology synchrotron radiation facilities for materials science. *J. Res - NIST*. **106**, 1141 (2002).

A Maiti, J Rodriguez, M Law, P Kung, J McKinney, P Yang. SnO2 Nanoribons as NO2 Sensors. *Nano Lett.*. **3**, 1025-1028 (2003).

A Marsh. Mechanisms of Deep Catalytic Oxidation of Aromatic Hydrocarbons on a Platinum Single Crystal Surface. Ph.D. Thesis. University of Michigan, Ann Arbor. (2003).

J McBreen, X Yang, M Balasubramanian, X Sun, H Lee. Synchrotron X-ray Studies of Lithium-Ion Battery Components. *The 43rd Battery Symposium in Japan*, Vol 2I, p. 46, sponsored by The Electrochemical Society of Japan. (2002).

G Meitzner, D Fischer. Distortions of fluoresence yield X-ray absorption spectra due to sample thickness. *Microchem. J.*. **71**, 281 (2002).

C Ober, J Youngblood, L Andruzzi, W Senaratne, X Li, A Hexemer, E Kramer. Block Copolymers as Surface Modifiers: Synthesis, Characterization and Relevance to Fouling Release and Biostability. *Polymeric Materials: Science & Engineering*, Vol 88, p. 612-613, sponsored by ACS. (2003).

D Pospiech, D Jehnichen, A Gottwald, L Häussler, U Scheler, P Friedel, W Kollig, C Ober, X Li, et al.. Investigation of the Microphase Separation in Semifluorinated Polyesters. *Polymeric Materials: Science & Engineering*, Vol 84, p. 314-315, sponsored by ACS. (2001).

J Rodriguez, P Liu, J Dvorak, T Jirsak, J Gomes, Y Takahashi, K Nakamura. Adsorption and decomposition of SO2 on TiC(001): An experimental and theoretical study. *Surf. Sci. Lett.*. **543**, L675-L682 (2003).

J Rodriguez, M Perez, T Jirsak, J Evans, J Hrbek, L Gonzalez. Activation of Au nanoparticles on oxide surfaces: reaction of SO2 with Au/MgO(100). *Chem. Phys. Lett.*. **378**, 526-532 (2003).

J Rodriguez, J Dvorak, T Jirsak, G Liu, J Hrbek, Y Aray, C Gonzalez. Coverage Effects and the Nature of the Metal-Sulfur Bond in S/Au(111): High Resolution Photoemission and Density-Functional Studies. *J. Am. Chem. Soc.*. **125**, 276-285 (2003).

W Senaratne, L Andruzzi, D Holowka, B Ilic, A Hexemer, B Baird, C Ober, E Kramer. Exploring the Potential of Surface Grown PEG-Polymer Brushes for Biotechnology Applications. *Polymeric Materials: Science & Engineering*, Vol 88, p. 337-338 , sponsored by ACS. (2003).

Z Song, T Cai, Z Chang, G Liu, J Rodriguez, J Hrbek. Molecular Level Study of the Formation and the Spread of MoO3 on Au (111) by Scanning Tunneling Microscopy and X-ray Photoelectron Spectroscopy. *J. Am. Chem. Soc.*. **125**, 8059-8066 (2003).

W Wallace, D Fischer. Resonant soft X-ray photofragmentation of propane. *J. Electron. Spectrosc. Relat. Phenom.*. **130**, 1-6 (2003).

T Wu, K Efimenko, P Vlcek, V Subr, J Genzer. Formation and Properties of Anchored Polymers with a Gradual Variation of Grafting Densities on Flat Substrates. *Macromolecules*. **36**, 2448-2453 (2003).

J Youngblood, L Andruzzi, C Ober, A Hexemer, E Kramer, J Callow, J Finley, M Callow. Coatings Based on Side-chain Ether-linked Poly(ethylene glycol) and Fluorocarbon Polymers for the Control of Marine Biofouling. *Biofouling*. **19** (supplement), 91-98 (2003).

Beamline U8B

K Miller. C-H and C-C Bond Activations of Organic Molecues by Stable Germylenes. Ph.D. Thesis. University of Michigan, Ann Arbor. (2002).

T Owens, S Süzer, M Banaszak Holl. Variable Energy X-ray Photoemission Studies of Alkylsilane Based Monolayers on Gold. *J. Phys. Chem. B*. **107** (14), 3177-3182 (2003).

K Schneider. Scanning Tunneling Microscopy Investigation of Spherosiloxane- and Alkylsilane-Based Monolayers. Ph.D. Thesis. University of Michigan, Ann Arbor. (2003).

K Schneider, K Nicholson, T Owens, B Orr, M Banaszak Holl. The differential reactivity of octahydridosilsesquioxane on Si(100)-2×1 and Si(111)-7×7: a comparitive experimental study. *Ultramicroscopy*. **97**, 35-43 (2003).

S Süzer, S Sayan, M Banaszak Holl, E Garfunkel, Z Hussain, N Hamdan. Soft X-ray photoemission studies of Hf oxidation. *J. Vac. Sci. Technol., A*. **21** (1), 106-109 (2003).

Beamline U10A

D Basov, A Bratkovsky, P Henning, B Zink, F Hellman, Y Wang, C Home, M Strongin. Infrared probe of metal-insulator transition in Si1-xGdx and Si1-xYx amorphous alloys in magnetic field. *Europhys. Lett.*. **57**, 240-246 (2002).

C Bernhard, T Holden, J Humlicek, D Munzar, A Golnik, M Klaser, T Wolf, L Carr, C Homes, et al.. In-plane polarized collective modes in detwined Yba2Cu3O6.95 observed by spectral ellipsometry. *Solid State Commun.*. **121**, 1963-1967 (2002).

C Homes, J Tranquada, Q Li, A Moodenbaugh. Mid-infrared conductivity from mid-gap states associated with charge stripes. *Phys. Rev. B*. **67**, 184516 (2003).
C Homes, Q Li, A Moodenbaugh, P Fournier, R Greene. Infrared optical properties of Pr2CuO4. *Phys. Rev. B: Condens. Matter*. **66**, 144511 (2002).
C Homes, T Vogt, S Shapiro, S Wakimoto, M Subramanian, A Ramirez. Charge transfer in high dielectric constant materials CaCu(3)Ti(4)O(12) and CdCu(3)Ti(4)O(12). *Phys. Rev. B: Condens. Matter*. **67**, 092106 (2003).
J Tu, C Homes, G Gu, D Basov, M Strongin. Optical studies of charge dynamics in the optimally doped Bi2Sr2CaCu2O8+delta. *Phys. Rev. B*. **66**, 144514 (2002).
J Tu, C Homes, G Gu, M Strongin. A systematic optical study of phonon properties in optimally doped Bi2Sr2CaCu2O8+delta. *Physica B*. **316-317**, 324-327 (2002).
G Tzamalis, N Zaidi, C Homes, A Monkman. Doping dependent studies of the Anderson-Mott localization in polyaniline at the metal-insulator boundary. *Phys. Rev. B*. **66**, 085202 (2002).

Beamline U10B

D Chidambaram, M Jaime Vasquez, G Halada, C Clayton. Studies on the repassivation behavior of aluminum and aluminum alloy exposed to chromate solutions. *Surf. Interface Anal.*. **35** (2), 226 (2003).
A Eilert, J Sweat, D Wetzel. Parabolic Concentration of Diffusely Transmitted Near-IR Radiation in an Acousto-Optic Tunable Filter Spectrometer. *J. Near Infrared Spectrosc.*. **8**, 239-250 (2000).
C Eng, G Halada, A Francis, C Dodge, J Gillow. Uranium Association with Corroding Carbon Steel Surfaces. *Surf. Interface Anal.*. **35**, 525-535 (2003).
S Federman, L Miller, I Sagi. Following Matrix Metalloproteinases Activity Near the Cell Boundary by Infrared Micro-Spectroscopy. *Matrix Biol.*. **21**, 567-577 (2002).
G Flynn, L Keller. Synchrotron FTIR Examination of Interplanetary Dust Particles: An Effort to Determine the Compounds and Minerals in Interstellar and Circumstellar Dust. *Laboratory Astrophysics Workshop*, Vol NASA CP-2002-211863 , p. 201-203, sponsored by NASA. (2002).
K Gough, D Zielinski, R Wiens, M Rak, I Dixon. Fourier transform infrared evaluation of microscopic scarring in the cardiomyopathic heart: Effect of chronic AT1 suppression. *Anal. Biochem.*. **316**, 232-242 (2003).
R Huang, L Miller, C Carlson, M Chance. FTIR Analysis of Tibia Bone from Ovariectomized Cynomolgus Monkeys (Macaca fascialaris) and the Effect of Nandrolone Deconoate Treatment. *Bone*. **30** (2), 492-497 (2002).
N Jamin, L Miller, J Moncuit, W Fridman, P Dumas, J Teillaud. Chemical Heterogeneity in Cell Death: Combined Synchrotron IR and Fluorescence Microscopy Studies of Single Apoptotic and Necrotic Cells. *Biopolymers*. **72** (5), 366-373 (2003).
V Joshi, R Powell, F Furuya, I Hainfeld. Metal carbonyl clusters as infrared labels for biosensing. *American Chemical Society National Meeting*, Vol Fall 2003, p. Inorg-73, sponsored by American Chemical Society. (2003).
S Judex, S Boyd, Y Qin, L Miller, R Muller, C Rubin. Combining High-Resolution MicroCT with Material Composition to Define the Quality of Bone Tissue. *Curr. Osteoporosis Reports*. **1**, 11-19 (2003).
A Lanzirotti, L Miller. Imaging and Microspectroscopy at the National Synchrotron Light Source. *Synch. Rad. News*. **15** (6), 17-26 (2003).
Y Mei, L Miller, W Gao, R Gross. Imaging the Distribution and Secondary Structure of Immobilized Enzymes using Infrared Microspectroscopy. *Biomacromolecules*. **4** (1), 70-74 (2003).
L Miller, P Dumas, N Jamin, J Teillaud, J Miklossy, L Forro. Combining IR Spectroscopy and Fluorescence Imaging in a Single Microscope: Biomedical Applications using a Synchrotron Infrared Source. *Rev. Sci. Instrum.*. **73**, 1357-1360 (2002).
L Miller, G Smith, G Carr. Synchrotron-based Biological Microspectroscopy: From the Mid- to the Far-Infrared Regimes. *J. Biol. Phys.*. **29** (1), 219-230 (2003).
L Miller, T Tague. Development and Biomedical Applications of Fluorescence-assisted Synchrotron Infrared Micro-Spectroscopy. *Vib. Spectrosc.*. **849**, 1-7 (2002).
J Radel, J Homan, D Wallace, D Wetzel, S LeVine. FT-IR Microspectroscopic Chemical Analysis of Photoreceptor Outer Segment Changes Resulting from Oxidative Stress. *Invest. Opht. Vis. Sci.*. **41** (4), S23 (2000).
D Wetzel, P Srivarin, J Finney. Revealing Protein Infrared Spectral Detail in a Heterogenous Matrix Dominated by Starch. *Vib. Spectrosc.*. **31**, 109-114 (2003).
D Wetzel, S LeVine. Biological Applications of Infrared Microspectroscopy. *Infrared and Raman Spectroscopy of Biological Materials*, p. 101-142, Marcel Dekkar, New York. (2000).
D Wetzel, J Reffner. Infrared Spectroscopy goes Microscopic. *Chem. Ind.*. **9** (8), 308-313 (2000).
P Yu, J McKinnon, C Christensen, D Christensen, N Marinkovic, L Miller. Chemical Imaging of Micro-Structures of Plant Tissues within Cellular Dimension Using Synchrotron Infrared Microspectroscopy. *J. Agr. Food Chem.*. **51** (20), 6062-6067 (2003).

Beamline U12A

K Adib, D Mullins, G Totir, N Camillone III, J Fitts, K Rim, G Flynn, R Osgood Jr. Dissociative adsorption of CCl4 on the Fe3O4(111)-(2x2) selvedge of alpha-Fe2O3(0001). *Surf. Sci.*. **524**, 113-128 (2003).

Beamline U12IR

S Kramer, B Podobedov. Coherent Microwave Synchrotron Radiation in the VUV Ring. *Proceedings of Eighth European Particle Accelerator Conference (EPAC'02)*, Vol , p. 1523, sponsored by EPAC-02. (2002).

Beamline U13UB

K Smith, J Xue, L Duda, A Fedorov, P Johnson, S Hulbert, W McCarroll, M Greenblatt. Recent high resolution photoemission studies of electronic structure in quasi-one dimensional conductors. *J. Electron. Spectrosc. Relat. Phenom.*. **117-118**, 517-526 (2001).

B Wells, Z Yusof, T Valla, A Fedorov, P Johnson, C Dendziora, S Jian, D Hinks. ARPES evidence for a quasiparticle liquid in overdoped Bi2Sr2CaCu2O8+delta. *Surf. Rev. Lett.*. **9** (2), 1091-1096 (2001).

Beamline X1A1

T Beetz, C Jacobsen. Soft X-ray Radiation-Damage Studies in PMMA using a Cryo-STXM. *J. Synch. Rad.*. **105**, 280-283 (2003).

G Flynn, L Keller, S Wirick, C Jacobsen, S Sutton. Analysis of interplanetary dust particles by soft and hard x-ray microscopy. *J. Phys. IV*. **104**, 367-372 (2003).

A Kilcoyne, T Tyliszczak, W Steele, S Fakra, P Hitchcock, K Franck, E Anderson, B Harteneck, E Rightor, et al. Interferometer-Controlled Scanning Transmission X-ray Microscopes at the Advanced Light Source. *J. Synch. Rad.*. **108**, 125-136 (2003).

J Rothe, M Plaschke, M Denecke. Soft x-ray spectromicroscopy investigation of the formation and ageing of Eu(III)-induced humic acid aggregates. *J. Phys. IV*. **104**, 421-424 (2003).

T Schaefer, F Claret, A Bauer, L Griffault, E Ferrage, B Lanson. Natural organic matter (NOM)-clay association and impact on Callovo-Oxfordian clay stability in high alkaline solution: Spectromicroscopic evidence. *J. Phys. IV*. **104**, 413-416 (2003).

T Schaefer, N Hertkorn, R Artinger, F Claret, A Bauer. Functional group analysis of natural organic colloids and clay association kinetics using C(1s) spectromicroscopy. *J. Phys. IV*. **104**, 409-412 (2003).

S Urquhart, H Ade. Trends in the Carbonyl Core (C 1s, O 1s) ® p*C=O Transition in the Near Edge X-ray Absorption Fine Structure Spectra of Organic Molecules. *J. Phys. Chem. B*. **106**, 8531-8538 (2002).

Beamline X1A2

T Schaefer, F Claret, A Bauer, L Griffault, E Ferrage, B Lanson. Natural organic matter (NOM)-clay association and impact on Callovo-Oxfordian clay stability in high alkaline solution: Spectromicroscopic evidence. *J. Phys. IV*. **104**, 413-416 (2003).

T Schaefer, N Hertkorn, R Artinger, F Claret, A Bauer. Functional group analysis of natural organic colloids and clay association kinetics using C(1s) spectromicroscopy. *J. Phys. IV*. **104**, 409-412 (2003).

Beamline X1B

T Beetz, C Jacobsen, C Kao, J Kirz, T Mentes, C Sanchez-Hanke, D Sayre, D Shapiro. Development of a Novel Apparatus for Experiments in Soft X-ray Diffraction Imaging and Diffraction Tomography. *J. Phys. IV*. **104**, 31-34 (2003).

U Hergenhahn, A Rüdel, K Maier, A Bradshaw, R Fink, A Wen. The Resonant Auger Spectra of Formic Acid, Acetaldehyde, Acetic Acid and Methyl formate. *Chem. Phys.*. **289**, 57-67 (2003).

C McGuinness, D Fu, J Downes, K Smith, G Hughes, J Roche. Electronic structure of thin film silicon oxynitrides measured using soft x-ray emission and absorption. *J. Appl. Phys.*. **94** (6), 3919-3922 (2003).

C McGuinness, J Downes, P Ryan, K Smith, D Doppalapudi, T Moustakas. X-ray Spectroscopic Studies of the Bulk Electronic Structure of InGaN Alloys. *GaN and Related Alloys, MRS Fall 2002 Meeting*, Vol 743, p. L10_11, sponsored by Materials Research Society. (2003).

Beamline X2B

R Seright, J Liang, B Lindquist, J Dunsmuir. Use of X-ray computed microtomography to understand why gels reduce relative permeability to water more than that to oil. *J. Petrol. Sci. Eng.*. **39**, 217-230 (2003).

Beamline X3A1

I Novozhilova, A Volkov, P Coppens. Theoretical Analysis of the Triplet Excited State of the [Pt2(H2P2O5)4]4- Ion and Comparison with Time-Resolved X-ray and Spectroscopic Results. *J. Am. Chem. Soc.*. **125**, 1079-1087 (2003).

J Overgaard, F Larsen, B Schiott, B Iverson. Electron Density Distributions of Redox Active Mixed Valence Carboxylate Bridged Trinuclear Iron Complexes. *J. Am. Chem. Soc.*. **125**, 11088-11099 (2003).

S Pillet, G Wu, V Kulsomphob, B Harvey, R Ernst, P Coppens. Investigation of Zr-C, Zr-N, and Potential Agostic Interactions in an Organozirconium Complex by Experimental Electron Density Analysis. *J. Am. Chem. Soc.*. **125**, 1937-1949 (2003).

Beamline X3A2

P Agarwal, R Somani, W Weng, A Mehta, L Yang, S Ran, L Liu, B Hsiao. Shear-Induced Crystallization in Novel Long Chain Branched Polypropylenes by in Situ Rheo-SAXS and -WAXD. *Macromolecules*. **36**, 5226-5235 (2003).

A Nogales, I Sics, T Ezquerra, Z Denchev, F Balta Calleja, B Hsiao. In-Situ Simultaneous Small- and Wide-Angle X-ray Scattering Study of Poly(ether ester) during Cold Drawing. *Macromolecules*. **36**, 4827-4832 (2003).

S Ran, Z Wang, C Burger, B Chu, B Hsiao. Mesophase as the Precursor for Strain-Induced Crystallization in Amorphous Poly(ethylene terephthalate) Film. *Macromolecules*. **35**, 10102-10107 (2002).

R Somani, L Yang, B Hsiao, P Agarwal, H Fruitwala, A Tsou. Shear-Induced Precursor Structures in Isotactic Polypropylene Melt by in-Situ Rheo-SAXS

and Rheo-WAXD Studies. *Macromolecules*. **35**, 9096-9104 (2002).

Beamline X3B1

M Bushey, T Nguyen, C Nuckolls. Synthesis, Self-Assembly, and Switching of One-Dimensional Nanostructures from New Crowded Aromatics. *J. Am. Chem. Soc.*. **125**, 8264-8269 (2003).

M Colle, R Dinnebier, W Brutting. The structure of the blue luminescent delta phase of tris(8-hydroxyquinoline)aluminum(III) (Alq3). *Chem. Commun.*. **2002**, 2908-2909 (2002).

R Dinnebier, S Vensky, M Panthöfer, M Jansen. Crystal and Molecular Structures of Alkali Oxalates - First Proof of a Staggered Oxalate Anion in the Solid State. *Z. Kristallogr.*. (Suppl. Iss. 20), 86 (2003).

R Dinnebier, S Vensky, M Panthöfer, M Jansen. Crystal and Molecular Structures of Alkali Oxalates: First Proof of a Staggered Oxalate Anion in the Solid State. *Inorg. Chem.*. **42** (5), 1499-1507 (2003).

A Le Bail, P Stephens, H Hubert. A crystal structure for the souzalite/gormanite series from synchrotron powder diffraction data. *Eur. J. Mineral.*. **15** (4), 719-723 (2003).

O Omotoso, R Mikula, P Stephens. Surface area of interstratified phyllosilicates in Athabasca oil sands from synchrotron XRD. *Advances in X-ray Analysis*, Vol 54, p. 391-396, sponsored by International Centre for Diffraction Data. (2002).

M Rajeswaran, T Blanton, N Zumbulyadis, D Giesen, C Conesa-Moratilla, S Misture, P Stephens, A Huq. Three-dimensional Structure Determination of N-(p-Tolyl)-dodecylsulfonamide from Powder Diffraction Data and Validation of Structure using Solid-State NMR Spectroscopy. *J. Am. Chem. Soc.*. **124**, 14450-14459 (2002).

M Viola, M Martinez-Lopez, J Alonso, J Martinez, J De Paoli, S Pagola, J Pedregosa, M Fernandez-Diaz, R Carbonio. Structure and Magnetic Properties of Sr2CoWO6: An Ordered Double Perovskite Containing Co2+(HS) with Unquenched Orbital Magnetic Moment. *Chem. Mater.*. **15**, 1655-1663 (2003).

Beamline X4A

M Aittaleb, R Rashid, Q Chen, J Palmer, C Daniels, H Li. Structure and Function of Archaeal Box C/D sRNP Core Proteins. *Nat. Struct. Biol.*. **106** (45), 256 (2003).

N Armstrong, M Mayer, E Gouaux. Tuning activation of the AMPA-sensitive GluR2 ion channel by genetic adjustment of agonist-induced conformational changes. *Proc Natl Acad Sci USA*. **100** (10), 5736-5741 (2003).

Y Chi, J Frantz, B Oh, L Hansen, S Shoelson. Diabetes mutations delineate an atypical POU domain in HNF1a.. *Mol. Cell*. **10**, 1129 (2002).

H Cho, K Mason, K Ramyar, A Stanley, S Gabelli, D Denney, D Leahy. Structure of the Extracellular Region of HER2 Alone and in Complex with the Herceptin Fab. *Nature*. **421**, 756-760 (2003).

N Friedland, H Liou, P Lobel, A Stock. Structure of a Cholesterol-Binding Protein Deficient in Niemann-Pick Type C2 Disease. *Proc Natl Acad Sci USA*. **100** (5), 2512-2517 (2003).

H Furukawa, E Gouaux. Mechanisms of activation, inhibition and specificity: crystal structures of the NMDA receptor NR1 ligand-binding core. *EMBO J.*. **22** (12), 2873-2885 (2003).

A Gogos, L Shapiro. Large Conformational Changes in the Catalytic Cycle of Glutathione Synthase. *Structure*. **10** (12), 1669-1676 (2002).

J Hunt, J Deisenhofer. Ping-Pong Cross-Validation in Real Space: a Method for Increasing the Phasing Power of a Partial Model Without Risk of Model Bias. *Acta Cryst. D*. **59**, 214-224 (2003).

R Jin, M Horning, M Mayer, E Gouaux. Mechanism of Activation and Selectivity in a Ligand-Gated Ion Channel: Structural and Functional Studies of GluR2 and Quisqualate. *Biochemistry*. **41**, 15635-15643 (2002).

R Jin, E Gouaux. Probing the Function, Conformational Plasticity, and Dimer-Dimer Contacts of the G1uR2 Ligand-Binding Core: Studies of 5-Substituted Willardiines and G1uR2 S1S2 in the Crystal. *Biochemistry*. **42**, 5201-5213 (2003).

G Jogl, L Tong. Crystal Structure of Carnitine Acetyltransferase and Implications for the Catalytic Mechanism and Fatty Acid Transport. *Cell*. **112**, 113-122 (2003).

Z Juo, G Kassavetis, J Wang, E Geiduschek, P Sigler. Crystal structure of a transcription factor IIIB core interface ternary complex. *Nature*. **422**, 534-539 (2003).

R Khayat, R Batra, C Qian, T Halmos, M Bailey, L Tong. Structural and Biochemical Studies of Inhibitor Binding to Human Cytomegalovirus Protease. *Biochemistry*. **42**, 885-891 (2003).

S Lahiri, G Zhang, D Dunaway-Mariano, K Allen. The Pentacovalent Phosphorus Intermediate of a Phosphoryl Transfer Reaction. *Science*. **299**, 2067 (2003).

I Levchenko, R Grant, D Wah, R Sauer, T Baker. Structure of a Delivery Protein for an AAA+ Protease in Complex with a Peptide Degradation Tag. *Mol. Cell*. **12**, 365-372 (2003).

S Majeed, G Ofek, A Belachew, C Huang, T Zhou, P Kwong. Enhancing Protein Crystallization Through Precipitant Synergy. *Structure*. **11**, 1061-1070 (2003).

Y Mao, J Chen, J Maynard, B Zhang, F Quiocho. A Novel A; Helix Fold of the AP180 Amino-Terminal Domain for Phoshoinositide. *Cell*. **104**, 433-440 (2001).

K Murthy, S Smith, V Ganesh, K Judge, N Mullin, P Barlow, C Ogata, G Kotwal. Crystal Structure of a Complement Control Protein that Regulates Both Pathways of Complement Activation and Binds Heparan Sulfate Proteoglycans. *Cell*. **104**, 301-311 (2001).

R Nagem, D Colau, L Dumoutier, J Renauld, C Ogata, I Polikarpov. Crystal Structure of Recombinant Human Interleukin-22. *Structure*. **10**, 1051-1062 (2002).

V Robinson, T Wu, A Stock. Structural analysis of the domain interface in DrrB, a response regulator of the OmpR/PhoB subfamily. *J. Bacteriol.*. **185** (14), 4186-4194 (2003).

V Robinson, J Hwang, E Fox, M Inouye, A Stock. Domain Arrangement of Der, a Switch Protein

Containing Two GTPase Domains.. *Structure*. **10** (12), 1649 (2002).

S Santagata, T Boggon, C Baird, C Gomez, J Zhao, W Shan, D Myszka, L Shapiro. G-Protein Signaling Through Tubby Proteins. *Science*. **292**, 2041-2050 (2001).

T Schwartz, G Blobel. Structural Basis for the Function of the beta Subunit of the Eukaryotic Signal Recognition Particle Receptor. *Cell*. **112** (6), 793-803 (2003).

I Shumilin, R Bauerle, R Kretsinger. The High-Resolution Structure of 3-Deoxy-D-arabino-heptulosonate-7-phosphate Synthase Reveals a Twist in the Plane of Bound Phosphoenolypyruvate. *Biochemistry*. **42**, 3766-3776 (2003).

S Sia, P Carr, A Cochran, V Malashkevich, P Kim. Short Constrained Peptides that Inhibit HIV-1 Entry. *Proc Natl Acad Sci USA*. **99** (23), 14664-14669 (2002).

X Tao, Y Xu, Y Zhang, A Beg, L Tong. An Extensively Associated Dimer in the Structure of the C713S Mutant of the TIR Domain of Human TLR2. *Biochem. Biophys. Res. Commun.*. **299**, 216-221 (2002).

A VanDemark, R Hofmann, C Tsui, C Pickart, C Wolberger. Molecular Insights into Polyubiquitin Chain Assembly:Crystal Structure of the Mms2/Ubc13 Heterodimer. *Cell*. **105**, 711-720 (2001).

H Yamaguchi, H Matsushita, A Nairn, J Kuriyan. Crystal Structure of the Atypical Protein Kinase Domain of a TRP Channel with Phophtransferase activity. *Mol. Cell*. **7**, 1047-1057 (2001).

B Yeh, M Igarashi, A Eliseenkova, A Plotnikov, I Sher, D Ron, S Aaronson, M Mohammadi. Structural Basis by Which Alternative Splicing Confers Specificity in Fibroblast Growth Factor Receptors. *Proc Natl Acad Sci USA*. **100** (5), 2266-2271 (2003).

Y Yuan, O Martsinkevich, J Hunt. Structural Characterizatin of an MJ1267 ATP-Binding Cassette Crystal with a Complex Pattern Twinning Caused by Promiscuous Fiber Packing. *Acta Cryst. D*. **59**, 225-238 (2003).

H Zhang, Z Yang, Y Shen, L Tong. Crystal Structure of the Carboxyltransferase Domain of Acetyl-Coenzyme A Carboxylase. *Science*. **299**, 2064 (2003).

Beamline X6A

J James, C Escalante, M Yoon-Robarts, T Edwards, R Linden, A Aggarwai. Crystal Structure of the SF3 Helicase from Adeno-Associated Virus Type 2. *Structure*. **11**, 1025-1035 (2003).

L Kang, S Gabelli, M Bianchet, W Xu, M Bessman, L Amzel. Structure of a coenzyme A pyrophosphatase from Deinococcus radiodurans: a member of the Nudix family. *J. Bacteriol.*. **185** (14), 4110-9 (2003).

Beamline X6B

A Mateja, Y Devedjiev, D Krowarsch, K Longenecker, Z Dauter, J Otlewski, Z Derewenda. The Impact of Glu>Ala and Glu>Asp Mutations on the Crystallization Properties of RhoGDI: The Structure of RhoGDI at 1.3 A Resolution. *Acta Cryst. D*. **58**, 1983-1991 (2002).

Beamline X7A

P Barnes, P Woodward, Y Lee, T Vogt, J Hriljac. Pressure-Induced Cation Migration and Volume Expansion in the Defect Pyrochlores ANbWO6 (A = NH4+, Rb+, H+m K+). *J. Am. Chem. Soc.*. **125**, 4572-4579 (2003).

A Burton, S Elomari, R Medrud, I Chan, C Chen, L Bull, E Vittoratos. The Synthesis, Characterization, and Structure Solution of SSZ-58: A Novel Two-Dimensional 10-Ring Pore Zeolite with Previously Unseen Double 5-Ring Subunits. *J. Am. Chem. Soc.*. **125**, 1633-1642 (2003).

W Dmowski, T Egami, K Swider-Lyons, C Love, D Rolison. Local Atomic Structure and Conduction Mechanism of Nanocrystalline Hydrous RuO2 from X-ray Scattering. *J. Phys. Chem. B*. **106**, 12677-12683 (2002).

E Irran, B Juergens, W Schnick. Synthesis, Crystal Structure Determination from X-ray Powder Diffractometry and Vibrational Spectroscopy of the Tricyanomelaminate Monohydrates M3[C6N9].H2O (M=K,Rb). *Solid State Sci.*. **4**, 1305-1311 (2002).

H Jeong, S Nair, T Vogt, L Dickinson, M Tsapatsis. A highly crystalline layered silicate with three dimensionally microporous layers. *Nat. Mater.*. **2**, 53-58 (2003).

J Lai, K Shafi, K Loos, A Ulman, Y Lee, T Vogt, C Estrones. Doping gamma-Fe2O3 Nanoparticles with Mn(III) Suppresses the Transition to the alpha-Fe2O3 Structure. *J. Am. Chem. Soc.*. **125**, 11470-11471 (2003).

Y Lee, D Mitzi, P Barnes, T Vogt. Pressure-Induced Phase Transitions and Templating Effect in Three-Dimensional Organic-Inorganic Hybrid Perovskites. *Phys. Rev. B: Condens. Matter*. **68**, 020103R (2003).

Y Lee, T Vogt, J Hriljac, J Parise, J Hanson, S Kim. Non-Framework Cation Migration and Irreversible Pressure-induced Hydration in a Zeolite. *Nature*. **420**, 485 (2002).

N Pereira, M Balasubramanian, L Dupont, J McBreen, L Klein, G Amatucci. The Electrochemistry of Germanium Nitride with Lithium. *J. Electrochem. Soc.*. **150** (8), A1118-A1128 (2003).

V Petkov, S Billinge, T Vogt, A Ichimura, J Dye. Structure of Intercalated Cs in Zeolite ITQ-4:An Array of Metal Ions and Correlated Electrons Confined in a Pseudo-1D Nanoporous Host. *Phys. Rev. Lett.*. **89**, 075502 (2002).

V Petkov, S Billinge, P Larson, S Mahanti, T Vogt, K Rangan, M Kanatzidis. Structure of Nanocrystalline Materials using Atomic Pair Distribution Function Analysis: Study of LiMoS2. *Phys. Rev. B*. **65**, 092105 (2002).

T Vogt, J Hriljac, N Hyatt, P Woodward. Pressure-induced intermediate-to-low spin state transition in LOaCoO3. *Phys. Rev. B*. **67**, 140401-1 - 140401-4 (2003).

X Yang, J McBreen, W Yoon, M Yoshio, H Wang, K Fukuda, T Umeno. Structural Studies of the New Carbon Coated Silicon Anode Using Synchrotron Based In Situ XRD. *Electrochem. Commun.*. **4** (11), 893-897 (2002).

Beamline X7B

A Christensen, T Jensen, N Scarlett, I Madsen. n-situ X-ray powder diffraction studies of hydrothermal and themal decomposition reactions of basic bismuth(III) nitrates in the temperature range 20-650C. *Dalton Trans.*. **16**, 3278-3282 (2003).

A Christensen, N Scarlett, I Madsen, T Jensen, J Hanson. Real Time study of cement and clinker phases hydration. *Dalton Trans.*. **2003**, 1529-1536 (2003).

P Chupas, D Corbin, V Rao, J Hanson, C Grey. A Combined Solid-State NMR and Diffraction Study of the Structures and Acidity of Fluorinated Aluminas: Implications for Catalysis. *J. Phys. Chem. B*. **107**, 8327-8336 (2003).

P Devi, Y Lee, J Margolis, J Parise, S Samath, H Herman, J Hanson. Comparison of citrate-nitrate gel combustion and precursor plasma spray processes for the synthesis of yttrium aluminum garnet. *J. Mater. Res.*. **17**, 2846-2851 (2002).

G Evans, R Fureaux, G Gainsford, J Hanson, G Kicska, A Sauve, V Schram, P Tyler. "8-Aza-Immuncillins as Transition State analogue Inhibitors of Purine Nucleoside Phosphorylase and Nucleoside Hydrolases. *J. Med. Chem.*. **46**, 155-160 (2003).

M Khoudiakov, A Parise, B Brunschwig. Interfacial Electron Transfer in FeII(CN)64-Sensitized TiO2 Nanoparticles: A Study of Direct Charge Injection by Electroabsorption Spectroscopy. *J. Am. Chem. Soc.*. **125**, 4637-4642 (2003).

J Kim, J Rodriquez, J Hanson, A Frenkel, P Lee. Reduction of CuO and Cu2O with H2: H Embedding and Kinetic Effects in the Formation of Suboxides. *J. Am. Chem. Soc.*. **125**, 10684-16092 (2003).

J Post, P Heany, J Hanson. Synchrotron x-ray diffraction study of the structure and dehydration behavior of todorokite. *Am. Mineral.*. **88**, 141-151 (2003).

J Post, P Heaney, R Von Dreele, J Hanson. Neutron and temperature-resolved synchrotron X-ray powder diffraction study of akaganeite. *Am. Mineral.*. **88**, 782-788 (2003).

J Rodriguez, X Wang, J Hanson, G Liu, A Iglesias-Juez, M Fernandez-Garcia. The behavior of mixed-metal oxides: Structural and electronic properties of Ce-Ca oxides. *J. Chem. Phys.*. **119**, 5659-5669 (2003).

J Rodriguez, J Kim, J Hanson, M Perez, A Frenkel. Reduction of CuO in H2: In Situ Time-Resolved XRD Studies. *Catal. Lett.*. **85**, 247-254 (2003).

J Rodriguez, J Kim, J Hanson, J Brito. Reduction of CoMoO4 and NiMoO4: In situ Time-Resolved XRD Studies. *Catal. Lett.*. **82** (1-2), 103-109 (2002).

J Rodriguez, J Kim, J Hanson, S Sawhill, M Bussell. Physical and Chemical Properties of MoP, Ni2P, and MoNiP Hydrodesulfurization Catalysts: Time-Resolved X-ray Diffractin, Density Functional, and Hydrodesulfurization Activity Studies. *J. Phys. Chem. B*. **107**, 6276-6285 (2003).

R Sullivan, H Liu, D Smith, J Hanson, D Osterhout, M Ciraolo, C Grey, J Martin. Sorptive Reconstruction of the CuAlCl4 Framework upon Reversible Ethylene Binding. *J. Am. Chem. Soc.*. **125**, 11065-11079 (2003).

J Wang, S Brankovic, Y Zhu, J Hanson, R Adzic. Kinetic Characterization of PtRu Fuel Cell Anode Catalysts Made by Spontaneous Pt Decomposition on Ru Nanoparticles. *J. Electrochem. Soc.*. **150**, a1108-a1117 (2003).

Beamline X8C

I Bosanac, J Alattia, T Mal, J Chan, S Talarico, F Tong, K Tong, F Yoshikawa, T Furuichi, et al. Structure of the Inositol 1,4,5-trisphosphate Receptor Binding Core in Complex with its Ligand. *Nature*. **420**, 696 (2002).

J Elam, A Taylor, R Strange, S Antonyuk, P Doucette, J Rodriguez, S Hasnain, L Hayward, J Selverston Valentine, et al. Amyloid-like Filaments and Water-filled Nanotubes formed by SOD1 Mutant Proteins Linked to Familial ALS. *Nat. Struct. Biol.*. **10** (6), 461-467 (2003).

S Eswaramoorthy, S Gerchman, V Graziano, H Kycia, F Studier, S Swaminathan. Structure of a Yeast Hypothetical Protein Selected by a Structural Genomics Approach. *Acta Cryst. D*. **59**, 127-135 (2003).

J Jiang, A Taylor, K Prasad, Y Ishikawa-Brush, P Hart, E Lafer, R Sousa. Structure-Function Analysis of the Auxilin J-Domain Reveals an Extended Hsc70 Interaction Interface. *Biochemistry*. **42**, 5748-5753 (2003).

V Kacer, S Scaringe, J Scarsdale, J Rife. Crystal Structures of r(GGUCACAGCCC)2. *Acta Cryst. D*. **59**, 423-432 (2003).

C Kerfeld, M Sawaya, V Brahmandam, D Cascio, K Ho, C Trevithick-Sutton, D Krogmann, T Yeates. The Crystal Structure of a Cyanobacterial Water-Soluble Carotenoid Binding Protein. *Structure*. **11**, 55-65 (2003).

P Kongsaeree, C Samanchart, P Laowanapiban, S Wiyakrutta, V Meevootisom. Crystallization and Preliminary X-ray Crystallographic Analysis of D-Phenylglycine Aminotransferase from Pseudomonas Stutzeri ST201. *Acta Cryst. D*. **59**, 953-954 (2003).

P Lario, A Vrielink. Sub-atomic resolution crystal structure of cholesterol oxidase: what atomic resolution crystallography reveals about enzyme mechanism and the role of the FAD cofactor in redox activity.. *J. Mol. Biol.*. **326** (5), 1635-50 (2003).

Y Lee, S Nadaraia, D Gu, D Becker, J Tanner. Structure of the Proline Dehydrogenase Domain of the Multifunctional PutA Flavoprotein. *Nat. Struct. Biol.*. **10** (2), 109 (2003).

J Liu, A Dermatakis, C Lukacs, F Konzelmann, Y Chen, U Kammlott, W Depinto, H Yang, X Yin, et al.. 3,5,6-Trisubstituted naphthostyrils as CDK2 inhibitors.. *BioOrg. Med. Chem.*. **13** (15), 2465-8 (2003).

C Mura, M Philips, A Kozhukhovsky, D Eisenberg. Structure and assembly of an augmented Sm-like archaeal protein 14-mer. *Proc Natl Acad Sci USA*. **100** (8), 4539-4544 (2003).

V Namboodiri, S Dutta, I Akey, J Head, C Akey. The Crystal Structure of Drosophila NLP-Core Porvids Insight into Pentamer Formation and Histone Binding. *Structure*. **11**, 175-186 (2003).

G Pal, T DeVeyra, J Elce, Z Jia. Purification, Crystallization and Preliminary X-ray Analysis of a u-like Calpain. *Acta Cryst. D*. **59**, 369-371 (2003).

X Qian, C Guan, H Guo. A Dual Role for an Aspartic Acid in Glycosylasparaginase Autoproteolysis. *Structure*. **11**, 997-1003 (2003).

M Sam, D Cascio, R Johnson, R Clubb. Crystallization and Prelimnary X-ray Crystallographic Analysis of the Excisionase-DNA Complex from Bacteriophage. *Acta Cryst. D*. **59**, 1238-1240 (2003).

X Yang, Y Hu, D Yin, M Turner, M Wang, R Borchardt, P Howell, K Kuczera, R Schowen. Catalytic Strategy of S-Adenosyl-L-homocysteine Hydrolase: Transition-State Stabilization and the Avoidance of Abortive Reactions. *Biochemistry*. **42**, 1900-1909 (2003).

J Yang, M Park, G Waldo, S Suh. Directed Evolution Approach to a Structural Genomics Project: Rv2002 from Mycobacterium tuberculosis. *Proc Natl Acad Sci USA*. **100** (2), 455-460 (2003).

Z Yang, C Lanks, L Tong. Molecular Mechanism for the Regulation of Human Mitochondrial NAD(P)+ - Dependent Malic Enzyme by ATP and Fumarate. *Structure*. **10**, 951-960 (2002).

Beamline X9A

C Albermann, A Soriano, J Jiang, H Vollmer, J Biggins, W Barton, J Lesniak, D Nikolov, J Thorson. Substrate Specificity of NovM: Implications for Novobiocin Biosynthesis and Glycorandomization. *Org. Lett.*. **5**, 933-936 (2003).

W Barton, B Liu, D Tzvetkova, P Jeffreey, A Fournier, D Sah, R Cate, S Strittmatter, D Nikolov. Structure and Axon Outgrowth Inhibitor Binding of the Nogo-66 Receptor and Related Proteins. *EMBO J.*. **22**, 3291-3302 (2003).

A Bobkov, A Muhlrad, K Kokabi, S Vorobiev, S Almo, E Reisler. Structural Effects of Cofilin on Longitudinal Contacts in F-Actin. *J. Mol. Biol.*. **323**, 739-750 (2002).

J Bonanno, S Burley. Structural Genomics of Proteins Contributing to Conserved Biochemical Pathways/Processes. *Curr. Opin. Struct. Biol.*. **12**, 383-391 (2002).

S Burley, J Bonanno. Structural Genomics. *Structural Bioinformatics*, p. 591-612, Academic Press, New York. (2002).

S Burley, J Bonanno. Structuring the Universe of Proteins. *Annu. Rev. Genomics and Human Genetics*. **3**, 243-262 (2002).

F Burling, R Kniewel, J Buglino, T Chadha, A Beckwith, C Lima. Structure of Escherichia Coli Uridine Phosphorylase at 2.0 Angstrom. *Acta Cryst. D*. **59**, 73-76 (2003).

E Campbell, J Tupy, T Gruber, S Wang, M Sharp, C Gross, S Darst. Crystal Structure of Escherichia Coli E with the Cytoplasmic Domain of its anti-RseA. *Mol. Cell*. **11**, 1067-078 (2003).

W Chan, S Roderick, D Cohen. Human Phosphatidylcholine Transfer Protein: Purification, Crystallization and Preliminary X-ray Diffraction. *Biochim Biophys Acta*. **1596** (1), 1-5 (2002).

J Coyle, D Nikolov. GABARAP: Lessons for Synaptogenesis. *The Neuroscientist*. **9**, 205-216 (2003).

A Deaconescu, A Roll-Mecak, S Gerchman, H Kycia, F Studier, J Bonanno, S Burley. X-Ray Structure of Saccharomyces Cerevisiae Homologous Mitochondrial Matrix Factor 1 (Hmf1). *Proteins: Struc. Func. Genet.*. **48**, 431-436 (2002).

J Dewan, A Feeling-Taylor, Y Puius, L Patskovska, Y Patskovsky, R Nagel, S Almo, R Hirsch. Structure of Mutant Human Carbonmonoxyhemoglobin C (betaE6K) at 2.0 A Resolution. *Acta Cryst. D*. **58**, 2038-2042 (2002).

C Fabrega, S Shuman, C Lima. Structure of Candida Albicans mRNA Guanylytransferase Bound to Phosphorylated CTD of RNA Polymerase II. *Mol. Cell*. **11**, 1549-1561 (2003).

C Groft, S Burley. Recognition of eIF4G by Rotavirus NSP3 Reveals a Basis for mRNA Circularization. *Mol. Cell*. **6**, 1273-1283 (2002).

J Himanen, D Nikolov. In Focus: Eph Receptors and Ephrins. *N/A*. **35**, 130-134 (2003).

J Himanen, D Nikolov. Eph Receptors and Ephrins a Structural View. *Trends Neurosci.*. **26**, 46-51 (2003).

W Joo, P Jeffrey, S Cantor, M Finnin, D Livingston, N Pavletich. Structure of the 53BP1 BRCT Region Bound to p53 and its Comparison to the Brcal BRCT Structure. *Genes Dev.*. **16**, 583-593 (2002).

K Kamada, F Hanoaka, S Burley. Crystal Structure of the MazE/MazF Complex: Molecular Bases of Antidote-Toxin Recognition. *Mol. Cell*. **11**, 875-884 (2003).

K Kamada, R Roeder, S Burley. Molecular Mechanism of Recruitment of TFIIF - Associating RNA Polymerase C-Terminal Domain Phosphatase (FCP1) by Transcription Factor IIF. *Proc Natl Acad Sci USA*. **100** (5), 2296-2299 (2003).

G Kicska, P Tyler, G Evans, R Furneaux, W Shi, A Fedorov, A Lewandowicz, S Cahill, S Almo, V Schramm. Atomic Dissection of the Hydrogen Bond Network for Transition-State Analogue Binding to Purine Nucleoside Phosphorylase. *Biochemistry*. **41**, 14489-14498 (2002).

R Kniewel, J Buglino, V Shen, T Chadna, A Beckwith, C Lima. Structural Analysis of Saccharomyces Cerevisiae Myo-Inositol Phosphate Synthase. *J. Struct. Funct. Genomics*. **3**, 129-134 (2002).

A Larsson, R Andersson, J Stahlberg, L Kenne, T Jones. Dextranase from Penicillium minioluteum: Reactin Course, Crystal Structure, and Product Complex. *Structure*. **11**, 1111-1121 (2003).

J Lesniak, W Barton, D Nikolov. Structural and Functional Characterization of the Pseudomonas Hydroperoxide Resistance Protein Ohr. *EMBO J.*. **21** (24), 6649-6659 (2002).

A Lewandowicz, W Shi, G Evans, P Tyler, R Furneaux, L Basso, D Santos, S Almo, V Schramm. Over-the-Barrier Transition State Analogues and Crystal Structure with Mycobacterium Tuberculosis Purine Nucleoside Phosphorylase. *Biochemistry*. **42**, 6057-6066 (2003).

M Lilic, V Galkin, A Orlova, M VanLoock, E Egelman, C Stebbins. Salmonella SipA Polymerizes Actin by Stapling Filaments with Nonglobular Protein Arms. *Science*. **301**, 1918-1921 (2003).

E Mossessova, L Bickford, J Goldberg. SNARE Selectivity of the COPII Coat. *Cell*. **114**, 483-495 (2003).

S Nair, S Burley. X-ray Structures of Myc-Max and Mad-Max Recognizing DNA: Molecular Bases of Regulation by Proto-Oncogenic Transcription Factors. *Cell*. **112**, 193-205 (2003).

A Niedzwiecka, J Marcotrigiano, J Stepinski, M Jankowska-Anyszka, A Wyslouch-Cieszynska, M Dadlez, A Gingras, P Mak, E Darzynkiewicz, et al.. Biophysical studies of eIF4E Cap-Binding Protein: Recognition of mRNA 5' Cap Structure and Synthetic Fragments of eIF4G and 4E-BP1 Proteins. *J. Mol. Biol.*. **319**, 615-635 (2002).

M Perbandt, E Guthohrlein, W Rypniewski, K Idakieva, S Stoeva, W Voelter, N Genov, C Betzel. The Structure of a Functional Unit from the Wall of a Gastropod Hemocyanin Offers a Possible Mechanism for Cooperativity. *Biochemistry*. **42**, 6341-6346 (2003).

D Pilloff, K Dabovic, M Romanowski, J Bonanno, M Doherty, S Burley, T Lehy. The Kinetic Mechanism of Phosphomevalonate Kinase. *J. Biol. Chem.*. **278**, 4510-4514 (2003).

S Ray, J Bonanno, H Chen, S Wu, H De Lencastre, A Tomasz, S Burley. Crystal Structure of a Methanococcus Jannaschii DNA-Binding Protein: Implications for Antibiotic Resistance in Staphyloccoccus Aureus. *Proteins: Struc. Func. Genet.*. **50**, 170-173 (2003).

K Schneibner, J DeAngelis, S Burley, P Cole. Investigation of the Roles of Catalytic Residues in Serotonin N-Acetyltransferase. *J. Biol. Chem.*. **277**, 18118-18126 (2002).

T Schwartz, G Blobel. Structural Basis for the Function of the beta Subunit of the Eukaryotic Signal Recognition Particle Receptor. *Cell*. **112** (6), 793-803 (2003).

W Shi, D Ostrov, S Gerchman, H Kycia, W Studier, W Edstrom, A Bresnick, J Ehrlich, J Blanchard, et al. High-Throughput Structural Biology & Proteomics. *Protein Arrays, Biochips & Proteomics: The Next Phase of Genomics Discovery*, p. 299-324, Marcel Dekker, New York. (2003).

B Shin, D Maag, A Roll-Mecak, M Arefin, S Burley, J Lorsch, T Dever. Uncoupling of Initiation Factor eIF5B/IF2 GTPase and Translational Activities by Mutations that Lower Ribosome Affinity. *Cell*. **111**, 1015-1025 (2002).

R Soccio, R Adams, M Romanowski, E Sehayek, S Burley, J Breslow. The Novel Cholesterol-Regulated StarD4 Gene Encodes a StAR-Related Lipid Transfer Protein with two Closely Related Homologues. *Proc Natl Acad Sci USA*. **99**, 6943-6948 (2002).

J Sun, A Fedorov, S Lee, X Guo, K Shen, D Lawrence, S Almo, Z Zhang. Crystal Structure of PTP1B Complexed with a Potent and Selective Bidentate Inhibitor. *J. Biol. Chem.*. **278**, 12406-12414 (2003).

J Sun, L Wu, A Fedorov, S Almo, Z Zhang. Crystal Structure of the Yersinia Protein-Tyrosine Phosphatase YopH Complexed with a Specific Small Molecule Inhibitor. *J. Biol. Chem.*. **278**, 33392-33399 (2003).

Y Tseng, B Schafer, S Almo, D Wirtz. Functional Synergy of Actin Filament Cross-Linking Proteins. *J. Biol. Chem.*. **277**, 25609-25616 (2002).

S Vorobiev, B Strokopytov, D Drubin, C Frieden, S Ono, J Condeelis, P Rubenstein, S Almo. The Structure of Non-Vertebrate Actin: Implications for the ATP Hydrolytic Mechanism. *Proc Natl Acad Sci USA*. **100** (10), 5760-5765 (2003).

E Wolf, J De Angelis, E Khalil, P Cole, S Burley. X-Ray Crystallographic Studies of Serotonin N-Acetyltransferase Catalysis and Inhibition. *J. Mol. Biol.*. **317**, 215-224 (2002).

G Wu, G Xu, B Schulman, P Jeffrey, J Harper, N Pavletich. Structure of a Beta-TrCPI-Skp1-Beta-Catenin Complex: Destruction Motif Binding and Lysine Specificity of the SCF(beta-TrCP1) Ubiquitin Ligase. *Mol. Cell*. **6**, 1445-1456 (2003).

X Zhang, J Schwartz, S Almo, S Nathenson. Expression, Refolding, Purification, Molecular Characterization, Crystallization and Preliminary X-Ray Analysis of the Receptor Binding Domain of Human B7-2. *Protein Expr. Purif.*. **25**, 105-113 (2003).

X Zhang, J Schwartz, S Almo, S Nathenson. Crystal Structure of the Receptor-Binding Domain of Human B7-2: Insights into Organization and Signaling. *Proc Natl Acad Sci USA*. **100** (5), 2586-2591 (2003).

Beamline X9B

M Andrykovitch, K Routzahn, M Li, Y Gu, D Waugh, X Ji. Characterization of four orthologs of stringent starvation protein A. *Acta Cryst. D*. **59**, 881-886 (2003).

O Asojo, S Cater, D Hoover, C Boulegue, W Lu, J Lubkowski. Crystallization and Preliminary X-ray Studies of Thymus and Activation-Regulated Chemokine (TARC). *Acta Cryst. D*. **59**, 163-165 (2003).

O Asojo, C Boulegue, D Hoover, W Lu, J Lubkowski. Structures of Thymus and Activation-regulated Chemokine (TARC). *Acta Cryst. D*. **59**, 1165-1173 (2003).

O Asojo, E Afonina, S Gulnik, J Erickson, R Randad, D Medjahed, A Silva. Novel Uncomplexed and Complexed Structures of Phasmepsin II, an Asparticprotease from Plasmodium Falciparum. *J. Mol. Biol.*. **327**, 173-181 (2003).

S Banumathi, M Dauter, Z Dauter. Phasing at High Resolution using Ta6Br12 Cluster. *Acta Cryst. D*. **59**, 492-498 (2003).

M Bernett, S Blaber, I Scarisbrick, P Dhanarajan, S Thompson, M Blaber. Crystal Structure and Biochemical Characterization of Human Kallikrein 6 Reveals a Trypsin-like Kallikrein is Expressed in the Central Nervous System. *J. Biol. Chem.*. **277**, 24562-24570 (2002).

M Bernett, S Blaber, I Scarisbrick, P Dhanarajan, S Thompson, M Blaber. Crystal Structure and Biochemical Characterization of Human Kallikrein 6 Reveals a Trypsin-like Kallikrein is Expressed in the Central Nervous System. *Protein Sci.*. **11**, 137 (2002).

J Blaszczyk, Y Li, G Shi, H Yan, X Ji. Dynamic Roles of Arginine Residues 82 and 92 of Escherichia coli 6-Hydroxymethyl-7,8-dihydropterin Pyrophophokinase: Crystallographic Studies. *Biochemistry*. **42**, 1573-1580 (2003).

C Boesen, S Radaev, S Motyka, A Patamawenu, P Sun. The 1.1 Angstrom Crystal Structure of Human TGF-beta Type II Receptor Ligand Binding Domain. *Structure*. **10**, 913-942 (2002).

C Boesen, S Motyka, A Patamawenu, P Sun. Crystallization and Preliminary Crystallographic Studies of Human TGF-Beta Type II Receptor Ligand-Binding Domain. *Acta Cryst. D*. **58**, 1214-1216 (2002).

P Carrington, P Chivers, F Al-Mjeni, R Sauer, M Maroney. Nickel Coordination is Regulated by the DNA-bound State of NikR. *Nat. Struct. Biol.*. **10** (2), 126 (2003).

P Carrington, F Al-Mjeni, M Zoroddu, M Costa, M Maroney. Use of XAS for the Elucidation of Metal Structure and Function: Applications to Nickel Biochemistry, Molecular Toxicology, and Carcinogenesis. *Environ. Health Perspect.*. **5**, 705-708 (2002).

C Chang, E Magracheva, S Kozlov, S Fong, G Tobin, S Kotenko, A Wlodawer, A Zdanov. Crystal Structure of Interleukin-19 Defines a New Subfamily of Helical Cytokines . *J. Biol. Chem.*. **278**, 3308-3313 (2003).

Z Dauter. One-and-a Half Wavelength Approach. *Acta Cryst. D*. **58**, 1958-1967 (2002).

Z Dauter. New Approaches to High-Throughput Phasing. *Curr. Opin. Struct. Biol.*. **12**, 674-678 (2002).

Z Dauter, R Nagem. Direct Way to Anomalous Scatterers. *Z. Kristallogr.*. **217**, 694-702 (2002).

C Deivanagagam, E Wann, W Chen, M Carson, K Rajashankar, M Hook, S Narayana. A Novel Variant of the Immunoglobulin Fold in Surface Adhesions of Staphylococcus Aureus: Crystal Structure of the Fibrinogen-Binding MSCRAMM, Clumping Factor A. *EMBO J.*. **21**, 6660-6672 (2002).

G Gainsford, A Kay, A Woolhouse. 1-(2-Hydroxyethyl)-4-{4,5,6,7-Tetrahydro--1-[1-(2-Hydroxyethyl)-Pyridin-4(1H)-YL-Idene]-1H-Inden-3-YL}Pyridinium Iodide. *Acta Cryst. E*. **E59** (04), o589-o590 (2003).

X Guo, X Wen, L Esser, B Quinn, L Yu, C Yu, D Xia. Structural Basis for the Quinone Reduction in the bc1 Complex: A Comparative Analysis of Crystal Structures of Mitochondrial Cytochrome bc1 with Bound Substrate and Inhibitors at the Qi Site. *Biochemistry*. **42**, 9067-9080 (2003).

F Guo, M Maurizi, L Esser, D Xia. Crystal Structure of ClpA, an Hsp100 Chaperone and Regulator of ClpAP Protease. *J. Biol. Chem.*. **277** (48), 46743-46752 (2002).

F Guo, L Esser, S Singh, M Maurizi, D Xia. Crystal Structure of the Heterodimeric Complex of the Adaptor, ClpS, with the N-domain of the AAA+ Chaperone, ClpA*. *J. Biol. Chem.*. **277** (48), 46753-46762 (2002).

Y Guo, B Xiao, H Wargo, M Bucher, S Singh, X Ji. Residues 207, 216, and 221 and the Catalytic Activity of mGSTA1-1 and MGSTA2-2 toward Benzo[a]pyrene-(7R,8S)-diol-(9S,10R)-epoxide. *Biochemistry*. **42**, 917-921 (2003).

P Hall, Y Wang, R Rivera-Hainaj, X Zheng, M Pustai-Carey, P Carey, V Yee. Transcarboxylase 12S crystal structure: hexamer assembly and substrate binding to a multienzyme core. *EMBO J.*. **22** (10), 2334-2347 (2003).

A Hofmann, H Iwai, S Hess, A Plucktuh, A Wlodawer. Structure of Cyclized Green Fluorescent Protein. *Acta Cryst. D*. **58**, 1400-1406 (2002).

A Hofmann, D Dolmer, A Wlodawer. The Crystal Structure of Annexin Gh1 from Gossypium Hirsutum Reveals an Unusual S3 Cluster. *Eur. J. Biochem.*. **270**, 2557-2564 (2003).

E Jaffe, J Kervinen, J Martins, F Stauffer, R Neier, A Wlodawer, A Zdanov. Species-Specific Inhibition of Porphobilinogen Synthase by 4-oxosebacic Acid. *J. Biol. Chem.*. **277**, 19792-19799 (2002).

B Kang, D Cooper, F Jelen, Y Devedjiev, U Derewenda, Z Dauter, J Otlewski, Z Derewenda. PDZ Tandem of Human Syntenin: Crystal Structure and Functional Properties. *Structure*. **11**, 459-468 (2003).

M Kim, T Cierpicki, U Derewenda, D Krowarsch, Y Feng, Y Devedjiev, Z Dauter, C Walsh, J Otlewski, et al.. The DCX-domain tandems of doublecortin and doublecortin-like kinase. *Nat. Struct. Biol.*. **10** (5), 324-333 (2003).

J Kim, I Yang, S Rhee, Z Dauter, Y Lee, S Park, K Kim. Crystal Structures of Glutaryl 7-Aminocephalosporanic Acid Acylase: Insight into Autoproteolytic Activation. *Biochemistry*. **42**, 4084-4093 (2003).

M Kim, U Derewenda, Y Devedjiev, Z Dauter, Z Derewenda. Purification and Crystallization of the N-Terminal Domain from the Human Doublecortin-like Kinase. *Acta Cryst. D*. **59**, 502-505 (2003).

O Kleifeld, A Frenkel, J Martin, I Sagi. Active Site Electronic Structure and Dynamics During Metalloenzyme Catalysis. *Nat. Struct. Biol.*. **10** (2), 98 (2003).

O Kleifeld, S Shi, R Zarivasch, M Eisenstein, I Sagi. The Conserved Glu-60 in the Active Site of Thermoanaerobacter Brockii Alcohol Dehydrogenase is not Essential for Catalysis. *Protein Sci.*. **12**, 468-479 (2003).

J Knowlton, M Bubunenko, M Andrykovitch, W Guo, K Routzahn, D Waugh, D Court, X Ji. A Spring-Loaded State of NusG in Its Functional Cycle is Suggested by X-ray Crystallography and Supported by Site-Directed Mutants. *Biochemistry*. **42**, 2275-2281 (2003).

C Lehmann, J Debreczeni, G Bunkoczi, M Dauter, Z Dauter, L Vertesy, G Sheldrick. Structures of Four Crystal Forms of Decaplanin. *Helv. Chim. Acta*. **86**, 1478-1486 (2003).

M Lim, J Rohde, A Stubna, M Bukowski, M Costas, R Ho, E Munck, W Nam, L Que. An FeIV==O complex of a tetradentate tripodal nonheme ligand. *Proc Natl Acad Sci USA*. **100** (7), 3665-3670 (2003).

K Longenecker, P Read, S Lin, A Somlyo, R Nakamoto, Z Derewenda. Structure of a Constitutively Activated RhoA Mutant (Q63L) at 1.55 Angstrom Resolution. *Acta Cryst. D*. **59**, 876-880 (2003).

J Lubkowski, M Dauter, K Aghaiypour, A Wlodawer, Z Dauter. Atomic Resolution Structure of Erwinia Chrysanthemi L-Asparaginase. *Acta Cryst. D*. **59**, 84-92 (2003).

T Martin, Z Dauter, Y Devedijiev, P Sheffield, F Jelen, M He, D Sherman, J Otlewski, Z Derewenda, U Derewenda. Molecular Basis of Mitomycin C Resistance in Streptomyces: Structure and Function of the MRD Protein. *Structure*. **10**, 933-942 (2002).

M Miller, J Shuman, T Sebastian, Z Dauter, P Johnson. Structural Basis for DNA Recognition by the Basic Region Leucine Zipper Transcription Factor CCAAT/Enhancer -Binding Protein Alpha. *J. Biol. Chem.*. **278**, 15178-15184 (2003).

W Nam, S Choi, M Lim, J Rohde, I Kim, J Kim, C Kim, L Que, Jr. Reversible Formation of Iodosylbenzene-Iron Porphyrin Intermediates in the Reaction of Oxoiron(IV) Porphyrin pi-Cation Radicals and Iodobenzene. *Angew. Chem. Int. Ed.*. **42**, 109-111 (2003).

P Natesh, K Manikandan, P Bhanumoorthy, M Viswamitra , S Ramakumar. Thermostable Xylanase from Thermoascus Aurantiacus at Ultrahigh Resolution (0.89 Angstrom) at 100 K and Atomic Resolution (1.11 Angstrom) at 293 K Refined Anisotropically to Small-molecule Accuracy. *Acta Cryst. D*. **59**, 105-117 (2003).

J Penner-Hahn. Snapshots of Transition States. *Nat. Struct. Biol.*. **10**, 75-77 (2002).

J Phan, A Zdanov, A Evdokimov, J Tropea, H Peters, R Kapust, M Li, A Wlodawer, D Waugh. Structural basis for the substrate specificity of tobacco etch virus protease. *J. Biol. Chem.*. **277** (52), 50564-50572 (2002).

T Pochapsky, S Pochapsky, T Ju, H Mo, F Al-Mjeni, M Maroney. Modeling and Experiment Yields the Structure of Acireductone Dioxygenase from Klebsiells Pneumoniae. *Nat. Struct. Biol.*. **9**, 966-972 (2002).

L Que, L Banci. Bioinorganic Chemistry. *Curr Opin Chem Biol*. **6**, 169-170 (2002).

U Ramagopal, M Dauter, Z Dauter. Phasing on Anomalous Signal of Sulfurs: What is the Limit?. *Acta Cryst. D*. **59**, 1020-1027 (2003).

U Ramagpal, M Dauter, Z Dauter. SAD Manganese in Two Crystal Forms of Glucose Isomerase. *Acta Cryst. D*. **59**, 868-875 (2003).

B Ramakrishnan, P Qasba. Comparison of the Closed Conformation of the Beta-1,4-Galactosyl-Transferase-I (beta 4Gal-T1) in the Presence and Absence of Alpha-Lactalbumin (LA). *J. Biomol. Struct. Dyn.*. **21** (1), 1-8 (2003).

V Ramasamy, B Ramakrishnan, E Boeggeman, P Qasba. The Role of Tryptophan 314 in the Conformational Changes of beta1,4-Galactosyltransferase-I. *J. Mol. Biol.*. **331**, 1065-1076 (2003).

G Roelfes, V Vrajmasu, K Chen, R Ho, J Rohde, C Zondervan, R la Crois, E Schudde, M Lutz, et al.. End-on and Side-on Peroxo Derivatives of Non-Heme Iron Complexes with Pentadentate Ligands: Models for Putative Intermediates in Biological Iron/Dioxygen Chemistry. *Inorg. Chem.*. **42**, 2639-2653 (2003).

P Sun, S Radaev. Generating Isomorphous Heavy-Atom Derivatives by a Quick Soak Method. Part II: Phasing of New Structures. *Acta Cryst. D*. **58**, 1099-1103 (2002).

C Taylor, S Watton, P Bryngelson, M Maroney. inner-Sphere Complexation of Cobalt(II) 2,9-dimethyl-1,10-Phenanthroline ([Co(neo)]2+) with Commercial and Sol-Gel Derived Silica Gel Surfaces. *Inorg. Chem.*. **42**, 312-320 (2003).

I Uson, B Schmidt, R von Bulow, S Grimme, K von Figura, M Dauter, K Rajashankar, Z Dauter, G Sheldrick. Locating the Anomalous Scatterer Substructures in Halide and Sulfur Phasing. *Acta Cryst. D*. **59**, 57-66 (2003).

M Weiss, Z Wan, M Zhao, Y Chu, S Nakagawa, G Burke, W Jia, R Hellmich, P Katsoyannis. Non-Standard Insulin Design: Structure-Activity Relationships at the Periphery of the Insulin Receptor. *J. Mol. Biol.*. **315**, 103-111 (2002).

Beamline X10A

Y Akpalu, Y Lin. Multivariable Structural Characterization of Semicrystalline Polymer Blends by Small-Angle Light Scattering. *J. Polym. Sci., Part B: Polym. Phys.*. **40**, 2714-2727 (2002).

D Coleman, J Fernsler, N Chattham, M Nakata, Y Takanishi, E Korblova, D Link, R Shao, W Jang, et al. Polarized-Modulated Smectic Liquid Crystal Phases. *Science*. **301**, 1204-1211 (2003).

Beamline X10B

D Vanderah, R Gates, V Silin, D Zeiger, J Woodward, C Meuse. Isostructural Self-Assembled Monolayers. 1. Octadecyl 1-Thiaoligo(ethylene oxides). *Langmuir*. **19**, 2612-2620 (2003).

Beamline X10C

T Das, G Jacobs, P Patterson, W Conner, J Li, B Davis. Fischer-Tropsch synthesis: characterization and catalytic properties of rhenium promoted cobalt alumina catalysts. *Fuel*. **82**, 805-815 (2003).

Beamline X11A

Y Arai, A Lanzirotti, S Sutton, J Davis, D Sparks. Arsenic Speciation and Reactivity in Poultry Litter. *Environ. Sci. Tech.*. **37** (18), 4083-4090 (2003).

A Argo, J Odzak, B Gates. Role of Cluster Size in Catalysis: Spectroscopic Investigation of ã-Al2O3-Supported Ir4 and Ir6 during Ethene Hydrogenation. *J. Am. Chem. Soc.*. **125**, 7107-7115 (2003).

A Argo, B Gates. MgO-Supported Rh6 and Irg: Structural Characterization during the Catalysis of Ethene Hydrogenation. *J. Phys. Chem. B*. **107**, 5519-5528 (2003).

S Calvin, E Carpenter, R Stroud, V Harris. Characterization of Core/Shell Nanoparticles by X-Ray Absorption Spectroscopy. *2003 Nanotechnology Conference and Trade Show*, Vol 3, p. 82-85, sponsored by Nano Science and Technology Institute. (2003).

S Calvin, E Carpenter, B Ravel, V Harris, S Morrison. Multiedge Refinement of Extended X-Ray-Absorption Fine Structure of Manganese Zinc Ferrite Nanoparticles. *Phys. Rev. B: Condens. Matter*. **66** (22), 224405-1 - 224405-13 (2002).

S Calvin, E Carpenter, V Harris. Characterization of passivated iron nanoparticles by x-ray absorption spectroscopy. *Phys. Rev. B: Condens. Matter*. **68** (3), 033411-1-033411-4 (2003).

S Calvin, M Miller, R Goswami, S Cheng, S Mulvaney, L Whitman, V Harris. Determination of crystallite size in a magnetic nanocomposite using extended x-ray absorption fine structure. *J. Appl. Phys.*. **94** (1), 778-783 (2003).

C Dodge, A Francis. Structural characterization of a ternary Fe(III)-U(VI)-citrate complex. *Radiochim. Acta*. **91**, 525-532 (2003).

J Goellner, B Gates. Synthesis and Characterization of Site-Isolated Hexarhodium Clusters on Titania Powder. *J. Phys. Chem. B*. **105** (16), 3269-3281 (2001).

A Mansour, P Smith, W Baker, M Balasubramanian, J McBreen. A Comparative In Situ X-Ray Absorption Spectroscopy Study of Nanophase V2O5 Aerogel and Ambigel Cathodes,. *J. Electrochem. Soc.*. **150** (4), A403-A413 (2003).

S Morrison, C Cahill, E Carpenter, S Calvin, V Harris. Preparation and Characterization of MnZn-Ferrite Nanoparticles Using Reverse Micelles. *J. Appl. Phys.*. **93** (10), 7489-7491 (2003).

M Nachtegaal, D Sparks. Nickel Sequestration in a Kaolinite-Humic Acid Complex. *Environ. Sci. Tech.*. **37**, 529-534 (2003).

D Roberts, A Scheinost, D Sparks. Zinc speciation in contaminated soils combing direct and indirect characterization methods. *Geochemical and Hydrological Reactivity of Heavy Metals in Soils*, p. 187-227, Lewis Publishers, Boca Raton. (2003).

D Roberts, R Ford, D Sparks. Kinetics and Mechanisms of Zn Complexation on Metal Oxides using EXAFS Spectroscopy. *J. Colloid Interface Sci.*. **263** (2), 364-376 (2003).

K Scheckel, C Impellitteri, J Ryan, T McEvoy. Assessment of a Sequential Extraction Procedure for Perturbed Lead-Contaminated Samples with and without Phosphorus Amendments. *Environ. Sci. Tech.*. **37**, 1892-1898 (2003).

A Scheinost, R Kretzschmar, S Pfister, D Roberts. Combining Selective Sequential Extractions, X-ray Absorption Spectroscopy, and Principal Component Analysis for Quantitative Zinc Speciation in Soil. *Environ. Sci. Tech.*. **36** (23), 5021 (2002).

P Trivedi, J Dyer, D Sparks. Lead Sorption onto Ferrihydrite. 1. A Macroscopic and Spectroscopic Assessment. *Environ. Sci. Tech.*. **37** (5), 908-914 (2003).

A Voegelin, A Scheinost, K Buehlmann, K Barmettler, R Kretzschmar. Slow formation and dissolution of Zn precipitates in soils: A combined column-transport and XAFS study. *Environ. Sci. Tech.*. **36** (17), 3749-3754 (2002).

W Yoon, Y Kim, X Yang, J McBreen, C Grey. 6Li MAS NMR and in situ X-ray Studies of Lithium Nickel Manganese Oxides. *J. Power Sources*. **119** (1), 649-653 (2003).

Beamline X12B

P Dai, P Cebe, M Capel, R Alamo, L Mandelkern. In Situ Wide- and Small-Angle X-ray Scattering Study of Melting Kinetics of Isotactic Poly(propylene). *Macromolecules*. **36**, 4042-4050 (2003).

S Eswaramoorthy, S Gerchman, V Graziano, H Kycia, F Studier, S Swaminathan. Structure of a Yeast Hypothetical Protein Selected by a Structural Genomics Approach. *Acta Cryst. D*. **59**, 127-135 (2003).

K Ferguson, M Berger, J Mendrola, H Cho, D Leahy, M Lemmon. EGF activates its receptor by removing interactions that auto-inhibit ectodomain dimerization. *Mol. Cell*. **11**, 507-517 (2003).

J Hansen, J Ippolito, N Ban, P Nissen. The Structures of Four Macrolide Antibiotics Bound to the Large Ribosomal Subunit. *Mol. Cell*. **10**, 117-128 (2002).

J Hunt, J Deisenhofer. Ping-Pong Cross-Validation in Real Space: a Method for Increasing the Phasing Power of a Partial Model Without Risk of Model Bias. *Acta Cryst. D*. **59**, 214-224 (2003).

S Johnson, J Taylor, L Beese. Processive DNA Synthesis Observed in a Polymerase Crystal Suggests a Mechanism for the Prevention of Frameshift Mutations. *Proc Natl Acad Sci USA*. **100** (7), 3895-3900 (2003).

Y Joly. Calculating X-ray Absorption Near-Edge Structure at Very Low Energy. *J. Synch. Rad.*. **10**, 58-63 (2003).

J Keller, P Smith, J Benach, D Christendat, G deTitta, J Hunt. The Crystal Structure of MT0146/CbiT Suggests that the Putative Precorrin-8w Decarboxylase Is a Methyltransferase. *Structure*. **10**, 1475-1487 (2002).

A Kilshtain-Vardi, M Glick, H Greenblatt, A Goldblum, G Shoham. Refined Structure of Bovine Carboxypeptidase A at 1.25 Angstrom Resolution. *Acta Cryst. D*. **59**, 323-333 (2003).

A Mavroudis, A Avgeropoulos, N Hadjichristidis, E Thomas, D Lohse. Synthesis and Morphological Behavior of Model Linear and Miktoarm Star Copolymers of 2-Methyl-1, 3-Pentadiene and Styrene. *Chem. Mater.*. **15**, 1976-1983 (2003).

P Paaventhan, J Joseph, S Nirthanan, G Rajaseger, P Gopalakrishnakone, R Kini, P Kolatkar. Crystallization and Preliminary X-ray Analysis of Candoxin, a Novel Reversible Neurotoxin from the Malayan Krait Bungarus Candidus. *Acta Cryst. D*. **59**, 584-586 (2003).

S Perez-Miller, T Hurley. Coenzyme Isomerization Is Integral to Catalysis in Aldehyde Dehydrogenase. *Biochemistry*. **42**, 7100-7109 (2003).

N Silvaggi, J Anderson, S Brinsmade, R Pratt, J Kelly. The Crystal Structure of Phosphonate-Inhibited D-Ala-D-Ala Peptidase Reveals an Analogue of a Tetrahedral Transition State. *Biochemistry*. **42** (5), 1199-1208 (2003).

E Sundberg, P Andersen, P Schlievert, K Karjalaine, R Mariuzza. Structural, Energetic, and Functional Analysis of a Protein-Protease Interface at Distinct Stages of Affinity Maturation. *Structure*. **11**, 1151-1161 (2003).

Beamline X12C

M Andrykovitch, K Routzahn, M Li, Y Gu, D Waugh, X Ji. Characterization of four orthologs of stringent starvation protein A. *Acta Cryst. D*. **59**, 881-886 (2003).

J Benach, I Lee, W Edstrom, A Kuzin, Y Chiang, T Acton, G Montelione, J Hunt. The 2.3-A crystal structure of the shikimate 5-dehydrogenase orthologue YdiB from Escherichia coli suggests a novel catalytic environment for an NAD-dependent dehydrogenase.. *J. Biol. Chem.*. **278** (21), 19176-82 (2003).

V Cherezov, K Riedl, M Caffrey. Too Hot to Handle? Synchrotron X-ray Damage of Lipid Membranes and Mesophases. *J. Synch. Rad.*. **9** (6), 333-341 (2002).

Y Chi, J Frantz, B Oh, L Hansen, S Shoelson. Diabetes mutations delineate an atypical POU domain in HNF1a.. *Mol. Cell*. **10**, 1129 (2002).

S Dutta, I Akey, C Dingwall, K Hartman, T Laue, R Nolte, J Head, C Akey. The crystal structure of nucleoplasmin-core: implications for histone binding and nucleosome assembly. *Mol. Cell*. **8** (4), 841-853 (2001).

B Eichman, E O'Rourke, J Radicella, T Ellenberger. Crystal structures of 3-methyladenine DNA glycosylase MagIII . *EMBO J.*. **22** (19), 4898-4909 (2003).
M Hu, P Li, M Li, W Li, T Yao, J Wu, W Gu, R Cohen, Y Shi. Crystal Structure of a UBP-Family Deubiquitinating Enzymen in Isolation and in Complex with Ubiquitin Aldehyde. *Cell*. **111**, 1041-1054 (2002).
Q Huai, H Wang, Y Sun, H Kim, Y Liu, H Ke. Three-dimensional Structures of PDE4D in Complex with Roliprams and Implication on Inhibitor Selectivity. *Structure*. **11**, 865-873 (2003).
M Huang, A Rigby. Structural basis of membrane binding by Gla domains of Vitamine-K dependent proteins. *Nat. Struct. Biol.*. **10** (9), 751 (2003).
S Kamtekar, W Kennedy, J Wang, C Strathopoulos, D Soll, T Steitz. The Structural Basis of Cysteine Aminoacylation of tRNA ^Pro by Prolyl-tRNA Synthetases. *Proc Natl Acad Sci USA*. **100** (4), 1673-1678 (2003).
N Karpowich, H Huang, P Smith, J Hunt. Crystal Structures of the BtuF Periplasmic-vinging Protein for Vitamin B12 Suggest a Functionally Important Reduction in Protein Mobility upon Ligand Binding. *J. Mol. Biol.*. **278** (10), 8429-8434 (2003).
R Khayat, R Batra, C Qian, T Halmos, M Bailey, L Tong. Structural and Biochemical Studies of Inhibitor Binding to Human Cytomegalovirus Protease. *Biochemistry*. **42**, 885-891 (2003).
S Kruse, R Zhao, D Smith, D Jones. Structure of a Specific Alcohol-Binding Site Defined by the Odorant Binding Protein LUSH from Drosophila melanogaster. *Nat. Struct. Biol.*. **10** (9), 694-700 (2003).
D M Himmel, S Gourinath, L Reshetnikova, Y Shen, A G Szent-Gyorgyi, C Cohen. Crystallographic Findings on the Internally-uncoupled and Near-rigor States of Myosin: Further Insights into the Mechanics of the Motor. *Proc Natl Acad Sci USA*. **99** (20), 12645-12650 (2002).
W McGrath, J Ding, A Didwania, R Sweet, W Mangel. Crystallographic structure at 1.6-A resolution of the human adenovirus proteinase in a covalent complex with its 11-amino-acid peptide cofactor: insights on a new fold. *Biochim Biophys Acta*. **1648** ((1-2)), 1-11 (2003).
P O'Neill, D Stevens, E Garman. Physical and Chemical Considerations of Damage Induced in Protein Crystals by Synchrotron Radiation: A Radiation Chemical Perspective. *J. Synch. Rad.*. **9** (6), 329-332 (2002).
S Perez-Miller, T Hurley. Coenzyme Isomerization Is Integral to Catalysis in Aldehyde Dehydrogenase. *Biochemistry*. **42**, 7100-7109 (2003).
P Stolt, H Jeon, H Song, J Herz, M Eck, S Blacklow. Origins of Peptide Selectivity and Phosphinositide Binding Revealed by Structures of Disabled-1 PTB Domain Complexes. *Structure*. **11**, 569-579 (2003).
L Xu, S Benson, S Butcher, D Bamford, R Burnett. The Receptor Binding Protein P2 of PRD1, A Virus Targeting Antibiotic-Resistant Bacteria, Has a Novel Fold Suggesting Multiple Functions. *Structure*. **11**, 309-322 (2003).
X Yang, R Skene, D McRee, P Schimmel. Crystal Structure of a Human Aminoacyl-tRNA Synthetase Cytokine. *Proc Natl Acad Sci USA*. **99** (24), 15369-15374 (2002).
P Yuan, G Jedd, D Kumaran, S Swaminathan, H Shio, D Hewitt, N Chua, K Swaminathan. A HEX-1 Crystal Lattice Required for Woronin Body Function in Neurospora Crassa. *Nat. Struct. Biol.*. **10** (4), 264 (2003).
J Yuvaniyama, P Chitnumsub, S Kamchonwongpaisan, J Vanichtananukul, W Sirawaraporn, P Taylor, M Walkinshaw, Y Yuthavong. Insights into antifolate resistance from malarial DHFR-TS structures . *Nat. Struct. Biol.*. **10** (5), 357-65 (2003).

Beamline X13A

F Castano, Y Hao, S Haratani, C Ross, B Vogeli, H Smith, C Sanchez-Hanke, C Kao, X Zhu, P Grutter. Magnetic force microscopy and x-ray scattering study of 70x550 nm2 pseudo-spin-valve nanomagnets. *J. Appl. Phys.*. **93** (10), 7927-7929 (2003).

Beamline X13B

K Evans-Lutterodt, J Ablett, A Stein, C Kao, D Tennant, F Klemens, A Taylor, C Jacobsen, P Gammel, et al.. Single-element Elliptical Hard X-ray Micro-optics. *Opt. Express*. **11** (8), 919-926 (2003).
K Evans-Lutterodt, A Stein, J Ablett, C Kao, D Tennant, F Klemens, A Taylor, C Jacobsen, P Gammel, et al.. From Lighthouses to Synchrotron Lightsources: Hard X-ray Micro-optics. *Synch. Rad. News*. **16** (3), 60-63 (2003).

Beamline X14A

D Arms, R Shah, R Simmons. X-ray Debye-Waller Factor Measurements of Solid He-3 and He-4. *Phys. Rev. B*. **67** (9), 094303 (2003).
R Benenson, J Bai, W Gibson. Transmission of x-ray polarization through glass capillary fibers. *Rev. Sci. Instrum.*. **74** (1), 23-27 (2003).
J Howe, C Rawn, L Jones, H Ow. Improved crystallographic data for graphite. *Powder Diffr.*. **18** (2), 150 (2003).
J Kim, R Ryba, J Bai. Effect of the Polyurethane Crystalline Interphase Formed at an Al Surface on Water-Vapor Absorption. *J. Appl. Polym. Sci.*. **89**, 1417 (2003).
J Kim, E Ryba, J Bai. Grazing incidence X-ray diffraction studies on the structures of polyurethane films and their effects on adhesion to Al substrates. *Polymer*. **44**, 6663 (2003).
D Klenov, W Donner, B Foran, S Stemmer. Impact of stress on oxygen vacancy ordering in epitaxial LSCO thin films. *Appl. Phys. Lett.*. **82** (20), 3427-3430 (2003).
J Kmetko, C Yu, G Evmenenko, S Kewalramani, P Dutta. Evidence of Registry at the Interface during Inorganic Nucleation at an Organic Template. *Phys. Rev. Lett.*. **89** (18), 186102 (2002).
J Kmetko. Effects of Divalent Ions on Langmuir Monolayers: Synchrotron X-ray Scattering Studies. Ph.D. Thesis. Northwestern University, Chicago. (2002).

J Li, S Moss, Y Zhang, A Mascarenhas, L Pfeiffer, K West, W Ge, J Bai. Layer Ordering and Faulting in (GaAs)n/(AlAs)n Ultrashort-Period Superlattices . *Phys. Rev. Lett.*. **91**, 106103 (2003).

Q Qian, T Tyson, C Dubourdieu, A Bossak, J Sénateur , M Deleon, J Bai, G BonFait, J Maria. Structural, magnetic, and transport studies of La0.8MnO3 films. *J. Appl. Phys.*. **92** (8), 4518 (2002).

Beamline X15A

L Chapman, M Hasnah, O Oltulu, Z Zhong, J Mollenhauer, C Muehleman, K Kuettner, M Aurich, E Pisano, et al.. Diffraction Enhanced X-ray Imaging of Articular Cartilage. US Patent No. 657,7708. (2003).

F Dilmanian, H Weinmann, Z Zhong, T Bacarian, L Rigon, T Buttone, B Ren, X Wu, N Zhong, H Atkins. Tailoring X-ray Beam Energy Spectrum to Enhance Image Quality of New Radiography Contrast Agents Based on Gd or Other Lanthanides. *SPIE: Physics of Medical Imaging*, Vol 4320, p. 417-426, sponsored by SPIE. (2001).

M Hasnah, Z Zhong, O Oltulu, E Pisano, R Johnston, D Sayers, W Thomlinson, D Chapman. Diffraction Enhanced Imaging Contrast Mechanisms in Breast Cancer Specimens. *Med. Phys.*. **29**, 2216-2221 (2002).

M Hasnah, O Oltulu, Z Zhong, D Chapman. Application of Absorption and Refraction Matching Techniques for Diffraction Enhanced Imaging. *Rev. Sci. Instrum.*. **73**, 1657-1659 (2002).

M Hasnah, O Oltulu, Z Zhong, D Chapman. Single Exposure Simultaneous Diffraction Enhanced Imaging. *Nucl. Instrum. Meth. A*. **492**, 236-240 (2002).

M Kiss. Application of diffraction enhanced imaging for obtaining improved contrast of calcifications in breast tissue. PhD Thesis. North Carolina State University, Raleigh. (2002).

M Kiss, D Sayers, Z Zhong. Measurement of image contrast using diffraction enhanced imaging. *Phys. Med. Biol.*. **48** (3), 325-340 (2003).

T Lee, C Kumpf, A Kazimirov, P Lyman, G Scherb, M Bedzyk, M Nielsen, R Feidenhansl, R Johnson, J Zegenhagen. Structural analysis of indium-stabilized GaAs(001)-c(8x2) surface. *Phys. Rev. B: Condens. Matter*. **66**, 235301-1-9 (2002).

J Li, Z Zhong, R Litdke, K Kuettner, C Peterfy, E Aleyeva, C Muehleman. Radiography of Soft Tissue of the Foot and Ankle with Diffraction Enhanced Imaging. *J. Anatomy*. **202**, 463-470 (2003).

J Mollenhauer, M Aurich, Z Zhong, C Muehleman, A Cole, M Hasnah, O Oltulu, K Kuettner, A Margulis, L Chapman. Diffraction Enhanced X-ray Imaging of Articular Cartilage. *Osteoarthr. Cartilage*. **10**, 168-171 (2002).

C Muehleman, L Chapman, K Kuettner, J Rieff, J Mollenhauer, K Massuda, Z Zhong. Radiography of Rabbit Articular Cartilage with Diffraction Enhanced Imaging. *Anatomical Record*. **272A**, 392-397 (2003).

C Muehleman, M Whiteside, Z Zhong, J Mollenhauer, M Aurich, K Kuettner, L Chapman. Diffraction enhanced imaging for articular cartilage. *Biophys. J.*. **82**, 2292-2292 (2002).

C Muehleman, Z Zhong, J Williams, K Kuettner, M Aurich, B Han, J Mollenhauer. Diffraction-enhanced X-ray Imaging of Articular Cartilage of Experimental Animals. *Proceedings Annual Meeting Othrop. Research Society*, Vol , p. 365, sponsored by Ann. Mtg. Orthop. Res. Soc.. (2002).

O Oltulu, Z Zhong, M Hasnah, D Chapman. Multiple Image Radiography in Diffraction Enhanced Imaging. *J. Phys. D: Appl. Phys.*. **36**, 2152-2156 (2003).

L Rigon, Z Zhong, F Arfelli, R Menk, A Pillon. Diffraction Enhanced Imaging utilizing different crystal reflections at Elettra and NSLS. *Proc. SPIE 4632: Physics of Medical Imaging*, Vol 4632, p. 29, sponsored by SPIE. (2002).

H Roberts, M Helba, J Carroll, J Burnett, T Drummond, J Lepak, R Propri, Z Zhong, F Agee. Gamma Spectroscopy of Hf-178m2 using Synchrotron X-rays. *Hyperfine Interact.*. **143**, 111-119 (2002).

B Tinkham, D Goodner, D Walko, M Bedzyk. X-ray studies of Si/Ge/Si(001) epitaxial growth with Te as a surfactant . *Phys. Rev. B: Condens. Matter*. **67**, 035404-1-6 (2003).

M Wernick, O Wirjadi, D Chapman, O Oltulu, Z Zhong, Y Yang. Preliminary investigation of a multiple-image radiography method. *IEEE. Intl. Symposium on Biomed. Imaging: Macro to Nano* , Vol (2002), p. 1435, sponsored by National Institute of Health. (2002).

Z Zhong, D Chapman, D Connor, A Dilmanian, N Gmur, M Hasnah, R Johnston, M Kiss, J Li, et al.. Diffraction Enhanced Imaging of Soft Tissues. *Synch. Rad. News*. **15** (6), 27-34 (2002).

Z Zhong, C Kao, D Siddons, H Zhong, J Hastings. X-ray reflectivity of sagittally bent Laue crystals. *Acta Cryst. A*. **59**, 1-6 (2003).

Z Zhong, D Chapman, M Hasnah, E Johnston, M Kiss, O Oltulu, L Rigon, N Zhong, E Pisano, D Sayers. X-ray Diffraction Order-selection with a Prism in DEI. *12th National Conference on Sychrotron Radiation Instrumentation*, Vol 73, p. 1614, sponsored by American Institute of Physics. (2002).

Z Zhong, C Kao, D Siddons, J Hastings. Rocking-curve width of sagittally bent Laue crystals. *Acta Cryst. A*. **58**, 487-493 (2002).

Z Zhong, D Siddons, D Chapman, C Kao, N Zhong, J Hastings. Model of Sagittally-bent Silicon Crystals Diffracting in the Laue Mode: the Effects of Elastic-Anisotropy on the Rocking-curve Widths. *12th National Conference on Sychrotron Radiation Instrumentation*, Vol 73, p. 1615, sponsored by University of Wisconsin-Madison. (2002).

Beamline X16C

A Frenkel, A Kolobov, I Robinson, J Cross, Y Maeda, C Bouldin. Direct Separation of Short Range Order in Intermixed Nanocrystalline and Amorphous Phases. *Phys. Rev. Lett.*. **89**, 285503 (2002).

Beamline X17B1

J Chen, D Weidner, M Vaughan, J Parise, J Zhang, Y Xu. A Combined CCD/IP Detection System for Monochromatic XRD Studies at High Pressure and Temperature. *Science and Technology of High*

Pressure, p. 1035-1038 , Universities Press Ltd., Hyderabad. (2000).

M Croft, I Zakharchenko, Z Zhong, T Tsakalakos, Y Gulak, Z Kalman, J Hastings, J Hu, R Holtz, K Sadananda. Stress Distribution and Tomographic Profiling with Energy Dispersive X-Ray Scattering. *MRS Proceedings: Applications of Synchrotron Radiation Techniques to Materials Science*, Vol 678, sponsored by Materials Research Society. (2002).

C Cui, T Tyson, Z Zhong, J P Carlo, Y Qin. Effects of Pressure on Electron Transport and Atomic Structure of Manganites: Low to High Pressure Regimes. *Phys. Rev. B: Condens. Matter*. **67**, 104107 (2003).

A Dilmanian, N Zhong, T Bacarian, J Tammam, J Kalef-Ezra, P Micca, M Miura, L Rigon, B Scharf, D Slatkin. Response of Subcutaneous Murine Mammary Carcinoma EMT-6 to Synchrotron-generated Segmented X-ray Microbeams. *Proceedings of the Joint Symposium on Bio-Sensing and Bio-Imaging, A. Akatsuka, Ed.*, p. 118-122, sponsored by Yamagata University. (2003).

A Dilmanian, T Button, G Le Duc, N Zhong, L Pena, J Smith, S Martinez, T Bacarian, J Tammam, B Ren. Response of rat intracranial 9L gliosarcoma to microbeam radiation therapy. *Neuro-Oncology*. **4**, 26-38 (2002).

F Dilmanian, H Weinmann, Z Zhong, T Bacarian, L Rigon, T Buttone, B Ren, X Wu, N Zhong, H Atkins. Tailoring X-ray Beam Energy Spectrum to Enhance Image Quality of New Radiography Contrast Agents Based on Gd or Other Lanthanides. *SPIE: Physics of Medical Imaging*, Vol 4320, p. 417-426, sponsored by SPIE. (2001).

A Dilmanian, G Morris, N Zhong, T Bacarian, J Hainfeld, J Kalef-Ezra, L Brewington, J Tammam, E Rosen. Murine EMT-6 carcinoma: high therapeutic efficacy of microbeam radiation therapy. *Radiat. Res.*. **159**, 632-641 (2003).

M Hasnah, O Oltulu, Z Zhong, D Chapman. Single Exposure Simultaneous Diffraction Enhanced Imaging. *Nucl. Instrum. Meth. A*. **492**, 236-240 (2002).

A Hennessy, G Graham, J Hastings, P Siddons, Z Zhong. New pressure flow cell to monitor BaSO4 precipitation using synchrotron in-situ angle dispersive X-ray diffraction. *J. Synch. Rad.*. **9**, 323-324 (2002).

J Hu, J Xu, M Somayazulu, Q Guo, D Herschbach, J Hemley, H Mao. X-ray diffraction and laser heating: application of moissanite anvil cell. *J. Phys.: Condens. Matter*. **14**, 10479 (2002).

B Noheda, Z Zhong, D Cox, G Shirane, S Park, P Rehring. Electric-field induced phase transitions in rhombohedral Pb(Zn1/3Nb2/3)1-xTixO3. *Phys. Rev. B*. **65**, art no. 224101 (2002).

L Rigon, Z Zhong, F Arfelli, R Menk, A Pillon. Diffraction Enhanced Imaging utilizing different crystal reflections at Elettra and NSLS. *Proc. SPIE 4632: Physics of Medical Imaging*, Vol 4632, p. 29, sponsored by SPIE. (2002).

H Roberts, M Helba, J Carroll, J Burnett, T Drummond, J Lepak, R Propri, Z Zhong, F Agee. Gamma Spectroscopy of Hf-178m2 using Synchrotron X-rays. *Hyperfine Interact.*. **143**, 111-119 (2002).

T Tsakalakos, M Croft, I Zakharchenko, Z Zhong, Y Gulak, M Desilva, R Holtz. On the Mechanical Stability of Nanostructured Coatings by Synchrotron Radiation. *AIAA 2002*, Vol AIAA-2002, p. 1314, sponsored by AIAA. (2002).

G Voronin, C Pantea, T Zerda, L Wang, Y Zhao. In situ X-ray diffraction study of silicon at pressures up to 15.5 GPa and temperatures up to 1073 K. *Phys. Rev. B: Condens. Matter*. **68**, 020102 (2003).

J Xu, H Mao, R Hemley, E Hines. Moissanite anvil cell: a new tool for high-pressure research. *J. Phys.: Condens. Matter*. **14**, 11543 (2002).

I Zakharchenko, Y Gulak, Z Zhong, M Croft, T Tsakalakos. Methodology of Synchrotron EDXRD Strain Profiling. *Advances in X-ray Analysis*, Vol 46, sponsored by International Centre for Diffraction Data. (2002).

I Zakharchenko, Y Gulak, Z Zhong, M Croft, T Tsakalakos. Application of Synchrotron EDXRD Strain Profiling in Shot Peened Materials. *Advances in X-ray Analysis*, Vol 46, sponsored by International Centre for Diffraction Data. (2002).

Z Zhong, D Siddons, D Chapman, C Kao, N Zhong, J Hastings. Model of Sagittally-bent Silicon Crystals Diffracting in the Laue Mode: the Effects of Elastic-Anisotropy on the Rocking-curve Widths. *12th National Conference on Sychrotron Radiation Instrumentation*, Vol 73, p. 1615, sponsored by University of Wisconsin-Madison. (2002).

Z Zhong, D Chapman, D Connor, A Dilmanian, N Gmur, M Hasnah, R Johnston, M Kiss, J Li, et al.. Diffraction Enhanced Imaging of Soft Tissues. *Synch. Rad. News*. **15** (6), 27-34 (2002).

N Zhong, G Morris, T Bacarian, E Rosen, A Dilmanian. Response of rat skin to high-dose unidirectional X-ray microbeams: a histological study. *Radiat. Res.*. **160**, 133-142 (2003).

Z Zhong, C Kao, D Siddons, H Zhong, J Hastings. X-ray reflectivity of sagittally bent Laue crystals. *Acta Cryst. A*. **59**, 1-6 (2003).

Z Zhong, D Chapman, M Hasnah, E Johnston, M Kiss, O Oltulu, L Rigon, N Zhong, E Pisano, D Sayers. X-ray Diffraction Order-selection with a Prism in DEI. *12th National Conference on Sychrotron Radiation Instrumentation*, Vol 73, p. 1614, sponsored by American Institute of Physics. (2002).

Z Zhong, C Kao, D Siddons, J Hastings. Rocking-curve width of sagittally bent Laue crystals. *Acta Cryst. A*. **58**, 487-493 (2002).

Beamline X17C

B Chen, D Penwell, L Benedetti, R Jeanloz, M Kruger. Particle-size effect on the compressibility of nanocrystalline alumina. *Phys. Rev. B: Condens. Matter*. **66**, 144101-4 (2002).

D Errandonea, M Somayazulu, D Hausermann. Phase transitions and amorphization of CaWO4 at high pressure. *Phys. Status Solidi B*. **235** (1), 162 - 169 (2003).

E Gregoryanz, A Goncharov, R Hemley, H Mao, M Somayazulu, G Shen. Raman, infrared, and x-ray evidence for new phases of. *Phys. Rev. B: Condens. Matter*. **66**, 224108 (2002).

Q Guo, H Mao, J Hu, J Shu, R Hemley. The phase transitions of CoO under static pressure to 104 GPa. *J. Phys.: Condens. Matter*. **14**, 11369 (2002).

D He, Y Zhao, T Sheng, R Schwarz, J Qian, K Lokshin, S Bobev, L Daemen, H Mao, J Hu. Bulk

metallic glass gasket for high pressure, in situ x-ray diffraction. *Rev. Sci. Instrum.*. **74**, 3012 (2003).
R Hemley, H Mao. New window on earth and planetary interiors. *Miner. Mag.*. **66**, 791-811 (2002).
R Hemley, H Mao. Overview of static high pressure science, in High-Pressure Phenomena. *Proceedings of the International School of Physics, "Enrico Fermi" Course CXLVII*, p. 3-40, IOS Press, Amsterdam. (2002).
J Hu, J Xu, M Somayazulu, Q Guo, D Herschbach, J Hemley, H Mao. X-ray diffraction and laser heating: application of moissanite anvil cell. *J. Phys.: Condens. Matter*. **14**, 10479 (2002).
A Kavner. Elasticity and strength of hydrous ringwoodite. *Earth Planet Sci. Lett.*. **214**, 645-654 (2003).
Y Lee, J Hriljac, S Kim, J Hanson, T Vogt. Pressure-Induced Hydration at 0.6 GPa in a Synthetic Gallosilicate Zeolite. *J. Am. Chem. Soc.*. **125**, 6036-6037 (2003).
K Lipinska-Kalita, B Chen, M Kruger, Y Ohki, J Murowchick, E Gogol. High-pressure x-ray diffraction studies of the nanostructured transparent vitroceramic medium K2O-SiO2-Ga2O3. *Phys. Rev. B: Condens. Matter*. **68**, 35209 (2003).
Z Liu, J Hu, H Yang, H Mao, R Hemley. High-pressure Synchrotron X-ray Diffraction and Infrared Microspectroscopy: Application to Dense Hydrous Phases. *J. Phys.: Condens. Matter*. **14**, 10641-10646 (2002).
Y Ma, C Prewitt, G Zou, H Mao, R Hemley. High-pressure high-temperature x-ray diffraction of beta-boron to 30 GPa. *Phys. Rev. B*. **67**, 174116 (2003).
S Merkel, A Jephcoat, J Shu, H Mao, P Gillet, R Hemley. Equation of state, elasticity, and shear strength of pyrite under high pressure. *Phys. Chem. Miner.*. **29**, 1-9 (2002).
C Sanloup, R Hemley, H Mao. Evidence for xenon silicates at high pressure and temperature. *Geophys. Res. Lett.*. **29**, 30 (2002).
S Shieh, T Duffy, B Li. Strength and Elasticity of SiO2 Across the Stishovite-CaCl2-type Structural Phase Boundary. *Phys. Rev. Lett.*. **89** (25), 255507-1 (2002).
S Shieh, T Duffy. Raman spectroscopy of Co(OH)2 to 30 GPa: Implications for amorphization and structural frustration. *Phys. Rev. B: Condens. Matter*. **66**, 134301 (2002).
Y Song, M Somayazulu, H Mao, R Hemley, D Herschbach. High-pressure structure and equation of state study of nitrosonium nitrate from synchrotron x-ray diffraction. *J. Chem. Phys.*. **118**, 8350 (2003).
J Xu, H Mao, R Hemley, E Hines. Moissanite anvil cell: a new tool for high-pressure research. *J. Phys.: Condens. Matter*. **14**, 11543 (2002).
G Xu, Z Zhong, Y Bing, Z Ye, C Stock, G Shirane. Ground State of the Relaxor Ferroelectric Pb(Zn1/3Nb2/3)O3. *Phys. Rev. B*. **67**, 104102 (2003).
J Xu, H Mao, R Hemley. Gem anvil cell: high-pressure behavior of diamond and related materials. *J. Phys.: Condens. Matter*. **14**, 11549 (2002).

Beamline X18A

H Mo, H Taub, U Volkmann, M Pino, S Ehrlich, F Hansen, E Lu, P Miceli. A Novel Growth Mode of Alkane Films on a SiO2 Surface. *Chem. Phys. Lett.*. **377**, 99-105 (2003).
X Yang, J McBreen, X Sun, M Balasubramanian. Structural studies of cathode and anode materials for lithium batteries using in situ XRD and X-ray absorption combined with NMR spectroscopy. *The 43rd Battery Symposium in Japan*, Vol 2I, p. 50, sponsored by The Electrochemical Society of Japan. (2002).
X Yang, J McBreen, M Balasubramanian, W Yoon, C Grey, M Yoshio, A Ueda, X Huang, L Chen, L Liu. Structural Studies of New Cathode and Anode Materials for Lithium Batteries Using In Situ XRD and x-ray Absorption Spectroscopy. *The 2002 Korean Battery Symposium*, Vol 1, p. 45, sponsored by The Korean Electrochemical Society. (2002).
W Yoon, Y Kim, X Yang, J McBreen, C Grey. 6Li MAS NMR and in situ X-ray Studies of Lithium Nickel Manganese Oxides. *J. Power Sources*. **119** (1), 649-653 (2003).
C Yu, A Richter, J Kmetko, S Dugan, A Datta, P Dutta. Structure of interfacial liquids: X-ray scattering studies. *Phys. Rev. E*. **63**, 021205 (2001).
Y Zhang, R Colella, S Kycia, A Goldman. Absolute Structure Factor Measurements of an Al-Pd-Mn Quasicrystal. *Acta Cryst. A*. **58**, 385-390 (2002).

Beamline X18B

O Adamopoulos, Z Yu, M Croft, I Zakharchenko, T Tsakalakos, M Muhammed. The characterisation and reactivity of nanostructured cerium-copper-oxide composites for environmental catalysis. *Synthesis, Functional Properties and Applications of Nanostructures. Symposium (Materials Research Society Symposium Proceedings Vol.676)*, Vol 676, p. Y8.11.1-6, sponsored by Mater. Res. Soc. (2002).
F Alamgir. The Structural Origins Of The Stability of Palladium-Nickel-Phosphorus Bulk Metallic Glasses. Ph.D. Thesis. Lehigh University, Bethlehem. (2003).
W Alvarez, B Kitiyanan, A Borgna, D Resasco. Synergism of Co and Mo in the catalytic production of single-wall carbon nanotubes by decomposition of CO. *Carbon*. **39**, 547-558 (2001).
G Chen, H Jain, M Vlcek, S Khalid, J Li, D Drabold, S Elliott. Observation of Light Polarization-dependent Structural Changes in Chalcogenide Glasses. *Appl. Phys. Lett.*. **82** (5), 706 (2003).
G Chen, H Jain, M Vlcek, J Li, D Drabold, S Khalid, S Elliott. Study of light-induced vector changes in the local atomic structure of As¨CSe glasses by EXAFS. *J. Non-Cryst. Solids*. **326-327**, 257 (2003).
G Chen, H Jain, S Khalid, J Li, D Drabold, S Elliott. Study of Structural Changes in Amorphous As2Se3 By EXAFS under In-Situ Laser Irradiation. *Solid State Commun.*. **120**, 149-153 (2001).
M Croft, W Caliebe, H Woo, T Tyson, D Sills, Y Hor, S Cheong, V Kiryukhin, S Oh. Metal-insulator transition in CuIr2S4: XAS results on the electronic structure. *Phys. Rev. B: Condens. Matter*. **67**, 201102-1-4 (2003).
T Das, G Jacobs, P Patterson, W Conner, J Li, B Davis. Fischer-Tropsch synthesis: characterization

and catalytic properties of rhenium promoted cobalt alumina catalysts. *Fuel*. **82**, 805-815 (2003).

R Egdal, A Hazell, F Larsen, C McKenzie, R Scarrow. A dihydroxo-bridged Fe(II)-Fe(III) complex: A new member of the diiron diamond core family.. *J. Am. Chem. Soc.*. **125** (1), 32-33 (2003).

K Galbreath, C Crocker, C Nyberg, F Huggins, G Huffman, K Larson. Nickel speciation measurements of urban particulate matter: method evaluation and relevance to risk assessment. *J. Environ. Monit.*. **5**, 56N-61N (2003).

M Giacomini, M Balasubramanian, S Khalid, J McBreen, E Ticianelli. Characterization of the Activity of Palladium-Modified Polythiophene Electrodes for the Hydrogen Oxidation and Oxygen Reduction Reactions. *J. Electrochem. Soc.*. **150** (5), A588-A593 (2003).

J Herrera, D Resasco. Role of Co-W Interaction in the Selective Growth of Single-Walled Carbon Nanotubes from CO Disproportionation. *J. Phys. Chem. B*. **107**, 3738-3746 (2003).

F Huggins, N Yap, G Huffman, C Senior. XAFS characterization of mercury captured from combustion gases on sorbents at low-temperature. *Fuel Process. Technol.*. **82**, 167-196 (2003).

G Jacobs, T Das, P Patterson, J Li, L Sanchez, B Davis. Fischer-Tropsch Synthesis: XAFS studies of the effect of water on a Pt-promoted Co/Al2O3 catalyst. *Appl. Catal. A*. **247** (2), 335 (2003).

G Popov, M Greenblatt, M Croft. Large effects of a-site average cation size on the properties of the double perovskites Ba2 xSrxMnReO6, a d5-d1 System. *Phys. Rev. B: Condens. Matter*. **B67**, 24406 (2003).

N Sakulchaicharoen , D Resasco. Temperature dependence of the quality of silicon nanowires produced over a titania-supported gold catalyst. *Chem. Phys. Lett.*. **377** (3), 377-383 (2003).

N Shah, S Pattanaik, F Huggins, D Panjala, G Huffman. XAFS and Mössbauer spectroscopy characterization of supported binary catalysts for nonoxidative dehydrogenation of methane. *Fuel Process. Technol.*. **83**, 163-173 (2003).

J Shearer, S Fitch, W Kaminsky, J Benedict, R Scarrow, J Kovacs. How does Cyanide Inhibit Superoxide Reductase? Insight from Synthetic Fe(III)N4S Model Complexes. *Proc Natl Acad Sci USA*. **100** (7), 3671-3676 (2003).

X Yang, J McBreen, X Sun, M Balasubramanian. Structural studies of cathode and anode materials for lithium batteries using in situ XRD and X-ray absorption combined with NMR spectroscopy. *The 43rd Battery Symposium in Japan*, Vol 2I, p. 50, sponsored by The Electrochemical Society of Japan. (2002).

X Yang, J McBreen, M Balasubramanian, W Yoon, C Grey, M Yoshio, A Ueda, X Huang, L Chen, L Liu. Structural Studies of New Cathode and Anode Materials for Lithium Batteries Using In Situ XRD and x-ray Absorption Spectroscopy. *The 2002 Korean Battery Symposium*, Vol 1, p. 45, sponsored by The Korean Electrochemical Society. (2002).

W Yoon, C Grey, M Balasubramanian, X Yang, J McBreen. In Situ X-ray Absorption Spectroscopic Study on LiNi0.5Mn0.5O2 Cathode Material during Electrochemical Cycling. *Chem. Mater.*. **15**, 3161-3169 (2003).

Beamline X19A

O Adamopoulos, Z Yu, M Croft, I Zakharchenko, T Tsakalakos, M Muhammed. The characterisation and reactivity of nanostructured cerium-copper-oxide composites for environmental catalysis. *Synthesis, Functional Properties and Applications of Nanostructures. Symposium (Materials Research Society Symposium Proceedings Vol.676)*, Vol 676, p. Y8.11.1-6, sponsored by Mater. Res. Soc. (2002).

S Beauchemin, D Hesterberg, J Chou, M Beauchemin, R Simard, D Sayers. Speciation of Phosphorus in Phosphorus-enriched Agricultural Soils using X-ray Absorption Near-edge Spectroscopy and Chemical Fractionation. *J. Environ. Qual.*. **32**, 1809-1819 (2003).

B Bostick, S Fendorf. Arsenite Sorption on Troilite (FeS) and Pyrite (FeS2). *Geochim. Cosmochim. Acta*. **67** (5), 909-921 (2003).

A Cady. Optical and resonant x-ray diffraction investigations of molecular ordering in chiral liquid crystals. Ph.D. Thesis. University of Minnesota, Minneapolis. (2003).

M Croft, W Caliebe, H Woo, T Tyson, D Sills, Y Hor, S Cheong, V Kiryukhin, S Oh. Metal-insulator transition in CuIr2S4: XAS results on the electronic structure. *Phys. Rev. B: Condens. Matter*. **67**, 201102-1-4 (2003).

G Liu, J Rodriguez, J Hrbek, B Long, D Chen. Interaction of Thiophene with Titania Surfaces. *J. Mol. Catal. A: Chem.*. **202**, 215-227 (2003).

J McBreen, X Yang, M Balasubramanian, X Sun, H Lee. Synchrotron X-ray Studies of Lithium-Ion Battery Components. *The 43rd Battery Symposium in Japan*, Vol 2I, p. 46, sponsored by The Electrochemical Society of Japan. (2002).

G Popov, M Greenblatt, M Croft. Large effects of a-site average cation size on the properties of the double perovskites Ba2 xSrxMnReO6, a d5-d1 System. *Phys. Rev. B: Condens. Matter*. **B67**, 24406 (2003).

J Qian, U Skyllberg, W Frech, W Bleam, P Bloom, P Petit. Bonding of Methyl Mercury to Reduced Sulfur Groups in Soil and Stream Organic Matter as Determined by X-ray Absorption Spectroscopy and Binding Affinity Studies. *Geochim. Cosmochim. Acta*. **66** (22), 3873-3885 (2002).

J Rodriguez, P Liu, J Dvorak, T Jirsak, J Gomes, Y Takahashi, K Nakamura. Adsorption and decomposition of SO2 on TiC(001): An experimental and theoretical study. *Surf. Sci. Lett.*. **543**, L675-L682 (2003).

J Rodriguez, X Wang, J Hanson, G Liu, A Iglesias-Juez, M Fernandez-Garcia. The behavior of mixed-metal oxides: Structural and electronic properties of Ce-Ca oxides. *J. Chem. Phys.*. **119**, 5659-5669 (2003).

J Rodriguez, J Hanson, J Kim, G Liu, A Iglesias-Juez, M Fernandez-Garcia. Properties of Ce2 and Ce1-xZrxO2 Nanoparticles: X-ray Absorption Near-Edge Spectroscopy, Density Functional, and Time-Resolved X-ray Diffraction Studies. *J. Phys. Chem. B*. **107**, 3535-3543 (2003).

N Shah, S Pattanaik, F Huggins, D Panjala, G Huffman. XAFS and Mössbauer spectroscopy characterization of supported binary catalysts for

nonoxidative dehydrogenation of methane. *Fuel Process. Technol.*. **83**, 163-173 (2003).
U Skyllberg, J Qian, W Frech, K Xia, W Bleam. Distribution of mercury, methyl mercury and organic sulphur species in soil, soil solution and stream of a boreal forest catchment. *Biogeochemistry*. **64**, 53-76 (2003).

Beamline X19C

M Dudley. Studies of Defects and Strains Using X-ray Topography and Diffraction. *2003 SEM Annual Conference & Exposition on Experimental and Applied Mechanics*, Vol 1, p. 348-355, sponsored by SEM. (2003).
M Dudley, X Huang, W Vetter, P Neudeck. Synchrotron White Beam X-ray Topography and High Resolution Triple Axis X-ray Diffraction Studies of Defects in SiC Substrates, Epilayers and Devices. *4th European Conference on Silicon Carbide and Related Materials*, Vol 433-436, p. 247-252, sponsored by European Commission. (2003).
D Gidalevitz, Y Ishitsuka, A Muresan, O Konovalov, A Waring, R Lehrer, K Lee. Interaction of antimicrobial peptide protegrin with biomembranes. *Proc Natl Acad Sci USA*. **100** (11), 6302-6307 (2003).
L Hanley, Y Choi, E Fuoco, F Akin, M Wijesundara, M Li, A Tikhonov, M Schlossman. Controlling the Nanoscale Morphology of Organic Films Deposited by Polyatomic Ions. *Nucl. Instrum. Meth. B*. **203**, 116 (2003).
J Hartwig, J Baruchel, H Kuhn, X Huang, M Dudley, E Pernot. X-ray "Magnifying" Imaging Investigation of Giant Burgers Vector Micropipe Dislocations in 4H-SiC. *Nucl. Instrum. Meth. B*. **200**, 323-328 (2003).
X Huang, M Dudley. A Universal Computation Method for Two-Beam Dynamical X-ray Diffraction. *Acta Cryst. A*. **59**, 163-167 (2003).
M Li, D Chaiko, M Schlossman. X-ray Reflectivity Study of a Monolayer of Ferritin Proteins at a Nanofilm Aqueous-Aqueous Interface. *J. Phys. Chem. B*. **107**, 9079-9085 (2003).
R Ma, H Zhang, V Prasad, M Dudley. Growth kinetics and thermal stress of silicon carbide. *Cryst. Growth Des.*. **2** (3), 213-220 (2002).
X Ma, M Dudley, W Vetter, T Sudharshan. Extended Defects: Polarized Light Microscopy Delineation and Synchrotron White Beam X-ray Topography Ratification. *Japanese J. Appl. Phys.*. **42**, L1077-L1079 (2003).
R Ma, H Zhang, M Dudley, V Prasad. Thermal System Design and Dislocation Reduction for Growth of Wide Band-gap Crystals: Application to SiC Growth. *J. Cryst. Growth*. **258**, 318-330 (2003).
R Ma, H Zhang, M Dudley, S Ha, M Skowronski. Modeling for mass transfer and Thermal Stress of Silicon carbide PVT growth. *2002 ASME International Mechanical Engineering Congress and Exposition*, Vol 1, p. 1-9, sponsored by ASME. (2003).
P Neudeck, J Powell, D Spry, A Trunek, X Huang, W Vetter, N Dudley, M Skowronski, J Liu. Characterization of 3C-SiC Films Grown on 4H- and 6H-SiC Substrate Mesas during Step-Free Surface Hetero-Epitaxy. *4th European Conference on Silicon Carbide and related Materials*, Vol 433-436, p. 213-216, sponsored by European Commission. (2003).
W Palosz, K Grasza, K Durose, D Halliday, N Boyall, M Dudley, B Raghothamachar, L Cai. The Effect of Wall Contact and Post-Growth Cool-Down on Defects in CdTe Crystals Grown by "Contactless" Physical Vapor Transport. *J. Cryst. Growth*. **254**, 316-328 (2003).
E Preble, P Miraglia, A Roskowski, W Vetter, M Dudley, R Davis. Domain Structures in 6H-SiC Wafers and Their Effect on the Microstructures of GaN Films Grown on AlN and Al0.2GaN0.8N Buffers Layers. *J. Cryst. Growth*. **258**, 75-83 (2003).
B Raghothamachar, M Dudley, J Rojo, K Morgan, L Schowalter. X-ray Characterization of Bulk AlN Single Crystals Grown by the Sublimation Technique. *J. Cryst. Growth*. **250**, 244-250 (2003).
A Tikhonov, M Schlossman. Surfactant and water ordering in triacontanol monolayers at the water-hexane interface. *J. Phys. Chem. B*. **107**, 3344 (2003).
W Vetter, J Liu, M Dudley, M Skowronski, H Lendenmann, C Hallin. Dislocation Loops Formed During the Degradation of Forward-Biased 4H-SiC p-n Junctions. *Mater. Sci. Eng. B*. **98**, 220-224 (2003).
B Wu, R Ma, H Zhang, M Dudley, R Schlesser, Z Sitar. Growth kinetics and thermal stress in AlN bulk crystal growth. *J. Cryst. Growth*. **253**, 326-339 (2003).
B Yang, D Li, S Rice. Structure of the liquid-vapor interface of a dilute ternary alloy: Pb and In in Ga. *Phys. Rev. B*. **67**, 05423 (2003).
B Yang, D Li, S Rice. Two Dimensional Freezing of Tl in the Liquid-Vapor Interface of a Dilute Tl in Ga Alloy. *Phys. Rev. B*. **67**, 212103 (2003).
U Zimmermann, J Osterman, D Kuylenstierna, A Hallen, A Konstantinov, W Vetter, M Dudley. Material Defects in 4H-Silicon Carbide Diodes. *J. Appl. Phys.*. **93** (1), 611 (2003).

Beamline X20A

S Anders, M Toney, T Thomson, J Thiele, B Terris, S Sun, C Murray. X-ray Studies of Magnetic Nanoparticle Assemblies. *J. Appl. Phys.*. **93** (10), 7343 (2003).
S Anders, M Toney, T Thomson, R Farrow, J Thiele, B Terris. X-ray Absorption and Diffraction Studies of Magnetic Nanoparticle Assemblies. *J. Appl. Phys.*. **93**, 6299 (2003).
R Bandhu, R Sooryyakumar, R Farrow, D Weller, M Toney, T Rabedeau. Elastic Properties of Chemically Ordered Co3Pt Thin Films. *J. Appl. Phys.*. **91**, 2737 (2002).
P Clegg, C Stock, R Birgeneau, C Garland, A Roshi, G Iannacchione. Effect of a quenched random field on a continuous symmetry breaking transition: Nematic to smectic-A transition in 8OCB-aerosil dispersions. *Phys. Rev. E*. **67**, 021703 (2003).
P Clegg, R Birgeneau, S Park, C Garland, G Iannacchione, R Leheny, M Neubert. High-resolution x-ray study of the nematic - smectic-A and smectic-A - smectic-C transitions in liquid-crystal - aerosil gels. *Phys. Rev. E*. **68**, 031706 (2003).
G Iannacchione, S Park, C Garland, R Birgeneau, R Leheny. Smectic ordering in liquid-crystal–aerosil

dispersions. II. Scaling analysis. *Phys. Rev. E*. **67** (1), 011709 (2003).
S Kaldor, C Noyan. Effects of Boundary Conditions and Anisotropy on Elastically Bent Silicon. *Exp. Mech.*. **42** (3), 353-358 (2002).
V Khmelenko, S Kiselev, D Lee, C Lee. Impurity-Helium Solids - Quantum Gels?. *Phys. Scr.*. **T102**, 118 (2002).
W Lee, M Toney, A Kellock, D Mauri, M Carey, J Hedstrom. Effects of Mn Concentration and Deposition Temperature on the Giantmagnetoresistance Properties of Ion Beam Deposited PtMn Spin Valves. *J. Appl. Phys.*. **91**, 2737 (2003).
R Leheny, S Park, R Birgeneau, J Gallani, C Garland, G Iannacchione. Smectic ordering in liquid-crystal–aerosil dispersions. I. X-ray scattering. *Phys. Rev. E*. **67** (1), 011708 (2003).
P Mooney. Materials for Strained Si Devices. *Selected Topics in Electronics and Systems*, p. 99-108, World Scientific, New Jersey. (2002).
P Mooney. Materials for Strained Si Devices. *Int. J. High Speed Electr. And Syst.*. **12**, 305-314 (2002).
M Toney, W Lee, J Hedstrom, A Kellock. Thickness and Growth Temperature Dependence of Structure and Magnetism in FePt Thin Films. *J. Appl. Phys.*. **93**, 9902 (2003).
M Toney, M Samant, T Lin, D Mauri. Thickness Dependence of Exchange Bias and Structure in PtMn and NiMn Spin Valves. *Appl. Phys. Lett.*. **81**, 4565 (2003).
W Zang, Y Yao. Laser Shock Processing (LSP) of Metal Thin Films. *Conference on Laser Materials Processing*, Vol 2002, p. CD, sponsored by 20th International Congress on Applications of Lasers and Electro-Optics, Scottsdale AZ. (2002).
W Zhang. Microscale Laser Ablative Processes. Ph.D. Thesis. Columbia University, New York. (2002).

Beamline X20C

S Anders, M Toney, T Thomson, J Thiele, B Terris, S Sun, C Murray. X-ray Studies of Magnetic Nanoparticle Assemblies. *J. Appl. Phys.*. **93** (10), 7343 (2003).
S Anders, M Toney, T Thomson, R Farrow, J Thiele, B Terris. X-ray Absorption and Diffraction Studies of Magnetic Nanoparticle Assemblies. *J. Appl. Phys.*. **93**, 6299 (2003).
R Bandhu, R Sooryyakumar, R Farrow, D Weller, M Toney, T Rabedeau. Elastic Properties of Chemically Ordered Co3Pt Thin Films. *J. Appl. Phys.*. **91**, 2737 (2002).
G Cohen, C Cabral, Jr., C Lavoie, P Soloman, K Guarini, K Chan, R Roy. A Self-aligned Silicide Process Utilizing Ion Implantation for Reduced Silicon Consumption and Control of the Silicide Formation Temperature . *Materials Research Society Symposium Proceedings*, Vol 716, p. 35, sponsored by Materials Research Society. (2002).
G Cohen, C Cabral, Jr., C Lavoie, P Soloman, K Guarini, K Chan, R Roy. A Self-aligned Process for Thin Silicon-on-insulator MOSFETS and Bulk MOSFETS with Shallow Junctions. *59th Annual Device Research Conference June 2001*, Vol 686, p. 89, sponsored by Material Research Symp. Proc.. (2002).
C Detavernier, C Lavoie, F d'Heurle. Thermal Expansion of the Isostructural PtSi and NiSi: Negative Expansion Coefficient in NiSi and Stress Effects in Thin Films. *J. Appl. Phys.*. **93** (5), 2510-2515 (2003).
A Gungor, K Barmak, A Rollett, C Cabral, Jr., J Harper. Texture and Resistivity of Dilute Binary Cu(Al), Cu(In), Cu(Ti), Cu(Nb), Cu(Ir), and Cu(W) Alkloy Thin Films. *J. Vac. Sci. Technol., A*. **20** (6), 2314 (2002).
G Iannacchione, S Park, C Garland, R Birgeneau, R Leheny. Smectic ordering in liquid-crystal–aerosil dispersions. II. Scaling analysis. *Phys. Rev. E*. **67** (1), 011709 (2003).
S Kaldor, C Noyan. Effects of Boundary Conditions and Anisotropy on Elastically Bent Silicon. *Exp. Mech.*. **42** (3), 353-358 (2002).
H Kim, C Cabral, Jr., C Lavoie, S Rossnagel. The Growth of Tantalum Thin Films by Plasma-Enhanced Atomic Layer Deposition and Diffusion Barrier Properties . *Materials Research Society Symposium Proceedings*, Vol 716, p. 407, sponsored by Materials Research Society. (2002).
C Lavoie, F d'Heurle, C Detavernier, C Cabral, Jr.. Towards Implementation of a Nickel Silicide Process for CMOS Technologies. *Microelectron. Eng.*. **70**, 144-157 (2003).
W Lee, M Toney, A Kellock, D Mauri, M Carey, J Hedstrom. Effects of Mn Concentration and Deposition Temperature on the Giantmagnetoresistance Properties of Ion Beam Deposited PtMn Spin Valves. *J. Appl. Phys.*. **91**, 2737 (2003).
R Leheny, S Park, R Birgeneau, J Gallani, C Garland, G Iannacchione. Smectic ordering in liquid-crystal–aerosil dispersions. I. X-ray scattering. *Phys. Rev. E*. **67** (1), 011708 (2003).
P Mooney. Materials for Strained Si Devices. *Int. J. High Speed Electr. And Syst.*. **12**, 305-314 (2002).
P Mooney. Materials for Strained Si Devices. *Selected Topics in Electronics and Systems*, p. 99-108, World Scientific, New Jersey. (2002).
A Ozcan, K Ludwig, C Cabral, Jr., C Lavoie, J Harper. Texture Formation in Ti-Ta Alloy Disilicide Thin Films. *J. Appl. Phys.*. **92** (12), 7210 (2002).
A Ozcan, K Ludwig, C Lavoie, C Cabral, Jr., J Harper, R Bradley. Nucleation and Growth Kinetics of Preferred C54 TiSi2 Orientation: Time-Resolved X-Ray Diffraction Measurements. *J. Appl. Phys.*. **92** (9), 5189 (2002).
S Rossnagel, I Noyan, C Cabral, Jr.. Phase Transformation of Thin Sputter-deposited Tungsten Films at Room Temperature. *J. Vac. Sci. Technol., B*. **20** (5), 2047 (2002).
P Solomon, K Guarini, Y Zhang, K Chan, E Jones, G Cohen, A Krasnoperova, M Ronay, O Dokumaci, H Hovel. A Planar, Self-Aligned, Double Gate MOSFET Technology. *IEEE Circuits Dev. Mag.*. **19** (1), 48 (2003).
S Sun, S Anders, T Thomson, J Baglin, M Toney, H Hamann, C Murray, B Terris. Controlled Synthesis and Assembly of FePt Nanoparticles. *J. Phys. Chem. B*. **107**, 5419-5425 (2003).
M Toney, W Lee, J Hedstrom, A Kellock. Thickness and Growth Temperature Dependence of Structure and Magnetism in FePt Thin Films. *J. Appl. Phys.*. **93**, 9902 (2003).

M Toney, M Samant, T Lin, D Mauri. Thickness Dependence of Exchange Bias and Structure in PtMn and NiMn Spin Valves. *Appl. Phys. Lett.*. **81**, 4565 (2003).
M Toney, E Marinero, M Doerner, P Rice. High Anisotropy CoPtCrB Magnetic Recording Media. *J. Appl. Phys.*. **94**, 4018 (2003).

Beamline X21

B Blank, T Kupp, A Deyhim, Y Cai, P Chow, C Kao. Development of a Spectrometer for Inelastic X-ray Measurements. *Proceedings of the 2nd International Workshop on Mechanical Engineering Design of Synchrotron Radiation Equipment and Instrumentation (MEDSI02)*, Vol , p. 308-314, sponsored by MEDSI02. (2002).
C Burns, P Giura, A Shukla, G Vanko, M Tuel-Benckendorf, E Isaacs, P Platzman. Probing Electronic Interactions in the Expanded Metal Compound Li-NH3. *Phys. Rev. Lett.*. **89**, 236404 (2002).
K Hamalainen, S Galambosi, H Sutinen, C Kao, R Sharon, M Deutsch. Near-threshold Mult-electronic Effects in the Cu K alpha 1,2 X-Ray Spectrum. *Phys. Rev. A*. **67**, 022510 (2003).
H Hayashi, Y Udagawa, J Gillet, W Caliebe, C Kao. Chemical Applications of Inelastic X-ray Scattering. *Chemical Application of Synchrotron Radiation*, p. 850, World Scientific, River Edge. (2002).
H Hayashi, N Wantanabe, Y Udagawa, C Kao. Momentum Dependence of ð-ð* Excitations of Benzene Rings in Condensed Phases. *J. Electron. Spectrosc. Relat. Phenom.*. **933**, 114-116 (2001).
H Hayashi, Y Udagawa, W Caliebe, C Kao. Lifetime-broadening Removed X-ray Absorption Near Edge Structure by Resonant Inelastic X-ray Scattering Spectroscopy. *Chem. Phys. Lett.*. **371**, 125 (2003).
H Mao, C Kao, R Hemley. Inelastic X-ray Scattering at Ultra-high Pressure. *J. Phys.: Condens. Matter*. **13**, 7847 (2001).
P Montano, D Price, A Macrander, B Cooper. Inelastic x-ray scattering from 6H-SiC. *Phys. Rev. B: Condens. Matter*. **66**, 165218 (2002).
Q Qian, T Tyson, S Savrassov, C Kao, M Croft. Electronic Structure of La(1-x)CaxMnO3 Determined by Spin-polarized X-ray Absorption Spectroscopy: Comparison of Experiments with Band-Structure Computations. *Phys. Rev. B*. **68**, 014429 (2003).
M v. Zimmermann, C Nelson, J Hill, D Gibbs, M Blume, D Casa, B Keimer, Y Murakami, C Kao, et al.. X-ray Resonant Scattering Studies of Orbital and Charge Ordering in Pr1-xCaxMnO3. *J. Magn. Magn. Mater.*. **233**, 31 (2001).
M v. Zimmermann, C Nelson, J Hill, D Gibbs, M Blume, D Casa, B Keimer, Y Murakami, C Kao, et al.. X-ray resonant scattering studies of orbital and charge ordering in Pr1-xCaxMnO3. *Phys. Rev. B*. **64**, 195133 (2001).
L Yang, L Ding, H Huang. New Phases of Phospholipids and Implications to the Membrane Fusion Problem. *Biochemistry*. **42** (22), 6631-6635 (2003).
L Yang, L Ding, H Huang. A Rhombohedral Phase of Lipid Containing a Membrane Fusion Intermediate Structure. *Biophys. J.*. **84**, 1808 (2003).

Beamline X22A

G da Silva, J Fossum, E DiMasi, K Maloy, S Lutnaes. Synchrotron x-ray scattering studies of water intercalation in a layered synthetic silicate. *Phys. Rev. E*. **66**, 011303 (2002).
G da Silva, J Fossum, E DiMasi, K Maloy. Hydration transitions in a nanolayered synthetic silicate: A synchrotron x-ray scattering study. *Phys. Rev. B*. **67**, 094114 (2003).
F He, B Wells, S Shapiro, M Zimmermann, A Clark, X Xi. Anomalous Phase Transition in Strained SrTiO3 Thin Films. *Appl. Phys. Lett.*. **83** (1), 123 (2003).
J Schearer, B Ocko, O Magnussen. Structure, dissolution, and passivation of Ni(111) electrodes in sulfuric acid solution: an in situ STM, x-ray scattering, and electrochemical study. *Electrochim. Acta*. **48**, 1169-1191 (2003).
H Schollmeyer, B Ocko, H Riegler. Surface Freezing of Triacontane at SiOx/Air Interfaces: Submonolayer Coverage. *Langmuir*. **18**, 4351 (2002).
J Wang, B Ocko, R Adzic. Overpotential Deposition of Ag Monolayer and Bilaer on Au(111) mediated by Pb Adlayer Unerpotential Deposition/Stripping Cysles. *Surf. Sci.*. **540** (2-3), 230 (2003).

Beamline X22B

J Blasie, S Zheng, J Strzalka. Solution to the phase problem for specular x-ray or neutron reflectivity from thin films on liquid surfaces. *Phys. Rev. B*. **67** (22), 224201 (2003).
E DiMasi, V Patel, M Sivakumar, M Olszta, Y Yang, L Gower. Polymer-Controlled Growth Rate of an Amorphous Mineral Film Nucleated at a Fatty Acid Monolayer. *Langmuir*. **18**, 8902-8909 (2002).
E DiMasi, M Olszta, V Patel, L Gower. When is template directed mineralization really template directed?. *Cryst. Eng.*. **5** (61), 346-350 (2003).
A Gibaud, D Grosso, B Smarsly, A Baptiste, J Bardeau, F Babonneau, D Doshi, Z Chen, C Brinker, C Sanchez. Evaporation-Controlled Self-Assembly of Silica Surfactant Mesophases. *J. Phys. Chem. B*. **107**, 6114-6118 (2003).
A Gibaud, D Doshi, B Ocko, V Goletto, C Brinker. Time-resolved in situ grazing incidence small angle x-ray scattering experiment of evaporation induced self-assembly. *Nanotechnology in Mesostructured Materials*, p. 351-354, Elsevier, St. Louis. (2003).
A Gibaud, A Baptiste, D Doshi, C Brinker, L Yang, B Ocko. Wall thickness and core radius determination in surfactant templated silica thin films using GISAXS and X-ray reflectivity. *Europhys. Lett.*. **63** (6), 833-839 (2003).
P Huber, O Shpyrko, P Pershan, B Ocko, H Tostmann, E DiMasi, M Deutsch. Short-range wetting at liquid gallium-bismuth alloy surfaces: X-ray measurements and square-gradient theory. *Phys. Rev. B: Condens. Matter*. **68**, 085409 (2003).
M Kent, H Kim, D Sasaki, J Majewski, G Smith, K Shin, S Satija, B Ocko. Segment concentration profile of myoglobin adsorbed tometal ion chelating lipid monolayers at the air-water interface by neutron reflection. *Langmuir*. **18**, 3754 (2002).

H Kraack, M Deutsch, B Ocko, P Pershan. The Structure of Organic Langmuir Films on liquid Metal Surfaces. *Nucl. Instrum. Meth. B*. **200**, 363-370 (2003).
H Kraack, B Ocko, P Pershan, E Sloutskin, M Deutsch. Structure of a Langmuir Film on a Liquid Metal Surface. *Science*. **298**, 1404 (2002).
H Lavoie, D Blaudez, D Vaknin, B Desbat, B Ocko, C Salesse. Spectroscopic and structural properties of valine gramicidin A in monolayers at the air-water interface. *Biophys. J.*. **83** (6), 3558-3569 (2002).
B Ocko, M Kelley, A Nikova, D Schwartz. Structure and Phase Behavior of Mixed Monolayers of Saturated and Unsaturated Fatty Acids. *Langmuir*. **18**, 9810-9815 (2002).
B Ocko, E Sirota, M Deutsch, E DiMasi, S Coburn, J Strzalka, S Zheng, A Tronin, T Gog, C Venkataraman. Positional order and thermal expansion of surface crystalline N-alkane monolayers. *Phys. Rev. E*. **6303** (3), 032602 (2001).
E Sloutskin, H Kraack, O Gang, B Ocko, E Sirota, M Deutsch. A Thin-thick Transition in the Surface-frozen Layer of a Binary Alcohol Mixture. *J. Chem. Phys.*. **118**, 10729 (2003).
E Sloutskin, O Gang, H Kraack, B Ocko, E Sirota, M Deutsch. Demixing transition in a quasi-two-dimensional surafce-frozen layer. *Phys. Rev. Lett.*. **89** (6), 065501 (2002).
A Tronin, J Strzalka, X Chen, P Dutton, B Ocko, J Blasie. Orientational distributions of the di-alpha-helical synthetic peptide ZnPPM-BBC16 in Langmuir monolayers by x-ray reflectivity and polarized epifluorescence. *Langmuir*. **17** (10), 3061-3066 (2001).
T Wandlowski, J Wang, B Ocko. Adsorption of bromide at the Ag(100) electrode surface. *J. Electroanal. Chem.*. **500** (1-2), 418-434 (2001).
S Ye, J Strzalka, X Chen, C Moser, P Dutton, J Blasie. Assembly of a Vectorially Oriented Four-Helix Bundle at the Air/Water Interface via Directed Electrostatic Interactions. *Langmuir*. **19**, 1515-1521 (2003).
S Zheng, J Strzalka, D Jones, S Opella, J Blasie. Comparative Structural Studies of Vpu Peptides in Phospholipid Monolayers by X-Ray Scattering . *Biophys. J.*. **84**, 2393-2415 (2003).

Beamline X22C

G Cao, L Balicas, Y Xin, J Crow, C Nelson. Quantum oscillations, colossal magnetoresistance, and the magnetoelastic interaction in bilayered Ca_3Ru_2O_7. *Phys. Rev. B: Condens. Matter*. **67** (18), 184405-1,8 (2003).
G Cao, L Balicas, Y Xin, E Dagotto, J Crow, C Nelson, D Agterberg. Tunneling Magnetoresistance and Quantum Oscillations in Bilayered Ca3Ru2O7. *Phys. Rev. B: Condens. Matter*. **67**, 060406(R) (2003).
D Gibbs. X-ray Magnetic Scattering. *Synch. Rad. News*. **14** (5), 4-10 (2001).
J Goff, R Sarthour, D McMorrow, F Yakhou, A Vigliante, D Gibbs, R Ward, M Wells. X-ray resonant scattering study of an intermediate-valence Ho-Ce alloy. *J. Magn. Magn. Mater.*. **226-230**, 1113-1115 (2001).
F He, B Wells, S Shapiro, M Zimmermann, A Clark, X Xi. Anomalous Phase Transition in Strained SrTiO3 Thin Films. *Appl. Phys. Lett.*. **83** (1), 123 (2003).
J Hill. Living on the K-edge: resonant scattering studies of electronic order in transition metal compounds. *Synch. Rad. News*. **14** (5), 21-26 (2001).
J Hill, C Nelson, M v. Zimmermann, Y Kim, D Gibbs, D Casa, B Keimer, Y Murakami, C Venkataraman, et al.. Orbital correlations in doped manganites. *Appl. Phys. A*. **73**, 723-730 (2001).
J Hill. Magnetic X-ray Scattering. *Characterization of Materials*, p. 752, John Wiley & Sons, New York. (2002).
V Kiryukhin, T Koo, H Ishibashi, J Hill, S Cheong. Average lattice symmetry and nanoscale structural correlations in magnetoresistive manganites. *Phys. Rev. B: Condens. Matter*. **67**, 064421 (2003).
H Nakao, Y Wakabayashi, T Kiyama, Y Murakami, M von Zimmerman, J Hill, D Gibbs, S Ishihara, Y Taguchi, Y Tokura. Quantitative Determination of the Atomic Scattering Tensor in Orbitally Ordered YTiO3 by using a Resonant X-ray Scattering Technique. *Phys. Rev. B*. **66**, 184419 (2002).
C Nelson, Y Kim, J Hill, D Gibbs, V Kiryukhin, T Koo, S Cheong. Structural distortions in the paramagnetic insulating phase of La0.7Ca0.3MnO3. *Materials Research Society 2001 Spring Meeting*, Vol 678, p. EE7.3, sponsored by MRS. (2001).
C Nelson, J Hill, D Gibbs. Resonant x-ray scattering as a probe of orbital and charge ordering. *Nanoscale Phase Separation and Colossal Magnetoresistance*, p. 179-183, Springer-Verlag, New York. (2002).
P Normile, W Stirling, D Mannix, G Lander, F Wastin, J Rebizant, S Coburn . (U1-xPux)Sb solid solutions. II. Energy dependencies. *Phys. Rev. B*. **66**, 014406 (2002).
M v. Zimmermann, C Nelson, J Hill, D Gibbs, M Blume, D Casa, B Keimer, Y Murakami, C Kao, et al.. X-ray resonant scattering studies of orbital and charge ordering in Pr1-xCaxMnO3. *Phys. Rev. B*. **64**, 195133 (2001).
M v. Zimmermann, C Nelson, Y Kim, J Hill, D Gibbs, H Nakao, Y Wakabayashi, Y Murakami, Y Tomioka, et al.. A resonant x-ray scattering study of octahedral tilt ordering in LaMnO3 and Pr1-xCaxMnO3. *Phys. Rev. B*. **64**, 1-9 (2001).
H Zajonz, D Gibbs, A Baddorf, D Zehner. Nanoscale strain distribution at the Ag/Ru(0001) interface. *Phys. Rev. B*. **67**, 155417-1 - 155417-8 (2003).

Beamline X23A2

F Alamgir. The Structural Origins Of The Stability of Palladium-Nickel-Phosphorus Bulk Metallic Glasses. Ph.D. Thesis. Lehigh University, Bethlehem. (2003).
D Brenner, S Sawant, P Hande, R Miller, C Elliston, Z Fu, G Randers-Pehrson, S Marino. Routine screening mammography: How important is the radiation-risk side of the benefit-risk equation?. *Int. J. Radiat. Biol.*. **78** (12), 1065-67 (2002).
C Dodge, A Francis. Structural characterization of a ternary Fe(III)-U(VI)-citrate complex. *Radiochim. Acta*. **91**, 525-532 (2003).

D McKeown, W Kot, I Pegg. X-ray Absorption Studies of the Local Strontium Environments in Borosilicate Waste Glasses. *J. Non-Cryst. Solids*. **317** (3), 290-300 (2003).

D McKeown, W Kot, I Pegg. X-ray Absorption Studies of Manganese Valence and Local Environment in Borosilicate Waste Glasses. *J. Non-Cryst. Solids*. **328**, 71-89 (2003).

F Ronci, P Stallworth, F Alamgir, T Schiros, J Sluytman, X Guo, P Reale, S Greenbaum, M denBoer, B Scrosati. Lithium-7 Nuclear Magnetic Resonance And Ti K-edge X-ray Absorption Spectroscopic Investigation Of Electrochemical Lithium Insertion In Li4/3+xTi5/3O4. *J. Power Sources*. **121**, 631-636 (2003).

Beamline X23B

S Calvin, E Carpenter, V Harris. Characterization of passivated iron nanoparticles by x-ray absorption spectroscopy. *Phys. Rev. B: Condens. Matter*. **68** (3), 033411-1-033411-4 (2003).

S Calvin, E Carpenter, B Ravel, V Harris, S Morrison. Multiedge Refinement of Extended X-Ray-Absorption Fine Structure of Manganese Zinc Ferrite Nanoparticles. *Phys. Rev. B: Condens. Matter*. **66** (22), 224405-1 - 224405-13 (2002).

G Chen, H Jain, M Vlcek, J Li, D Drabold, S Khalid, S Elliott. Study of light-induced vector changes in the local atomic structure of As¨CSe glasses by EXAFS. *J. Non-Cryst. Solids*. **326-327**, 257 (2003).

J Cui, Q Huang, J Vienot, H Yan, Q Wang, G Hutchison, A Richter, G Evmenenko, P Dutta, T Marks. Anode Interfacial Engineering Approaches to Enhancing Anode/Hole Transport Layer Interfacial Stability and Charge Injection Efficiency in Organic Light-Emitting Diodes. *Langmuir*. **18**, 9958-9970 (2002).

G Evmenenko, M van der Boom, C Yu, J Kmetko, P Dutta. Specular X-Ray Reflectivity Analysis of Adhesion Interface-Dependent Density Profiles in Nanometer-Scale Siloxane-Based Liquid Films. *Polymer*. **44** (4), 1051-1056 (2003).

A Facchetti, A Abbotto, L Beverina, M van der Boom, P Dutta, G Evmenenko, T Marks, G Pagani. Azinium-(ð-Bridge)-Pyrrole NLO-Phores: Influence of Heterocycle Acceptors on Chromophoric and Self-Assembled Thin-Film Properties. *Chem. Mater.*. **14**, 4996-5005 (2002).

A Facchetti, A Abbotto, L Beverina, M van der Boom, P Dutta, G Evmenenko, G Pagani, T Marks. Layer-by-layer self-assembled pyrrole-based donor-acceptor chromophores as electro-optic materials. *Chem. Mater.*. **15** (5), 1064-1072 (2003).

Y Koide, M Such, R Basu, G Evmenenko, J Cui, P Dutta, M Hersam, T Marks. Hot Microcontact Printing for Patterning ITO Surfaces. Methodology, Morphology, Microstructure, and OLED Charge Injectin Barrier Imaging. *Langmuir*. **19**, 86-93 (2002).

S Morrison, C Cahill, E Carpenter, S Calvin, V Harris. Preparation and Characterization of MnZn-Ferrite Nanoparticles Using Reverse Micelles. *J. Appl. Phys.*. **93** (10), 7489-7491 (2003).

F Ronci, P Stallworth, F Alamgir, T Schiros, J Sluytman, X Guo, P Reale, S Greenbaum, M denBoer, B Scrosati. Lithium-7 Nuclear Magnetic Resonance And Ti K-edge X-ray Absorption Spectroscopic Investigation Of Electrochemical Lithium Insertion In Li4/3+xTi5/3O4. *J. Power Sources*. **121**, 631-636 (2003).

S Yoon, P Helmke, J Amonette, W Bleam. X-ray Absorption and Magnetic Studies of Trivalent Lanthanide Ioins Sorbed on Pristine and Phosphate-Modifed Boehmite Surfaces. *Langmuir*. **18**, 10128-10136 (2002).

P Zhu, H Kang, A Facchetti, G Evmenenko, P Dutta, T Marks. Vapor Phase Self-Assembly of Electrooptic Thin Films via Triple Hydrogen Bonds. *J. Am. Chem. Soc.*. **125** (38), 11496-11497 (2003).

P Zhu, M van der Boom, H Kang, G Evmenenko, P Dutta , T Marks. Realization of Expeditious Layer-by-Layer Siloxane-Based Self-assembly as an Efficient Route to Structurally Regular Acentric Superlattices with Large Electro-optic Responses. *Chem. Mater.*. **14**, 4982-4989 (2002).

Beamline X24A

K McCarthy, U Arp, A Baciero, B Zurro, B Karlin. Response of chromium-doped alumina screens to soft x-rays using synchrotron radiation. *J. Appl. Phys.*. **94**, 958 (2003).

Beamline X24C

L Goray, J Seely. Efficiencies of Master, Replica, and Multilayer Gratings for the Soft X-Ray - Extreme Ultraviolet Range: Modeling Based on the Modified Intergral Method and Comparisons with Measurements. *Appl. Optics-OT*. **41**, 1434 (2002).

M Kowalski, R Cruddace, K Wood, D Yentis, H Gursky, T Barbee, Jr., W Goldstein, J Kordas, G Fritz, et al.. The Astrophysical Plasmadynamic Explorer (APEX): a high-resolution spectroscopic observatory. *Astronomical Telescopes and Instrumentation*, Vol 4854, p. 640-652, sponsored by SPIE. (2002).

B Sae-Lao, S Bajt, C Montcalm, J Seely. Performance of Normal-Incidence Molybdenum/Yttrium Multilayer-Coated Diffraction Grating at a Wavelength of 9 nm. *Appl. Optics-OT*. **41**, 2394 (2002).

J Seely. Extreme Ultraviolet Thin-Film Interference in an Al-Mg-Al Multiple-Layer Transmission Filter. *Appl. Optics-OT*. **41**, 5979 (2002).

J Seely, C Montcalm, S Bajt. High-Efficiency MoRu/Be Multilayer Grating Operating near Normal Incidence in the 11.1-12.0 nm Wavelength Range. *Appl. Optics-OT*. **40**, 5565 (2001).

J Seely, Y Uspenskii, Y Pershin, V Kondratenko, A Vinogradov. Skylab 3600 groove/mm Replica Grating with a Scandium-Silicon Multilayer Coating and High Normal-Incidence Efficiency at 38 nm Wavelength. *Appl. Optics-OT*. **41**, 1846 (2002).

J Seely, C Boyer, G Holland, J Weaver. X-Ray Absolute Calibration of the Time Response of a Silicon Photodiode. *Appl. Optics-OT*. **41**, 5209 (2002).

Beamline X25

J Alexander, C Nelson, V van Berkel, E Lau, J Studts, T Brett, S Spe, T Handel, H Virgin, D Fremont. Structural Basis of Chemokine Sequestration by a Herpesvirus Decoy Receptor. *Cell*. **111**, 343-356 (2002).

J Avalos, I Celic, S Muhammad, M Cosgrove, J Boeke, C Wolberger. Structure of a Sir2 Enzyme Bound to an Acetylated p53 Peptide. *Mol. Cell*. **10** (3), 523-535 (2002).

M Bertero, R Rothery, M Palak, C Hou, D Lim, F Blasco, J Weiner, N Strynadka. Insights into the Respiratory Electron Transfer Pathway from the Structure of Nitrate Reductase A. *Nat. Struct. Biol.*. **10** (9), 681-687 (2003).

I Bosanac, J Alattia, T Mal, J Chan, S Talarico, F Tong, K Tong, F Yoshikawa, T Furuichi, et al. Structure of the Inositol 1,4,5-trisphosphate Receptor Binding Core in Complex with its Ligand. *Nature*. **420**, 696 (2002).

T Brett, L Traub, D Fremont. Accessory Protein Recruitment Motifs in Clathrin-Mediated Endocytosis. *Structure*. **10** (6), 797-809 (2002).

G Cao, L Balicas, Y Xin, E Dagotto, J Crow, C Nelson, D Agterberg. Tunneling Magnetoresistance and Quantum Oscillations in Bilayered Ca3Ru2O7. *Phys. Rev. B: Condens. Matter*. **67**, 060406(R) (2003).

G Cao, L Balicas, Y Xin, J Crow, C Nelson. Quantum oscillations, colossal magnetoresistance, and the magnetoelastic interaction in bilayered Ca_3Ru_2O_7. *Phys. Rev. B: Condens. Matter*. **67** (18), 184405-1,8 (2003).

D Chimento, A Mohanty, R Kadner, M Wiener. Substrate-induced transmembrane signaling in the cobalamin transporter BtuB. *Nat. Struct. Biol.*. **10** (5), 394-401 (2003).

H Cho, K Mason, K Ramyar, A Stanley, S Gabelli, D Denney, D Leahy. Structure of the Extracellular Region of HER2 Alone and in Complex with the Herceptin Fab. *Nature*. **421**, 756-760 (2003).

J Ding, A Smith, S Geisler, X Ma, G Arnold, E Arnold. Crystal Structure of a Human Rhinovirus that Displays Part of the HIV-1 V3 Loop and Induces Neutralizing Antibodies against HIV-1. *Structure*. **10**, 999-1011 (2002).

R Dutzler, E Campbell, R MacKinnon. Gating the Selectivity Filter in ClC Chloride Channels. *Science*. **300**, 108-112 (2003).

C Escalante, L Shen, D Thanos, A Aggarwal. Structure of NF-kB p50/p65 Heterodimer Bound to the PRDII DNA Element fro mthe Interferon-beta Promoter. *Structure*. **10**, 383-391 (2002).

K Ferguson, M Berger, J Mendrola, H Cho, D Leahy, M Lemmon. EGF activates its receptor by removing interactions that auto-inhibit ectodomain dimerization. *Mol. Cell*. **11**, 507-517 (2003).

J Hansen, J Ippolito, N Ban, P Nissen. The Structures of Four Macrolide Antibiotics Bound to the Large Ribosomal Subunit. *Mol. Cell*. **10**, 117-128 (2002).

A Hodel, M Hodel, E Griffis, K Hennig, G Ratner, S Xu, M Powers. The Three-Dimensional Structure of the Autoproteolytic, Nuclear Pore-Targeting Domain of the Human Nucleoporin Nup98. *Mol. Cell*. **10**, 347-358 (2002).

M Hu, P Li, M Li, W Li, T Yao, J Wu, W Gu, R Cohen, Y Shi. Crystal Structure of a UBP-Family Deubiquitinating Enzymen in Isolation and in Complex with Ubiquitin Aldehyde. *Cell*. **111**, 1041-1054 (2002).

Q Huai, H Wang, Y Sun, H Kim, Y Liu, H Ke. Three-dimensional Structures of PDE4D in Complex with Roliprams and Implication on Inhibitor Selectivity. *Structure*. **11**, 865-873 (2003).

M Huang, A Rigby. Structural basis of membrane binding by Gla domains of Vitamine-K dependent proteins. *Nat. Struct. Biol.*. **10** (9), 751 (2003).

Y Huang, M Lemineux, J Song, M Auer, D Wang. Structure and Mechanism of the Glycerol-3-Phosphate Transporter from Escherichia coli. *Science*. **301**, 616-620 (2003).

J Jiang, A Lee, J Chen, V Ruta, M Cadene, B Chait, R MacKinnon. X-ray structure of a voltage-dependent K+ channel. *Nature*. **423**, 33-41 (2003).

S Johnson, J Taylor, L Beese. Processive DNA Synthesis Observed in a Polymerase Crystal Suggests a Mechanism for the Prevention of Frameshift Mutations. *Proc Natl Acad Sci USA*. **100** (7), 3895-3900 (2003).

Z Juo, G Kassavetis, J Wang, E Geiduschek, P Sigler. Crystal structure of a transcription factor IIIB core interface ternary complex. *Nature*. **422**, 534-539 (2003).

L Kang, S Gabelli, M Bianchet, W Xu, M Bessman, L Amzel. Structure of a coenzyme A pyrophosphatase from Deinococcus radiodurans: a member of the Nudix family. *J. Bacteriol.*. **185** (14), 4110-9 (2003).

C Kielkopf, N Rodionova, M Green, S Burley. A Novel Peptide Recognition Mode Revealed by the X-Ray Structure of a Core U2AF 35/U2AF 65 Heterodimer. *Cell*. **106**, 595-605 (2001).

A Klon, A Heroux, L Ross, V Pathak, C Johnson, J Piper, D Borhani. Atomic Structures of Human Dihydrofolate Reductase Complexed with NADPH and Two Lipophilic Antifolates at 1.09 Å and 1.05 Å Resolution. *J. Mol. Biol.*. **320** (3), 677-693 (2002).

F Li, Y Xiong, J Wang, H Cho, K Tomita, A Weiner, T Steitz. Crystal Structures of the Bacillus sterothermophilus CCA-Adding Enzyme and its Complexes with ATP or CTP. *Cell*. **111**, 815-824 (2002).

J Liu, M Lu. An Alanine-Zipper Structure Determined by Long Range Intermolecular Interactions. *J. Biol. Chem.*. **277** (50), 48708-48713 (2002).

E Mains, Y Xiong, M Cocco, L D'Andrea, L Regan. Design of Stable alpha-Helical Arrays from an Idealized TPR Motif. *Structure*. **11** (5), 497-508 (2003).

A Mulichak, C Bonin, W Reiter, R Garavito. Structure of the MUR1 GDP-Mannose 4,6-Dehydratase from Arabidopsis thaliana: Implicatins for Ligand Binding and Specificity. *Biochemistry*. **41**, 15578-15589 (2002).

A Mulichak, H Losey, W Lu, Z Wawrzak, C Walsh, R Garavito. Structure of the TDP-epi-vancosaminyltransferase GtfA from the chloroeremomycin biosynthetic pathway. *Proc Natl Acad Sci USA*. **100** (16), 9238-9243 (2003).

S Nair, S Burley. X-ray Structures of Myc-Max and Mad-Max Recognizing DNA: Molecular Bases of Regulation by Proto-Oncogenic Transcription Factors. *Cell*. **112**, 193-205 (2003).

A Prota, J Campbell, P Schelling, J Forrest, M Watson, T Peters, M Aurrand-Lions, B Imhof, T Dermody, T Stehle. Crystal structure of human junctional adhesion molecule 1: Implications for

reovirus binding. *Proc Natl Acad Sci USA*. **100** (9), 5366-5371 (2003).

S Ray, J Bonanno, K Rajashankar, M Pinho, G He, H De Lencastre, A Tomasz, S Burley. Cocrystal Structures of Diaminopimelate Decarboxylase: Mechanism, Evolution, and Inhibition of an Antibiotic Resistance Accessory Factor. *Structure*. **10**, 1499-1508 (2002).

N Schrader, K Fischer, K Theis, R Mendel, G Schwarz, C Kisker. The Crystal Structure of Plant Sulfite Oxidase Provides Insights into Sulfite Oxidation in Plants and Animals. *Structure*. **11** (10), 1251-1263 (2003).

B Staker, K Hjerrild, M Feese, C Behnke, A Burgin, Jr., L Stewart. The Mechanism of Topoisomerase I Poisoning by a Camptothecin Analog. *Proc Natl Acad Sci USA*. **99** (24), 15387-15392 (2002).

H Walden, M Podgorski, B Schulman. Insights into the Ubiquitin Transfer Cascade from the Structure of the Activating Enzyme for NEDD8. *Nature*. **422**, 330 (2003).

J Wilson, O Matsushita, A Okabe, J Sakon. A Bacterial Collagen-Binding Domain with Novel Calcium-Binding Motif Controls Domain Orientation. *EMBO J.*. **22** (8), 1743-1752 (2003).

J Wu, A Krawitz, J Chai, W Li, F Zhang, K Luo, Y Shi. Structural Mechanism of Smad4 Recognition by the Nuclear Oncoprotein Ski: Insights on Ski-Mediated Repression of TGF-beta Signaling. *Cell*. **111**, 357-367 (2002).

Y Yin, T Steitz. Structural Basis for the Transition from Initiation to Elongation Transcription in T7 RNA Polymerase. *Science*. **298**, 1387 (2002).

F Zalfa, M Giorgi, B Primerano, A Moro, A Di Penta, S Reis, B Oostra, C Bagni. The Fragile X Syndrome Protein FMRP Associates with BC1 RNA and Regulates the Translation of Specific mRNAs at Synapses . *Cell*. **112**, 317-327 (2003).

Beamline X26A

A Aerts, B Velde, K Janssens, W Dijkman. Change in Silica Sources in Roman and Post-Roman Glass. *Spectrochim. Acta B*. **58**, 659-667 (2003).

Y Arai, A Lanzirotti, S Sutton, J Davis, D Sparks. Arsenic Speciation and Reactivity in Poultry Litter. *Environ. Sci. Tech.*. **37** (18), 4083-4090 (2003).

M Dyar, M Gunter, J Delaney, A Lanzirotti, S Sutton. Systematics in the structure and XANES spectra of pyroxenes, amphiboles, and micas as derived from oriented single crystals. *Can. Mineral*. **40**, 1375-1393 (2002).

G Flynn, L Keller, S Wirick, C Jacobsen, S Sutton. Analysis of interplanetary dust particles by soft and hard x-ray microscopy. *J. Phys. IV*. **104**, 367-372 (2003).

J Howe, R Loeppert, V Derose, D Hunter, P Bertsch. Localization and Speciation of Chromium in Subterranean Clover Using XRF, XANES, and EPR Spectroscopy. *Environ. Sci. Tech.*. **37** (18), 4091-4097 (2003).

B Jones, C Conko, J Flinn, D Linkous, A Lanzirotti, C Frederickson, P Bertsch, A Friedlich, A Bush. The Effect of enhanced zinc in drinking water on brain and memory. *Natural Science and the Environment:Prescription for a Better Environment*, Vol 1, p. 3, sponsored by USGS. (2003).

K Kehm, G Flynn, S Sutton, C Hohenberg. Combined noble gas and trace element measurements on individual stratospheric interplanetary dust particles. *Meteoritics & Planet. Sci.*. **37** (10), 1323-1335 (2002).

H Li, L Lee, D Schulze, C Guest. Role of Soil Manganese in the Oxidation of Aromatic Amines. *Environ. Sci. Tech.*. **37**, 2686-2693 (2003).

D Linkous, J Flinn, A Lanzirotti, C Frederickson, B Jones, P Bertsch. Use of Synchrotron X-ray Fluorescence to Measure race Metal Distribution in the Brain. *Transactions of the American Geophysical Union*, Vol F202, p. 81, sponsored by American Geophysical Union. (2002).

R Muller, E Weckert, J Zellner, M Drakopoulos. Investigation of Radiation-dose-induced Changes in Organic Light-atom Crystals by Accurate d-spacing Measurements. *J. Synch. Rad.*. **9** (6), 368-374 (2002).

A Neufeld, H Isaacs, I Cole, A Bond, S Furman. Characterisation of salt particle induced corrosion processes by synchrotron generated X-ray fluorescence and complementary surface analysis tools. *199th Electrochemical Society Meeting*, Vol 2001-5, p. 187-196, (2001).

T Punshon, P Bertsch, A Lanzirotti, K McLeod, J Burger. Geochemical signature of contaminated sediment remobilization by spatially resolved X-ray microanalysis of annual rings of Salix nigra. *Environ. Sci. Tech.*. **37**, 1766-1774 (2003).

D Roberts, A Scheinost, D Sparks. Zinc speciation in contaminated soils combing direct and indirect characterization methods. *Geochemical and Hydrological Reactivity of Heavy Metals in Soils*, p. 187-227, Lewis Publishers, Boca Raton. (2003).

D Roberts, R Ford, D Sparks. Kinetics and Mechanisms of Zn Complexation on Metal Oxides using EXAFS Spectroscopy. *J. Colloid Interface Sci.*. **263** (2), 364-376 (2003).

S Sutton, P Bertsch, M Newville, M Rivers, A Lanzirotti, P Eng. Microfluorescence and microtomography analyses of heterogeneous earth and environmental materials. *Applications of Synchrotron Radiation in Low-Temperature Geochemistry and Environmental Science*, p. Chapter 8, Mineralogical Society of America, Washington, D.C. (2002).

T Tokunaga, J Wan, M Firestone, T Hazen, K Olson, D Herman, S Sutton, A Lanzirotti. In situ reduction of chromium(VI) in heavily contaminated soils through organic carbon amendment. *J. Environ. Qual.*. **32**, 1641-1649 (2003).

T Tokunaga, J Wan, T Hazen, E Schwartz, M Firestone, S Sutton, M Newville, K Olson, A Lanzirotti, W Rao. Distribution of Chromium Contamination and Microbial Activity in Soil Aggregates. *J. Environ. Qual.*. **32**, 541-549 (2003).

T Tokunaga, K Olson, J Wan. Moisture characteristics of Hanford gravels: Bulk, grain-surface, and intragranular components. *Vadose Zone J.*. **2**, 322-329 (2003).

J Twilley. Pigment Analyses for the Grave Stelae and Architectural Fragments from Chersonesos. *Color in Ancient Greece: The Role of Color in Ancient Greek Art and Architecture 700 – 31 B.C*, p. 171-178, Lamrakis Research Foundation, Aristotle University, Thessaloniki. (2002).

D Vantelon, A Lanzirotti, B Aeschlimann, D Guenther, A Scheinost, R Kretzschmar. Micro-scale Pb distribution and oxidation in a shooting range soil. *Geochim. Cosmochim. Acta*. **66** (S1), A-799 (2002).

Beamline X26C

K Bateman, E Brownie, W Wolodko, M Fraser. Structure of the Mammalian CoA Transferase from Pig Heart. *Biochemistry*. **417**, 14455-14462 (2002).

A Hodel, M Hodel, E Griffis, K Hennig, G Ratner, S Xu, M Powers. The Three-Dimensional Structure of the Autoproteolytic, Nuclear Pore-Targeting Domain of the Human Nucleoporin Nup98. *Mol. Cell*. **10**, 347-358 (2002).

A Kilshtain-Vardi, M Glick, H Greenblatt, A Goldblum, G Shoham. Refined Structure of Bovine Carboxypeptidase A at 1.25 Angstrom Resolution. *Acta Cryst. D*. **59**, 323-333 (2003).

J Liu, J Dai, M Lu. Zinc-Mediated Helix Capping in A Triple-Helical Protein. *Biochemistry*. **42**, 5657-5664 (2003).

D M Himmel, S Gourinath, L Reshetnikova, Y Shen, A G Szent-Gyorgyi, C Cohen. Crystallographic Findings on the Internally-uncoupled and Near-rigor States of Myosin: Further Insights into the Mechanics of the Motor. *Proc Natl Acad Sci USA*. **99** (20), 12645-12650 (2002).

J Min, Q Feng, Z Li, Y Zhang, R Xu. Structure of the Catalytic Domain of Human DOT1L, A Non-SET Domain Nucleosomal Histone Methyltransferase. *Cell*. **112**, 711-723 (2003).

M Rudolph, J Johnson, K Rajagopalan, C Kisker. The 1.2 Angstrom Structure of the Human Sulfite Oxidase Cytochrome b5 Domain. *Acta Cryst. D*. **59**, 1183-1191 (2003).

N Schrader, K Fischer, K Theis, R Mendel, G Schwarz, C Kisker. The Crystal Structure of Plant Sulfite Oxidase Provides Insights into Sulfite Oxidation in Plants and Animals. *Structure*. **11** (10), 1251-1263 (2003).

Beamline X27C

Y Cohen, E Thomas. Effect of Defects on the Response of a Layered Block Copolymer to Perpendicular Deformation: One-Dimensional Necking. *Macromolecules*. **36**, 5265-5270 (2003).

G Floudas, P Papadopoulos, H Klok, G Vandermeulen, J Rodriguez-Hernandez. Hierarchical Self-Assembly of Poly(ã-benzyl-L-glutamate)-Poly(ethylene glycol)-Poly(ã-benzyl-L-glutamate) Rod-Coil-Rod Triblock Copolymers. *Macromolecules*. **36**, 3673-3683 (2003).

L Liu, B Hsiao, B Fu, S Ran, S Toki, B Chu, A Tsou, P Agarwal. Structure Changes During Uiaxial Deformation of Ethylene-Based Semicrystalline Ethylene-Propylene Copolymer. 1. SAXS Study. *Macromolecules*. **36**, 1920-1929 (2003).

L Liu, Q Wan, T Liu, B Hsiao, B Chu. Salt-Induced Polymer Gelation and Formation of Nanocrystals in a Polymer-Salt System. *Langmuir*. **18**, 10402-10406 (2002).

S Ran, C Burger, D Fang, X Zong, B Chu, B Hsiao, Y Ohta, K Yabuki, P Cunniff. A Synchrotron WAXD Study on the Early Stages of Coagulation during PBO Fiber Spinning. *Macromolecules*. **35**, 9851 (2002).

R Somani, L Yang, B Hsiao, P Agarwal, H Fruitwala, A Tsou. Shear-Induced Precursor Structures in Isotactic Polypropylene Melt by in-Situ Rheo-SAXS and Rheo-WAXD Studies. *Macromolecules*. **35**, 9096-9104 (2002).

S Toki, B Hsiao. Nature of Strain-Induced Structures in Natural and Synthetic Rubbers Under Stretching. *Macromolecules*. **36**, 5915-5917 (2003).

S Xu, G Offer, J Gu, H White, L Yu. Temperature and Ligand Dependence of Conformation and Helical Order in Myosin Filaments. *Biochemistry*. **42**, 390-401 (2003).

F Yeh, B Hsiao, B Sauer, S Michel, H Siesler. In-Situ Studies of Structure Development During Deformation of a Segmented Poly(urethane-urea) Elastomer. *Macromolecules*. **36**, 1940-1954 (2003).

L Zhu, P Huang, W Chen, X Weng, S Cheng, Q Ge, R Quirk, T Senador, M Shaw, et al.. "Plastic Deformation" Mechanism and Phase Transformation in a Shear-Induced Metastable Hexagonally Perforated Layer Phase of a Polystyrene-b-poy(ethylene oxide) Diblock Copolymer. *Macromolecules*. **36**, 3180-3188 (2003).

Beamline X28C

M Brenowitz, M Chance, G Dhavan, K Takamoto. Probing the Structural Dynamics of Nucleic Acid Structure by Quantitive Time-Resolved and Equilibrium Hydroxyl Radical "Footprinting". *Curr. Opin. Struct. Biol.*. **12**, 648-653 (2002).

G Dhavan, M Chance, M Brenowitz. Kinetics Analysis of DNA-Protein Interactions by Time-Resolved Synchrotron X-Ray Footprinting . *Analysis of Macromolecules: A Practical Approach*, p. 75-86, IRL Press at Oxford University Press, Oxford. (2003).

J Kiselar, P Janmey, S Almo, M Chance. Visualizing the Ca2+-dependent activation of gelsolin by using synchrotron footprinting. *Proc Natl Acad Sci USA*. **100** (7), 3942-3947 (2003).

P Rangan, B Masquida, E Westhof, S Woodson. Assembly of Core Helices and Rapid Tertiary Folding of a Small Bacterial Group I Ribozyme. *Proc Natl Acad Sci USA*. **100** (4), 1574-1579 (2003).

H Rashidzadeh, S Khrapunov, M Chance, M Brenowitz. Solution Structure and Interdomain Interactions of the Saccharomyces cerevisiae "TATA Binding Protein" (TBP) Probed by Radiolytic Protein Footprinting. *Biochemistry*. **42**, 3655-3665 (2003).

K Takamoto, Q He, S Morris, M Chance, M Brenowitz. Monovalent Cations Mediate Formation of Native Tertiary Structure of the Tetrahymena Thermophila Ribozyme: Implications for the Kinetics of Folding. *Nat. Struct. Biol.*. **9**, 928-933 (2002).

T Ucida, K Takamoto, Q He, M Chance, M Brenowitz. Multiple Monovalent Ion-Dependent Pathways for the Folding of the L-21 Tetrahymena Thermophila Ribozyme. *J. Mol. Biol.*. **328**, 463-478 (2003).

S Woodson. Folding Mechanisms of Group I Ribozymes: Role of Stability and Contact Order. *Biochem Soc Trans*. **30**, 1166-1169 (2002).

NSLS Staff

B Acharya, K Baldwin, R MacHarrie, J Rogers, C Huang, R Pindak. High-speed In-fiber Nematic Liquid Crystal Optical Modulator Based on In-plane Switching with Microsecond Response Time. *Appl. Phys. Lett.*. **81** (27), 5243 (2002).

O Adamopoulos, Z Yu, M Croft, I Zakharchenko, T Tsakalakos, M Muhammed. The characterisation and reactivity of nanostructured cerium-copper-oxide composites for environmental catalysis. *Synthesis, Functional Properties and Applications of Nanostructures. Symposium (Materials Research Society Symposium Proceedings Vol.676)*, Vol 676, p. Y8.11.1-6, sponsored by Mater. Res. Soc. (2002).

T Beetz, C Jacobsen, C Kao, J Kirz, T Mentes, C Sanchez-Hanke, D Sayre, D Shapiro. Development of a Novel Apparatus for Experiments in Soft X-ray Diffraction Imaging and Diffraction Tomography. *J. Phys. IV*. **104**, 31-34 (2003).

C Bernhard, T Holden, J Humlicek, D Munzar, A Golnik, M Klaser, T Wolf, L Carr, C Homes, et al.. In-plane polarized collective modes in detwined Yba2Cu3O6.95 observed by spectral ellipsometry. *Solid State Commun.*. **121**, 1963-1967 (2002).

B Blank, T Kupp, A Deyhim, Y Cai, P Chow, C Kao. Development of a Spectrometer for Inelastic X-ray Measurements. *Proceedings of the 2nd International Workshop on Mechanical Engineering Design of Synchrotron Radiation Equipment and Instrumentation (MEDSI02)*, Vol , p. 308-314, sponsored by MEDSI02. (2002).

G Carr. Dynamics of GaAs photocarriers probed with pulsed infrared synchrotron radiation. *Nucl. Instrum. Meth. B*. **199**, 323 (2003).

F Castano, Y Hao, S Haratani, C Ross, B Vogeli, H Smith, C Sanchez-Hanke, C Kao, X Zhu, P Grutter. Magnetic force microscopy and x-ray scattering study of 70x550 nm2 pseudo-spin-valve nanomagnets. *J. Appl. Phys.*. **93** (10), 7927-7929 (2003).

L Chapman, M Hasnah, O Oltulu, Z Zhong, J Mollenhauer, C Muehleman, K Kuettner, M Aurich, E Pisano, et al.. Diffraction Enhanced X-ray Imaging of Articular Cartilage. US Patent No. 657,7708. (2003).

G Chen, H Jain, M Vlcek, S Khalid, J Li, D Drabold, S Elliott. Observation of Light Polarization-dependent Structural Changes in Chalcogenide Glasses. *Appl. Phys. Lett.*. **82** (5), 706 (2003).

G Chen, H Jain, S Khalid, J Li, D Drabold, S Elliott. Study of Structural Changes in Amorphous As2Se3 By EXAFS under In-Situ Laser Irradiation. *Solid State Commun.*. **120**, 149-153 (2001).

M Croft, W Caliebe, H Woo, T Tyson, D Sills, Y Hor, S Cheong, V Kiryukhin, S Oh. Metal-insulator transition in CuIr2S4: XAS results on the electronic structure. *Phys. Rev. B: Condens. Matter*. **67**, 201102-1-4 (2003).

M Croft, I Zakharchenko, Z Zhong, T Tsakalakos, Y Gulak, Z Kalman, J Hastings, J Hu, R Holtz, K Sadananda. Stress Distribution and Tomographic Profiling with Energy Dispersive X-Ray Scattering. *MRS Proceedings: Applications of Synchrotron Radiation Techniques to Materials Science*, Vol 678, sponsored by Materials Research Society. (2002).

C Cui, T Tyson, Z Zhong, J P Carlo, Y Qin. Effects of Pressure on Electron Transport and Atomic Structure of Manganites: Low to High Pressure Regimes. *Phys. Rev. B: Condens. Matter*. **67**, 104107 (2003).

G De Geronimo, P O'Connor, R Beuttenmuller, Z Li, A Kuczewski, D Siddons. Development of a High-Rate High-Resolution Detector for EXAFS Experiments. *IEEE Trans. Nucl. Sci.*. **50** (4), 885 - 897 (2003).

F Dilmanian, H Weinmann, Z Zhong, T Bacarian, L Rigon, T Buttone, B Ren, X Wu, N Zhong, H Atkins. Tailoring X-ray Beam Energy Spectrum to Enhance Image Quality of New Radiography Contrast Agents Based on Gd or Other Lanthanides. *SPIE: Physics of Medical Imaging*, Vol 4320, p. 417-426, sponsored by SPIE. (2001).

A Doyuran, L DiMauro, E Johnson, S Krinsky, H Loos, J Murphy, G Rakowsky, J Rose, T Shaftan, et al.. Saturation of the NSLS DUV-FEL at BNL. *2003 Particle Accelerator Conference*, Vol 20, p. TOAC012, sponsored by IEEE. (2003).

A Doyuran, W Graves, E Johnson, S Krinsky, H Loos, G Rakowsky, J Rose, T Shaftan, B Sheehy, et al.. Diagnostics System for the NISUS Wiggler and FEL Observations at the BNL Source Development Lab. *European Particle Acclerator Conference, Paris 2002*, Vol 8, p. 802, sponsored by CEA/DSM and CNRS/IN2P3. (2002).

A Doyuran, L DiMauro, W Graves, R Heese, E Johnson, S Krinksy, H Loos, J Murphy, G Rakowsky, et al.. Observation of SASE and Amplified Seed of the DUV-FEL at BNL. *Nucl. Instrum. Meth. A*. **507**, 392-395 (2003).

A Doyuran, M Babzien, T Shaftan, S Biedron, L Yu, I Ben-Zvi, L DiMauro, J Galayda, E Gluskin, et al.. New Results of the High-Gain Harmonic Generation Free-Electon Laser Experiment. *Nucl. Instrum. Meth. A*. **475**, 260-265 (2001).

K Evans-Lutterodt, J Ablett, A Stein, C Kao, D Tennant, F Klemens, A Taylor, C Jacobsen, P Gammel, et al.. Single-element Elliptical Hard X-ray Micro-optics. *Opt. Express*. **11** (8), 919-926 (2003).

K Evans-Lutterodt, A Stein, J Ablett, C Kao, D Tennant, F Klemens, A Taylor, C Jacobsen, P Gammel, et al.. From Lighthouses to Synchrotron Lightsources: Hard X-ray Micro-optics. *Synch. Rad. News*. **16** (3), 60-63 (2003).

S Federman, L Miller, I Sagi. Following Matrix Metalloproteinases Activity Near the Cell Boundary by Infrared Micro-Spectroscopy. *Matrix Biol.*. **21**, 567-577 (2002).

N Gmur. Brookhaven's Free electron Laser at the NSLS Reaches a New Milestone. *Synch. Rad. News*. **16** (1), 32-33 (2003).

N Gmur. Brookhaven National Laboratory DUV-FEL Achieves Important Milestone. *Synch. Rad. News*. **15** (3), 29 (2002).

K Hamalainen, S Galambosi, H Sutinen, C Kao, R Sharon, M Deutsch. Near-threshold Mult-electronic Effects in the Cu K alpha 1,2 X-Ray Spectrum. *Phys. Rev. A*. **67**, 022510 (2003).

M Hasnah, Z Zhong, O Oltulu, E Pisano, R Johnston, D Sayers, W Thomlinson, D Chapman. Diffraction Enhanced Imaging Contrast Mechanisms in Breast

Cancer Specimens. *Med. Phys.*. **29**, 2216-2221 (2002).

M Hasnah, O Oltulu, Z Zhong, D Chapman. Single Exposure Simultaneous Diffraction Enhanced Imaging. *Nucl. Instrum. Meth. A*. **492**, 236-240 (2002).

M Hasnah, O Oltulu, Z Zhong, D Chapman. Application of Absorption and Refraction Matching Techniques for Diffraction Enhanced Imaging. *Rev. Sci. Instrum.*. **73**, 1657-1659 (2002).

H Hayashi, Y Udagawa, W Caliebe, C Kao. Lifetime-broadening Removed X-ray Absorption Near Edge Structure by Resonant Inelastic X-ray Scattering Spectroscopy. *Chem. Phys. Lett.*. **371**, 125 (2003).

H Hayashi, N Wantanabe, Y Udagawa, C Kao. Momentum Dependence of ð-ð* Excitations of Benzene Rings in Condensed Phases. *J. Electron. Spectrosc. Relat. Phenom.*. **933**, 114-116 (2001).

H Hayashi, Y Udagawa, J Gillet, W Caliebe, C Kao. Chemical Applications of Inelastic X-ray Scattering. *Chemical Application of Synchrotron Radiation*, p. 850, World Scientific, River Edge. (2002).

A Hennessy, G Graham, J Hastings, P Siddons, Z Zhong. New pressure flow cell to monitor BaSO4 precipitation using synchrotron in-situ angle dispersive X-ray diffraction. *J. Synch. Rad.*. **9**, 323-324 (2002).

R Huang, L Miller, C Carlson, M Chance. FTIR Analysis of Tibia Bone from Ovariectomized Cynomolgus Monkeys (Macaca fascialaris) and the Effect of Nandrolone Deconoate Treatment. *Bone*. **30** (2), 492-497 (2002).

N Jamin, L Miller, J Moncuit, W Fridman, P Dumas, J Teillaud. Chemical Heterogeneity in Cell Death: Combined Synchrotron IR and Fluorescence Microscopy Studies of Single Apoptotic and Necrotic Cells. *Biopolymers*. **72** (5), 366-373 (2003).

B Jones, C Conko, J Flinn, D Linkous, A Lanzirotti, C Frederickson, P Bertsch, A Friedlich, A Bush. The Effect of enhanced zinc in drinking water on brain and memory. *Natural Science and the Environment:Prescription for a Better Environment*, Vol 1, p. 3, sponsored by USGS. (2003).

S Judex, S Boyd, Y Qin, L Miller, R Muller, C Rubin. Combining High-Resolution MicroCT with Material Composition to Define the Quality of Bone Tissue. *Curr. Osteoporosis Reports*. **1**, 11-19 (2003).

S Kramer, B Podobedov. Coherent Microwave Synchrotron Radiation in the VUV Ring. *Proceedings of Eighth European Particle Accelerator Conference (EPAC'02)*, p. 1523, sponsored by EPAC-02. (2002).

S Krinsky, R Gluckstern. Analysis of Statistical Correlations and Intensity Spiking In The Self-Amplified Spontaneous-Emission Free-Electron Laser. *Phys. Rev. ST AB*. **6**, 050701 (2003).

S Krinsky, Z Huang. Frequency Chirped Self-Amplified Spontaneous-emission Free-electron Laser. *Phys. Rev. ST AB*. **6**, 050702 (2003).

A Lanzirotti, L Miller. Imaging and Microspectroscopy at the National Synchrotron Light Source. *Synch. Rad. News*. **15** (6), 17-26 (2003).

J Li, Z Zhong, R Litdke, K Kuettner, C Peterfy, E Aleyeva, C Muehleman. Radiography of Soft Tissue of the Foot and Ankle with Diffraction Enhanced Imaging. *J. Anatomy*. **202**, 463-470 (2003).

C Limborg, P Bolton, J Clendenin, D Dowell, P Emma, S Gierman, W Graves, H Loos, B Murphy, et al.. PARMELA vs Measurements for GTF and DUVFEL. *European Particle Acclerator Conference, Paris 2002*, Vol 8, p. 1786, sponsored by CEA/DSM and CNRS/IN2P3. (2002).

D Linkous, J Flinn, A Lanzirotti, C Frederickson, B Jones, P Bertsch. Use of Synchrotron X-ray Fluorescence to Measure race Metal Distribution in the Brain. *Transactions of the American Geophysical Union*, Vol F202, p. 81, sponsored by American Geophysical Union. (2002).

H Loos, L DiMauro, A Doyuran, W Graves, E Johnson, S Krinsky, J Rakowsky, J Rose, T Shaftan, et al.. Beam-based Trajectory Alignment in the NISUS Wiggler. *European Particle Accelerator Conference, Paris 2002*, Vol 8, p. 837, sponsored by CEA/DSM and CNRS/IN2P3. (2002).

H Loos, G Carr, A Doyuran, W Graves, E Johnson, S Krinsky, J Rose, B Sheehy, T Shaftan, et al.. Electron Bunch Compression and Coherent Effects at the SDL. *AIP Conference Proceedings*, Vol 647, p. 849-857, (2002).

H Loos, T Shaftan. Beam-Based Undulator Field Characterization and Correction at DUV-FEL. *2003 Particle Accelerator Conference*, Vol 20, p. MPPB038, sponsored by IEEE. (2003).

H Loos, A Doyuran, J Murphy, J Rose, T Shaftan, B Sheehy, Y Shen, J Skaritka, X Wang, et al.. Electro-Optic Longitudinal Electron Beam Diagnostic at SDL. *2003 Particle Accelerator Conference*, Vol 20, p. WPPB021, sponsored by IEEE. (2003).

H Loos, A Doyuran, W Graves, E Johnson, S Krinsky, J Rose, T Shaftan, B Sheehy, J Skaritka, et al.. Experiments in Coherent Radiation at SDL. *European Particle Acclerator Conference, Paris 2002*, Vol 8, p. 814, sponsored by CEA/DSM and CNRS/IN2P3. (2002).

H Mao, C Kao, R Hemley. Inelastic X-ray Scattering at Ultra-high Pressure. *J. Phys.: Condens. Matter*. **13**, 7847 (2001).

Y Mei, L Miller, W Gao, R Gross. Imaging the Distribution and Secondary Structure of Immobilized Enzymes using Infrared Microspectroscopy. *Biomacromolecules*. **4** (1), 70-74 (2003).

L Miller. National Synchrotron Light Source Activity Report 2002. Government Printing Office, Washington. Prepared for Department of Energy. (2003).

L Miller, T Tague. Development and Biomedical Applications of Fluorescence-assisted Synchrotron Infrared Micro-Spectroscopy. *Vib. Spectrosc.*. **849**, 1-7 (2002).

L Miller, G Smith, G Carr. Synchrotron-based Biological Microspectroscopy: From the Mid- to the Far-Infrared Regimes. *J. Biol. Phys.*. **29** (1), 219-230 (2003).

L Miller, P Dumas, N Jamin, J Teillaud, J Miklossy, L Forro. Combining IR Spectroscopy and Fluorescence Imaging in a Single Microscope: Biomedical Applications using a Synchrotron Infrared Source. *Rev. Sci. Instrum.*. **73**, 1357-1360 (2002).

H Mo, H Taub, U Volkmann, M Pino, S Ehrlich, F Hansen, E Lu, P Miceli. A Novel Growth Mode of Alkane Films on a SiO2 Surface. *Chem. Phys. Lett.*. **377**, 99-105 (2003).

J Mollenhauer, M Aurich, Z Zhong, C Muehleman, A Cole, M Hasnah, O Oltulu, K Kuettner, A Margulis, L

Chapman. Diffraction Enhanced X-ray Imaging of Articular Cartilage. *Osteoarthr. Cartilage*. **10**, 168-171 (2002).

C Muehleman, Z Zhong, J Williams, K Kuettner, M Aurich, B Han, J Mollenhauer. Diffraction-enhanced X-ray Imaging of Articular Cartilage of Experimental Animals. *Proceedings Annual Meeting Othrop. Research Society*, Vol , p. 365, sponsored by Ann. Mtg. Orthop. Res. Soc.. (2002).

C Muehleman, L Chapman, K Kuettner, J Rieff, J Mollenhauer, K Massuda, Z Zhong. Radiography of Rabbit Articular Cartilage with Diffraction Enhanced Imaging. *Anatomical Record*. **272A**, 392-397 (2003).

C Muehleman, M Whiteside, Z Zhong, J Mollenhauer, M Aurich, K Kuettner, L Chapman. Diffraction enhanced imaging for articular cartilage. *Biophys. J.*. **82**, 2292-2292 (2002).

J Neumann, D Demske, R Fiorito, P O'Shea, L Carr, H Loos, T Shaftan, B Sheehy, Z Wu. Study of Coherent Radiation from an Electron Beam Prebunched at the Photocathode. *2003 Particle Accelerator Conference*, Vol 20, p. TPAG030, sponsored by IEEE. (2003).

J Neumann, P O'Shea, D Demske, W Graves, B Sheehy, H Loos, G Carr. Electron beam modulation using a laser-driven photocathode . *Nucl. Instrum. Meth. A*. **57** (1-2), 498-501 (2003).

B Noheda, Z Zhong, D Cox, G Shirane, S Park, P Rehring. Electric-field induced phase transitions in rhombohedral Pb(Zn1/3Nb2/3)1-xTixO3. *Phys. Rev. B*. **65**, art no. 224101 (2002).

O Oltulu, Z Zhong, M Hasnah, D Chapman. Multiple Image Radiography in Diffraction Enhanced Imaging. *J. Phys. D: Appl. Phys.*. **36**, 2152-2156 (2003).

P Piot, L Carr, W Graves, H Loos. Subpicosecond compression by velocity bunching in a photoinjector. *Phys. Rev. ST AB*. **6**, 033503 (2003).

B Podobedov, J Ablett, L Berman, R Biscardi, L Carr, B Casey, S Dierker, A Doyuran, R Heese, et al.. NSLS Upgrade Concept. *2003 Particle Accelerator Conference*, Vol 20, p. TOPA007, sponsored by IEEE. (2003).

G Popov, M Greenblatt, M Croft. Large effects of a-site average cation size on the properties of the double perovskites Ba2 xSrxMnReO6, a d5-d1 System. *Phys. Rev. B: Condens. Matter*. **B67**, 24406 (2003).

D Pospiech, D Jehnichen, A Gottwald, L Häussler, U Scheler, P Friedel, W Kollig, C Ober, X Li, et al.. Investigation of the Microphase Separation in Semifluorinated Polyesters. *Polymeric Materials: Science & Engineering*, Vol 84, p. 314-315, sponsored by ACS. (2001).

Q Qian, T Tyson, S Savrassov, C Kao, M Croft. Electronic Structure of La(1-x)CaxMnO3 Determined by Spin-polarized X-ray Absorption Spectroscopy: Comparison of Experiments with Band-Structure Computations. *Phys. Rev. B*. **68**, 014429 (2003).

L Rigon, Z Zhong, F Arfelli, R Menk, A Pillon. Diffraction Enhanced Imaging utilizing different crystal reflections at Elettra and NSLS. *Proc. SPIE 4632: Physics of Medical Imaging*, Vol 4632, p. 29, sponsored by SPIE. (2002).

H Roberts, M Helba, J Carroll, J Burnett, T Drummond, J Lepak, R Propri, Z Zhong, F Agee. Gamma Spectroscopy of Hf-178m2 using Synchrotron X-rays. *Hyperfine Interact.*. **143**, 111-119 (2002).

J Rose, A Doyuran, W Graves, H Loos, T Shaftan, B Sheehy, Z Wu. Radio-Frequency Control System for the DUVFEL. *2003 Particle Accelerator Conference*, Vol 20, p. TPAB006, sponsored by IEEE. (2003).

T Shaftan, A Doyuran, W Graves, E Johnson, S Krinsky, H Loos, J Rose, B Sheehy, J Wu, et al.. Electron Bunch Compression in the SDL Linac. *European Particle Acclerator Conference, Paris 2002*, Vol 8, p. 834, sponsored by CEA/DSM and CNRS/IN2P3. (2002).

T Shaftan, M Babzien, I Ben-Zvi, S Biedron, L DiMauro, A Doyuran, W Graves, J Jagger, E Johnson, et al.. High Gain Harmonic Generation Free-Electron Laser at Saturation. *2001 Particle Accelerator Conference*, p. 246, sponsored by PAC. (2001).

T Shaftan, L Carr, H Loos, B Sheehy, W Graves, Z Huang, C Limborg. Microbunching and Beam Break-up in DUV FEL Accelerator. *2003 Particle Accelerator Conference*, Vol 20, p. TOPD005, sponsored by IEEE. (2003).

T Shaften, L DiMauro, A Doyuran, W Graves, R Heese, E Johnson, S Krinsky, H Loos, J Murphy, et al.. First Sase and Seeded FEL Lasing of NSLS DUV Fel at 266 and 400 nm. *Nucl. Instrum. Meth. A*. **507**, 15-18 (2003).

B Sheehy, G Carr, A Doyuran, W Graves, R Heese, E Johnson, S Krinsky, H Loos, J Murphy, G Rakowsky. Ultrafast Deep UV FEL Source for AMO Physics at Brookhaven National Laboratory. *Annual (2003) Meeting of the Division of Atomic, Molecular, and Optical Physics of the APS*, Vol 48, p. 61, sponsored by American Physical Society. (2003).

B Sheehy, G Carr, L DiMauro, A Doyuran, W Graves, R Heese, E Johnson, S Krinsky, H Loos, J Murphy. A Deep Ultraviolet Ultrafast Source Driven by High Gain. *CLEO/QELS 2003: Conference on Lasers and Electro-optics / Quantum Electronics and Laser Science Conference*, Vol 2003, p. QWC2, sponsored by Optical Society of America. (2003).

K Smith, J Xue, L Duda, A Fedorov, P Johnson, S Hulbert, W McCarroll, M Greenblatt. Recent high resolution photoemission studies of electronic structure in quasi-one dimensional conductors. *J. Electron. Spectrosc. Relat. Phenom.*. **117-118**, 517-526 (2001).

T Tsakalakos, M Croft, I Zakharchenko, Z Zhong, Y Gulak, M Desilva, R Holtz. On the Mechanical Stability of Nanostructured Coatings by Synchrotron Radiation. *AIAA 2002*, Vol AIAA-2002, p. 1314, sponsored by AIAA. (2002).

M v. Zimmermann, C Nelson, J Hill, D Gibbs, M Blume, D Casa, B Keimer, Y Murakami, C Kao, et al.. X-ray resonant scattering studies of orbital and charge ordering in Pr1-xCaxMnO3. *Phys. Rev. B*. **64**, 195133 (2001).

M v. Zimmermann, C Nelson, J Hill, D Gibbs, M Blume, D Casa, B Keimer, Y Murakami, C Kao, et al.. X-ray Resonant Scattering Studies of Orbital and Charge Ordering in Pr1-xCaxMnO3. *J. Magn. Magn. Mater.*. **233**, 31 (2001).

M Wernick, O Wirjadi, D Chapman, O Oltulu, Z Zhong, Y Yang. Preliminary investigation of a multiple-image radiography method. *IEEE. Intl. Symposium on Biomed. Imaging: Macro to Nano* , Vol (2002), p. 1435, sponsored by National Institute of Health. (2002).

J Wu, L Yu. Coherent Hard X-ray Productin by Cascading Stages of High Gain Harmonic

Generation X-ray FEL. *Nucl. Instrum. Meth. A*. **475** (1-3), 104 (2001).

Y Yacoby, M Sowman, E Stern, J Cross, D Brewer, R Pindak, J Pitney, E Dufresne, R Clarke. Direct determination of epitaxial interface structure: Gd2O3 passivation of GaAs, Nature Materials. *Nat. Mater.*. **1**, 99 (2002).

L Yang, L Ding, H Huang. New Phases of Phospholipids and Implications to the Membrane Fusion Problem. *Biochemistry*. **42** (22), 6631-6635 (2003).

L Yang, L Ding, H Huang. A Rhombohedral Phase of Lipid Containing a Membrane Fusion Intermediate Structure. *Biophys. J.*. **84**, 1808 (2003).

L Yu, L DiMauro, A Doyuran, W Graves, E Johnson, R Heese, S Krinsky, H Loos, J Murphy, et al. First Ultraviolet High-Gain Harmonic-Generation Free-Electron Laser. *Phys. Rev. Lett.*. **91** (7), 074801-1 (2003).

L Yu, J Wu. Theory of High Gain Harmonic Generation - an Analytical Estimate. *Nucl. Instrum. Meth. A*. **483**, 493 (2002).

L Yu, M Babzien, I Ben-Zvi, L DiMauro, A Doyuran, W Graves, E Johnson, S Krinsky, R Malone, et al.. First Lasing of a High Gain Harmonic Generation Free-Electron Laser Experiment. *Nucl. Instrum. Meth. A*. **445**, 301 (2000).

I Zakharchenko, Y Gulak, Z Zhong, M Croft, T Tsakalakos. Methodology of Synchrotron EDXRD Strain Profiling. *Advances in X-ray Analysis*, Vol 46, sponsored by International Centre for Diffraction Data. (2002).

I Zakharchenko, Y Gulak, Z Zhong, M Croft, T Tsakalakos. Application of Synchrotron EDXRD Strain Profiling in Shot Peened Materials. *Advances in X-ray Analysis*, Vol 46, sponsored by International Centre for Diffraction Data. (2002).

Z Zhong, C Kao, D Siddons, H Zhong, J Hastings. X-ray reflectivity of sagittally bent Laue crystals. *Acta Cryst. A*. **59**, 1-6 (2003).

Z Zhong, D Chapman, D Connor, A Dilmanian, N Gmur, M Hasnah, R Johnston, M Kiss, J Li, et al.. Diffraction Enhanced Imaging of Soft Tissues. *Synch. Rad. News*. **15** (6), 27-34 (2002).

Z Zhong, D Siddons, D Chapman, C Kao, N Zhong, J Hastings. Model of Sagittally-bent Silicon Crystals Diffracting in the Laue Mode: the Effects of Elastic-Anisotropy on the Rocking-curve Widths. *12th National Conference on Sychrotron Radiation Instrumentation*, Vol 73, p. 1615, sponsored by University of Wisconsin-Madison. (2002).

Z Zhong, D Chapman, M Hasnah, E Johnston, M Kiss, O Oltulu, L Rigon, N Zhong, E Pisano, D Sayers. X-ray Diffraction Order-selection with a Prism in DEI. *12th National Conference on Sychrotron Radiation Instrumentation*, Vol 73, p. 1614, sponsored by American Institute of Physics. (2002).

Z Zhong, C Kao, D Siddons, J Hastings. Rocking-curve width of sagittally bent Laue crystals. *Acta Cryst. A*. **58**, 487-493 (2002).

F Zhou, I Ben-Zvi, M Babzien, X Chang, A Doyuran, R Malone, X Wang, V Yakimenko. Experimental Characterization of Emittance Growth Induced the the Nonuniform Transverse Laser Distribution in a Photoinjector. *Phys. Rev. ST AB*. **5**, 094203 (2002).

The following pages list all publication citations reported to the NSLS in FY 2003 (October 1, 2002 through September 30, 2003). Citations are listed in order of beamline number and then alphabetically by the last name of the first author. This list contains unique citations for journal, published conference proceedings, books, chapters in books, formal reports, informal reports, technical reports, theses, dissertations, and patents when reported. For citation submissions where research was performed on more than one beamline, the citation is listed under each beamline. However, each citation was only counted once. Citations bearing publication dates prior to the Year 2003 are listed only if they had not been previously reported to the NSLS and did not appear in a prior fiscal year's activity report. Diligent effort has been made to ensure that each reference is unique and complete. For journal articles, online searches were performed to locate missing reference information (e.g., year of publication, volume, issue or page numbers). With regard to conference papers, considerable effort was put into ensuring that the citations appeared in published proceedings. Many citations for conferences papers have been omitted from this list if verification could not be made. We apologize to our users and authors for any citations incorrectly omitted.

Several types of journal articles are reported in this list, including premiere journals, peer-reviewed journals and a few that are not peer-reviewed. Premiere journals include: Physical Review Letters, Science, Nature, Cell, EMBO Journal, Nature Structural Biology, Proceedings of the National Academy of Sciences of the United States of America, Structure, and Applied Physics Letters.

In FY 2003, the following types and numbers of publication citations were reported to the NSLS where research was performed in part or in whole at the NSLS.

Journals, peer-reviewed, premiere	113
Journals, other peer-reviewed	440
Journals, non peer-reviewed	22
Total Journals and Magazines	575
Books/Chapters in Books	17
Published Conference Proceedings	59
Reports: Technical, Formal, Informal	1
Theses/Dissertations	9
Patents	1
Total Misc. Publications	87
Total Citations Listed	**662**

NSLS VUV User Publications	76
NSLS X-Ray User Publications	489
NSLS Staff Publications	97
	662

NSLS Users

Beamline U1A

M Zwahlen, D Brovelli, W Caseri, G Haehner. Orientation and Electronic Structure of Ion-Exchanged Pyridinium Compounds on Mica. *J. Colloid Interface Sci.*. **256**, 262 (2002).

Beamline U2A

B Chen, D Muthu, Z Liu, A Sleight, M Kruger. High-pressure Optical Study of HfW2O8. *J. Phys.: Condens. Matter*. **14**, 13911-13916 (2002).

E Gregoryanz, A Goncharov, R Hemley, H Mao, M Somayazulu, G Shen. Raman. Infrared, and x-ray evidence for new phases of. *Phys. Rev. B: Condens. Matter*. **66**, 224108 (2002).

R Hemley, Z Liu, E Gregoryanz, H Mao. Infrared and Raman Microspectroscopy of Materials Under Pressure. *Microscopy and Microanalysis*, Vol 9, p. 1098, (2003).

R Hemley, H Mao. Overview of static high pressure science, in High-Pressure Phenomena. *Proceedings of the International School of Physics, "Enrico Fermi" Course CXLVII*, p. 3-40, IOS Press, Amsterdam. (2002).

R Hemley, H Mao. New window on earth and planetary interiors. *Miner. Mag.*. **66**, 791-811 (2002).

Z Liu, J Hu, H Yang, H Mao, R Hemley. High-pressure Synchrotron X-ray Diffraction and Infrared Microspectroscopy: Application to Dense Hydrous Phases. *J. Phys.: Condens. Matter*. **14**, 10641-10646 (2002).

Z Liu, G Lager, R Hemley, N Ross. Synchrotron Infrared Spectroscopic Study of OH-chondrodite and OH-clinohumite at High Pressure. *Am. Mineral.*. **88**, 1412 (2003).

Y Song, R Hemley, Z Liu, M Mosayazulu, H Mao, D Herschbach. High-pressure stability, transformations, and vibrational dynamics of nitrosonium nitrate from synchrotron infrared and Raman spectroscopy. *J. Chem. Phys.*. **119** (4), 2232 (2002).

H Yang, C Prewitt, Z Liu. Crystal structures and infrared spectra of two Fe-bearing hydrous magnesium silicates synthesized at high temperature and pressure. *J. Miner. Petrological Sci.*. **97**, 137-143 (2002).

Beamline U2B

L Cho, J Reffner, B Gatewood, D Wetzel. Single Fiber Analysis by Internal Reflection Infrared Microspectroscopy. *J. of Forsensic Sci.*. **46** (6), 1309-1314 (2001).

A Eilert, J Sweat, D Wetzel. Parabolic Concentration of Diffusely Transmitted Near-IR Radiation in an Acousto-Optic Tunable Filter Spectrometer. *J. Near Infrared Spectrosc.*. **8**, 239-250 (2000).

A Eilert, D Wetzel. Optics and Sample Handling for Near-Infrared Diffuse Reflection. *Handbook of Vibrational Spectroscopy*, p. 436-452, Wiley, Chichester. (2002).

R Huang, L Miller, C Carlson, M Chance. FTIR Analysis of Tibia Bone from Ovariectomized Cynomolgus Monkeys (Macaca fascialaris) and the Effect of Nandrolone Deconoate Treatment. *Bone*. **30** (2), 492-497 (2002).

S Judex, S Boyd, Y Qin, L Miller, R Muller, C Rubin. Combining High-Resolution MicroCT with Material Composition to Define the Quality of Bone Tissue. *Curr. Osteoporosis Reports*. **1**, 11-19 (2003).

J Radel, J Homan, D Wallace, D Wetzel, S LeVine. FT-IR Microspectroscopic Chemical Analysis of Photoreceptor Outer Segment Changes Resulting from Oxidative Stress. *Invest. Opht. Vis. Sci.*. **41** (4), S23 (2000).

J Sweat, D Wetzel. Near Infrared Acousto-Optic Tunable Filter Based Instrumentation for the Measurement of Dynamic Spectra of Polymers. *Rev. Sci. Instrum.*. **72** (4), 2153-2158 (2001).

D Wetzel, A Eilert, J Sweat. Tunable Filter and Discrete Filter Near-IR Spectrometers. *Handbook of Vibrational Spectroscopy*, p. 436-452, Wiley, Chichester. (2002).

D Wetzel, S LeVine. Biological Applications of Infrared Microspectroscopy. *Infrared and Raman Spectroscopy of Biological Materials*, p. 101-142, Marcel Dekkar, New York. (2000).

D Wetzel, J Reffner. Infrared Spectroscopy goes Microscopic. *Chem. Ind.*. **9** (8), 308-313 (2000).

D Wetzel, P Srivarin, J Finney. Revealing Protein Infrared Spectral Detail in a Heterogenous Matrix Dominated by Starch. *Vib. Spectrosc.*. **31**, 109-114 (2003).

D Wetzel, S LeVine. Spatially Resolved Improved FT-IR Microspectroscopy of Deuterated Species in Tissue. *Microscopy and Microanalysis*, Vol 8, p. 1502, (2002).

D Wetzel, G Williams. Synchrotron Infrared Microspectroscopy of Retinal Layers. *Vib. Spectrosc.*. **30**, 101-109 (2002).

D Wetzel. A New Approach to the Problem of Dispersive Windows in Infrared Microspectroscopy. *Vib. Spectrosc.*. **29**, 291-297 (2002).

D Wetzel. Sensitive Infrared Narrow Band Optimized Microspectrometer. *Vib. Spectrosc.*. **29**, 291-297 (2002).

D Wetzel. Contemporary Near-Infrared Instrumentation. *Near Infrared Technology in the Agricultural and Food Industries*, p. 129-144, Am. Assoc. Cereal Chem., St. Paul. (2001).

Beamline U4B

M Harris, G Appel, H Ade. Surface Morphology of Annealed Polystyrene and Poly(methyl methacrylate) Thin Film Blends and Bilayers. *Macromolecules*. **36**, 3307-3314 (2003).

A Lussier, Y Idzerda, S Stadler, S Ogale, S Shinde, V Venkatesan. Characterization for Strontium Titanate/Fe3O4 and TiN/Fe3O4 Interfaces. *J. Vac. Sci. Technol., B*. **20** (4), 1609-1613 (2002).

Beamline U4IR

A Boris, D Munzar, N Kovaleva, B Liang, C Lin, A Dubroka, T Holden, B Keimer, C Bernhard, et al.. Josephson Plasma Resonanse and Phonon Anomalies in Trilayer Bi2Sr2Ca2Cu3O10. *Phys. Rev. Lett.*. **89** (27), 277001 (2002).

G Carr. Dynamics of GaAs photocarriers probed with pulsed infrared synchrotron radiation. *Nucl. Instrum. Meth. B*. **199**, 323 (2003).

G Flynn, L Keller. Synchrotron FTIR Examination of Interplanetary Dust Particles: An Effort to Determine the Compounds and Minerals in Interstellar and Circumstellar Dust. *Laboratory Astrophysics Workshop*, Vol NASA CP-2002-211863, p. 201-203, sponsored by NASA. (2002).

L Miller, G Smith, G Carr. Synchrotron-based Biological Microspectroscopy: From the Mid- to the Far-Infrared Regimes. *J. Biol. Phys.*. **29** (1), 219-230 (2003).

Beamline U5UA

I Baek, H Lee, H Kim, E Vescovo. Spin Reorientation Transition in Fe(110) Thin Films: The Role of Surface Anisotropy. *Phys. Lett. B*. **67**, 075401 (2003).

Beamline U7A

D Abraham, R Twesten, M Balasubramanian, J Kropf, D Fischer, J McBreen, I Petrov, K Amine. The Electrochemistry of Germanium Nitride with Lithium. *J. Electrochem. Soc.*. **150** (11), A1450-A1456 (2003).

L Andruzzi, W Senaratne, A Hexemer, C Ober, E Kramer. PEG-Based Biostable Surfaces by Controlled Radical Polymerization. *Polymeric Materials: Science & Engineering*, Vol 88, p. 604-605, sponsored by ACS. (2003).

R Bhat, J Genzer, B Chaney, H Sugg, A Liebmann-Vinson. Controlling the Assemblies of Nanoparticles using Molecular and Macromolecular Gradients. *Nanotech.*. **14**, 1145-1152 (2003).

R Bubeck, L Thomas, W Burghardt, S Rendon, A Hexemer, B Hart. Mechanical and Morphological Anisotropy in a Thermotropic Liquid Crystalline Polymer. *12th International Conference on Deformation, Yield, and Fracture of Polymers*, Vol 12, p. 155 - 158, sponsored by The Plastics and Rubber Division of the Institute of Materials, Minerals, and Mining. (2003).

J Genzer, D Fischer, K Efimenko. Combinatorial near-edge x-ray absorption fine structure: Simultaneous determination of molecular orientation and bond concentration on chemically heterogeneous surfaces. *Appl. Phys. Lett.*. **82**, 266 (2003).

J Genzer, K Efimenko, D Fischer. Molecular Orientation and Grafting Density in Semifluorinated Self-Assembled Monolayers of Mono-, Di-, and Trichloro Silanes on Silica Substrates. *Langmuir*. **18**, 9307-9311 (2002).

J Genzer, D Fischer, K Efimenko. Fabricating Two-Dimensional Molecular Gradients via Asymmetric Deformation of Uniformly-Coated Elastomer Sheets. *Advanced Materials*. **15** (18), 1545-1547 (2003).

J Genzer, E Kramer, D Fischer. Application of near-edge absorption fine structure (NEXAFS) to studies of surface molecular orientation of model organic molecules. *J. Appl. Phys.*. **92**, 7070 (2002).

S Kang, M Liang, X Li, F Chiellini, C Ober, E Kramer. Surface Active Block Copolymers (SABC): Biofouling Resistant Coatings from Chemically Modified Polymers. *Polymeric Materials: Science & Engineering*, Vol 84, p. 14-15, sponsored by ACS. (2001).

J Lenhart, R Jones, E Lin, C Soles, W Wu, S Sambasivan, D Goldfarb, M Angelopoulos. Probing Surface and Bulk Chemistry in Resist Films using near-edge x-ray absorption fine structure. *J. Vac. Sci. Technol., B*. **20** (6), 2920-2926 (2002).

Q Li, L Wu, Y Zhu, A Moodenbaugh, G Gu, M Suenaga, Z Ye, D Fischer. Comparitive studies fo MgB2/Mg Nano-composites and press-sintered MgB2 pellets. *IEEE Trans. Appl. Superconductivity*. **13**, 3051-3055 (2003).

X Li. Studies of Block Copolymers in Surface Engineering and Nanotechnology. Ph.D. Thesis. Cornell University, Ithaca. (2003).

G Liu, J Rodriguez, J Hrbek, B Long, D Chen. Interaction of Thiophene with Titania Surfaces. *J. Mol. Catal. A: Chem.*. **202**, 215-227 (2003).

P Liu, J Rodriguez, J Muckerman, J Hrbek. Interaction of CO, O, and S with metal nanoparticles on Au(111): A theoretical study. *Phys. Rev. B*. **67**, 155416-1-155416-10 (2003).

G Long, A Allen, D Black, H Burdette, D Fischer, R Spal, J Woicik. National Institute of Standards and Technology synchrotron radiation facilities for materials science. *J. Res - NIST*. **106**, 1141 (2002).

A Maiti, J Rodriguez, M Law, P Kung, J McKinney, P Yang. SnO2 Nanoribons as NO2 Sensors. *Nano Lett.*. **3**, 1025-1028 (2003).

A Marsh. Mechanisms of Deep Catalytic Oxidation of Aromatic Hydrocarbons on a Platinum Single Crystal Surface. Ph.D. Thesis. University of Michigan, Ann Arbor. (2003).

J McBreen, X Yang, M Balasubramanian, X Sun, H Lee. Synchrotron X-ray Studies of Lithium-Ion Battery Components. *The 43rd Battery Symposium in Japan*, Vol 2I, p. 46, sponsored by The Electrochemical Society of Japan. (2002).

G Meitzner, D Fischer. Distortions of fluoresence yield X-ray absorption spectra due to sample thickness. *Microchem. J.*. **71**, 281 (2002).

C Ober, J Youngblood, L Andruzzi, W Senaratne, X Li, A Hexemer, E Kramer. Block Copolymers as Surface Modifiers: Synthesis, Characterization and Relevance to Fouling Release and Biostability. *Polymeric Materials: Science & Engineering*, Vol 88, p. 612-613, sponsored by ACS. (2003).

D Pospiech, D Jehnichen, A Gottwald, L Häussler, U Scheler, P Friedel, W Kollig, C Ober, X Li, et al.. Investigation of the Microphase Separation in Semifluorinated Polyesters. *Polymeric Materials: Science & Engineering*, Vol 84, p. 314-315, sponsored by ACS. (2001).

J Rodriguez, P Liu, J Dvorak, T Jirsak, J Gomes, Y Takahashi, K Nakamura. Adsorption and decomposition of SO2 on TiC(001): An experimental and theoretical study. *Surf. Sci. Lett.*. **543**, L675-L682 (2003).

J Rodriguez, M Perez, T Jirsak, J Evans, J Hrbek, L Gonzalez. Activation of Au nanoparticles on oxide surfaces: reaction of SO2 with Au/MgO(100). *Chem. Phys. Lett.*. **378**, 526-532 (2003).

J Rodriguez, J Dvorak, T Jirsak, G Liu, J Hrbek, Y Aray, C Gonzalez. Coverage Effects and the Nature of the Metal-Sulfur Bond in S/Au(111): High Resolution Photoemission and Density-Functional Studies. *J. Am. Chem. Soc.*. **125**, 276-285 (2003).

W Senaratne, L Andruzzi, D Holowka, B Ilic, A Hexemer, B Baird, C Ober, E Kramer. Exploring the Potential of Surface Grown PEG-Polymer Brushes for Biotechnology Applications. *Polymeric Materials: Science & Engineering*, Vol 88, p. 337-338 , sponsored by ACS. (2003).

Z Song, T Cai, Z Chang, G Liu, J Rodriguez, J Hrbek. Molecular Level Study of the Formation and the Spread of MoO3 on Au (111) by Scanning Tunneling Microscopy and X-ray Photoelectron Spectroscopy. *J. Am. Chem. Soc.*. **125**, 8059-8066 (2003).

W Wallace, D Fischer. Resonant soft X-ray photofragmentation of propane. *J. Electron. Spectrosc. Relat. Phenom.*. **130**, 1-6 (2003).

T Wu, K Efimenko, P Vlcek, V Subr, J Genzer. Formation and Properties of Anchored Polymers with a Gradual Variation of Grafting Densities on Flat Substrates. *Macromolecules*. **36**, 2448-2453 (2003).

J Youngblood, L Andruzzi, C Ober, A Hexemer, E Kramer, J Callow, J Finley, M Callow. Coatings Based on Side-chain Ether-linked Poly(ethylene glycol) and Fluorocarbon Polymers for the Control of Marine Biofouling. *Biofouling*. **19** (supplement), 91-98 (2003).

Beamline U8B

K Miller. C-H and C-C Bond Activations of Organic Molecues by Stable Germylenes. Ph.D. Thesis. University of Michigan, Ann Arbor. (2002).

T Owens, S Süzer, M Banaszak Holl. Variable Energy X-ray Photoemission Studies of Alkylsilane Based Monolayers on Gold. *J. Phys. Chem. B*. **107** (14), 3177-3182 (2003).

K Schneider. Scanning Tunneling Microscopy Investigation of Spherosiloxane- and Alkylsilane-Based Monolayers. Ph.D. Thesis. University of Michigan, Ann Arbor. (2003).

K Schneider, K Nicholson, T Owens, B Orr, M Banaszak Holl. The differential reactivity of octahydridosilsesquioxane on Si(100)-2×1 and Si(111)-7×7: a comparitive experimental study. *Ultramicroscopy*. **97**, 35-43 (2003).

S Süzer, S Sayan, M Banaszak Holl, E Garfunkel, Z Hussain, N Hamdan. Soft X-ray photoemission studies of Hf oxidation. *J. Vac. Sci. Technol., A*. **21** (1), 106-109 (2003).

Beamline U10A

D Basov, A Bratkovsky, P Henning, B Zink, F Hellman, Y Wang, C Home, M Strongin. Infrared probe of metal-insulator transition in Si1-xGdx and Si1-xYx amorphous alloys in magnetic field. *Europhys. Lett.*. **57**, 240-246 (2002).

C Bernhard, T Holden, J Humlicek, D Munzar, A Golnik, M Klaser, T Wolf, L Carr, C Homes, et al.. In-plane polarized collective modes in detwined Yba2Cu3O6.95 observed by spectral ellipsometry. *Solid State Commun.*. **121**, 1963-1967 (2002).

C Homes, J Tranquada, Q Li, A Moodenbaugh. Mid-infrared conductivity from mid-gap states associated with charge stripes. *Phys. Rev. B*. **67**, 184516 (2003).
C Homes, Q Li, A Moodenbaugh, P Fournier, R Greene. Infrared optical properties of Pr2CuO4. *Phys. Rev. B: Condens. Matter*. **66**, 144511 (2002).
C Homes, T Vogt, S Shapiro, S Wakimoto, M Subramanian, A Ramirez. Charge transfer in high dielectric constant materials CaCu(3)Ti(4)O(12) and CdCu(3)Ti(4)O(12). *Phys. Rev. B: Condens. Matter*. **67**, 092106 (2003).
J Tu, C Homes, G Gu, D Basov, M Strongin. Optical studies of charge dynamics in the optimally doped Bi2Sr2CaCu2O8+delta. *Phys. Rev. B*. **66**, 144514 (2002).
J Tu, C Homes, G Gu, M Strongin. A systematic optical study of phonon properties in optimally doped Bi2Sr2CaCu2O8+delta. *Physica B*. **316-317**, 324-327 (2002).
G Tzamalis, N Zaidi, C Homes, A Monkman. Doping dependent studies of the Anderson-Mott localization in polyaniline at the metal-insulator boundary. *Phys. Rev. B*. **66**, 085202 (2002).

Beamline U10B

D Chidambaram, M Jaime Vasquez, G Halada, C Clayton. Studies on the repassivation behavior of aluminum and aluminum alloy exposed to chromate solutions. *Surf. Interface Anal.*. **35** (2), 226 (2003).
A Eilert, J Sweat, D Wetzel. Parabolic Concentration of Diffusely Transmitted Near-IR Radiation in an Acousto-Optic Tunable Filter Spectrometer. *J. Near Infrared Spectrosc.*. **8**, 239-250 (2000).
C Eng, G Halada, A Francis, C Dodge, J Gillow. Uranium Association with Corroding Carbon Steel Surfaces. *Surf. Interface Anal.*. **35**, 525-535 (2003).
S Federman, L Miller, I Sagi. Following Matrix Metalloproteinases Activity Near the Cell Boundary by Infrared Micro-Spectroscopy. *Matrix Biol.*. **21**, 567-577 (2002).
G Flynn, L Keller. Synchrotron FTIR Examination of Interplanetary Dust Particles: An Effort to Determine the Compounds and Minerals in Interstellar and Circumstellar Dust. *Laboratory Astrophysics Workshop*, Vol NASA CP-2002-211863 , p. 201-203, sponsored by NASA. (2002).
K Gough, D Zielinski, R Wiens, M Rak, I Dixon. Fourier transform infrared evaluation of microscopic scarring in the cardiomyopathic heart: Effect of chronic AT1 suppression. *Anal. Biochem.*. **316**, 232-242 (2003).
R Huang, L Miller, C Carlson, M Chance. FTIR Analysis of Tibia Bone from Ovariectomized Cynomolgus Monkeys (Macaca fascialaris) and the Effect of Nandrolone Deconoate Treatment. *Bone*. **30** (2), 492-497 (2002).
N Jamin, L Miller, J Moncuit, W Fridman, P Dumas, J Teillaud. Chemical Heterogeneity in Cell Death: Combined Synchrotron IR and Fluorescence Microscopy Studies of Single Apoptotic and Necrotic Cells. *Biopolymers*. **72** (5), 366-373 (2003).
V Joshi, R Powell, F Furuya, I Hainfeld. Metal carbonyl clusters as infrared labels for biosensing. *American Chemical Society National Meeting*, Vol Fall 2003, p. Inorg-73, sponsored by American Chemical Society. (2003).
S Judex, S Boyd, Y Qin, L Miller, R Muller, C Rubin. Combining High-Resolution MicroCT with Material Composition to Define the Quality of Bone Tissue. *Curr. Osteoporosis Reports*. **1**, 11-19 (2003).
A Lanzirotti, L Miller. Imaging and Microspectroscopy at the National Synchrotron Light Source. *Synch. Rad. News*. **15** (6), 17-26 (2003).
Y Mei, L Miller, W Gao, R Gross. Imaging the Distribution and Secondary Structure of Immobilized Enzymes using Infrared Microspectroscopy. *Biomacromolecules*. **4** (1), 70-74 (2003).
L Miller, P Dumas, N Jamin, J Teillaud, J Miklossy, L Forro. Combining IR Spectroscopy and Fluorescence Imaging in a Single Microscope: Biomedical Applications using a Synchrotron Infrared Source. *Rev. Sci. Instrum.*. **73**, 1357-1360 (2002).
L Miller, G Smith, G Carr. Synchrotron-based Biological Microspectroscopy: From the Mid- to the Far-Infrared Regimes. *J. Biol. Phys.*. **29** (1), 219-230 (2003).
L Miller, T Tague. Development and Biomedical Applications of Fluorescence-assisted Synchrotron Infrared Micro-Spectroscopy. *Vib. Spectrosc.*. **849**, 1-7 (2002).
J Radel, J Homan, D Wallace, D Wetzel, S LeVine. FT-IR Microspectroscopic Chemical Analysis of Photoreceptor Outer Segment Changes Resulting from Oxidative Stress. *Invest. Opht. Vis. Sci.*. **41** (4), S23 (2000).
D Wetzel, P Srivarin, J Finney. Revealing Protein Infrared Spectral Detail in a Heterogenous Matrix Dominated by Starch. *Vib. Spectrosc.*. **31**, 109-114 (2003).
D Wetzel, S LeVine. Biological Applications of Infrared Microspectroscopy. *Infrared and Raman Spectroscopy of Biological Materials*, p. 101-142, Marcel Dekkar, New York. (2000).
D Wetzel, J Reffner. Infrared Spectroscopy goes Microscopic. *Chem. Ind.*. **9** (8), 308-313 (2000).
P Yu, J McKinnon, C Christensen, D Christensen, N Marinkovic, L Miller. Chemical Imaging of Micro-Structures of Plant Tissues within Cellular Dimension Using Synchrotron Infrared Microspectroscopy. *J. Agr. Food Chem.*. **51** (20), 6062-6067 (2003).

Beamline U12A

K Adib, D Mullins, G Totir, N Camillone III, J Fitts, K Rim, G Flynn, R Osgood Jr. Dissociative adsorption of CCl4 on the Fe3O4(111)-(2x2) selvedge of alpha-Fe2O3(0001). *Surf. Sci.*. **524**, 113-128 (2003).

Beamline U12IR

S Kramer, B Podobedov. Coherent Microwave Synchrotron Radiation in the VUV Ring. *Proceedings of Eighth European Particle Accelerator Conference (EPAC'02)*, Vol , p. 1523, sponsored by EPAC-02. (2002).

Beamline U13UB

K Smith, J Xue, L Duda, A Fedorov, P Johnson, S Hulbert, W McCarroll, M Greenblatt. Recent high resolution photoemission studies of electronic structure in quasi-one dimensional conductors. *J. Electron. Spectrosc. Relat. Phenom.*. **117-118**, 517-526 (2001).

B Wells, Z Yusof, T Valla, A Fedorov, P Johnson, C Dendziora, S Jian, D Hinks. ARPES evidence for a quasiparticle liquid in overdoped Bi2Sr2CaCu2O8+delta. *Surf. Rev. Lett.*. **9** (2), 1091-1096 (2001).

Beamline X1A1

T Beetz, C Jacobsen. Soft X-ray Radiation-Damage Studies in PMMA using a Cryo-STXM. *J. Synch. Rad.*. **105**, 280-283 (2003).

G Flynn, L Keller, S Wirick, C Jacobsen, S Sutton. Analysis of interplanetary dust particles by soft and hard x-ray microscopy. *J. Phys. IV*. **104**, 367-372 (2003).

A Kilcoyne, T Tyliszczak, W Steele, S Fakra, P Hitchcock, K Franck, E Anderson, B Harteneck, E Rightor, et al. Interferometer-Controlled Scanning Transmission X-ray Microscopes at the Advanced Light Source. *J. Synch. Rad.*. **108**, 125-136 (2003).

J Rothe, M Plaschke, M Denecke. Soft x-ray spectromicroscopy investigation of the formation and ageing of Eu(III)-induced humic acid aggregates. *J. Phys. IV*. **104**, 421-424 (2003).

T Schaefer, F Claret, A Bauer, L Griffault, E Ferrage, B Lanson. Natural organic matter (NOM)-clay association and impact on Callovo-Oxfordian clay stability in high alkaline solution: Spectromicroscopic evidence. *J. Phys. IV*. **104**, 413-416 (2003).

T Schaefer, N Hertkorn, R Artinger, F Claret, A Bauer. Functional group analysis of natural organic colloids and clay association kinetics using C(1s) spectromicroscopy. *J. Phys. IV*. **104**, 409-412 (2003).

S Urquhart, H Ade. Trends in the Carbonyl Core (C 1s, O 1s) ® p*C=O Transition in the Near Edge X-ray Absorption Fine Structure Spectra of Organic Molecules. *J. Phys. Chem. B*. **106**, 8531-8538 (2002).

Beamline X1A2

T Schaefer, F Claret, A Bauer, L Griffault, E Ferrage, B Lanson. Natural organic matter (NOM)-clay association and impact on Callovo-Oxfordian clay stability in high alkaline solution: Spectromicroscopic evidence. *J. Phys. IV*. **104**, 413-416 (2003).

T Schaefer, N Hertkorn, R Artinger, F Claret, A Bauer. Functional group analysis of natural organic colloids and clay association kinetics using C(1s) spectromicroscopy. *J. Phys. IV*. **104**, 409-412 (2003).

Beamline X1B

T Beetz, C Jacobsen, C Kao, J Kirz, T Mentes, C Sanchez-Hanke, D Sayre, D Shapiro. Development of a Novel Apparatus for Experiments in Soft X-ray Diffraction Imaging and Diffraction Tomography. *J. Phys. IV*. **104**, 31-34 (2003).

U Hergenhahn, A Rüdel, K Maier, A Bradshaw, R Fink, A Wen. The Resonant Auger Spectra of Formic Acid, Acetaldehyde, Acetic Acid and Methyl formate. *Chem. Phys.*. **289**, 57-67 (2003).

C McGuinness, D Fu, J Downes, K Smith, G Hughes, J Roche. Electronic structure of thin film silicon oxynitrides measured using soft x-ray emission and absorption. *J. Appl. Phys.*. **94** (6), 3919-3922 (2003).

C McGuinness, J Downes, P Ryan, K Smith, D Doppalapudi, T Moustakas. X-ray Spectroscopic Studies of the Bulk Electronic Structure of InGaN Alloys. *GaN and Related Alloys, MRS Fall 2002 Meeting*, Vol 743, p. L10_11, sponsored by Materials Research Society. (2003).

Beamline X2B

R Seright, J Liang, B Lindquist, J Dunsmuir. Use of X-ray computed microtomography to understand why gels reduce relative permeability to water more than that to oil. *J. Petrol. Sci. Eng.*. **39**, 217-230 (2003).

Beamline X3A1

I Novozhilova, A Volkov, P Coppens. Theoretical Analysis of the Triplet Excited State of the [Pt2(H2P2O5)4]4- Ion and Comparison with Time-Resolved X-ray and Spectroscopic Results. *J. Am. Chem. Soc.*. **125**, 1079-1087 (2003).

J Overgaard, F Larsen, B Schiott, B Iverson. Electron Density Distributions of Redox Active Mixed Valence Carboxylate Bridged Trinuclear Iron Complexes. *J. Am. Chem. Soc.*. **125**, 11088-11099 (2003).

S Pillet, G Wu, V Kulsomphob, B Harvey, R Ernst, P Coppens. Investigation of Zr-C, Zr-N, and Potential Agostic Interactions in an Organozirconium Complex by Experimental Electron Density Analysis. *J. Am. Chem. Soc.*. **125**, 1937-1949 (2003).

Beamline X3A2

P Agarwal, R Somani, W Weng, A Mehta, L Yang, S Ran, L Liu, B Hsiao. Shear-Induced Crystallization in Novel Long Chain Branched Polypropylenes by in Situ Rheo-SAXS and -WAXD. *Macromolecules*. **36**, 5226-5235 (2003).

A Nogales, I Sics, T Ezquerra, Z Denchev, F Balta Calleja, B Hsiao. In-Situ Simultaneous Small- and Wide-Angle X-ray Scattering Study of Poly(ether ester) during Cold Drawing. *Macromolecules*. **36**, 4827-4832 (2003).

S Ran, Z Wang, C Burger, B Chu, B Hsiao. Mesophase as the Precursor for Strain-Induced Crystallization in Amorphous Poly(ethylene terephthalate) Film. *Macromolecules*. **35**, 10102-10107 (2002).

R Somani, L Yang, B Hsiao, P Agarwal, H Fruitwala, A Tsou. Shear-Induced Precursor Structures in Isotactic Polypropylene Melt by in-Situ Rheo-SAXS

and Rheo-WAXD Studies. *Macromolecules*. **35**, 9096-9104 (2002).

Beamline X3B1

M Bushey, T Nguyen, C Nuckolls. Synthesis, Self-Assembly, and Switching of One-Dimensional Nanostructures from New Crowded Aromatics. *J. Am. Chem. Soc.*. **125**, 8264-8269 (2003).

M Colle, R Dinnebier, W Brutting. The structure of the blue luminescent delta phase of tris(8-hydroxyquinoline)aluminum(III) (Alq3). *Chem. Commun.*. **2002**, 2908-2909 (2002).

R Dinnebier, S Vensky, M Panthöfer, M Jansen. Crystal and Molecular Structures of Alkali Oxalates - First Proof of a Staggered Oxalate Anion in the Solid State. *Z. Kristallogr.*. (Suppl. Iss. 20), 86 (2003).

R Dinnebier, S Vensky, M Panthöfer, M Jansen. Crystal and Molecular Structures of Alkali Oxalates: First Proof of a Staggered Oxalate Anion in the Solid State. *Inorg. Chem.*. **42** (5), 1499-1507 (2003).

A Le Bail, P Stephens, H Hubert. A crystal structure for the souzalite/gormanite series from synchrotron powder diffraction data. *Eur. J. Mineral.*. **15** (4), 719-723 (2003).

O Omotoso, R Mikula, P Stephens. Surface area of interstratified phyllosilicates in Athabasca oil sands from synchrotron XRD. *Advances in X-ray Analysis*, Vol 54, p. 391-396, sponsored by International Centre for Diffraction Data. (2002).

M Rajeswaran, T Blanton, N Zumbulyadis, D Giesen, C Conesa-Moratilla, S Misture, P Stephens, A Huq. Three-dimensional Structure Determination of N-(p-Tolyl)-dodecylsulfonamide from Powder Diffraction Data and Validation of Structure using Solid-State NMR Spectroscopy. *J. Am. Chem. Soc.*. **124**, 14450-14459 (2002).

M Viola, M Martinez-Lopez, J Alonso, J Martinez, J De Paoli, S Pagola, J Pedregosa, M Fernandez-Diaz, R Carbonio. Structure and Magnetic Properties of Sr2CoWO6: An Ordered Double Perovskite Containing Co2+(HS) with Unquenched Orbital Magnetic Moment. *Chem. Mater.*. **15**, 1655-1663 (2003).

Beamline X4A

M Aittaleb, R Rashid, Q Chen, J Palmer, C Daniels, H Li. Structure and Function of Archaeal Box C/D sRNP Core Proteins. *Nat. Struct. Biol.*. **106** (45), 256 (2003).

N Armstrong, M Mayer, E Gouaux. Tuning activation of the AMPA-sensitive GluR2 ion channel by genetic adjustment of agonist-induced conformational changes. *Proc Natl Acad Sci USA*. **100** (10), 5736-5741 (2003).

Y Chi, J Frantz, B Oh, L Hansen, S Shoelson. Diabetes mutations delineate an atypical POU domain in HNF1a.. *Mol. Cell*. **10**, 1129 (2002).

H Cho, K Mason, K Ramyar, A Stanley, S Gabelli, D Denney, D Leahy. Structure of the Extracellular Region of HER2 Alone and in Complex with the Herceptin Fab. *Nature*. **421**, 756-760 (2003).

N Friedland, H Liou, P Lobel, A Stock. Structure of a Cholesterol-Binding Protein Deficient in Niemann-Pick Type C2 Disease. *Proc Natl Acad Sci USA*. **100** (5), 2512-2517 (2003).

H Furukawa, E Gouaux. Mechanisms of activation, inhibition and specificity: crystal structures of the NMDA receptor NR1 ligand-binding core. *EMBO J.*. **22** (12), 2873-2885 (2003).

A Gogos, L Shapiro. Large Conformational Changes in the Catalytic Cycle of Glutathione Synthase. *Structure*. **10** (12), 1669-1676 (2002).

J Hunt, J Deisenhofer. Ping-Pong Cross-Validation in Real Space: a Method for Increasing the Phasing Power of a Partial Model Without Risk of Model Bias. *Acta Cryst. D*. **59**, 214-224 (2003).

R Jin, M Horning, M Mayer, E Gouaux. Mechanism of Activation and Selectivity in a Ligand-Gated Ion Channel: Structural and Functional Studies of GluR2 and Quisqualate. *Biochemistry*. **41**, 15635-15643 (2002).

R Jin, E Gouaux. Probing the Function, Conformational Plasticity, and Dimer-Dimer Contacts of the G1uR2 Ligand-Binding Core: Studies of 5-Substituted Willardiines and G1uR2 S1S2 in the Crystal. *Biochemistry*. **42**, 5201-5213 (2003).

G Jogl, L Tong. Crystal Structure of Carnitine Acetyltransferase and Implications for the Catalytic Mechanism and Fatty Acid Transport. *Cell*. **112**, 113-122 (2003).

Z Juo, G Kassavetis, J Wang, E Geiduschek, P Sigler. Crystal structure of a transcription factor IIIB core interface ternary complex. *Nature*. **422**, 534-539 (2003).

R Khayat, R Batra, C Qian, T Halmos, M Bailey, L Tong. Structural and Biochemical Studies of Inhibitor Binding to Human Cytomegalovirus Protease. *Biochemistry*. **42**, 885-891 (2003).

S Lahiri, G Zhang, D Dunaway-Mariano, K Allen. The Pentacovalent Phosphorus Intermediate of a Phosphoryl Transfer Reaction. *Science*. **299**, 2067 (2003).

I Levchenko, R Grant, D Wah, R Sauer, T Baker. Structure of a Delivery Protein for an AAA+ Protease in Complex with a Peptide Degradation Tag. *Mol. Cell*. **12**, 365-372 (2003).

S Majeed, G Ofek, A Belachew, C Huang, T Zhou, P Kwong. Enhancing Protein Crystallization Through Precipitant Synergy. *Structure*. **11**, 1061-1070 (2003).

Y Mao, J Chen, J Maynard, B Zhang, F Quiocho. A Novel A; Helix Fold of the AP180 Amino-Terminal Domain for Phoshoinositide. *Cell*. **104**, 433-440 (2001).

K Murthy, S Smith, V Ganesh, K Judge, N Mullin, P Barlow, C Ogata, G Kotwal. Crystal Structure of a Complement Control Protein that Regulates Both Pathways of Complement Activation and Binds Heparan Sulfate Proteoglycans. *Cell*. **104**, 301-311 (2001).

R Nagem, D Colau, L Dumoutier, J Renauld, C Ogata, I Polikarpov. Crystal Structure of Recombinant Human Interleukin-22. *Structure*. **10**, 1051-1062 (2002).

V Robinson, T Wu, A Stock. Structural analysis of the domain interface in DrrB, a response regulator of the OmpR/PhoB subfamily. *J. Bacteriol.*. **185** (14), 4186-4194 (2003).

V Robinson, J Hwang, E Fox, M Inouye, A Stock. Domain Arrangement of Der, a Switch Protein

Containing Two GTPase Domains.. *Structure*. **10** (12), 1649 (2002).
S Santagata, T Boggon, C Baird, C Gomez, J Zhao, W Shan, D Myszka, L Shapiro. G-Protein Signaling Through Tubby Proteins. *Science*. **292**, 2041-2050 (2001).
T Schwartz, G Blobel. Structural Basis for the Function of the beta Subunit of the Eukaryotic Signal Recognition Particle Receptor. *Cell*. **112** (6), 793-803 (2003).
I Shumilin, R Bauerle, R Kretsinger. The High-Resolution Structure of 3-Deoxy-D-arabino-heptulosonate-7-phosphate Synthase Reveals a Twist in the Plane of Bound Phosphoenolypyruvate. *Biochemistry*. **42**, 3766-3776 (2003).
S Sia, P Carr, A Cochran, V Malashkevich, P Kim. Short Constrained Peptides that Inhibit HIV-1 Entry. *Proc Natl Acad Sci USA*. **99** (23), 14664-14669 (2002).
X Tao, Y Xu, Y Zhang, A Beg, L Tong. An Extensively Associated Dimer in the Structure of the C713S Mutant of the TIR Domain of Human TLR2. *Biochem. Biophys. Res. Commun.*. **299**, 216-221 (2002).
A VanDemark, R Hofmann, C Tsui, C Pickart, C Wolberger. Molecular Insights into Polyubiquitin Chain Assembly:Crystal Structure of the Mms2/Ubc13 Heterodimer. *Cell*. **105**, 711-720 (2001).
H Yamaguchi, H Matsushita, A Nairn, J Kuriyan. Crystal Structure of the Atypical Protein Kinase Domain of a TRP Channel with Phophtransferase activity. *Mol. Cell*. **7**, 1047-1057 (2001).
B Yeh, M Igarashi, A Eliseenkova, A Plotnikov, I Sher, D Ron, S Aaronson, M Mohammadi. Structural Basis by Which Alternative Splicing Confers Specificity in Fibroblast Growth Factor Receptors. *Proc Natl Acad Sci USA*. **100** (5), 2266-2271 (2003).
Y Yuan, O Martsinkevich, J Hunt. Structural Characterizatin of an MJ1267 ATP-Binding Cassette Crystal with a Complex Pattern Twinning Caused by Promiscuous Fiber Packing. *Acta Cryst. D*. **59**, 225-238 (2003).
H Zhang, Z Yang, Y Shen, L Tong. Crystal Structure of the Carboxyltransferase Domain of Acetyl-Coenzyme A Carboxylase. *Science*. **299**, 2064 (2003).

Beamline X6A

J James, C Escalante, M Yoon-Robarts, T Edwards, R Linden, A Aggarwai. Crystal Structure of the SF3 Helicase from Adeno-Associated Virus Type 2. *Structure*. **11**, 1025-1035 (2003).
L Kang, S Gabelli, M Bianchet, W Xu, M Bessman, L Amzel. Structure of a coenzyme A pyrophosphatase from Deinococcus radiodurans: a member of the Nudix family. *J. Bacteriol.*. **185** (14), 4110-9 (2003).

Beamline X6B

A Mateja, Y Devedjiev, D Krowarsch, K Longenecker, Z Dauter, J Otlewski, Z Derewenda. The Impact of Glu>Ala and Glu>Asp Mutations on the Crystallization Properties of RhoGDI: The Structure of RhoGDI at 1.3 A Resolution. *Acta Cryst. D*. **58**, 1983-1991 (2002).

Beamline X7A

P Barnes, P Woodward, Y Lee, T Vogt, J Hriljac. Pressure-Induced Cation Migration and Volume Expansion in the Defect Pyrochlores ANbWO6 (A = NH4+, Rb+, H+m K+). *J. Am. Chem. Soc.*. **125**, 4572-4579 (2003).
A Burton, S Elomari, R Medrud, I Chan, C Chen, L Bull, E Vittoratos. The Synthesis, Characterization, and Structure Solution of SSZ-58: A Novel Two-Dimensional 10-Ring Pore Zeolite with Previously Unseen Double 5-Ring Subunits. *J. Am. Chem. Soc.*. **125**, 1633-1642 (2003).
W Dmowski, T Egami, K Swider-Lyons, C Love, D Rolison. Local Atomic Structure and Conduction Mechanism of Nanocrystalline Hydrous RuO2 from X-ray Scattering. *J. Phys. Chem. B*. **106**, 12677-12683 (2002).
E Irran, B Juergens, W Schnick. Synthesis, Crystal Structure Determination from X-ray Powder Diffractometry and Vibrational Spectroscopy of the Tricyanomelaminate Monohydrates M3[C6N9].H2O (M=K,Rb). *Solid State Sci.*. **4**, 1305-1311 (2002).
H Jeong, S Nair, T Vogt, L Dickinson, M Tsapatsis. A highly crystalline layered silicate with three dimensionally microporous layers. *Nat. Mater.*. **2**, 53-58 (2003).
J Lai, K Shafi, K Loos, A Ulman, Y Lee, T Vogt, C Estrones. Doping gamma-Fe2O3 Nanoparticles with Mn(III) Suppresses the Transition to the alpha-Fe2O3 Structure. *J. Am. Chem. Soc.*. **125**, 11470-11471 (2003).
Y Lee, D Mitzi, P Barnes, T Vogt. Pressure-Induced Phase Transitions and Templating Effect in Three-Dimensional Organic-Inorganic Hybrid Perovskites. *Phys. Rev. B: Condens. Matter*. **68**, 020103R (2003).
Y Lee, T Vogt, J Hriljac, J Parise, J Hanson, S Kim. Non-Framework Cation Migration and Irreversible Pressure-induced Hydration in a Zeolite. *Nature*. **420**, 485 (2002).
N Pereira, M Balasubramanian, L Dupont, J McBreen, L Klein, G Amatucci. The Electrochemistry of Germanium Nitride with Lithium. *J. Electrochem. Soc.*. **150** (8), A1118-A1128 (2003).
V Petkov, S Billinge, T Vogt, A Ichimura, J Dye. Structure of Intercalated Cs in Zeolite ITQ-4:An Array of Metal Ions and Correlated Electrons Confined in a Pseudo-1D Nanoporous Host. *Phys. Rev. Lett.*. **89**, 075502 (2002).
V Petkov, S Billinge, P Larson, S Mahanti, T Vogt, K Rangan, M Kanatzidis. Structure of Nanocrystalline Materials using Atomic Pair Distribution Function Analysis: Study of LiMoS2. *Phys. Rev. B*. **65**, 092105 (2002).
T Vogt, J Hriljac, N Hyatt, P Woodward. Pressure-induced intermediate-to-low spin state transition in LOaCoO3. *Phys. Rev. B*. **67**, 140401-1 - 140401-4 (2003).
X Yang, J McBreen, W Yoon, M Yoshio, H Wang, K Fukuda, T Umeno. Structural Studies of the New Carbon Coated Silicon Anode Using Synchrotron Based In Situ XRD. *Electrochem. Commun.*. **4** (11), 893-897 (2002).

Beamline X7B

A Christensen, T Jensen, N Scarlett, I Madsen. n-situ X-ray powder diffraction studies of hydrothermal and themal decomposition reactions of basic bismuth(III) nitrates in the temperature range 20-650C. *Dalton Trans.*. **16**, 3278-3282 (2003).

A Christensen, N Scarlett, I Madsen, T Jensen, J Hanson. Real Time study of cement and clinker phases hydration. *Dalton Trans.*. **2003**, 1529-1536 (2003).

P Chupas, D Corbin, V Rao, J Hanson, C Grey. A Combined Solid-State NMR and Diffraction Study of the Structures and Acidity of Fluorinated Aluminas: Implications for Catalysis. *J. Phys. Chem. B*. **107**, 8327-8336 (2003).

P Devi, Y Lee, J Margolis, J Parise, S Samath, H Herman, J Hanson. Comparison of citrate-nitrate gel combustion and precursor plasma spray processes for the synthesis of yttrium aluminum garnet. *J. Mater. Res.*. **17**, 2846-2851 (2002).

G Evans, R Fureaux, G Gainsford, J Hanson, G Kicska, A Sauve, V Schram, P Tyler. "8-Aza-Immuncillins as Transition State analogue Inhibitors of Purine Nucleoside Phosphorylase and Nucleoside Hydrolases. *J. Med. Chem.*. **46**, 155-160 (2003).

M Khoudiakov, A Parise, B Brunschwig. Interfacial Electron Transfer in FeII(CN)64-Sensitized TiO2 Nanoparticles: A Study of Direct Charge Injection by Electroabsorption Spectroscopy. *J. Am. Chem. Soc.*. **125**, 4637-4642 (2003).

J Kim, J Rodriquez, J Hanson, A Frenkel, P Lee. Reduction of CuO and Cu2O with H2: H Embedding and Kinetic Effects in the Formation of Suboxides. *J. Am. Chem. Soc.*. **125**, 10684-16092 (2003).

J Post, P Heany, J Hanson. Synchrotron x-ray diffraction study of the structure and dehydration behavior of todorokite. *Am. Mineral.*. **88**, 141-151 (2003).

J Post, P Heaney, R Von Dreele, J Hanson. Neutron and temperature-resolved synchrotron X-ray powder diffraction study of akaganeite. *Am. Mineral.*. **88**, 782-788 (2003).

J Rodriguez, X Wang, J Hanson, G Liu, A Iglesias-Juez, M Fernandez-Garcia. The behavior of mixed-metal oxides: Structural and electronic properties of Ce-Ca oxides. *J. Chem. Phys.*. **119**, 5659-5669 (2003).

J Rodriguez, J Kim, J Hanson, M Perez, A Frenkel. Reduction of CuO in H2: In Situ Time-Resolved XRD Studies. *Catal. Lett.*. **85**, 247-254 (2003).

J Rodriguez, J Kim, J Hanson, J Brito. Reduction of CoMoO4 and NiMoO4: In situ Time-Resolved XRD Studies. *Catal. Lett.*. **82** (1-2), 103-109 (2002).

J Rodriguez, J Kim, J Hanson, S Sawhill, M Bussell. Physical and Chemical Properties of MoP, Ni2P, and MoNiP Hydrodesulfurization Catalysts: Time-Resolved X-ray Diffractin, Density Functional, and Hydrodesulfurization Activity Studies. *J. Phys. Chem. B*. **107**, 6276-6285 (2003).

R Sullivan, H Liu, D Smith, J Hanson, D Osterhout, M Ciraolo, C Grey, J Martin. Sorptive Reconstruction of the CuAlCl4 Framework upon Reversible Ethylene Binding. *J. Am. Chem. Soc.*. **125**, 11065-11079 (2003).

J Wang, S Brankovic, Y Zhu, J Hanson, R Adzic. Kinetic Characterization of PtRu Fuel Cell Anode Catalysts Made by Spontaneous Pt Decomposition on Ru Nanoparticles. *J. Electrochem. Soc.*. **150**, a1108-a1117 (2003).

Beamline X8C

I Bosanac, J Alattia, T Mal, J Chan, S Talarico, F Tong, K Tong, F Yoshikawa, T Furuichi, et al. Structure of the Inositol 1,4,5-trisphosphate Receptor Binding Core in Complex with its Ligand. *Nature*. **420**, 696 (2002).

J Elam, A Taylor, R Strange, S Antonyuk, P Doucette, J Rodriguez, S Hasnain, L Hayward, J Selverston Valentine, et al. Amyloid-like Filaments and Water-filled Nanotubes formed by SOD1 Mutant Proteins Linked to Familial ALS. *Nat. Struct. Biol.*. **10** (6), 461-467 (2003).

S Eswaramoorthy, S Gerchman, V Graziano, H Kycia, F Studier, S Swaminathan. Structure of a Yeast Hypothetical Protein Selected by a Structural Genomics Approach. *Acta Cryst. D*. **59**, 127-135 (2003).

J Jiang, A Taylor, K Prasad, Y Ishikawa-Brush, P Hart, E Lafer, R Sousa. Structure-Function Analysis of the Auxilin J-Domain Reveals an Extended Hsc70 Interaction Interface. *Biochemistry*. **42**, 5748-5753 (2003).

V Kacer, S Scaringe, J Scarsdale, J Rife. Crystal Structures of r(GGUCACAGCCC)2. *Acta Cryst. D*. **59**, 423-432 (2003).

C Kerfeld, M Sawaya, V Brahmandam, D Cascio, K Ho, C Trevithick-Sutton, D Krogmann, T Yeates. The Crystal Structure of a Cyanobacterial Water-Soluble Carotenoid Binding Protein. *Structure*. **11**, 55-65 (2003).

P Kongsaeree, C Samanchart, P Laowanapiban, S Wiyakrutta, V Meevootisom. Crystallization and Preliminary X-ray Crystallographic Analysis of D-Phenylglycine Aminotransferase from Pseudomonas Stutzeri ST201. *Acta Cryst. D*. **59**, 953-954 (2003).

P Lario, A Vrielink. Sub-atomic resolution crystal structure of cholesterol oxidase: what atomic resolution crystallography reveals about enzyme mechanism and the role of the FAD cofactor in redox activity.. *J. Mol. Biol.*. **326** (5), 1635-50 (2003).

Y Lee, S Nadaraia, D Gu, D Becker, J Tanner. Structure of the Proline Dehydrogenase Domain of the Multifunctional PutA Flavoprotein. *Nat. Struct. Biol.*. **10** (2), 109 (2003).

J Liu, A Dermatakis, C Lukacs, F Konzelmann, Y Chen, U Kammlott, W Depinto, H Yang, X Yin, et al.. 3,5,6-Trisubstituted naphthostyrils as CDK2 inhibitors.. *BioOrg. Med. Chem.*. **13** (15), 2465-8 (2003).

C Mura, M Philips, A Kozhukhovsky, D Eisenberg. Structure and assembly of an augmented Sm-like archaeal protein 14-mer. *Proc Natl Acad Sci USA*. **100** (8), 4539-4544 (2003).

V Namboodiri, S Dutta, I Akey, J Head, C Akey. The Crystal Structure of Drosophila NLP-Core Porvids Insight into Pentamer Formation and Histone Binding. *Structure*. **11**, 175-186 (2003).

G Pal, T DeVeyra, J Elce, Z Jia. Purification, Crystallization and Preliminary X-ray Analysis of a u-like Calpain. *Acta Cryst. D*. **59**, 369-371 (2003).

X Qian, C Guan, H Guo. A Dual Role for an Aspartic Acid in Glycosylasparaginase Autoproteolysis. *Structure*. **11**, 997-1003 (2003).

M Sam, D Cascio, R Johnson, R Clubb. Crystallization and Prelimnary X-ray Crystallographic Analysis of the Excisionase-DNA Complex from Bacteriophage. *Acta Cryst. D*. **59**, 1238-1240 (2003).

X Yang, Y Hu, D Yin, M Turner, M Wang, R Borchardt, P Howell, K Kuczera, R Schowen. Catalytic Strategy of S-Adenosyl-L-homocysteine Hydrolase: Transition-State Stabilization and the Avoidance of Abortive Reactions. *Biochemistry*. **42**, 1900-1909 (2003).

J Yang, M Park, G Waldo, S Suh. Directed Evolution Approach to a Structural Genomics Project: Rv2002 from Mycobacterium tuberculosis. *Proc Natl Acad Sci USA*. **100** (2), 455-460 (2003).

Z Yang, C Lanks, L Tong. Molecular Mechanism for the Regulation of Human Mitochondrial NAD(P)+ - Dependent Malic Enzyme by ATP and Fumarate. *Structure*. **10**, 951-960 (2002).

Beamline X9A

C Albermann, A Soriano, J Jiang, H Vollmer, J Biggins, W Barton, J Lesniak, D Nikolov, J Thorson. Substrate Specificity of NovM: Implications for Novobiocin Biosynthesis and Glycorandomization. *Org. Lett.*. **5**, 933-936 (2003).

W Barton, B Liu, D Tzvetkova, P Jeffreey, A Fournier, D Sah, R Cate, S Strittmatter, D Nikolov. Structure and Axon Outgrowth Inhibitor Binding of the Nogo-66 Receptor and Related Proteins. *EMBO J.*. **22**, 3291-3302 (2003).

A Bobkov, A Muhlrad, K Kokabi, S Vorobiev, S Almo, E Reisler. Structural Effects of Cofilin on Longitudinal Contacts in F-Actin. *J. Mol. Biol.*. **323**, 739-750 (2002).

J Bonanno, S Burley. Structural Genomics of Proteins Contributing to Conserved Biochemical Pathways/Processes. *Curr. Opin. Struct. Biol.*. **12**, 383-391 (2002).

S Burley, J Bonanno. Structural Genomics. *Structural Bioinformatics*, p. 591-612, Academic Press, New York. (2002).

S Burley, J Bonanno. Structuring the Universe of Proteins. *Annu. Rev. Genomics and Human Genetics*. **3**, 243-262 (2002).

F Burling, R Kniewel, J Buglino, T Chadha, A Beckwith, C Lima. Structure of Escherichia Coli Uridine Phosphorylase at 2.0 Angstrom. *Acta Cryst. D*. **59**, 73-76 (2003).

E Campbell, J Tupy, T Gruber, S Wang, M Sharp, C Gross, S Darst. Crystal Structure of Escherichia Coli E with the Cytoplasmic Domain of its anti-RseA. *Mol. Cell*. **11**, 1067-078 (2003).

W Chan, S Roderick, D Cohen. Human Phosphatidylcholine Transfer Protein: Purification, Crystallization and Preliminary X-ray Diffraction. *Biochim Biophys Acta*. **1596** (1), 1-5 (2002).

J Coyle, D Nikolov. GABARAP: Lessons for Synaptogenesis. *The Neuroscientist*. **9**, 205-216 (2003).

A Deaconescu, A Roll-Mecak, S Gerchman, H Kycia, F Studier, J Bonanno, S Burley. X-Ray Structure of Saccharomyces Cerevisiae Homologous Mitochondrial Matrix Factor 1 (Hmf1). *Proteins: Struc. Func. Genet.*. **48**, 431-436 (2002).

J Dewan, A Feeling-Taylor, Y Puius, L Patskovska, Y Patskovsky, R Nagel, S Almo, R Hirsch. Structure of Mutant Human Carbonmonoxyhemoglobin C (betaE6K) at 2.0 A Resolution. *Acta Cryst. D*. **58**, 2038-2042 (2002).

C Fabrega, S Shuman, C Lima. Structure of Candida Albicans mRNA Guanylytransferase Bound to Phosphorylated CTD of RNA Polymerase II. *Mol. Cell*. **11**, 1549-1561 (2003).

C Groft, S Burley. Recognition of eIF4G by Rotavirus NSP3 Reveals a Basis for mRNA Circularization. *Mol. Cell*. **6**, 1273-1283 (2002).

J Himanen, D Nikolov. In Focus: Eph Receptors and Ephrins. *N/A*. **35**, 130-134 (2003).

J Himanen, D Nikolov. Eph Receptors and Ephrins a Structural View. *Trends Neurosci.*. **26**, 46-51 (2003).

W Joo, P Jeffrey, S Cantor, M Finnin, D Livingston, N Pavletich. Structure of the 53BP1 BRCT Region Bound to p53 and its Comparison to the Brcal BRCT Structure. *Genes Dev.*. **16**, 583-593 (2002).

K Kamada, F Hanoaka, S Burley. Crystal Structure of the MazE/MazF Complex: Molecular Bases of Antidote-Toxin Recognition. *Mol. Cell*. **11**, 875-884 (2003).

K Kamada, R Roeder, S Burley. Molecular Mechanism of Recruitment of TFIIF - Associating RNA Polymerase C-Terminal Domain Phosphatase (FCP1) by Transcription Factor IIF. *Proc Natl Acad Sci USA*. **100** (5), 2296-2299 (2003).

G Kicska, P Tyler, G Evans, R Furneaux, W Shi, A Fedorov, A Lewandowicz, S Cahill, S Almo, V Schramm. Atomic Dissection of the Hydrogen Bond Network for Transition-State Analogue Binding to Purine Nucleoside Phosphorylase. *Biochemistry*. **41**, 14489-14498 (2002).

R Kniewel, J Buglino, V Shen, T Chadna, A Beckwith, C Lima. Structural Analysis of Saccharomyces Cerevisiae Myo-Inositol Phosphate Synthase. *J. Struct. Funct. Genomics*. **3**, 129-134 (2002).

A Larsson, R Andersson, J Stahlberg, L Kenne, T Jones. Dextranase from Penicillium minioluteum: Reactin Course, Crystal Structure, and Product Complex. *Structure*. **11**, 1111-1121 (2003).

J Lesniak, W Barton, D Nikolov. Structural and Functional Characterization of the Pseudomonas Hydroperoxide Resistance Protein Ohr. *EMBO J.*. **21** (24), 6649-6659 (2002).

A Lewandowicz, W Shi, G Evans, P Tyler, R Furneaux, L Basso, D Santos, S Almo, V Schramm. Over-the-Barrier Transition State Analogues and Crystal Structure with Mycobacterium Tuberculosis Purine Nucleoside Phosphorylase. *Biochemistry*. **42**, 6057-6066 (2003).

M Lilic, V Galkin, A Orlova, M VanLoock, E Egelman, C Stebbins. Salmonella SipA Polymerizes Actin by Stapling Filaments with Nonglobular Protein Arms. *Science*. **301**, 1918-1921 (2003).

E Mossessova, L Bickford, J Goldberg. SNARE Selectivity of the COPII Coat. *Cell*. **114**, 483-495 (2003).

S Nair, S Burley. X-ray Structures of Myc-Max and Mad-Max Recognizing DNA: Molecular Bases of Regulation by Proto-Oncogenic Transcription Factors. *Cell*. **112**, 193-205 (2003).

A Niedzwiecka, J Marcotrigiano, J Stepinski, M Jankowska-Anyszka, A Wyslouch-Cieszynska, M Dadlez, A Gingras, P Mak, E Darzynkiewicz, et al.. Biophysical studies of eIF4E Cap-Binding Protein: Recognition of mRNA 5' Cap Structure and Synthetic Fragments of eIF4G and 4E-BP1 Proteins. *J. Mol. Biol.*. **319**, 615-635 (2002).

M Perbandt, E Guthohrlein, W Rypniewski, K Idakieva, S Stoeva, W Voelter, N Genov, C Betzel. The Structure of a Functional Unit from the Wall of a Gastropod Hemocyanin Offers a Possible Mechanism for Cooperativity. *Biochemistry*. **42**, 6341-6346 (2003).

D Pilloff, K Dabovic, M Romanowski, J Bonanno, M Doherty, S Burley, T Lehy. The Kinetic Mechanism of Phosphomevalonate Kinase. *J. Biol. Chem.*. **278**, 4510-4514 (2003).

S Ray, J Bonanno, H Chen, S Wu, H De Lencastre, A Tomasz, S Burley. Crystal Structure of a Methanococcus Jannaschii DNA-Binding Protein: Implications for Antibiotic Resistance in Staphyloccoccus Aureus. *Proteins: Struc. Func. Genet.*. **50**, 170-173 (2003).

K Schneibner, J DeAngelis, S Burley, P Cole. Investigation of the Roles of Catalytic Residues in Serotonin N-Acetyltransferase. *J. Biol. Chem.*. **277**, 18118-18126 (2002).

T Schwartz, G Blobel. Structural Basis for the Function of the beta Subunit of the Eukaryotic Signal Recognition Particle Receptor. *Cell*. **112** (6), 793-803 (2003).

W Shi, D Ostrov, S Gerchman, H Kycia, W Studier, W Edstrom, A Bresnick, J Ehrlich, J Blanchard, et al. High-Throughput Structural Biology & Proteomics. *Protein Arrays, Biochips & Proteomics: The Next Phase of Genomics Discovery*, p. 299-324, Marcel Dekker, New York. (2003).

B Shin, D Maag, A Roll-Mecak, M Arefin, S Burley, J Lorsch, T Dever. Uncoupling of Initiation Factor eIF5B/IF2 GTPase and Translational Activities by Mutations that Lower Ribosome Affinity. *Cell*. **111**, 1015-1025 (2002).

R Soccio, R Adams, M Romanowski, E Sehayek, S Burley, J Breslow. The Novel Cholesterol-Regulated StarD4 Gene Encodes a StAR-Related Lipid Transfer Protein with two Closely Related Homologues. *Proc Natl Acad Sci USA*. **99**, 6943-6948 (2002).

J Sun, A Fedorov, S Lee, X Guo, K Shen, D Lawrence, S Almo, Z Zhang. Crystal Structure of PTP1B Complexed with a Potent and Selective Bidentate Inhibitor. *J. Biol. Chem.*. **278**, 12406-12414 (2003).

J Sun, L Wu, A Fedorov, S Almo, Z Zhang. Crystal Structure of the Yersinia Protein-Tyrosine Phosphatase YopH Complexed with a Specific Small Molecule Inhibitor. *J. Biol. Chem.*. **278**, 33392-33399 (2003).

Y Tseng, B Schafer, S Almo, D Wirtz. Functional Synergy of Actin Filament Cross-Linking Proteins. *J. Biol. Chem.*. **277**, 25609-25616 (2002).

S Vorobiev, B Strokopytov, D Drubin, C Frieden, S Ono, J Condeelis, P Rubenstein, S Almo. The Structure of Non-Vertebrate Actin: Implications for the ATP Hydrolytic Mechanism. *Proc Natl Acad Sci USA*. **100** (10), 5760-5765 (2003).

E Wolf, J De Angelis, E Khalil, P Cole, S Burley. X-Ray Crystallographic Studies of Serotonin N-Acetyltransferase Catalysis and Inhibition. *J. Mol. Biol.*. **317**, 215-224 (2002).

G Wu, G Xu, B Schulman, P Jeffrey, J Harper, N Pavletich. Structure of a Beta-TrCPI-Skp1-Beta-Catenin Complex: Destruction Motif Binding and Lysine Specificity of the SCF(beta-TrCP1) Ubiquitin Ligase. *Mol. Cell*. **6**, 1445-1456 (2003).

X Zhang, J Schwartz, S Almo, S Nathenson. Expression, Refolding, Purification, Molecular Characterization, Crystallization and Preliminary X-Ray Analysis of the Receptor Binding Domain of Human B7-2. *Protein Expr. Purif.*. **25**, 105-113 (2003).

X Zhang, J Schwartz, S Almo, S Nathenson. Crystal Structure of the Receptor-Binding Domain of Human B7-2: Insights into Organization and Signaling. *Proc Natl Acad Sci USA*. **100** (5), 2586-2591 (2003).

Beamline X9B

M Andrykovitch, K Routzahn, M Li, Y Gu, D Waugh, X Ji. Characterization of four orthologs of stringent starvation protein A. *Acta Cryst. D*. **59**, 881-886 (2003).

O Asojo, S Cater, D Hoover, C Boulegue, W Lu, J Lubkowski. Crystallization and Preliminary X-ray Studies of Thymus and Activation-Regulated Chemokine (TARC). *Acta Cryst. D*. **59**, 163-165 (2003).

O Asojo, C Boulegue, D Hoover, W Lu, J Lubkowski. Structures of Thymus and Activation-regulated Chemokine (TARC). *Acta Cryst. D*. **59**, 1165-1173 (2003).

O Asojo, E Afonina, S Gulnik, J Erickson, R Randad, D Medjahed, A Silva. Novel Uncomplexed and Complexed Structures of Phasmepsin II, an Asparticprotease from Plasmodium Falciparum. *J. Mol. Biol.*. **327**, 173-181 (2003).

S Banumathi, M Dauter, Z Dauter. Phasing at High Resolution using Ta6Br12 Cluster. *Acta Cryst. D*. **59**, 492-498 (2003).

M Bernett, S Blaber, I Scarisbrick, P Dhanarajan, S Thompson, M Blaber. Crystal Structure and Biochemical Characterization of Human Kallikrein 6 Reveals a Trypsin-like Kallikrein is Expressed in the Central Nervous System. *J. Biol. Chem.*. **277**, 24562-24570 (2002).

M Bernett, S Blaber, I Scarisbrick, P Dhanarajan, S Thompson, M Blaber. Crystal Structure and Biochemical Characterization of Human Kallikrein 6 Reveals a Trypsin-like Kallikrein is Expressed in the Central Nervous System. *Protein Sci.*. **11**, 137 (2002).

J Blaszczyk, Y Li, G Shi, H Yan, X Ji. Dynamic Roles of Arginine Residues 82 and 92 of Escherichia coli 6-Hydroxymethyl-7,8-dihydropterin Pyrophophokinase: Crystallographic Studies. *Biochemistry*. **42**, 1573-1580 (2003).

C Boesen, S Radaev, S Motyka, A Patamawenu, P Sun. The 1.1 Angstrom Crystal Structure of Human TGF-beta Type II Receptor Ligand Binding Domain. *Structure*. **10**, 913-942 (2002).

C Boesen, S Motyka, A Patamawenu, P Sun. Crystallization and Preliminary Crystallographic Studies of Human TGF-Beta Type II Receptor Ligand-Binding Domain. *Acta Cryst. D*. **58**, 1214-1216 (2002).

P Carrington, P Chivers, F Al-Mjeni, R Sauer, M Maroney. Nickel Coordination is Regulated by the DNA-bound State of NikR. *Nat. Struct. Biol.*. **10** (2), 126 (2003).

P Carrington, F Al-Mjeni, M Zoroddu, M Costa, M Maroney. Use of XAS for the Elucidation of Metal Structure and Function: Applications to Nickel Biochemistry, Molecular Toxicology, and Carcinogenesis. *Environ. Health Perspect.*. **5**, 705-708 (2002).

C Chang, E Magracheva, S Kozlov, S Fong, G Tobin, S Kotenko, A Wlodawer, A Zdanov. Crystal Structure of Interleukin-19 Defines a New Subfamily of Helical Cytokines . *J. Biol. Chem.*. **278**, 3308-3313 (2003).

Z Dauter. One-and-a Half Wavelength Approach. *Acta Cryst. D*. **58**, 1958-1967 (2002).

Z Dauter. New Approaches to High-Throughput Phasing. *Curr. Opin. Struct. Biol.*. **12**, 674-678 (2002).

Z Dauter, R Nagem. Direct Way to Anomalous Scatterers. *Z. Kristallogr.*. **217**, 694-702 (2002).

C Deivanagagam, E Wann, W Chen, M Carson, K Rajashankar, M Hook, S Narayana. A Novel Variant of the Immunoglobulin Fold in Surface Adhesions of Staphylococcus Aureus: Crystal Structure of the Fibrinogen-Binding MSCRAMM, Clumping Factor A. *EMBO J.*. **21**, 6660-6672 (2002).

G Gainsford, A Kay, A Woolhouse. 1-(2-Hydroxyethyl)-4-{4,5,6,7-Tetrahydro--1-[1-(2-Hydroxyethyl)-Pyridin-4(1H)-YL-Idene]-1H-Inden-3-YL}Pyridinium Iodide. *Acta Cryst. E*. **E59** (04), o589-o590 (2003).

X Guo, X Wen, L Esser, B Quinn, L Yu, C Yu, D Xia. Structural Basis for the Quinone Reduction in the bc1 Complex: A Comparative Analysis of Crystal Structures of Mitochondrial Cytochrome bc1 with Bound Substrate and Inhibitors at the Qi Site. *Biochemistry*. **42**, 9067-9080 (2003).

F Guo, M Maurizi, L Esser, D Xia. Crystal Structure of ClpA, an Hsp100 Chaperone and Regulator of ClpAP Protease. *J. Biol. Chem.*. **277** (48), 46743-46752 (2002).

F Guo, L Esser, S Singh, M Maurizi, D Xia. Crystal Structure of the Heterodimeric Complex of the Adaptor, ClpS, with the N-domain of the AAA+ Chaperone, ClpA*. *J. Biol. Chem.*. **277** (48), 46753-46762 (2002).

Y Guo, B Xiao, H Wargo, M Bucher, S Singh, X Ji. Residues 207, 216, and 221 and the Catalytic Activity of mGSTA1-1 and MGSTA2-2 toward Benzo[a]pyrene-(7R,8S)-diol-(9S,10R)-epoxide. *Biochemistry*. **42**, 917-921 (2003).

P Hall, Y Wang, R Rivera-Hainaj, X Zheng, M Pustai-Carey, P Carey, V Yee. Transcarboxylase 12S crystal structure: hexamer assembly and substrate binding to a multienzyme core. *EMBO J.*. **22** (10), 2334-2347 (2003).

A Hofmann, H Iwai, S Hess, A Plucktuh, A Wlodawer. Structure of Cyclized Green Fluorescent Protein. *Acta Cryst. D*. **58**, 1400-1406 (2002).

A Hofmann, D Dolmer, A Wlodawer. The Crystal Structure of Annexin Gh1 from Gossypium Hirsutum Reveals an Unusual S3 Cluster. *Eur. J. Biochem.*. **270**, 2557-2564 (2003).

E Jaffe, J Kervinen, J Martins, F Stauffer, R Neier, A Wlodawer, A Zdanov. Species-Specific Inhibition of Porphobilinogen Synthase by 4-oxosebacic Acid. *J. Biol. Chem.*. **277**, 19792-19799 (2002).

B Kang, D Cooper, F Jelen, Y Devedjiev, U Derewenda, Z Dauter, J Otlewski, Z Derewenda. PDZ Tandem of Human Syntenin: Crystal Structure and Functional Properties. *Structure*. **11**, 459-468 (2003).

M Kim, T Cierpicki, U Derewenda, D Krowarsch, Y Feng, Y Devedjiev, Z Dauter, C Walsh, J Otlewski, et al.. The DCX-domain tandems of doublecortin and doublecortin-like kinase. *Nat. Struct. Biol.*. **10** (5), 324-333 (2003).

J Kim, I Yang, S Rhee, Z Dauter, Y Lee, S Park, K Kim. Crystal Structures of Glutaryl 7-Aminocephalosporanic Acid Acylase: Insight into Autoproteolytic Activation. *Biochemistry*. **42**, 4084-4093 (2003).

M Kim, U Derewenda, Y Devedjiev, Z Dauter, Z Derewenda. Purification and Crystallization of the N-Terminal Domain from the Human Doublecortin-like Kinase. *Acta Cryst. D*. **59**, 502-505 (2003).

O Kleifeld, A Frenkel, J Martin, I Sagi. Active Site Electronic Structure and Dynamics During Metalloenzyme Catalysis. *Nat. Struct. Biol.*. **10** (2), 98 (2003).

O Kleifeld, S Shi, R Zarivasch, M Eisenstein, I Sagi. The Conserved Glu-60 in the Active Site of Thermoanaerobacter Brockii Alcohol Dehydrogenase is not Essential for Catalysis. *Protein Sci.*. **12**, 468-479 (2003).

J Knowlton, M Bubunenko, M Andrykovitch, W Guo, K Routzahn, D Waugh, D Court, X Ji. A Spring-Loaded State of NusG in Its Functional Cycle is Suggested by X-ray Crystallography and Supported by Site-Directed Mutants. *Biochemistry*. **42**, 2275-2281 (2003).

C Lehmann, J Debreczeni, G Bunkoczi, M Dauter, Z Dauter, L Vertesy, G Sheldrick. Structures of Four Crystal Forms of Decaplanin. *Helv. Chim. Acta*. **86**, 1478-1486 (2003).

M Lim, J Rohde, A Stubna, M Bukowski, M Costas, R Ho, E Munck, W Nam, L Que. An FeIV==O complex of a tetradentate tripodal nonheme ligand. *Proc Natl Acad Sci USA*. **100** (7), 3665-3670 (2003).

K Longenecker, P Read, S Lin, A Somlyo, R Nakamoto, Z Derewenda. Structure of a Constitutively Activated RhoA Mutant (Q63L) at 1.55 Angstrom Resolution. *Acta Cryst. D*. **59**, 876-880 (2003).

J Lubkowski, M Dauter, K Aghaiypour, A Wlodawer, Z Dauter. Atomic Resolution Structure of Erwinia Chrysanthemi L-Asparaginase. *Acta Cryst. D*. **59**, 84-92 (2003).

T Martin, Z Dauter, Y Devedijiev, P Sheffield, F Jelen, M He, D Sherman, J Otlewski, Z Derewenda, U Derewenda. Molecular Basis of Mitomycin C Resistance in Streptomyces: Structure and Function of the MRD Protein. *Structure*. **10**, 933-942 (2002).

M Miller, J Shuman, T Sebastian, Z Dauter, P Johnson. Structural Basis for DNA Recognition by the Basic Region Leucine Zipper Transcription Factor CCAAT/Enhancer -Binding Protein Alpha. *J. Biol. Chem.*. **278**, 15178-15184 (2003).

W Nam, S Choi, M Lim, J Rohde, I Kim, J Kim, C Kim, L Que, Jr. Reversible Formation of Iodosylbenzene-Iron Porphyrin Intermediates in the Reaction of Oxoiron(IV) Porphyrin pi-Cation Radicals and Iodobenzene. *Angew. Chem. Int. Ed.*. **42**, 109-111 (2003).

P Natesh, K Manikandan, P Bhanumoorthy, M Viswamitra , S Ramakumar. Thermostable Xylanase from Thermoascus Aurantiacus at Ultrahigh Resolution (0.89 Angstrom) at 100 K and Atomic Resolution (1.11 Angstrom) at 293 K Refined Anisotropically to Small-molecule Accuracy. *Acta Cryst. D*. **59**, 105-117 (2003).

J Penner-Hahn. Snapshots of Transition States. *Nat. Struct. Biol.*. **10**, 75-77 (2002).

J Phan, A Zdanov, A Evdokimov, J Tropea, H Peters, R Kapust, M Li, A Wlodawer, D Waugh. Structural basis for the substrate specificity of tobacco etch virus protease. *J. Biol. Chem.*. **277** (52), 50564-50572 (2002).

T Pochapsky, S Pochapsky, T Ju, H Mo, F Al-Mjeni, M Maroney. Modeling and Experiment Yields the Structure of Acireductone Dioxygenase from Klebsiells Pneumoniae. *Nat. Struct. Biol.*. **9**, 966-972 (2002).

L Que, L Banci. Bioinorganic Chemistry. *Curr Opin Chem Biol*. **6**, 169-170 (2002).

U Ramagopal, M Dauter, Z Dauter. Phasing on Anomalous Signal of Sulfurs: What is the Limit?. *Acta Cryst. D*. **59**, 1020-1027 (2003).

U Ramagpal, M Dauter, Z Dauter. SAD Manganese in Two Crystal Forms of Glucose Isomerase. *Acta Cryst. D*. **59**, 868-875 (2003).

B Ramakrishnan, P Qasba. Comparison of the Closed Conformation of the Beta-1,4-Galactosyl-Transferase-I (beta 4Gal-T1) in the Presence and Absence of Alpha-Lactalbumin (LA). *J. Biomol. Struct. Dyn.*. **21** (1), 1-8 (2003).

V Ramasamy, B Ramakrishnan, E Boeggeman, P Qasba. The Role of Tryptophan 314 in the Conformational Changes of beta1,4-Galactosyltransferase-I. *J. Mol. Biol.*. **331**, 1065-1076 (2003).

G Roelfes, V Vrajmasu, K Chen, R Ho, J Rohde, C Zondervan, R la Crois, E Schudde, M Lutz, et al.. End-on and Side-on Peroxo Derivatives of Non-Heme Iron Complexes with Pentadentate Ligands: Models for Putative Intermediates in Biological Iron/Dioxygen Chemistry. *Inorg. Chem.*. **42**, 2639-2653 (2003).

P Sun, S Radaev. Generating Isomorphous Heavy-Atom Derivatives by a Quick Soak Method. Part II: Phasing of New Structures. *Acta Cryst. D*. **58**, 1099-1103 (2002).

C Taylor, S Watton, P Bryngelson, M Maroney. inner-Sphere Complexation of Cobalt(II) 2,9-dimethyl-1,10-Phenanthroline ([Co(neo)]2+) with Commercial and Sol-Gel Derived Silica Gel Surfaces. *Inorg. Chem.*. **42**, 312-320 (2003).

I Uson, B Schmidt, R von Bulow, S Grimme, K von Figura, M Dauter, K Rajashankar, Z Dauter, G Sheldrick. Locating the Anomalous Scatterer Substructures in Halide and Sulfur Phasing. *Acta Cryst. D*. **59**, 57-66 (2003).

M Weiss, Z Wan, M Zhao, Y Chu, S Nakagawa, G Burke, W Jia, R Hellmich, P Katsoyannis. Non-Standard Insulin Design: Structure-Activity Relationships at the Periphery of the Insulin Receptor. *J. Mol. Biol.*. **315**, 103-111 (2002).

Beamline X10A

Y Akpalu, Y Lin. Multivariable Structural Characterization of Semicrystalline Polymer Blends by Small-Angle Light Scattering. *J. Polym. Sci., Part B: Polym. Phys.*. **40**, 2714-2727 (2002).

D Coleman, J Fernsler, N Chattham, M Nakata, Y Takanishi, E Korblova, D Link, R Shao, W Jang, et al. Polarized-Modulated Smectic Liquid Crystal Phases. *Science*. **301**, 1204-1211 (2003).

Beamline X10B

D Vanderah, R Gates, V Silin, D Zeiger, J Woodward, C Meuse. Isostructural Self-Assembled Monolayers. 1. Octadecyl 1-Thiaoligo(ethylene oxides). *Langmuir*. **19**, 2612-2620 (2003).

Beamline X10C

T Das, G Jacobs, P Patterson, W Conner, J Li, B Davis. Fischer-Tropsch synthesis: characterization and catalytic properties of rhenium promoted cobalt alumina catalysts. *Fuel*. **82**, 805-815 (2003).

Beamline X11A

Y Arai, A Lanzirotti, S Sutton, J Davis, D Sparks. Arsenic Speciation and Reactivity in Poultry Litter. *Environ. Sci. Tech.*. **37** (18), 4083-4090 (2003).

A Argo, J Odzak, B Gates. Role of Cluster Size in Catalysis: Spectroscopic Investigation of ã-Al2O3-Supported Ir4 and Ir6 during Ethene Hydrogenation. *J. Am. Chem. Soc.*. **125**, 7107-7115 (2003).

A Argo, B Gates. MgO-Supported Rh6 and Irg: Structural Characterization during the Catalysis of Ethene Hydrogenation. *J. Phys. Chem. B*. **107**, 5519-5528 (2003).

S Calvin, E Carpenter, R Stroud, V Harris. Characterization of Core/Shell Nanoparticles by X-Ray Absorption Spectroscopy. *2003 Nanotechnology Conference and Trade Show*, Vol 3, p. 82-85, sponsored by Nano Science and Technology Institute. (2003).

S Calvin, E Carpenter, B Ravel, V Harris, S Morrison. Multiedge Refinement of Extended X-Ray-Absorption Fine Structure of Manganese Zinc Ferrite Nanoparticles. *Phys. Rev. B: Condens. Matter*. **66** (22), 224405-1 - 224405-13 (2002).

S Calvin, E Carpenter, V Harris. Characterization of passivated iron nanoparticles by x-ray absorption spectroscopy. *Phys. Rev. B: Condens. Matter*. **68** (3), 033411-1-033411-4 (2003).

S Calvin, M Miller, R Goswami, S Cheng, S Mulvaney, L Whitman, V Harris. Determination of crystallite size in a magnetic nanocomposite using extended x-ray absorption fine structure. *J. Appl. Phys.*. **94** (1), 778-783 (2003).

C Dodge, A Francis. Structural characterization of a ternary Fe(III)-U(VI)-citrate complex. *Radiochim. Acta*. **91**, 525-532 (2003).

J Goellner, B Gates. Synthesis and Characterization of Site-Isolated Hexarhodium Clusters on Titania Powder. *J. Phys. Chem. B*. **105** (16), 3269-3281 (2001).

A Mansour, P Smith, W Baker, M Balasubramanian, J McBreen. A Comparative In Situ X-Ray Absorption Spectroscopy Study of Nanophase V2O5 Aerogel and Ambigel Cathodes,. *J. Electrochem. Soc.*. **150** (4), A403-A413 (2003).

S Morrison, C Cahill, E Carpenter, S Calvin, V Harris. Preparation and Characterization of MnZn-Ferrite Nanoparticles Using Reverse Micelles. *J. Appl. Phys.*. **93** (10), 7489-7491 (2003).

M Nachtegaal, D Sparks. Nickel Sequestration in a Kaolinite-Humic Acid Complex. *Environ. Sci. Tech.*. **37**, 529-534 (2003).

D Roberts, A Scheinost, D Sparks. Zinc speciation in contaminated soils combing direct and indirect characterization methods. *Geochemical and Hydrological Reactivity of Heavy Metals in Soils*, p. 187-227, Lewis Publishers, Boca Raton. (2003).

D Roberts, R Ford, D Sparks. Kinetics and Mechanisms of Zn Complexation on Metal Oxides using EXAFS Spectroscopy. *J. Colloid Interface Sci.*. **263** (2), 364-376 (2003).

K Scheckel, C Impellitteri, J Ryan, T McEvoy. Assessment of a Sequential Extraction Procedure for Perturbed Lead-Contaminated Samples with and without Phosphorus Amendments. *Environ. Sci. Tech.*. **37**, 1892-1898 (2003).

A Scheinost, R Kretzschmar, S Pfister, D Roberts. Combining Selective Sequential Extractions, X-ray Absorption Spectroscopy, and Principal Component Analysis for Quantitative Zinc Speciation in Soil. *Environ. Sci. Tech.*. **36** (23), 5021 (2002).

P Trivedi, J Dyer, D Sparks. Lead Sorption onto Ferrihydrite. 1. A Macroscopic and Spectroscopic Assessment. *Environ. Sci. Tech.*. **37** (5), 908-914 (2003).

A Voegelin, A Scheinost, K Buehlmann, K Barmettler, R Kretzschmar. Slow formation and dissolution of Zn precipitates in soils: A combined column-transport and XAFS study. *Environ. Sci. Tech.*. **36** (17), 3749-3754 (2002).

W Yoon, Y Kim, X Yang, J McBreen, C Grey. 6Li MAS NMR and in situ X-ray Studies of Lithium Nickel Manganese Oxides. *J. Power Sources*. **119** (1), 649-653 (2003).

Beamline X12B

P Dai, P Cebe, M Capel, R Alamo, L Mandelkern. In Situ Wide- and Small-Angle X-ray Scattering Study of Melting Kinetics of Isotactic Poly(propylene). *Macromolecules*. **36**, 4042-4050 (2003).

S Eswaramoorthy, S Gerchman, V Graziano, H Kycia, F Studier, S Swaminathan. Structure of a Yeast Hypothetical Protein Selected by a Structural Genomics Approach. *Acta Cryst. D*. **59**, 127-135 (2003).

K Ferguson, M Berger, J Mendrola, H Cho, D Leahy, M Lemmon. EGF activates its receptor by removing interactions that auto-inhibit ectodomain dimerization. *Mol. Cell*. **11**, 507-517 (2003).

J Hansen, J Ippolito, N Ban, P Nissen. The Structures of Four Macrolide Antibiotics Bound to the Large Ribosomal Subunit. *Mol. Cell*. **10**, 117-128 (2002).

J Hunt, J Deisenhofer. Ping-Pong Cross-Validation in Real Space: a Method for Increasing the Phasing Power of a Partial Model Without Risk of Model Bias. *Acta Cryst. D*. **59**, 214-224 (2003).

S Johnson, J Taylor, L Beese. Processive DNA Synthesis Observed in a Polymerase Crystal Suggests a Mechanism for the Prevention of Frameshift Mutations. *Proc Natl Acad Sci USA*. **100** (7), 3895-3900 (2003).

Y Joly. Calculating X-ray Absorption Near-Edge Structure at Very Low Energy. *J. Synch. Rad.*. **10**, 58-63 (2003).

J Keller, P Smith, J Benach, D Christendat, G deTitta, J Hunt. The Crystal Structure of MT0146/CbiT Suggests that the Putative Precorrin-8w Decarboxylase Is a Methyltransferase. *Structure*. **10**, 1475-1487 (2002).

A Kilshtain-Vardi, M Glick, H Greenblatt, A Goldblum, G Shoham. Refined Structure of Bovine Carboxypeptidase A at 1.25 Angstrom Resolution. *Acta Cryst. D*. **59**, 323-333 (2003).

A Mavroudis, A Avgeropoulos, N Hadjichristidis, E Thomas, D Lohse. Synthesis and Morphological Behavior of Model Linear and Miktoarm Star Copolymers of 2-Methyl-1, 3-Pentadiene and Styrene. *Chem. Mater.*. **15**, 1976-1983 (2003).

P Paaventhan, J Joseph, S Nirthanan, G Rajaseger, P Gopalakrishnakone, R Kini, P Kolatkar. Crystallization and Preliminary X-ray Analysis of Candoxin, a Novel Reversible Neurotoxin from the Malayan Krait Bungarus Candidus. *Acta Cryst. D*. **59**, 584-586 (2003).

S Perez-Miller, T Hurley. Coenzyme Isomerization Is Integral to Catalysis in Aldehyde Dehydrogenase. *Biochemistry*. **42**, 7100-7109 (2003).

N Silvaggi, J Anderson, S Brinsmade, R Pratt, J Kelly. The Crystal Structure of Phosphonate-Inhibited D-Ala-D-Ala Peptidase Reveals an Analogue of a Tetrahedral Transition State. *Biochemistry*. **42** (5), 1199-1208 (2003).

E Sundberg, P Andersen, P Schlievert, K Karjalaine, R Mariuzza. Structural, Energetic, and Functional Analysis of a Protein-Protease Interface at Distinct Stages of Affinity Maturation. *Structure*. **11**, 1151-1161 (2003).

Beamline X12C

M Andrykovitch, K Routzahn, M Li, Y Gu, D Waugh, X Ji. Characterization of four orthologs of stringent starvation protein A. *Acta Cryst. D*. **59**, 881-886 (2003).

J Benach, I Lee, W Edstrom, A Kuzin, Y Chiang, T Acton, G Montelione, J Hunt. The 2.3-A crystal structure of the shikimate 5-dehydrogenase orthologue YdiB from Escherichia coli suggests a novel catalytic environment for an NAD-dependent dehydrogenase.. *J. Biol. Chem.*. **278** (21), 19176-82 (2003).

V Cherezov, K Riedl, M Caffrey. Too Hot to Handle? Synchrotron X-ray Damage of Lipid Membranes and Mesophases. *J. Synch. Rad.*. **9** (6), 333-341 (2002).

Y Chi, J Frantz, B Oh, L Hansen, S Shoelson. Diabetes mutations delineate an atypical POU domain in HNF1a.. *Mol. Cell*. **10**, 1129 (2002).

S Dutta, I Akey, C Dingwall, K Hartman, T Laue, R Nolte, J Head, C Akey. The crystal structure of nucleoplasmin-core: implications for histone binding and nucleosome assembly. *Mol. Cell*. **8** (4), 841-853 (2001).

B Eichman, E O'Rourke, J Radicella, T Ellenberger. Crystal structures of 3-methyladenine DNA glycosylase MagIII . *EMBO J.*. **22** (19), 4898-4909 (2003).

M Hu, P Li, M Li, W Li, T Yao, J Wu, W Gu, R Cohen, Y Shi. Crystal Structure of a UBP-Family Deubiquitinating Enzymen in Isolation and in Complex with Ubiquitin Aldehyde. *Cell*. **111**, 1041-1054 (2002).

Q Huai, H Wang, Y Sun, H Kim, Y Liu, H Ke. Three-dimensional Structures of PDE4D in Complex with Roliprams and Implication on Inhibitor Selectivity. *Structure*. **11**, 865-873 (2003).

M Huang, A Rigby. Structural basis of membrane binding by Gla domains of Vitamine-K dependent proteins. *Nat. Struct. Biol.*. **10** (9), 751 (2003).

S Kamtekar, W Kennedy, J Wang, C Strathopoulos, D Soll, T Steitz. The Structural Basis of Cysteine Aminoacylation of tRNA ^Pro by Prolyl-tRNA Synthetases. *Proc Natl Acad Sci USA*. **100** (4), 1673-1678 (2003).

N Karpowich, H Huang, P Smith, J Hunt. Crystal Structures of the BtuF Periplasmic-vinging Protein for Vitamin B12 Suggest a Functionally Important Reduction in Protein Mobility upon Ligand Binding. *J. Mol. Biol.*. **278** (10), 8429-8434 (2003).

R Khayat, R Batra, C Qian, T Halmos, M Bailey, L Tong. Structural and Biochemical Studies of Inhibitor Binding to Human Cytomegalovirus Protease. *Biochemistry*. **42**, 885-891 (2003).

S Kruse, R Zhao, D Smith, D Jones. Structure of a Specific Alcohol-Binding Site Defined by the Odorant Binding Protein LUSH from Drosophila melanogaster. *Nat. Struct. Biol.*. **10** (9), 694-700 (2003).

D M Himmel, S Gourinath, L Reshetnikova, Y Shen, A G Szent-Gyorgyi, C Cohen. Crystallographic Findings on the Internally-uncoupled and Near-rigor States of Myosin: Further Insights into the Mechanics of the Motor. *Proc Natl Acad Sci USA*. **99** (20), 12645-12650 (2002).

W McGrath, J Ding, A Didwania, R Sweet, W Mangel. Crystallographic structure at 1.6-A resolution of the human adenovirus proteinase in a covalent complex with its 11-amino-acid peptide cofactor: insights on a new fold. *Biochim Biophys Acta*. **1648** ((1-2)), 1-11 (2003).

P O'Neill, D Stevens, E Garman. Physical and Chemical Considerations of Damage Induced in Protein Crystals by Synchrotron Radiation: A Radiation Chemical Perspective. *J. Synch. Rad.*. **9** (6), 329-332 (2002).

S Perez-Miller, T Hurley. Coenzyme Isomerization Is Integral to Catalysis in Aldehyde Dehydrogenase. *Biochemistry*. **42**, 7100-7109 (2003).

P Stolt, H Jeon, H Song, J Herz, M Eck, S Blacklow. Origins of Peptide Selectivity and Phosphinositide Binding Revealed by Structures of Disabled-1 PTB Domain Complexes. *Structure*. **11**, 569-579 (2003).

L Xu, S Benson, S Butcher, D Bamford, R Burnett. The Receptor Binding Protein P2 of PRD1, A Virus Targeting Antibiotic-Resistant Bacteria, Has a Novel Fold Suggesting Multiple Functions. *Structure*. **11**, 309-322 (2003).

X Yang, R Skene, D McRee, P Schimmel. Crystal Structure of a Human Aminoacyl-tRNA Synthetase Cytokine. *Proc Natl Acad Sci USA*. **99** (24), 15369-15374 (2002).

P Yuan, G Jedd, D Kumaran, S Swaminathan, H Shio, D Hewitt, N Chua, K Swaminathan. A HEX-1 Crystal Lattice Required for Woronin Body Function in Neurospora Crassa. *Nat. Struct. Biol.*. **10** (4), 264 (2003).

J Yuvaniyama, P Chitnumsub, S Kamchonwongpaisan, J Vanichtanankul, W Sirawaraporn, P Taylor, M Walkinshaw, Y Yuthavong. Insights into antifolate resistance from malarial DHFR-TS structures . *Nat. Struct. Biol.*. **10** (5), 357-65 (2003).

Beamline X13A

F Castano, Y Hao, S Haratani, C Ross, B Vogeli, H Smith, C Sanchez-Hanke, C Kao, X Zhu, P Grutter. Magnetic force microscopy and x-ray scattering study of 70x550 nm2 pseudo-spin-valve nanomagnets. *J. Appl. Phys.*. **93** (10), 7927-7929 (2003).

Beamline X13B

K Evans-Lutterodt, J Ablett, A Stein, C Kao, D Tennant, F Klemens, A Taylor, C Jacobsen, P Gammel, et al.. Single-element Elliptical Hard X-ray Micro-optics. *Opt. Express*. **11** (8), 919-926 (2003).

K Evans-Lutterodt, A Stein, J Ablett, C Kao, D Tennant, F Klemens, A Taylor, C Jacobsen, P Gammel, et al.. From Lighthouses to Synchrotron Lightsources: Hard X-ray Micro-optics. *Synch. Rad. News*. **16** (3), 60-63 (2003).

Beamline X14A

D Arms, R Shah, R Simmons. X-ray Debye-Waller Factor Measurements of Solid He-3 and He-4. *Phys. Rev. B*. **67** (9), 094303 (2003).

R Benenson, J Bai, W Gibson. Transmission of x-ray polarization through glass capillary fibers. *Rev. Sci. Instrum.*. **74** (1), 23-27 (2003).

J Howe, C Rawn, L Jones, H Ow. Improved crystallographic data for graphite. *Powder Diffr.*. **18** (2), 150 (2003).

J Kim, R Ryba, J Bai. Effect of the Polyurethane Crystalline Interphase Formed at an Al Surface on Water-Vapor Absorption. *J. Appl. Polym. Sci.*. **89**, 1417 (2003).

J Kim, E Ryba, J Bai. Grazing incidence X-ray diffraction studies on the structures of polyurethane films and their effects on adhesion to Al substrates. *Polymer*. **44**, 6663 (2003).

D Klenov, W Donner, B Foran, S Stemmer. Impact of stress on oxygen vacancy ordering in epitaxial LSCO thin films. *Appl. Phys. Lett.*. **82** (20), 3427-3430 (2003).

J Kmetko, C Yu, G Evmenenko, S Kewalramani, P Dutta. Evidence of Registry at the Interface during Inorganic Nucleation at an Organic Template. *Phys. Rev. Lett.*. **89** (18), 186102 (2002).

J Kmetko. Effects of Divalent Ions on Langmuir Monolayers: Synchrotron X-ray Scattering Studies. Ph.D. Thesis. Northwestern University, Chicago. (2002).

J Li, S Moss, Y Zhang, A Mascarenhas, L Pfeiffer, K West, W Ge, J Bai. Layer Ordering and Faulting in (GaAs)n/(AlAs)n Ultrashort-Period Superlattices . *Phys. Rev. Lett.*. **91**, 106103 (2003).

Q Qian, T Tyson, C Dubourdieu, A Bossak, J Sénateur , M Deleon, J Bai, G BonFait, J Maria. Structural, magnetic, and transport studies of La0.8MnO3 films. *J. Appl. Phys.*. **92** (8), 4518 (2002).

Beamline X15A

L Chapman, M Hasnah, O Oltulu, Z Zhong, J Mollenhauer, C Muehleman, K Kuettner, M Aurich, E Pisano, et al.. Diffraction Enhanced X-ray Imaging of Articular Cartilage. US Patent No. 657,7708. (2003).

F Dilmanian, H Weinmann, Z Zhong, T Bacarian, L Rigon, T Buttone, B Ren, X Wu, N Zhong, H Atkins. Tailoring X-ray Beam Energy Spectrum to Enhance Image Quality of New Radiography Contrast Agents Based on Gd or Other Lanthanides. *SPIE: Physics of Medical Imaging*, Vol 4320, p. 417-426, sponsored by SPIE. (2001).

M Hasnah, Z Zhong, O Oltulu, E Pisano, R Johnston, D Sayers, W Thomlinson, D Chapman. Diffraction Enhanced Imaging Contrast Mechanisms in Breast Cancer Specimens. *Med. Phys.*. **29**, 2216-2221 (2002).

M Hasnah, O Oltulu, Z Zhong, D Chapman. Application of Absorption and Refraction Matching Techniques for Diffraction Enhanced Imaging. *Rev. Sci. Instrum.*. **73**, 1657-1659 (2002).

M Hasnah, O Oltulu, Z Zhong, D Chapman. Single Exposure Simultaneous Diffraction Enhanced Imaging. *Nucl. Instrum. Meth. A*. **492**, 236-240 (2002).

M Kiss. Application of diffraction enhanced imaging for obtaining improved contrast of calcifications in breast tissue. PhD Thesis. North Carolina State University, Raleigh. (2002).

M Kiss, D Sayers, Z Zhong. Measurement of image contrast using diffraction enhanced imaging. *Phys. Med. Biol.*. **48** (3), 325-340 (2003).

T Lee, C Kumpf, A Kazimirov, P Lyman, G Scherb, M Bedzyk, M Nielsen, R Feidenhansl, R Johnson, J Zegenhagen. Structural analysis of indium-stabilized GaAs(001)-c(8x2) surface. *Phys. Rev. B: Condens. Matter*. **66**, 235301-1-9 (2002).

J Li, Z Zhong, R Litdke, K Kuettner, C Peterfy, E Aleyeva, C Muehleman. Radiography of Soft Tissue of the Foot and Ankle with Diffraction Enhanced Imaging. *J. Anatomy*. **202**, 463-470 (2003).

J Mollenhauer, M Aurich, Z Zhong, C Muehleman, A Cole, M Hasnah, O Oltulu, K Kuettner, A Margulis, L Chapman. Diffraction Enhanced X-ray Imaging of Articular Cartilage. *Osteoarthr. Cartilage*. **10**, 168-171 (2002).

C Muehleman, L Chapman, K Kuettner, J Rieff, J Mollenhauer, K Massuda, Z Zhong. Radiography of Rabbit Articular Cartilage with Diffraction Enhanced Imaging. *Anatomical Record*. **272A**, 392-397 (2003).

C Muehleman, M Whiteside, Z Zhong, J Mollenhauer, M Aurich, K Kuettner, L Chapman. Diffraction enhanced imaging for articular cartilage. *Biophys. J.*. **82**, 2292-2292 (2002).

C Muehleman, Z Zhong, J Williams, K Kuettner, M Aurich, B Han, J Mollenhauer. Diffraction-enhanced X-ray Imaging of Articular Cartilage of Experimental Animals. *Proceedings Annual Meeting Othrop. Research Society*, Vol , p. 365, sponsored by Ann. Mtg. Orthop. Res. Soc.. (2002).

O Oltulu, Z Zhong, M Hasnah, D Chapman. Multiple Image Radiography in Diffraction Enhanced Imaging. *J. Phys. D: Appl. Phys.*. **36**, 2152-2156 (2003).

L Rigon, Z Zhong, F Arfelli, R Menk, A Pillon. Diffraction Enhanced Imaging utilizing different crystal reflections at Elettra and NSLS. *Proc. SPIE 4632: Physics of Medical Imaging*, Vol 4632, p. 29, sponsored by SPIE. (2002).

H Roberts, M Helba, J Carroll, J Burnett, T Drummond, J Lepak, R Propri, Z Zhong, F Agee. Gamma Spectroscopy of Hf-178m2 using Synchrotron X-rays. *Hyperfine Interact.*. **143**, 111-119 (2002).

B Tinkham, D Goodner, D Walko, M Bedzyk. X-ray studies of Si/Ge/Si(001) epitaxial growth with Te as a surfactant . *Phys. Rev. B: Condens. Matter*. **67**, 035404-1-6 (2003).

M Wernick, O Wirjadi, D Chapman, O Oltulu, Z Zhong, Y Yang. Preliminary investigation of a multiple-image radiography method. *IEEE. Intl. Symposium on Biomed. Imaging: Macro to Nano* , Vol (2002), p. 1435, sponsored by National Institute of Health. (2002).

Z Zhong, D Chapman, D Connor, A Dilmanian, N Gmur, M Hasnah, R Johnston, M Kiss, J Li, et al.. Diffraction Enhanced Imaging of Soft Tissues. *Synch. Rad. News*. **15** (6), 27-34 (2002).

Z Zhong, C Kao, D Siddons, H Zhong, J Hastings. X-ray reflectivity of sagittally bent Laue crystals. *Acta Cryst. A*. **59**, 1-6 (2003).

Z Zhong, D Chapman, M Hasnah, E Johnston, M Kiss, O Oltulu, L Rigon, N Zhong, E Pisano, D Sayers. X-ray Diffraction Order-selection with a Prism in DEI. *12th National Conference on Sychrotron Radiation Instrumentation*, Vol 73, p. 1614, sponsored by American Institute of Physics. (2002).

Z Zhong, C Kao, D Siddons, J Hastings. Rocking-curve width of sagittally bent Laue crystals. *Acta Cryst. A*. **58**, 487-493 (2002).

Z Zhong, D Siddons, D Chapman, C Kao, N Zhong, J Hastings. Model of Sagittally-bent Silicon Crystals Diffracting in the Laue Mode: the Effects of Elastic-Anisotropy on the Rocking-curve Widths. *12th National Conference on Sychrotron Radiation Instrumentation*, Vol 73, p. 1615, sponsored by University of Wisconsin-Madison. (2002).

Beamline X16C

A Frenkel, A Kolobov, I Robinson, J Cross, Y Maeda, C Bouldin. Direct Separation of Short Range Order in Intermixed Nanocrystalline and Amorphous Phases. *Phys. Rev. Lett.*. **89**, 285503 (2002).

Beamline X17B1

J Chen, D Weidner, M Vaughan, J Parise, J Zhang, Y Xu. A Combined CCD/IP Detection System for Monochromatic XRD Studies at High Pressure and Temperature. *Science and Technology of High*

Pressure, p. 1035-1038 , Universities Press Ltd., Hyderabad. (2000).

M Croft, I Zakharchenko, Z Zhong, T Tsakalakos, Y Gulak, Z Kalman, J Hastings, J Hu, R Holtz, K Sadananda. Stress Distribution and Tomographic Profiling with Energy Dispersive X-Ray Scattering. *MRS Proceedings: Applications of Synchrotron Radiation Techniques to Materials Science*, Vol 678, sponsored by Materials Research Society. (2002).

C Cui, T Tyson, Z Zhong, J P Carlo, Y Qin. Effects of Pressure on Electron Transport and Atomic Structure of Manganites: Low to High Pressure Regimes. *Phys. Rev. B: Condens. Matter*. **67**, 104107 (2003).

A Dilmanian, N Zhong, T Bacarian, J Tammam, J Kalef-Ezra, P Micca, M Miura, L Rigon, B Scharf, D Slatkin. Response of Subcutaneous Murine Mammary Carcinoma EMT-6 to Synchrotron-generated Segmented X-ray Microbeams. *Proceedings of the Joint Symposium on Bio-Sensing and Bio-Imaging, A. Akatsuka, Ed.*, p. 118-122, sponsored by Yamagata University. (2003).

A Dilmanian, T Button, G Le Duc, N Zhong, L Pena, J Smith, S Martinez, T Bacarian, J Tammam, B Ren. Response of rat intracranial 9L gliosarcoma to microbeam radiation therapy. *Neuro-Oncology*. **4**, 26-38 (2002).

F Dilmanian, H Weinmann, Z Zhong, T Bacarian, L Rigon, T Buttone, B Ren, X Wu, N Zhong, H Atkins. Tailoring X-ray Beam Energy Spectrum to Enhance Image Quality of New Radiography Contrast Agents Based on Gd or Other Lanthanides. *SPIE: Physics of Medical Imaging*, Vol 4320, p. 417-426, sponsored by SPIE. (2001).

A Dilmanian, G Morris, N Zhong, T Bacarian, J Hainfeld, J Kalef-Ezra, L Brewington, J Tammam, E Rosen. Murine EMT-6 carcinoma: high therapeutic efficacy of microbeam radiation therapy. *Radiat. Res.*. **159**, 632-641 (2003).

M Hasnah, O Oltulu, Z Zhong, D Chapman. Single Exposure Simultaneous Diffraction Enhanced Imaging. *Nucl. Instrum. Meth. A*. **492**, 236-240 (2002).

A Hennessy, G Graham, J Hastings, P Siddons, Z Zhong. New pressure flow cell to monitor BaSO4 precipitation using synchrotron in-situ angle dispersive X-ray diffraction. *J. Synch. Rad.*. **9**, 323-324 (2002).

J Hu, J Xu, M Somayazulu, Q Guo, D Herschbach, J Hemley, H Mao. X-ray diffraction and laser heating: application of moissanite anvil cell. *J. Phys.: Condens. Matter*. **14**, 10479 (2002).

B Noheda, Z Zhong, D Cox, G Shirane, S Park, P Rehring. Electric-field induced phase transitions in rhombohedral Pb(Zn1/3Nb2/3)1-xTixO3. *Phys. Rev. B*. **65**, art no. 224101 (2002).

L Rigon, Z Zhong, F Arfelli, R Menk, A Pillon. Diffraction Enhanced Imaging utilizing different crystal reflections at Elettra and NSLS. *Proc. SPIE 4632: Physics of Medical Imaging*, Vol 4632, p. 29, sponsored by SPIE. (2002).

H Roberts, M Helba, J Carroll, J Burnett, T Drummond, J Lepak, R Propri, Z Zhong, F Agee. Gamma Spectroscopy of Hf-178m2 using Synchrotron X-rays. *Hyperfine Interact.*. **143**, 111-119 (2002).

T Tsakalakos, M Croft, I Zakharchenko, Z Zhong, Y Gulak, M Desilva, R Holtz. On the Mechanical Stability of Nanostructured Coatings by Synchrotron Radiation. *AIAA 2002*, Vol AIAA-2002, p. 1314, sponsored by AIAA. (2002).

G Voronin, C Pantea, T Zerda, L Wang, Y Zhao. In situ X-ray diffraction study of silicon at pressures up to 15.5 GPa and temperatures up to 1073 K. *Phys. Rev. B: Condens. Matter*. **68**, 020102 (2003).

J Xu, H Mao, R Hemley, E Hines. Moissanite anvil cell: a new tool for high-pressure research. *J. Phys.: Condens. Matter*. **14**, 11543 (2002).

I Zakharchenko, Y Gulak, Z Zhong, M Croft, T Tsakalakos. Methodology of Synchrotron EDXRD Strain Profiling. *Advances in X-ray Analysis*, Vol 46, sponsored by International Centre for Diffraction Data. (2002).

I Zakharchenko, Y Gulak, Z Zhong, M Croft, T Tsakalakos. Application of Synchrotron EDXRD Strain Profiling in Shot Peened Materials. *Advances in X-ray Analysis*, Vol 46, sponsored by International Centre for Diffraction Data. (2002).

Z Zhong, D Siddons, D Chapman, C Kao, N Zhong, J Hastings. Model of Sagittally-bent Silicon Crystals Diffracting in the Laue Mode: the Effects of Elastic-Anisotropy on the Rocking-curve Widths. *12th National Conference on Sychrotron Radiation Instrumentation*, Vol 73, p. 1615, sponsored by University of Wisconsin-Madison. (2002).

Z Zhong, D Chapman, D Connor, A Dilmanian, N Gmur, M Hasnah, R Johnston, M Kiss, J Li, et al.. Diffraction Enhanced Imaging of Soft Tissues. *Synch. Rad. News*. **15** (6), 27-34 (2002).

N Zhong, G Morris, T Bacarian, E Rosen, A Dilmanian. Response of rat skin to high-dose unidirectional X-ray microbeams: a histological study. *Radiat. Res.*. **160**, 133-142 (2003).

Z Zhong, C Kao, D Siddons, H Zhong, J Hastings. X-ray reflectivity of sagittally bent Laue crystals. *Acta Cryst. A*. **59**, 1-6 (2003).

Z Zhong, D Chapman, M Hasnah, E Johnston, M Kiss, O Oltulu, L Rigon, N Zhong, E Pisano, D Sayers. X-ray Diffraction Order-selection with a Prism in DEI. *12th National Conference on Sychrotron Radiation Instrumentation*, Vol 73, p. 1614, sponsored by American Institute of Physics. (2002).

Z Zhong, C Kao, D Siddons, J Hastings. Rocking-curve width of sagittally bent Laue crystals. *Acta Cryst. A*. **58**, 487-493 (2002).

Beamline X17C

B Chen, D Penwell, L Benedetti, R Jeanloz, M Kruger. Particle-size effect on the compressibility of nanocrystalline alumina. *Phys. Rev. B: Condens. Matter*. **66**, 144101-4 (2002).

D Errandonea, M Somayazulu, D Hausermann. Phase transitions and amorphization of CaWO4 at high pressure. *Phys. Status Solidi B*. **235** (1), 162 - 169 (2003).

E Gregoryanz, A Goncharov, R Hemley, H Mao, M Somayazulu, G Shen. Raman, infrared, and x-ray evidence for new phases of. *Phys. Rev. B: Condens. Matter*. **66**, 224108 (2002).

Q Guo, H Mao, J Hu, J Shu, R Hemley. The phase transitions of CoO under static pressure to 104 GPa. *J. Phys.: Condens. Matter*. **14**, 11369 (2002).

D He, Y Zhao, T Sheng, R Schwarz, J Qian, K Lokshin, S Bobev, L Daemen, H Mao, J Hu. Bulk

metallic glass gasket for high pressure, in situ x-ray diffraction. *Rev. Sci. Instrum.*. **74**, 3012 (2003).
R Hemley, H Mao. New window on earth and planetary interiors. *Miner. Mag.*. **66**, 791-811 (2002).
R Hemley, H Mao. Overview of static high pressure science, in High-Pressure Phenomena. *Proceedings of the International School of Physics, "Enrico Fermi" Course CXLVII*, p. 3-40, IOS Press, Amsterdam. (2002).
J Hu, J Xu, M Somayazulu, Q Guo, D Herschbach, J Hemley, H Mao. X-ray diffraction and laser heating: application of moissanite anvil cell. *J. Phys.: Condens. Matter*. **14**, 10479 (2002).
A Kavner. Elasticity and strength of hydrous ringwoodite. *Earth Planet Sci. Lett.*. **214**, 645-654 (2003).
Y Lee, J Hriljac, S Kim, J Hanson, T Vogt. Pressure-Induced Hydration at 0.6 GPa in a Synthetic Gallosilicate Zeolite. *J. Am. Chem. Soc.*. **125**, 6036-6037 (2003).
K Lipinska-Kalita, B Chen, M Kruger, Y Ohki, J Murowchick, E Gogol. High-pressure x-ray diffraction studies of the nanostructured transparent vitroceramic medium K2O-SiO2-Ga2O3. *Phys. Rev. B: Condens. Matter*. **68**, 35209 (2003).
Z Liu, J Hu, H Yang, H Mao, R Hemley. High-pressure Synchrotron X-ray Diffraction and Infrared Microspectroscopy: Application to Dense Hydrous Phases. *J. Phys.: Condens. Matter*. **14**, 10641-10646 (2002).
Y Ma, C Prewitt, G Zou, H Mao, R Hemley. High-pressure high-temperature x-ray diffraction of beta-boron to 30 GPa. *Phys. Rev. B*. **67**, 174116 (2003).
S Merkel, A Jephcoat, J Shu, H Mao, P Gillet, R Hemley. Equation of state, elasticity, and shear strength of pyrite under high pressure. *Phys. Chem. Miner.*. **29**, 1-9 (2002).
C Sanloup, R Hemley, H Mao. Evidence for xenon silicates at high pressure and temperature. *Geophys. Res. Lett.*. **29**, 30 (2002).
S Shieh, T Duffy, B Li. Strength and Elasticity of SiO2 Across the Stishovite-CaCl2-type Structural Phase Boundary. *Phys. Rev. Lett.*. **89** (25), 255507-1 (2002).
S Shieh, T Duffy. Raman spectroscopy of Co(OH)2 to 30 GPa: Implications for amorphization and structural frustration. *Phys. Rev. B: Condens. Matter*. **66**, 134301 (2002).
Y Song, M Somayazulu, H Mao, R Hemley, D Herschbach. High-pressure structure and equation of state study of nitrosonium nitrate from synchrotron x-ray diffraction. *J. Chem. Phys.*. **118**, 8350 (2003).
J Xu, H Mao, R Hemley, E Hines. Moissanite anvil cell: a new tool for high-pressure research. *J. Phys.: Condens. Matter*. **14**, 11543 (2002).
G Xu, Z Zhong, Y Bing, Z Ye, C Stock, G Shirane. Ground State of the Relaxor Ferroelectric Pb(Zn1/3Nb2/3)O3. *Phys. Rev. B*. **67**, 104102 (2003).
J Xu, H Mao, R Hemley. Gem anvil cell: high-pressure behavior of diamond and related materials. *J. Phys.: Condens. Matter*. **14**, 11549 (2002).

Beamline X18A

H Mo, H Taub, U Volkmann, M Pino, S Ehrlich, F Hansen, E Lu, P Miceli. A Novel Growth Mode of Alkane Films on a SiO2 Surface. *Chem. Phys. Lett.*. **377**, 99-105 (2003).
X Yang, J McBreen, X Sun, M Balasubramanian. Structural studies of cathode and anode materials for lithium batteries using in situ XRD and X-ray absorption combined with NMR spectroscopy. *The 43rd Battery Symposium in Japan*, Vol 2I, p. 50, sponsored by The Electrochemical Society of Japan. (2002).
X Yang, J McBreen, M Balasubramanian, W Yoon, C Grey, M Yoshio, A Ueda, X Huang, L Chen, L Liu. Structural Studies of New Cathode and Anode Materials for Lithium Batteries Using In Situ XRD and x-ray Absorption Spectroscopy. *The 2002 Korean Battery Symposium*, Vol 1, p. 45, sponsored by The Korean Electrochemical Society. (2002).
W Yoon, Y Kim, X Yang, J McBreen, C Grey. 6Li MAS NMR and in situ X-ray Studies of Lithium Nickel Manganese Oxides. *J. Power Sources*. **119** (1), 649-653 (2003).
C Yu, A Richter, J Kmetko, S Dugan, A Datta, P Dutta. Structure of interfacial liquids: X-ray scattering studies. *Phys. Rev. E*. **63**, 021205 (2001).
Y Zhang, R Colella, S Kycia, A Goldman. Absolute Structure Factor Measurements of an Al-Pd-Mn Quasicrystal. *Acta Cryst. A*. **58**, 385-390 (2002).

Beamline X18B

O Adamopoulos, Z Yu, M Croft, I Zakharchenko, T Tsakalakos, M Muhammed. The characterisation and reactivity of nanostructured cerium-copper-oxide composites for environmental catalysis. *Synthesis, Functional Properties and Applications of Nanostructures. Symposium (Materials Research Society Symposium Proceedings Vol.676)*, Vol 676, p. Y8.11.1-6, sponsored by Mater. Res. Soc. (2002).
F Alamgir. The Structural Origins Of The Stability of Palladium-Nickel-Phosphorus Bulk Metallic Glasses. Ph.D. Thesis. Lehigh University, Bethlehem. (2003).
W Alvarez, B Kitiyanan, A Borgna, D Resasco. Synergism of Co and Mo in the catalytic production of single-wall carbon nanotubes by decomposition of CO. *Carbon*. **39**, 547-558 (2001).
G Chen, H Jain, M Vlcek, S Khalid, J Li, D Drabold, S Elliott. Observation of Light Polarization-dependent Structural Changes in Chalcogenide Glasses. *Appl. Phys. Lett.*. **82** (5), 706 (2003).
G Chen, H Jain, M Vlcek, J Li, D Drabold, S Khalid, S Elliott. Study of light-induced vector changes in the local atomic structure of As¨CSe glasses by EXAFS. *J. Non-Cryst. Solids*. **326-327**, 257 (2003).
G Chen, H Jain, S Khalid, J Li, D Drabold, S Elliott. Study of Structural Changes in Amorphous As2Se3 By EXAFS under In-Situ Laser Irradiation. *Solid State Commun.*. **120**, 149-153 (2001).
M Croft, W Caliebe, H Woo, T Tyson, D Sills, Y Hor, S Cheong, V Kiryukhin, S Oh. Metal-insulator transition in CuIr2S4: XAS results on the electronic structure. *Phys. Rev. B: Condens. Matter*. **67**, 201102-1-4 (2003).
T Das, G Jacobs, P Patterson, W Conner, J Li, B Davis. Fischer-Tropsch synthesis: characterization

and catalytic properties of rhenium promoted cobalt alumina catalysts. *Fuel*. **82**, 805-815 (2003).
R Egdal, A Hazell, F Larsen, C McKenzie, R Scarrow. A dihydroxo-bridged Fe(II)-Fe(III) complex: A new member of the diiron diamond core family.. *J. Am. Chem. Soc.*. **125** (1), 32-33 (2003).
K Galbreath, C Crocker, C Nyberg, F Huggins, G Huffman, K Larson. Nickel speciation measurements of urban particulate matter: method evaluation and relevance to risk assessment. *J. Environ. Monit.*. **5**, 56N-61N (2003).
M Giacomini, M Balasubramanian, S Khalid, J McBreen, E Ticianelli. Characterization of the Activity of Palladium-Modified Polythiophene Electrodes for the Hydrogen Oxidation and Oxygen Reduction Reactions. *J. Electrochem. Soc.*. **150** (5), A588-A593 (2003).
J Herrera, D Resasco. Role of Co-W Interaction in the Selective Growth of Single-Walled Carbon Nanotubes from CO Disproportionation. *J. Phys. Chem. B*. **107**, 3738-3746 (2003).
F Huggins, N Yap, G Huffman, C Senior. XAFS characterization of mercury captured from combustion gases on sorbents at low-temperature. *Fuel Process. Technol.*. **82**, 167-196 (2003).
G Jacobs, T Das, P Patterson, J Li, L Sanchez, B Davis. Fischer-Tropsch Synthesis: XAFS studies of the effect of water on a Pt-promoted Co/Al2O3 catalyst. *Appl. Catal. A*. **247** (2), 335 (2003).
G Popov, M Greenblatt, M Croft. Large effects of a-site average cation size on the properties of the double perovskites Ba2 xSrxMnReO6, a d5-d1 System. *Phys. Rev. B: Condens. Matter*. **B67**, 24406 (2003).
N Sakulchaicharoen , D Resasco. Temperature dependence of the quality of silicon nanowires produced over a titania-supported gold catalyst. *Chem. Phys. Lett.*. **377** (3), 377-383 (2003).
N Shah, S Pattanaik, F Huggins, D Panjala, G Huffman. XAFS and Mössbauer spectroscopy characterization of supported binary catalysts for nonoxidative dehydrogenation of methane. *Fuel Process. Technol.*. **83**, 163-173 (2003).
J Shearer, S Fitch, W Kaminsky, J Benedict, R Scarrow, J Kovacs. How does Cyanide Inhibit Superoxide Reductase? Insight from Synthetic Fe(III)N4S Model Complexes. *Proc Natl Acad Sci USA*. **100** (7), 3671-3676 (2003).
X Yang, J McBreen, X Sun, M Balasubramanian. Structural studies of cathode and anode materials for lithium batteries using in situ XRD and X-ray absorption combined with NMR spectroscopy. *The 43rd Battery Symposium in Japan*, Vol 2I, p. 50, sponsored by The Electrochemical Society of Japan. (2002).
X Yang, J McBreen, M Balasubramanian, W Yoon, C Grey, M Yoshio, A Ueda, X Huang, L Chen, L Liu. Structural Studies of New Cathode and Anode Materials for Lithium Batteries Using In Situ XRD and x-ray Absorption Spectroscopy. *The 2002 Korean Battery Symposium*, Vol 1, p. 45, sponsored by The Korean Electrochemical Society. (2002).
W Yoon, C Grey, M Balasubramanian, X Yang, J McBreen. In Situ X-ray Absorption Spectroscopic Study on LiNi0.5Mn0.5O2 Cathode Material during Electrochemical Cycling. *Chem. Mater.*. **15**, 3161-3169 (2003).

Beamline X19A

O Adamopoulos, Z Yu, M Croft, I Zakharchenko, T Tsakalakos, M Muhammed. The characterisation and reactivity of nanostructured cerium-copper-oxide composites for environmental catalysis. *Synthesis, Functional Properties and Applications of Nanostructures. Symposium (Materials Research Society Symposium Proceedings Vol.676)*, Vol 676, p. Y8.11.1-6, sponsored by Mater. Res. Soc. (2002).
S Beauchemin, D Hesterberg, J Chou, M Beauchemin, R Simard, D Sayers. Speciation of Phosphorus in Phosphorus-enriched Agricultural Soils using X-ray Absorption Near-edge Spectroscopy and Chemical Fractionation. *J. Environ. Qual.*. **32**, 1809-1819 (2003).
B Bostick, S Fendorf. Arsenite Sorption on Troilite (FeS) and Pyrite (FeS2). *Geochim. Cosmochim. Acta*. **67** (5), 909-921 (2003).
A Cady. Optical and resonant x-ray diffraction investigations of molecular ordering in chiral liquid crystals. Ph.D. Thesis. University of Minnesota, Minneapolis. (2003).
M Croft, W Caliebe, H Woo, T Tyson, D Sills, Y Hor, S Cheong, V Kiryukhin, S Oh. Metal-insulator transition in CuIr2S4: XAS results on the electronic structure. *Phys. Rev. B: Condens. Matter*. **67**, 201102-1-4 (2003).
G Liu, J Rodriguez, J Hrbek, B Long, D Chen. Interaction of Thiophene with Titania Surfaces. *J. Mol. Catal. A: Chem.*. **202**, 215-227 (2003).
J McBreen, X Yang, M Balasubramanian, X Sun, H Lee. Synchrotron X-ray Studies of Lithium-Ion Battery Components. *The 43rd Battery Symposium in Japan*, Vol 2I, p. 46, sponsored by The Electrochemical Society of Japan. (2002).
G Popov, M Greenblatt, M Croft. Large effects of a-site average cation size on the properties of the double perovskites Ba2 xSrxMnReO6, a d5-d1 System. *Phys. Rev. B: Condens. Matter*. **B67**, 24406 (2003).
J Qian, U Skyllberg, W Frech, W Bleam, P Bloom, P Petit. Bonding of Methyl Mercury to Reduced Sulfur Groups in Soil and Stream Organic Matter as Determined by X-ray Absorption Spectroscopy and Binding Affinity Studies. *Geochim. Cosmochim. Acta*. **66** (22), 3873-3885 (2002).
J Rodriguez, P Liu, J Dvorak, T Jirsak, J Gomes, Y Takahashi, K Nakamura. Adsorption and decomposition of SO2 on TiC(001): An experimental and theoretical study. *Surf. Sci. Lett.*. **543**, L675-L682 (2003).
J Rodriguez, X Wang, J Hanson, G Liu, A Iglesias-Juez, M Fernandez-Garcia. The behavior of mixed-metal oxides: Structural and electronic properties of Ce-Ca oxides. *J. Chem. Phys.*. **119**, 5659-5669 (2003).
J Rodriguez, J Hanson, J Kim, G Liu, A Iglesias-Juez, M Fernandez-Garcia. Properties of Ce2 and Ce1-xZrxO2 Nanoparticles: X-ray Absorption Near-Edge Spectroscopy, Density Functional, and Time-Resolved X-ray Diffraction Studies. *J. Phys. Chem. B*. **107**, 3535-3543 (2003).
N Shah, S Pattanaik, F Huggins, D Panjala, G Huffman. XAFS and Mössbauer spectroscopy characterization of supported binary catalysts for

nonoxidative dehydrogenation of methane. *Fuel Process. Technol.*. **83**, 163-173 (2003).
U Skyllberg, J Qian, W Frech, K Xia, W Bleam. Distribution of mercury, methyl mercury and organic sulphur species in soil, soil solution and stream of a boreal forest catchment. *Biogeochemistry*. **64**, 53-76 (2003).

Beamline X19C

M Dudley. Studies of Defects and Strains Using X-ray Topography and Diffraction. *2003 SEM Annual Conference & Exposition on Experimental and Applied Mechanics*, Vol 1, p. 348-355, sponsored by SEM. (2003).
M Dudley, X Huang, W Vetter, P Neudeck. Synchrotron White Beam X-ray Topography and High Resolution Triple Axis X-ray Diffraction Studies of Defects in SiC Substrates, Epilayers and Devices. *4th European Conference on Silicon Carbide and Related Materials*, Vol 433-436, p. 247-252, sponsored by European Commission. (2003).
D Gidalevitz, Y Ishitsuka, A Muresan, O Konovalov, A Waring, R Lehrer, K Lee. Interaction of antimicrobial peptide protegrin with biomembranes. *Proc Natl Acad Sci USA*. **100** (11), 6302-6307 (2003).
L Hanley, Y Choi, E Fuoco, F Akin, M Wijesundara, M Li, A Tikhonov, M Schlossman. Controlling the Nanoscale Morphology of Organic Films Deposited by Polyatomic Ions. *Nucl. Instrum. Meth. B*. **203**, 116 (2003).
J Hartwig, J Baruchel, H Kuhn, X Huang, M Dudley, E Pernot. X-ray "Magnifying" Imaging Investigation of Giant Burgers Vector Micropipe Dislocations in 4H-SiC. *Nucl. Instrum. Meth. B*. **200**, 323-328 (2003).
X Huang, M Dudley. A Universal Computation Method for Two-Beam Dynamical X-ray Diffraction. *Acta Cryst. A*. **59**, 163-167 (2003).
M Li, D Chaiko, M Schlossman. X-ray Reflectivity Study of a Monolayer of Ferritin Proteins at a Nanofilm Aqueous-Aqueous Interface. *J. Phys. Chem. B*. **107**, 9079-9085 (2003).
R Ma, H Zhang, V Prasad, M Dudley. Growth kinetics and thermal stress of silicon carbide. *Cryst. Growth Des.*. **2** (3), 213-220 (2002).
X Ma, M Dudley, W Vetter, T Sudharshan. Extended Defects: Polarized Light Microscopy Delineation and Synchrotron White Beam X-ray Topography Ratification. *Japanese J. Appl. Phys.*. **42**, L1077-L1079 (2003).
R Ma, H Zhang, M Dudley, V Prasad. Thermal System Design and Dislocation Reduction for Growth of Wide Band-gap Crystals: Application to SiC Growth. *J. Cryst. Growth*. **258**, 318-330 (2003).
R Ma, H Zhang, M Dudley, S Ha, M Skowronski. Modeling for mass transfer and Thermal Stress of Silicon carbide PVT growth. *2002 ASME International Mechanical Engineering Congress and Exposition*, Vol 1, p. 1-9, sponsored by ASME. (2003).
P Neudeck, J Powell, D Spry, A Trunek, X Huang, W Vetter, N Dudley, M Skowronski, J Liu. Characterization of 3C-SiC Films Grown on 4H- and 6H-SiC Substrate Mesas during Step-Free Surface Hetero-Epitaxy. *4th European Conference on Silicon Carbide and related Materials*, Vol 433-436, p. 213-216, sponsored by European Commission. (2003).
W Palosz, K Grasza, K Durose, D Halliday, N Boyall, M Dudley, B Raghothamachar, L Cai. The Effect of Wall Contact and Post-Growth Cool-Down on Defects in CdTe Crystals Grown by "Contactless" Physical Vapor Transport. *J. Cryst. Growth*. **254**, 316-328 (2003).
E Preble, P Miraglia, A Roskowski, W Vetter, M Dudley, R Davis. Domain Structures in 6H-SiC Wafers and Their Effect on the Microstructures of GaN Films Grown on AlN and Al0.2GaN0.8N Buffers Layers. *J. Cryst. Growth*. **258**, 75-83 (2003).
B Raghothamachar, M Dudley, J Rojo, K Morgan, L Schowalter. X-ray Characterization of Bulk AlN Single Crystals Grown by the Sublimation Technique. *J. Cryst. Growth*. **250**, 244-250 (2003).
A Tikhonov, M Schlossman. Surfactant and water ordering in triacontanol monolayers at the water-hexane interface. *J. Phys. Chem. B*. **107**, 3344 (2003).
W Vetter, J Liu, M Dudley, M Skowronski, H Lendenmann, C Hallin. Dislocation Loops Formed During the Degradation of Forward-Biased 4H-SiC p-n Junctions. *Mater. Sci. Eng. B*. **98**, 220-224 (2003).
B Wu, R Ma, H Zhang, M Dudley, R Schlesser, Z Sitar. Growth kinetics and thermal stress in AlN bulk crystal growth. *J. Cryst. Growth*. **253**, 326-339 (2003).
B Yang, D Li, S Rice. Structure of the liquid-vapor interface of a dilute ternary alloy: Pb and In in Ga. *Phys. Rev. B*. **67**, 05423 (2003).
B Yang, D Li, S Rice. Two Dimensional Freezing of Tl in the Liquid-Vapor Interface of a Dilute Tl in Ga Alloy. *Phys. Rev. B*. **67**, 212103 (2003).
U Zimmermann, J Osterman, D Kuylenstierna, A Hallen, A Konstantinov, W Vetter, M Dudley. Material Defects in 4H-Silicon Carbide Diodes. *J. Appl. Phys.*. **93** (1), 611 (2003).

Beamline X20A

S Anders, M Toney, T Thomson, J Thiele, B Terris, S Sun, C Murray. X-ray Studies of Magnetic Nanoparticle Assemblies. *J. Appl. Phys.*. **93** (10), 7343 (2003).
S Anders, M Toney, T Thomson, R Farrow, J Thiele, B Terris. X-ray Absorption and Diffraction Studies of Magnetic Nanoparticle Assemblies. *J. Appl. Phys.*. **93**, 6299 (2003).
R Bandhu, R Sooryyakumar, R Farrow, D Weller, M Toney, T Rabedeau. Elastic Properties of Chemically Ordered Co3Pt Thin Films. *J. Appl. Phys.*. **91**, 2737 (2002).
P Clegg, C Stock, R Birgeneau, C Garland, A Roshi, G Iannacchione. Effect of a quenched random field on a continuous symmetry breaking transition: Nematic to smectic-A transition in 8OCB-aerosil dispersions. *Phys. Rev. E*. **67**, 021703 (2003).
P Clegg, R Birgeneau, S Park, C Garland, G Iannacchione, R Leheny, M Neubert. High-resolution x-ray study of the nematic - smectic-A and smectic-A - smectic-C transitions in liquid-crystal - aerosil gels. *Phys. Rev. E*. **68**, 031706 (2003).
G Iannacchione, S Park, C Garland, R Birgeneau, R Leheny. Smectic ordering in liquid-crystal–aerosil

dispersions. II. Scaling analysis. *Phys. Rev. E*. **67** (1), 011709 (2003).
S Kaldor, C Noyan. Effects of Boundary Conditions and Anisotropy on Elastically Bent Silicon. *Exp. Mech.*. **42** (3), 353-358 (2002).
V Khmelenko, S Kiselev, D Lee, C Lee. Impurity-Helium Solids - Quantum Gels?. *Phys. Scr.*. **T102**, 118 (2002).
W Lee, M Toney, A Kellock, D Mauri, M Carey, J Hedstrom. Effects of Mn Concentration and Deposition Temperature on the Giantmagnetoresistance Properties of Ion Beam Deposited PtMn Spin Valves. *J. Appl. Phys.*. **91**, 2737 (2003).
R Leheny, S Park, R Birgeneau, J Gallani, C Garland, G Iannacchione. Smectic ordering in liquid-crystal–aerosil dispersions. I. X-ray scattering. *Phys. Rev. E*. **67** (1), 011708 (2003).
P Mooney. Materials for Strained Si Devices. *Selected Topics in Electronics and Systems*, p. 99-108, World Scientific, New Jersey. (2002).
P Mooney. Materials for Strained Si Devices. *Int. J. High Speed Electr. And Syst.*. **12**, 305-314 (2002).
M Toney, W Lee, J Hedstrom, A Kellock. Thickness and Growth Temperature Dependence of Structure and Magnetism in FePt Thin Films. *J. Appl. Phys.*. **93**, 9902 (2003).
M Toney, M Samant, T Lin, D Mauri. Thickness Dependence of Exchange Bias and Structure in PtMn and NiMn Spin Valves. *Appl. Phys. Lett.*. **81**, 4565 (2003).
W Zang, Y Yao. Laser Shock Processing (LSP) of Metal Thin Films. *Conference on Laser Materials Processing*, Vol 2002, p. CD, sponsored by 20th International Congress on Applications of Lasers and Electro-Optics, Scottsdale AZ. (2002).
W Zhang. Microscale Laser Ablative Processes. Ph.D. Thesis. Columbia University, New York. (2002).

Beamline X20C

S Anders, M Toney, T Thomson, J Thiele, B Terris, S Sun, C Murray. X-ray Studies of Magnetic Nanoparticle Assemblies. *J. Appl. Phys.*. **93** (10), 7343 (2003).
S Anders, M Toney, T Thomson, R Farrow, J Thiele, B Terris. X-ray Absorption and Diffraction Studies of Magnetic Nanoparticle Assemblies. *J. Appl. Phys.*. **93**, 6299 (2003).
R Bandhu, R Sooryyakumar, R Farrow, D Weller, M Toney, T Rabedeau. Elastic Properties of Chemically Ordered Co3Pt Thin Films. *J. Appl. Phys.*. **91**, 2737 (2002).
G Cohen, C Cabral, Jr., C Lavoie, P Soloman, K Guarini, K Chan, R Roy. A Self-aligned Silicide Process Utilizing Ion Implantation for Reduced Silicon Consumption and Control of the Silicide Formation Temperature . *Materials Research Society Symposium Proceedings*, Vol 716, p. 35, sponsored by Materials Research Society. (2002).
G Cohen, C Cabral, Jr., C Lavoie, P Soloman, K Guarini, K Chan, R Roy. A Self-aligned Process for Thin Silicon-on-insulator MOSFETS and Bulk MOSFETS with Shallow Junctions. *59th Annual Device Research Conference June 2001*, Vol 686, p. 89, sponsored by Material Research Symp. Proc.. (2002).
C Detavernier, C Lavoie, F d'Heurle. Thermal Expansion of the Isostructural PtSi and NiSi: Negative Expansion Coefficient in NiSi and Stress Effects in Thin Films. *J. Appl. Phys.*. **93** (5), 2510-2515 (2003).
A Gungor, K Barmak, A Rollett, C Cabral, Jr., J Harper. Texture and Resistivity of Dilute Binary Cu(Al), Cu(In), Cu(Ti), Cu(Nb), Cu(Ir), and Cu(W) Alkloy Thin Films. *J. Vac. Sci. Technol., A*. **20** (6), 2314 (2002).
G Iannacchione, S Park, C Garland, R Birgeneau, R Leheny. Smectic ordering in liquid-crystal–aerosil dispersions. II. Scaling analysis. *Phys. Rev. E*. **67** (1), 011709 (2003).
S Kaldor, C Noyan. Effects of Boundary Conditions and Anisotropy on Elastically Bent Silicon. *Exp. Mech.*. **42** (3), 353-358 (2002).
H Kim, C Cabral, Jr., C Lavoie, S Rossnagel. The Growth of Tantalum Thin Films by Plasma-Enhanced Atomic Layer Deposition and Diffusion Barrier Properties . *Materials Research Society Symposium Proceedings*, Vol 716, p. 407, sponsored by Materials Research Society. (2002).
C Lavoie, F d'Heurle, C Detavernier, C Cabral, Jr.. Towards Implementation of a Nickel Silicide Process for CMOS Technologies. *Microelectron. Eng.*. **70**, 144-157 (2003).
W Lee, M Toney, A Kellock, D Mauri, M Carey, J Hedstrom. Effects of Mn Concentration and Deposition Temperature on the Giantmagnetoresistance Properties of Ion Beam Deposited PtMn Spin Valves. *J. Appl. Phys.*. **91**, 2737 (2003).
R Leheny, S Park, R Birgeneau, J Gallani, C Garland, G Iannacchione. Smectic ordering in liquid-crystal–aerosil dispersions. I. X-ray scattering. *Phys. Rev. E*. **67** (1), 011708 (2003).
P Mooney. Materials for Strained Si Devices. *Int. J. High Speed Electr. And Syst.*. **12**, 305-314 (2002).
P Mooney. Materials for Strained Si Devices. *Selected Topics in Electronics and Systems*, p. 99-108, World Scientific, New Jersey. (2002).
A Ozcan, K Ludwig, C Cabral, Jr., C Lavoie, J Harper. Texture Formation in Ti-Ta Alloy Disilicide Thin Films. *J. Appl. Phys.*. **92** (12), 7210 (2002).
A Ozcan, K Ludwig, C Lavoie, C Cabral, Jr., J Harper, R Bradley. Nucleation and Growth Kinetics of Preferred C54 TiSi2 Orientation: Time-Resolved X-Ray Diffraction Measurements. *J. Appl. Phys.*. **92** (9), 5189 (2002).
S Rossnagel, I Noyan, C Cabral, Jr.. Phase Transformation of Thin Sputter-deposited Tungsten Films at Room Temperature. *J. Vac. Sci. Technol., B*. **20** (5), 2047 (2002).
P Solomon, K Guarini, Y Zhang, K Chan, E Jones, G Cohen, A Krasnoperova, M Ronay, O Dokumaci, H Hovel. A Planar, Self-Aligned, Double Gate MOSFET Technology. *IEEE Circuits Dev. Mag.*. **19** (1), 48 (2003).
S Sun, S Anders, T Thomson, J Baglin, M Toney, H Hamann, C Murray, B Terris. Controlled Synthesis and Assembly of FePt Nanoparticles. *J. Phys. Chem. B*. **107**, 5419-5425 (2003).
M Toney, W Lee, J Hedstrom, A Kellock. Thickness and Growth Temperature Dependence of Structure and Magnetism in FePt Thin Films. *J. Appl. Phys.*. **93**, 9902 (2003).

M Toney, M Samant, T Lin, D Mauri. Thickness Dependence of Exchange Bias and Structure in PtMn and NiMn Spin Valves. *Appl. Phys. Lett.*. **81**, 4565 (2003).
M Toney, E Marinero, M Doerner, P Rice. High Anisotropy CoPtCrB Magnetic Recording Media. *J. Appl. Phys.*. **94**, 4018 (2003).

Beamline X21

B Blank, T Kupp, A Deyhim, Y Cai, P Chow, C Kao. Development of a Spectrometer for Inelastic X-ray Measurements. *Proceedings of the 2nd International Workshop on Mechanical Engineering Design of Synchrotron Radiation Equipment and Instrumentation (MEDSI02)*, Vol , p. 308-314, sponsored by MEDSI02. (2002).
C Burns, P Giura, A Shukla, G Vanko, M Tuel-Benckendorf, E Isaacs, P Platzman. Probing Electronic Interactions in the Expanded Metal Compound Li-NH3. *Phys. Rev. Lett.*. **89**, 236404 (2002).
K Hamalainen, S Galambosi, H Sutinen, C Kao, R Sharon, M Deutsch. Near-threshold Mult-electronic Effects in the Cu K alpha 1,2 X-Ray Spectrum. *Phys. Rev. A*. **67**, 022510 (2003).
H Hayashi, Y Udagawa, J Gillet, W Caliebe, C Kao. Chemical Applications of Inelastic X-ray Scattering. *Chemical Application of Synchrotron Radiation*, p. 850, World Scientific, River Edge. (2002).
H Hayashi, N Wantanabe, Y Udagawa, C Kao. Momentum Dependence of ð-ð* Excitations of Benzene Rings in Condensed Phases. *J. Electron. Spectrosc. Relat. Phenom.*. **933**, 114-116 (2001).
H Hayashi, Y Udagawa, W Caliebe, C Kao. Lifetime-broadening Removed X-ray Absorption Near Edge Structure by Resonant Inelastic X-ray Scattering Spectroscopy. *Chem. Phys. Lett.*. **371**, 125 (2003).
H Mao, C Kao, R Hemley. Inelastic X-ray Scattering at Ultra-high Pressure. *J. Phys.: Condens. Matter*. **13**, 7847 (2001).
P Montano, D Price, A Macrander, B Cooper. Inelastic x-ray scattering from 6H-SiC. *Phys. Rev. B: Condens. Matter*. **66**, 165218 (2002).
Q Qian, T Tyson, S Savrassov, C Kao, M Croft. Electronic Structure of La(1-x)CaxMnO3 Determined by Spin-polarized X-ray Absorption Spectroscopy: Comparison of Experiments with Band-Structure Computations. *Phys. Rev. B*. **68**, 014429 (2003).
M v. Zimmermann, C Nelson, J Hill, D Gibbs, M Blume, D Casa, B Keimer, Y Murakami, C Kao, et al.. X-ray Resonant Scattering Studies of Orbital and Charge Ordering in Pr1-xCaxMnO3. *J. Magn. Magn. Mater.*. **233**, 31 (2001).
M v. Zimmermann, C Nelson, J Hill, D Gibbs, M Blume, D Casa, B Keimer, Y Murakami, C Kao, et al.. X-ray resonant scattering studies of orbital and charge ordering in Pr1-xCaxMnO3. *Phys. Rev. B*. **64**, 195133 (2001).
L Yang, L Ding, H Huang. New Phases of Phospholipids and Implications to the Membrane Fusion Problem. *Biochemistry*. **42** (22), 6631-6635 (2003).
L Yang, L Ding, H Huang. A Rhombohedral Phase of Lipid Containing a Membrane Fusion Intermediate Structure. *Biophys. J.*. **84**, 1808 (2003).

Beamline X22A

G da Silva, J Fossum, E DiMasi, K Maloy, S Lutnaes. Synchrotron x-ray scattering studies of water intercalation in a layered synthetic silicate. *Phys. Rev. E*. **66**, 011303 (2002).
G da Silva, J Fossum, E DiMasi, K Maloy. Hydration transitions in a nanolayered synthetic silicate: A synchrotron x-ray scattering study. *Phys. Rev. B*. **67**, 094114 (2003).
F He, B Wells, S Shapiro, M Zimmermann, A Clark, X Xi. Anomalous Phase Transition in Strained SrTiO3 Thin Films. *Appl. Phys. Lett.*. **83** (1), 123 (2003).
J Schearer, B Ocko, O Magnussen. Structure, dissolution, and passivation of Ni(111) electrodes in sulfuric acid solution: an in situ STM, x-ray scattering, and electrochemical study. *Electrochim. Acta*. **48**, 1169-1191 (2003).
H Schollmeyer, B Ocko, H Riegler. Surface Freezing of Triacontane at SiOx/Air Interfaces: Submonolayer Coverage. *Langmuir*. **18**, 4351 (2002).
J Wang, B Ocko, R Adzic. Overpotential Deposition of Ag Monolayer and Bilaer on Au(111) mediated by Pb Adlayer Unerpotential Deposition/Stripping Cysles. *Surf. Sci.*. **540** (2-3), 230 (2003).

Beamline X22B

J Blasie, S Zheng, J Strzalka. Solution to the phase problem for specular x-ray or neutron reflectivity from thin films on liquid surfaces. *Phys. Rev. B*. **67** (22), 224201 (2003).
E DiMasi, V Patel, M Sivakumar, M Olszta, Y Yang, L Gower. Polymer-Controlled Growth Rate of an Amorphous Mineral Film Nucleated at a Fatty Acid Monolayer. *Langmuir*. **18**, 8902-8909 (2002).
E DiMasi, M Olszta, V Patel, L Gower. When is template directed mineralization really template directed?. *Cryst. Eng.*. **5** (61), 346-350 (2003).
A Gibaud, D Grosso, B Smarsly, A Baptiste, J Bardeau, F Babonneau, D Doshi, Z Chen, C Brinker, C Sanchez. Evaporation-Controlled Self-Assembly of Silica Surfactant Mesophases. *J. Phys. Chem. B*. **107**, 6114-6118 (2003).
A Gibaud, D Doshi, B Ocko, V Goletto, C Brinker. Time-resolved in situ grazing incidence small angle x-ray scattering experiment of evaporation induced self-assembly. *Nanotechnology in Mesostructured Materials*, p. 351-354, Elsevier, St. Louis. (2003).
A Gibaud, A Baptiste, D Doshi, C Brinker, L Yang, B Ocko. Wall thickness and core radius determination in surfactant templated silica thin films using GISAXS and X-ray reflectivity. *Europhys. Lett.*. **63** (6), 833-839 (2003).
P Huber, O Shpyrko, P Pershan, B Ocko, H Tostmann, E DiMasi, M Deutsch. Short-range wetting at liquid gallium-bismuth alloy surfaces: X-ray measurements and square-gradient theory. *Phys. Rev. B: Condens. Matter*. **68**, 085409 (2003).
M Kent, H Kim, D Sasaki, J Majewski, G Smith, K Shin, S Satija, B Ocko. Segment concentration profile of myoglobin adsorbed tometal ion chelating lipid monolayers at the air-water interface by neutron reflection. *Langmuir*. **18**, 3754 (2002).

H Kraack, M Deutsch, B Ocko, P Pershan. The Structure of Organic Langmuir Films on liquid Metal Surfaces. *Nucl. Instrum. Meth. B*. **200**, 363-370 (2003).

H Kraack, B Ocko, P Pershan, E Sloutskin, M Deutsch. Structure of a Langmuir Film on a Liquid Metal Surface. *Science*. **298**, 1404 (2002).

H Lavoie, D Blaudez, D Vaknin, B Desbat, B Ocko, C Salesse. Spectroscopic and structural properties of valine gramicidin A in monolayers at the air-water interface. *Biophys. J.*. **83** (6), 3558-3569 (2002).

B Ocko, M Kelley, A Nikova, D Schwartz. Structure and Phase Behavior of Mixed Monolayers of Saturated and Unsaturated Fatty Acids. *Langmuir*. **18**, 9810-9815 (2002).

B Ocko, E Sirota, M Deutsch, E DiMasi, S Coburn, J Strzalka, S Zheng, A Tronin, T Gog, C Venkataraman. Positional order and thermal expansion of surface crystalline N-alkane monolayers. *Phys. Rev. E*. **6303** (3), 032602 (2001).

E Sloutskin, H Kraack, O Gang, B Ocko, E Sirota, M Deutsch. A Thin-thick Transition in the Surface-frozen Layer of a Binary Alcohol Mixture. *J. Chem. Phys.*. **118**, 10729 (2003).

E Sloutskin, O Gang, H Kraack, B Ocko, E Sirota, M Deutsch. Demixing transition in a quasi-two-dimensional surafce-frozen layer. *Phys. Rev. Lett.*. **89** (6), 065501 (2002).

A Tronin, J Strzalka, X Chen, P Dutton, B Ocko, J Blasie. Orientational distributions of the di-alpha-helical synthetic peptide ZnPPM-BBC16 in Langmuir monolayers by x-ray reflectivity and polarized epifluorescence. *Langmuir*. **17** (10), 3061-3066 (2001).

T Wandlowski, J Wang, B Ocko. Adsorption of bromide at the Ag(100) electrode surface. *J. Electroanal. Chem.*. **500** (1-2), 418-434 (2001).

S Ye, J Strzalka, X Chen, C Moser, P Dutton, J Blasie. Assembly of a Vectorially Oriented Four-Helix Bundle at the Air/Water Interface via Directed Electrostatic Interactions. *Langmuir*. **19**, 1515-1521 (2003).

S Zheng, J Strzalka, D Jones, S Opella, J Blasie. Comparative Structural Studies of Vpu Peptides in Phospholipid Monolayers by X-Ray Scattering . *Biophys. J.*. **84**, 2393-2415 (2003).

Beamline X22C

G Cao, L Balicas, Y Xin, J Crow, C Nelson. Quantum oscillations, colossal magnetoresistance, and the magnetoelastic interaction in bilayered Ca_3Ru_2O_7. *Phys. Rev. B: Condens. Matter*. **67** (18), 184405-1,8 (2003).

G Cao, L Balicas, Y Xin, E Dagotto, J Crow, C Nelson, D Agterberg. Tunneling Magnetoresistance and Quantum Oscillations in Bilayered Ca3Ru2O7. *Phys. Rev. B: Condens. Matter*. **67**, 060406(R) (2003).

D Gibbs. X-ray Magnetic Scattering. *Synch. Rad. News*. **14** (5), 4-10 (2001).

J Goff, R Sarthour, D McMorrow, F Yakhou, A Vigliante, D Gibbs, R Ward, M Wells. X-ray resonant scattering study of an intermediate-valence Ho-Ce alloy. *J. Magn. Magn. Mater.*. **226-230**, 1113-1115 (2001).

F He, B Wells, S Shapiro, M Zimmermann, A Clark, X Xi. Anomalous Phase Transition in Strained SrTiO3 Thin Films. *Appl. Phys. Lett.*. **83** (1), 123 (2003).

J Hill. Living on the K-edge: resonant scattering studies of electronic order in transition metal compounds. *Synch. Rad. News*. **14** (5), 21-26 (2001).

J Hill, C Nelson, M v. Zimmermann, Y Kim, D Gibbs, D Casa, B Keimer, Y Murakami, C Venkataraman, et al.. Orbital correlations in doped manganites. *Appl. Phys. A*. **73**, 723-730 (2001).

J Hill. Magnetic X-ray Scattering. *Characterization of Materials*, p. 752, John Wiley & Sons, New York. (2002).

V Kiryukhin, T Koo, H Ishibashi, J Hill, S Cheong. Average lattice symmetry and nanoscale structural correlations in magnetoresistive manganites. *Phys. Rev. B: Condens. Matter*. **67**, 064421 (2003).

H Nakao, Y Wakabayashi, T Kiyama, Y Murakami, M von Zimmerman, J Hill, D Gibbs, S Ishihara, Y Taguchi, Y Tokura. Quantitative Determination of the Atomic Scattering Tensor in Orbitally Ordered YTiO3 by using a Resonant X-ray Scattering Technique. *Phys. Rev. B*. **66**, 184419 (2002).

C Nelson, Y Kim, J Hill, D Gibbs, V Kiryukhin, T Koo, S Cheong. Structural distortions in the paramagnetic insulating phase of La0.7Ca0.3MnO3. *Materials Research Society 2001 Spring Meeting*, Vol 678, p. EE7.3, sponsored by MRS. (2001).

C Nelson, J Hill, D Gibbs. Resonant x-ray scattering as a probe of orbital and charge ordering. *Nanoscale Phase Separation and Colossal Magnetoresistance*, p. 179-183, Springer-Verlag, New York. (2002).

P Normile, W Stirling, D Mannix, G Lander, F Wastin, J Rebizant, S Coburn . (U1-xPux)Sb solid solutions. II. Energy dependencies. *Phys. Rev. B*. **66**, 014406 (2002).

M v. Zimmermann, C Nelson, J Hill, D Gibbs, M Blume, D Casa, B Keimer, Y Murakami, C Kao, et al.. X-ray resonant scattering studies of orbital and charge ordering in Pr1-xCaxMnO3. *Phys. Rev. B*. **64**, 195133 (2001).

M v. Zimmermann, C Nelson, Y Kim, J Hill, D Gibbs, H Nakao, Y Wakabayashi, Y Murakami, Y Tomioka, et al.. A resonant x-ray scattering study of octahedral tilt ordering in LaMnO3 and Pr1-xCaxMnO3. *Phys. Rev. B*. **64**, 1-9 (2001).

H Zajonz, D Gibbs, A Baddorf, D Zehner. Nanoscale strain distribution at the Ag/Ru(0001) interface. *Phys. Rev. B*. **67**, 155417-1 - 155417-8 (2003).

Beamline X23A2

F Alamgir. The Structural Origins Of The Stability of Palladium-Nickel-Phosphorus Bulk Metallic Glasses. Ph.D. Thesis. Lehigh University, Bethlehem. (2003).

D Brenner, S Sawant, P Hande, R Miller, C Elliston, Z Fu, G Randers-Pehrson, S Marino. Routine screening mammography: How important is the radiation-risk side of the benefit-risk equation?. *Int. J. Radiat. Biol.*. **78** (12), 1065-67 (2002).

C Dodge, A Francis. Structural characterization of a ternary Fe(III)-U(VI)-citrate complex. *Radiochim. Acta*. **91**, 525-532 (2003).

D McKeown, W Kot, I Pegg. X-ray Absorption Studies of the Local Strontium Environments in Borosilicate Waste Glasses. *J. Non-Cryst. Solids*. **317** (3), 290-300 (2003).

D McKeown, W Kot, I Pegg. X-ray Absorption Studies of Manganese Valence and Local Environment in Borosilicate Waste Glasses. *J. Non-Cryst. Solids*. **328**, 71-89 (2003).

F Ronci, P Stallworth, F Alamgir, T Schiros, J Sluytman, X Guo, P Reale, S Greenbaum, M denBoer, B Scrosati. Lithium-7 Nuclear Magnetic Resonance And Ti K-edge X-ray Absorption Spectroscopic Investigation Of Electrochemical Lithium Insertion In Li4/3+xTi5/3O4. *J. Power Sources*. **121**, 631-636 (2003).

Beamline X23B

S Calvin, E Carpenter, V Harris. Characterization of passivated iron nanoparticles by x-ray absorption spectroscopy. *Phys. Rev. B: Condens. Matter*. **68** (3), 033411-1-033411-4 (2003).

S Calvin, E Carpenter, B Ravel, V Harris, S Morrison. Multiedge Refinement of Extended X-Ray-Absorption Fine Structure of Manganese Zinc Ferrite Nanoparticles. *Phys. Rev. B: Condens. Matter*. **66** (22), 224405-1 - 224405-13 (2002).

G Chen, H Jain, M Vlcek, J Li, D Drabold, S Khalid, S Elliott. Study of light-induced vector changes in the local atomic structure of As¨CSe glasses by EXAFS. *J. Non-Cryst. Solids*. **326-327**, 257 (2003).

J Cui, Q Huang, J Vienot, H Yan, Q Wang, G Hutchison, A Richter, G Evmenenko, P Dutta, T Marks. Anode Interfacial Engineering Approaches to Enhancing Anode/Hole Transport Layer Interfacial Stability and Charge Injection Efficiency in Organic Light-Emitting Diodes. *Langmuir*. **18**, 9958-9970 (2002).

G Evmenenko, M van der Boom, C Yu, J Kmetko, P Dutta. Specular X-Ray Reflectivity Analysis of Adhesion Interface-Dependent Density Profiles in Nanometer-Scale Siloxane-Based Liquid Films. *Polymer*. **44** (4), 1051-1056 (2003).

A Facchetti, A Abbotto, L Beverina, M van der Boom, P Dutta, G Evmenenko, T Marks, G Pagani. Azinium-(ð-Bridge)-Pyrrole NLO-Phores: Influence of Heterocycle Acceptors on Chromophoric and Self-Assembled Thin-Film Properties. *Chem. Mater.*. **14**, 4996-5005 (2002).

A Facchetti, A Abbotto, L Beverina, M van der Boom, P Dutta, G Evmenenko, G Pagani, T Marks. Layer-by-layer self-assembled pyrrole-based donor-acceptor chromophores as electro-optic materials. *Chem. Mater.*. **15** (5), 1064-1072 (2003).

Y Koide, M Such, R Basu, G Evmenenko, J Cui, P Dutta, M Hersam, T Marks. Hot Microcontact Printing for Patterning ITO Surfaces. Methodology, Morphology, Microstructure, and OLED Charge Injectin Barrier Imaging. *Langmuir*. **19**, 86-93 (2002).

S Morrison, C Cahill, E Carpenter, S Calvin, V Harris. Preparation and Characterization of MnZn-Ferrite Nanoparticles Using Reverse Micelles. *J. Appl. Phys.*. **93** (10), 7489-7491 (2003).

F Ronci, P Stallworth, F Alamgir, T Schiros, J Sluytman, X Guo, P Reale, S Greenbaum, M denBoer, B Scrosati. Lithium-7 Nuclear Magnetic Resonance And Ti K-edge X-ray Absorption Spectroscopic Investigation Of Electrochemical Lithium Insertion In Li4/3+xTi5/3O4. *J. Power Sources*. **121**, 631-636 (2003).

S Yoon, P Helmke, J Amonette, W Bleam. X-ray Absorption and Magnetic Studies of Trivalent Lanthanide Ioins Sorbed on Pristine and Phosphate-Modifed Boehmite Surfaces. *Langmuir*. **18**, 10128-10136 (2002).

P Zhu, H Kang, A Facchetti, G Evmenenko, P Dutta, T Marks. Vapor Phase Self-Assembly of Electrooptic Thin Films via Triple Hydrogen Bonds. *J. Am. Chem. Soc.*. **125** (38), 11496-11497 (2003).

P Zhu, M van der Boom, H Kang, G Evmenenko, P Dutta , T Marks. Realization of Expeditious Layer-by-Layer Siloxane-Based Self-assembly as an Efficient Route to Structurally Regular Acentric Superlattices with Large Electro-optic Responses. *Chem. Mater.*. **14**, 4982-4989 (2002).

Beamline X24A

K McCarthy, U Arp, A Baciero, B Zurro, B Karlin. Response of chromium-doped alumina screens to soft x-rays using synchrotron radiation. *J. Appl. Phys.*. **94**, 958 (2003).

Beamline X24C

L Goray, J Seely. Efficiencies of Master, Replica, and Multilayer Gratings for the Soft X-Ray - Extreme Ultraviolet Range: Modeling Based on the Modified Intergral Method and Comparisons with Measurements. *Appl. Optics-OT*. **41**, 1434 (2002).

M Kowalski, R Cruddace, K Wood, D Yentis, H Gursky, T Barbee, Jr., W Goldstein, J Kordas, G Fritz, et al.. The Astrophysical Plasmadynamic Explorer (APEX): a high-resolution spectroscopic observatory. *Astronomical Telescopes and Instrumentation*, Vol 4854, p. 640-652, sponsored by SPIE. (2002).

B Sae-Lao, S Bajt, C Montcalm, J Seely. Performance of Normal-Incidence Molybdenum/Yttrium Multilayer-Coated Diffraction Grating at a Wavelength of 9 nm. *Appl. Optics-OT*. **41**, 2394 (2002).

J Seely. Extreme Ultraviolet Thin-Film Interference in an Al-Mg-Al Multiple-Layer Transmission Filter. *Appl. Optics-OT*. **41**, 5979 (2002).

J Seely, C Montcalm, S Bajt. High-Efficiency MoRu/Be Multilayer Grating Operating near Normal Incidence in the 11.1-12.0 nm Wavelength Range. *Appl. Optics-OT*. **40**, 5565 (2001).

J Seely, Y Uspenskii, Y Pershin, V Kondratenko, A Vinogradov. Skylab 3600 groove/mm Replica Grating with a Scandium-Silicon Multilayer Coating and High Normal-Incidence Efficiency at 38 nm Wavelength. *Appl. Optics-OT*. **41**, 1846 (2002).

J Seely, C Boyer, G Holland, J Weaver. X-Ray Absolute Calibration of the Time Response of a Silicon Photodiode. *Appl. Optics-OT*. **41**, 5209 (2002).

Beamline X25

J Alexander, C Nelson, V van Berkel, E Lau, J Studts, T Brett, S Spe, T Handel, H Virgin, D Fremont. Structural Basis of Chemokine Sequestration by a Herpesvirus Decoy Receptor. *Cell*. **111**, 343-356 (2002).

J Avalos, I Celic, S Muhammad, M Cosgrove, J Boeke, C Wolberger. Structure of a Sir2 Enzyme Bound to an Acetylated p53 Peptide. *Mol. Cell*. **10** (3), 523-535 (2002).

M Bertero, R Rothery, M Palak, C Hou, D Lim, F Blasco, J Weiner, N Strynadka. Insights into the Respiratory Electron Transfer Pathway from the Structure of Nitrate Reductase A. *Nat. Struct. Biol.*. **10** (9), 681-687 (2003).

I Bosanac, J Alattia, T Mal, J Chan, S Talarico, F Tong, K Tong, F Yoshikawa, T Furuichi, et al. Structure of the Inositol 1,4,5-trisphosphate Receptor Binding Core in Complex with its Ligand. *Nature*. **420**, 696 (2002).

T Brett, L Traub, D Fremont. Accessory Protein Recruitment Motifs in Clathrin-Mediated Endocytosis. *Structure*. **10** (6), 797-809 (2002).

G Cao, L Balicas, Y Xin, E Dagotto, J Crow, C Nelson, D Agterberg. Tunneling Magnetoresistance and Quantum Oscillations in Bilayered Ca3Ru2O7. *Phys. Rev. B: Condens. Matter*. **67**, 060406(R) (2003).

G Cao, L Balicas, Y Xin, J Crow, C Nelson. Quantum oscillations, colossal magnetoresistance, and the magnetoelastic interaction in bilayered Ca_3Ru_2O_7. *Phys. Rev. B: Condens. Matter*. **67** (18), 184405-1,8 (2003).

D Chimento, A Mohanty, R Kadner, M Wiener. Substrate-induced transmembrane signaling in the cobalamin transporter BtuB. *Nat. Struct. Biol.*. **10** (5), 394-401 (2003).

H Cho, K Mason, K Ramyar, A Stanley, S Gabelli, D Denney, D Leahy. Structure of the Extracellular Region of HER2 Alone and in Complex with the Herceptin Fab. *Nature*. **421**, 756-760 (2003).

J Ding, A Smith, S Geisler, X Ma, G Arnold, E Arnold. Crystal Structure of a Human Rhinovirus that Displays Part of the HIV-1 V3 Loop and Induces Neutralizing Antibodies against HIV-1. *Structure*. **10**, 999-1011 (2002).

R Dutzler, E Campbell, R MacKinnon. Gating the Selectivity Filter in ClC Chloride Channels. *Science*. **300**, 108-112 (2003).

C Escalante, L Shen, D Thanos, A Aggarwal. Structure of NF-kB p50/p65 Heterodimer Bound to the PRDII DNA Element fro mthe Interferon-beta Promoter. *Structure*. **10**, 383-391 (2002).

K Ferguson, M Berger, J Mendrola, H Cho, D Leahy, M Lemmon. EGF activates its receptor by removing interactions that auto-inhibit ectodomain dimerization. *Mol. Cell*. **11**, 507-517 (2003).

J Hansen, J Ippolito, N Ban, P Nissen. The Structures of Four Macrolide Antibiotics Bound to the Large Ribosomal Subunit. *Mol. Cell*. **10**, 117-128 (2002).

A Hodel, M Hodel, E Griffis, K Hennig, G Ratner, S Xu, M Powers. The Three-Dimensional Structure of the Autoproteolytic, Nuclear Pore-Targeting Domain of the Human Nucleoporin Nup98. *Mol. Cell*. **10**, 347-358 (2002).

M Hu, P Li, M Li, W Li, T Yao, J Wu, W Gu, R Cohen, Y Shi. Crystal Structure of a UBP-Family Deubiquitinating Enzymen in Isolation and in Complex with Ubiquitin Aldehyde. *Cell*. **111**, 1041-1054 (2002).

Q Huai, H Wang, Y Sun, H Kim, Y Liu, H Ke. Three-dimensional Structures of PDE4D in Complex with Roliprams and Implication on Inhibitor Selectivity. *Structure*. **11**, 865-873 (2003).

M Huang, A Rigby. Structural basis of membrane binding by Gla domains of Vitamine-K dependent proteins. *Nat. Struct. Biol.*. **10** (9), 751 (2003).

Y Huang, M Lemineux, J Song, M Auer, D Wang. Structure and Mechanism of the Glycerol-3-Phosphate Transporter from Escherichia coli. *Science*. **301**, 616-620 (2003).

J Jiang, A Lee, J Chen, V Ruta, M Cadene, B Chait, R MacKinnon. X-ray structure of a voltage-dependent K+ channel. *Nature*. **423**, 33-41 (2003).

S Johnson, J Taylor, L Beese. Processive DNA Synthesis Observed in a Polymerase Crystal Suggests a Mechanism for the Prevention of Frameshift Mutations. *Proc Natl Acad Sci USA*. **100** (7), 3895-3900 (2003).

Z Juo, G Kassavetis, J Wang, E Geiduschek, P Sigler. Crystal structure of a transcription factor IIIB core interface ternary complex. *Nature*. **422**, 534-539 (2003).

L Kang, S Gabelli, M Bianchet, W Xu, M Bessman, L Amzel. Structure of a coenzyme A pyrophosphatase from Deinococcus radiodurans: a member of the Nudix family. *J. Bacteriol.*. **185** (14), 4110-9 (2003).

C Kielkopf, N Rodionova, M Green, S Burley. A Novel Peptide Recognition Mode Revealed by the X-Ray Structure of a Core U2AF 35/U2AF 65 Heterodimer. *Cell*. **106**, 595-605 (2001).

A Klon, A Heroux, L Ross, V Pathak, C Johnson, J Piper, D Borhani. Atomic Structures of Human Dihydrofolate Reductase Complexed with NADPH and Two Lipophilic Antifolates at 1.09 Å and 1.05 Å Resolution. *J. Mol. Biol.*. **320** (3), 677-693 (2002).

F Li, Y Xiong, J Wang, H Cho, K Tomita, A Weiner, T Steitz. Crystal Structures of the Bacillus sterothermophilus CCA-Adding Enzyme and its Complexes with ATP or CTP. *Cell*. **111**, 815-824 (2002).

J Liu, M Lu. An Alanine-Zipper Structure Determined by Long Range Intermolecular Interactions. *J. Biol. Chem.*. **277** (50), 48708-48713 (2002).

E Mains, Y Xiong, M Cocco, L D'Andrea, L Regan. Design of Stable alpha-Helical Arrays from an Idealized TPR Motif. *Structure*. **11** (5), 497-508 (2003).

A Mulichak, C Bonin, W Reiter, R Garavito. Structure of the MUR1 GDP-Mannose 4,6-Dehydratase from Arabidopsis thaliana: Implicatins for Ligand Binding and Specificity. *Biochemistry*. **41**, 15578-15589 (2002).

A Mulichak, H Losey, W Lu, Z Wawrzak, C Walsh, R Garavito. Structure of the TDP-epi-vancosaminyltransferase GtfA from the chloroeremomycin biosynthetic pathway. *Proc Natl Acad Sci USA*. **100** (16), 9238-9243 (2003).

S Nair, S Burley. X-ray Structures of Myc-Max and Mad-Max Recognizing DNA: Molecular Bases of Regulation by Proto-Oncogenic Transcription Factors. *Cell*. **112**, 193-205 (2003).

A Prota, J Campbell, P Schelling, J Forrest, M Watson, T Peters, M Aurrand-Lions, B Imhof, T Dermody, T Stehle. Crystal structure of human junctional adhesion molecule 1: Implications for

reovirus binding. *Proc Natl Acad Sci USA*. **100** (9), 5366-5371 (2003).

S Ray, J Bonanno, K Rajashankar, M Pinho, G He, H De Lencastre, A Tomasz, S Burley. Cocrystal Structures of Diaminopimelate Decarboxylase: Mechanism, Evolution, and Inhibition of an Antibiotic Resistance Accessory Factor. *Structure*. **10**, 1499-1508 (2002).

N Schrader, K Fischer, K Theis, R Mendel, G Schwarz, C Kisker. The Crystal Structure of Plant Sulfite Oxidase Provides Insights into Sulfite Oxidation in Plants and Animals. *Structure*. **11** (10), 1251-1263 (2003).

B Staker, K Hjerrild, M Feese, C Behnke, A Burgin, Jr., L Stewart. The Mechanism of Topoisomerase I Poisoning by a Camptothecin Analog. *Proc Natl Acad Sci USA*. **99** (24), 15387-15392 (2002).

H Walden, M Podgorski, B Schulman. Insights into the Ubiquitin Transfer Cascade from the Structure of the Activating Enzyme for NEDD8. *Nature*. **422**, 330 (2003).

J Wilson, O Matsushita, A Okabe, J Sakon. A Bacterial Collagen-Binding Domain with Novel Calcium-Binding Motif Controls Domain Orientation. *EMBO J.*. **22** (8), 1743-1752 (2003).

J Wu, A Krawitz, J Chai, W Li, F Zhang, K Luo, Y Shi. Structural Mechanism of Smad4 Recognition by the Nuclear Oncoprotein Ski: Insights on Ski-Mediated Repression of TGF-beta Signaling. *Cell*. **111**, 357-367 (2002).

Y Yin, T Steitz. Structural Basis for the Transition from Initiation to Elongation Transcription in T7 RNA Polymerase. *Science*. **298**, 1387 (2002).

F Zalfa, M Giorgi, B Primerano, A Moro, A Di Penta, S Reis, B Oostra, C Bagni. The Fragile X Syndrome Protein FMRP Associates with BC1 RNA and Regulates the Translation of Specific mRNAs at Synapses . *Cell*. **112**, 317-327 (2003).

Beamline X26A

A Aerts, B Velde, K Janssens, W Dijkman. Change in Silica Sources in Roman and Post-Roman Glass. *Spectrochim. Acta B*. **58**, 659-667 (2003).

Y Arai, A Lanzirotti, S Sutton, J Davis, D Sparks. Arsenic Speciation and Reactivity in Poultry Litter. *Environ. Sci. Tech.*. **37** (18), 4083-4090 (2003).

M Dyar, M Gunter, J Delaney, A Lanzirotti, S Sutton. Systematics in the structure and XANES spectra of pyroxenes, amphiboles, and micas as derived from oriented single crystals. *Can. Mineral*. **40**, 1375-1393 (2002).

G Flynn, L Keller, S Wirick, C Jacobsen, S Sutton. Analysis of interplanetary dust particles by soft and hard x-ray microscopy. *J. Phys. IV*. **104**, 367-372 (2003).

J Howe, R Loeppert, V Derose, D Hunter, P Bertsch. Localization and Speciation of Chromium in Subterranean Clover Using XRF, XANES, and EPR Spectroscopy. *Environ. Sci. Tech.*. **37** (18), 4091-4097 (2003).

B Jones, C Conko, J Flinn, D Linkous, A Lanzirotti, C Frederickson, P Bertsch, A Friedlich, A Bush. The Effect of enhanced zinc in drinking water on brain and memory. *Natural Science and the Environment:Prescription for a Better Environment*, Vol 1, p. 3, sponsored by USGS. (2003).

K Kehm, G Flynn, S Sutton, C Hohenberg. Combined noble gas and trace element measurements on individual stratospheric interplanetary dust particles. *Meteoritics & Planet. Sci.*. **37** (10), 1323-1335 (2002).

H Li, L Lee, D Schulze, C Guest. Role of Soil Manganese in the Oxidation of Aromatic Amines. *Environ. Sci. Tech.*. **37**, 2686-2693 (2003).

D Linkous, J Flinn, A Lanzirotti, C Frederickson, B Jones, P Bertsch. Use of Synchrotron X-ray Fluorescence to Measure race Metal Distribution in the Brain. *Transactions of the American Geophysical Union*, Vol F202, p. 81, sponsored by American Geophysical Union. (2002).

R Muller, E Weckert, J Zellner, M Drakopoulos. Investigation of Radiation-dose-induced Changes in Organic Light-atom Crystals by Accurate d-spacing Measurements. *J. Synch. Rad.*. **9** (6), 368-374 (2002).

A Neufeld, H Isaacs, I Cole, A Bond, S Furman. Characterisation of salt particle induced corrosion processes by synchrotron generated X-ray fluorescence and complementary surface analysis tools. *199th Electrochemical Society Meeting*, Vol 2001-5, p. 187-196, (2001).

T Punshon, P Bertsch, A Lanzirotti, K McLeod, J Burger. Geochemical signature of contaminated sediment remobilization by spatially resolved X-ray microanalysis of annual rings of Salix nigra. *Environ. Sci. Tech.*. **37**, 1766-1774 (2003).

D Roberts, A Scheinost, D Sparks. Zinc speciation in contaminated soils combing direct and indirect characterization methods. *Geochemical and Hydrological Reactivity of Heavy Metals in Soils*, p. 187-227, Lewis Publishers, Boca Raton. (2003).

D Roberts, R Ford, D Sparks. Kinetics and Mechanisms of Zn Complexation on Metal Oxides using EXAFS Spectroscopy. *J. Colloid Interface Sci.*. **263** (2), 364-376 (2003).

S Sutton, P Bertsch, M Newville, M Rivers, A Lanzirotti, P Eng. Microfluorescence and microtomography analyses of heterogeneous earth and environmental materials. *Applications of Synchrotron Radiation in Low-Temperature Geochemistry and Environmental Science*, p. Chapter 8, Mineralogical Society of America, Washington, D.C. (2002).

T Tokunaga, J Wan, M Firestone, T Hazen, K Olson, D Herman, S Sutton, A Lanzirotti. In situ reduction of chromium(VI) in heavily contaminated soils through organic carbon amendment. *J. Environ. Qual.*. **32**, 1641-1649 (2003).

T Tokunaga, J Wan, T Hazen, E Schwartz, M Firestone, S Sutton, M Newville, K Olson, A Lanzirotti, W Rao. Distribution of Chromium Contamination and Microbial Activity in Soil Aggregates. *J. Environ. Qual.*. **32**, 541-549 (2003).

T Tokunaga, K Olson, J Wan. Moisture characteristics of Hanford gravels: Bulk, grain-surface, and intragranular components. *Vadose Zone J.*. **2**, 322-329 (2003).

J Twilley. Pigment Analyses for the Grave Stelae and Architectural Fragments from Chersonesos. *Color in Ancient Greece: The Role of Color in Ancient Greek Art and Architecture 700 – 31 B.C*, p. 171-178, Lamrakis Research Foundation, Aristotle University, Thessaloniki. (2002).

D Vantelon, A Lanzirotti, B Aeschlimann, D Guenther, A Scheinost, R Kretzschmar. Micro-scale Pb distribution and oxidation in a shooting range soil. *Geochim. Cosmochim. Acta*. **66** (S1), A-799 (2002).

Beamline X26C

K Bateman, E Brownie, W Wolodko, M Fraser. Structure of the Mammalian CoA Transferase from Pig Heart. *Biochemistry*. **417**, 14455-14462 (2002).

A Hodel, M Hodel, E Griffis, K Hennig, G Ratner, S Xu, M Powers. The Three-Dimensional Structure of the Autoproteolytic, Nuclear Pore-Targeting Domain of the Human Nucleoporin Nup98. *Mol. Cell*. **10**, 347-358 (2002).

A Kilshtain-Vardi, M Glick, H Greenblatt, A Goldblum, G Shoham. Refined Structure of Bovine Carboxypeptidase A at 1.25 Angstrom Resolution. *Acta Cryst. D*. **59**, 323-333 (2003).

J Liu, J Dai, M Lu. Zinc-Mediated Helix Capping in A Triple-Helical Protein. *Biochemistry*. **42**, 5657-5664 (2003).

D M Himmel, S Gourinath, L Reshetnikova, Y Shen, A G Szent-Gyorgyi, C Cohen. Crystallographic Findings on the Internally-uncoupled and Near-rigor States of Myosin: Further Insights into the Mechanics of the Motor. *Proc Natl Acad Sci USA*. **99** (20), 12645-12650 (2002).

J Min, Q Feng, Z Li, Y Zhang, R Xu. Structure of the Catalytic Domain of Human DOT1L, A Non-SET Domain Nucleosomal Histone Methyltransferase. *Cell*. **112**, 711-723 (2003).

M Rudolph, J Johnson, K Rajagopalan, C Kisker. The 1.2 Angstrom Structure of the Human Sulfite Oxidase Cytochrome b5 Domain. *Acta Cryst. D*. **59**, 1183-1191 (2003).

N Schrader, K Fischer, K Theis, R Mendel, G Schwarz, C Kisker. The Crystal Structure of Plant Sulfite Oxidase Provides Insights into Sulfite Oxidation in Plants and Animals. *Structure*. **11** (10), 1251-1263 (2003).

Beamline X27C

Y Cohen, E Thomas. Effect of Defects on the Response of a Layered Block Copolymer to Perpendicular Deformation: One-Dimensional Necking. *Macromolecules*. **36**, 5265-5270 (2003).

G Floudas, P Papadopoulos, H Klok, G Vandermeulen, J Rodriguez-Hernandez. Hierarchical Self-Assembly of Poly(ã-benzyl-L-glutamate)-Poly(ethylene glycol)-Poly(ã-benzyl-L-glutamate) Rod-Coil-Rod Triblock Copolymers. *Macromolecules*. **36**, 3673-3683 (2003).

L Liu, B Hsiao, B Fu, S Ran, S Toki, B Chu, A Tsou, P Agarwal. Structure Changes During Uiaxial Deformation of Ethylene-Based Semicrystalline Ethylene-Propylene Copolymer. 1. SAXS Study. *Macromolecules*. **36**, 1920-1929 (2003).

L Liu, Q Wan, T Liu, B Hsiao, B Chu. Salt-Induced Polymer Gelation and Formation of Nanocrystals in a Polymer-Salt System. *Langmuir*. **18**, 10402-10406 (2002).

S Ran, C Burger, D Fang, X Zong, B Chu, B Hsiao, Y Ohta, K Yabuki, P Cunniff. A Synchrotron WAXD Study on the Early Stages of Coagulation during PBO Fiber Spinning. *Macromolecules*. **35**, 9851 (2002).

R Somani, L Yang, B Hsiao, P Agarwal, H Fruitwala, A Tsou. Shear-Induced Precursor Structures in Isotactic Polypropylene Melt by in-Situ Rheo-SAXS and Rheo-WAXD Studies. *Macromolecules*. **35**, 9096-9104 (2002).

S Toki, B Hsiao. Nature of Strain-Induced Structures in Natural and Synthetic Rubbers Under Stretching. *Macromolecules*. **36**, 5915-5917 (2003).

S Xu, G Offer, J Gu, H White, L Yu. Temperature and Ligand Dependence of Conformation and Helical Order in Myosin Filaments. *Biochemistry*. **42**, 390-401 (2003).

F Yeh, B Hsiao, B Sauer, S Michel, H Siesler. In-Situ Studies of Structure Development During Deformation of a Segmented Poly(urethane-urea) Elastomer. *Macromolecules*. **36**, 1940-1954 (2003).

L Zhu, P Huang, W Chen, X Weng, S Cheng, Q Ge, R Quirk, T Senador, M Shaw, et al.. "Plastic Deformation" Mechanism and Phase Transformation in a Shear-Induced Metastable Hexagonally Perforated Layer Phase of a Polystyrene-b-poy(ethylene oxide) Diblock Copolymer. *Macromolecules*. **36**, 3180-3188 (2003).

Beamline X28C

M Brenowitz, M Chance, G Dhavan, K Takamoto. Probing the Structural Dynamics of Nucleic Acid Structure by Quantitive Time-Resolved and Equilibrium Hydroxyl Radical "Footprinting". *Curr. Opin. Struct. Biol.*. **12**, 648-653 (2002).

G Dhavan, M Chance, M Brenowitz. Kinetics Analysis of DNA-Protein Interactions by Time-Resolved Synchrotron X-Ray Footprinting . *Analysis of Macromolecules: A Practical Approach*, p. 75-86, IRL Press at Oxford University Press, Oxford. (2003).

J Kiselar, P Janmey, S Almo, M Chance. Visualizing the Ca2+-dependent activation of gelsolin by using synchrotron footprinting. *Proc Natl Acad Sci USA*. **100** (7), 3942-3947 (2003).

P Rangan, B Masquida, E Westhof, S Woodson. Assembly of Core Helices and Rapid Tertiary Folding of a Small Bacterial Group I Ribozyme. *Proc Natl Acad Sci USA*. **100** (4), 1574-1579 (2003).

H Rashidzadeh, S Khrapunov, M Chance, M Brenowitz. Solution Structure and Interdomain Interactions of the Saccharomyces cerevisiae "TATA Binding Protein" (TBP) Probed by Radiolytic Protein Footprinting. *Biochemistry*. **42**, 3655-3665 (2003).

K Takamoto, Q He, S Morris, M Chance, M Brenowitz. Monovalent Cations Mediate Formation of Native Tertiary Structure of the Tetrahymena Thermophila Ribozyme: Implications for the Kinetics of Folding. *Nat. Struct. Biol.*. **9**, 928-933 (2002).

T Ucida, K Takamoto, Q He, M Chance, M Brenowitz. Multiple Monovalent Ion-Dependent Pathways for the Folding of the L-21 Tetrahymena Thermophila Ribozyme. *J. Mol. Biol.*. **328**, 463-478 (2003).

S Woodson. Folding Mechanisms of Group I Ribozymes: Role of Stability and Contact Order. *Biochem Soc Trans*. **30**, 1166-1169 (2002).

NSLS Staff

B Acharya, K Baldwin, R MacHarrie, J Rogers, C Huang, R Pindak. High-speed In-fiber Nematic Liquid Crystal Optical Modulator Based on In-plane Switching with Microsecond Response Time. *Appl. Phys. Lett.*. **81** (27), 5243 (2002).

O Adamopoulos, Z Yu, M Croft, I Zakharchenko, T Tsakalakos, M Muhammed. The characterisation and reactivity of nanostructured cerium-copper-oxide composites for environmental catalysis. *Synthesis, Functional Properties and Applications of Nanostructures. Symposium (Materials Research Society Symposium Proceedings Vol.676)*, Vol 676, p. Y8.11.1-6, sponsored by Mater. Res. Soc. (2002).

T Beetz, C Jacobsen, C Kao, J Kirz, T Mentes, C Sanchez-Hanke, D Sayre, D Shapiro. Development of a Novel Apparatus for Experiments in Soft X-ray Diffraction Imaging and Diffraction Tomography. *J. Phys. IV*. **104**, 31-34 (2003).

C Bernhard, T Holden, J Humlicek, D Munzar, A Golnik, M Klaser, T Wolf, L Carr, C Homes, et al.. In-plane polarized collective modes in detwined Yba2Cu3O6.95 observed by spectral ellipsometry. *Solid State Commun.*. **121**, 1963-1967 (2002).

B Blank, T Kupp, A Deyhim, Y Cai, P Chow, C Kao. Development of a Spectrometer for Inelastic X-ray Measurements. *Proceedings of the 2nd International Workshop on Mechanical Engineering Design of Synchrotron Radiation Equipment and Instrumentation (MEDSI02)*, Vol , p. 308-314, sponsored by MEDSI02. (2002).

G Carr. Dynamics of GaAs photocarriers probed with pulsed infrared synchrotron radiation. *Nucl. Instrum. Meth. B*. **199**, 323 (2003).

F Castano, Y Hao, S Haratani, C Ross, B Vogeli, H Smith, C Sanchez-Hanke, C Kao, X Zhu, P Grutter. Magnetic force microscopy and x-ray scattering study of 70x550 nm2 pseudo-spin-valve nanomagnets. *J. Appl. Phys.*. **93** (10), 7927-7929 (2003).

L Chapman, M Hasnah, O Oltulu, Z Zhong, J Mollenhauer, C Muehleman, K Kuettner, M Aurich, E Pisano, et al.. Diffraction Enhanced X-ray Imaging of Articular Cartilage. US Patent No. 657,7708. (2003).

G Chen, H Jain, M Vlcek, S Khalid, J Li, D Drabold, S Elliott. Observation of Light Polarization-dependent Structural Changes in Chalcogenide Glasses. *Appl. Phys. Lett.*. **82** (5), 706 (2003).

G Chen, H Jain, S Khalid, J Li, D Drabold, S Elliott. Study of Structural Changes in Amorphous As2Se3 By EXAFS under In-Situ Laser Irradiation. *Solid State Commun.*. **120**, 149-153 (2001).

M Croft, W Caliebe, H Woo, T Tyson, D Sills, Y Hor, S Cheong, V Kiryukhin, S Oh. Metal-insulator transition in CuIr2S4: XAS results on the electronic structure. *Phys. Rev. B: Condens. Matter*. **67**, 201102-1-4 (2003).

M Croft, I Zakharchenko, Z Zhong, T Tsakalakos, Y Gulak, Z Kalman, J Hastings, J Hu, R Holtz, K Sadananda. Stress Distribution and Tomographic Profiling with Energy Dispersive X-Ray Scattering. *MRS Proceedings: Applications of Synchrotron Radiation Techniques to Materials Science*, Vol 678, sponsored by Materials Research Society. (2002).

C Cui, T Tyson, Z Zhong, J P Carlo, Y Qin. Effects of Pressure on Electron Transport and Atomic Structure of Manganites: Low to High Pressure Regimes. *Phys. Rev. B: Condens. Matter*. **67**, 104107 (2003).

G De Geronimo, P O'Connor, R Beuttenmuller, Z Li, A Kuczewski, D Siddons. Development of a High-Rate High-Resolution Detector for EXAFS Experiments. *IEEE Trans. Nucl. Sci.*. **50** (4), 885 - 897 (2003).

F Dilmanian, H Weinmann, Z Zhong, T Bacarian, L Rigon, T Buttone, B Ren, X Wu, N Zhong, H Atkins. Tailoring X-ray Beam Energy Spectrum to Enhance Image Quality of New Radiography Contrast Agents Based on Gd or Other Lanthanides. *SPIE: Physics of Medical Imaging*, Vol 4320, p. 417-426, sponsored by SPIE. (2001).

A Doyuran, L DiMauro, E Johnson, S Krinsky, H Loos, J Murphy, G Rakowsky, J Rose, T Shaftan, et al.. Saturation of the NSLS DUV-FEL at BNL. *2003 Particle Accelerator Conference*, Vol 20, p. TOAC012, sponsored by IEEE. (2003).

A Doyuran, W Graves, E Johnson, S Krinsky, H Loos, G Rakowsky, J Rose, T Shaftan, B Sheehy, et al.. Diagnostics System for the NISUS Wiggler and FEL Observations at the BNL Source Development Lab. *European Particle Acclerator Conference, Paris 2002*, Vol 8, p. 802, sponsored by CEA/DSM and CNRS/IN2P3. (2002).

A Doyuran, L DiMauro, W Graves, R Heese, E Johnson, S Krinksy, H Loos, J Murphy, G Rakowsky, et al.. Observation of SASE and Amplified Seed of the DUV-FEL at BNL. *Nucl. Instrum. Meth. A*. **507**, 392-395 (2003).

A Doyuran, M Babzien, T Shaftan, S Biedron, L Yu, I Ben-Zvi, L DiMauro, J Galayda, E Gluskin, et al.. New Results of the High-Gain Harmonic Generation Free-Electon Laser Experiment. *Nucl. Instrum. Meth. A*. **475**, 260-265 (2001).

K Evans-Lutterodt, J Ablett, A Stein, C Kao, D Tennant, F Klemens, A Taylor, C Jacobsen, P Gammel, et al.. Single-element Elliptical Hard X-ray Micro-optics. *Opt. Express*. **11** (8), 919-926 (2003).

K Evans-Lutterodt, A Stein, J Ablett, C Kao, D Tennant, F Klemens, A Taylor, C Jacobsen, P Gammel, et al.. From Lighthouses to Synchrotron Lightsources: Hard X-ray Micro-optics. *Synch. Rad. News*. **16** (3), 60-63 (2003).

S Federman, L Miller, I Sagi. Following Matrix Metalloproteinases Activity Near the Cell Boundary by Infrared Micro-Spectroscopy. *Matrix Biol.*. **21**, 567-577 (2002).

N Gmur. Brookhaven's Free electron Laser at the NSLS Reaches a New Milestone. *Synch. Rad. News*. **16** (1), 32-33 (2003).

N Gmur. Brookhaven National Laboratory DUV-FEL Achieves Important Milestone. *Synch. Rad. News*. **15** (3), 29 (2002).

K Hamalainen, S Galambosi, H Sutinen, C Kao, R Sharon, M Deutsch. Near-threshold Mult-electronic Effects in the Cu K alpha 1,2 X-Ray Spectrum. *Phys. Rev. A*. **67**, 022510 (2003).

M Hasnah, Z Zhong, O Oltulu, E Pisano, R Johnston, D Sayers, W Thomlinson, D Chapman. Diffraction Enhanced Imaging Contrast Mechanisms in Breast

Cancer Specimens. *Med. Phys.*. **29**, 2216-2221 (2002).

M Hasnah, O Oltulu, Z Zhong, D Chapman. Single Exposure Simultaneous Diffraction Enhanced Imaging. *Nucl. Instrum. Meth. A*. **492**, 236-240 (2002).

M Hasnah, O Oltulu, Z Zhong, D Chapman. Application of Absorption and Refraction Matching Techniques for Diffraction Enhanced Imaging. *Rev. Sci. Instrum.*. **73**, 1657-1659 (2002).

H Hayashi, Y Udagawa, W Caliebe, C Kao. Lifetime-broadening Removed X-ray Absorption Near Edge Structure by Resonant Inelastic X-ray Scattering Spectroscopy. *Chem. Phys. Lett.*. **371**, 125 (2003).

H Hayashi, N Wantanabe, Y Udagawa, C Kao. Momentum Dependence of ð-ð* Excitations of Benzene Rings in Condensed Phases. *J. Electron. Spectrosc. Relat. Phenom.*. **933**, 114-116 (2001).

H Hayashi, Y Udagawa, J Gillet, W Caliebe, C Kao. Chemical Applications of Inelastic X-ray Scattering. *Chemical Application of Synchrotron Radiation*, p. 850, World Scientific, River Edge. (2002).

A Hennessy, G Graham, J Hastings, P Siddons, Z Zhong. New pressure flow cell to monitor BaSO4 precipitation using synchrotron in-situ angle dispersive X-ray diffraction. *J. Synch. Rad.*. **9**, 323-324 (2002).

R Huang, L Miller, C Carlson, M Chance. FTIR Analysis of Tibia Bone from Ovariectomized Cynomolgus Monkeys (Macaca fascialaris) and the Effect of Nandrolone Deconoate Treatment. *Bone*. **30** (2), 492-497 (2002).

N Jamin, L Miller, J Moncuit, W Fridman, P Dumas, J Teillaud. Chemical Heterogeneity in Cell Death: Combined Synchrotron IR and Fluorescence Microscopy Studies of Single Apoptotic and Necrotic Cells. *Biopolymers*. **72** (5), 366-373 (2003).

B Jones, C Conko, J Flinn, D Linkous, A Lanzirotti, C Frederickson, P Bertsch, A Friedlich, A Bush. The Effect of enhanced zinc in drinking water on brain and memory. *Natural Science and the Environment:Prescription for a Better Environment*, Vol 1, p. 3, sponsored by USGS. (2003).

S Judex, S Boyd, Y Qin, L Miller, R Muller, C Rubin. Combining High-Resolution MicroCT with Material Composition to Define the Quality of Bone Tissue. *Curr. Osteoporosis Reports*. **1**, 11-19 (2003).

S Kramer, B Podobedov. Coherent Microwave Synchrotron Radiation in the VUV Ring. *Proceedings of Eighth European Particle Accelerator Conference (EPAC'02)*, p. 1523, sponsored by EPAC-02. (2002).

S Krinsky, R Gluckstern. Analysis of Statistical Correlations and Intensity Spiking In The Self-Amplified Spontaneous-Emission Free-Electron Laser. *Phys. Rev. ST AB*. **6**, 050701 (2003).

S Krinsky, Z Huang. Frequency Chirped Self-Amplified Spontaneous-emission Free-electron Laser. *Phys. Rev. ST AB*. **6**, 050702 (2003).

A Lanzirotti, L Miller. Imaging and Microspectroscopy at the National Synchrotron Light Source. *Synch. Rad. News*. **15** (6), 17-26 (2003).

J Li, Z Zhong, R Litdke, K Kuettner, C Peterfy, E Aleyeva, C Muehleman. Radiography of Soft Tissue of the Foot and Ankle with Diffraction Enhanced Imaging. *J. Anatomy*. **202**, 463-470 (2003).

C Limborg, P Bolton, J Clendenin, D Dowell, P Emma, S Gierman, W Graves, H Loos, B Murphy, et al.. PARMELA vs Measurements for GTF and DUVFEL. *European Particle Acclerator Conference, Paris 2002*, Vol 8, p. 1786, sponsored by CEA/DSM and CNRS/IN2P3. (2002).

D Linkous, J Flinn, A Lanzirotti, C Frederickson, B Jones, P Bertsch. Use of Synchrotron X-ray Fluorescence to Measure race Metal Distribution in the Brain. *Transactions of the American Geophysical Union*, Vol F202, p. 81, sponsored by American Geophysical Union. (2002).

H Loos, L DiMauro, A Doyuran, W Graves, E Johnson, S Krinsky, J Rakowsky, J Rose, T Shaftan, et al.. Beam-based Trajectory Alignment in the NISUS Wiggler. *European Particle Accelerator Conference, Paris 2002*, Vol 8, p. 837, sponsored by CEA/DSM and CNRS/IN2P3. (2002).

H Loos, G Carr, A Doyuran, W Graves, E Johnson, S Krinsky, J Rose, B Sheehy, T Shaftan, et al.. Electron Bunch Compression and Coherent Effects at the SDL. *AIP Conference Proceedings*, Vol 647, p. 849-857, (2002).

H Loos, T Shaftan. Beam-Based Undulator Field Characterization and Correction at DUV-FEL. *2003 Particle Accelerator Conference*, Vol 20, p. MPPB038, sponsored by IEEE. (2003).

H Loos, A Doyuran, J Murphy, J Rose, T Shaftan, B Sheehy, Y Shen, J Skaritka, X Wang, et al.. Electro-Optic Longitudinal Electron Beam Diagnostic at SDL. *2003 Particle Accelerator Conference*, Vol 20, p. WPPB021, sponsored by IEEE. (2003).

H Loos, A Doyuran, W Graves, E Johnson, S Krinsky, J Rose, T Shaftan, B Sheehy, J Skaritka, et al.. Experiments in Coherent Radiation at SDL. *European Particle Acclerator Conference, Paris 2002*, Vol 8, p. 814, sponsored by CEA/DSM and CNRS/IN2P3. (2002).

H Mao, C Kao, R Hemley. Inelastic X-ray Scattering at Ultra-high Pressure. *J. Phys.: Condens. Matter*. **13**, 7847 (2001).

Y Mei, L Miller, W Gao, R Gross. Imaging the Distribution and Secondary Structure of Immobilized Enzymes using Infrared Microspectroscopy. *Biomacromolecules*. **4** (1), 70-74 (2003).

L Miller. National Synchrotron Light Source Activity Report 2002. Government Printing Office, Washington. Prepared for Department of Energy. (2003).

L Miller, T Tague. Development and Biomedical Applications of Fluorescence-assisted Synchrotron Infrared Micro-Spectroscopy. *Vib. Spectrosc.*. **849**, 1-7 (2002).

L Miller, G Smith, G Carr. Synchrotron-based Biological Microspectroscopy: From the Mid- to the Far-Infrared Regimes. *J. Biol. Phys.*. **29** (1), 219-230 (2003).

L Miller, P Dumas, N Jamin, J Teillaud, J Miklossy, L Forro. Combining IR Spectroscopy and Fluorescence Imaging in a Single Microscope: Biomedical Applications using a Synchrotron Infrared Source. *Rev. Sci. Instrum.*. **73**, 1357-1360 (2002).

H Mo, H Taub, U Volkmann, M Pino, S Ehrlich, F Hansen, E Lu, P Miceli. A Novel Growth Mode of Alkane Films on a SiO2 Surface. *Chem. Phys. Lett.*. **377**, 99-105 (2003).

J Mollenhauer, M Aurich, Z Zhong, C Muehleman, A Cole, M Hasnah, O Oltulu, K Kuettner, A Margulis, L

Chapman. Diffraction Enhanced X-ray Imaging of Articular Cartilage. *Osteoarthr. Cartilage*. **10**, 168-171 (2002).

C Muehleman, Z Zhong, J Williams, K Kuettner, M Aurich, B Han, J Mollenhauer. Diffraction-enhanced X-ray Imaging of Articular Cartilage of Experimental Animals. *Proceedings Annual Meeting Othrop. Research Society*, Vol , p. 365, sponsored by Ann. Mtg. Orthop. Res. Soc.. (2002).

C Muehleman, L Chapman, K Kuettner, J Rieff, J Mollenhauer, K Massuda, Z Zhong. Radiography of Rabbit Articular Cartilage with Diffraction Enhanced Imaging. *Anatomical Record*. **272A**, 392-397 (2003).

C Muehleman, M Whiteside, Z Zhong, J Mollenhauer, M Aurich, K Kuettner, L Chapman. Diffraction enhanced imaging for articular cartilage. *Biophys. J.*. **82**, 2292-2292 (2002).

J Neumann, D Demske, R Fiorito, P O'Shea, L Carr, H Loos, T Shaftan, B Sheehy, Z Wu. Study of Coherent Radiation from an Electron Beam Prebunched at the Photocathode. *2003 Particle Accelerator Conference*, Vol 20, p. TPAG030, sponsored by IEEE. (2003).

J Neumann, P O'Shea, D Demske, W Graves, B Sheehy, H Loos, G Carr. Electron beam modulation using a laser-driven photocathode . *Nucl. Instrum. Meth. A*. **57** (1-2), 498-501 (2003).

B Noheda, Z Zhong, D Cox, G Shirane, S Park, P Rehring. Electric-field induced phase transitions in rhombohedral Pb(Zn1/3Nb2/3)1-xTixO3. *Phys. Rev. B*. **65**, art no. 224101 (2002).

O Oltulu, Z Zhong, M Hasnah, D Chapman. Multiple Image Radiography in Diffraction Enhanced Imaging. *J. Phys. D: Appl. Phys.*. **36**, 2152-2156 (2003).

P Piot, L Carr, W Graves, H Loos. Subpicosecond compression by velocity bunching in a photoinjector. *Phys. Rev. ST AB*. **6**, 033503 (2003).

B Podobedov, J Ablett, L Berman, R Biscardi, L Carr, B Casey, S Dierker, A Doyuran, R Heese, et al.. NSLS Upgrade Concept. *2003 Particle Accelerator Conference*, Vol 20, p. TOPA007, sponsored by IEEE. (2003).

G Popov, M Greenblatt, M Croft. Large effects of a-site average cation size on the properties of the double perovskites Ba2 xSrxMnReO6, a d5-d1 System. *Phys. Rev. B: Condens. Matter*. **B67**, 24406 (2003).

D Pospiech, D Jehnichen, A Gottwald, L Häussler, U Scheler, P Friedel, W Kollig, C Ober, X Li, et al.. Investigation of the Microphase Separation in Semifluorinated Polyesters. *Polymeric Materials: Science & Engineering*, Vol 84, p. 314-315, sponsored by ACS. (2001).

Q Qian, T Tyson, S Savrassov, C Kao, M Croft. Electronic Structure of La(1-x)CaxMnO3 Determined by Spin-polarized X-ray Absorption Spectroscopy: Comparison of Experiments with Band-Structure Computations. *Phys. Rev. B*. **68**, 014429 (2003).

L Rigon, Z Zhong, F Arfelli, R Menk, A Pillon. Diffraction Enhanced Imaging utilizing different crystal reflections at Elettra and NSLS. *Proc. SPIE 4632: Physics of Medical Imaging*, Vol 4632, p. 29, sponsored by SPIE. (2002).

H Roberts, M Helba, J Carroll, J Burnett, T Drummond, J Lepak, R Propri, Z Zhong, F Agee. Gamma Spectroscopy of Hf-178m2 using Synchrotron X-rays. *Hyperfine Interact.*. **143**, 111-119 (2002).

J Rose, A Doyuran, W Graves, H Loos, T Shaftan, B Sheehy, Z Wu. Radio-Frequency Control System for the DUVFEL. *2003 Particle Accelerator Conference*, Vol 20, p. TPAB006, sponsored by IEEE. (2003).

T Shaftan, A Doyuran, W Graves, E Johnson, S Krinsky, H Loos, J Rose, B Sheehy, J Wu, et al.. Electron Bunch Compression in the SDL Linac. *European Particle Acclerator Conference, Paris 2002*, Vol 8, p. 834, sponsored by CEA/DSM and CNRS/IN2P3. (2002).

T Shaftan, M Babzien, I Ben-Zvi, S Biedron, L DiMauro, A Doyuran, W Graves, J Jagger, E Johnson, et al.. High Gain Harmonic Generation Free-Electron Laser at Saturation. *2001 Particle Accelerator Conference*, p. 246, sponsored by PAC. (2001).

T Shaftan, L Carr, H Loos, B Sheehy, W Graves, Z Huang, C Limborg. Microbunching and Beam Break-up in DUV FEL Accelerator. *2003 Particle Accelerator Conference*, Vol 20, p. TOPD005, sponsored by IEEE. (2003).

T Shaften, L DiMauro, A Doyuran, W Graves, R Heese, E Johnson, S Krinsky, H Loos, J Murphy, et al.. First Sase and Seeded FEL Lasing of NSLS DUV Fel at 266 and 400 nm. *Nucl. Instrum. Meth. A*. **507**, 15-18 (2003).

B Sheehy, G Carr, A Doyuran, W Graves, R Heese, E Johnson, S Krinsky, H Loos, J Murphy, G Rakowsky. Ultrafast Deep UV FEL Source for AMO Physics at Brookhaven National Laboratory. *Annual (2003) Meeting of the Division of Atomic, Molecular, and Optical Physics of the APS*, Vol 48, p. 61, sponsored by American Physical Society. (2003).

B Sheehy, G Carr, L DiMauro, A Doyuran, W Graves, R Heese, E Johnson, S Krinsky, H Loos, J Murphy. A Deep Ultraviolet Ultrafast Source Driven by High Gain. *CLEO/QELS 2003: Conference on Lasers and Electro-optics / Quantum Electronics and Laser Science Conference*, Vol 2003, p. QWC2, sponsored by Optical Society of America. (2003).

K Smith, J Xue, L Duda, A Fedorov, P Johnson, S Hulbert, W McCarroll, M Greenblatt. Recent high resolution photoemission studies of electronic structure in quasi-one dimensional conductors. *J. Electron. Spectrosc. Relat. Phenom.*. **117-118**, 517-526 (2001).

T Tsakalakos, M Croft, I Zakharchenko, Z Zhong, Y Gulak, M Desilva, R Holtz. On the Mechanical Stability of Nanostructured Coatings by Synchrotron Radiation. *AIAA 2002*, Vol AIAA-2002, p. 1314, sponsored by AIAA. (2002).

M v. Zimmermann, C Nelson, J Hill, D Gibbs, M Blume, D Casa, B Keimer, Y Murakami, C Kao, et al.. X-ray resonant scattering studies of orbital and charge ordering in Pr1-xCaxMnO3. *Phys. Rev. B*. **64**, 195133 (2001).

M v. Zimmermann, C Nelson, J Hill, D Gibbs, M Blume, D Casa, B Keimer, Y Murakami, C Kao, et al.. X-ray Resonant Scattering Studies of Orbital and Charge Ordering in Pr1-xCaxMnO3. *J. Magn. Magn. Mater.*. **233**, 31 (2001).

M Wernick, O Wirjadi, D Chapman, O Oltulu, Z Zhong, Y Yang. Preliminary investigation of a multiple-image radiography method. *IEEE. Intl. Symposium on Biomed. Imaging: Macro to Nano* , Vol (2002), p. 1435, sponsored by National Institute of Health. (2002).

J Wu, L Yu. Coherent Hard X-ray Productin by Cascading Stages of High Gain Harmonic

Generation X-ray FEL. *Nucl. Instrum. Meth. A*. **475** (1-3), 104 (2001).

Y Yacoby, M Sowman, E Stern, J Cross, D Brewer, R Pindak, J Pitney, E Dufresne, R Clarke. Direct determination of epitaxial interface structure: Gd2O3 passivation of GaAs, Nature Materials. *Nat. Mater.*. **1**, 99 (2002).

L Yang, L Ding, H Huang. New Phases of Phospholipids and Implications to the Membrane Fusion Problem. *Biochemistry*. **42** (22), 6631-6635 (2003).

L Yang, L Ding, H Huang. A Rhombohedral Phase of Lipid Containing a Membrane Fusion Intermediate Structure. *Biophys. J.*. **84**, 1808 (2003).

L Yu, L DiMauro, A Doyuran, W Graves, E Johnson, R Heese, S Krinsky, H Loos, J Murphy, et al. First Ultraviolet High-Gain Harmonic-Generation Free-Electron Laser. *Phys. Rev. Lett.*. **91** (7), 074801-1 (2003).

L Yu, J Wu. Theory of High Gain Harmonic Generation - an Analytical Estimate. *Nucl. Instrum. Meth. A*. **483**, 493 (2002).

L Yu, M Babzien, I Ben-Zvi, L DiMauro, A Doyuran, W Graves, E Johnson, S Krinsky, R Malone, et al.. First Lasing of a High Gain Harmonic Generation Free-Electron Laser Experiment. *Nucl. Instrum. Meth. A*. **445**, 301 (2000).

I Zakharchenko, Y Gulak, Z Zhong, M Croft, T Tsakalakos. Methodology of Synchrotron EDXRD Strain Profiling. *Advances in X-ray Analysis*, Vol 46, sponsored by International Centre for Diffraction Data. (2002).

I Zakharchenko, Y Gulak, Z Zhong, M Croft, T Tsakalakos. Application of Synchrotron EDXRD Strain Profiling in Shot Peened Materials. *Advances in X-ray Analysis*, Vol 46, sponsored by International Centre for Diffraction Data. (2002).

Z Zhong, C Kao, D Siddons, H Zhong, J Hastings. X-ray reflectivity of sagittally bent Laue crystals. *Acta Cryst. A*. **59**, 1-6 (2003).

Z Zhong, D Chapman, D Connor, A Dilmanian, N Gmur, M Hasnah, R Johnston, M Kiss, J Li, et al.. Diffraction Enhanced Imaging of Soft Tissues. *Synch. Rad. News*. **15** (6), 27-34 (2002).

Z Zhong, D Siddons, D Chapman, C Kao, N Zhong, J Hastings. Model of Sagittally-bent Silicon Crystals Diffracting in the Laue Mode: the Effects of Elastic-Anisotropy on the Rocking-curve Widths. *12th National Conference on Sychrotron Radiation Instrumentation*, Vol 73, p. 1615, sponsored by University of Wisconsin-Madison. (2002).

Z Zhong, D Chapman, M Hasnah, E Johnston, M Kiss, O Oltulu, L Rigon, N Zhong, E Pisano, D Sayers. X-ray Diffraction Order-selection with a Prism in DEI. *12th National Conference on Sychrotron Radiation Instrumentation*, Vol 73, p. 1614, sponsored by American Institute of Physics. (2002).

Z Zhong, C Kao, D Siddons, J Hastings. Rocking-curve width of sagittally bent Laue crystals. *Acta Cryst. A*. **58**, 487-493 (2002).

F Zhou, I Ben-Zvi, M Babzien, X Chang, A Doyuran, R Malone, X Wang, V Yakimenko. Experimental Characterization of Emittance Growth Induced the the Nonuniform Transverse Laser Distribution in a Photoinjector. *Phys. Rev. ST AB*. **5**, 094203 (2002).